NISTIR 8271 DRAFT SUPPLEMENT

Face Recognition Vendor Test (FRVT)

Part 2: Identification

Patrick Grother
Mei Ngan
Kayee Hanaoka
Information Access Division
Information Technology Laboratory

This document is a draft supplement of NIST Interagency Report 8271

2020/03/27

National Institute of Standards and Technology
U.S. Department of Commerce

NISTIR 8271 DRAFT SUPPLEMENT

Face Recognition Vendor Test (FRVT)

Part 2: Identification

Patrick Grother
Mei Ngan
Kayee Hanaoka
Information Access Division
Information Technology Laboratory

This document is a draft supplement of NIST Interagency Report 8271

January 2020

U.S. Department of Commerce
Wilbur Ross, Secretary

National Institute of Standards and Technology
Walter Copan, Director

RELEASE NOTES

2020-03-24: The second draft of the update to NIST Interagency Report 8271:

- ▷ Adds results for three algorithms from three developers, Dermalog, Innovatrics, and Synesis.
- ▷ Adds Table 7 on ageing showing the increase in false negative rates with time elapsed between two photos. Some of the results were contained in graphs in prior editions of this report, but the table adds results for some newly submitted algorithms.
- ▷ Adjusts frontal mugshot results (for recent and lifetime consolidated galleries) to include the effect of removing some images that should not have been included in image test sets. These images were mostly profile views, images of tattoos containing faces, images of faces on tee shirts, and images of photographs on walls behind the intended subject. This affects many tables and reduces false negative identification rates for all algorithms. The reduction is larger for "recent" enrollments than for "lifetime consolidated" ones with the consequence that accuracy on recent images is now superior.
- ▷ We plan to retire use of mugshot galleries of sizes 6 and 12 million. Instead we expect to use a newer non-mugshot dataset to show scalability to large N. We also expect to primarily state mugshot accuracy using the ageing results given in Table 7. The introduction of these changes will depend on the duration of restrictions related to SARS-COV-19.

2020-02-26: The first draft of the update to NIST Interagency Report 8271:

- ▷ Adds results for 38 algorithms from 31 different developers, eleven of whom are entirely new to the 1:N track of FRVT. These are Allgovision, Cyberlink, Deepsea Tencent, Farbar F8, Imperial College London, Intsys MSU, Kedacom, Kneron, Pixelall, and Scanovate.

DISCLAIMER

Specific hardware and software products identified in this report were used in order to perform the evaluations described in this document. In no case does identification of any commercial product, trade name, or vendor, imply recommendation or endorsement by the National Institute of Standards and Technology, nor does it imply that the products and equipment identified are necessarily the best available for the purpose.

INSTITUTIONAL REVIEW BOARD

The National Institute of Standards and Technology's Research Protections Office reviewed the protocol for this project and determined it is not human subjects research as defined in Department of Commerce Regulations, 15 CFR 27, also known as the Common Rule for the Protection of Human Subjects (45 CFR 46, Subpart A).

Executive Summary

This report supplements the September 2019 report NIST Interagency Report 8271 that, in turn, replaced the NIST Interagency Report 8238. **This report adds partial results for algorithms submitted to NIST since those reports were prepared. This report will be updated on an approximately monthly basis with results from newly submitted algorithms. It will additionally be updated with results currently being computed in ongoing recognition tests, and with new results and analyses.**

The algorithms, which implement one-to-many identification of faces appearing in two-dimensional images, are prototypes from the research and development laboratories of mostly commercial suppliers, and are submitted to NIST as compiled black-box libraries implementing a NIST-specified C++ test interface. The report therefore does not describe how algorithms operate.

The evaluation used three datasets - frontal mugshots, profile views, and webcam photos - and the report lists accuracy results alongside developer names. It will therefore be useful for comparison of face recognition algorithms and assessment of absolute capability. The primary dataset is comprised of 26.6 million reasonably well-controlled live portrait photos of 12.3 million individuals. The three smaller datasets contain more unconstrained photos: 3.2 million webcam images; and 200 thousand side-view images. NIST Interagency Report 8271 includes results also for 2.5 million photojournalism and amateur photographer photos. These datasets are sequestered at NIST, meaning that developers do not have access to them for training or testing. The last dataset, however, consists of images drawn from the internet for testing purposes so while it is not truly sequestered, its composition is unknown to the developers.

The major result in NIST IRs 8238 and 8271 was that massive gains in accuracy have been achieved in the years 2013 to 2018 and these far exceed improvements made in the prior period, 2010 to 2013. While the industry gains were broad - at least 30 developers' algorithms outperformed the most accurate algorithm from late 2013 - there remains a wide range of capability. While this report shows accuracy gains only over the course of 2018, the most accurate algorithm reported here is substantially more accurate than anything reported in NIST IR 8238. This is evidence that face recognition development continues apace, and that FRVT reports are but a snapshot of contemporary capability.

From discussion with developers, the accuracy gains stem from the adoption of deep convolutional neural networks. As such, face recognition has undergone an industrial revolution, with algorithms increasingly tolerant of poorly illuminated and other low quality images, and poorly posed subjects. One related result is that a few algorithms correctly match side-view photographs to galleries of frontal photos, with search accuracy approaching that of the best c. 2010 algorithms executing frontal-frontal search. The capability to recognize under a 90-degree change in viewpoint - pose invariance - has been a long-sought milestone in face recognition research.

With good quality portrait photos, the most accurate algorithms will find matching entries, when present, in galleries containing 12 million individuals, with rank one miss rates of approaching 0.1%. The remaining errors are in large part attributable to long-run ageing, facial injury and poor image quality. Given this impressive achievement - close to perfect recognition - an advocate might claim that frontal face recognition is a solved problem, a statement that should be refuted with the following context and caveats:

- ▷ **Algorithm accuracy spectrum:** Many algorithms do not achieve the low error rates tabulated above, and while many of those may still be useful and valuable to end-users, only the most accurate excel on poor quality images and those collected long after the initial enrollment sample.
- ▷ **Versioning:** While results for up to seven algorithms from each developer are reported here, the intra-provider accuracy variations are usually smaller than the inter-provider variations. That said different versions give order of magnitude fewer misses. Some developers demonstrate speed-accuracy tradeoffs[1]. See Figs. 16, 17.

[1]NEC-0 prepares templates much faster than NEC-2 but gives twenty times more misses. Dermalog-5 executes a template search much more quickly than Dermalog-6 but is also much less accurate.

- ▷ **Quality:** The low error rates here are attained using mostly excellent cooperative live-capture mugshot images collected with an attendant present. Recognition in other circumstances, particularly those without a dedicated photographic environment and human or automated quality control checks, will lead to declines in accuracy. This is documented here for poorer quality webcam images and unconstrained "wild" images.

- ▷ **Low similarity scores:** In thousands of cases the correct gallery image is returned at rank 1 but its similarity score is nevertheless low, below some operationally required score threshold. This does not matter when face recognition is used for "lead generation" in investigational applications because human reviewers are specifically required to review potentially long candidate lists and the threshold is effectively 0. In applications where search volumes are higher and labor is not available to review the results from searches, a higher threshold can be applied. This reduces the length of candidate lists and false positive identification rates at the expense of increased false negative miss rates. The tradeoff between the two error rates is reported extensively later.

- ▷ **Population size:** As the number of enrolled subjects grows, some mates are displaced from rank one, decreasing accuracy. As tabulated later for N up to 12 million, false negative rates generally rise slowly with population size.

- ▷ **Database integrity:** An operational error rate should be added to all false negative rates in this report reflecting the proportion of images in a real database that are un-matchable. Such anomalies arise from images that: do not contain a face; include multiple persons; cannot be decoded; are rotated by 90° or 180°; depict a face on clothing; and others introduced by a long tail of various clerical errors. While the mugshot trials in this report have been constructed to minimize such effects, they are a real problem in actual operations.

Recognition accuracy is very strongly dependent on the algorithm and, more generally, on the developer of the algorithm. False negative error rates in a particular scenario range from a few tenths of one percent to beyond fifty percent. This is tabulated exhaustively later: For example Table 26 shows accuracy across datasets. Figure 1 here compares algorithms on mugshot searches in a consolidated gallery of 12 million subjects and 26.1 million photos. In positive or negative identification applications, a score threshold is set to limit the rate at which non-mate searches produce false positives. This has the consequence that some mated searches will report the mate below threshold, i.e. a miss, even if it is at rank 1. The utility of this is that many non-mated searches will usually not return any candidate identities at all. As the figure error-tradeoff characteristic shows, investigational miss rates on the right side are very low but then rise steadily (in the center region) as threshold is increased to support "lights-out" applications, and ultimately rise quickly (left side) as discussed below. Thus, if we demand that just one in one thousand non-mate searches produce any false positives, the most accurate algorithms there (Sensetime-003 and NEC-3) would fail on between 4 and 7% of mated searches. Even though the graph shows results for the most accurate algorithms, all but two would fail to find the mate in more than 10% of mated searches. While the NEC algorithm produces a relatively flat error tradeoff until the threshold is raised to limit false positives to about 1 in 400 non-mated searches[2]

Thereafter, as the threshold is raised to further reduce false positives, miss rates rise rapidly. This means that low false positive identification rates are inaccesible with these algorithms, a result that does not apply for ten-finger identification algorithms. The rapid rise occurs because the lower mate scores are mixed with very high non-mate scores, the low scores from poor image quality and ageing, the high non-mates from the presence of lookalikes persons (doppelgangers), twins (discussed next) and, ultimately, the presence of a few unconsolidated subjects i.e. persons present under multiple IDs.

▷ **False positives from twins:** By enrolling 640 000 mugshots, adding photos of one twin, and then searching photos

[2]The gallery size here is 12 million people, 26.1 million images. Given 331 254 non-mated searches, an exhaustive implementation of one-too-many search would execute 8.6 trillion comparisons. At a false positive identification rate of 0.0025 the number of false positives is, to first order, 828 corresponding to single-comparison false match rate of 828 / 8.6 trillion = 9.6 10^{-11} i.e. about 1 in 10 billion. Strictly this FMR computation is meaningful only for algorithms that implement 1:N search using N 1:1 comparisons, which is not always the case.

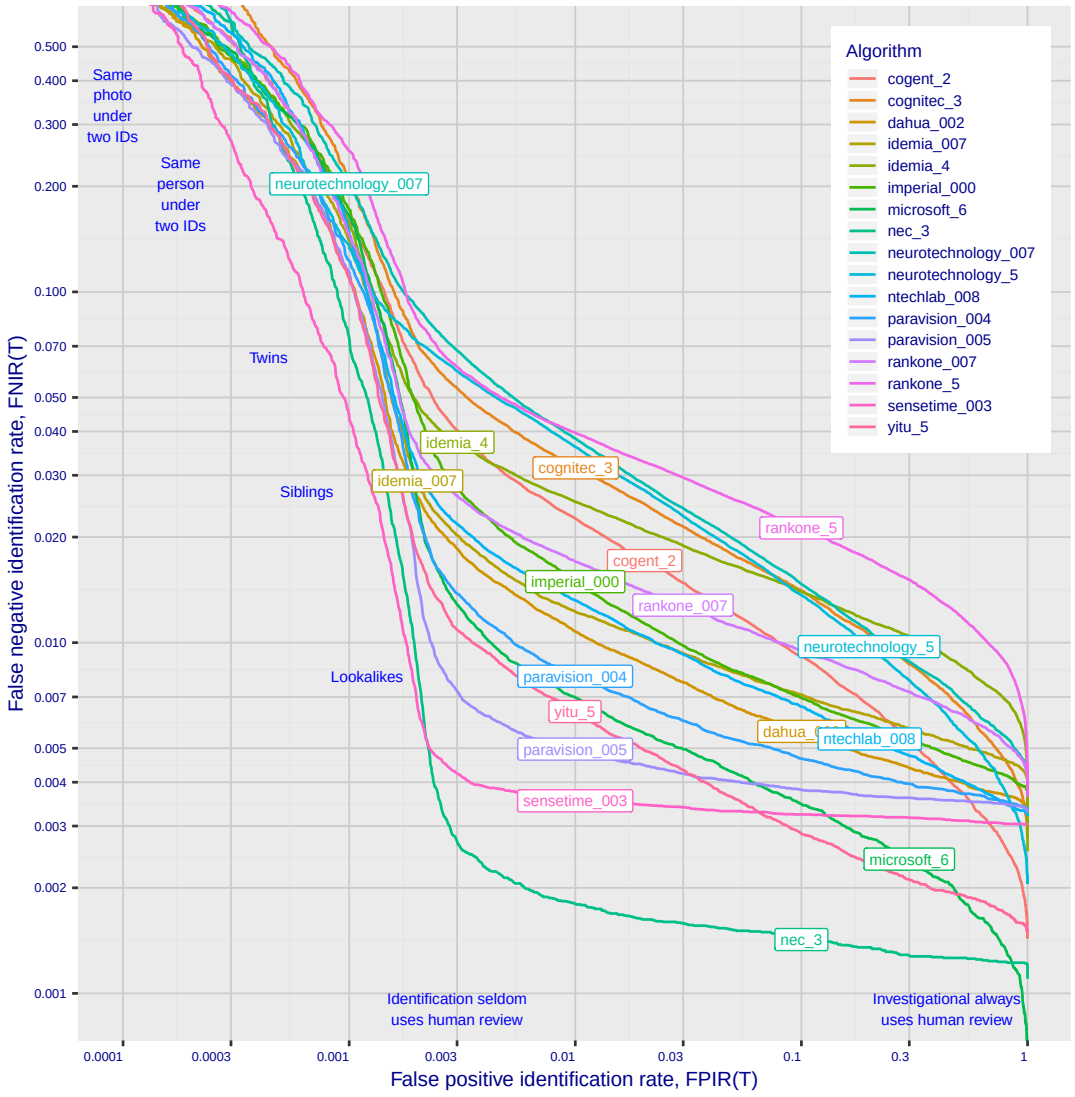

Figure 1: Identification Miss rates across the false positive range. N = 12 million individuals are enrolled with a total of 26.1 million images.

of those subjects and their twin the inset figure shows, for one typical algorithm, the similarity is generally greater when searching twins against themselves (A) than when searching twins against their sibling (B) but very often still above even stringent thresholds i.e. those corresponding to one in one thousand searches producing a false positive. Thus twins will very often produce a high-scoring non-match on a candidate list and a false alarm in an online identification system. The plot shows that some fraternal twins are correctly rejected at those thresholds - these are largely from different sex twins (at center). Figure 20 shows substantially similar behavior for all algorithms tested. In an investigative search, a twin would typically appear at rank 1, or rank 2 if their sibling happened to also be

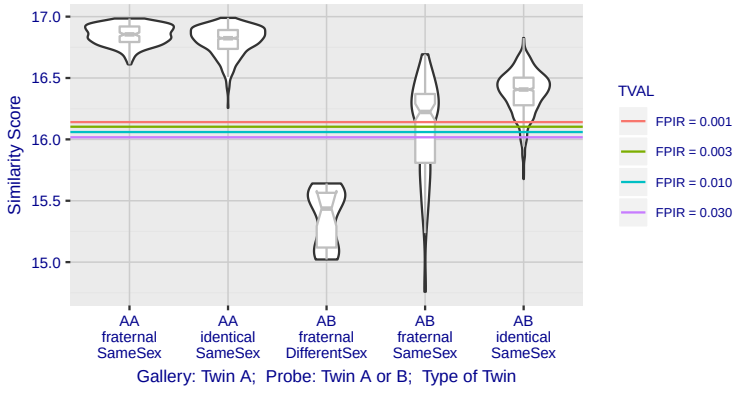

Figure 2: Intra- and inter-twin scores

the gallery. Twins (and triplets etc.) constituted 3.3%
of all live births [16] in recent years[3], and because that number is higher today than when the individuals in current adult databases were born, the false positives that arise from twins are now, and will increasingly be, an operational problem. Relative to the United States, twins are born with considerable regional variation. For example they are much less common in East Asia, and much more common in Sub-Saharan Africa [20]. The presence of twins in the mugshot database is inevitable given its size, around 12.3 million people. As this is not an insignificant sample of the domestic United States population, people with other familial ties will be present also. The data was collected over an extended period and because location information is not available, we are unable to estimate the proportion of the domestic population that is present in the dataset. However, if we assume twins are neither more or less disposed to arrest than the general population, we can estimate that hundreds of thousands of individuals in the dataset are twins. This will affect false positive rates because we randomly set aside 331 254 individuals for nonmate searches, and some proportion of those will be twins with siblings in the gallery.

From early 2020 this report is being updated continuously as new algorithms are submitted to FRVT, and run on new datasets. Participation in the one-to-many identification track requires a developer to first demonstrate high accuracy in the one-to-one verification track of FRVT.

[3]See the CDC's National Vital Statistics Report for 2017: https://www.cdc.gov/nchs/data/nvsr/nvsr67/nvsr67_08-508.pdf

Scope and Context

Audience: This report is intended for developers, integrators, end users, policy makers and others who have some familiarity with biometrics applications. The methods and metrics documented here will be of interest to organizations engaged in tests of face recognition algorithms. Some of these have been incorporated in the ISO/IEC 19795 Part 1 Biometric Testing and Reporting Framework standard, now under revision.

Prior benchmarks: Automated face recognition accuracy has improved massively in the two decades since initial commercialization of the various technologies. NIST has tracked that improvement through its conduct of regular independent, free, open, and public evaluations. These have fostered improvements in the state of the art. This report serves as an update to the NIST Interagency Report 8271 on performance of face identification algorithms, published in September 2019.

Demographics: In December 2019, NIST published a first report on demographic dependencies in face recognition, NIST Interagency Report 8280 that documented age, sex and race differentials in one-to-one and one-to-many false positive and false negative rates.

Scope: NIST IR 8271 documented recognition results for four databases containing in excess of 30.2 million still photographs of 14.4 million individuals. That constituted the largest public and independent evaluation of face recognition ever conducted. It includes results for accuracy, speed, investigative vs. identification applications, scalability to large populations, use of multiple images per person, images of cooperative and non-cooperative subjects.

The report also includes results for ageing, recognition of twins, and recognition of profile-view images against frontal galleries. It otherwise does not address causes of recognition failure, neither image-specific problems nor subject-specific factors including demographics. Separate reports on demographic dependencies in face recognition will be published in the future. Additionally out of scope are: performance of live human-in-the-loop transactional systems like automated border control gates; human recognition accuracy as used in forensic applications; and recognition of persons in video sequences (which NIST evaluated separately [8]). Some of those applications share core matching technologies that *are* tested in this report.

Images: Three kinds of images are employed. The primary dataset is a set of law enforcement mugshot images (Fig. 3) which are enrolled and then searched with three kinds of images: 1) other mugshots (i.e. within-domain); 2) profile-view photographs (90 degree cross-view); 3) lower quality webcam images (Fig. 4) collected in similar detention operations (cross-domain);

Participation and industry coverage: The report includes performance figures for prototype algorithms from the research laboratories of commercial developers and a few universities. This represents a substantial majority of the face recognition industry, but only a tiny minority of the academic community. Participation was open worldwide. While there is no charge for participation, developers incur some software engineering expense in implementing their algorithms behind the NIST application programming interface (API). The test is a black-box test where the function of the algorithm, and the intellectual property associated with it, is hidden inside pre-compiled libraries.

Recent technology development: Most face recognition research with deep convolutional neural networks (CNNs) has been aimed at achieving invariance to pose, illumination and expression variations that characterize photojournalism and social media images. The initial research [17, 21] employed large numbers of images of relatively few ($\sim 10^4$) individuals to learn invariance. Inevitably much larger populations ($\sim 10^7$) were employed for training [10, 19] but the benchmark, Labeled Faces in the Wild with (essentially) an equal error rate metric [11], represents an easy task, one-to-one verification at very high false match rates. While a larger scale identification benchmark duly followed, Megaface [14], its primary metric, rank one hit rate, contrasts with the high threshold discrimination task required in most large-population applications of face recognition, namely credential de-duplication, and background checks. There, identification in galleries containing up to 10^8 individuals must be performed using a) very few images per

individual and b) stringent thresholds to afford very low false positive identification rates. This track of FRVT was launched to measure the capability of the new technologies, including in these two cases. FRVT has included open-set identification tests since 2002, reporting both false negative and positive identification rates [6].

Performance metrics for applications: This report documents the performance of one-to-many face recognition algorithms. The word "performance" here refers to recognition accuracy and computational resource usage, as measured by executing those algorithms on massive sequestered datasets.

This report includes extensive tabulation of recognition error rates germane to the main use-cases for face search technology. The Figure below, inspired by the Figure 1 in [22] differentiates different applications of the technolgy. The last row directs readers to the main tables relevant to those applications, respectively threshold-based and rank-based metrics that are special cases of the metrics given in section 3. The terms negative identification and positive identification are taken from the ISO/IEC 2382-37:2017 standardized biometrics vocabulary.

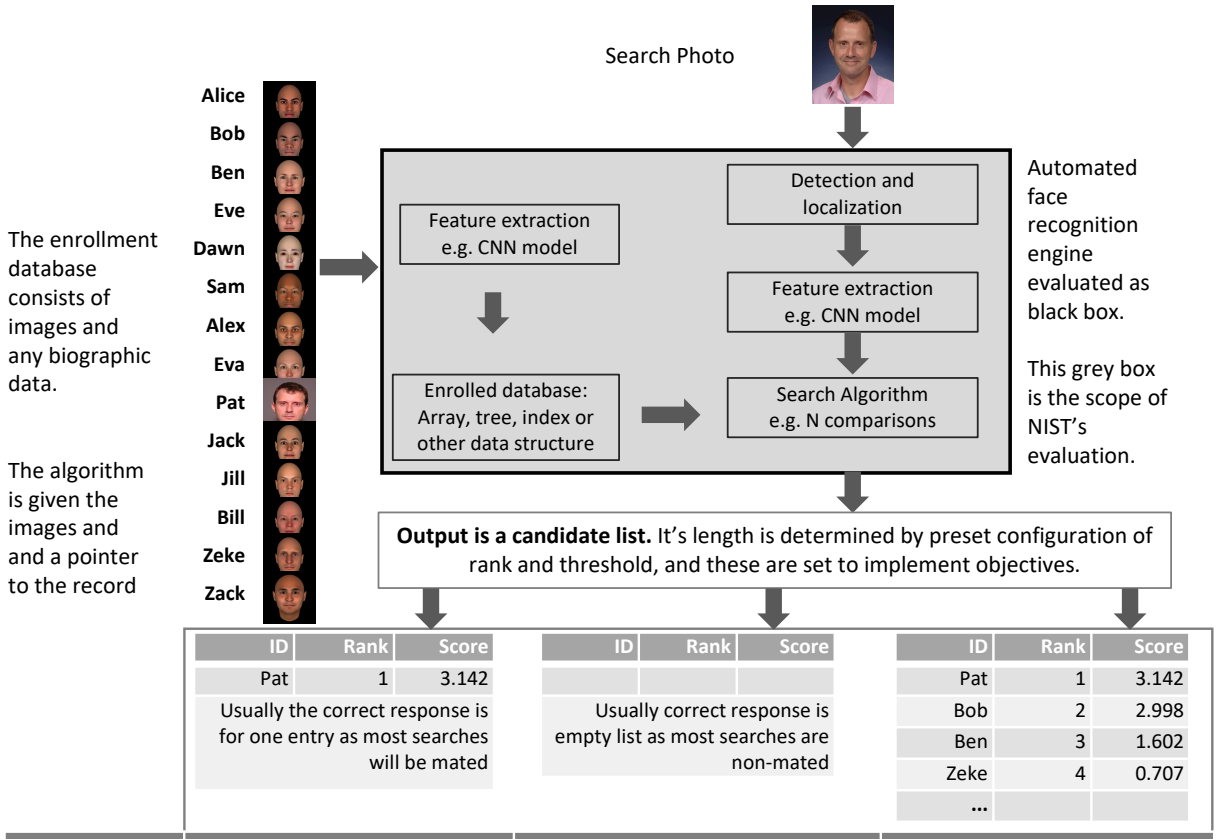

	Positive identification	Negative identification	Post-event investigation
Example	Access to a gym or cruise ship	Watchlist e.g. Detection of deportee or duplicate drivers license applications	Crime scene photos, or of detainee without ID documents.
Claim of identity	Implicit claim to be enrolled	Implicit claim to not be enrolled	No claim: Inquiry
Threshold	High, to implement security objective	High, to limit false positives	Zero
Num. candidates	1	0	L, set by request to algorithm
Human role	Review candidate to assist user in resolution of false negatives, or to detect impostor	Review candidate to determine false positive or correct hit	Review multiple candidates, refer possible hits to examiners see [26]
Intended human involvement frequency	Rare – approx. the false negative identification rate plus prior probability of impostor	Rare – approx. the false positive identification rate plus prior probability of an actual mate	Always
Performance metric of interest	**FNIR at low FPIR. See sec. 3.1, 3.2 and Tables 10, 19**	**FNIR at low FPIR. See sec. 3.1, 3.2 and Tables 10, 19**	**FNIR at ranks 1... 50, say. FPIR = 1. See sec. 3.2 and Table 12, 14, 16**

The algorithms are specifically configured for these applications by setting thresholds and candidate list lengths. Both rank-based metrics and threshold-based metrics include tradeoffs. In investigation, overall accuracy will be reduced if labor is only available to review a few candidates from the automated system. Note that when a fixed number of candidates are returned, the false positive identification rate of the automated face recognition engine will be 100%, because a probe image of anyone not enrolled will still return candidates. In identification applications where false positives must be limited to satisfy reviewer labor availability or a security objective, higher false negative rates are implied. This report includes extensive quantification of this threshold-based tradeoff. See Sec. 3

Template diversity: The FRVT is designed to evaluate black-box technologies with the consequence that the templates that hold features extracted from face images are entirely proprietary opaque binary data that embed considerable

intellectual property of the developer. Despite migration to CNN-based technologies there is no consensus on the optimal feature vector dimension. This is evidenced by template sizes ranging from below 100 bytes to more than four kilobytes. This diversity of approaches, suggests there is no prospect of a standard template something that would require a common feature set to be extracted from faces. Interoperability in automated face recognition remains solidly based on images and documentary standards for those, in particular the ICAO portrait [26] specification deriving from the ISO/IEC 19794-5 Token frontal [23] standard, which are similar to certain ANSI/NIST Type 10 [25] formats.

Training: The algorithms submitted to NIST have been developed using image datasets that developers do not disclose. The development will often include application of machine learning techniques and will additionally involve iterative training and testing cycles. NIST itself does not perform any training and does not refine or alter the algorithm in any way. Thus the model, data files, and libraries that define an algorithm are fixed for the duration of the tests. This reflects typical operational reality where recognition software, once installed, is fixed and constant until upgraded. This situation persists because on-site training of algorithms on customer data is atypical essentially because training is not a turnkey process.

Automated search and human review: Virtually all applications using automated face search require human review of the outputs at some frequency: Always for investigational applications; rarely in positive identification applications, after rejection (false or otherwise); and rarely in negative identification applications, after an alarm (false or otherwise). The human role is usually to compare a reference image with the query image or the live-subject if present, to render either a definitive decision on "exclusion" (different subjects), or "identification" (same subject), or a declaration that one or both images have "no value" and that no decision can be made. Note that automated face recognition algorithms are not built to do exclusion - low scores from a face comparison arise from different faces *and* poor quality images of the same face.

Human reviewers make recognition errors [4, 18, 24] and are sensitive to image acquisition and quality. Accurate human review is supported by high resolution - as specified in the Type 50, 51 acquisition profiles of the ANSI/NIST Type 10 record [25], and by multiple non-frontal views as specified in the same standard. These often afford views of the ear. Organizations involved in image collection should consider supporting human adjudication by collecting high-resolution frontal and non-frontal views, preparing low resolution versions for automated face recognition [23], and retaining both for any subsequent resolution of candidate matches. Along these lines, the ISO/IEC Joint Technical Committee 1 subcommittee 37 on biometrics has just initiated projects on image quality assessment and face-aware capture.

Release Notes

FRVT Activities: Since February 2017, NIST has been evaluating one-to-one verification algorithms on an ongoing basis. NIST then restarted FRVT's one-to-many track in February 2018, inviting participants to send up to prototype algorithms. Both tracks allows developers to submit updated algorithms to NIST at any time but no more frequently than four calendar months. This more closely aligns development and evaluation schedules. Results are posted to the web within a few weeks of submission. Details and full report are linked from the Ongoing FRVT site.

FRVT Reports: The results of the FRVT appear in the series NIST Interagency Reports tabulated below. The reports were developed separately and released on different schedules. In prior years NIST has mostly reported FRVT results as a single report; this had the disadvantage that results from completed sub-studies were not published until all other studies were complete.

Date	Link	Title	No.
2014-03-20	PDF	FRVT Performance of Automated Age Estimation Algorithms	7995
2015-04-20	PDF	Face Recognition Vendor Test (FRVT) Performance of Automated Gender Classification Algorithms	8052
2014-05-21	PDF	FRVT Performance of face identification algorithms	8009
2017-03-07	PDF	Face In Video Evaluation (FIVE) Face Recognition of Non-Cooperative Subjects	8173
2017-11-23	PDF	The 2017 IARPA Face Recognition Prize Challenge (FRPC)	8197
2018-11-27	PDF	Face Recognition Vendor Test - Part 2: Identification	8271
2019-09-11	PDF	Face Recognition Vendor Test - Part 2: Identification	8271
2019-12-11	PDF	Face Recognition Vendor Test - Part 3: Demographic Effects	8280
2020-01-03	WWW	Face Recognition Vendor Test (FRVT) - Part 1 Verification	Draft

Details appear on pages linked from `https://www.nist.gov/programs-projects/face-projects`.

Appendices: This report is accompanied by appendices which present exhaustive results on a per-algorithm basis. These are machine-generated and are included because the authors believe that visualization of such data is broadly informative and vital to understanding the context of the report.

Typesetting: Virtually all of the tabulated content in this report was produced automatically. This involved the use of scripting tools to generate directly type-settable LaTeX content. This improves timeliness, flexibility, maintainability, and reduces transcription errors.

Graphics: Many of the Figures in this report were produced using the ggplot2 package running under R, the capabilities of which extend beyond those evident in this document.

Contents

1 Introduction

One-to-many identification represents the largest market for face recognition technology. Algorithms are used across the world in a diverse range of biometric applications: detection of duplicates in databases, detection of fraudulent applications for credentials such as passports and driving licenses, token-less access control, surveillance, social media tagging, lookalike discovery, criminal investigation, and forensic clustering.

This report contains a breadth of performance measurements relevant to many applications. Performance here refers to accuracy and resource consumption. In most applications, the core accuracy of a facial recognition algorithm is the most important performance variable. Resource consumption will be important also as it drives the amount of hardware, power, and cooling necessary to accommodate high volume workflows. Algorithms consume processing time, they require computer memory, and their static template data requires storage space. This report documents these variables.

1.1 Open-set searches

FRVT tested open-set identification algorithms. Real-world applications are almost always "open-set", meaning that some searches have an enrolled mate, but some do not. For example, some subjects have truly not been issued a visa or drivers license before; some law enforcement searches are from first-time arrestees[4]. In an "open-set" application, algorithms make no prior assumption about whether or not to return a high-scoring result, and for a mated search, the ideal behaviour is that the search produces the correct mate at high score and first rank. For a non-mate search, the ideal behavior is that the search produces zero high-scoring candidates.

Many academic benchmarks execute only closed-set searches. The proportion of mates found in the rank one position is the default accuracy metric. This hit rate metric ignores the score with which a mate is found; weak hits count as much as strong hits. This ignores the real-world imperative that in many applications it is necessary to elevate a threshold to reduce the number of false positives.

2 Evaluation datasets

This report documents accuracy for four kinds of images - mugshots, webcam, profiles and wild - as described in the following sections.

2.1 Mugshot images

The main mugshot dataset used is referred to as the FRVT 2018 set. This set was collected over the period 2002 to 2017 in routine United States law enforcement operations. This set has been extracted from a larger operational parent set by excluding non-face images, and setting aside webcam and profile-view images, for use in separate tests.

NIST Interagency Report 8238 includes a comparison of this set of mugshots with the smaller and easier sets of mugshots used in tests run in 2010 and 2014.

[4]Operationally closed-set applications are rare because it is usually not the case that all searches have an enrolled mate. One counter-example, however, is a cruise ship in which all passengers are enrolled and all searches should produce exactly one identity. Another example is forensic identification of dental records from an aircraft crash.

- **Mugshots**: Mugshots comprise about 86% of the database. They have reasonable compliance with the ANSI/NIST ITL1-2011 Type 10 standard's subject acquisition profiles levels 10-20 for frontal images [25]. The most common departure from the standard's requirements is the presence of mild pose variations around frontal - the images of Figure 3 are typical. The images vary in size, with many being 480x600 pixels with JPEG compression applied to produce filesizes of between 18 and 36KB with many images outside this range, implying that about 0.5 bits are being encoded per pixel.

- **Profile images**: Profile-view images have been collected in law enforcement for more than 100 years, as human capability is improved with orthogonal information. The profile images used in this report were collected during the same session as the frontal mugshot photograph, in the same standardized photographic setup. These would not therefore be used with automated face recognition. A small subset, 200 000 images, were set aside for testing.

- **Webcam images**: The remaining 14% of the images were collected using an inexpensive webcam attached to a flexible operator-directed mount. These images are all of size 240x240 pixels, that are in considerable violation of most quality-related clauses of all face recognition standards. As evident in the figure, the most common defects are non-frontal pose (associated with the rotational degrees of freedom of the camera mount), low contrast (due to varying and intense background lights), and poor spatial resolution (due to inexpensive camera optics) - see examples in Fig 4. The images are overly JPEG compressed, to between 4 and 7KB, implying that only 0.5 to 1 bits are being encoded per color pixel.

Example images are shown in Figures 3, 4 and 5 These are drawn from NIST Special Database 32 which may be downloaded here.

These images were partitioned in galleries and probesets for the various experiment listed in Table 1.

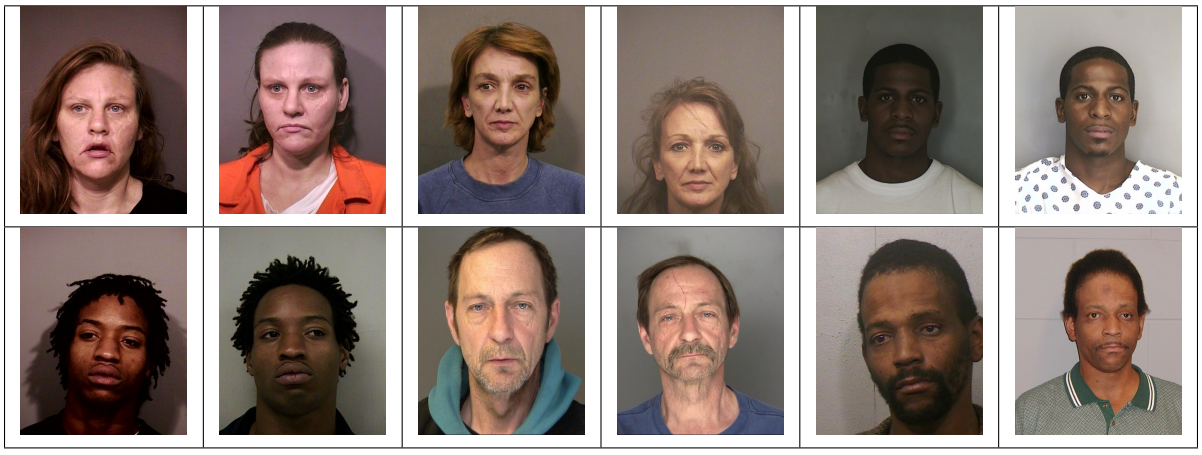

Figure 3: Six mated mugshot pairs representative of the FRVT-2014 (LEO) and FRVT-2018 datasets. The images are collected live, i.e. not scanned from paper. Image source: NIST Special Database 32 the Multiple Encounter Deceased Subjects dataset.

Figure 5: **[Profile views]** *The three images are a frontal enrollment, subsequent frontal probe, and same-session ninety degree profile view. While collection of both frontal and profile views has been typical in law enforcement for more than a century, the recognition of profile to frontal views has essentially been impossible. However, reasonbly high accuracy results is now possible - see section E.*

Figure 4: Twelve webcam images representative of probes against the FRVT-2018 mugshot gallery. The first eight images are four mated pairs. Such images present challenges to recognition including pose, non-uniform illumination, low contrast, compression, cropping, and low spatial sampling rate. Image source: NIST Special Database 32 the Multiple Encounter Deceased Subjects dataset.

2.2 Enrollment strategies

Many operational applications include collection and enrollment of biometric data from subjects on more than one occasion. This might be done on a regular basis, as might occur in credential (re-)issuance, or irregularly, as might happen in a criminal recidivist situation [3]. The number of images per person will depend on the application area. In civil identity credentialing (e.g. passports, driver's licenses), the images will be acquired approximately uniformly over time (e.g. ten years for a passport). While the distribution of dates for such images of a person might be assumed uniform, a number of factors might undermine this assumption[5]. In criminal applications, the number of images would depend on the number of arrests. The distribution of dates for arrest records for a person (i.e. the recidivism distribution) has been modeled using the exponential distribution but is recognized to be more complicated[6].

In any case, the 2010 NIST evaluation of face recognition showed that considerable accuracy benefits accrue with retention and use of *all* historical images [5].

[5]For example, a person might skip applying for a passport for one cycle, letting it expire. In addition, a person might submit identical images (from the same photography session) to consecutive passport applications at five year intervals.
[6]A number of distributions have been considered to model recidivism, see for example [2].

Image		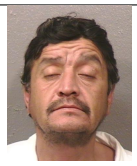		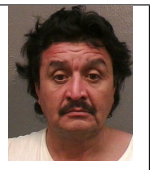
Encounter	1	...	$K_i - 1$	K_i
Capture Time	T_1	...	T_{K_i-1}	T_{K_i}
Role RECENT	Not used	Not used	Enrolled	Search
Role LIFETIME	Enrolled	Enrolled	Enrolled	Search

Figure 6: Depiction of the "recent" and "lifetime" enrollment types. Image source: NIST Special Database 32

To this end, the FRVT API document provides $K \geq 1$ images of an individual to the enrollment software. The software is tasked with producing a single proprietary undocumented "black-box" template[7] from the K images. This affords the algorithm an ability to generate a *model* of the individual, rather than to simply extract features from each image on a sequential basis.

As depicted in Figure 6, the i-th individual in the FRVT 2018 dataset has K_i images. These are labelled as x_k for $k = 1 \ldots K_i$ in chronological order of capture date. To measure the utility of having multiple enrollment images, this report evaluates three kinds of enrollment:

- **Recent**: Only the second most recent image, x_{K_i-1} is enrolled. This strategy of enrollment mimics the operational policy of retaining the imagery from the most recent encounter. This might be done operationally to ameliorate the effects of face ageing. Obviously retaining only the most recent image should only be done if the identity of the person is trusted to be correct. For example, in an access control situation retention of the most recent successful *authentication* image would be hazardous if it could be a false positive.

- **Lifetime-consolidated**: All but the most recent image are enrolled, $x_1 \ldots x_{K_i-1}$. This subject-centric strategy might be adopted if quality variations exist where an older image might be more suitable for matching, despite the ageing effect.

- **Lifetime-unconsolidated**: Again all but the most recent image are enrolled $x_1 \ldots x_{K_i-1}$ but now separately, with different identifiers, such that the algorithm is not aware that the images are from the same face. This kind of event- or encounter-centric enrollment is very common when operational constraints preclude reliable consolidation of the historical encounters into a single identity. This aspect also prevents the recognition algorithm from a) building a holistic model of identity (as is common in speaker recognition systems) and b) implementing fusion, for example template-level fusion of feature vectors, or post-search score-level fusion. The result is that searches will typically yield more than one image of a person in the top ranks. This has consequences for appropriate metrics, as detailed in section 3.2.1

  NIST first evaluated this kind of enrollment in mid 2018, and the results tables include some comparison of accuracy available from all three enrollment styles.

In all cases, the most recent image, x_{K_i}, is reserved as the search image. For the 1.6 million subject enrollment partition of the FRVT 2018 data, $1 \leq K_i \leq 33$ with $K_i = 1$ in 80.1% of the individuals, $K_i = 2$ in 13.4%, $K_i = 3$ in 3.7%, $K_i = 4$ in

[7] There are no formal face template standards. Template standards only exist for fingerprint minutiae - see ISO/IEC 19794-2:2011.

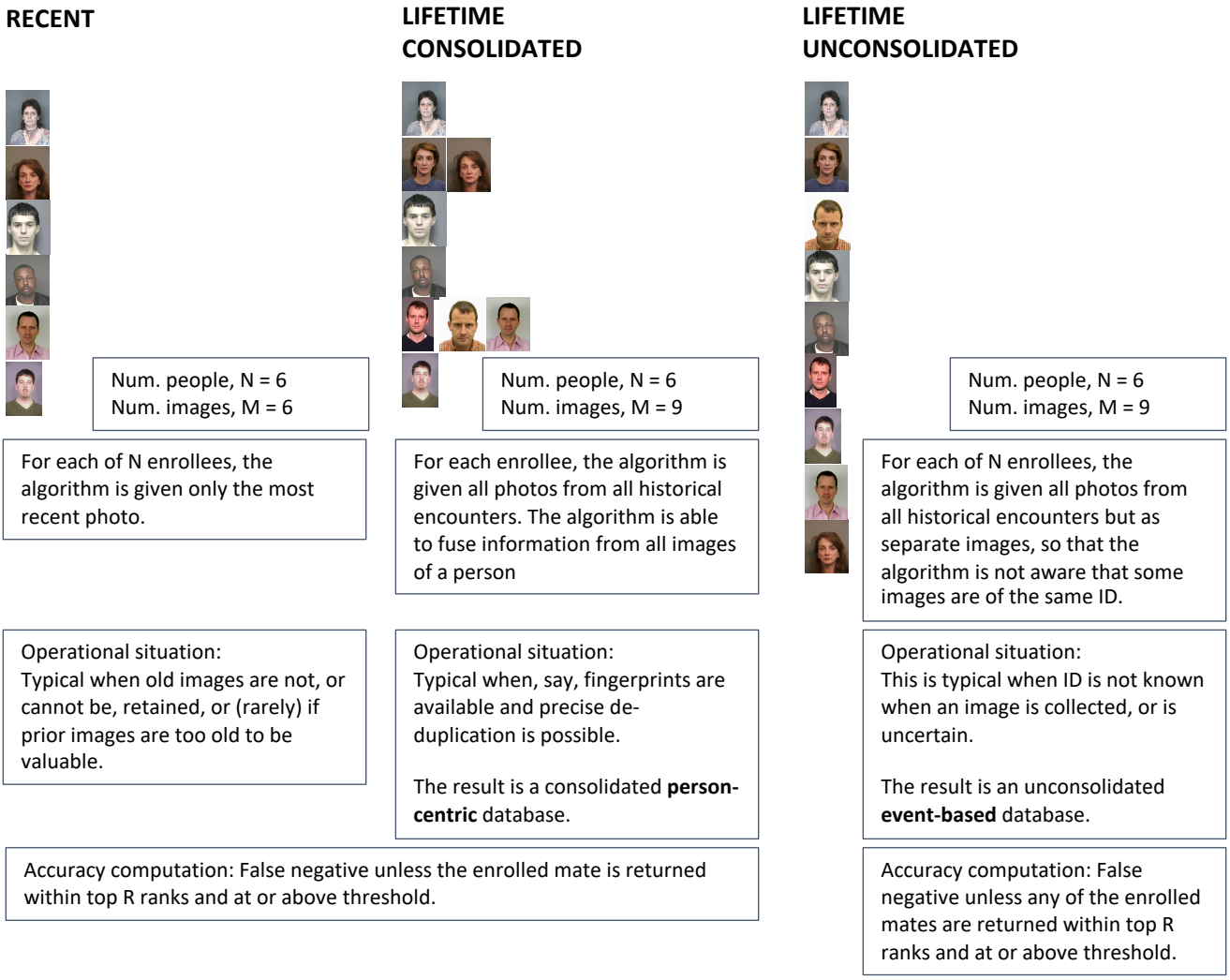

Figure 7: **Enrollment strategies**. *The figure shows the three kinds of enrollment databases examined in this report. Image source: NIST Special Database 32*

	ENROLLMENT				SEARCH			
	TYPE SEE	POPULATION			MATE		NON-MATE	
	SECTION 2.2	FILTER	N-SUBJECTS	N-IMAGES	N-SUBJECTS	N-IMAGES	N-SUBJECTS	N-IMAGES
Mugshot trials from enrollment of single images								
1	RECENT	NATURAL	640 000	640 000	154 549	154 549	331 254	331 254
2	RECENT	NATURAL	1 600 000	1 600 000				
3	RECENT	NATURAL	3 000 000	3 000 000				
4	RECENT	NATURAL	6 000 000	6 000 000				
5	RECENT	NATURAL	12 000 000	12 000 000				
Mugshot trials from enrollment of lifetime images								
6	CONSOL	NATURAL	640 000	1 247 331				
7	CONSOL	NATURAL	1 600 000	3 351 206				
8	CONSOL	NATURAL	3 000 000	6 417 057				
9	CONSOL	NATURAL	6 000 000	12 976 185				
10	CONSOL	NATURAL	12 000 000	26 107 917				
11	UN-CONSOL	NATURAL	640 000	1 247 331				
12	UN-CONSOL	NATURAL	1 600 000	3 351 206				
Cross-domain								
13	MUGSHOTS AS ON ROW 2				82 106 WEBCAM	82 106 WEBCAM	331 254 WEBCAM	331 254 WEBCAM
Cross-view								
14	MUGSHOTS AS ON ROW 2				100 000 PROFILE	100 000 PROFILE	100 000 PROFILE	100 000 PROFILE
Ageing								
17	OLDEST	NATURAL	3 068 801	3 068 801	2 853 221	10 951 064	0	0

Table 1: **Enrollment and search sets**. *Each row summarizes one identification trial. Unless stated otherwise, all entries refer to mugshot images. The term "natural" means that subjects were selected without heed to demographics, i.e. in the distribution native to this dataset. The probe images were collected in a different calendar year to the enrollment image. Missing values in rows 2-12 are the same as in row 1.*

1.4%, $K_i = 5$ in 0.6%, $K_i = 6$ in 0.3%, and $K_i > 6$ is 0.2% for everyone else. This distribution is substantially dependent on United States recidivism rates.

We did not evaluate the case of retaining only the highest quality image, since automated quality assessment is out of scope for this report. We do not anticipate that such strategies will prove beneficial when the quality assessment apparatus is imperfect and unvalidated.

3 Performance metrics

This section gives specific definitions for accuracy and timing metrics. Tests of open-set biometric algorithms must quantify frequency of two error conditions:

- ▷ **False positives**: Type I errors occur when search data from a person who has never been seen before is incorrectly associated with one or more enrollees' data.
- ▷ **Misses**: Type II errors arise when a search of an enrolled person's biometric does not return the correct identity.

Many practitioners prefer to talk about "hit rates" instead of "miss rates" - the first is simply one minus the other as detailed below. Sections 3.1 and 3.2 define metrics for the Type I and Type II performance variables.

Additionally, because recognition algorithms sometimes fail to produce a template from an image, or fail to execute a one-to-many search, the occurrence of such events must be recorded. Further because algorithms might elect to not

produce a template from, for example, a poor quality image, these failure rates must be combined with the recognition error rates to support algorithm comparison. This is addressed in section 3.5.

Finally, section 3.7 discusses measurement of computation duration, and section 3.8 addresses the uncertainty associated with various measurements. Template size measurement is included with the results.

3.1 Quantifying false positives

It is typical for a search to be conducted into an enrolled population of N identities, and for the algorithm to be configured to return the closest L candidate identities. These candidates are ranked by their score, in descending order, with all scores required to be greater than or equal to zero. A human analyst might examine either all L candidates, or just the top $R \leq L$ identities, or only those with score greater than threshold, T. The workload associated with such examination is discussed later, in 3.6.

False alarm performance is quantified in two related ways. These express how many searches produces false positives, and then, how many false positives are produced in a search.

False positive identification rate: The first quantity, FPIR, is the proportion of non-mate searches that produce an adverse outcome:

$$\text{FPIR}(N,T) = \frac{\text{Num. non-mate searches where one or more enrolled candidates are returned with score at or above threshold}}{\text{Num. non-mate searches attempted.}} \quad (1)$$

Under this definition, FPIR can be computed from the highest non-mate candidate produced in a search - it is not necessary to consider candidates at rank 2 and above. FPIR is the primary measure of Type I errors in this report.

Selectivity: However, note that in any given search, several non-mate may be returned above threshold. In order to quantify such events, a second quantity, selectivity (SEL), is defined as the *number* of non-mates returned on a candidate list, averaged over all searches.

$$\text{SEL}(N,T) = \frac{\text{Num. non-mate enrolled candidates returned with score at or above threshold}}{\text{Num. non-mate searches attempted.}} \quad (2)$$

where $0 \leq$ SEL(N, T) $\leq$L. Both of these metrics are useful operationally. FPIR is useful for targeting how often an adverse false positive outcome can occur, while SEL as a number is related to workload associated with adjudicating candidate lists. The relationship between the two quantities is complicated - it depends on whether an algorithm concentrates the false alarms in the results of a few searches or whether it disburses them across many. This was detailed in FRVT 2014, NISTIR 8009. It has not yet been detailed in FRVT 2018.

3.2 Quantifying hits and misses

If L candidates are returned in a search, a shorter candidate list can be prepared by taking the top $R \leq L$ candidates for which the score is above some threshold, $T \geq 0$. This reduction of the candidate list is done because thresholds may be applied, and only short lists might be reviewed (according to policy or labor availability, for example). It is useful then to state accuracy in terms of R and T, so we define a "miss rate" with the general name **false negative identification**

rate (FNIR), as follows:

$$\text{FNIR}(N, R, T) = \frac{\text{Num. mate searches with enrolled mate found outside top R ranks or score below threshold}}{\text{Num. mate searches attempted.}} \quad (3)$$

This formulation is simple for evaluation in that it does not distinguish between causes of misses. Thus a mate that is not reported on a candidate list is treated the same as a miss arising from face finding failure, algorithm intolerance of poor quality, or software crashes. Thus if the algorithm fails to produce a candidate list, either because the search failed, or because a search template was not made, the result is regarded as a miss, adding to FNIR.

Hit rates, and true positive identification rates: While FNIR states the "miss rate" as how often the correct candidate is either not above threshold or not at good rank, many communities prefer to talk of "hit rates". This is simply the **true positive identification rate**(TPIR) which is the complement of FNIR giving a positive statement of how often mated searches are successful:

$$\text{TPIR}(N, R, T) = 1 - \text{FNIR}(N, R, T) \quad (4)$$

This report does not report true positive "hit" rates, preferring false negative miss rates for two reasons. First, costs rise linearly with error rates. For example, if we double FNIR in an access control system, then we double user inconvenience and delay. If we express that as decrease of TPIR from, say 98.5% to 97%, then we mentally have to invert the scale to see a doubling in costs. More subtly, readers don't perceive differences in numbers near 100% well, becoming inured to the "high nineties" effect where numbers close to 100 are perceived indifferently.

Reliability is a corresponding term, typically being identical to TPIR, and often cited in automated (fingerprint) identification system (AFIS) evaluations.

An important special case is the **cumulative match characteristic**(CMC) which summarizes accuracy of mated-searches only. It ignores similarity scores by relaxing the threshold requirement, and just reports the fraction of mated searches returning the mate at rank R or better.

$$\text{CMC}(N, R) = 1 - \text{FNIR}(N, R, 0) \quad (5)$$

We primarily cite the complement of this quantity, $\text{FNIR}(N, R, 0)$, the fraction of mates *not* in the top R ranks.

The **rank one hit rate** is the fraction of mated searches yielding the correct candidate at best rank, i.e. CMC(N, 1). While this quantity is the most common summary indicator of an algorithm's efficacy, it is not dependent on similarity scores, so it does not distinguish between strong (high scoring) and weak hits. It also ignores that an adjudicating reviewer is often willing to look at many candidates.

3.2.1 False negative rates for unconsolidated galleries

As detailed in section 2.2 a common type of gallery, here referred to as the lifetime unconsolidate type, is populated with all images of an individual without any association between them. That is, the gallery construction algorithm is not provided with any ID labels that would support processing of a person's images jointly. This constrasts with the lifetime consolidate type where an algorithm may explicitly fuse features from multiple images of a person, or select a best image. In such cases, where the number of enrolled images is a random variable, we define two false negative rates as follows.

The first demands that the algorithm place any of the K_i mates in the top $R \geq 1$ ranks. The proportion of searches for

which this does not occur forms a false negative identification rate:

$$\text{FNIR}_{\text{any}}(N, R, T) = 1 - \frac{\text{Num. mate searches where any enrolled mate is found in the top R ranks and at-or-above threshold}}{\text{Num. mate searches attempted.}} \quad (6)$$

The second demands that the algorithm place all K_i mates in the top $R \geq K_i$ ranks. The proportion of searches for which this does not occur forms a false negative identification rate:

$$\text{FNIR}_{\text{all}}(N, R, T) = 1 - \frac{\text{Num. mate searches where all enrolled mates are found in the top R ranks and at-or-above threshold}}{\text{Num. mate searches attempted.}} \quad (7)$$

Placing all mates in the top ranks is a more difficult task than correctly retrieving any image, so it holds that: $\text{FNIR}_{\text{all}} \geq \text{FNIR}_{\text{any}}$. This is evident in the results presented for November 2018 algorithms in Tables starting at 30.

The information retrieval community might prefer to compute and plot *precision* and *recall*; this is a valid approach, but we advance the two metrics above because they relate to our normal definition of consolidated FNIR, and they cover the two extreme use-cases of wanting any hit vs. all hits.

3.3 DET interpretation

In biometrics, a false negative occurs when an algorithm fails to match two samples of one person – a Type II error. Correspondingly, a false positive occurs when samples from two persons are improperly associated – a Type I error.

Matches are declared by a biometric system when the native comparison score from the recognition algorithm meets some threshold. Comparison scores can be either similarity scores, in which case higher values indicate that the samples are more likely to come from the same person, or dissimilarity scores, in which case higher values indicate different people. Similarity scores are traditionally computed by fingerprint and face recognition algorithms, while dissimilarities are used in iris recognition. In some cases, the dissimilarity score is a distance possessing metric properties. In any case, scores can be either mate scores, coming from a comparison of one person's samples, or nonmate scores, coming from comparison of different persons' samples.

The words "genuine" or "authentic" are synonyms for mate, and the word "impostor" is used as a synonym for nonmate. The words "mate" and "nonmate" are traditionally used in identification applications (such as law enforcement search, or background checks) while genuine and impostor are used in verification applications (such as access control).

An error tradeoff characteristic represents the tradeoff between Type II and Type I classification errors. For identification this plots false negative vs. false positive identification rates i.e. FNIR vs. FPIR parametrically with T. Such plots are often called detection error tradeoff (DET) characteristics or receiver operating characteristic (ROC). These serve the same function − to show error tradeoff − but differ, for example, in plotting the complement of an error rate (e.g. TPIR = 1 − FNIR) and in transforming the axes, most commonly using logarithms, to show multiple decades of FPIR. More rarely, the function might be the inverse of the Gaussian cumulative distribution function.

The slides of Figures 8 through 15 discuss presentation and interpretation of DETs used in this document for reporting face identification accuracy. Further detail is provided in formal biometrics testing standards, see the various parts of ISO/IEC 19795 Biometrics Testing and Reporting. More terms, including and beyond those to do with accuracy, appear in ISO/IEC 2382-37 Information technology – Vocabulary – Part 37: Harmonized biometric vocabulary.

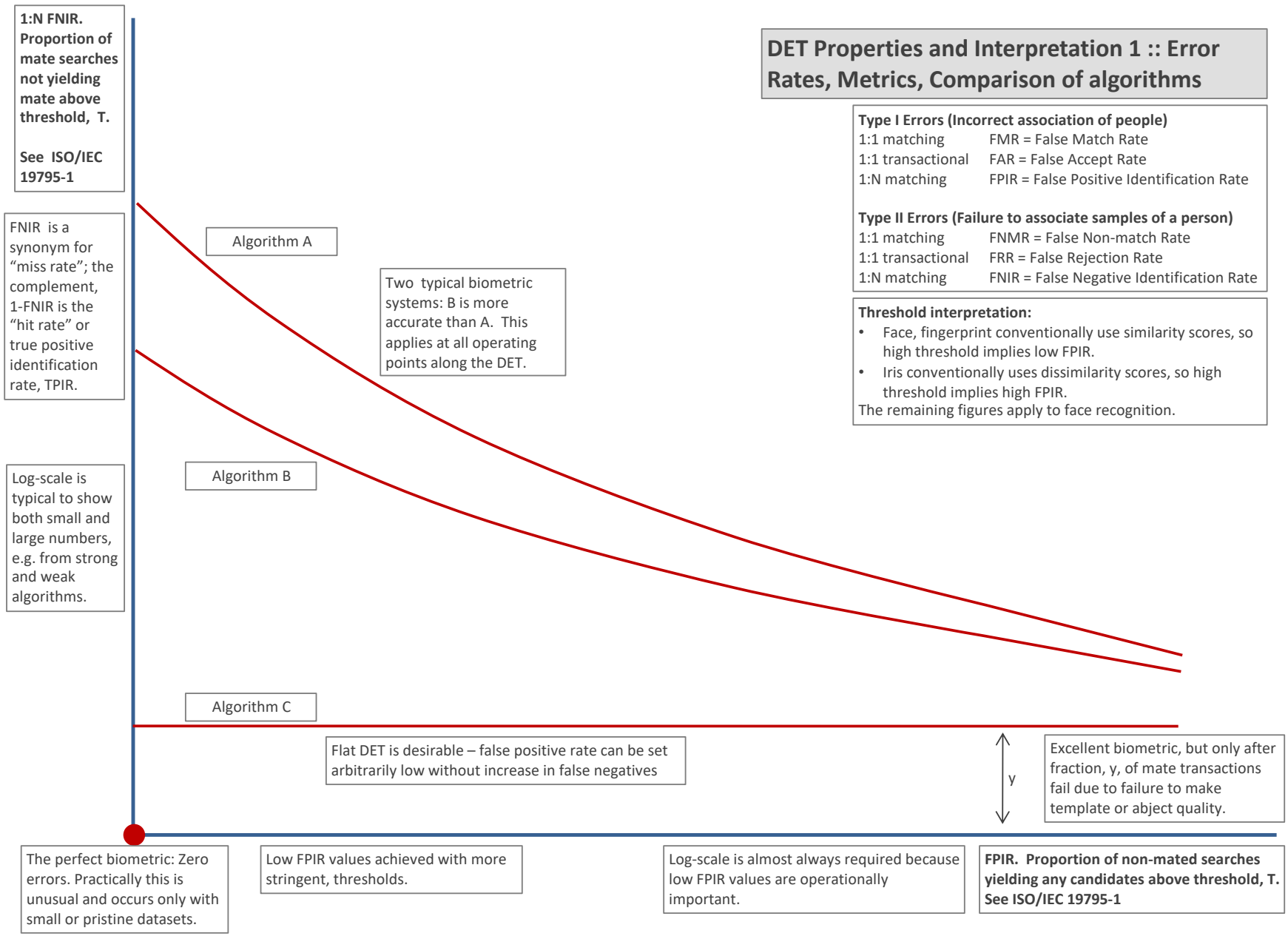

Figure 8: **DET as the primary performance reporting mechanism**.

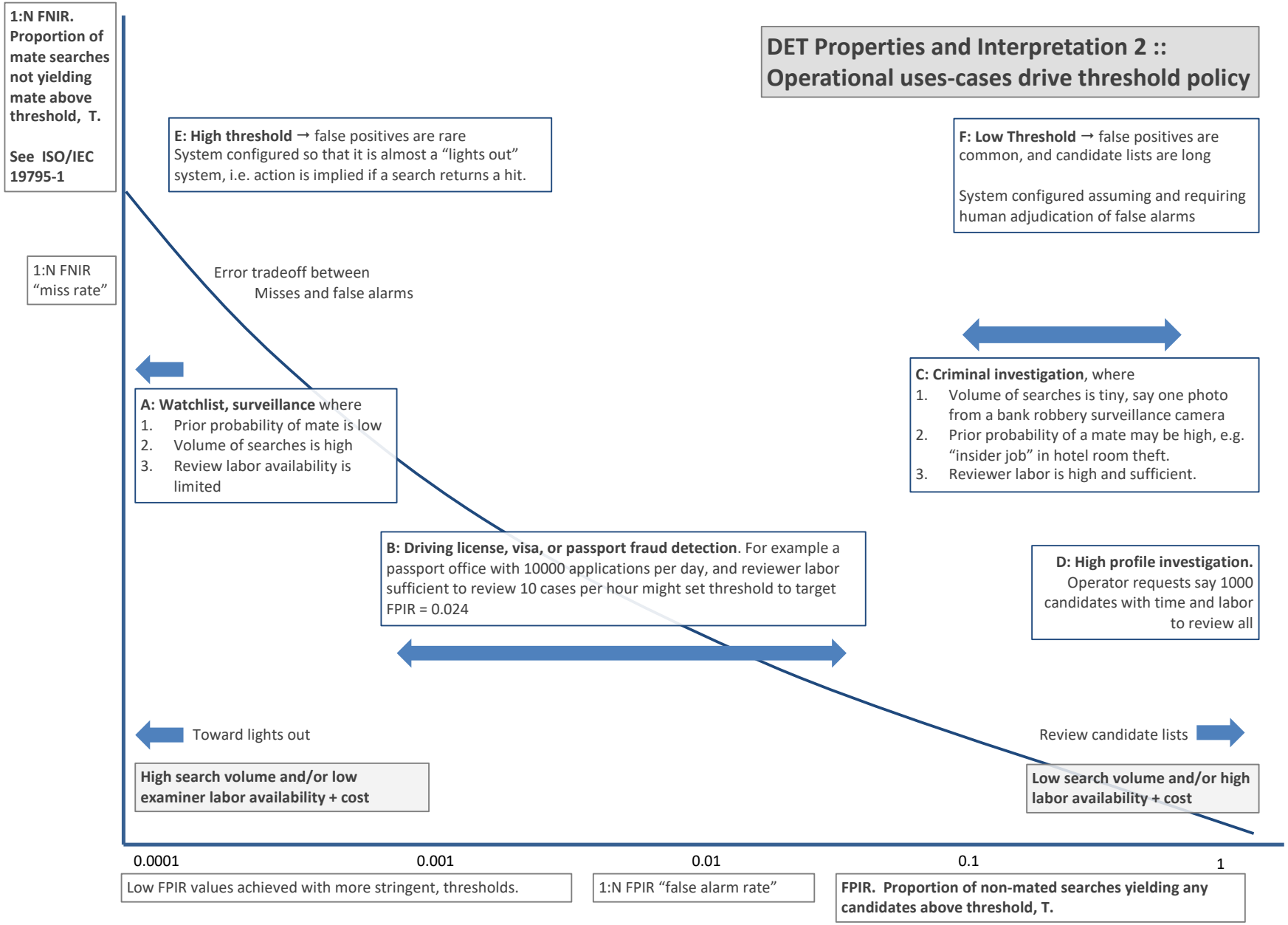

Figure 9: **DET as the primary performance reporting mechanism**.

FNIR(N, R, T) = False neg. identification rate
FPIR(N, T) = False pos. identification rate
N = Num. enrolled subjects
R = Num. candidates examined
T = Threshold
T = 0 → Investigation
T > 0 → Identification

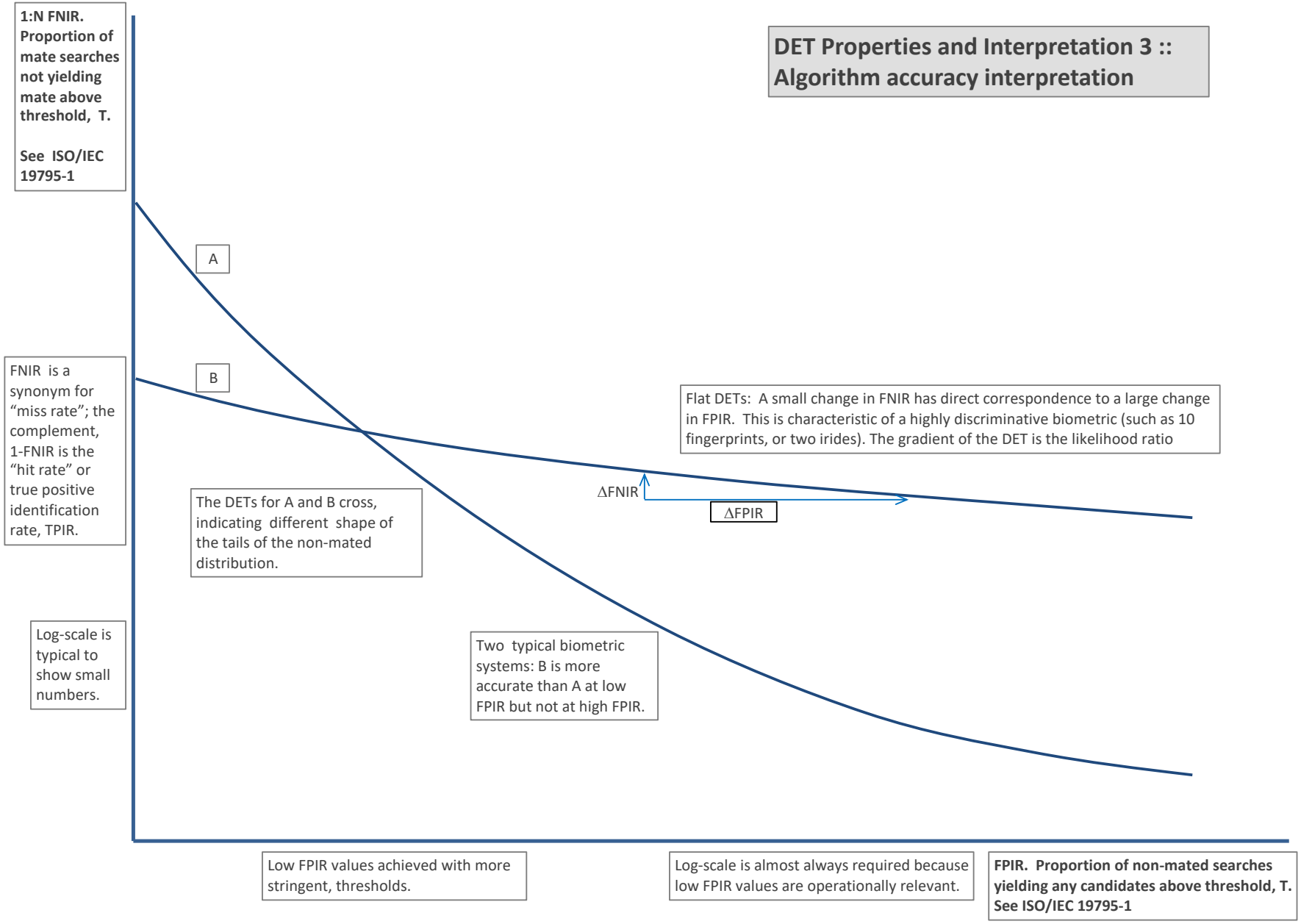

Figure 10: **DET as the primary performance reporting mechanism**.

2020/03/27 10:40:09

FNIR(N, R, T) = False neg. identification rate
FPIR(N, T) = False pos. identification rate
N = Num. enrolled subjects
R = Num. candidates examined
T = Threshold
T = 0 → Investigation
T > 0 → Identification

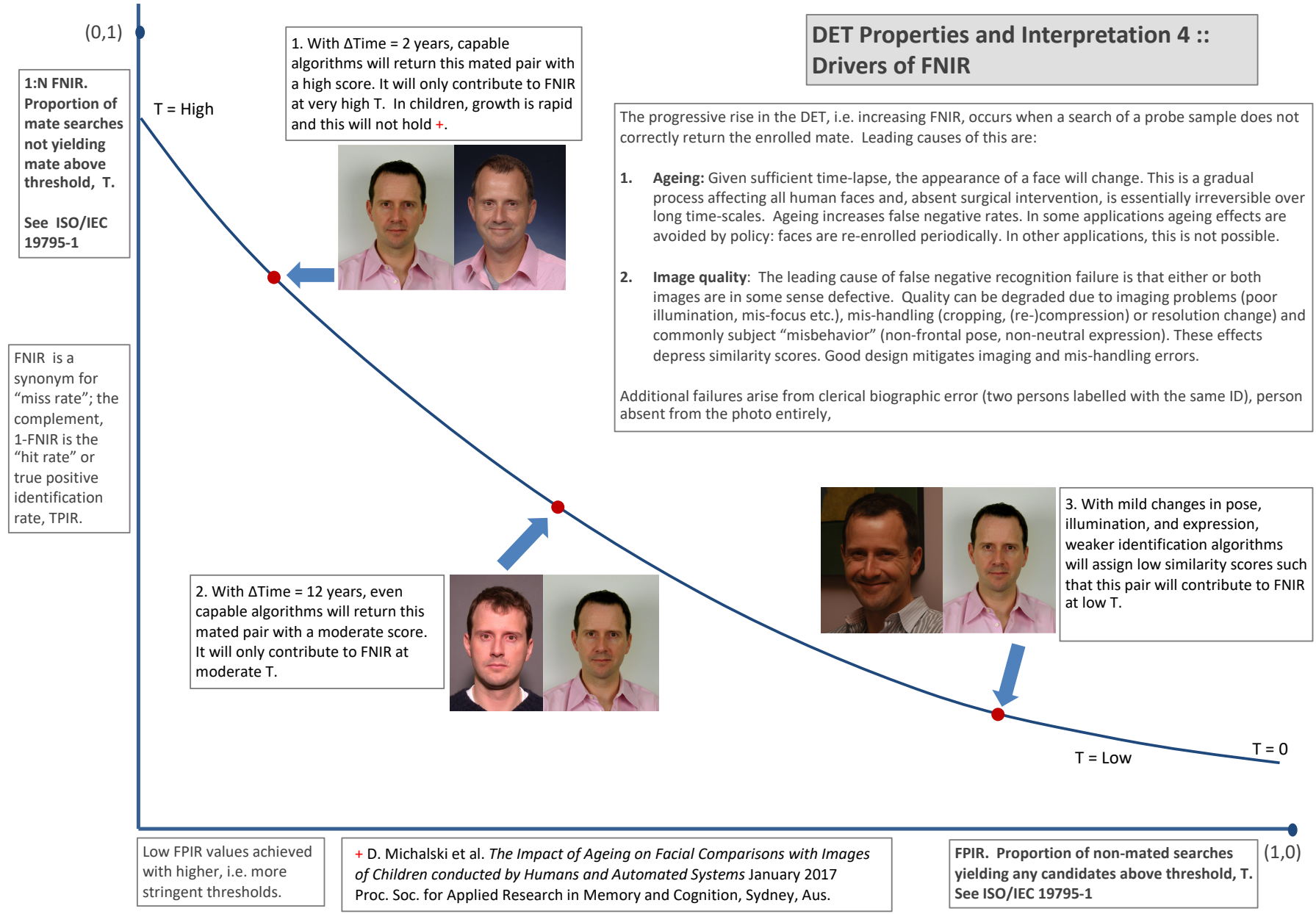

Figure 11: **DET as the primary performance reporting mechanism**.

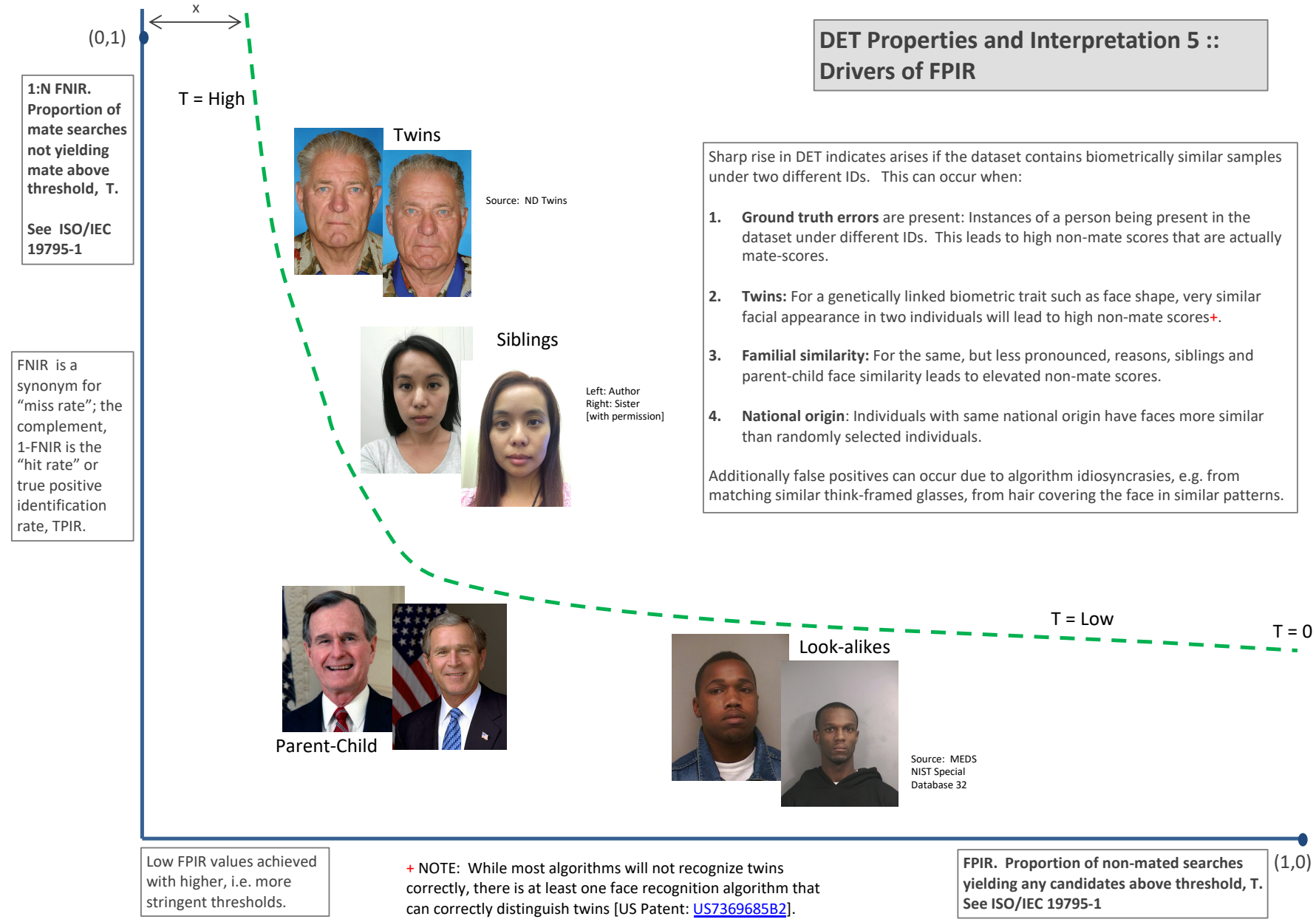

Figure 12: **DET as the primary performance reporting mechanism**.

2020/03/27 10:40:09
FNIR(N, R, T) = False neg. identification rate
FPIR(N, T) = False pos. identification rate
N = Num. enrolled subjects
R = Num. candidates examined
T = Threshold
T = 0 → Investigation
T > 0 → Identification

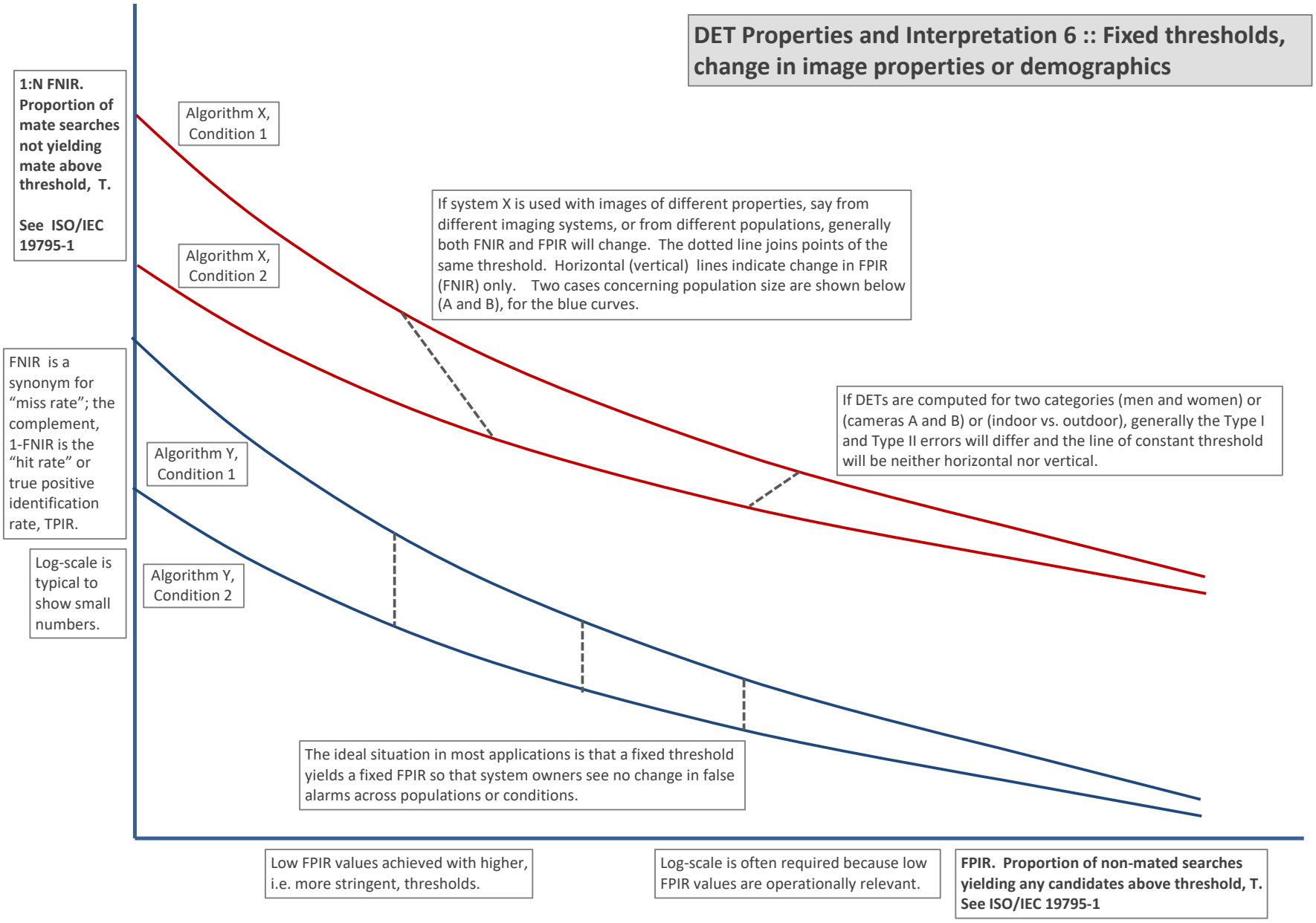

Figure 13: **DET as the primary performance reporting mechanism**.

FNIR(N, R, T) = False neg. identification rate
FPIR(N, T) = False pos. identification rate
N = Num. enrolled subjects
R = Num. candidates examined
T = Threshold
T = 0 → Investigation
T > 0 → Identification

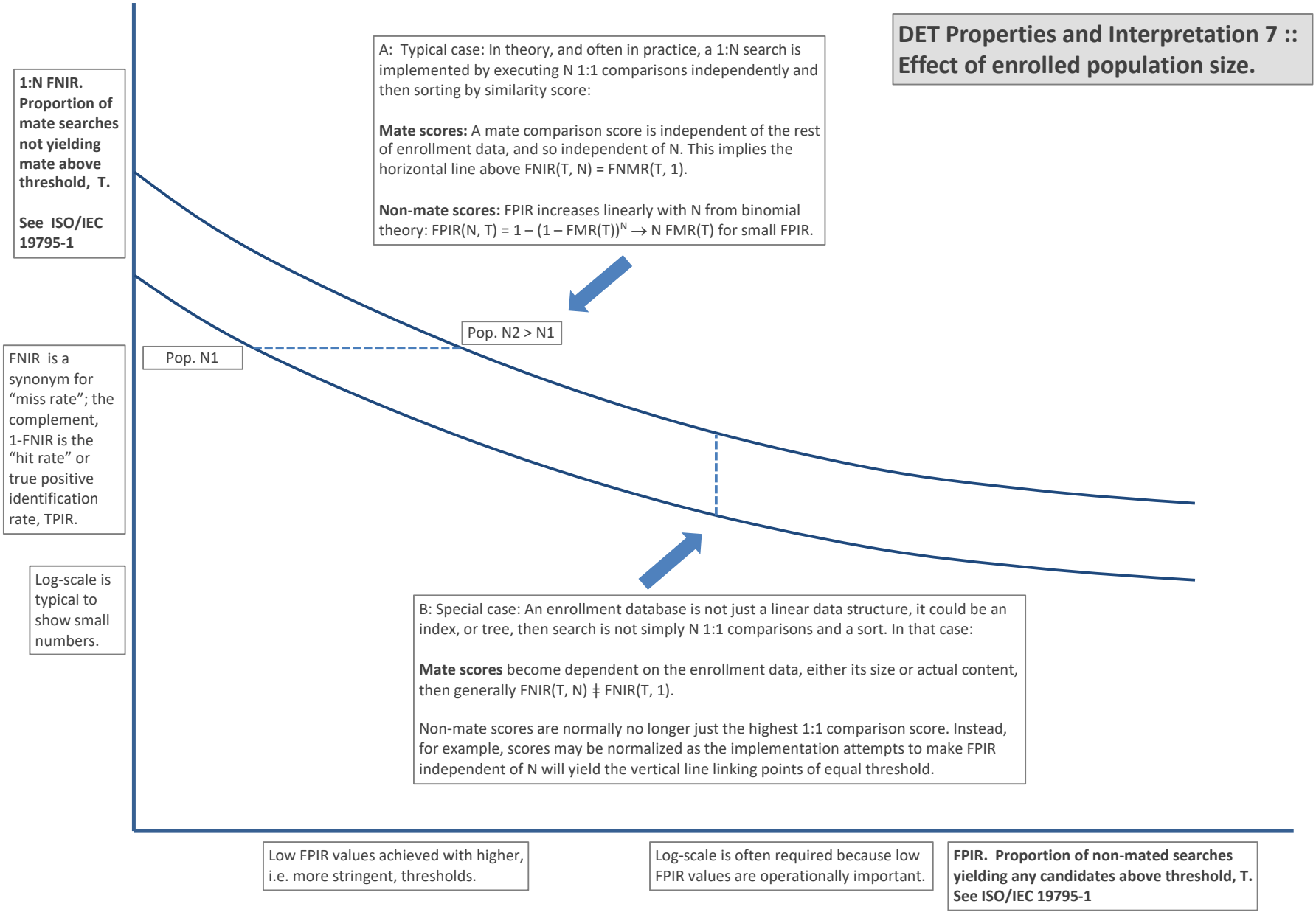

Figure 14: **DET as the primary performance reporting mechanism**.

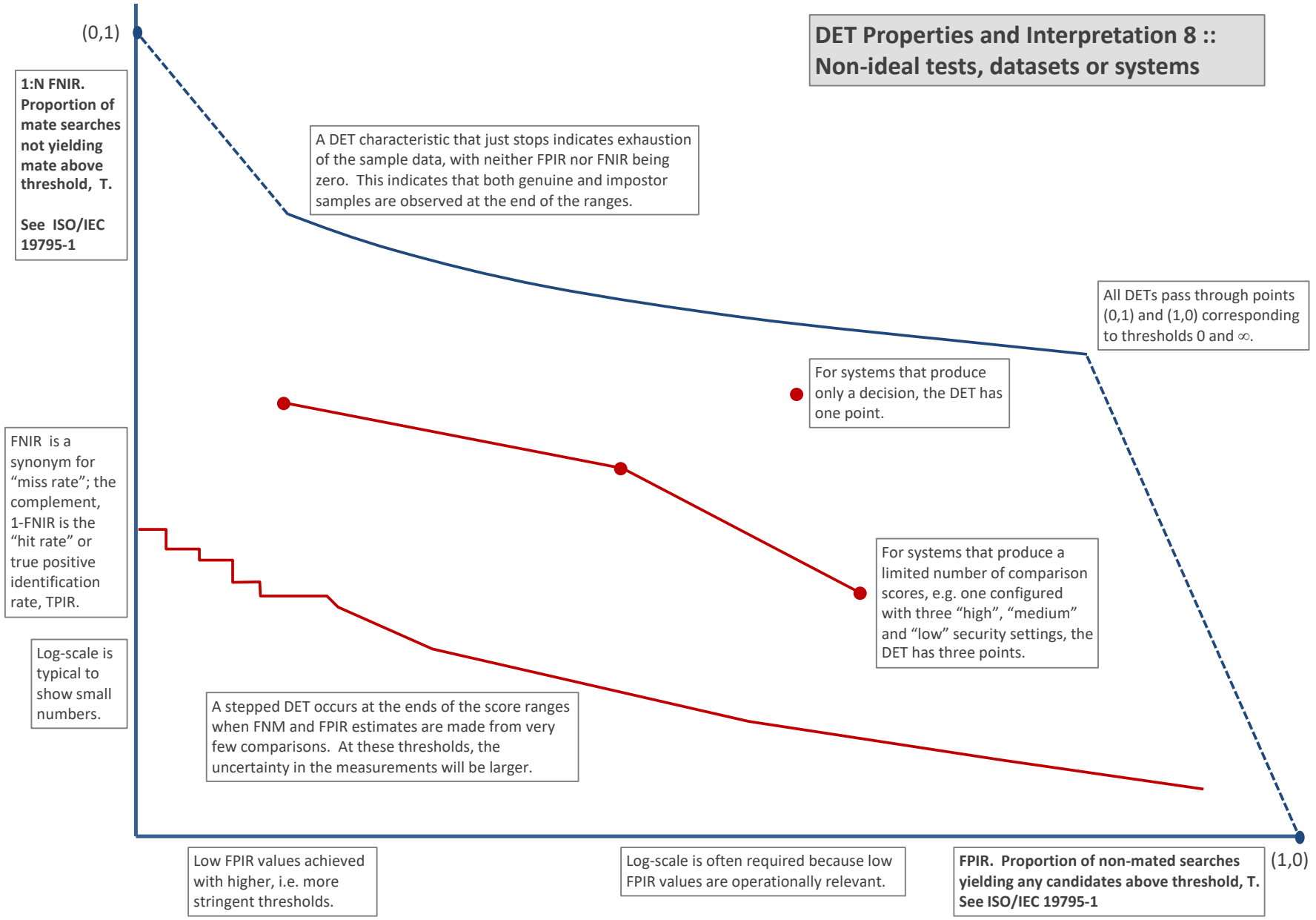

Figure 15: **DET as the primary performance reporting mechanism**.

3.4 Best practice testing requires execution of searches with and without mates

FRVT embeds 1:N searches of two kinds: Those for which there is an enrolled mate, and those for which there is not. The respective numbers for these types of searches appear in Table 1. However, it is common to conduct only mated searches[8]. The cumulative match characteristic is computed from candidate lists produced in mated searches. Even if the CMC is the only metric of interest, the actual trials executed in a test should nevertheless include searches for which no mate exists. As detailed in Table 1 the FRVT reserved disjoint populations of subjects for executing true non-mate searches.

3.5 Failure to extract features

During enrollment some algorithms fail to convert a face image to a template. The proportion of failures is the failure-to-enroll rate, denoted by FTE. Similarly, some search images are not converted to templates. The corresponding proportion is termed failure-to-extract, denoted by FTX.

We do not report FTX because we assume that the same underlying algorithm is used for template generation for enrollment and search.

Failure to extract rates are incorporated into FNIR and FPIR measurements as follows.

- **Enrollment templates**: Any failed enrollment is regarded as producing a zero length template. Algorithms are required by the API [9] to transparently process zero length templates. The effect of template generation failure on search accuracy depends on whether subsequent searches are mated, or non-mated: Mated searches will fail giving elevated FNIR; non-mated searches will not produce false positives so, to first order, FPIR will be reduced by a factor of $1-\text{FTE}$.

- **Search templates and 1:N search**: In cases where the algorithm fails to produce a search template from input imagery, the result is taken to be a candidate list whose entries have no hypothesized identities and zero score. The effect of template generation failure on search accuracy depends on whether searches are mated, or non-mated: Mated searches will fail giving elevated FNIR; Non-mated searches will not produce false positives, so FPIR will be reduced. Thus given a measurement of false negative and positive rates made over only those where failures-to-extract did not occur, those rates - call them $\text{FNIR}^{\dagger}$ and $\text{FPIR}^{\dagger}$ - could be adjusted by an explicit measurement of FTX as follows

$$\text{FNIR} = \text{FTX} + (1 - \text{FTX})\text{FNIR}^{\dagger} \tag{8}$$

$$\text{FPIR} = (1 - \text{FTX})\text{FPIR}^{\dagger} \tag{9}$$

This approach is the correct treatment for positive-identification applications such as access control where cooperative users are enrolled and make attempts at recognition. This approach is not appropriate to negative identification applications, such as visa fraud detection, in which hostile individuals may attempt to evade detection by submitting poor quality samples. In those cases, template generation failures should be investigated as though a false alarm had occurred.

[8]For example, the Megaface benchmark. This is bad practice for several reasons: First, if a developer knows, or can reasonably assume, that a mate always exists, then unrealistic gaming of the test is possible. A second reason is that it does not put FPIR on equal footing with FNIR and that matters because in most applications, not all searches have mates - not everyone has been previously enrolled in a driving license issuance or a criminal justice system - so addressing between-class separation becomes necessary.

3.6 Fixed length candidate lists, threshold independent workload

Suppose an automated face identification algorithm returns L candidates, and a human reviewer is retained to examine up to R candidates, where $R \leq L$ might be set by policy, preference or labor availability. For now, assume also that the reviewer is not provided with, or ignores, similarity scores, and thresholds are not applied. Given the algorithm typically places mates at low (good) ranks, the number of candidates a reviewer can be expected to review can be derived as follows. Note that the reviewer will:

- ▷ Always inspect the first ranked image — Frac. reviewed = 1
- ▷ Then inspect those candidates where mate not confirmed at rank 1 — Frac. reviewed = 1-CMC(1)
- ▷ Then inspect those candidates where mate not confirmed at rank 1 or 2 — Frac. reviewed = 1-CMC(2)

etc. Thus if the reviewer will stop after a maximum of R candidates, the expected number of candidate reviews is

$$M(R) = 1 + (1 - CMC(1)) + (1 - CMC(2)) + \ldots + (1 - CMC(R-1)) \tag{10}$$

$$= R - \sum_{r=1}^{R-1} CMC(r) \tag{11}$$

A recognition algorithm that front-loads the cumulative match characteristic will offer reduced workload for the reviewer. This workload is defined only over the searches for which a mate exists. In the cases where there truly is no mate, the reviewer would review all R candidates. Thus, if the proportion of searches for which a mate does exist is β, which in the law enforcement context would be the recidivism rate [2], the full expression for workload becomes:

$$M(R) = \beta \left(R - \sum_{r=1}^{R-1} CMC(r) \right) \quad + \quad (1 - \beta)R \tag{12}$$

$$= R - \beta \sum_{r=1}^{R-1} CMC(r) \tag{13}$$

3.7 Timing measurement

Algorithms were submitted to NIST as implementations of the application programming interface(API) specified by NIST in the Evaluation Plan [9]. The API includes functions for initialization, template generation, finalization, search, gallery insert, and gallery delete. Two template generation functions are required, one for the preparation of an enrollment template, and one for a search template.

In NIST's test harness, all functions were wrapped by calls to the C++ std::chrono::high resolution clock which on the dedicated timing machine counts 1ns clock ticks. Precision is somewhat worse than that however.

3.8 Uncertainty estimation

3.8.1 Random error

This study leverages operational datasets for measurement of recognition error rates. This affords several advantages. First, large numbers of searches are conducted (see Table 1) giving precision to the measurements. Moreover, for the two mugshot datasets, these do not involve reuse of individuals so binomial statistics can be expected to apply to recognition error counts. In that case, an observed count of a particular recognition outcome (i.e. a false negative or false positive) in M trials will sustain 95% confidence that the actual error rate is no larger than some value.

As an example, the minimum number of mugshot searches conducted in this report is M =154 549, and for an observed FNIR around 0.002, the measurement supports a conclusion that the actual FNIR is no higher than 0.00228 at 99% confidence level. On the false positive side, we tabulate FNIR at FPIR values as low as 0.001. Given estimates based on 331 254 non-mate trials, the actual FPIR values will be below 0.00115 at 99% confidence. In conclusion, large scale evaluation, without reuse of subjects, supports tight uncertainty bounds on the measured error rates.

3.8.2 Systematic error

The FRVT 2018 dataset includes anomalies discovered as a result of inspecting images involved in recognition failures from the most accurate algorithms. Two kinds of failure occur: False negatives (which, for the purpose here, include failures to make templates) and false positives.

False negative errors: We reviewed 600 false negative pairs for which either or both of the leading two algorithms did not put the correct mate in the top 50 candidates. Given 154 549 searches, this number represents 0.39% of the total, resulting in FNIR ~ 0.0039. Of the 600 pairs:

- **A: Poor quality**: About 20% of the pairs included images of very low quality, often greyscale, low resolution, blurred, low contrast, partially cropped, interlaced, or noisy scans of paper images. Additionally, in a few cases, the face is injured or occluded by bandages or heavy cosmetics.
- **B: Ground truth identity label bugs**: About 15% of the pairs are not actually mated. We only assigned this outcome when a pair is clearly not mated.
- **C: Profile views**: About 35% included an image of a profile (side) view of the face, or, more rarely, an image that was rotated 90 degrees in-plane (roll).
- **D: Tattoos**: About 30% included an image of a tattoo that contained a face image. These arise from mis-labelling in the parent dataset metadata.
- **E: Ageing**: There is considerable time-lapse between the two captures.

All these estimates are approximate. Of these, the tattoo and mislabled images can never be matched. These constitute an accuracy floor in the sample implying that FNIR cannot be below 0.0018[9]. The profile-views, low-quality images, and images with considerable ageing can, in principle, be successfully matched - indeed some algorithms do so - so are not part of the accuracy floor.

[9]This value is the sum of two partial false negative rates: FNIR_B = 0.15 * 0.0039 plus FNIR_D = 0.3 * 0.0039

For the microsoft-4 algorithm the lowest miss rate from (recent entry in Table 18) is FNIR(640 000, 50, 0) = 0.0018. This is close to the value estimated from the inspection of misses. It is below the 0.0039 figure because the algorithm does match some profile and poor quality images, that the yitu-2 algorithm does not.

For many tables (e.g. Table 18), the FNIR values obtained for the FRVT-2018 mugshots could be corrected by reducing them by 0.0018. The best values would then be indistinct from zero. The results in this report *were not* adjusted to account for this systematic error.

False positive errors: As depicted in Figure 8 many of the DET characteristics in this report exhibit a pronounced turn upward at low false positive rates. The shape can be caused by identity labelling errors in the ground truth of a dataset, specifically persons present in the database under two IDs such that some proportion of non-mate pairs are actually mated. We merged the highest 1000 non-mate pairs produced by three different algorithms which resulted in 1839 unique pairs. This constitutes 0.56% of all non-mate searches. We assert that it is *very* difficult for human reviewers to assign the pairs into the following three categories: twins; doppelgangers; or ground-truth errors (instances of the same person under two IDs). Given this difficulty we made no attempt to correct any ground truth except by removing 57 pairs in the following categories:

- **A: Profile views**: Thirteen pairs included one or two profile-view images. As described in Figure 111, these can cause false positives.
- **B: Same-session photographs**: For twelve pairs, the images were identical or trivially altered (e.g. cropped) versions of the same photo. These were present under a different ID likely due to some clerical or procedural mistake.
- **C: Tattoos of faces**: There were fourteen instances of tattoo photographs that contained faces causing false matches.
- **D: T-shirt faces**: There were six instances of T-shirt photographs (of Bob Marley and Che Guevara) being detected instead of the face and causing false positives.
- **E: Background faces**: There were twelve instances of one subject appearing in the background of two otherwise correct portrait photos.

Note we did not remove any images where there was a chance that the pair was actually a different person.

In any case, the results in this report have not been adjusted for this systematic error.

4 Results

This section gives extensive results for algorithms submitted to FRVT 2018. Three page "report cards" for each algorithm are contained in a separate supplement. Performance metrics were described in section 3. The main results are summarized in tabular form with more exhaustive data included as DET, CMC and related graphs in appendices as follows:

- The three tables 2-4 list algorithms alongside full developer names, acceptance date, size of the provided configuration data, template size and generation time, and search duration data.
  - The **template generation duration** is most important to applications that require fast response. For example, an eGate taking more than two seconds to produce a template might be unacceptable. Note that GPUs may be of utility in expediting this operation for some algorithms, though at additional expense. Two additional factors should be considered[10][11].
  - The **search duration** is the time taken for a search of a search template into a gallery of N enrollment templates. This performance variable, together with the volume of searches, is influential on the amount of hardware needed to sustain an operational deployment. This is measured here with the algorithm running on a single core of a contemporary CPU. Search is most simply implemented as N computations of a distance metric followed by a sort operation to find the closest enrollments. However, considerable optimization of this process is possible, up to and including fast-search algorithms that, by various means, avoid computation of all N distances.
  - The **template size** is the size of the extracted feature vector (or vectors) and any needed header information. Large template sizes may be influential on bus or network bandwidth, storage requirements, and on search duration. While the template itself is an opaque data blob, the feature dimensionality might be estimated by assuming a four-bytes-per-float encoding. There is a wide range of encodings. For the more accurate algorithm, sizes range from 256 bytes to about 2KB bytes, indicating essentially no consensus on face modeling and template design.
  - The **template size multiplier** column shows how, given k input images, the size of the template grows. Most implementations internally extract features from each image and concatenate them, and implement some score-level fusion logic during search. Other implementations, including many of the most accurate algorithms, produce templates whose size does not grow with k. This could be achieved via selection of the best quality image - but this is not optimal in handling ageing where the oldest image could be the best quality. Another mechanism would be feature-level fusion where information is fused from all k inputs. In any case, as a black-box test, the fusion scheme is proprietary and unknown.
  - The size of the **configuration data** is the total size of all files resident in a vendor-provided directory that contains arbitrary read-only files such as parameters, recognition models (e.g caffe). Generally a large value for this quantity may prohibit the use of the algorithm on a resource-constrained device.

[10] The FRVT 2018 API prohibited threading, so some gains from parallelism may be available on multiple-cores or multiple processors, if the feature extraction code could be distributed across them.

[11] Note also that factors of two or more may be realizable by exploiting modern vector processing instructions on CPUs. It is not clear in our measurements whether all developers exploited Intel's AVX2 instructions, for example. Our machine was so equipped, but we insisted that the same compiled library should also run on older machines lacking that instruction. The more sophisticated implementations may have detected AVX2 presence and branched accordingly. The less sophisticated may be defaulted to the reduced instruction set. Readers should see the FRVT 2018 API document for the specific chip details.

▷ Tables 18-19 report core rank-based accuracy for mugshot images. The population size is limited to N = 1.6 million identities because this is the largest gallery size on which all algorithms were executed. Notable observations from these tables are as follows:

- **Accuracy gains during 2018**: NIST Interagency Report 8238 documented massive gains over those reported in the FRVT 2014 report, NIST Interagency Report 8009.

  Further gains are documented in this report. Comparing the most accurate algorithm in June 2018, Microsoft-4, with the most accurate in November 2018, NEC-2, the value of FNIR(N, 1, 0) reduced from 0.0031 to 0.0028 with N = 1.6 million recent images. For lifetime enrollments, Microsoft-4 remained the most accurate algorithm as the newer variants from Microsoft did not reduce this error rate.

  We further note that the revolution is not over: Figure 18 shows that many developers have made great advances in the four months between Phases 1 and 2 of FRVT 2018, Feburary to June. Most developers saw a two-fold reduction in errors, with Neurotechnology seeing a five fold reduction.

- **Wide range in accuracy**: The rank-1 miss rates vary from FNIR(N, 1, 0) = 0.001 for nec-3 up to about 0.5 for the very fast but inaccurate microfocus-x algorithms. Among the developers who are superior to NEC in 2013, the range is from 0.002 to 0.035 for camvi-3. This large accuracy range is consistent with the buyer-beware maxim, and indicates that face recognition software is far from being commoditized.

▷ Tables 22-23 report threshold-based error rates, FNIR(N, L, T), for N = 1.6 million for mugshot-mugshot accuracy on FRVT 2014, FRVT 2018, and also (in pink) mugshot-webcam accuracy using FRVT 2018 enrollments. Notable observations from these tables are as follows:

- **Order of magnitude accuracy gains since 2014**: As with rank-based results, the gains in accuracy are substantial, though somewhat reduced. At FPIR = 0.01, the best improvement over NEC in 2014 is a 27 fold reduction in FNIR using the NEC_2 algorithm. At FPIR = 0.001, the largest gain is a six-fold reduction in FNIR via the NEC_3 algorithm.

- **Broad gains across the industry**: About 19 companies realize accuracy better than the NEC benchmark from 2014. This is somewhat lower than the 28 developers who succeeded on the rank-1 metric. This may be due to the ubiquity of, and emphasis on, the rank-1 metric in many published algorithm development papers.

- **Webcam images**: Searches of webcam images give FNIR(N, T) values around 2 to 3 times higher than mugshot searches. Notably the leading developers with mugshots are approximately the same with poorer quality webcams. But some developers e.g. Camvi, Megvii, TongYi, and Neurotechnology do improve their relative rankings on webcams, perhaps indicating their algorithms were tailored to less constrained images.

▷ Tables 9, 12, 13 and show, respectively, high-threshold, rank 1, nd rank 50 FNIR values for all algorithms performing searches into five different gallery sizes, N = 640 000, N = 1 600 000, N = 3 000 000, N = 6 000 000 and 12 000 000. The FPIR = 0.001 table is included to inform high-volume duplicate detection applications. The Rank-1 table is included as a primary accuracy indicator. The Rank-50 table is included to inform agencies who routinely produce 50 candidates for human-review. The notable results are:

- **Slow growth in rank-based miss rates:** FNIR(N, R) generally grows as a power law, aN^b. From the straight lines of many graphs of Figure 21 this is clearly a reasonable model for most, but not all, algorithms. The coefficient a can be interpreted as FNIR in a gallery of size 1. The more important coefficient b indicates

scalability, and often, $b \ll 1$, implies very benign growth in FNIR. The coefficients of the models appear in the Tables 12 and 13.

- **Slow growth in threshold-based miss rates:** FNIR(N, T) also generally grows as a power law, aN^b except at the high threshold values corresponding to low FPIR values. This is visible in the plots of Figure 37 which show straight lines except for FPIR = 0.001, which increase more rapidly with N above 3 000 000. Each trace in those figures shows FNIR(N, T) at fixed FPIR with both N and T varying. Thus at large N, it is usually necessary to elevate T to maintain fixed FPIR. This causes increased FNIR. Why that would no-longer obey a power-law is not known. However, if we expect large galleries to contain individuals with familial relations to the non-mate search images - in the most extreme case, twins - then suppression of false positives becomes more difficult. This is discussed in the Figures starting at Fig. 8

▷ Figure 20 shows false positives from twins against their enrolled siblings, broken out by type of twin: fraternal or identical. The Figure is based on the enrollment of 104 single images on one of a pair of twins, and then the search of 2354 second images. Note that the dataset is heavily skewed towards identical twins which is not representative of the true population. There is also a skew towards same sex fraternal twin pairs compared to different sex fraternal twin pairs again not representative of the true population.

The notable results are:

- For all algorithms tested, the 1087 mated searches (Twin A vs. Twin A) produce scores almost always above typical operational thresholds, with (not shown) matches at rank 1. The images are of good quality, so this is the result expected from the rest of this report.
- For the 1066 identical twin searches (AB), almost all produce the twin at rank 1, with a few producing the mate at further down the candidate lists rank and low score.
- For the 169 fraternal searches (AB) from same sex pairs, most algorithms give a large number of very high scores, implying false positives at all thresholds. However, there there are long tails containing lower scores that are correctly below threshold. In general, scores that are higher in this distribution are all rank 1 whereas the lower scores have much higher ranks.
- (Not shown) Of the 169, there are 24 fraternal searches (AB) involving different sex twins. Here most algorithms correctly report scores well below the lowest threshold, and usually not on the candidate list at all.

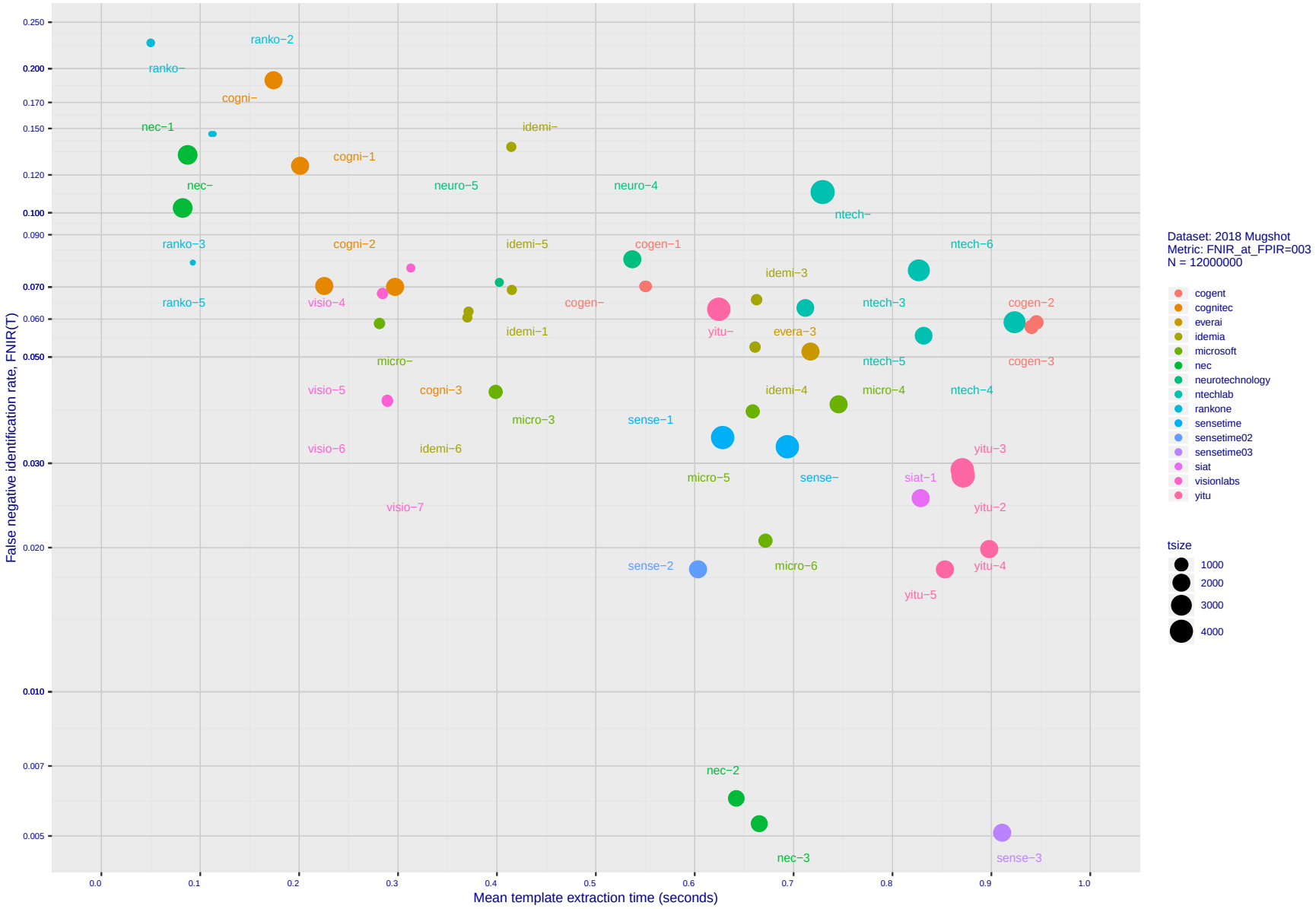

Figure 16: **[Mugshot Dataset] Speed-accuracy tradeoff**. *For developers of the more accurate algorithms the plot shows the tradeoff of high-threshold recognition miss-rates, FNIR(N, N, T) for FPIR(N, T) = 0.003, and template generation time. Developers are coded by color. Template size is encoded by the size of the circle. Some labels are quite distant from the respective point, to avoid superposing text. Without any other influences, the assumption would be that taking time to localize the face, and extract features, would lead to better accuracy. The most notable result, for NEC, is that their slower algorithms are much more accurate than the version that extract features in fewer than 90 milliseconds.*

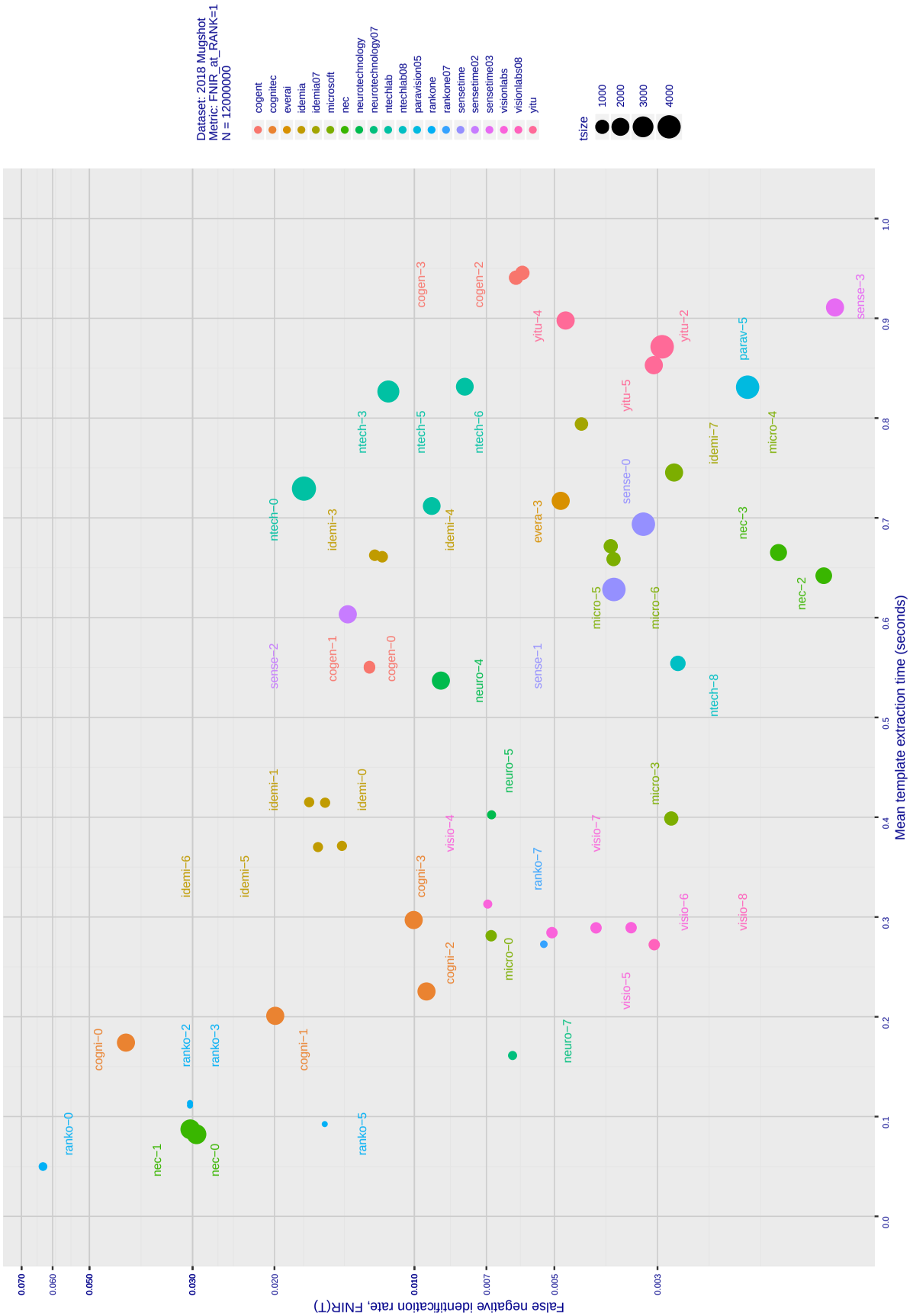

Figure 17: **[Mugshot Dataset] Speed-accuracy tradeoff**. *For developers of the more accurate algorithms the plot shows the tradeoff of rank-one recognition miss-rates, FNIR(N, 1, 0), and template generation time. Developers are coded by color. Template size is encoded by the size of the circle. Some labels are quite distant from the respective point, to avoid superposing text. Without any other influences, the assumption would be that taking time to localize the face, and extract features, would lead to better accuracy. This occurs for NEC with their slower algorithm being much accurate than the version that extract features in fewer than 90 milliseconds.*

	DEVELOPER	SHORT	SEQ.	VALIDATION	CONFIG[1]	TEMPLATE GENERATION			SEARCH DURATION[4] MILLISEC					
	FULL NAME	NAME	NUM.	DATE	DATA (MB)	SIZE (B)	MULT[2]	TIME (MS)[3]	L=1 N=1.6M	L=50 N=1.6M	L=50 N=3M	L=50 N=6M	L=50 N=12M	POWER LAW (μs)
1	3Divi	3divi	0	2018-02-09	186	[217]4096	k	[101]426	-	[122]553	-	-	-	
2	3Divi	3divi	1	2018-02-15	187	[230]4224	k	[105]428	-	[21]37	-	-	-	
3	3Divi	3divi	2	2018-02-15	187	[53]528	k	[103]428	-	[19]33	-	-	-	
4	3Divi	3divi	3	2018-06-19	165	[47]512	k	[147]625	[17]76	[25]76	-	-	-	
5	3Divi	3divi	4	2018-06-19	186	[213]4096	k	[148]628	[89]604	[148]801	-	-	-	
6	3Divi	3divi	5	2018-10-26	186	[211]4096	k	[157]653	[81]537	[119]537	[63]1376	[60]2612	[53]5524	[88]0.07 $N^{1.1}$
7	3Divi	3divi	6	2018-10-26	187	[55]528	k	[159]653	[12]33	[17]33	-	-	-	
8	Alchera Inc	alchera	0	2018-06-30	168	[169]2048	k	[48]263	[150]3296	[226]5420	-	-	-	
9	Alchera Inc	alchera	1	2018-06-30	46	[143]2048	k	[8]66	[151]3516	[227]5489	-	-	-	
10	Alchera Inc	alchera	2	2018-10-30	7	[166]2048	k	[16]115	[147]2920	[210]2926	-	-	-	
11	Alchera Inc	alchera	3	2018-10-30	251	[126]2048	k	[133]548	[148]2952	[212]2953	[106]6540	[101]14998	[97]35227	[103]0.10 $N^{1.2}$
12	AllGoVision	allgovision	000	2019-07-30	168	[157]2048	k	[100]425	[149]3217	[216]3184	[104]6111	[98]12411	[94]25758	[48]1.40 $N^{1.0}$
13	Anke Investments	anke	0	2018-10-30	779	[193]2072	k	[107]431	[91]675	[143]748	[67]1482	[64]2965	[55]6142	[70]0.21 $N^{1.1}$
14	Anke Investments	anke	002	2019-06-27	341	[186]2056	k	[152]641	[90]624	[138]682	[61]1306	[57]2403	[51]5082	[43]0.30 $N^{1.0}$
15	Anke Investments	anke	1	2018-10-30	779	[192]2072	k	[108]433	[95]707	[146]769	-	-	-	
16	Aware	aware	0	2018-02-16	261	[109]1564	k	[158]653	-	[66]251	-	-	-	
17	Aware	aware	1	2018-02-16	232	[110]1564	k	[155]651	-	[67]251	-	-	-	
18	Aware	aware	2	2018-02-16	349	[195]2076	k	[231]912	-	[68]252	-	-	-	
19	Aware	aware	3	2018-06-22	350	[194]2076	k	[189]716	[143]2426	[205]2508	[99]4495	-	-	[46]1.09 $N^{1.0}$
20	Aware	aware	4	2018-06-22	349	[2]92	k	[185]712	[114]1232	[167]1187	-	-	-	
21	Aware	aware	5	2018-10-30	368	[204]3100	k	[212]827	[20]94	[29]97	[14]202	[12]370	[10]251	[12]4.13 $N^{0.7}$
22	Aware	aware	6	2018-10-30	368	[3]124	k	[205]818	[31]157	[44]162	-	-	-	
23	Ayonix	ayonix	0	2018-06-21	57	[85]1036	k	[1]10	[53]283	[82]298	-	-	-	
24	Ayonix	ayonix	1	2018-10-29	74	[89]1036	k	[3]12	[50]277	[77]277	-	-	-	
25	Ayonix	ayonix	2	2018-10-30	74	[87]1036	1	[2]11	[49]277	[76]274	[31]531	[29]1079	[27]2268	[56]0.11 $N^{1.0}$
26	Camvi Technologies	camvitech	1	2018-02-16	94	[77]1024	1	[25]177	-	[13]23	-	-	-	
27	Camvi Technologies	camvitech	2	2018-02-16	442	[82]1024	1	[200]774	-	[12]20	-	-	-	
28	Camvi Technologies	camvitech	3	2018-06-30	233	[80]1024	1	[183]707	[8]10	[10]11	-	-	-	
29	Camvi Technologies	camvitech	4	2018-10-30	233	[74]1024	1	[191]718	[13]33	[16]32	[9]38	[7]40	[5]48	[2]8492.66 $N^{0.1}$
30	Camvi Technologies	camvitech	5	2018-10-30	257	[69]1024	1	[198]769	[11]31	[15]30	-	-	-	
31	Thales	cogent	0	2018-06-20	533	[52]525	k	[134]551	[77]494	[125]558	[49]1047	[50]2060	[41]4141	[22]0.46 $N^{1.0}$
32	Thales	cogent	1	2018-06-20	533	[51]525	k	[135]552	[78]498	[123]556	[50]1048	[51]2082	[43]4263	[27]0.39 $N^{1.0}$
33	Thales	cogent	2	2018-10-30	681	[92]1043	k	[238]987	[137]2017	[197]2144	[98]4298	[94]8472	[90]16429	[40]1.08 $N^{1.0}$
34	Thales	cogent	3	2018-10-30	681	[91]1043	k	[237]960	[113]1230	[174]1311	[87]2687	[81]5398	[73]10184	[44]0.62 $N^{1.0}$
35	Cognitec Systems GmbH	cognitec	0	2018-06-21	364	[179]2052	k	[24]176	[129]1748	[185]1780	[93]3672	[89]7093	[88]15224	[66]0.57 $N^{1.0}$
36	Cognitec Systems GmbH	cognitec	1	2018-06-21	412	[173]2052	k	[32]202	[132]1835	[187]1805	[96]3971	[92]7484	[89]16249	[74]0.49 $N^{1.1}$
37	Cognitec Systems GmbH	cognitec	2	2018-10-30	463	[175]2052	k	[39]227	[128]1733	[184]1763	[92]3660	[91]7279	[83]13895	[45]0.83 $N^{1.0}$
38	Cognitec Systems GmbH	cognitec	3	2018-10-30	465	[181]2052	k	[60]297	[127]1719	[186]1791	[91]3638	[90]7277	[86]14904	[62]0.66 $N^{1.0}$
39	Cyberlink Corp	cyberlink	000	2019-06-12	217	[171]2052	1	[177]699	[93]694	[140]699	[64]1376	[61]2633	[56]6201	[58]0.28 $N^{1.0}$
40	Cyberlink Corp	cyberlink	001	2019-10-07	459	[182]2052	1	[109]433	[94]698	[141]700	[62]1350	[83]5524	[78]12031	[108]0.00 $N^{1.3}$
41	Dahua Technology Co Ltd	dahua	0	2018-10-29	276	[152]2048	k	[80]378	-	[71]256	-	-	-	
43	Dahua Technology Co Ltd	dahua	1	2018-10-29	276	[129]2048	k	[76]371	-	[70]256	[37]601	[35]1199	[36]3001	[96]0.02 $N^{1.2}$
42	Dahua Technology Co Ltd	dahua	002	2019-12-02	607	[137]2048	k	[178]699	[46]243	[75]269	[55]1189	[63]2950	[58]6732	[112]0.00 $N^{1.5}$
44	Deepglint	deepglint	001	2019-11-15	448	[215]4096	1	[176]696	[76]484	[113]493	[69]1687	[37]1246	[12]686	[5]76694.70 $N^{0.2}$
45	Tencent Deepsea Lab	deepsea	001	2019-07-29	250	[131]2048	1	[202]780	[107]1021	[157]1020	[88]2774	[84]5767	[79]12341	[101]0.06 $N^{1.2}$
46	Dermalog	dermalog	0	2018-02-16	0	[5]128	1	[73]344	-	[99]404	-	-	-	
48	Dermalog	dermalog	1	2018-02-16	0	[9]128	1	[23]171	-	[102]407	-	-	-	
49	Dermalog	dermalog	2	2018-02-16	0	[21]256	k	[72]344	-	[136]640	-	-	-	
50	Dermalog	dermalog	3	2018-06-21	0	[7]128	1	[35]211	[19]92	[26]92	-	-	-	
51	Dermalog	dermalog	4	2018-06-21	0	[4]128	1	[33]208	[18]91	[27]93	-	-	-	
52	Dermalog	dermalog	5	2018-10-26	0	[6]128	1	[124]532	[3]0	[2]0	[2]0	[2]0	[2]0	[4]66.21 $N^{0.2}$

Notes	
1	Configuration size does not capture static data present in libraries. Libraries are not counted because most implementations include common ancillary libraries for image processing (e.g. openCV) or numerical computation (e.g. blas).
2	This multiplier expresses the increase in template size when k images are passed to the template generation function.
3	All durations are measured on Intel®Xeon®CPU E5-2630 v4 @ 2.20GHz processors. Estimates are made by wrapping the API function call in calls to std::chrono::high_resolution_clock which on the machine in (3) counts 1ns clock ticks. Precision is somewhat worse than that however.
4	Search durations are measured as in the prior note. The power-law model in the final column mostly fits the empirical results in Figure 112. However in certain cases the model is not correct and should not be used numerically.

Table 2: Summary of algorithms and properties included in this report. The blue superscripts give ranking for the quantity in that column. Missing search durations, denoted by "-", are absent because those runs were not executed, usually because we did not run on the larger galleries. Caution: The power-law model is sometimes an incorrect model. It is included here only to show broad sublinear behavior, which is flagged in green. The models should not be used for prediction.

FNIR(N, R, T) = False neg. identification rate
FPIR(N, T) = False pos. identification rate

N = Num. enrolled subjects
R = Num. candidates examined

T = Threshold

T = 0 → Investigation
T > 0 → Identification

	DEVELOPER	SHORT	SEQ.	VALIDATION	CONFIG[1]	TEMPLATE GENERATION			SEARCH DURATION[4] MILLISEC					
	FULL NAME	NAME	NUM.	DATE	DATA (MB)	SIZE (B)	MULT[2]	TIME (MS)[3]	L=1 N=1.6M	L=50 N=1.6M	L=50 N=3M	L=50 N=6M	L=50 N=12M	POWER LAW (μs)
53	Dermalog	dermalog	6	2018-10-26	0	[27]256	1	[119]514	[28]141	[39]143	[21]267	[19]527	[18]1285	[63]0.05 $N^{1.0}$
47	Dermalog	dermalog	007	2020-02-12	0	[8]128	-	[94]413	-	[28]96	[16]218	[13]427	[14]1010	[84]0.01 $N^{1.1}$
54	Paravision (EverAI)	everai	0	2018-06-21	142	[163]2048	1	[111]438	[5]4	[6]3	[3]5	-	-	[10]42.41 $N^{0.3}$
55	Paravision (EverAI)	everai	1	2018-06-21	200	[123]2048	1	[142]590	[58]336	[89]356	[39]651	-	-	[91]0.03 $N^{1.1}$
56	Paravision (EverAI)	everai	2	2018-10-30	224	[152]2048	1	[79]377	[52]278	[79]283	-	-	-	
57	Paravision (EverAI)	everai	3	2018-10-30	438	[125]2048	1	[195]735	[51]278	[78]281	[34]572	[33]1146	[28]2278	[54]0.12 $N^{1.0}$
58	Paravision (EverAI)	everai-paravision	004	2019-06-19	527	[209]4096	1	[193]720	[84]559	[126]559	[86]2611	[87]6445	[84]14519	[111]0.00 $N^{1.5}$
151	Paravision (EverAI)	paravision	005	2019-12-11	543	[219]4096	1	[222]858	[85]561	[128]564	[51]1056	[53]2298	[47]4966	[71]0.16 $N^{1.1}$
59	Eyedea Recognition	eyedea	0	2018-02-16	644	[229]4152	k	[99]424	-	[137]640	-	-	-	
60	Eyedea Recognition	eyedea	1	2018-02-16	287	[90]1036	k	[64]311	-	[84]307	-	-	-	
61	Eyedea Recognition	eyedea	2	2018-02-16	287	[86]1036	k	[106]429	-	[83]305	-	-	-	
62	Eyedea Recognition	eyedea	3	2018-06-18	284	[88]1036	k	[81]385	[55]309	[86]311	-	-	-	
63	FarBar Inc	f8	001	2019-10-03	266	[136]2048	k	[220]851	[1]0	[1]0	[1]0	[1]0	[1]0	
64	Glory Ltd	glory	0	2018-06-30	0	[38]418	k	[18]160	[86]575	[129]575	-	-	-	
65	Glory Ltd	glory	1	2018-06-30	0	[113]1726	k	[90]405	[133]1864	[190]1978	-	-	-	
66	Gorilla Technology	gorilla	0	2018-02-01	95	[237]8300	k	[102]427	-	[234]10426	-	-	-	
68	Gorilla Technology	gorilla	1	2018-06-19	91	[198]2156	k	[21]169	[159]5254	[223]5156	-	-	-	
69	Gorilla Technology	gorilla	2	2018-10-29	91	[95]1132	k	[70]341	[29]145	[41]146	[22]293	[20]612	[22]1509	[82]0.02 $N^{1.1}$
70	Gorilla Technology	gorilla	3	2018-10-26	94	[197]2156	k	[141]563	[134]1934	[192]2047	-	-	-	
67	Gorilla Technology	gorilla	004	2020-01-06	182	[199]2192	k	[84]395	[54]286	[81]285	[56]1191	[59]2416	[50]5036	[107]0.00 $N^{1.3}$
71	loginface Corp	hbinno	0	2018-02-01	88	[50]520	-	[49]265	-	[106]419	-	-	-	
72	Hikvision Research Institute	hikvision	0	2018-02-12	378	[115]1808	1	[227]875	-	[202]2360	-	-	-	
73	Hikvision Research Institute	hikvision	1	2018-02-12	378	[117]1808	1	[208]820	-	[203]2403	-	-	-	
74	Hikvision Research Institute	hikvision	2	2018-02-12	378	[116]1808	1	[206]820	-	[204]2408	-	-	-	
75	Hikvision Research Institute	hikvision	3	2018-06-30	408	[100]1408	1	[150]633	[104]904	[162]1108	[80]2377	[68]3785	[60]7570	[21]0.91 $N^{1.0}$
76	Hikvision Research Institute	hikvision	4	2018-06-30	334	[96]1152	1	[117]510	[99]784	[158]1024	[75]2094	[67]3254	[59]7117	[20]0.86 $N^{1.0}$
77	Hikvision Research Institute	hikvision	5	2018-10-29	593	[99]1408	1	[146]619	[103]883	[154]895	[71]1908	[69]3792	[69]9387	[89]0.10 $N^{1.1}$
78	Hikvision Research Institute	hikvision	6	2018-10-29	593	[98]1408	1	[143]610	[102]871	[153]877	-	-	-	
79	Idemia	idemia	0	2018-02-16	371	[37]364	1	[96]416	-	[32]133	[17]249	[15]502	-	[35]0.08 $N^{1.0}$
81	Idemia	idemia	1	2018-02-16	371	[35]364	1	[97]417	-	[37]138	-	-	-	
82	Idemia	idemia	2	2018-02-16	371	[36]364	1	[98]417	-	[38]138	-	-	-	
83	Idemia	idemia	3	2018-06-21	472	[54]528	1	[170]689	[57]318	[90]361	[38]631	[32]1104	[29]2332	[13]5.03 $N^{0.8}$
84	Idemia	idemia	4	2018-06-21	472	[56]528	1	[167]669	[33]168	[59]211	[29]475	[27]995	[26]2225	[90]0.02 $N^{1.1}$
85	Idemia	idemia	5	2018-10-29	417	[33]352	1	[78]374	[23]137	[36]138	[27]437	[23]724	[24]1630	[100]0.01 $N^{1.2}$
86	Idemia	idemia	6	2018-10-29	417	[34]352	1	[77]373	[24]137	[35]138	[28]442	[26]827	[25]1646	[102]0.01 $N^{1.2}$
80	Idemia	idemia	007	2020-01-17	738	[66]860	1	[204]807	[30]151	[42]152	[41]683	[40]1481	[37]3022	[110]0.00 $N^{1.4}$
88	Imagus Technology Pty Ltd	imagus	0	2018-02-14	35	[43]512	k	[5]43	-	[54]202	-	-	-	
89	Imagus Technology Pty Ltd	imagus	2	2018-06-21	35	[39]512	k	[9]76	[42]200	[58]208	-	-	-	
90	Imagus Technology Pty Ltd	imagus	3	2018-06-21	46	[45]512	k	[7]57	[43]201	[56]206	-	-	-	
91	Imperial College London	imperial	000	2019-08-28	461	[145]2048	1	[161]654	[60]360	[93]379	[68]1626	[71]4057	[74]10291	[113]0.00 $N^{1.5}$
92	Incode Technologies Inc	incode	0	2018-06-29	23	[83]1024	k	[30]190	[119]1293	[217]3510	-	-	-	
94	Incode Technologies Inc	incode	1	2018-06-29	151	[167]2048	k	[172]690	[123]1542	[220]4497	-	-	-	
95	Incode Technologies Inc	incode	2	2018-10-29	71	[139]2048	1	[57]291	[71]411	[100]404	-	-	-	
96	Incode Technologies Inc	incode	3	2018-10-29	133	[162]2048	1	[181]704	[70]408	[105]412	[44]846	[41]1606	[44]4482	[86]0.05 $N^{1.1}$
93	Incode Technologies Inc	incode	004	2019-06-24	254	[135]2048	1	[116]508	[61]365	[92]377	[66]1481	[42]1658	[35]2951	[72]0.12 $N^{1.1}$
97	Innovatrics	innovatrics	0	2018-02-16	0	[59]530	k	[112]455	-	[135]625	-	-	-	
98	Innovatrics	innovatrics	1	2018-02-16	0	[57]530	k	[66]316	-	[134]625	-	-	-	
99	Innovatrics	innovatrics	2	2018-06-21	0	[58]530	k	[45]255	[4]1	[4]2	-	-	-	
100	Innovatrics	innovatrics	3	2018-06-21	0	[60]530	k	[46]255	[138]2020	[188]1882	-	-	-	
101	Innovatrics	innovatrics	4	2018-10-30	0	[93]1076	k	[92]406	[7]8	[9]8	[5]11	[4]9	[3]13	[8]668.38 $N^{0.2}$
102	Lomonosov Moscow State University	intsysmsu	000	2019-08-19	375	[134]2048	1	[169]675	[72]430	[109]431	[46]860	[43]1730	[52]5353	[95]0.03 $N^{1.1}$

Notes	
1	Configuration size does not capture static data present in libraries. Libraries are not counted because most implementations include common ancillary libraries for image processing (e.g. openCV) or numerical computation (e.g. blas).
2	This multiplier expresses the increase in template size when k images are passed to the template generation function.
3	All durations are measured on Intel®Xeon®CPU E5-2630 v4 @ 2.20GHz processors. Estimates are made by wrapping the API function call in calls to std::chrono::high_resolution_clock which on the machine in (3) counts 1ns clock ticks. Precision is somewhat worse than that however.
4	Search durations are measured as in the prior note. The power-law model in the final column mostly fits the empirical results in Figure 112. However in certain cases the model is not correct and should not be used numerically.

Table 3: Summary of algorithms and properties included in this report. The blue superscripts give ranking for the quantity in that column. Missing search durations, denoted by "-", are absent because those runs were not executed, usually because we did not run on the larger galleries. Caution: The power-law model is sometimes an incorrect model. It is included here only to show broad sublinear behavior, which is flagged in green. The models should not be used for prediction.

FNIR(N, R, T) = False neg. identification rate
FPIR(N, T) = False pos. identification rate
N = Num. enrolled subjects
R = Num. candidates examined
T = Threshold
T = 0 → Investigation
T > 0 → Identification

	DEVELOPER	SHORT	SEQ.	VALIDATION	CONFIG[1]	TEMPLATE GENERATION			SEARCH DURATION[4] MILLISEC					
	FULL NAME	NAME	NUM.	DATE	DATA (MB)	SIZE (B)	MULT[2]	TIME (MS)[3]	L=1 N=1.6M	L=50 N=1.6M	L=50 N=3M	L=50 N=6M	L=50 N=12M	POWER LAW (μs)
103	Alivia / Innovation Sys	isystems	0	2018-02-14	262	[155]2048	1	[38]222	-	[96]393	-	-	-	
104	Alivia / Innovation Sys	isystems	1	2018-02-14	263	[71]1024	1	[37]222	-	[61]240	-	-	-	
105	Alivia / Innovation Sys	isystems	2	2018-06-25	268	[146]2048	1	[67]316	[66]385	[112]484	[60]1275	[48]1770	[38]3063	[17]0.68 $N^{0.9}$
106	Alivia / Innovation Sys	isystems	3	2018-10-30	350	[165]2048	1	[221]856	[65]384	[95]387	[48]976	[49]1817	[68]9319	[109]0.00 $N^{1.3}$
107	Kedacom International Pte	kedacom	001	2019-09-16	239	[31]292	1	[128]537	[97]764	[144]760	[73]1940	[65]2983	[57]6623	[60]0.31 $N^{1.0}$
109	Lookman Electroplast Industries	lookman	3	2018-10-28	203	[30]292	1	[71]342	[96]739	[142]745	[65]1394	[62]2817	[61]8286	[80]0.13 $N^{1.1}$
110	Lookman Electroplast Industries	lookman	4	2018-10-28	184	[61]548	1	[68]325	[105]981	[155]998	-	-	-	
108	Lookman Electroplast Industries	lookman	005	2019-09-16	239	[62]548	1	[118]514	[106]1005	[156]1008	[85]2597	[82]5446	[65]8939	[78]0.19 $N^{1.1}$
111	Megvii/Face++	megvii	0	2018-02-15	1327	[160]2048	1	[203]794	-	[80]284	[30]530	[28]1060	-	[31]0.18 $N^{1.0}$
112	Megvii/Face++	megvii	1	2018-10-28	1703	[218]4096	1	[156]652	[82]551	[127]560	[59]1219	[55]2316	[54]5956	[85]0.08 $N^{1.1}$
113	Megvii/Face++	megvii	2	2018-10-28	1735	[216]4096	1	[162]656	[83]552	[124]557	-	-	-	
114	MicroFocus	microfocus	0	2018-02-12	101	[24]256	k	[121]525	-	[48]184	-	-	-	
115	MicroFocus	microfocus	1	2018-02-16	101	[16]256	k	[122]527	-	[22]39	-	-	-	
116	MicroFocus	microfocus	2	2018-02-16	101	[25]256	k	[123]529	-	[5]2	-	-	-	
117	MicroFocus	microfocus	3	2018-06-22	101	[17]256	k	[52]269	[38]185	[51]188	-	-	-	
118	MicroFocus	microfocus	4	2018-06-22	102	[23]256	k	[53]270	[39]186	[52]189	-	-	-	
119	MicroFocus	microfocus	5	2018-10-29	94	[29]256	k	[51]266	[36]182	[50]186	[24]353	[22]706	[20]1422	[37]0.11 $N^{1.0}$
120	MicroFocus	microfocus	6	2018-10-29	94	[22]256	k	[50]265	[37]182	[49]186	-	-	-	
121	Microsoft	microsoft	0	2018-01-30	126	[49]512	1	[56]283	-	[131]593	[57]1193	[56]2395	[46]4936	[61]0.22 $N^{1.0}$
122	Microsoft	microsoft	1	2018-02-12	165	[76]1024	1	[74]349	-	[152]869	-	-	-	
123	Microsoft	microsoft	2	2018-02-12	228	[81]1024	1	[136]555	-	[151]869	-	-	-	
124	Microsoft	microsoft	3	2018-06-20	230	[73]1024	1	[89]404	[125]1638	[179]1603	[90]3260	[88]6730	[82]13833	[68]0.51 $N^{1.1}$
125	Microsoft	microsoft	4	2018-06-20	437	[148]2048	1	[199]773	[146]2662	[208]2691	[101]5260	[97]11070	[93]22748	[69]0.83 $N^{1.1}$
126	Microsoft	microsoft	5	2018-10-29	381	[78]1024	1	[168]673	[124]1604	[181]1671	[89]3073	[85]6296	[81]13147	[42]0.79 $N^{1.0}$
127	Microsoft	microsoft	6	2018-10-29	478	[70]1024	1	[174]695	[126]1640	[180]1617	[94]3707	[86]6394	[80]12879	[53]0.68 $N^{1.0}$
128	NEC	nec	0	2018-06-21	131	[203]2592	k	[10]82	[56]317	[107]426	[42]738	[38]1315	[32]2737	[15]0.73 $N^{0.9}$
129	NEC	nec	1	2018-06-29	131	[202]2592	k	[11]88	[41]193	[57]208	[26]388	[24]750	[23]1577	[19]0.21 $N^{1.0}$
130	NEC	nec	2	2018-10-30	705	[111]1616	k	[160]653	[69]405	[104]409	[52]1072	[45]1755	[42]4255	[87]0.06 $N^{1.1}$
131	NEC	nec	3	2018-10-30	774	[112]1712	k	[171]690	[6]7	[8]7	[6]14	[6]40	[7]82	[98]0.00 $N^{1.2}$
132	Neurotechnology	neurotech	0	2018-02-16	331	[232]5214	k	[179]702	-	[213]3040	-	-	-	
134	Neurotechnology	neurotech	1	2018-02-16	331	[233]5214	k	[165]661	-	[215]3054	-	-	-	
135	Neurotechnology	neurotech	2	2018-02-16	331	[234]5214	k	[164]658	-	[214]3051	-	-	-	
136	Neurotechnology	neurotech	3	2018-06-27	265	[130]2048	k	[132]547	[109]1084	[159]1059	[76]2111	[75]4779	[64]8793	[32]0.73 $N^{1.0}$
137	Neurotechnology	neurotech	4	2018-06-27	265	[168]2048	k	[131]543	[108]1060	[160]1061	[74]2091	[72]4263	[62]8736	[18]1.22 $N^{1.0}$
138	Neurotechnology	neurotech	5	2018-10-30	266	[20]256	k	[93]412	[100]835	[149]839	[70]1690	[66]3219	[66]8955	[76]0.19 $N^{1.1}$
139	Neurotechnology	neurotech	6	2018-10-30	564	[19]256	k	[197]746	[101]839	[150]842	-	-	-	
133	Neurotechnology	neurotech	007	2019-10-03	57	[28]256	k	[22]169	[110]1118	[163]1110	[78]2143	[73]4397	[67]9045	[41]0.55 $N^{1.0}$
140	Newland Computer Co Ltd	newland	2	2018-10-30	96	[122]2048	-	[224]868	[166]8653	[233]8765	[114]17713	[109]38963	-	[83]1.32 $N^{1.1}$
141	Noblis	noblis	1	2018-10-30	114	[149]2048	1	[34]211	[117]1273	[170]1272	-	-	-	
142	Noblis	noblis	2	2018-10-30	153	[235]6144	1	[125]535	[145]2513	[206]2522	[102]5649	[99]12432	[100]44262	[105]0.04 $N^{1.3}$
143	N-Tech Lab	ntech	0	2018-02-16	2124	[231]4442	k	[194]730	-	[94]382	[40]673	[39]1344	-	[23]0.27 $N^{1.0}$
146	N-Tech Lab	ntech	1	2018-02-16	851	[114]1736	k	[91]405	-	[43]161	-	-	-	
147	N-Tech Lab	ntech	3	2018-06-21	3664	[206]3484	k	[214]831	[64]384	[88]326	[35]596	[34]1192	[30]2411	[25]0.24 $N^{1.0}$
148	N-Tech Lab	ntech	4	2018-06-21	3766	[207]3484	k	[232]929	[62]378	[87]312	[36]597	[36]1204	[31]2416	[30]0.21 $N^{1.0}$
149	N-Tech Lab	ntech	5	2018-10-30	1685	[120]1940	k	[190]717	[48]243	[63]246	[32]538	[30]1100	[33]2867	[92]0.02 $N^{1.1}$
150	N-Tech Lab	ntech	6	2018-10-30	1686	[121]1940	k	[218]841	[47]243	[62]246	[33]546	[31]1104	[34]2873	[94]0.02 $N^{1.1}$
144	N-Tech Lab	ntechlab	007	2019-06-25	2450	[205]3348	k	[217]834	[67]393	[108]427	[43]780	[46]1768	[40]3499	[59]0.16 $N^{1.0}$
145	N-Tech Lab	ntechlab	008	2020-01-06	1111	[97]1300	k	[140]562	[35]179	[47]184	[23]341	[21]683	[19]1395	[34]0.11 $N^{1.0}$
152	Guangzhou Pixel Solutions Co Ltd	pixelall	002	2019-07-01	0	[200]2560	k	[31]198	[120]1296	[176]1334	[84]2526	[77]5136	[76]11045	[57]0.52 $N^{1.0}$
153	Guangzhou Pixel Solutions Co Ltd	pixelall	003	2019-11-05	0	[201]2560	k	[192]719	[116]1273	[173]1307	[82]2474	[78]5198	[77]11141	[64]0.46 $N^{1.0}$
154	Quantasoft	quantasoft	1	2018-10-30	276	[132]2048	k	[85]396	[167]15422	[235]14858	[113]14717	-	[91]18323	

Notes	
1	Configuration size does not capture static data present in libraries. Libraries are not counted because most implementations include common ancillary libraries for image processing (e.g. openCV) or numerical computation (e.g. blas).
2	This multiplier expresses the increase in template size when k images are passed to the template generation function.
3	All durations are measured on Intel®Xeon®CPU E5-2630 v4 @ 2.20GHz processors. Estimates are made by wrapping the API function call in calls to std::chrono::high_resolution_clock which on the machine in (3) counts 1ns clock ticks. Precision is somewhat worse than that however.
4	Search durations are measured as in the prior note. The power-law model in the final column mostly fits the empirical results in Figure 112. However in certain cases the model is not correct and should not be used numerically.

Table 4: Summary of algorithms and properties included in this report. The blue superscripts give ranking for the quantity in that column. Missing search durations, denoted by "-", are absent because those runs were not executed, usually because we did not run on the larger galleries. Caution: The power-law model is sometimes an incorrect model. It is included here only to show broad sublinear behavior, which is flagged in green. The models should not be used for prediction.

	DEVELOPER	SHORT	SEQ.	VALIDATION	CONFIG[1]	TEMPLATE GENERATION			SEARCH DURATION[4] MILLISEC					
	FULL NAME	NAME	NUM.	DATE	DATA (MB)	SIZE (B)	MULT[2]	TIME (MS)[3]	L=1 N=1.6M	L=50 N=1.6M	L=50 N=3M	L=50 N=6M	L=50 N=12M	POWER LAW (μs)
155	Rank One Computing	rankone	0	2018-02-07	0	[15]228	k	[6]50	-	[24]75	[12]142	[11]220	[11]502	[16]0.12 $N^{0.9}$
158	Rank One Computing	rankone	1	2018-02-15	0	[32]324	k	[17]136	-	[46]169	-	-	-	
159	Rank One Computing	rankone	2	2018-06-19	0	[11]133	k	[14]113	[25]138	[33]137	[19]258	[17]517	[16]1029	[26]0.10 $N^{1.0}$
160	Rank One Computing	rankone	3	2018-06-19	0	[12]133	k	[15]114	[26]138	[34]137	[18]258	[16]515	[15]1027	[29]0.09 $N^{1.0}$
161	Rank One Computing	rankone	4	2018-10-09	0	[1]85	k	[4]36	[21]101	[30]101	[13]190	-	-	[28]0.07 $N^{1.0}$
162	Rank One Computing	rankone	5	2018-10-24	0	[10]133	k	[12]94	[27]140	[40]144	[20]266	[18]525	[17]1049	[24]0.11 $N^{1.0}$
156	Rank One Computing	rankone	006	2019-06-03	0	[14]165	k	[47]261	-	-	-	-	-	
157	Rank One Computing	rankone	007	2019-11-12	0	[13]165	k	[55]278	[22]116	[31]115	[15]215	[14]439	[13]877	[36]0.07 $N^{1.0}$
163	Realnetworks Inc	realnetworks	0	2018-06-21	96	[220]4100	1	[43]244	[153]4257	[209]2740	-	-	-	
166	Realnetworks Inc	realnetworks	1	2018-06-21	105	[224]4104	k	[42]243	[152]3568	[195]2107	-	-	-	
167	Realnetworks Inc	realnetworks	2	2018-10-30	105	[222]4104	k	[44]245	[136]2006	[191]2046	[97]4190	[95]8633	[87]15020	[39]1.08 $N^{1.0}$
164	Realnetworks Inc	realnetworks	003	2019-06-12	93	[119]1848	k	[26]178	[112]1143	[164]1130	[77]2139	[79]5235	[75]10485	[77]0.21 $N^{1.1}$
165	Realnetworks Inc	realnetworks	004	2019-10-17	94	[118]1848	1	[27]185	[111]1142	[166]1136	[79]2147	[74]4735	[72]9683	[67]0.36 $N^{1.0}$
168	Remark Holdings	remarkai	0	2018-10-30	187	[150]2048	k	[144]615	[162]5685	[229]5723	-	-	-	
170	Remark Holdings	remarkai	1	2018-10-30	187	[128]2048	k	[110]434	[161]5680	[230]5761	[112]12475	[107]28726	[103]59618	[99]0.37 $N^{1.2}$
169	Remark Holdings	remarkai	000	2019-06-12	234	[124]2048	k	[173]691	[163]5776	[228]5703	[110]11604	[108]32133	-	[104]0.16 $N^{1.2}$
171	Scanovate Ltd	scanovate	000	2020-01-15	250	[161]2048	1	[186]712	[122]1419	[178]1412	-	-	-	
172	Sensetime Group	sensetime	0	2018-10-30	525	[221]4104	k	[188]715	[79]498	[114]501	[58]1212	[52]2281	[49]5032	[81]0.09 $N^{1.1}$
173	Sensetime Group	sensetime	002	2019-06-03	523	[185]2056	k	[154]650	[59]359	[91]370	-	-	-	
174	Sensetime Group	sensetime	003	2019-12-02	769	[184]2056	1	[236]940	[156]4885	[222]4989	-	-	-	
175	Sensetime Group	sensetime	1	2018-10-30	525	[223]4104	k	[163]656	[80]516	[115]502	[53]1146	[54]2301	[45]4765	[79]0.09 $N^{1.1}$
176	Shaman Software	shaman	0	2018-02-12	0	[214]4096	k	[129]538	-	[117]523	-	-	-	
177	Shaman Software	shaman	1	2018-02-12	0	[212]4096	k	[137]557	-	[118]524	-	-	-	
178	Shaman Software	shaman	2	2018-02-12	0	[236]8192	k	[138]557	-	[139]688	-	-	-	
179	Shaman Software	shaman	3	2018-06-30	0	[144]2048	k	[180]704	[92]692	[85]310	-	-	-	
180	Shaman Software	shaman	4	2018-06-30	0	[158]2048	k	[153]642	[74]434	[72]267	-	-	-	
181	Shaman Software	shaman	6	2018-10-26	0	[154]2048	k	[182]706	[88]594	[132]603	-	-	-	
182	Shaman Software	shaman	7	2018-10-26	0	[142]2048	k	[184]709	[87]593	[133]605	[54]1169	[58]2411	[48]5007	[55]0.25 $N^{1.0}$
183	Shenzhen Inst Adv Integrated Tech CAS	SIAT	0	2018-02-14	306	[94]1096	k	[75]358	-	[177]1343	-	-	-	
184	Shenzhen Inst Adv Integrated Tech CAS	SIAT	1	2018-06-30	521	[170]2052	1	[219]842	[155]4512	[218]4402	[108]9103	[103]18391	[98]38745	[50]2.06 $N^{1.0}$
185	Shenzhen Inst Adv Integrated Tech CAS	SIAT	2	2018-02-30	521	[177]2052	1	[229]906	[157]5101	[221]4884	[109]9556	[104]18834	[99]39717	[51]2.08 $N^{1.0}$
186	Smilart	smilart	0	2018-02-15	105	[72]1024	k	[20]168	-	[171]1285	-	-	-	
187	Smilart	smilart	1	2018-02-15	120	[79]1024	k	[166]662	-	[165]1135	-	-	-	
188	Smilart	smilart	2	2018-02-15	109	[75]1024	k	[139]560	-	[172]1302	-	-	-	
189	Smilart	smilart	4	2018-10-30	65	[41]512	k	[19]167	[168]15879	[236]15382	-	-	-	
190	Smilart	smilart	5	2018-10-30	562	[151]2048	k	[113]464	-	-	-	-	-	
191	Synesis	synesis	0	2018-02-15	332	[44]512	k	[41]237	-	[45]162	-	-	-	
192	Synesis	synesis	003	2019-07-04	143	[127]2048	-	[36]215	-	[116]502	-	-	-	
193	Synesis	synesis	3	2018-10-30	237	[210]4096	k	[13]103	[98]784	[147]796	[72]1928	[70]3861	[63]8748	[93]0.07 $N^{1.1}$
194	Tech5 SA	tech5	001	2019-08-19	1394	[101]1536	k	[228]898	[63]383	[145]765	-	-	-	
195	Tevian	tevian	0	2018-02-16	666	[141]2048	1	[83]394	-	[101]405	-	-	-	
196	Tevian	tevian	1	2018-02-16	666	[159]2048	1	[88]398	-	[98]403	-	-	-	
197	Tevian	tevian	2	2018-02-16	666	[156]2048	1	[86]397	-	[97]402	-	-	-	
198	Tevian	tevian	3	2018-06-20	707	[133]2048	1	[62]300	[75]473	[121]539	-	-	-	
199	Tevian	tevian	4	2018-06-20	707	[164]2048	1	[61]299	[73]434	[120]537	-	-	-	
200	Tevian	tevian	5	2018-10-30	773	[140]2048	1	[95]416	[68]405	[103]407	[45]852	[44]1753	[39]3373	[65]0.14 $N^{1.0}$
201	TigerIT Americas LLC	tiger	0	2018-06-29	333	[176]2052	k	[104]428	[131]1822	[211]2942	-	-	-	
202	TigerIT Americas LLC	tiger	1	2018-06-27	333	[172]2052	k	[87]398	[2]0	[3]1	-	-	-	
203	TigerIT Americas LLC	tiger	2	2018-10-29	416	[180]2052	k	[115]464	[130]1814	[189]1919	[95]3829	[93]7519	[85]14805	[49]0.83 $N^{1.0}$
204	TigerIT Americas LLC	tiger	3	2018-10-30	416	[178]2052	k	[114]464	[40]191	[53]189	-	-	-	
205	TongYi Transportation Technology	tongyi	0	2018-06-29	1701	[191]2070	k	[29]190	[142]2256	[200]2272	-	-	-	
206	TongYi Transportation Technology	tongyi	1	2018-06-29	1701	[189]2070	1	[28]189	[141]2238	[199]2257	-	-	-	

Notes	
1	Configuration size does not capture static data present in libraries. Libraries are not counted because most implementations include common ancillary libraries for image processing (e.g. openCV) or numerical computation (e.g. blas).
2	This multiplier expresses the increase in template size when k images are passed to the template generation function.
3	All durations are measured on Intel®Xeon®CPU E5-2630 v4 @ 2.20GHz processors. Estimates are made by wrapping the API function call in calls to std::chrono::high_resolution_clock which on the machine in (3) counts 1ns clock ticks. Precision is somewhat worse than that however.
4	Search durations are measured as in the prior note. The power-law model in the final column mostly fits the empirical results in Figure 112. However in certain cases the model is not correct and should not be used numerically.

Table 5: Summary of algorithms and properties included in this report. The blue superscripts give ranking for the quantity in that column. Missing search durations, denoted by "-", are absent because those runs were not executed, usually because we did not run on the larger galleries. Caution: The power-law model is sometimes an incorrect model. It is included here only to show broad sublinear behavior, which is flagged in green. The models should not be used for prediction.

FNIR(N, R, T) = False neg. identification rate
FPIR(N, T) = False pos. identification rate
N = Num. enrolled subjects
R = Num. candidates examined
T = Threshold
T = 0 → Investigation
T > 0 → Identification

	DEVELOPER	SHORT	SEQ.	VALIDATION	CONFIG[1]	TEMPLATE GENERATION			SEARCH DURATION[4] MILLISEC					
	FULL NAME	NAME	NUM.	DATE	DATA (MB)	SIZE (B)	MULT[2]	TIME (MS)[3]	L=1 N=1.6M	L=50 N=1.6M	L=50 N=3M	L=50 N=6M	L=50 N=12M	POWER LAW (μs)
207	Toshiba	toshiba	0	2018-10-30	961	[108]1548	k	[234]930	[165]6147	[231]6230	[111]12209	[106]25330	[102]49398	[97]0.36 $N^{1.2}$
208	Toshiba	toshiba	1	2018-10-30	961	[187]2060	k	[235]931	[164]6001	[232]6349	-	-	-	
209	Visidon	visidon	0	2018-06-20	208	[84]1028	k	[69]337	[133]2006	[207]2566	-	-	-	
210	Visidon	visidon	1	2018-10-30	166	[174]2052	k	[175]695	[154]4357	[219]4458	[107]8429	[102]17210	[96]34185	[38]2.40 $N^{1.0}$
211	Vigilant Solutions	vigilant	0	2018-02-08	335	[105]1544	k	[210]823	-	[193]2058	-	-	-	
212	Vigilant Solutions	vigilant	1	2018-02-14	249	[183]2056	k	[196]739	-	[194]2075	-	-	-	
213	Vigilant Solutions	vigilant	2	2018-02-14	335	[107]1544	k	[207]820	-	[196]2121	-	-	-	
214	Vigilant Solutions	vigilant	3	2018-06-21	335	[104]1544	k	[215]832	[144]2453	[201]2307	-	-	-	
215	Vigilant Solutions	vigilant	4	2018-06-21	337	[103]1544	k	[213]830	[139]2050	[198]2251	-	-	-	
216	Vigilant Solutions	vigilant	5	2018-10-30	335	[106]1544	k	[201]778	-	[183]1720	-	-	-	
217	Vigilant Solutions	vigilant	6	2018-10-30	337	[102]1544	k	[216]834	-	[182]1713	-	-	-	
219	VisionLabs	visionlabs	3	2018-02-16	624	[18]256	1	[40]228	-	[7]5	[4]5	[3]6	-	[7]417.37 $N^{0.2}$
220	VisionLabs	visionlabs	4	2018-06-22	299	[26]256	1	[65]315	[9]19	[11]17	[7]20	[5]26	[4]29	[3]2663.29 $N^{0.1}$
221	VisionLabs	visionlabs	5	2018-06-22	305	[40]512	1	[63]300	[15]54	[18]33	[8]37	[9]56	[8]88	[11]166.84 $N^{0.4}$
222	VisionLabs	visionlabs	6	2018-10-30	360	[46]512	1	[58]292	[14]36	[20]36	[10]39	[8]44	[6]53	[6]3211.93 $N^{0.2}$
223	VisionLabs	visionlabs	7	2018-10-30	360	[48]512	1	[59]293	[16]63	[23]63	[11]72	[10]80	[9]115	[9]2076.32 $N^{0.2}$
218	VisionLabs	visionlabs	008	2019-06-18	348	[42]512	1	[54]277	[10]23	[14]24	-	-	-	
224	Vocord	vocord	0	2018-02-16	872	[63]608	k	[126]536	-	[73]268	-	-	-	
225	Vocord	vocord	1	2018-02-16	872	[64]608	k	[127]536	-	[74]268	-	-	-	
226	Vocord	vocord	2	2018-02-16	924	[138]2048	k	[151]635	-	[65]248	-	-	-	
227	Vocord	vocord	3	2018-06-30	627	[62]896	k	[187]714	[44]215	[64]247	-	-	-	
228	Vocord	vocord	4	2018-06-30	627	[68]896	k	[130]538	[45]216	[69]253	-	-	-	
229	Vocord	vocord	5	2018-10-30	1035	[65]768	k	[209]822	[32]158	[55]204	[25]383	[25]767	[21]1466	[33]0.12 $N^{1.0}$
230	Vocord	vocord	6	2018-10-30	1035	[238]10240	k	[211]825	[34]170	[60]216	-	-	-	
231	Zhuhai Yisheng Electronics Technology	yisheng	0	2018-02-14	473	[196]2108	k	[145]615	-	[130]587	-	-	-	
232	Zhuhai Yisheng Electronics Technology	yisheng	1	2018-06-19	474	[208]3704	k	[82]387	[140]2228	[161]1108	-	-	-	
233	Shanghai Yitu Technology	yitu	0	2018-02-12	1774	[226]4136	1	[149]633	-	[111]464	[47]868	[47]1769	-	[73]0.12 $N^{1.1}$
234	Shanghai Yitu Technology	yitu	1	2018-02-12	1944	[225]4136	1	[233]930	-	[110]463	-	-	-	
235	Shanghai Yitu Technology	yitu	2	2018-06-21	2077	[228]4138	1	[228]870	[160]5516	[225]5417	[103]6101	[100]13264	[95]33047	[14]9.25 $N^{0.9}$
236	Shanghai Yitu Technology	yitu	3	2018-06-21	2077	[227]4138	1	[226]871	[158]5248	[224]5242	[105]6286	[105]19829	[101]45621	[75]1.08 $N^{1.1}$
237	Shanghai Yitu Technology	yitu	4	2018-10-30	2119	[190]2070	1	[230]910	[118]1288	[169]1203	[81]2440	[80]5241	[71]9671	[52]0.52 $N^{1.0}$
238	Shanghai Yitu Technology	yitu	5	2018-10-30	2043	[188]2070	1	[223]861	[115]1235	[168]1197	[83]2508	[76]5003	[70]9601	[47]0.55 $N^{1.0}$

Notes	
1	Configuration size does not capture static data present in libraries. Libraries are not counted because most implementations include common ancillary libraries for image processing (e.g. openCV) or numerical computation (e.g. blas).
2	This multiplier expresses the increase in template size when k images are passed to the template generation function.
3	All durations are measured on Intel®Xeon®CPU E5-2630 v4 @ 2.20GHz processors. Estimates are made by wrapping the API function call in calls to std::chrono::high_resolution_clock which on the machine in (3) counts 1ns clock ticks. Precision is somewhat worse than that however.
4	Search durations are measured as in the prior note. The power-law model in the final column mostly fits the empirical results in Figure 112. However in certain cases the model is not correct and should not be used numerically.

Table 6: Summary of algorithms and properties included in this report. The blue superscripts give ranking for the quantity in that column. Missing search durations, denoted by "-", are absent because those runs were not executed, usually because we did not run on the larger galleries. Caution: The power-law model is sometimes an incorrect model. It is included here only to show broad sublinear behavior, which is flagged in green. The models should not be used for prediction.

MISS RATES		INVESTIGATION, FNIR(N, R = 1, T = 0)								IDENTIFICATION, FNIR(N, R = L, T $\geq$ 0) FOR FPIR = 0.001							
#	ALGORITHM	(0, 2]	(2, 4]	(4, 6]	(6, 8]	(8, 10]	(10, 12]	(12, 14]	(14, 18]	(0, 2]	(2, 4]	(4, 6]	(6, 8]	(8, 10]	(10, 12]	(12, 14]	(14, 18]
1	3DIVI-005	[61]0.0207	[60]0.0304	[60]0.0415	[60]0.0533	[60]0.0646	[59]0.0735	[59]0.0884	[60]0.1148	[62]0.1580	[61]0.2316	[61]0.3033	[61]0.3740	[61]0.4285	[61]0.4742	[62]0.5329	[60]0.5975
2	ANKE-000	[58]0.0162	[58]0.0245	[58]0.0333	[58]0.0428	[57]0.0515	[57]0.0615	[56]0.0780	[55]0.1028	[60]0.1132	[60]0.1761	[60]0.2402	[60]0.3057	[58]0.3640	[57]0.4200	[57]0.4928	[57]0.5680
3	AWARE-005	[67]0.0328	[67]0.0519	[67]0.0712	[67]0.0910	[67]0.1078	[67]0.1235	[67]0.1457	[68]0.1831	[68]0.3605	[69]0.4949	[69]0.5948	[69]0.6783	[69]0.7393	[69]0.7905	[69]0.8408	[70]0.8831
4	AWARE-006	[72]0.0702	[72]0.1110	[72]0.1502	[72]0.1899	[72]0.2253	[73]0.2614	[72]0.3045	[72]0.3659								
5	AYONIX-002	[75]0.3360	[76]0.4389	[76]0.5144	[76]0.5814	[76]0.6340	[76]0.6818	[76]0.7297	[76]0.7774	[71]0.8288	[72]0.9013	[72]0.9375	[72]0.9603	[72]0.9744	[73]0.9837	[73]0.9893	[73]0.9927
6	CAMVI-004	[71]0.0623	[71]0.0944	[71]0.1243	[71]0.1548	[70]0.1812	[70]0.2056	[70]0.2344	[70]0.2672	[53]0.0810	[52]0.1267	[50]0.1721	[50]0.2203	[50]0.2619	[48]0.3040	[46]0.3543	[43]0.4124
7	CAMVI-005	[73]0.0849	[73]0.1255	[73]0.1631	[73]0.1989	[73]0.2298	[72]0.2585	[71]0.2915	[71]0.3246								
8	COGENT-000	[54]0.0128	[52]0.0184	[54]0.0250	[52]0.0327	[52]0.0407	[52]0.0488	[50]0.0611	[50]0.0794	[41]0.0559	[43]0.0923	[41]0.1342	[41]0.1812	[39]0.2243	[37]0.2675	[37]0.3240	[41]0.3992
9	COGENT-001	[53]0.0128	[53]0.0184	[53]0.0250	[53]0.0327	[53]0.0407	[51]0.0488	[51]0.0611	[49]0.0794	[42]0.0559	[42]0.0923	[40]0.1342	[40]0.1812	[38]0.2243	[38]0.2675	[36]0.3240	[40]0.3992
10	COGENT-002	[32]0.0081	[30]0.0105	[27]0.0123	[27]0.0137	[25]0.0157	[25]0.0175	[23]0.0215	[23]0.0280	[34]0.0499	[33]0.0827	[32]0.1207	[31]0.1639	[31]0.2037	[31]0.2432	[32]0.2972	[33]0.3638
11	COGENT-003	[33]0.0082	[31]0.0108	[29]0.0128	[29]0.0145	[29]0.0168	[31]0.0191	[32]0.0239	[29]0.0312	[43]0.0582	[44]0.0971	[44]0.1417	[44]0.1918	[44]0.2380	[44]0.2836	[44]0.3440	[45]0.4207
12	COGNITEC-000	[66]0.0265	[66]0.0423	[66]0.0588	[66]0.0757	[65]0.0894	[65]0.1014	[65]0.1169	[63]0.1381	[61]0.1522	[62]0.2330	[62]0.3051	[62]0.3751	[62]0.4300	[62]0.4779	[61]0.5307	[59]0.5913
13	COGNITEC-001	[56]0.0149	[57]0.0228	[57]0.0312	[56]0.0399	[56]0.0479	[55]0.0546	[54]0.0656	[51]0.0806	[56]0.0963	[55]0.1562	[55]0.2157	[55]0.2771	[54]0.3287	[54]0.3771	[54]0.4343	[52]0.4959
14	COGNITEC-002	[40]0.0101	[40]0.0138	[41]0.0170	[41]0.0201	[40]0.0237	[40]0.0264	[40]0.0309	[39]0.0389	[36]0.0517	[35]0.0879	[36]0.1269	[37]0.1707	[35]0.2098	[32]0.2463	[31]0.2919	[31]0.3535
15	COGNITEC-003	[42]0.0104	[41]0.0140	[42]0.0174	[42]0.0205	[41]0.0238	[41]0.0266	[41]0.0311	[41]0.0401	[35]0.0504	[34]0.0855	[34]0.1235	[33]0.1662	[32]0.2045	[30]0.2403	[30]0.2854	[29]0.3451
16	DAHUA-002	[12]0.0035	[9]0.0047	[8]0.0058	[7]0.0067	[7]0.0074	[7]0.0082	[8]0.0100	[8]0.0108	[11]0.0169	[12]0.0294	[11]0.0449	[11]0.0635	[11]0.0817	[12]0.1013	[10]0.1291	[9]0.1638
17	DEEPGLINT-001	[79]0.9395	[79]0.9397	[79]0.9382	[79]0.9388	[79]0.9388	[79]0.9392	[79]0.9396	[79]0.9409								
18	DERMALOG-006	[46]0.0113	[42]0.0142	[38]0.0163	[37]0.0183	[36]0.0200	[35]0.0218	[34]0.0251	[32]0.0329	[39]0.0545	[37]0.0889	[37]0.1271	[35]0.1697	[34]0.2090	[34]0.2498	[34]0.3028	[34]0.3670
19	DERMALOG-007	[50]0.0125	[49]0.0170	[48]0.0214	[48]0.0264	[47]0.0309	[46]0.0356	[46]0.0432	[46]0.0579	[54]0.0910	[54]0.1453	[54]0.2009	[53]0.2602	[53]0.3134	[53]0.3649	[53]0.4289	[54]0.5007
20	GORILLA-002	[63]0.0213	[63]0.0359	[64]0.0528	[65]0.0716	[66]0.0895	[66]0.1088	[66]0.1367	[66]0.1765	[64]0.1828	[65]0.2787	[65]0.3654	[65]0.4485	[66]0.5168	[66]0.5823	[66]0.6508	[66]0.7180
21	IDEMIA-000	[52]0.0126	[54]0.0190	[55]0.0265	[54]0.0341	[54]0.0419	[53]0.0497	[52]0.0621	[53]0.0852	[58]0.1062	[58]0.1668	[58]0.2311	[58]0.2990	[57]0.3582	[56]0.4140	[56]0.4825	[56]0.5599
22	IDEMIA-003	[45]0.0110	[46]0.0151	[46]0.0196	[45]0.0238	[44]0.0281	[43]0.0313	[44]0.0368	[43]0.0504	[49]0.0717	[49]0.1147	[49]0.1614	[49]0.2113	[47]0.2553	[46]0.2976	[45]0.3537	[46]0.4334
23	IDEMIA-004	[44]0.0107	[44]0.0148	[45]0.0192	[44]0.0233	[43]0.0277	[42]0.0312	[43]0.0367	[44]0.0512	[25]0.0373	[23]0.0587	[23]0.0833	[23]0.1100	[22]0.1340	[20]0.1580	[17]0.1911	[17]0.2482
24	IDEMIA-005	[47]0.0118	[48]0.0167	[50]0.0218	[49]0.0270	[48]0.0317	[47]0.0357	[45]0.0425	[45]0.0579	[31]0.0440	[29]0.0689	[26]0.0964	[25]0.1254	[25]0.1513	[24]0.1762	[20]0.2113	[20]0.2698
25	IDEMIA-006	[49]0.0124	[50]0.0171	[49]0.0218	[47]0.0263	[46]0.0302	[44]0.0321	[42]0.0356	[42]0.0471	[27]0.0409	[25]0.0620	[24]0.0850	[22]0.1097	[20]0.1309	[17]0.1486	[14]0.1738	[14]0.2200
26	IDEMIA-007	[19]0.0050	[19]0.0071	[18]0.0089	[19]0.0106	[19]0.0124	[18]0.0142	[18]0.0171	[19]0.0220	[14]0.0202	[15]0.0335	[13]0.0491	[12]0.0663	[12]0.0825	[11]0.0999	[9]0.1240	[10]0.1645
27	IMPERIAL-000	[14]0.0040	[14]0.0054	[14]0.0067	[12]0.0079	[12]0.0093	[13]0.0112	[12]0.0139	[13]0.0178	[21]0.0286	[22]0.0503	[22]0.0779	[24]0.1116	[24]0.1455	[25]0.1844	[26]0.2341	[25]0.2951
28	INCODE-003	[57]0.0155	[59]0.0247	[59]0.0348	[59]0.0463	[58]0.0571	[58]0.0674	[58]0.0856	[59]0.1114	[63]0.1627	[63]0.2507	[63]0.3322	[63]0.4122	[62]0.4772	[64]0.5368	[64]0.6059	[64]0.6766
29	INCODE-004	[23]0.0061	[24]0.0087	[24]0.0110	[25]0.0136	[27]0.0161	[27]0.0185	[30]0.0236	[28]0.0309	[37]0.0532	[38]0.0908	[39]0.1334	[39]0.1809	[40]0.2245	[39]0.2675	[38]0.3249	[37]0.3932
30	INNOVATRICS-004	[76]0.3594	[75]0.3629	[75]0.3688	[74]0.3754	[74]0.3813	[74]0.3870	[74]0.3960	[74]0.4135	[69]0.4234	[68]0.4642	[68]0.5073	[68]0.5522	[67]0.5902	[67]0.6274	[67]0.6736	[67]0.7253
31	ISYSTEMS-002	[39]0.0101	[39]0.0135	[40]0.0169	[39]0.0197	[39]0.0228	[39]0.0256	[39]0.0304	[40]0.0398	[52]0.0779	[51]0.1258	[52]0.1759	[52]0.2299	[52]0.2758	[51]0.3204	[50]0.3763	[48]0.4401
32	ISYSTEMS-003	[37]0.0089	[33]0.0115	[32]0.0139	[31]0.0158	[32]0.0177	[33]0.0198	[29]0.0234	[26]0.0303	[47]0.0647	[47]0.1056	[47]0.1502	[47]0.1986	[46]0.2402	[42]0.2819	[41]0.3351	[39]0.3976
33	LOOKMAN-003	[48]0.0123	[43]0.0144	[37]0.0158	[33]0.0168	[33]0.0178	[29]0.0188	[22]0.0212	[22]0.0260	[30]0.0438	[27]0.0687	[27]0.0978	[27]0.1296	[26]0.1581	[26]0.1879	[25]0.2294	[23]0.2756
34	MEGVII-000	[38]0.0094	[47]0.0157	[51]0.0236	[55]0.0343	[55]0.0466	[56]0.0609	[57]0.0830	[58]0.1114	[55]0.0962	[56]0.1617	[59]0.2329	[59]0.3053	[60]0.3676	[58]0.4254	[58]0.4960	[58]0.5712
35	MICROFOCUS-005	[77]0.4269	[77]0.5527	[77]0.6355	[77]0.7024	[77]0.7503	[77]0.7876	[77]0.8234	[78]0.8601	[72]0.8338	[73]0.9113	[73]0.9468	[73]0.9667	[73]0.9771	[72]0.9836	[72]0.9880	[72]0.9924
36	MICROSOFT-000	[27]0.0071	[29]0.0103	[30]0.0131	[32]0.0158	[34]0.0187	[36]0.0221	[36]0.0271	[37]0.0354	[28]0.0418	[30]0.0698	[29]0.1025	[28]0.1390	[28]0.1752	[28]0.2126	[28]0.2610	[28]0.3232
37	MICROSOFT-003	[10]0.0034	[13]0.0050	[11]0.0064	[11]0.0078	[10]0.0092	[10]0.0107	[11]0.0135	[12]0.0166	[22]0.0288	[21]0.0503	[21]0.0763	[21]0.1067	[23]0.1359	[22]0.1680	[21]0.2116	[19]0.2644
38	MICROSOFT-004	[7]0.0032	[8]0.0047	[9]0.0060	[10]0.0075	[9]0.0087	[9]0.0103	[10]0.0131	[10]0.0159	[19]0.0268	[20]0.0470	[20]0.0716	[19]0.1007	[19]0.1291	[21]0.1610	[19]0.2052	[18]0.2590
39	MICROSOFT-005	[6]0.0031	[10]0.0047	[13]0.0066	[15]0.0084	[15]0.0103	[16]0.0131	[17]0.0164	[14]0.0185	[17]0.0243	[17]0.0432	[17]0.0658	[17]0.0913	[17]0.1172	[15]0.1476	[16]0.1874	[15]0.2272
40	MICROSOFT-006	[8]0.0032	[12]0.0049	[12]0.0065	[14]0.0081	[14]0.0096	[14]0.0117	[13]0.0144	[11]0.0160	[8]0.0134	[8]0.0233	[9]0.0346	[7]0.0462	[6]0.0578	[6]0.0713	[6]0.0903	[6]0.1156
41	NEC-000	[60]0.0195	[62]0.0316	[62]0.0445	[62]0.0581	[61]0.0699	[62]0.0817	[61]0.0998	[61]0.1237	[51]0.0759	[50]0.1245	[51]0.1729	[51]0.2240	[51]0.2671	[50]0.3117	[47]0.3639	[47]0.4348
42	NEC-001	[65]0.0246	[65]0.0382	[63]0.0524	[63]0.0672	[64]0.0793	[64]0.0904	[62]0.1076	[62]0.1317	[57]0.1019	[57]0.1623	[56]0.2214	[56]0.2834	[55]0.3341	[55]0.3844	[55]0.4440	[55]0.5183
43	NEC-002	[9]0.0033	[6]0.0041	[4]0.0043	[3]0.0044	[2]0.0045	[2]0.0049	[2]0.0056	[2]0.0041	[4]0.0066	[3]0.0090	[3]0.0111	[3]0.0131	[3]0.0149	[3]0.0171	[4]0.0207	[4]0.0267
44	NEC-003	[13]0.0036	[7]0.0046	[6]0.0051	[6]0.0055	[6]0.0059	[5]0.0067	[5]0.0077	[6]0.0073	[2]0.0056	[2]0.0076	[2]0.0091	[2]0.0105	[2]0.0119	[2]0.0137	[2]0.0162	[2]0.0209

Table 7: **Accuracy for the FRVT 2018 mugshot sets under ageing**. *The second row shows the time lapse between gallery and subsequent probe images, in years. The first two columns identify the algorithm The next 8 values give rank-based FNIR with R = 1, T = 0 and FPIR = 1. All these are relevant to investigational uses where candidates from all searches would need human review. The second 8 values give threshold-based FNIR with T $\geq$ 0, FPIR = 0.001 and no rank criterion. The shaded cells indictate indicate the three most accurate algorithms for that elapsed time. The gallery size is 3068801. The total number of searches is 10951064.*

2020/03/27 10:40:09

FNIR(N, R, T) = FPIR(N, T) = False neg. identification rate / False pos. identification rate

N = Num. enrolled subjects
R = Num. candidates examined

T = Threshold

T = 0 → Investigation
T > 0 → Identification

MISS RATES		INVESTIGATION, FNIR(N, R = 1, T = 0)								IDENTIFICATION, FNIR(N, R = L, T $\geq$ 0) FOR FPIR = 0.001							
#	ALGORITHM	(0, 2]	(2, 4]	(4, 6]	(6, 8]	(8, 10]	(10, 12]	(12, 14]	(14, 18]	(0, 2]	(2, 4]	(4, 6]	(6, 8]	(8, 10]	(10, 12]	(12, 14]	(14, 18]
45	NEUROTECHNOLOGY-003	[64]0.0234	[64]0.0379	[65]0.0549	[64]0.0682	[63]0.0720	[60]0.0747	[60]0.0886	[57]0.1066	[70]0.6802	[70]0.8187	[71]0.8920	[71]0.9355	[71]0.9594	[71]0.9738	[71]0.9828	[71]0.9885
46	NEUROTECHNOLOGY-004	[43]0.0104	[38]0.0134	[36]0.0156	[34]0.0173	[35]0.0195	[34]0.0212	[33]0.0245	[30]0.0320	[46]0.0642	[45]0.1015	[45]0.1426	[43]0.1881	[41]0.2299	[40]0.2722	[39]0.3269	[38]0.3943
47	NEUROTECHNOLOGY-005	[36]0.0089	[34]0.0116	[31]0.0136	[30]0.0152	[31]0.0173	[32]0.0196	[28]0.0233	[27]0.0306	[40]0.0556	[40]0.0913	[38]0.1315	[38]0.1766	[37]0.2192	[36]0.2617	[35]0.3174	[35]0.3843
48	NEUROTECHNOLOGY-007	[30]0.0078	[28]0.0103	[28]0.0124	[28]0.0140	[26]0.0161	[26]0.0185	[25]0.0225	[24]0.0290	[45]0.0641	[48]0.1069	[48]0.1546	[48]0.2075	[48]0.2572	[49]0.3081	[49]0.3713	[49]0.4421
49	NOBLIS-002	[74]0.1520	[74]0.2419	[74]0.3296	[75]0.4114	[75]0.4856	[75]0.5528	[75]0.6061	[75]0.6532	[74]0.9984	[74]0.9996	[74]0.9998	[74]0.9999	[74]0.9999	[74]1.0000	[79]1.0000	[78]1.0000
50	NTECHLAB-000	[41]0.0103	[51]0.0179	[56]0.0285	[57]0.0422	[59]0.0578	[61]0.0790	[63]0.1099	[64]0.1488	[50]0.0731	[53]0.1299	[53]0.1989	[54]0.2756	[56]0.3493	[59]0.4294	[59]0.5156	[61]0.6021
51	NTECHLAB-003	[29]0.0078	[37]0.0131	[47]0.0202	[50]0.0295	[51]0.0405	[54]0.0543	[55]0.0761	[56]0.1035	[33]0.0491	[36]0.0881	[43]0.1384	[46]0.1985	[49]0.2594	[52]0.3270	[52]0.4065	[51]0.4891
52	NTECHLAB-004	[26]0.0068	[32]0.0110	[39]0.0167	[46]0.0239	[49]0.0330	[50]0.0447	[53]0.0641	[54]0.0891	[26]0.0379	[28]0.0688	[30]0.1108	[30]0.1629	[36]0.2192	[45]0.2846	[48]0.3657	[50]0.4524
53	NTECHLAB-006	[20]0.0056	[26]0.0095	[33]0.0148	[43]0.0218	[45]0.0301	[48]0.0413	[49]0.0591	[52]0.0814	[23]0.0349	[26]0.0636	[28]0.1023	[29]0.1506	[30]0.2024	[35]0.2617	[42]0.3374	[44]0.4185
54	NTECHLAB-007	[15]0.0044	[16]0.0066	[19]0.0089	[23]0.0118	[24]0.0150	[30]0.0189	[35]0.0255	[35]0.0342	[18]0.0256	[18]0.0450	[19]0.0705	[20]0.1012	[21]0.1334	[23]0.1692	[22]0.2170	[22]0.2752
55	NTECHLAB-008	[4]0.0025	[5]0.0038	[7]0.0052	[9]0.0074	[16]0.0104	[19]0.0146	[31]0.0236	[36]0.0348	[9]0.0143	[11]0.0267	[12]0.0459	[13]0.0733	[14]0.1062	[14]0.1469	[18]0.2044	[21]0.2698
56	PARAVISION-002	[21]0.0058	[23]0.0083	[25]0.0111	[26]0.0137	[28]0.0162	[28]0.0187	[27]0.0229	[25]0.0295								
57	PARAVISION-003	[18]0.0048	[17]0.0067	[20]0.0090	[21]0.0109	[21]0.0128	[20]0.0148	[19]0.0178	[18]0.0219	[24]0.0354	[24]0.0618	[25]0.0931	[26]0.1290	[27]0.1625	[27]0.1964	[27]0.2408	[24]0.2924
58	PARAVISION-004	[3]0.0024	[3]0.0032	[3]0.0040	[4]0.0047	[4]0.0053	[4]0.0061	[4]0.0073	[5]0.0072	[5]0.0118	[7]0.0209	[8]0.0327	[8]0.0465	[7]0.0613	[7]0.0779	[7]0.1008	[7]0.1285
59	PARAVISION-005	[2]0.0021	[2]0.0028	[2]0.0035	[2]0.0041	[3]0.0046	[3]0.0054	[3]0.0067	[4]0.0070	[3]0.0057	[4]0.0093	[4]0.0144	[4]0.0207	[5]0.0278	[5]0.0368	[5]0.0508	[5]0.0715
60	RANKONE-000	[69]0.0400	[68]0.0591	[68]0.0786	[68]0.0994	[68]0.1166	[68]0.1312	[68]0.1512	[67]0.1818	[66]0.2134	[66]0.3003	[66]0.3776	[66]0.4518	[65]0.5104	[65]0.5616	[65]0.6195	[65]0.6830
61	RANKONE-002	[62]0.0212	[61]0.0313	[61]0.0431	[61]0.0562	[62]0.0712	[63]0.0881	[64]0.1130	[65]0.1543	[59]0.1111	[59]0.1707	[57]0.2305	[57]0.2968	[59]0.3646	[60]0.4345	[60]0.5172	[62]0.6110
62	RANKONE-004	[70]0.0424	[69]0.0643	[69]0.0875	[69]0.1127	[69]0.1364	[69]0.1579	[69]0.1914	[69]0.2378	[65]0.1855	[64]0.2681	[64]0.3431	[64]0.4155	[64]0.4785	[63]0.5350	[63]0.5980	[63]0.6722
63	RANKONE-005	[55]0.0136	[56]0.0192	[52]0.0246	[51]0.0303	[50]0.0362	[49]0.0422	[48]0.0521	[47]0.0694	[44]0.0582	[39]0.0910	[35]0.1260	[32]0.1645	[29]0.2005	[29]0.2353	[29]0.2816	[30]0.3522
64	RANKONE-007	[31]0.0078	[27]0.0099	[26]0.0113	[24]0.0123	[23]0.0139	[24]0.0156	[21]0.0191	[20]0.0242	[16]0.0242	[16]0.0376	[16]0.0542	[14]0.0737	[13]0.0935	[13]0.1130	[11]0.1416	[11]0.1811
65	REALNETWORKS-002	[68]0.0381	[70]0.0687	[70]0.1062	[70]0.1495	[71]0.1963	[71]0.2513	[73]0.3206	[73]0.3927	[67]0.2153	[67]0.3323	[67]0.4444	[67]0.5485	[68]0.6355	[68]0.7132	[68]0.7855	[68]0.8437
66	SENSETIME-002	[59]0.0186	[55]0.0191	[44]0.0183	[36]0.0179	[30]0.0173	[17]0.0133	[7]0.0089	[3]0.0059	[15]0.0220	[9]0.0236	[5]0.0237	[5]0.0240	[4]0.0245	[4]0.0219	[3]0.0195	[3]0.0222
67	SENSETIME-003	[1]0.0021	[1]0.0028	[1]0.0031	[1]0.0033	[1]0.0035	[1]0.0040	[1]0.0047	[1]0.0033	[1]0.0046	[1]0.0064	[1]0.0076	[1]0.0086	[1]0.0101	[1]0.0122	[1]0.0155	[1]0.0196
68	SIAT-002	[78]0.8309	[78]0.8310	[78]0.8311	[78]0.8306	[78]0.8296	[78]0.8302	[78]0.8300	[77]0.8301	[73]0.8340	[71]0.8368	[70]0.8404	[70]0.8445	[70]0.8480	[70]0.8532	[70]0.8595	[69]0.8691
69	SYNESIS-003	[51]0.0125	[45]0.0151	[43]0.0174	[40]0.0199	[38]0.0223	[37]0.0240	[37]0.0279	[33]0.0331	[48]0.0658	[46]0.1052	[46]0.1483	[45]0.1968	[45]0.2399	[43]0.2834	[43]0.3405	[42]0.4046
70	TOSHIBA-001	[34]0.0086	[35]0.0119	[34]0.0150	[35]0.0178	[37]0.0209	[38]0.0241	[38]0.0292	[38]0.0365								
71	VISIONLABS-004	[17]0.0048	[18]0.0069	[21]0.0091	[22]0.0111	[22]0.0130	[22]0.0152	[20]0.0187	[21]0.0242	[38]0.0540	[41]0.0916	[42]0.1358	[42]0.1855	[42]0.2303	[41]0.2745	[40]0.3312	[36]0.3913
72	VISIONLABS-005	[16]0.0044	[15]0.0063	[15]0.0081	[17]0.0095	[17]0.0109	[15]0.0125	[14]0.0151	[15]0.0187	[32]0.0479	[32]0.0812	[33]0.1212	[34]0.1664	[33]0.2078	[33]0.2473	[33]0.2999	[32]0.3577
73	VISIONLABS-006	[11]0.0035	[11]0.0048	[10]0.0061	[8]0.0069	[8]0.0077	[8]0.0087	[9]0.0105	[9]0.0120	[20]0.0273	[19]0.0465	[18]0.0702	[18]0.0970	[18]0.1228	[16]0.1486	[15]0.1847	[16]0.2295
74	VISIONLABS-008	[5]0.0028	[4]0.0037	[5]0.0047	[5]0.0053	[5]0.0058	[6]0.0067	[6]0.0081	[7]0.0085	[10]0.0143	[10]0.0241	[10]0.0373	[10]0.0519	[10]0.0677	[8]0.0850	[8]0.1104	[8]0.1444
75	YITU-000	[35]0.0088	[36]0.0119	[35]0.0153	[38]0.0193	[42]0.0253	[45]0.0338	[47]0.0501	[48]0.0732	[29]0.0433	[31]0.0748	[31]0.1164	[36]0.1701	[43]0.2306	[47]0.3029	[51]0.3969	[53]0.4969
76	YITU-002	[24]0.0066	[22]0.0083	[22]0.0094	[18]0.0101	[18]0.0121	[21]0.0150	[24]0.0223	[31]0.0328	[12]0.0189	[13]0.0317	[14]0.0494	[15]0.0750	[15]0.1066	[18]0.1494	[23]0.2171	[26]0.2958
77	YITU-003	[28]0.0072	[25]0.0089	[23]0.0100	[20]0.0107	[20]0.0125	[23]0.0153	[26]0.0226	[34]0.0334	[13]0.0194	[14]0.0321	[15]0.0500	[16]0.0756	[16]0.1071	[19]0.1500	[24]0.2177	[27]0.2964
78	YITU-004	[22]0.0061	[20]0.0075	[16]0.0081	[13]0.0081	[11]0.0092	[11]0.0107	[16]0.0154	[17]0.0207	[7]0.0125	[6]0.0204	[7]0.0314	[9]0.0469	[9]0.0671	[10]0.0955	[13]0.1421	[13]0.2006
79	YITU-005	[25]0.0067	[21]0.0080	[17]0.0087	[16]0.0085	[13]0.0094	[12]0.0108	[15]0.0151	[16]0.0204	[6]0.0124	[5]0.0198	[6]0.0308	[6]0.0462	[8]0.0667	[9]0.0953	[12]0.1418	[12]0.1930

Table 8: **Accuracy for the FRVT 2018 mugshot sets under ageing**. *The second row shows the time lapse between gallery and subsequent probe images, in years. The first two columns identify the algorithm The next 8 values give rank-based FNIR with R = 1, T = 0 and FPIR = 1. All these are relevant to investigational uses where candidates from all searches would need human review. The second 8 values give threshold-based FNIR with T $\geq$ 0, FPIR = 0.001 and no rank criterion. The shaded cells indictate indicate the three most accurate algorithms for that elapsed time. The gallery size is 3068801. The total number of searches is 10951064.*

2020/03/27 10:40:09

FNIR(N, R, T) = FPIR(N, T) = False neg. identification rate / False pos. identification rate

N = Num. enrolled subjects
R = Num. candidates examined

T = Threshold

T = 0 → Investigation
T > 0 → Identification

MISSES BELOW THRESHOLD, T		ENROL LIFETIME					ENROL MOST RECENT				
FNIR(N, T> 0, R >L)		DATASET: FRVT 2018					DATASET: FRVT 2018				
#	ALGORITHM	N=0.64M	N=1.6M	N=3.0M	N=6.0M	N=12.0M	N=0.64M	N=1.6M	N=3.0M	N=6.0M	N=12.0M
1	3DIVI-003	[168]0.2998	[152]0.3495	[74]0.3853	[71]0.4340		[181]0.3531	[180]0.4005			
2	3DIVI-005	[122]0.1041	[120]0.1334				[135]0.1358	[135]0.1664	[104]0.1915	[98]0.2370	[94]0.3054
3	ALCHERA-000	[111]0.0848	[110]0.1097	[62]0.1352	[60]0.1880		[126]0.1103	[125]0.1380			
4	ALCHERA-003	[120]0.1014	[118]0.1290				[128]0.1176	[128]0.1553	[100]0.1853	[99]0.2409	[101]0.3553
5	ALLGOVISION-000	[92]0.0555	[91]0.0733				[99]0.0688	[99]0.0881	[81]0.1084	[76]0.1389	[68]0.2129
6	ANKE-000	[105]0.0762	[102]0.0982				[115]0.0942	[113]0.1169	[94]0.1404	[89]0.1776	[88]0.2559
7	ANKE-002	[29]0.0200	[29]0.0275				[31]0.0229	[31]0.0318	[31]0.0406	[31]0.0605	[26]0.1466
8	AWARE-003	[110]0.0843	[103]0.0987	[59]0.1143	[55]0.1450		[125]0.1098	[123]0.1283	[95]0.1471	[90]0.1793	[80]0.2364
9	AWARE-005	[160]0.2569	[146]0.2895				[177]0.3389	[173]0.3643	[112]0.3993	[108]0.4526	[87]0.2531
10	AYONIX-000	[202]0.8262	[169]0.8490	[80]0.8639	[75]0.8808		[216]0.7789	[213]0.8109			
11	AYONIX-002	[198]0.7602	[167]0.8038				[217]0.7862	[215]0.8242	[117]0.8508	[112]0.8704	[110]0.8939
12	CAMVI-003	[56]0.0278	[69]0.0505	[45]0.0675	[59]0.1868		[60]0.0388	[82]0.0711			
13	CAMVI-004	[48]0.0254	[68]0.0501				[57]0.0367	[83]0.0716	[75]0.0983	[101]0.2508	[91]0.2701
14	COGENT-000	[73]0.0384	[64]0.0425	[39]0.0515	[36]0.0773	[21]0.1556	[75]0.0430	[62]0.0527	[62]0.0734	[65]0.1194	[59]0.1960
15	COGENT-001	[94]0.0594	[70]0.0510				[76]0.0430	[63]0.0527	[63]0.0734	[66]0.1194	[60]0.1960
16	COGENT-002	[33]0.0216	[32]0.0296	[25]0.0381	[35]0.0692	[24]0.1592	[42]0.0322	[46]0.0444	[44]0.0610	[61]0.1116	[70]0.2180
17	COGENT-003	[46]0.0251	[45]0.0337	[32]0.0436	[39]0.0819	[36]0.1861	[43]0.0328	[49]0.0463	[55]0.0683	[69]0.1294	[82]0.2445
18	COGNITEC-000	[119]0.0986	[117]0.1251				[139]0.1377	[132]0.1606	[103]0.1892	[94]0.2205	[93]0.2831
19	COGNITEC-001	[93]0.0592	[92]0.0770	[53]0.0937	[52]0.1281	[49]0.2504	[108]0.0807	[106]0.1017	[87]0.1244	[81]0.1561	[74]0.2238
20	COGNITEC-002	[60]0.0291	[57]0.0396	[38]0.0509	[40]0.0833	[46]0.2213	[67]0.0406	[64]0.0531	[52]0.0666	[51]0.0935	[53]0.1874
21	COGNITEC-003	[57]0.0285	[56]0.0393	[37]0.0494	[37]0.0792	[44]0.2100	[65]0.0400	[61]0.0526	[48]0.0650	[46]0.0895	[47]0.1772
22	CYBERLINK-000	[64]0.0308	[63]0.0423				[69]0.0414	[70]0.0565	[60]0.0707	[58]0.1031	[65]0.2050
23	CYBERLINK-001	[58]0.0287	[55]0.0393				[61]0.0392	[65]0.0536	[57]0.0695	[55]0.0973	[48]0.1794
24	DAHUA-001	[77]0.0407	[71]0.0518				[87]0.0569	[85]0.0727	[71]0.0878	[63]0.1148	[52]0.1867
25	DAHUA-002	[12]0.0095	[10]0.0126	[10]0.0156	[8]0.0257	[6]0.1113	[12]0.0108	[12]0.0151	[12]0.0191	[11]0.0291	[13]0.1153
26	DEEPSEA-001	[40]0.0245	[42]0.0322				[50]0.0347	[48]0.0462	[43]0.0586	[42]0.0802	[45]0.1708
27	DERMALOG-004	[171]0.3403	[157]0.3890	[76]0.4179	[72]0.4531		[188]0.4365	[186]0.4798			
28	DERMALOG-005	[87]0.0487	[84]0.0646				[104]0.0700	[98]0.0880	[83]0.1144	[83]0.1578	[83]0.2451
29	DERMALOG-006	[54]0.0273	[54]0.0380				[62]0.0395	[59]0.0517	[50]0.0659	[54]0.0973	[46]0.1745
30	DERMALOG-007						[100]0.0691	[94]0.0863	[82]0.1107		[78]0.2299
31	EYEDEA-003	[166]0.2908	[150]0.3279	[73]0.3670	[70]0.4151		[180]0.3480	[177]0.3877			
32	F8-001	[189]0.5795	[163]0.5947				[120]0.1140	[133]0.1658	[99]0.1658	[86]0.1658	[44]0.1658
33	GLORY-001	[152]0.2157	[138]0.2444	[68]0.2613	[65]0.2878		[171]0.2771	[166]0.3049			
34	GORILLA-002	[128]0.1085	[125]0.1376				[142]0.1539	[141]0.1880	[107]0.2184	[102]0.2596	[100]0.3398
35	GORILLA-004	[89]0.0510	[85]0.0653	[51]0.0789	[49]0.1057	[33]0.1762	[103]0.0699	[102]0.0892	[79]0.1048	[75]0.1370	[62]0.1969
36	HIK-002	[129]0.1099	[134]0.1359	[64]0.1598	[61]0.2047	[53]0.3043	[120]0.0959	[118]0.1187			
37	HIK-003	[112]0.0882	[109]0.1093				[109]0.0828	[107]0.1028	[86]0.1228	[80]0.1552	[85]0.2480
38	HIK-004	[109]0.0836	[107]0.1025	[60]0.1222	[58]0.1515	[51]0.2615	[107]0.0796	[103]0.0988	[84]0.1173	[79]0.1498	[86]0.2483
39	HIK-005	[32]0.0215	[35]0.0304	[28]0.0392	[32]0.0656		[40]0.0312	[42]0.0436	[42]0.0560	[48]0.0911	[69]0.2129
40	IDEMIA-000	[96]0.0642	[93]0.0798	[54]0.0983	[51]0.1234	[37]0.1869	[112]0.0896	[111]0.1112	[90]0.1332	[85]0.1628	[71]0.2181
41	IDEMIA-001	[63]0.0300	[53]0.0374	[35]0.0462	[27]0.0620	[23]0.1575	[70]0.0418	[58]0.0515	[47]0.0647	[43]0.0856	[37]0.1587
42	IDEMIA-002	[80]0.0450	[76]0.0561	[43]0.0665	[43]0.0892	[29]0.1703	[73]0.0424	[60]0.0518			
43	IDEMIA-003	[37]0.0235	[34]0.0303				[48]0.0346	[51]0.0471	[73]0.0927	[104]0.2887	[105]0.4311
44	IDEMIA-004	[34]0.0220	[28]0.0273	[20]0.0334	[19]0.0475	[20]0.1554	[37]0.0300	[36]0.0373	[33]0.0447	[32]0.0617	[42]0.1635
45	IDEMIA-005	[51]0.0257	[39]0.0315	[27]0.0391	[24]0.0584	[32]0.1761	[54]0.0360	[44]0.0440	[38]0.0537	[40]0.0764	[55]0.1915
46	IDEMIA-006	[43]0.0249	[38]0.0312	[24]0.0379	[23]0.0577	[42]0.2043	[51]0.0351	[41]0.0433	[37]0.0525	[37]0.0734	[72]0.2201
47	IDEMIA-007	[17]0.0118	[15]0.0151	[13]0.0192	[12]0.0305	[14]0.1403	[15]0.0136	[15]0.0181	[13]0.0228	[13]0.0357	[25]0.1402
48	IMAGUS-002	[194]0.6603	[164]0.7119	[78]0.7481	[73]0.7855		[211]0.7077	[209]0.7491			
49	IMPERIAL-000	[25]0.0153	[24]0.0215	[19]0.0285	[28]0.0623	[30]0.1723	[26]0.0187	[25]0.0259	[28]0.0358	[36]0.0733	[49]0.1794
50	INCODE-001	[136]0.1395	[132]0.1788	[66]0.2147	[64]0.2729		[148]0.1739	[147]0.2116			
51	INCODE-003	[117]0.0945	[115]0.1222				[134]0.1324	[136]0.1672	[105]0.1961	[97]0.2345	[96]0.3123
52	INCODE-004	[61]0.0296	[60]0.0405				[66]0.0403	[67]0.0538	[51]0.0662	[49]0.0917	[38]0.1619
53	INNOVATRICS-004	[108]0.0834	[98]0.0925				[124]0.1082	[124]0.1317	[93]0.1394	[77]0.1394	[24]0.1394
54	INNOVATRICS-005						[33]0.0251	[32]0.0340	[32]0.0424	[23]0.0482	
55	INTSYSMSU-000	[218]0.9978	[178]0.9981				[234]0.9982	[230]0.9984	[121]0.9985	[115]0.9987	[112]0.9988
56	ISYSTEMS-000	[85]0.0481	[83]0.0629	[50]0.0789	[48]0.1051	[43]0.2054	[97]0.0681	[100]0.0887			
57	ISYSTEMS-001	[83]0.0476	[82]0.0622	[49]0.0777	[47]0.1043	[41]0.2039	[96]0.0673	[96]0.0878			
58	ISYSTEMS-002	[74]0.0390	[74]0.0542	[44]0.0673			[89]0.0584	[88]0.0783	[76]0.1006	[78]0.1405	[77]0.2295
59	ISYSTEMS-003	[62]0.0297	[58]0.0396	[41]0.0550	[42]0.0873	[39]0.1979	[78]0.0438	[74]0.0590	[68]0.0807	[68]0.1259	[29]0.2357
60	KEDACOM-001	[28]0.0190	[26]0.0225				[23]0.0181	[22]0.0227	[16]0.0265	[20]0.0422	[23]0.1340
61	LOOKMAN-003	[69]0.0332	[62]0.0421				[49]0.0346	[43]0.0437	[36]0.0514	[35]0.0724	[39]0.1620
62	LOOKMAN-005	[45]0.0250	[37]0.0311				[32]0.0240	[30]0.0301	[27]0.0356	[26]0.0512	[22]0.1334
63	MEGVII-000	[107]0.0819	[106]0.1020	[61]0.1224	[52]0.1485	[48]0.2346	[111]0.0868	[110]0.1061	[89]0.1287	[84]0.1606	[76]0.2255
64	MEGVII-001						[85]0.0562	[84]0.0722	[70]0.0872	[72]0.1309	[92]0.2713
65	MICROFOCUS-003	[210]0.9000	[173]0.9213	[82]0.9342			[222]0.9116	[220]0.9308			
66	MICROFOCUS-005	[213]0.9679	[175]0.9835				[220]0.9732	[217]0.8354	[118]0.8555	[113]0.8755	[111]0.8954
67	MICROSOFT-000	[30]0.0204	[30]0.0287	[22]0.0357	[21]0.0519	[15]0.1460	[38]0.0302	[38]0.0410	[40]0.0544	[41]0.0767	[43]0.1637
68	MICROSOFT-001	[31]0.0211	[31]0.0295	[23]0.0368	[22]0.0532	[22]0.1556	[39]0.0310	[39]0.0418			
69	MICROSOFT-002	[42]0.0248	[46]0.0341	[29]0.0422	[25]0.0595	[19]0.1544	[52]0.0359	[53]0.0475			
70	MICROSOFT-003	[23]0.0131	[22]0.0190				[30]0.0198	[29]0.0278	[30]0.0384	[30]0.0570	[34]0.1539
71	MICROSOFT-004	[18]0.0126	[19]0.0176	[16]0.0238	[17]0.0395	[25]0.1617	[25]0.0185	[26]0.0259	[29]0.0360	[29]0.0550	[31]0.1510
72	MICROSOFT-005	[16]0.0117	[17]0.0169	[14]0.0216	[15]0.0381	[26]0.1637	[24]0.0181	[24]0.0256	[24]0.0320	[25]0.0512	[30]0.1491

Table 9: **Identification-mode: Effect of N on FNIR at high threshold.** *Values are threshold-based miss rates i.e.* FNIR *at* FPIR *= 0.001 for five enrollment population sizes, N. The left six columns apply for enrollment of a variable number of images per subject. The right six columns apply for enrollment of one image. Missing entries usually apply because another algorithm from the same developer was run instead. Some developers are missing because less accurate algorithms were not run on galleries with* $N \geq 3\,000\,000$*. Throughout blue superscripts indicate the rank of the algorithm for that column.*

MISSES BELOW THRESHOLD, T		ENROL LIFETIME					ENROL MOST RECENT				
FNIR(N, T> 0, R >L)		DATASET: FRVT 2018					DATASET: FRVT 2018				
#	ALGORITHM	N=0.64M	N=1.6M	N=3.0M	N=6.0M	N=12.0M	N=0.64M	N=1.6M	N=3.0M	N=6.0M	N=12.0M
73	MICROSOFT-006	[8]0.0057	[7]0.0079	[7]0.0107	[11]0.0269	[27]0.1651	[9]0.0091	[8]0.0120	[9]0.0162	[12]0.0301	[29]0.1482
74	NEC-000	[84]0.0480	[79]0.0600	[48]0.0718	[45]0.0969	[47]0.2339	[91]0.0637	[89]0.0789	[74]0.0961	[67]0.1199	[58]0.1941
75	NEC-001	[99]0.0707	[97]0.0893				[110]0.0863	[109]0.1055	[88]0.1276	[82]0.1565	[75]0.2253
76	NEC-002	[1]0.0016	[2]0.0021	[2]0.0031	[4]0.0167	[4]0.0948	[2]0.0020	[3]0.0026	[3]0.0033	[3]0.0135	[3]0.0653
77	NEC-003	[2]0.0017	[1]0.0020	[1]0.0024	[2]0.0089	[2]0.0747	[3]0.0021	[2]0.0024	[2]0.0028	[2]0.0059	[2]0.0540
78	NEUROTECHNOLOGY-003	[187]0.5357	[162]0.5928				[201]0.5698	[203]0.6362	[116]0.7217	[111]0.7852	[109]0.8336
79	NEUROTECHNOLOGY-004	[79]0.0424	[77]0.0570	[47]0.0704	[44]0.0949	[35]0.1832	[80]0.0466	[78]0.0629	[69]0.0810	[64]0.1167	[67]0.2102
80	NEUROTECHNOLOGY-005	[72]0.0381	[73]0.0522	[40]0.0542	[38]0.0808	[12]0.1361	[63]0.0396	[68]0.0538	[53]0.0675	[53]0.0950	[61]0.1966
81	NEUROTECHNOLOGY-007	[76]0.0402	[196]1.0000	[46]0.0694	[46]0.0973	[40]0.2032	[77]0.0436	[77]0.0623	[65]0.0802	[73]0.1320	[81]0.2393
82	NEWLAND-002						[184]0.3996	[183]0.4385	[113]0.4702	[109]0.5119	
83	NOBLIS-002	[216]0.9941	[177]0.9959				[233]0.9962	[229]0.9973	[120]0.9979	[114]0.9985	
84	NTECHLAB-000	[90]0.0514	[86]0.0663	[52]0.0847	[50]0.1153		[95]0.0652	[90]0.0804	[77]0.1029	[71]0.1306	[57]0.1926
85	NTECHLAB-001	[95]0.0631	[94]0.0815	[56]0.1003	[54]0.1332	[45]0.2148	[106]0.0777	[105]0.0997			
86	NTECHLAB-003	[67]0.0326	[65]0.0430				[72]0.0421	[66]0.0537	[58]0.0699	[50]0.0933	[36]0.1582
87	NTECHLAB-004	[44]0.0250	[43]0.0333	[30]0.0428	[34]0.0684	[34]0.1816	[41]0.0312	[37]0.0405	[41]0.0545	[38]0.0749	[33]0.1528
88	NTECHLAB-005	[53]0.0265	[48]0.0344				[45]0.0334	[40]0.0424	[39]0.0537	[39]0.0760	[35]0.1543
89	NTECHLAB-006	[35]0.0225	[33]0.0298	[26]0.0391	[31]0.0650	[38]0.1883	[35]0.0288	[34]0.0367	[35]0.0471	[34]0.0670	[32]0.1523
90	NTECHLAB-007	[26]0.0167	[25]0.0219	[18]0.0284	[20]0.0475	[28]0.1677	[27]0.0188	[23]0.0256	[23]0.0317	[24]0.0495	[21]0.1306
91	NTECHLAB-008	[14]0.0108	[14]0.0148	[12]0.0185	[13]0.0306	[18]0.1485	[11]0.0107	[10]0.0145	[11]0.0187	[9]0.0286	[5]0.0995
92	PARAVISION-000	[81]0.0456	[88]0.0670				[94]0.0652	[101]0.0888	[85]0.1223		
93	PARAVISION-001	[47]0.0252	[51]0.0356				[53]0.0359	[55]0.0491	[56]0.0686		
94	PARAVISION-003	[27]0.0188	[27]0.0254	[21]0.0335	[16]0.0386		[34]0.0260	[33]0.0351	[34]0.0447	[33]0.0657	[41]0.1630
95	PARAVISION-004	[9]0.0075	[8]0.0097	[8]0.0127	[7]0.0245	[10]0.1231	[7]0.0074	[7]0.0101	[7]0.0136	[8]0.0267	[18]0.1256
96	PARAVISION-005	[5]0.0046	[4]0.0052	[4]0.0063	[3]0.0145	[7]0.1144	[5]0.0032	[4]0.0041	[4]0.0057	[4]0.0174	[7]0.1037
97	PIXELALL-002	[113]0.0889	[114]0.1203				[105]0.0716	[108]0.1052	[97]0.1475	[100]0.2489	[103]0.3904
98	PIXELALL-003	[38]0.0237	[40]0.0317				[20]0.0158	[19]0.0218	[21]0.0288	[22]0.0474	[12]0.1138
99	QUANTASOFT-001	[215]0.9915	[176]0.9915				[207]0.6387	[204]0.6387	[115]0.6387		[107]0.6387
100	RANKONE-000	[139]0.1480	[131]0.1782	[67]0.2189	[66]0.3223	[55]0.4688	[150]0.1876	[148]0.2169	[110]0.2635	[105]0.2992	[104]0.4275
101	RANKONE-001	[131]0.1202	[129]0.1543	[65]0.1786	[63]0.2341	[54]0.3508	[141]0.1518	[134]0.1659			
102	RANKONE-002	[103]0.0741	[100]0.0936				[122]0.0973	[115]0.1175	[92]0.1382	[87]0.1744	[90]0.2636
103	RANKONE-003	[102]0.0741	[99]0.0936	[58]0.1115	[56]0.1480	[52]0.2930	[123]0.0973	[116]0.1175	[91]0.1382	[88]0.1744	[89]0.2613
104	RANKONE-004	[134]0.1260	[128]0.1539				[143]0.1608	[142]0.1929	[108]0.2189		
105	RANKONE-005	[70]0.0343	[66]0.0443	[42]0.0566	[41]0.0841	[50]0.2526	[81]0.0473	[75]0.0592	[59]0.0700	[52]0.0944	[63]0.1998
106	RANKONE-007	[24]0.0150	[23]0.0191	[15]0.0231	[14]0.0374	[16]0.1464	[22]0.0168	[21]0.0222	[17]0.0266	[15]0.0381	[11]0.1132
107	REALNETWORKS-000	[148]0.2087	[139]0.2469	[70]0.2830			[153]0.1965	[151]0.2335			
108	REALNETWORKS-002	[130]0.1682	[134]0.2037				[152]0.1943	[150]0.2314	[111]0.2656	[107]0.3134	[98]0.3208
109	REALNETWORKS-003	[130]0.1114	[126]0.1402				[133]0.1300	[131]0.1594	[102]0.1858	[95]0.2246	[95]0.3076
110	REALNETWORKS-004	[116]0.0938	[113]0.1176				[132]0.1279	[130]0.1581	[101]0.1857	[96]0.2329	[97]0.3179
111	REMARKAI-000	[68]0.0331	[67]0.0457				[68]0.0406	[69]0.0552	[54]0.0676	[57]0.1028	[64]0.2003
112	REMARKAI-002	[101]0.0726	[101]0.0982				[117]0.0946	[121]0.1239	[96]0.1472	[92]0.1895	
113	SCANOVATE-000	[199]0.7848	[168]0.7901	[79]0.7906	[74]0.7906	[56]0.7906	[82]0.0498	[81]0.0667	[66]0.0804	[60]0.1097	[10]0.1109
114	SENSETIME-000	[12]0.0115	[16]0.0161				[17]0.0158	[17]0.0208	[19]0.0270	[18]0.0398	[14]0.1232
115	SENSETIME-001	[19]0.0126	[18]0.0172				[21]0.0161	[20]0.0219	[20]0.0277	[19]0.0420	[20]0.1304
116	SENSETIME-002	[20]0.0128	[12]0.0131	[9]0.0135	[9]0.0258	[3]0.0823	[17]0.0146	[11]0.0148	[8]0.0153	[6]0.0234	[4]0.0657
117	SENSETIME-003	[3]0.0035	[3]0.0037	[3]0.0039	[1]0.0063	[1]0.0451	[1]0.0016	[1]0.0018	[1]0.0021	[1]0.0054	[1]0.0451
118	SHAMAN-003	[174]0.3504	[158]0.3916	[77]0.4292			[185]0.4163	[184]0.4513			
119	SHAMAN-007	[115]0.0921	[112]0.1109				[131]0.1212	[127]0.1413	[98]0.1587	[91]0.1879	[84]0.2460
120	SIAT-001	[161]0.2693	[145]0.2725	[69]0.2755			[14]0.0136	[13]0.0176	[15]0.0260	[14]0.0380	[6]0.1035
121	SIAT-002	[154]0.2195	[136]0.2236				[18]0.0154	[18]0.0216	[22]0.0301	[21]0.0434	[19]0.1283
122	SMILART-004	[203]0.8381	[174]0.9569				[226]0.9258	[224]0.9682	[119]0.9913		
123	SYNESIS-003	[183]0.4747	[160]0.5294				[198]0.5341	[197]0.5821	[114]0.6113	[110]0.6479	[108]0.6822
124	SYNESIS-003						[83]0.0499	[79]0.0652	[67]0.0804	[59]0.1095	[56]0.1916
125	TECH5-001	[78]0.0422	[78]0.0587				[71]0.0420	[71]0.0574	[72]0.0911	[93]0.2106	[102]0.3725
126	TEVIAN-004	[98]0.0681	[96]0.0875	[57]0.1029			[113]0.0924	[114]0.1170			
127	TEVIAN-005	[91]0.0515	[87]0.0663				[101]0.0692	[95]0.0873	[80]0.1066	[70]0.1301	[51]0.1840
128	TIGER-000	[165]0.2857	[151]0.3356	[72]0.3654	[69]0.4129		[179]0.3435	[179]0.3904			
129	TIGER-002	[88]0.0507	[89]0.0690				[93]0.0647	[92]0.0861	[78]0.1036	[74]0.1332	[73]0.2231
130	TONGYITRANS-001	[97]0.0653	[95]0.0830	[55]0.1000	[53]0.1305		[84]0.0519	[80]0.0665			
131	TOSHIBA-000	[71]0.0366	[72]0.0519				[79]0.0460	[76]0.0620	[64]0.0780	[62]0.1117	[66]0.2082
132	VD-000	[207]0.8686	[172]0.9048	[81]0.9241	[76]0.9378		[220]0.8889	[219]0.9169			
133	VD-001	[135]0.1309	[130]0.1650				[144]0.1642	[146]0.2015	[109]0.2351	[103]0.2736	[99]0.3293
134	VIGILANTSOLUTIONS-003	[169]0.3059	[153]0.3565	[75]0.3859	[67]0.3859		[183]0.3631	[182]0.4082			
135	VISIONLABS-003	[40]0.0256	[47]0.0343	[34]0.0440	[33]0.0670		[56]0.0367	[54]0.0480	[46]0.0629	[47]0.0902	
136	VISIONLABS-004	[59]0.0291	[59]0.0399				[74]0.0427	[72]0.0578	[61]0.0733	[56]0.0982	[54]0.1893
137	VISIONLABS-005	[41]0.0247	[49]0.0350	[33]0.0438	[29]0.0625	[31]0.1726	[59]0.0369	[57]0.0502	[49]0.0654	[45]0.0878	[50]0.1815
138	VISIONLABS-006	[22]0.0129	[21]0.0182				[29]0.0188	[28]0.0267	[26]0.0336	[28]0.0542	[27]0.1478
139	VISIONLABS-007	[21]0.0129	[20]0.0182	[17]0.0240	[18]0.0407	[17]0.1478	[28]0.0188	[27]0.0266	[25]0.0335	[27]0.0540	[28]0.1479
140	VISIONLABS-008	[10]0.0089	[9]0.0114				[10]0.0096	[9]0.0131	[10]0.0166	[10]0.0291	[16]0.1247
141	VOCORD-003	[118]0.0955	[116]0.1250	[63]0.1580	[62]0.2275		[116]0.0944	[120]0.1222			
142	VOCORD-005	[100]0.0717	[108]0.1043				[129]0.1179	[129]0.1577	[106]0.2183	[106]0.3122	[106]0.4490
143	YISHENG-001	[159]0.2528	[147]0.2972	[71]0.3352	[68]0.3879		[173]0.3001	[170]0.3464			
144	YITU-000	[55]0.0276	[50]0.0354	[36]0.0464	[30]0.0630	[13]0.1383	[55]0.0362	[52]0.0474	[45]0.0622	[44]0.0862	[40]0.1621

Table 10: **Identification-mode: Effect of N on FNIR at high threshold.** *Values are threshold-based miss rates i.e.* FNIR *at* FPIR *= 0.001 for five enrollment population sizes, N. The left six columns apply for enrollment of a variable number of images per subject. The right six columns apply for enrollment of one image. Missing entries usually apply because another algorithm from the same developer was run instead. Some developers are missing because less accurate algorithms were not run on galleries with* $N \geq 3\,000\,000$*. Throughout blue superscripts indicate the rank of the algorithm for that column.*

MISSES BELOW THRESHOLD, T		ENROL LIFETIME					ENROL MOST RECENT				
FNIR(N, T> 0, R >L)		DATASET: FRVT 2018					DATASET: FRVT 2018				
#	ALGORITHM	N=0.64M	N=1.6M	N=3.0M	N=6.0M	N=12.0M	N=0.64M	N=1.6M	N=3.0M	N=6.0M	N=12.0M
145	YITU-001	[50]0.0257	[44]0.0337	[31]0.0429	[26]0.0606	[11]0.1343	[47]0.0340	[45]0.0444			
146	YITU-002	[11]0.0092	[11]0.0129	[11]0.0171	[10]0.0268	[9]0.1174	[13]0.0129	[14]0.0177	[14]0.0258	[16]0.0382	[15]0.1241
147	YITU-003	[13]0.0100	[13]0.0136				[16]0.0138	[16]0.0185	[18]0.0266	[17]0.0389	[17]0.1248
148	YITU-004	[6]0.0048	[5]0.0070	[5]0.0094	[5]0.0180	[8]0.1144	[6]0.0067	[5]0.0096	[5]0.0129	[5]0.0232	[8]0.1046
149	YITU-005	[7]0.0054	[6]0.0072	[6]0.0097	[6]0.0183	[5]0.1100	[8]0.0074	[6]0.0101	[6]0.0135	[7]0.0255	[9]0.1057

Table 11: **Identification-mode: Effect of N on FNIR at high threshold.** *Values are threshold-based miss rates i.e.* FNIR *at* FPIR *= 0.001 for five enrollment population sizes, N. The left six columns apply for enrollment of a variable number of images per subject. The right six columns apply for enrollment of one image. Missing entries usually apply because another algorithm from the same developer was run instead. Some developers are missing because less accurate algorithms were not run on galleries with* $N \geq 3\,000\,000$*. Throughout blue superscripts indicate the rank of the algorithm for that column.*

MISSES NOT AT RANK 1 FNIR(N, T= 0, R =1)		ENROL LIFETIME DATASET: FRVT 2018						ENROL MOST RECENT DATASET: FRVT 2018					
#	ALGORITHM	N=0.64M	N=1.6M	N=3.0M	N=6.0M	N=12.0M	aN^b	N=0.64M	N=1.6M	N=3.0M	N=6.0M	N=12.0M	aN^b
1	3DIVI-003	169 0.0491	150 0.0641	73 0.0756	69 0.0895		106 0.0014 $N^{0.269}$ 91	187 0.0655	186 0.0833				120 0.0020 $N^{0.261}$ 97
2	3DIVI-005	109 0.0097	111 0.0130				46 0.0001 $N^{0.317}$ 124	131 0.0137	128 0.0176	96 0.0210	93 0.0253	92 0.0302	93 0.0004 $N^{0.271}$ 103
3	ALCHERA-000	115 0.0103	106 0.0119	59 0.0132	57 0.0167		83 0.0006 $N^{0.211}$ 69	132 0.0143	123 0.0161				122 0.0024 $N^{0.134}$ 28
4	ALCHERA-003	121 0.0117	116 0.0156				51 0.0002 $N^{0.316}$ 122	96 0.0079	100 0.0104	78 0.0123	82 0.0147	84 0.0180	65 0.0002 $N^{0.278}$ 112
5	ALLGOVISION-000	104 0.0092	99 0.0102				113 0.0019 $N^{0.117}$ 34	112 0.0101	109 0.0114	80 0.0127	81 0.0145	81 0.0166	110 0.0010 $N^{0.171}$ 40
6	ANKE-000	94 0.0074	92 0.0097				47 0.0001 $N^{0.295}$ 112	115 0.0102	116 0.0132	90 0.0155	89 0.0188	88 0.0225	81 0.0003 $N^{0.270}$ 101
7	ANKE-002	56 0.0041	48 0.0044				105 0.0013 $N^{0.084}$ 23	30 0.0024	29 0.0028	22 0.0032	22 0.0037	23 0.0043	54 0.0002 $N^{0.203}$ 53
8	AWARE-003	136 0.0161	127 0.0205	64 0.0243	62 0.0293		80 0.0005 $N^{0.267}$ 90	154 0.0238	150 0.0306	109 0.0387	107 0.0456	105 0.0506	107 0.0008 $N^{0.256}$ 92
9	AWARE-005	135 0.0159	125 0.0205				76 0.0004 $N^{0.275}$ 96	156 0.0245	151 0.0311	108 0.0366	105 0.0434	96 0.0312	134 0.0056 $N^{0.118}$ 24
10	AYONIX-000	209 0.4196	173 0.4647	80 0.4967	75 0.5316		138 0.1020 $N^{0.106}$ 32	229 0.4080	226 0.4505				147 0.0961 $N^{0.108}$ 16
11	AYONIX-002	202 0.2189	166 0.2603				132 0.0175 $N^{0.189}$ 56	223 0.2935	222 0.3414	120 0.3736	115 0.4101	112 0.4465	144 0.0440 $N^{0.143}$ 31
12	CAMVI-003	125 0.0141	139 0.0365	69 0.0525	72 0.1788		3 0.0000 $N^{1.084}$ 143	149 0.0199	174 0.0520				2 0.0000 $N^{1.048}$ 149
13	CAMVI-004	99 0.0081	137 0.0324				1 0.0000 $N^{1.514}$ 144	124 0.0124	171 0.0468	114 0.0719	114 0.2363	111 0.2367	1 0.0000 $N^{1.055}$ 150
14	COGENT-000	113 0.0100	100 0.0102	52 0.0106	47 0.0111	42 0.0119	120 0.0045 $N^{0.059}$ 17	113 0.0101	101 0.0105	86 0.0136	78 0.0141	68 0.0125	127 0.0037 $N^{0.075}$ 8
15	COGENT-001	114 0.0100	101 0.0102				124 0.0071 $N^{0.026}$ 11	114 0.0101	102 0.0105	85 0.0136	79 0.0141	69 0.0125	128 0.0037 $N^{0.075}$ 9
16	COGENT-002	19 0.0019	19 0.0024	12 0.0029	13 0.0034	14 0.0040	29 0.0001 $N^{0.251}$ 85	35 0.0029	37 0.0036	29 0.0041	30 0.0049	31 0.0059	34 0.0001 $N^{0.244}$ 82
17	COGENT-003	31 0.0029	30 0.0034	21 0.0038	21 0.0045	21 0.0052	52 0.0002 $N^{0.208}$ 68	41 0.0031	39 0.0038	33 0.0043	34 0.0051	34 0.0060	45 0.0001 $N^{0.230}$ 72
18	COGNITEC-000	126 0.0142	121 0.0186				63 0.0003 $N^{0.291}$ 108	147 0.0195	146 0.0252	106 0.0323	104 0.0378	100 0.0417	103 0.0006 $N^{0.258}$ 93
19	COGNITEC-001	85 0.0065	86 0.0086	51 0.0103	50 0.0124	47 0.0150	48 0.0001 $N^{0.284}$ 103	106 0.0090	108 0.0117	94 0.0165	91 0.0192	86 0.0199	75 0.0002 $N^{0.271}$ 102
20	COGNITEC-002	33 0.0032	40 0.0040	31 0.0049	31 0.0058	30 0.0071	33 0.0001 $N^{0.271}$ 94	67 0.0048	64 0.0057	52 0.0067	51 0.0079	53 0.0094	69 0.0002 $N^{0.232}$ 73
21	COGNITEC-003	46 0.0037	49 0.0045	35 0.0052	34 0.0061	33 0.0075	49 0.0001 $N^{0.240}$ 82	71 0.0053	68 0.0062	55 0.0072	54 0.0085	55 0.0100	79 0.0003 $N^{0.222}$ 64
22	CYBERLINK-000	72 0.0049	62 0.0053				107 0.0014 $N^{0.091}$ 24	48 0.0034	42 0.0040	36 0.0046	36 0.0054	36 0.0063	67 0.0002 $N^{0.209}$ 58
23	CYBERLINK-001	58 0.0043	52 0.0047				101 0.0011 $N^{0.101}$ 29	39 0.0030	34 0.0035	31 0.0042	32 0.0050	33 0.0060	35 0.0001 $N^{0.243}$ 81
24	DAHUA-001	50 0.0038	53 0.0048				44 0.0001 $N^{0.251}$ 86	73 0.0053	72 0.0067	58 0.0079	60 0.0093	61 0.0112	60 0.0002 $N^{0.256}$ 91
25	DAHUA-002	42 0.0035	34 0.0037	19 0.0038	18 0.0040	15 0.0042	109 0.0015 $N^{0.063}$ 18	18 0.0017	14 0.0018	9 0.0021	7 0.0023	7 0.0027	66 0.0002 $N^{0.156}$ 35
26	DEEPSEA-001	63 0.0044	60 0.0051				81 0.0005 $N^{0.163}$ 44	47 0.0033	48 0.0043	42 0.0052	46 0.0065	47 0.0081	16 0.0001 $N^{0.311}$ 135
27	DERMALOG-004	172 0.0757	153 0.0958	76 0.1102	71 0.1257		119 0.0037 $N^{0.227}$ 76	192 0.1017	191 0.1251				133 0.0050 $N^{0.226}$ 68
28	DERMALOG-005	97 0.0080	104 0.0110				30 0.0001 $N^{0.357}$ 137	121 0.0114	122 0.0149	95 0.0201	98 0.0289	103 0.0447	7 0.0000 $N^{0.470}$ 147
29	DERMALOG-006	77 0.0053	67 0.0058				108 0.0015 $N^{0.095}$ 25	91 0.0075	85 0.0081	65 0.0086	61 0.0093	57 0.0104	119 0.0017 $N^{0.109}$ 17
30	DERMALOG-007						-	98 0.0080	93 0.0092	72 0.0102		73 0.0140	102 0.0006 $N^{0.192}$ 49
31	EYEDEA-003	168 0.0477	149 0.0610	72 0.0714	68 0.0827		112 0.0018 $N^{0.247}$ 84	185 0.0638	185 0.0800				121 0.0024 $N^{0.247}$ 85
32	F8-001	215 0.5359	175 0.5362				141 0.5316 $N^{0.001}$ 6	119 0.0113	113 0.0120	77 0.0120	70 0.0120	66 0.0120	135 0.0090 $N^{0.019}$ 3
33	GLORY-001	178 0.0815	152 0.0929	74 0.1004	70 0.1088		131 0.0146 $N^{0.129}$ 39	197 0.1130	193 0.1268				142 0.0211 $N^{0.126}$ 25
34	GORILLA-002	112 0.0100	112 0.0134				43 0.0001 $N^{0.326}$ 131	133 0.0147	134 0.0197	98 0.0238	95 0.0288	97 0.0351	83 0.0003 $N^{0.295}$ 124
35	GORILLA-004	80 0.0056	75 0.0066	42 0.0075	39 0.0087	36 0.0101	72 0.0004 $N^{0.204}$ 64	68 0.0048	69 0.0063	56 0.0075	57 0.0091	63 0.0114	32 0.0001 $N^{0.292}$ 121
36	HIK-002	132 0.0152	119 0.0182	62 0.0206	60 0.0237	54 0.0269	102 0.0011 $N^{0.195}$ 60	122 0.0122	119 0.0147				108 0.0008 $N^{0.204}$ 57
37	HIK-003	101 0.0082	102 0.0105				61 0.0003 $N^{0.261}$ 88	107 0.0091	109 0.0117	93 0.0164	92 0.0194	87 0.0203	71 0.0002 $N^{0.274}$ 106
38	HIK-004	98 0.0080	97 0.0101	55 0.0119	53 0.0144	48 0.0174	58 0.0002 $N^{0.264}$ 89	104 0.0088	106 0.0113	91 0.0159	88 0.0188	85 0.0195	72 0.0002 $N^{0.271}$ 104
39	HIK-005	27 0.0025	26 0.0032	20 0.0038	23 0.0047		24 0.0001 $N^{0.283}$ 101	52 0.0036	52 0.0046	45 0.0053	45 0.0065	46 0.0081	30 0.0001 $N^{0.274}$ 107
40	IDEMIA-000	65 0.0045	69 0.0059	40 0.0073	40 0.0092	38 0.0113	27 0.0001 $N^{0.317}$ 123	86 0.0067	88 0.0088	82 0.0131	83 0.0153	77 0.0156	48 0.0001 $N^{0.287}$ 118
41	IDEMIA-001	67 0.0046	72 0.0062	43 0.0077	42 0.0097	44 0.0121	21 0.0001 $N^{0.334}$ 133	88 0.0070	90 0.0090	84 0.0135	84 0.0162	82 0.0168	40 0.0001 $N^{0.303}$ 130
42	IDEMIA-002	93 0.0072	91 0.0096	53 0.0116	55 0.0145	51 0.0180	40 0.0001 $N^{0.312}$ 119	97 0.0079	99 0.0100				80 0.0003 $N^{0.252}$ 89
43	IDEMIA-003	51 0.0038	59 0.0051				22 0.0001 $N^{0.318}$ 125	74 0.0054	76 0.0069	74 0.0110	72 0.0127	67 0.0122	43 0.0001 $N^{0.280}$ 113
44	IDEMIA-004	52 0.0039	55 0.0049	37 0.0058	36 0.0071	35 0.0085	39 0.0001 $N^{0.270}$ 93	77 0.0054	71 0.0066	59 0.0079	64 0.0097	65 0.0117	47 0.0001 $N^{0.270}$ 100
45	IDEMIA-005	61 0.0044	68 0.0059	39 0.0070	38 0.0085	37 0.0104	34 0.0001 $N^{0.293}$ 110	83 0.0064	84 0.0081	70 0.0097	69 0.0118	75 0.0143	52 0.0002 $N^{0.277}$ 111
46	IDEMIA-006	75 0.0052	76 0.0067	45 0.0080	43 0.0097	41 0.0115	45 0.0001 $N^{0.272}$ 95	94 0.0076	97 0.0096	76 0.0113	76 0.0135	80 0.0161	73 0.0002 $N^{0.259}$ 94
47	IDEMIA-007	48 0.0037	41 0.0041	27 0.0044	25 0.0048	22 0.0054	89 0.0007 $N^{0.125}$ 38	22 0.0021	26 0.0026	20 0.0030	20 0.0036	24 0.0044	21 0.0001 $N^{0.250}$ 87
48	IMAGUS-002	192 0.1467	162 0.1830	72 0.2083	73 0.2377		127 0.0083 $N^{0.216}$ 71	212 0.1817	212 0.2203				138 0.0109 $N^{0.210}$ 60
49	IMPERIAL-000	55 0.0040	42 0.0041	26 0.0043	22 0.0046	19 0.0048	110 0.0016 $N^{0.068}$ 19	29 0.0022	25 0.0024	18 0.0027	18 0.0030	18 0.0035	78 0.0003 $N^{0.157}$ 36
50	INCODE-001	107 0.0096	109 0.0128	66 0.0283	65 0.0463		4 0.0000 $N^{0.737}$ 141	125 0.0128	125 0.0166				82 0.0003 $N^{0.286}$ 116
51	INCODE-003	84 0.0065	88 0.0086				38 0.0001 $N^{0.313}$ 120	111 0.0098	115 0.0129	89 0.0154	90 0.0191	89 0.0233	63 0.0002 $N^{0.296}$ 125
52	INCODE-004	60 0.0044	56 0.0049				99 0.0009 $N^{0.117}$ 35	37 0.0029	35 0.0035	30 0.0041	31 0.0049	32 0.0060	33 0.0001 $N^{0.244}$ 83
53	INNOVATRICS-004	87 0.0067	80 0.0078				90 0.0007 $N^{0.167}$ 49	108 0.0093	114 0.0123	83 0.0132	73 0.0132	71 0.0132	123 0.0024 $N^{0.110}$ 19
54	INNOVATRICS-005						-	23 0.0021	24 0.0024	19 0.0028	19 0.0031		91 0.0004 $N^{0.136}$ 30
55	INTSYSMSU-000	186 0.1237	157 0.1291				135 0.0670 $N^{0.046}$ 16	199 0.1395	197 0.1457	116 0.1498	111 0.1544	108 0.1591	146 0.0768 $N^{0.045}$ 4
56	ISYSTEMS-000	91 0.0071	85 0.0082	48 0.0091	46 0.0102	40 0.0115	93 0.0008 $N^{0.166}$ 47	110 0.0096	104 0.0110				113 0.0013 $N^{0.149}$ 34
57	ISYSTEMS-001	92 0.0071	84 0.0082	47 0.0091	45 0.0101	39 0.0115	95 0.0008 $N^{0.164}$ 45	109 0.0096	103 0.0110				114 0.0013 $N^{0.148}$ 33
58	ISYSTEMS-002	47 0.0037	46 0.0044	32 0.0049			67 0.0003 $N^{0.183}$ 54	72 0.0053	70 0.0064	69 0.0096	67 0.0108	54 0.0096	88 0.0003 $N^{0.204}$ 54
59	ISYSTEMS-003	36 0.0033	35 0.0037	25 0.0041	24 0.0048	23 0.0054	66 0.0003 $N^{0.174}$ 53	63 0.0046	60 0.0052	47 0.0057	47 0.0066	44 0.0076	97 0.0004 $N^{0.174}$ 42
60	KEDACOM-001	110 0.0097	95 0.0099				126 0.0077 $N^{0.017}$ 8	93 0.0076	80 0.0077	60 0.0079	53 0.0083	48 0.0087	130 0.0040 $N^{0.047}$ 5
61	KNERON-000						-	66 0.0048	65 0.0059	53 0.0067	52 0.0079	52 0.0093	70 0.0002 $N^{0.226}$ 69
62	LOOKMAN-003	100 0.0082	87 0.0086				121 0.0046 $N^{0.044}$ 15	101 0.0083	89 0.0088	67 0.0091	62 0.0096	58 0.0104	126 0.0030 $N^{0.076}$ 10
63	LOOKMAN-005	111 0.0100	98 0.0102				125 0.0073 $N^{0.023}$ 10	95 0.0078	83 0.0080	63 0.0083	55 0.0086	50 0.0092	129 0.0038 $N^{0.053}$ 7
64	MEGVII-000	90 0.0070	93 0.0097	57 0.0121	56 0.0147	50 0.0179	37 0.0001 $N^{0.321}$ 126	78 0.0055	79 0.0073	75 0.0111	75 0.0134	74 0.0140	24 0.0001 $N^{0.318}$ 137
65	MEGVII-001						-	117 0.0105	110 0.0118	81 0.0128	80 0.0142	79 0.0161	117 0.0015 $N^{0.143}$ 32
66	MICROFOCUS-003	211 0.4789	176 0.5387	81 0.5770			137 0.0950 $N^{0.121}$ 37	231 0.5405	229 0.5942				148 0.1358 $N^{0.103}$ 15
67	MICROFOCUS-005	206 0.3152	170 0.3699				133 0.0306 $N^{0.174}$ 52	226 0.3700	224 0.4242	121 0.4610	116 0.5000	113 0.5391	145 0.0674 $N^{0.128}$ 27
68	MICROSOFT-000	20 0.0020	20 0.0025	14 0.0030	17 0.0038	18 0.0046	17 0.0000 $N^{0.293}$ 111	42 0.0031	40 0.0038	51 0.0066	50 0.0077	39 0.0068	23 0.0001 $N^{0.275}$ 108
69	MICROSOFT-001	17 0.0019	18 0.0024	13 0.0029	14 0.0036	16 0.0045	14 0.0000 $N^{0.298}$ 115	36 0.0029	36 0.0035				39 0.0001 $N^{0.238}$ 77
70	MICROSOFT-002	21 0.0021	22 0.0028	16 0.0033	19 0.0040	20 0.0049	20 0.0000 $N^{0.283}$ 102	43 0.0031	43 0.0040				31 0.0001 $N^{0.260}$ 96
71	MICROSOFT-003	3 0.0008	4 0.0011				15 0.0000 $N^{0.239}$ 81	5 0.0013	7 0.0016	25 0.0035	24 0.0039	11 0.0028	13 0.0000 $N^{0.276}$ 110
72	MICROSOFT-004	2 0.0008	2 0.0010	3 0.0012	4 0.0015	4 0.0018	9 0.0000 $N^{0.290}$ 105	4 0.0012	5 0.0015	23 0.0034	23 0.0038	10 0.0028	11 0.0000 $N^{0.288}$ 119

Table 12: **Investigation-mode: Effect of N on FNIR at rank 1** *For five enrollment population sizes, N, with T = 0 and FPIR = 1. The left five columns apply for consolidated enrollment of a variable number of lifetime images from each subject. The right five columns apply for enrollment of one recent image. Missing entries usually apply because another algorithm from the same developer was run instead. Some developers are missing because less accurate algorithms were not run on galleries with $N > 1\,600\,000$. Throughout blue superscripts indicate the rank of the algorithm for that column, and yellow highlighting indicates the most accurate value. Caution: The Power-low models are mostly intended to draw attention to the kind of behavior, not as a model to be used for prediction.*

MISSES NOT AT RANK 1 FNIR(N, T= 0, R =1)		ENROL LIFETIME DATASET: FRVT 2018						ENROL MOST RECENT DATASET: FRVT 2018					
#	ALGORITHM	N=0.64M	N=1.6M	N=3.0M	N=6.0M	N=12.0M	aN^b	N=0.64M	N=1.6M	N=3.0M	N=6.0M	N=12.0M	aN^b
73	MICROSOFT-005	5 0.0010	7 0.0013	7 0.0015	7 0.0019	8 0.0024	8 0.0000 N^0.310 118	10 0.0015	16 0.0019	12 0.0023	16 0.0030	20 0.0037	8 0.0000 N^0.320 138
74	MICROSOFT-006	6 0.0010	8 0.0013	8 0.0016	8 0.0020	9 0.0025	7 0.0000 N^0.321 127	12 0.0016	17 0.0020	15 0.0025	17 0.0030	21 0.0038	12 0.0000 N^0.305 132
75	NEC-000	106 0.0094	108 0.0124	60 0.0151	58 0.0181	52 0.0219	54 0.0002 N^0.290 107	127 0.0131	126 0.0170	97 0.0229	94 0.0270	91 0.0294	86 0.0003 N^0.276 109
76	NEC-001	124 0.0133	117 0.0160				96 0.0008 N^0.206 66	142 0.0180	138 0.0209	101 0.0259	99 0.0292	93 0.0304	118 0.0016 N^0.179 46
77	NEC-002	4 0.0009	3 0.0010	2 0.0010	1 0.0011	1 0.0012	60 0.0002 N^0.098 27	1 0.0009	2 0.0010	2 0.0011	2 0.0012	2 0.0013	68 0.0002 N^0.113 23
78	NEC-003	8 0.0011	6 0.0012	4 0.0012	3 0.0013	2 0.0014	77 0.0004 N^0.076 22	6 0.0013	4 0.0014	3 0.0015	3 0.0016	3 0.0016	98 0.0005 N^0.079 11
79	NEUROTECHNOLOGY-003	130 0.0157	124 0.0196				86 0.0007 N^0.238 80	141 0.0179	141 0.0225	103 0.0288	100 0.0331	98 0.0361	106 0.0007 N^0.239 79
80	NEUROTECHNOLOGY-004	69 0.0046	63 0.0055	38 0.0062	37 0.0072	34 0.0084	65 0.0003 N^0.204 63	64 0.0046	61 0.0056	66 0.0090	65 0.0100	49 0.0088	74 0.0002 N^0.221 63
81	NEUROTECHNOLOGY-005	35 0.0032	39 0.0039	23 0.0040	26 0.0050	24 0.0058	59 0.0002 N^0.194 59	51 0.0035	47 0.0043	39 0.0049	39 0.0057	38 0.0068	61 0.0002 N^0.223 66
82	NEUROTECHNOLOGY-007	71 0.0048	184 1.0000	36 0.0057	35 0.0064	31 0.0072	144 20.0319 N^-0.476 1	45 0.0032	41 0.0039	34 0.0044	35 0.0052	35 0.0062	56 0.0002 N^0.222 65
83	NEWLAND-002						-	186 0.0646	184 0.0786	115 0.0889	110 0.1015		131 0.0044 N^0.202 52
84	NOBLIS-002	187 0.1257	161 0.1562				122 0.0053 N^0.237 79	203 0.1486	204 0.1794	118 0.2018	113 0.2356		132 0.0097 N^0.204 55
85	NTECHLAB-000	78 0.0054	79 0.0075	49 0.0092	48 0.0113	46 0.0139	31 0.0001 N^0.328 132	89 0.0071	95 0.0094	88 0.0137	85 0.0164	83 0.0173	41 0.0001 N^0.303 131
86	NTECHLAB-001	88 0.0069	90 0.0095	54 0.0117	52 0.0144	49 0.0177	36 0.0001 N^0.322 128	105 0.0088	112 0.0119				37 0.0001 N^0.323 140
87	NTECHLAB-003	43 0.0036	58 0.0050				13 0.0000 N^0.360 138	65 0.0046	66 0.0062	68 0.0096	68 0.0115	62 0.0114	22 0.0001 N^0.308 134
88	NTECHLAB-004	30 0.0028	37 0.0038	29 0.0047	33 0.0059	32 0.0073	16 0.0000 N^0.323 130	54 0.0037	57 0.0048	57 0.0078	58 0.0092	60 0.0107	19 0.0001 N^0.297 126
89	NTECHLAB-005	29 0.0027	36 0.0038				10 0.0000 N^0.369 139	49 0.0035	54 0.0047	48 0.0058	48 0.0073	51 0.0092	15 0.0000 N^0.334 143
90	NTECHLAB-006	24 0.0023	28 0.0033	24 0.0041	27 0.0051	27 0.0064	11 0.0000 N^0.350 136	38 0.0030	46 0.0041	41 0.0050	42 0.0062	45 0.0078	14 0.0000 N^0.326 141
91	NTECHLAB-007	53 0.0039	45 0.0043	28 0.0047	28 0.0052	25 0.0058	84 0.0006 N^0.136 41	26 0.0022	27 0.0027	21 0.0031	21 0.0037	25 0.0044	26 0.0001 N^0.245 84
92	NTECHLAB-008	38 0.0034	33 0.0037	22 0.0039	20 0.0042	17 0.0045	100 0.0009 N^0.097 26	8 0.0014	9 0.0017	7 0.0020	9 0.0024	8 0.0027	20 0.0001 N^0.224 67
93	PARAVISION-000	83 0.0063	118 0.0165				2 0.0000 N^1.043 142	100 0.0082	131 0.0188	107 0.0348			3 0.0000 N^0.910 148
94	PARAVISION-001	22 0.0022	21 0.0026				41 0.0001 N^0.218 72	40 0.0030	38 0.0038	50 0.0061			38 0.0001 N^0.242 80
95	PARAVISION-003	18 0.0019	17 0.0022	11 0.0025	11 0.0027		55 0.0002 N^0.167 50	32 0.0026	31 0.0031	24 0.0035	25 0.0042	27 0.0048	53 0.0002 N^0.210 59
96	PARAVISION-004	40 0.0034	32 0.0035	18 0.0036	16 0.0037	12 0.0039	115 0.0020 N^0.040 14	11 0.0015	8 0.0016	6 0.0017	6 0.0019	5 0.0021	87 0.0003 N^0.111 20
97	PARAVISION-005	37 0.0034	31 0.0034	17 0.0035	15 0.0037	11 0.0038	114 0.0019 N^0.040 13	9 0.0015	6 0.0015	5 0.0016	5 0.0018	4 0.0019	96 0.0004 N^0.094 14
98	PIXELALL-002	89 0.0069	82 0.0080				91 0.0007 N^0.166 48	56 0.0037	50 0.0045	43 0.0052	44 0.0062	43 0.0075	51 0.0002 N^0.238 78
99	PIXELALL-003	62 0.0044	50 0.0047				111 0.0018 N^0.069 20	20 0.0019	19 0.0021	13 0.0024	12 0.0028	16 0.0032	57 0.0002 N^0.182 47
100	QUANTASOFT-001	220 0.9857	180 0.9857				143 0.9857 N^-0.000 2	218 0.2177	211 0.2177	119 0.2177		109 0.2177	149 0.2177 N^0.000 1
101	RANKONE-000	151 0.0252	135 0.0316	67 0.0362	64 0.0422	56 0.0482	104 0.0013 N^0.222 75	172 0.0349	167 0.0429	113 0.0514	109 0.0564	107 0.0629	124 0.0024 N^0.200 51
102	RANKONE-001	130 0.0149	123 0.0191	63 0.0221	61 0.0257	55 0.0299	85 0.0006 N^0.236 78	150 0.0200	140 0.0221				132 0.0046 N^0.110 18
103	RANKONE-002	119 0.0113	113 0.0146				62 0.0003 N^0.275 97	137 0.0155	132 0.0194	100 0.0250	96 0.0288	94 0.0304	104 0.0007 N^0.229 70
104	RANKONE-003	120 0.0113	114 0.0146	61 0.0168	59 0.0197	53 0.0232	79 0.0005 N^0.242 83	138 0.0155	133 0.0194	99 0.0250	97 0.0288	95 0.0304	105 0.0007 N^0.229 71
105	RANKONE-004	148 0.0243	134 0.0315				82 0.0005 N^0.285 104	167 0.0326	166 0.0415	112 0.0483			111 0.0011 N^0.255 90
106	RANKONE-005	79 0.0054	78 0.0069	46 0.0083	44 0.0099	43 0.0119	50 0.0001 N^0.269 92	92 0.0075	96 0.0094	73 0.0110	74 0.0132	78 0.0156	77 0.0003 N^0.251 88
107	RANKONE-007	59 0.0044	54 0.0048	34 0.0052	30 0.0057	26 0.0064	92 0.0008 N^0.129 40	34 0.0028	32 0.0034	26 0.0038	28 0.0045	29 0.0053	58 0.0002 N^0.211 61
108	REALNETWORKS-000	161 0.0334	142 0.0440	68 0.0524			88 0.0007 N^0.292 109	162 0.0306	165 0.0402				100 0.0006 N^0.298 128
109	REALNETWORKS-002	146 0.0238	136 0.0318				71 0.0004 N^0.315 121	160 0.0299	159 0.0393	111 0.0470	108 0.0562	106 0.0580	115 0.0013 N^0.236 76
110	REALNETWORKS-003	137 0.0166	128 0.0216				69 0.0003 N^0.290 106	143 0.0183	144 0.0242	104 0.0291	102 0.0352	102 0.0423	94 0.0004 N^0.287 117
111	REALNETWORKS-004	129 0.0146	122 0.0188				68 0.0003 N^0.281 100	140 0.0175	142 0.0236	102 0.0284	101 0.0347	99 0.0416	89 0.0003 N^0.295 123
112	REMARKAI-000	57 0.0042	51 0.0047				97 0.0009 N^0.118 36	33 0.0027	33 0.0034	27 0.0040	29 0.0048	30 0.0058	28 0.0001 N^0.260 95
113	REMARKAI-002	64 0.0045	70 0.0060				26 0.0001 N^0.322 129	82 0.0062	86 0.0081	71 0.0098	71 0.0121		36 0.0001 N^0.298 127
114	SCANOVATE-000	216 0.7782	177 0.7786	82 0.7787	76 0.7787	57 0.7787	142 0.7766 N^0.000 3	57 0.0038	58 0.0050	49 0.0059	49 0.0073	42 0.0073	59 0.0002 N^0.235 75
115	SENSETIME-000	13 0.0015	12 0.0016				73 0.0004 N^0.104 31	25 0.0022	21 0.0023	17 0.0026	14 0.0028	13 0.0032	90 0.0003 N^0.135 29
116	SENSETIME-001	12 0.0015	11 0.0016				74 0.0004 N^0.100 28	24 0.0022	22 0.0023	16 0.0025	15 0.0029	19 0.0037	64 0.0002 N^0.177 44
117	SENSETIME-002	122 0.0120	107 0.0120	56 0.0121	49 0.0122	45 0.0123	130 0.0107 N^0.008 7	130 0.0136	118 0.0137	87 0.0137	77 0.0138	72 0.0139	140 0.0124 N^0.007 2
118	SENSETIME-003	32 0.0030	24 0.0030	15 0.0031	12 0.0031	10 0.0032	116 0.0022 N^0.022 9	2 0.0010	1 0.0010	1 0.0010	1 0.0011	1 0.0012	85 0.0003 N^0.085 13
119	SHAMAN-003	179 0.0805	154 0.0966	75 0.1088			123 0.0059 N^0.195 61	194 0.1050	189 0.1243				136 0.0090 N^0.184 48
120	SHAMAN-007	154 0.0286	132 0.0307				129 0.0104 N^0.076 21	174 0.0371	162 0.0396	110 0.0416	106 0.0443	104 0.0473	139 0.0122 N^0.083 12
121	SIAT-001	204 0.2636	167 0.2637	78 0.2638			140 0.2618 N^0.001 5	17 0.0017	11 0.0018	28 0.0041	26 0.0044	9 0.0027	50 0.0001 N^0.178 45
122	SIAT-002	201 0.2126	165 0.2127				130 0.2114 N^0.000 4	16 0.0016	12 0.0018	32 0.0042	27 0.0045	6 0.0027	55 0.0002 N^0.173 41
123	SMILART-004	218 0.8188	178 0.9530				136 0.0893 N^0.166 46	235 0.9174	233 0.9648	122 0.9908			150 0.4696 N^0.050 6
124	SYNESIS-003	183 0.1130	159 0.1347				128 0.0087 N^0.191 57	203 0.1456	202 0.1700	117 0.1876	112 0.2088	110 0.2317	141 0.0177 N^0.158 37
125	SYNESIS-003						-	139 0.0161	124 0.0162	92 0.0163	86 0.0165	90 0.0254	125 0.0027 N^0.127 26
126	TECH5-001	73 0.0049	65 0.0055				94 0.0008 N^0.137 42	44 0.0032	44 0.0040	38 0.0047	38 0.0057	41 0.0071	27 0.0001 N^0.271 105
127	TEVIAN-004	81 0.0056	81 0.0078	50 0.0095			23 0.0001 N^0.345 135	103 0.0085	105 0.0113				46 0.0001 N^0.306 133
128	TEVIAN-005	54 0.0039	61 0.0052				28 0.0001 N^0.305 117	79 0.0056	78 0.0073	64 0.0084	66 0.0105	70 0.0130	42 0.0001 N^0.283 115
129	TIGER-000	163 0.0361	144 0.0478	70 0.0562	67 0.0675		98 0.0009 N^0.279 98	178 0.0472	179 0.0616				109 0.0010 N^0.289 120
130	TIGER-002	34 0.0032	43 0.0042				25 0.0001 N^0.299 116	61 0.0044	62 0.0056	54 0.0068	56 0.0086	59 0.0105	25 0.0001 N^0.299 129
131	TONGYITRANS-001	105 0.0092	103 0.0110	58 0.0124	54 0.0144		87 0.0007 N^0.197 62	75 0.0054	74 0.0069				49 0.0001 N^0.269 99
132	TOSHIBA-000	25 0.0023	25 0.0031				19 0.0000 N^0.298 114	50 0.0035	49 0.0045	44 0.0052	41 0.0061	76 0.0154	5 0.0000 N^0.449 146
133	VD-000	208 0.3580	172 0.4301	79 0.4774	74 0.5279		134 0.0354 N^0.174 51	228 0.4058	227 0.4737				143 0.0423 N^0.169 39
134	VD-001	142 0.0180	129 0.0218				103 0.0012 N^0.204 65	153 0.0230	149 0.0276	105 0.0315	103 0.0363	101 0.0418	116 0.0015 N^0.204 56
135	VIGILANTSOLUTIONS-003	165 0.0407	148 0.0545	71 0.0651	66 0.0651		117 0.0023 N^0.220 74	183 0.0535	182 0.0694				112 0.0012 N^0.283 114
136	VISIONLABS-003	41 0.0035	57 0.0049	41 0.0074	51 0.0128		5 0.0000 N^0.576 140	70 0.0051	73 0.0068	79 0.0124	87 0.0185		18 0.0001 N^0.323 139
137	VISIONLABS-004	14 0.0015	15 0.0019				32 0.0001 N^0.218 73	27 0.0022	28 0.0027	40 0.0049	43 0.0062	40 0.0070	6 0.0000 N^0.406 144
138	VISIONLABS-005	11 0.0014	13 0.0017	10 0.0019	10 0.0026	13 0.0039	6 0.0000 N^0.345 134	21 0.0020	23 0.0024	35 0.0046	37 0.0054	28 0.0051	10 0.0000 N^0.332 142
139	VISIONLABS-006	10 0.0012	10 0.0014				53 0.0002 N^0.140 43	15 0.0016	13 0.0018	11 0.0022	13 0.0028	22 0.0041	9 0.0000 N^0.314 136
140	VISIONLABS-007	9 0.0012	9 0.0014	6 0.0015	6 0.0018	6 0.0021	35 0.0001 N^0.189 55	14 0.0016	10 0.0018	8 0.0020	8 0.0023	17 0.0034	17 0.0001 N^0.248 86
141	VISIONLABS-008	40 0.0038	38 0.0039				118 0.0025 N^0.032 12	19 0.0019	18 0.0020	10 0.0021	10 0.0025	13 0.0030	62 0.0002 N^0.169 38
142	VOCORD-003	74 0.0050	74 0.0064	44 0.0077	41 0.0094		42 0.0001 N^0.279 99	69 0.0049	67 0.0062				44 0.0001 N^0.268 98
143	VOCORD-005	68 0.0046	64 0.0055				70 0.0003 N^0.193 58	81 0.0060	77 0.0070	61 0.0082	63 0.0097	64 0.0117	76 0.0003 N^0.232 74
144	YISHENG-001	131 0.0152	126 0.0205	65 0.0245	63 0.0295		64 0.0003 N^0.297 113	151 0.0203	148 0.0265				95 0.0004 N^0.293 122

Table 13: **Investigation-mode: Effect of N on FNIR at rank 1** *For five enrollment population sizes, N, with T = 0 and FPIR = 1. The left five columns apply for consolidated enrollment of a variable number of lifetime images from each subject. The right five columns apply for enrollment of one recent image. Missing entries usually apply because another algorithm from the same developer was run instead. Some developers are missing because less accurate algorithms were not run on galleries with N > 1 600 000. Throughout blue superscripts indicate the rank of the algorithm for that column, and yellow highlighting indicates the most accurate value. Caution: The Power-low models are mostly intended to draw attention to the kind of behavior, not as a model to be used for prediction.*

MISSES NOT AT RANK 1		ENROL LIFETIME						ENROL MOST RECENT					
FNIR(N, T= 0, R =1)		DATASET: FRVT 2018						DATASET: FRVT 2018					
#	ALGORITHM	N=0.64M	N=1.6M	N=3.0M	N=6.0M	N=12.0M	aN^b	N=0.64M	N=1.6M	N=3.0M	N=6.0M	N=12.0M	aN^b
145	YITU-000	[45] 0.0037	[47] 0.0044	[33] 0.0050	[32] 0.0058	[29] 0.0068	[56] 0.0002 $N^{0.212}$ [70]	[59] 0.0040	[55] 0.0047	[62] 0.0082	[59] 0.0092	[56] 0.0103	[84] 0.0003 $N^{0.195}$ [50]
146	YITU-001	[44] 0.0036	[44] 0.0043	[30] 0.0048	[29] 0.0056	[28] 0.0066	[57] 0.0002 $N^{0.206}$ [67]	[58] 0.0039	[51] 0.0045				[92] 0.0004 $N^{0.177}$ [43]
147	YITU-002	[7] 0.0010	[5] 0.0012	[5] 0.0014	[5] 0.0016	[5] 0.0020	[18] 0.0000 $N^{0.233}$ [77]	[13] 0.0016	[15] 0.0018	[37] 0.0047	[33] 0.0050	[12] 0.0029	[29] 0.0001 $N^{0.217}$ [62]
148	YITU-003	[16] 0.0019	[16] 0.0021				[78] 0.0004 $N^{0.112}$ [33]	[31] 0.0026	[30] 0.0029	[46] 0.0057	[40] 0.0061	[37] 0.0065	[101] 0.0006 $N^{0.111}$ [21]
149	YITU-004	[1] 0.0007	[1] 0.0008	[1] 0.0010	[2] 0.0012	[3] 0.0016	[12] 0.0000 $N^{0.254}$ [87]	[3] 0.0011	[3] 0.0013	[4] 0.0015	[4] 0.0017	[26] 0.0047	[4] 0.0000 $N^{0.438}$ [145]
150	YITU-005	[15] 0.0016	[14] 0.0017	[9] 0.0018	[9] 0.0020	[7] 0.0022	[75] 0.0004 $N^{0.104}$ [30]	[28] 0.0022	[20] 0.0023	[14] 0.0025	[11] 0.0027	[14] 0.0031	[99] 0.0005 $N^{0.113}$ [22]

Table 14: **Investigation-mode: Effect of N on FNIR at rank 1** *For five enrollment population sizes, N, with T = 0 and FPIR = 1. The left five columns apply for consolidated enrollment of a variable number of lifetime images from each subject. The right five columns apply for enrollment of one recent image. Missing entries usually apply because another algorithm from the same developer was run instead. Some developers are missing because less accurate algorithms were not run on galleries with $N > 1\,600\,000$. Throughout blue superscripts indicate the rank of the algorithm for that column, and yellow highlighting indicates the most accurate value. Caution: The Power-low models are mostly intended to draw attention to the kind of behavior, not as a model to be used for prediction.*

MISSES NOT AT RANK 50 FNIR(N, T= 0, R =50)		ENROL LIFETIME DATASET: FRVT 2018						ENROL MOST RECENT DATASET: FRVT 2018					
#	ALGORITHM	N=0.64M	N=1.6M	N=3.0M	N=6.0M	N=12.0M	aN^b	N=0.64M	N=1.6M	N=3.0M	N=6.0M	N=12.0M	aN^b
1	3DIVI-003	155 0.0100	142 0.0148	71 0.0189	67 0.0238		38 0.0001 $N^{0.389}$ 135	168 0.0133	172 0.0191				34 0.0001 $N^{0.399}$ 140
2	3DIVI-005	78 0.0028	86 0.0035				60 0.0001 $N^{0.249}$ 97	117 0.0040	111 0.0049	80 0.0057	82 0.0068	85 0.0081	62 0.0002 $N^{0.240}$ 98
3	ALCHERA-000	142 0.0071	124 0.0074	63 0.0077	60 0.0098		96 0.0011 $N^{0.136}$ 67	162 0.0101	153 0.0105				138 0.0058 $N^{0.041}$ 15
4	ALCHERA-003	80 0.0028	98 0.0038				25 0.0000 $N^{0.317}$ 115	94 0.0027	90 0.0032	62 0.0035	63 0.0042	65 0.0048	66 0.0002 $N^{0.199}$ 85
5	ALLGOVISION-000	138 0.0066	121 0.0069				122 0.0030 $N^{0.059}$ 41	141 0.0063	132 0.0067	90 0.0071	86 0.0075	84 0.0081	125 0.0020 $N^{0.086}$ 41
6	ANKE-000	62 0.0021	70 0.0027				47 0.0001 $N^{0.255}$ 100	103 0.0032	103 0.0040	70 0.0046	70 0.0056	76 0.0066	53 0.0001 $N^{0.247}$ 101
7	ANKE-002	105 0.0035	91 0.0036				113 0.0026 $N^{0.024}$ 24	45 0.0016	42 0.0017	25 0.0017	21 0.0018	22 0.0019	100 0.0006 $N^{0.067}$ 33
8	AWARE-003	111 0.0036	111 0.0047	59 0.0058	58 0.0073		35 0.0001 $N^{0.316}$ 113	131 0.0055	139 0.0075	104 0.0118	102 0.0139	102 0.0143	39 0.0001 $N^{0.325}$ 127
9	AWARE-005	114 0.0038	113 0.0049				54 0.0001 $N^{0.284}$ 108	139 0.0062	146 0.0082	101 0.0101	100 0.0128	86 0.0089	105 0.0007 $N^{0.169}$ 75
10	AYONIX-000	207 0.1720	172 0.2139	79 0.2464	75 0.2847		132 0.0085 $N^{0.226}$ 92	229 0.1946	229 0.2381				143 0.0102 $N^{0.221}$ 91
11	AYONIX-002	197 0.0643	162 0.0870				89 0.0008 $N^{0.330}$ 118	221 0.0950	221 0.1274	120 0.1524	114 0.1828	111 0.2150	128 0.0023 $N^{0.279}$ 112
12	CAMVI-003	163 0.0139	153 0.0364	75 0.0524	73 0.1787		4 0.0000 $N^{1.088}$ 141	179 0.0196	194 0.0517				3 0.0000 $N^{1.059}$ 148
13	CAMVI-004	148 0.0077	151 0.0321				1 0.0000 $N^{1.559}$ 144	166 0.0117	191 0.0464	116 0.0715	115 0.2361	112 0.2364	2 0.0000 $N^{1.071}$ 149
14	COGENT-000	51 0.0017	52 0.0021	29 0.0024	29 0.0028	42 0.0042	22 0.0000 $N^{0.283}$ 107	74 0.0021	74 0.0024	75 0.0054	77 0.0062	89 0.0095	5 0.0000 $N^{0.539}$ 146
15	COGENT-001	50 0.0017	53 0.0021				57 0.0001 $N^{0.217}$ 89	75 0.0021	75 0.0024	76 0.0054	78 0.0062	90 0.0095	6 0.0000 $N^{0.539}$ 147
16	COGENT-002	16 0.0009	17 0.0010	15 0.0011	14 0.0013	13 0.0014	50 0.0001 $N^{0.180}$ 79	38 0.0014	36 0.0015	22 0.0017	25 0.0019	30 0.0021	67 0.0002 $N^{0.144}$ 67
17	COGENT-003	29 0.0011	29 0.0013	19 0.0015	19 0.0017	16 0.0020	45 0.0001 $N^{0.209}$ 85	41 0.0015	43 0.0017	34 0.0018	32 0.0020	35 0.0022	72 0.0002 $N^{0.143}$ 65
18	COGNITEC-000	106 0.0035	108 0.0047				41 0.0001 $N^{0.304}$ 110	126 0.0050	131 0.0065	102 0.0104	98 0.0123	98 0.0122	45 0.0001 $N^{0.307}$ 120
19	COGNITEC-001	60 0.0021	64 0.0025	39 0.0029	42 0.0033	41 0.0040	61 0.0001 $N^{0.221}$ 91	99 0.0030	97 0.0034	88 0.0066	83 0.0072	70 0.0054	64 0.0002 $N^{0.209}$ 88
20	COGNITEC-002	47 0.0017	43 0.0018	23 0.0019	22 0.0022	18 0.0024	72 0.0003 $N^{0.130}$ 66	85 0.0024	81 0.0026	48 0.0028	48 0.0030	49 0.0034	93 0.0005 $N^{0.117}$ 57
21	COGNITEC-003	59 0.0020	54 0.0022	28 0.0023	25 0.0025	22 0.0028	80 0.0005 $N^{0.109}$ 58	96 0.0028	88 0.0030	53 0.0032	54 0.0035	55 0.0037	108 0.0008 $N^{0.097}$ 47
22	CYBERLINK-000	117 0.0039	101 0.0040				112 0.0025 $N^{0.034}$ 32	71 0.0021	66 0.0022	43 0.0023	43 0.0025	44 0.0027	97 0.0006 $N^{0.092}$ 45
23	CYBERLINK-001	101 0.0034	88 0.0035				115 0.0026 $N^{0.020}$ 20	48 0.0016	46 0.0017	30 0.0018	29 0.0020	33 0.0022	87 0.0004 $N^{0.109}$ 52
24	DAHUA-001	56 0.0019	51 0.0021				84 0.0005 $N^{0.102}$ 57	93 0.0027	83 0.0029	52 0.0031	52 0.0034	57 0.0038	95 0.0005 $N^{0.121}$ 60
25	DAHUA-002	92 0.0033	82 0.0033	48 0.0033	44 0.0034	32 0.0034	116 0.0028 $N^{0.011}$ 13	31 0.0013	26 0.0013	15 0.0014	13 0.0014	14 0.0015	102 0.0007 $N^{0.043}$ 17
26	DEEPSEA-001	88 0.0032	81 0.0033				110 0.0023 $N^{0.024}$ 25	28 0.0012	29 0.0014	18 0.0015	18 0.0017	26 0.0020	58 0.0001 $N^{0.157}$ 73
27	DERMALOG-004	168 0.0184	148 0.0269	73 0.0338	70 0.0424		64 0.0001 $N^{0.374}$ 131	184 0.0240	187 0.0343				54 0.0001 $N^{0.390}$ 138
28	DERMALOG-005	137 0.0065	131 0.0091				32 0.0000 $N^{0.365}$ 129	159 0.0094	159 0.0122	110 0.0171	108 0.0254	107 0.0406	9 0.0000 $N^{0.505}$ 144
29	DERMALOG-006	125 0.0045	107 0.0046				126 0.0034 $N^{0.020}$ 21	140 0.0062	130 0.0063	85 0.0064	80 0.0065	77 0.0068	134 0.0043 $N^{0.028}$ 12
30	DERMALOG-007						-	128 0.0051	119 0.0054	78 0.0056		74 0.0063	126 0.0020 $N^{0.070}$ 34
31	EYEDEA-003	158 0.0110	144 0.0157	72 0.0206	68 0.0249		51 0.0001 $N^{0.370}$ 130	174 0.0150	173 0.0211				51 0.0001 $N^{0.372}$ 135
32	F8-001	215 0.5353	176 0.5354				141 0.5348 $N^{0.000}$ 4	160 0.0098	151 0.0099	100 0.0099	94 0.0099	92 0.0099	142 0.0093 $N^{0.004}$ 3
33	GLORY-001	187 0.0412	156 0.0486	76 0.0536	71 0.0596		128 0.0046 $N^{0.165}$ 73	208 0.0579	205 0.0673				141 0.0064 $N^{0.165}$ 74
34	GORILLA-002	64 0.0021	73 0.0028				23 0.0000 $N^{0.297}$ 109	102 0.0032	105 0.0041	72 0.0049	76 0.0062	83 0.0080	25 0.0000 $N^{0.315}$ 122
35	GORILLA-004	100 0.0034	90 0.0035	52 0.0038	49 0.0040	45 0.0043	95 0.0011 $N^{0.085}$ 51	43 0.0015	50 0.0018	41 0.0021	42 0.0025	47 0.0029	41 0.0001 $N^{0.222}$ 93
36	HIK-002	151 0.0082	130 0.0089	64 0.0095	61 0.0103	54 0.0115	103 0.0018 $N^{0.114}$ 59	142 0.0063	133 0.0069				127 0.0020 $N^{0.087}$ 42
37	HIK-003	67 0.0021	67 0.0026				58 0.0001 $N^{0.232}$ 93	84 0.0024	87 0.0030	82 0.0058	81 0.0066	69 0.0053	31 0.0001 $N^{0.279}$ 113
38	HIK-004	68 0.0022	68 0.0027	42 0.0031	46 0.0037	46 0.0046	46 0.0001 $N^{0.257}$ 102	88 0.0024	84 0.0030	81 0.0058	79 0.0065	68 0.0052	37 0.0001 $N^{0.263}$ 108
39	HIK-005	15 0.0008	18 0.0010	14 0.0011	15 0.0013		34 0.0001 $N^{0.207}$ 84	24 0.0012	31 0.0015	20 0.0016	26 0.0019	32 0.0022	44 0.0001 $N^{0.202}$ 87
40	IDEMIA-000	37 0.0013	39 0.0016	24 0.0020	23 0.0023	23 0.0028	26 0.0000 $N^{0.257}$ 103	68 0.0020	77 0.0025	77 0.0055	74 0.0060	62 0.0041	38 0.0001 $N^{0.249}$ 102
41	IDEMIA-001	46 0.0016	50 0.0021	37 0.0026	38 0.0033	44 0.0043	12 0.0000 $N^{0.340}$ 120	86 0.0024	93 0.0032	87 0.0065	87 0.0076	75 0.0064	16 0.0000 $N^{0.335}$ 129
42	IDEMIA-002	81 0.0028	95 0.0036	54 0.0045	54 0.0055	51 0.0070	29 0.0000 $N^{0.309}$ 112	108 0.0035	106 0.0043				63 0.0002 $N^{0.225}$ 94
43	IDEMIA-003	44 0.0015	44 0.0019				55 0.0001 $N^{0.212}$ 87	81 0.0023	82 0.0027	29 0.0057	75 0.0062	61 0.0041	59 0.0002 $N^{0.200}$ 86
44	IDEMIA-004	34 0.0012	34 0.0014	21 0.0017	21 0.0020	19 0.0025	30 0.0000 $N^{0.243}$ 95	64 0.0018	61 0.0021	46 0.0025	47 0.0030	54 0.0036	36 0.0001 $N^{0.241}$ 99
45	IDEMIA-005	42 0.0015	47 0.0020	26 0.0023	33 0.0030	38 0.0039	15 0.0000 $N^{0.325}$ 116	78 0.0022	86 0.0030	64 0.0036	65 0.0044	71 0.0055	23 0.0000 $N^{0.300}$ 118
46	IDEMIA-006	55 0.0019	61 0.0025	41 0.0031	48 0.0040	47 0.0051	14 0.0000 $N^{0.346}$ 124	95 0.0028	100 0.0037	69 0.0046	72 0.0059	81 0.0076	18 0.0000 $N^{0.341}$ 131
47	IDEMIA-007	87 0.0031	77 0.0032	44 0.0032	41 0.0033	33 0.0034	107 0.0021 $N^{0.030}$ 29	14 0.0011	14 0.0012	10 0.0012	12 0.0014	15 0.0015	76 0.0002 $N^{0.110}$ 54
48	IMAGUS-002	183 0.0345	157 0.0507	72 0.0638	72 0.0800		71 0.0002 $N^{0.377}$ 132	200 0.0442	200 0.0632				75 0.0002 $N^{0.390}$ 137
49	IMPERIAL-000	107 0.0036	92 0.0036	51 0.0037	45 0.0037	37 0.0037	118 0.0029 $N^{0.016}$ 18	51 0.0016	44 0.0017	26 0.0017	20 0.0018	19 0.0018	113 0.0009 $N^{0.041}$ 16
50	INCODE-001	74 0.0025	76 0.0032	70 0.0166	69 0.0322		2 0.0000 $N^{1.242}$ 143	109 0.0035	107 0.0043				68 0.0002 $N^{0.215}$ 89
51	INCODE-003	45 0.0015	46 0.0020				28 0.0000 $N^{0.266}$ 104	87 0.0024	89 0.0031	66 0.0036	66 0.0046	72 0.0056	29 0.0001 $N^{0.285}$ 115
52	INCODE-004	110 0.0036	93 0.0036				123 0.0031 $N^{0.012}$ 15	61 0.0018	53 0.0019	36 0.0020	36 0.0021	34 0.0022	99 0.0006 $N^{0.077}$ 38
53	INNOVATRICS-004	48 0.0017	45 0.0019				73 0.0003 $N^{0.129}$ 64	90 0.0026	92 0.0032	60 0.0035	55 0.0035	52 0.0035	103 0.0007 $N^{0.100}$ 49
54	INNOVATRICS-005						-	36 0.0013	30 0.0014	19 0.0016	17 0.0017		89 0.0004 $N^{0.085}$ 39
55	INTSYSMSU-000	202 0.0962	164 0.1024				137 0.0388 $N^{0.068}$ 45	223 0.1098	219 0.1163	119 0.1206	113 0.1252	110 0.1296	148 0.0519 $N^{0.056}$ 24
56	ISYSTEMS-000	123 0.0044	109 0.0047	56 0.0050	53 0.0052	49 0.0056	100 0.0015 $N^{0.080}$ 49	134 0.0059	129 0.0063				130 0.0026 $N^{0.063}$ 30
57	ISYSTEMS-001	121 0.0045	110 0.0047	55 0.0049	52 0.0052	50 0.0056	101 0.0015 $N^{0.079}$ 46	135 0.0059	128 0.0063				131 0.0027 $N^{0.059}$ 27
58	ISYSTEMS-002	72 0.0024	65 0.0025	38 0.0027			92 0.0010 $N^{0.063}$ 42	105 0.0033	98 0.0034	83 0.0058	73 0.0060	60 0.0041	121 0.0012 $N^{0.074}$ 35
59	ISYSTEMS-003	71 0.0024	60 0.0025	32 0.0025	26 0.0026	21 0.0028	99 0.0012 $N^{0.050}$ 35	101 0.0031	94 0.0033	57 0.0034	57 0.0035	56 0.0037	123 0.0013 $N^{0.063}$ 31
60	KEDACOM-001	152 0.0093	132 0.0094				133 0.0089 $N^{0.004}$ 9	145 0.0071	135 0.0072	91 0.0072	84 0.0073	78 0.0073	140 0.0063 $N^{0.009}$ 4
61	KNERON-000						-	123 0.0048	122 0.0059	89 0.0067	90 0.0079	88 0.0093	74 0.0002 $N^{0.226}$ 95
62	LOOKMAN-003	144 0.0072	123 0.0073				129 0.0057 $N^{0.017}$ 19	148 0.0072	138 0.0074	94 0.0075	88 0.0076	82 0.0077	137 0.0054 $N^{0.022}$ 11
63	LOOKMAN-005	153 0.0094	133 0.0094				131 0.0084 $N^{0.008}$ 11	146 0.0072	136 0.0072	92 0.0073	85 0.0073	79 0.0074	139 0.0060 $N^{0.013}$ 7
64	MEGVII-000	27 0.0011	42 0.0018	27 0.0023	35 0.0030	40 0.0040	6 0.0000 $N^{0.439}$ 138	26 0.0012	38 0.0016	58 0.0034	61 0.0039	48 0.0031	11 0.0000 $N^{0.317}$ 123
65	MEGVII-001						-	152 0.0077	145 0.0080	95 0.0082	93 0.0086	87 0.0089	133 0.0040 $N^{0.048}$ 20
66	MICROFOCUS-003	209 0.2045	174 0.2622	81 0.3015			130 0.0070 $N^{0.253}$ 99	231 0.2498	229 0.3095				144 0.0110 $N^{0.234}$ 96
67	MICROFOCUS-005	204 0.1037	168 0.1419				93 0.0011 $N^{0.342}$ 123	226 0.1300	225 0.1724	121 0.2046	116 0.2425	113 0.2810	132 0.0040 $N^{0.263}$ 107
68	MICROSOFT-000	9 0.0007	11 0.0009	11 0.0010	11 0.0011	10 0.0012	49 0.0001 $N^{0.170}$ 75	16 0.0011	23 0.0013	55 0.0032	56 0.0035	20 0.0019	52 0.0001 $N^{0.176}$ 77
69	MICROSOFT-001	10 0.0007	10 0.0009	10 0.0010	9 0.0011	11 0.0012	48 0.0001 $N^{0.172}$ 76	13 0.0011	18 0.0013				47 0.0001 $N^{0.190}$ 82
70	MICROSOFT-002	11 0.0008	12 0.0009	9 0.0010	12 0.0011	12 0.0013	43 0.0001 $N^{0.187}$ 81	15 0.0011	24 0.0013				43 0.0001 $N^{0.198}$ 84
71	MICROSOFT-003	2 0.0004	4 0.0004				27 0.0000 $N^{0.160}$ 71	2 0.0006	2 0.0006	39 0.0021	39 0.0022	4 0.0009	40 0.0001 $N^{0.153}$ 71
72	MICROSOFT-004	1 0.0004	1 0.0004	1 0.0004	1 0.0005	1 0.0005	36 0.0001 $N^{0.143}$ 69	1 0.0006	1 0.0006	37 0.0020	37 0.0021	2 0.0009	46 0.0001 $N^{0.144}$ 66

Table 15: **Investigation-mode: Effect of N on FNIR at rank 50** *For five enrollment population sizes, N, with T = 0 and FPIR = 1. The left five columns apply for consolidated enrollment of a variable number of lifetime images from each subject. The right five columns apply for enrollment of one recent image. Missing entries usually apply because another algorithm from the same developer was run instead. Some developers are missing because less accurate algorithms were not run on galleries with $N > 1\,600\,000$. Throughout blue superscripts indicate the rank of the algorithm for that column, and yellow highlighting indicates the most accurate value. Caution: The Power-low models are mostly intended to draw attention to the kind of behavior, not as a model to be used for prediction.*

MISSES NOT AT RANK 50		ENROL LIFETIME						ENROL MOST RECENT					
FNIR(N, T= 0, R =50)		DATASET: FRVT 2018						DATASET: FRVT 2018					
#	ALGORITHM	N=0.64M	N=1.6M	N=3.0M	N=6.0M	N=12.0M	aN^b	N=0.64M	N=1.6M	N=3.0M	N=6.0M	N=12.0M	aN^b
73	MICROSOFT-005	3 0.0004	3 0.0004	3 0.0005	2 0.0005	2 0.0006	40 0.0001 $N^{0.139}$ 68	3 0.0006	3 0.0006	1 0.0007	1 0.0008	3 0.0009	48 0.0001 $N^{0.136}$ 63
74	MICROSOFT-006	4 0.0004	2 0.0004	2 0.0005	3 0.0006	3 0.0006	21 0.0000 $N^{0.173}$ 77	4 0.0006	4 0.0007	2 0.0007	3 0.0009	6 0.0010	26 0.0000 $N^{0.184}$ 81
75	NEC-000	58 0.0020	72 0.0027	49 0.0034	51 0.0043	48 0.0056	13 0.0000 $N^{0.356}$ 128	98 0.0029	102 0.0038	93 0.0074	92 0.0085	80 0.0074	22 0.0000 $N^{0.320}$ 125
76	NEC-001	145 0.0073	126 0.0076				127 0.0036 $N^{0.053}$ 38	164 0.0109	154 0.0113	108 0.0142	103 0.0147	99 0.0129	136 0.0050 $N^{0.058}$ 25
77	NEC-002	12 0.0008	9 0.0008	7 0.0008	6 0.0008	6 0.0009	83 0.0005 $N^{0.036}$ 33	5 0.0008	5 0.0008	3 0.0008	2 0.0008	1 0.0008	90 0.0005 $N^{0.038}$ 14
78	NEC-003	25 0.0010	21 0.0010	12 0.0010	10 0.0011	8 0.0011	88 0.0008 $N^{0.021}$ 22	21 0.0012	13 0.0012	8 0.0012	7 0.0012	9 0.0012	112 0.0009 $N^{0.019}$ 9
79	NEUROTECHNOLOGY-003	102 0.0034	112 0.0048				19 0.0000 $N^{0.349}$ 126	120 0.0042	121 0.0057	97 0.0097	97 0.0116	97 0.0112	27 0.0001 $N^{0.332}$ 128
80	NEUROTECHNOLOGY-004	49 0.0017	49 0.0021	31 0.0024	30 0.0028	27 0.0032	59 0.0001 $N^{0.214}$ 88	76 0.0022	76 0.0025	74 0.0054	71 0.0057	51 0.0034	81 0.0003 $N^{0.151}$ 68
81	NEUROTECHNOLOGY-005	40 0.0014	38 0.0016	20 0.0016	20 0.0018	17 0.0020	74 0.0003 $N^{0.116}$ 62	73 0.0021	69 0.0023	45 0.0024	44 0.0025	45 0.0028	98 0.0006 $N^{0.092}$ 46
82	NEUROTECHNOLOGY-007	115 0.0038	216 1.0000	53 0.0040	50 0.0041	43 0.0042	144 118.4579 $N^{-0.617}$ 1	69 0.0020	64 0.0022	42 0.0023	40 0.0024	39 0.0026	104 0.0007 $N^{0.076}$ 36
83	NEWLAND-002						-	181 0.0211	178 0.0263	112 0.0307	110 0.0366		109 0.0008 $N^{0.247}$ 100
84	NOBLIS-002	185 0.0363	158 0.0516				70 0.0002 $N^{0.386}$ 134	197 0.0377	196 0.0535	115 0.0657	111 0.0915		69 0.0002 $N^{0.390}$ 136
85	NTECHLAB-000	32 0.0012	35 0.0015	22 0.0019	24 0.0024	29 0.0032	10 0.0000 $N^{0.335}$ 119	54 0.0017	62 0.0021	68 0.0043	68 0.0051	59 0.0039	19 0.0000 $N^{0.295}$ 117
86	NTECHLAB-001	33 0.0012	40 0.0017	25 0.0021	28 0.0028	36 0.0037	7 0.0000 $N^{0.382}$ 133	63 0.0018	71 0.0023				21 0.0000 $N^{0.285}$ 116
87	NTECHLAB-003	20 0.0009	26 0.0011				37 0.0001 $N^{0.211}$ 86	34 0.0013	39 0.0016	61 0.0035	60 0.0039	40 0.0026	28 0.0001 $N^{0.239}$ 97
88	NTECHLAB-004	13 0.0008	13 0.0009	13 0.0011	13 0.0012	15 0.0015	24 0.0000 $N^{0.220}$ 90	18 0.0011	25 0.0013	54 0.0032	53 0.0035	58 0.0039	50 0.0001 $N^{0.183}$ 80
89	NTECHLAB-005	8 0.0006	8 0.0008				17 0.0000 $N^{0.255}$ 101	7 0.0008	11 0.0011	9 0.0012	16 0.0015	21 0.0019	12 0.0000 $N^{0.283}$ 114
90	NTECHLAB-006	6 0.0006	7 0.0007	6 0.0008	7 0.0010	9 0.0012	16 0.0000 $N^{0.251}$ 98	6 0.0008	7 0.0009	7 0.0011	8 0.0013	18 0.0016	13 0.0000 $N^{0.253}$ 103
91	NTECHLAB-007	86 0.0031	78 0.0032	46 0.0033	43 0.0034	34 0.0035	106 0.0020 $N^{0.033}$ 30	17 0.0011	15 0.0012	12 0.0013	14 0.0014	16 0.0015	77 0.0003 $N^{0.109}$ 53
92	NTECHLAB-008	84 0.0031	75 0.0031	43 0.0031	37 0.0032	28 0.0032	111 0.0025 $N^{0.016}$ 17	11 0.0010	10 0.0010	6 0.0011	6 0.0011	8 0.0012	88 0.0004 $N^{0.065}$ 32
93	PARAVISION-000	127 0.0050	143 0.0149				3 0.0000 $N^{1.198}$ 142	136 0.0060	170 0.0164	113 0.0317			1 0.0000 $N^{1.097}$ 150
94	PARAVISION-001	35 0.0012	30 0.0013				75 0.0003 $N^{0.094}$ 54	62 0.0018	54 0.0019	59 0.0034			111 0.0008 $N^{0.058}$ 26
95	PARAVISION-003	31 0.0012	28 0.0012	17 0.0013	16 0.0014		28 0.0004 $N^{0.079}$ 47	50 0.0016	46 0.0017	33 0.0018	31 0.0020	29 0.0021	91 0.0005 $N^{0.089}$ 43
96	PARAVISION-004	90 0.0032	80 0.0033	47 0.0033	40 0.0033	31 0.0033	117 0.0029 $N^{0.009}$ 12	33 0.0013	21 0.0013	13 0.0013	10 0.0013	12 0.0014	116 0.0010 $N^{0.020}$ 10
97	PARAVISION-005	89 0.0032	79 0.0032	45 0.0033	39 0.0033	30 0.0033	121 0.0030 $N^{0.007}$ 10	35 0.0013	22 0.0013	14 0.0013	11 0.0013	11 0.0014	117 0.0011 $N^{0.015}$ 8
98	PIXELALL-002	122 0.0043	106 0.0045				108 0.0021 $N^{0.053}$ 39	56 0.0017	57 0.0019	40 0.0021	41 0.0024	41 0.0027	71 0.0002 $N^{0.154}$ 72
99	PIXELALL-003	112 0.0037	97 0.0037				114 0.0026 $N^{0.027}$ 27	37 0.0014	29 0.0014	16 0.0014	15 0.0015	17 0.0016	107 0.0007 $N^{0.045}$ 19
100	QUANTASOFT-001	220 0.9843	180 0.9843				143 0.9843 $N^{-0.000}$ 2	224 0.1116	218 0.1116	118 0.1116		109 0.1116	149 0.1116 $N^{-0.000}$ 1
101	RANKONE-000	141 0.0070	135 0.0097	66 0.0117	65 0.0143	56 0.0173	63 0.0001 $N^{0.306}$ 111	163 0.0101	161 0.0133	111 0.0185	107 0.0206	104 0.0226	78 0.0003 $N^{0.273}$ 110
102	RANKONE-001	116 0.0038	114 0.0052	61 0.0064	59 0.0079	53 0.0097	39 0.0001 $N^{0.317}$ 114	129 0.0052	123 0.0059				101 0.0007 $N^{0.153}$ 70
103	RANKONE-002	98 0.0034	103 0.0043				53 0.0001 $N^{0.276}$ 105	124 0.0048	126 0.0060	98 0.0098	95 0.0111	94 0.0102	60 0.0002 $N^{0.255}$ 105
104	RANKONE-003	97 0.0034	104 0.0043	57 0.0052	55 0.0063	52 0.0075	52 0.0001 $N^{0.276}$ 106	125 0.0048	127 0.0060	99 0.0098	96 0.0111	95 0.0102	61 0.0002 $N^{0.255}$ 106
105	RANKONE-004	131 0.0055	125 0.0076				33 0.0000 $N^{0.352}$ 127	147 0.0072	152 0.0102	105 0.0126			30 0.0001 $N^{0.364}$ 134
106	RANKONE-005	52 0.0018	55 0.0022	34 0.0026	36 0.0031	35 0.0036	44 0.0001 $N^{0.248}$ 96	92 0.0026	91 0.0032	65 0.0036	64 0.0043	67 0.0050	56 0.0001 $N^{0.221}$ 92
107	RANKONE-007	99 0.0034	89 0.0035	50 0.0036	47 0.0038	39 0.0040	102 0.0017 $N^{0.052}$ 37	42 0.0015	41 0.0017	29 0.0018	27 0.0019	31 0.0021	80 0.0003 $N^{0.123}$ 61
108	REALNETWORKS-000	133 0.0057	128 0.0081	65 0.0106			18 0.0000 $N^{0.398}$ 136	132 0.0056	142 0.0077				33 0.0001 $N^{0.339}$ 130
109	REALNETWORKS-002	118 0.0040	118 0.0060				9 0.0000 $N^{0.431}$ 137	130 0.0054	140 0.0076	96 0.0097	99 0.0126	100 0.0132	42 0.0001 $N^{0.320}$ 126
110	REALNETWORKS-003	132 0.0056	120 0.0067				29 0.0004 $N^{0.195}$ 82	119 0.0041	116 0.0054	86 0.0064	91 0.0080	93 0.0101	35 0.0001 $N^{0.307}$ 119
111	REALNETWORKS-004	128 0.0052	117 0.0058				90 0.0009 $N^{0.128}$ 63	115 0.0040	114 0.0050	84 0.0061	89 0.0078	91 0.0099	32 0.0001 $N^{0.315}$ 121
112	REMARKAI-000	94 0.0033	83 0.0034				109 0.0023 $N^{0.029}$ 28	40 0.0014	35 0.0015	21 0.0016	19 0.0018	23 0.0020	83 0.0003 $N^{0.108}$ 51
113	REMARKAI-002	30 0.0012	33 0.0014				31 0.0000 $N^{0.241}$ 94	58 0.0018	60 0.0021	44 0.0024	46 0.0028		49 0.0001 $N^{0.216}$ 90
114	SCANOVATE-000	217 0.7780	177 0.7780	82 0.7780	76 0.7780	57 0.7780	142 0.7777 $N^{0.000}$ 3	39 0.0014	37 0.0015	24 0.0017	34 0.0020	27 0.0020	70 0.0002 $N^{0.142}$ 64
115	SENSETIME-000	28 0.0011	27 0.0012				81 0.0005 $N^{0.063}$ 43	52 0.0016	47 0.0017	31 0.0018	23 0.0018	24 0.0020	106 0.0007 $N^{0.060}$ 28
116	SENSETIME-001	26 0.0010	24 0.0011				87 0.0007 $N^{0.027}$ 26	49 0.0016	40 0.0016	23 0.0017	22 0.0018	38 0.0024	79 0.0003 $N^{0.125}$ 62
117	SENSETIME-002	161 0.0120	141 0.0120	67 0.0120	63 0.0120	55 0.0120	134 0.0119 $N^{0.000}$ 7	171 0.0136	162 0.0136	106 0.0136	101 0.0136	101 0.0136	145 0.0135 $N^{0.001}$ 2
118	SENSETIME-003	83 0.0030	74 0.0030	40 0.0030	34 0.0030	24 0.0030	119 0.0029 $N^{0.002}$ 8	9 0.0009	8 0.0009	5 0.0009	5 0.0010	5 0.0010	110 0.0008 $N^{0.013}$ 6
119	SHAMAN-003	181 0.0341	154 0.0401	74 0.0449			125 0.0031 $N^{0.178}$ 78	201 0.0443	195 0.0518				135 0.0044 $N^{0.172}$ 76
120	SHAMAN-007	176 0.0240	147 0.0245				136 0.0180 $N^{0.022}$ 23	195 0.0308	183 0.0314	114 0.0319	109 0.0326	106 0.0337	146 0.0207 $N^{0.029}$ 13
121	SIAT-001	213 0.2634	175 0.2634	80 0.2634			140 0.2626 $N^{0.000}$ 6	12 0.0010	12 0.0011	51 0.0031	49 0.0032	10 0.0013	84 0.0003 $N^{0.085}$ 40
122	SIAT-002	211 0.2123	171 0.2123				139 0.2117 $N^{0.000}$ 5	19 0.0011	17 0.0012	56 0.0032	50 0.0033	13 0.0014	94 0.0005 $N^{0.062}$ 29
123	SMILART-004	218 0.8160	179 0.9521				138 0.0858 $N^{0.168}$ 74	236 0.9157	234 0.9638	122 0.9905			150 0.4623 $N^{0.051}$ 23
124	SYNESIS-003	194 0.0579	159 0.0629				135 0.0172 $N^{0.091}$ 53	214 0.0828	209 0.0869	117 0.0920	112 0.0998	108 0.1104	147 0.0218 $N^{0.098}$ 48
125	SYNESIS-003						-	175 0.0160	169 0.0160	109 0.0160	105 0.0245		114 0.0009 $N^{0.192}$ 83
126	TECH5-001	96 0.0034	87 0.0035				105 0.0020 $N^{0.039}$ 34	44 0.0016	45 0.0017	32 0.0018	28 0.0020	36 0.0023	82 0.0003 $N^{0.119}$ 58
127	TEVIAN-004	54 0.0018	48 0.0021	30 0.0024			66 0.0001 $N^{0.185}$ 80	89 0.0025	85 0.0030				73 0.0002 $N^{0.181}$ 79
128	TEVIAN-005	38 0.0014	37 0.0016				67 0.0002 $N^{0.163}$ 72	67 0.0020	68 0.0023	47 0.0025	45 0.0028	50 0.0034	65 0.0002 $N^{0.178}$ 78
129	TIGER-000	134 0.0059	134 0.0095	68 0.0124	66 0.0162		11 0.0000 $N^{0.449}$ 139	154 0.0080	157 0.0120				14 0.0000 $N^{0.446}$ 141
130	TIGER-002	18 0.0009	25 0.0011				42 0.0001 $N^{0.202}$ 83	29 0.0013	33 0.0015	28 0.0018	35 0.0021	42 0.0027	24 0.0000 $N^{0.253}$ 104
131	TONGYITRANS-001	130 0.0054	116 0.0057	60 0.0059	56 0.0064		104 0.0018 $N^{0.080}$ 48	83 0.0023	79 0.0026				92 0.0005 $N^{0.116}$ 56
132	TOSHIBA-000	21 0.0009	23 0.0011				65 0.0001 $N^{0.143}$ 70	47 0.0016	51 0.0018	35 0.0019	38 0.0021	96 0.0105	4 0.0000 $N^{0.539}$ 145
133	VD-000	203 0.1003	167 0.1419	78 0.1749	74 0.2144		94 0.0011 $N^{0.341}$ 122	225 0.1226	224 0.1678				122 0.0013 $N^{0.342}$ 132
134	VD-001	154 0.0095	136 0.0102				120 0.0030 $N^{0.087}$ 52	167 0.0120	160 0.0130	107 0.0140	104 0.0154	103 0.0170	129 0.0024 $N^{0.120}$ 59
135	VIGILANTSOLUTIONS-003	140 0.0069	137 0.0107	69 0.0140	64 0.0140		56 0.0001 $N^{0.329}$ 117	158 0.0092	164 0.0140				13 0.0000 $N^{0.458}$ 142
136	VISIONLABS-003	82 0.0029	102 0.0041	62 0.0065	62 0.0117		5 0.0000 $N^{0.624}$ 140	116 0.0040	120 0.0055	103 0.0106	106 0.0166		20 0.0000 $N^{0.353}$ 133
137	VISIONLABS-004	24 0.0009	20 0.0010				69 0.0002 $N^{0.114}$ 60	27 0.0012	28 0.0014	50 0.0030	59 0.0039	64 0.0045	7 0.0000 $N^{0.464}$ 143
138	VISIONLABS-005	19 0.0009	15 0.0010	16 0.0011	18 0.0015	20 0.0026	8 0.0000 $N^{0.347}$ 125	25 0.0012	20 0.0013	49 0.0029	51 0.0033	46 0.0029	10 0.0000 $N^{0.318}$ 124
139	VISIONLABS-006	23 0.0009	16 0.0010				82 0.0005 $N^{0.051}$ 36	22 0.0012	19 0.0013	17 0.0015	24 0.0019	43 0.0027	17 0.0000 $N^{0.275}$ 111
140	VISIONLABS-007	17 0.0009	14 0.0009	8 0.0010	8 0.0010	7 0.0011	76 0.0004 $N^{0.066}$ 44	20 0.0012	16 0.0012	11 0.0013	9 0.0013	25 0.0020	57 0.0001 $N^{0.152}$ 69
141	VISIONLABS-008	109 0.0036	94 0.0036				124 0.0031 $N^{0.012}$ 14	53 0.0016	49 0.0017	27 0.0017	30 0.0020	37 0.0023	86 0.0003 $N^{0.114}$ 55
142	VOCORD-003	65 0.0021	57 0.0023	33 0.0026	32 0.0028		27 0.0004 $N^{0.130}$ 65	72 0.0021	70 0.0023				96 0.0005 $N^{0.100}$ 50
143	VOCORD-005	75 0.0025	69 0.0027				98 0.0012 $N^{0.057}$ 40	106 0.0033	99 0.0035	67 0.0037	62 0.0040	63 0.0043	115 0.0010 $N^{0.090}$ 44
144	YISHENG-001	91 0.0033	105 0.0045	58 0.0055	57 0.0070		20 0.0000 $N^{0.340}$ 121	121 0.0047	124 0.0059				55 0.0001 $N^{0.267}$ 109

Table 16: **Investigation-mode: Effect of N on FNIR at rank 50** *For five enrollment population sizes, N, with T = 0 and FPIR = 1. The left five columns apply for consolidated enrollment of a variable number of lifetime images from each subject. The right five columns apply for enrollment of one recent image. Missing entries usually apply because another algorithm from the same developer was run instead. Some developers are missing because less accurate algorithms were not run on galleries with N > 1 600 000. Throughout blue superscripts indicate the rank of the algorithm for that column, and yellow highlighting indicates the most accurate value. Caution: The Power-low models are mostly intended to draw attention to the kind of behavior, not as a model to be used for prediction.*

MISSES NOT AT RANK 50		ENROL LIFETIME						ENROL MOST RECENT					
FNIR(N, T= 0, R =50)		DATASET: FRVT 2018						DATASET: FRVT 2018					
#	ALGORITHM	N=0.64M	N=1.6M	N=3.0M	N=6.0M	N=12.0M	aN^b	N=0.64M	N=1.6M	N=3.0M	N=6.0M	N=12.0M	aN^b
145	YITU-000	[70] 0.0023	[59] 0.0024	[36] 0.0026	[31] 0.0028	[26] 0.0031	[86] 0.0006 $N^{0.099}$ [55]	[80] 0.0023	[73] 0.0024	[73] 0.0052	[69] 0.0054	[73] 0.0057	[120] 0.0012 $N^{0.049}$ [21]
146	YITU-001	[69] 0.0023	[58] 0.0024	[35] 0.0026	[27] 0.0028	[25] 0.0031	[85] 0.0006 $N^{0.100}$ [56]	[79] 0.0023	[72] 0.0024				[119] 0.0012 $N^{0.049}$ [22]
147	YITU-002	[7] 0.0006	[6] 0.0006	[5] 0.0007	[5] 0.0007	[4] 0.0008	[68] 0.0002 $N^{0.082}$ [50]	[10] 0.0009	[9] 0.0010	[63] 0.0036	[58] 0.0036	[7] 0.0012	[85] 0.0003 $N^{0.077}$ [37]
148	YITU-003	[43] 0.0015	[36] 0.0015				[91] 0.0010 $N^{0.033}$ [31]	[70] 0.0020	[63] 0.0021	[71] 0.0047	[67] 0.0048	[66] 0.0049	[118] 0.0011 $N^{0.044}$ [18]
149	YITU-004	[5] 0.0006	[5] 0.0006	[4] 0.0006	[4] 0.0006	[5] 0.0008	[62] 0.0001 $N^{0.115}$ [61]	[8] 0.0008	[6] 0.0009	[4] 0.0009	[4] 0.0009	[53] 0.0036	[8] 0.0000 $N^{0.395}$ [139]
150	YITU-005	[39] 0.0014	[32] 0.0014	[18] 0.0014	[17] 0.0015	[14] 0.0015	[97] 0.0012 $N^{0.016}$ [16]	[66] 0.0020	[58] 0.0020	[38] 0.0020	[33] 0.0020	[28] 0.0020	[124] 0.0017 $N^{0.012}$ [5]

Table 17: **Investigation-mode: Effect of N on FNIR at rank 50** *For five enrollment population sizes, N, with T = 0 and FPIR = 1. The left five columns apply for consolidated enrollment of a variable number of lifetime images from each subject. The right five columns apply for enrollment of one recent image. Missing entries usually apply because another algorithm from the same developer was run instead. Some developers are missing because less accurate algorithms were not run on galleries with $N > 1\,600\,000$. Throughout blue superscripts indicate the rank of the algorithm for that column, and yellow highlighting indicates the most accurate value. Caution: The Power-low models are mostly intended to draw attention to the kind of behavior, not as a model to be used for prediction.*

MISSES OUTSIDE RANK R FNIR(N, T=0, R)		RESOURCE USAGE TEMPLATE		ENROLL LIFETIME CONSOLIDATED = 1.6M FRVT 2018 MUGSHOTS				ENROL MOST RECENT, N = 1.6M FRVT 2018 MUGSHOTS			
#	ALGORITHM	BYTES	MSEC	R=1	R=10	R=50	WORK-10	R=1	R=10	R=50	WORK-10
1	3DIVI-000	[239] -	[239] -				[224] 10.000	[152] 0.0318	[146] 0.0130	[143] 0.0080	[151] 1.166
2	3DIVI-001	[239] -	[239] -				[236] 10.000	[153] 0.0349	[162] 0.0187	[167] 0.0155	[157] 1.210
3	3DIVI-002	[239] -	[239] -				[203] 10.000	[158] 0.0379	[166] 0.0216	[171] 0.0186	[163] 1.235
4	3DIVI-003	[239] -	[239] -	[150] 0.0641	[145] 0.0266	[142] 0.0148	[148] 1.342	[186] 0.0833	[179] 0.0349	[172] 0.0191	[182] 1.447
5	3DIVI-004	[239] -	[239] -	[110] 0.0130	[102] 0.0053	[84] 0.0034	[103] 1.067	[127] 0.0175	[117] 0.0075	[110] 0.0049	[122] 1.092
6	3DIVI-005	[239] -	[239] -	[111] 0.0130	[101] 0.0053	[86] 0.0035	[102] 1.067	[128] 0.0176	[115] 0.0074	[111] 0.0049	[124] 1.092
7	3DIVI-006	[239] -	[239] -	[120] 0.0183	[131] 0.0123	[139] 0.0114	[128] 1.124	[143] 0.0240	[154] 0.0160	[166] 0.0148	[149] 1.162
8	ALCHERA-000	[239] -	[239] -	[106] 0.0119	[118] 0.0083	[124] 0.0074	[111] 1.083	[123] 0.0161	[142] 0.0117	[153] 0.0105	[134] 1.116
9	ALCHERA-001	[239] -	[239] -	[179] 0.9824	[179] 0.9647	[178] 0.9458	[179] 9.748	[234] 0.9869	[234] 0.9735	[233] 0.9590	[234] 9.811
10	ALCHERA-002	[239] -	[239] -	[151] 0.0910	[153] 0.0465	[150] 0.0289	[152] 1.549	[187] 0.0949	[184] 0.0443	[174] 0.0254	[186] 1.544
11	ALCHERA-003	[239] -	[239] -	[116] 0.0156	[105] 0.0066	[98] 0.0038	[112] 1.084	[100] 0.0104	[90] 0.0045	[90] 0.0032	[92] 1.055
12	ALLGOVISION-000	[239] -	[239] -	[99] 0.0102	[112] 0.0076	[121] 0.0069	[108] 1.075	[107] 0.0114	[120] 0.0078	[132] 0.0067	[113] 1.079
13	ANKE-000	[239] -	[239] -	[93] 0.0097	[85] 0.0042	[70] 0.0027	[88] 1.052	[116] 0.0132	[104] 0.0060	[103] 0.0040	[108] 1.072
14	ANKE-001	[239] -	[239] -	[94] 0.0097	[86] 0.0042	[71] 0.0027	[89] 1.052	[117] 0.0132	[106] 0.0061	[104] 0.0040	[109] 1.073
15	ANKE-002	[239] -	[239] -	[48] 0.0044	[77] 0.0037	[91] 0.0036	[62] 1.035	[29] 0.0028	[31] 0.0018	[42] 0.0017	[29] 1.019
16	AWARE-000	[239] -	[239] -				[215] 10.000	[178] 0.0614	[182] 0.0396	[186] 0.0335	[180] 1.416
17	AWARE-001	[239] -	[239] -				[211] 10.000	[175] 0.0562	[176] 0.0329	[179] 0.0264	[177] 1.359
18	AWARE-002	[239] -	[239] -				[212] 10.000	[176] 0.0575	[181] 0.0379	[185] 0.0327	[179] 1.393
19	AWARE-003	[239] -	[239] -	[127] 0.0205	[115] 0.0083	[111] 0.0047	[123] 1.107	[150] 0.0306	[144] 0.0127	[139] 0.0075	[150] 1.163
20	AWARE-004	[239] -	[239] -	[146] 0.0526	[141] 0.0208	[138] 0.0110	[142] 1.272	[181] 0.0679	[171] 0.0274	[165] 0.0145	[175] 1.354
21	AWARE-005	[239] -	[239] -	[125] 0.0205	[117] 0.0083	[113] 0.0049	[122] 1.107	[151] 0.0311	[147] 0.0134	[146] 0.0082	[152] 1.167
22	AWARE-006	[239] -	[239] -	[147] 0.0535	[142] 0.0221	[140] 0.0119	[144] 1.283	[183] 0.0697	[174] 0.0288	[168] 0.0158	[178] 1.371
23	AYONIX-000	[239] -	[239] -	[173] 0.4647	[173] 0.3059	[172] 0.2139	[173] 4.266	[226] 0.4505	[227] 0.3176	[227] 0.2381	[227] 4.288
24	AYONIX-001	[239] -	[239] -	[169] 0.3361	[167] 0.1758	[165] 0.1040	[165] 3.071	[221] 0.3414	[221] 0.1977	[220] 0.1274	[221] 3.226
25	AYONIX-002	[239] -	[239] -	[166] 0.2603	[164] 0.1392	[162] 0.0870	[165] 2.617	[222] 0.3414	[222] 0.1977	[221] 0.1274	[222] 3.226
26	CAMVI-001	[239] -	[239] -				[186] 10.000	[214] 0.2247	[208] 0.1220	[208] 0.0833	[211] 2.399
27	CAMVI-002	[239] -	[239] -				[209] 10.000	[194] 0.1269	[194] 0.0659	[193] 0.0478	[193] 1.760
28	CAMVI-003	[239] -	[239] -	[139] 0.0365	[149] 0.0364	[153] 0.0364	[146] 1.328	[174] 0.0520	[186] 0.0517	[194] 0.0517	[184] 1.466
29	CAMVI-004	[239] -	[239] -	[137] 0.0324	[147] 0.0321	[151] 0.0321	[145] 1.290	[171] 0.0468	[185] 0.0465	[191] 0.0464	[181] 1.419
30	CAMVI-005	[239] -	[239] -	[143] 0.0456	[151] 0.0453	[155] 0.0453	[150] 1.408	[180] 0.0652	[192] 0.0648	[203] 0.0647	[187] 1.584
31	COGENT-000	[239] -	[239] -	[100] 0.0102	[57] 0.0031	[52] 0.0021	[97] 1.059	[101] 0.0105	[133] 0.0095	[74] 0.0024	[119] 1.088
32	COGENT-001	[239] -	[239] -	[101] 0.0102	[58] 0.0031	[53] 0.0021	[98] 1.059	[102] 0.0105	[134] 0.0095	[75] 0.0024	[120] 1.088
33	COGENT-002	[239] -	[239] -	[19] 0.0024	[21] 0.0014	[17] 0.0010	[18] 1.015	[37] 0.0036	[37] 0.0020	[36] 0.0015	[36] 1.021
34	COGENT-003	[239] -	[239] -	[30] 0.0034	[33] 0.0019	[29] 0.0013	[31] 1.021	[39] 0.0038	[43] 0.0021	[43] 0.0017	[43] 1.023
35	COGNITEC-000	[239] -	[239] -	[121] 0.0186	[114] 0.0080	[108] 0.0047	[117] 1.100	[146] 0.0252	[141] 0.0107	[131] 0.0065	[144] 1.136
36	COGNITEC-001	[239] -	[239] -	[86] 0.0086	[72] 0.0036	[64] 0.0025	[83] 1.045	[108] 0.0117	[97] 0.0051	[97] 0.0034	[98] 1.062
37	COGNITEC-002	[239] -	[239] -	[40] 0.0040	[37] 0.0022	[43] 0.0018	[35] 1.025	[64] 0.0057	[69] 0.0032	[81] 0.0026	[66] 1.035
38	COGNITEC-003	[239] -	[239] -	[49] 0.0045	[43] 0.0026	[54] 0.0022	[40] 1.028	[68] 0.0062	[78] 0.0036	[88] 0.0030	[73] 1.039
39	CYBERLINK-000	[239] -	[239] -	[62] 0.0053	[90] 0.0043	[101] 0.0040	[77] 1.041	[42] 0.0040	[58] 0.0026	[66] 0.0022	[53] 1.027
40	CYBERLINK-001	[239] -	[239] -	[52] 0.0047	[76] 0.0037	[88] 0.0035	[68] 1.036	[34] 0.0035	[42] 0.0021	[48] 0.0017	[38] 1.022
41	DAHUA-000	[239] -	[239] -	[77] 0.0068	[92] 0.0044	[100] 0.0039	[82] 1.045	[94] 0.0093	[105] 0.0061	[117] 0.0054	[99] 1.062
42	DAHUA-001	[239] -	[239] -	[53] 0.0048	[41] 0.0026	[51] 0.0021	[42] 1.028	[72] 0.0067	[76] 0.0036	[83] 0.0029	[74] 1.040
43	DAHUA-002	[239] -	[239] -	[34] 0.0037	[69] 0.0034	[82] 0.0033	[51] 1.031	[14] 0.0018	[19] 0.0014	[26] 0.0013	[17] 1.014
44	DEEPGLINT-001	[239] -	[239] -	[160] 0.1422	[165] 0.1421	[169] 0.1421	[163] 2.279				[239] 10.000
45	DEEPSEA-001	[239] -	[239] -	[60] 0.0051	[71] 0.0036	[81] 0.0033	[63] 1.036	[48] 0.0043	[29] 0.0018	[27] 0.0014	[39] 1.022
46	DERMALOG-000	[239] -	[239] -				[225] 10.000	[195] 0.1286	[191] 0.0629	[189] 0.0375	[192] 1.758
47	DERMALOG-001	[239] -	[239] -				[222] 10.000	[198] 0.1541	[196] 0.0777	[192] 0.0476	[197] 1.924
48	DERMALOG-002	[239] -	[239] -				[217] 10.000	[196] 0.1355	[193] 0.0657	[190] 0.0391	[195] 1.797
49	DERMALOG-003	[239] -	[239] -	[155] 0.0967	[154] 0.0467	[149] 0.0272	[154] 1.564	[192] 0.1259	[190] 0.0603	[188] 0.0347	[191] 1.731
50	DERMALOG-004	[239] -	[239] -	[153] 0.0958	[152] 0.0464	[148] 0.0269	[153] 1.559	[191] 0.1251	[189] 0.0598	[187] 0.0343	[190] 1.727
51	DERMALOG-005	[239] -	[239] -	[104] 0.0110	[122] 0.0093	[131] 0.0091	[114] 1.088	[122] 0.0149	[143] 0.0125	[159] 0.0122	[135] 1.118
52	DERMALOG-006	[239] -	[239] -	[67] 0.0058	[96] 0.0047	[107] 0.0046	[84] 1.045	[85] 0.0081	[107] 0.0066	[130] 0.0063	[101] 1.063
53	DERMALOG-007	[239] -	[239] -				[181] 10.000	[93] 0.0092	[103] 0.0060	[119] 0.0054	[100] 1.062
54	EYEDEA-000	[239] -	[239] -				[206] 10.000	[219] 0.2981	[219] 0.1577	[212] 0.0951	[219] 2.845
55	EYEDEA-001	[239] -	[239] -				[234] 10.000	[207] 0.1960	[204] 0.1030	[199] 0.0625	[206] 2.206
56	EYEDEA-002	[239] -	[239] -				[227] 10.000	[208] 0.1979	[206] 0.1049	[204] 0.0648	[207] 2.226
57	EYEDEA-003	[239] -	[239] -	[149] 0.0610	[146] 0.0275	[144] 0.0157	[147] 1.340	[185] 0.0800	[180] 0.0362	[175] 0.0211	[183] 1.448
58	F8-001	[239] -	[239] -	[175] 0.5362	[176] 0.5355	[176] 0.5354	[176] 5.821	[113] 0.0120	[139] 0.0102	[151] 0.0099	[127] 1.096
59	GLORY-000	[239] -	[239] -	[158] 0.1332	[160] 0.0932	[161] 0.0734	[158] 1.962	[203] 0.1781	[210] 0.1266	[214] 0.1007	[208] 2.298
60	GLORY-001	[239] -	[239] -	[152] 0.0929	[156] 0.0627	[156] 0.0486	[156] 1.653	[193] 0.1268	[197] 0.0869	[205] 0.0673	[196] 1.903
61	GORILLA-000	[239] -	[239] -				[197] 10.000				[236] 10.000
62	GORILLA-001	[239] -	[239] -	[141] 0.0411	[136] 0.0154	[127] 0.0079	[137] 1.208	[177] 0.0603	[162] 0.0230	[155] 0.0117	[170] 1.309
63	GORILLA-002	[239] -	[239] -	[112] 0.0134	[99] 0.0049	[73] 0.0028	[101] 1.066	[134] 0.0197	[110] 0.0070	[105] 0.0041	[126] 1.096
64	GORILLA-003	[239] -	[239] -	[130] 0.0242	[109] 0.0073	[96] 0.0037	[124] 1.107	[155] 0.0361	[140] 0.0106	[118] 0.0054	[148] 1.158
65	GORILLA-004	[239] -	[239] -	[75] 0.0066	[83] 0.0041	[90] 0.0035	[80] 1.043	[69] 0.0063	[60] 0.0026	[50] 0.0018	[63] 1.033
66	HBINNO-000	[239] -	[239] -				[216] 10.000	[218] 0.2726	[216] 0.1500	[213] 0.0956	[218] 2.724
67	HIK-000	[239] -	[239] -				[205] 10.000	[139] 0.0210	[152] 0.0152	[163] 0.0139	[146] 1.152
68	HIK-001	[239] -	[239] -				[219] 10.000	[120] 0.0147	[125] 0.0086	[134] 0.0070	[125] 1.093
69	HIK-002	[239] -	[239] -	[119] 0.0182	[127] 0.0109	[130] 0.0089	[126] 1.117	[119] 0.0147	[124] 0.0085	[133] 0.0069	[123] 1.092
70	HIK-003	[239] -	[239] -	[102] 0.0105	[89] 0.0043	[67] 0.0026	[93] 1.055	[109] 0.0117	[94] 0.0048	[87] 0.0030	[97] 1.061
71	HIK-004	[239] -	[239] -	[97] 0.0101	[84] 0.0041	[68] 0.0027	[91] 1.053	[106] 0.0113	[93] 0.0047	[84] 0.0030	[96] 1.060
72	HIK-005	[239] -	[239] -	[26] 0.0032	[22] 0.0014	[18] 0.0010	[26] 1.017	[52] 0.0046	[38] 0.0020	[31] 0.0015	[49] 1.025

Table 18: **Rank-based accuracy for the FRVT 2018 mugshot sets**. *In columns 3 and 4 are template size and template generation duration. Thereafter values are rank-based FNIR with T = 0 and FPIR = 1. This is appropriate to investigational uses but not those with higher volumes where candidates from all searches would need review. Columns 5 - 9 show FRVT 2018 accuracy for various ranks for galleries unenrolled with all lifetime images. Column 10 is a workload statistic, a small value shows an algorithm front-loads mates into the first 10 candidates. The last four columns gives analogous results for enrollment only of the most recent image - see Figure 7. Throughout, blue superscripts indicate the rank of the algorithm for that column, and the best value is highlighted in yellow.*

MISSES OUTSIDE RANK R		RESOURCE USAGE		ENROLL LIFETIME CONSOLIDATED = 1.6M				ENROL MOST RECENT, N = 1.6M			
FNIR(N, T=0, R)		TEMPLATE		FRVT 2018 MUGSHOTS							
#	ALGORITHM	BYTES	MSEC	R=1	R=10	R=50	WORK-10	R=1	R=10	R=50	WORK-10
73	HIK-006	[239] -	[239] -	[27] 0.0032	[23] 0.0014	[19] 0.0010	[25] 1.017	[53] 0.0046	[40] 0.0020	[32] 0.0015	[48] 1.025
74	IDEMIA-000	[239] -	[239] -	[69] 0.0059	[40] 0.0025	[39] 0.0016	[52] 1.031	[88] 0.0088	[81] 0.0038	[77] 0.0025	[84] 1.046
75	IDEMIA-001	[239] -	[239] -	[72] 0.0062	[45] 0.0027	[50] 0.0021	[55] 1.032	[90] 0.0090	[85] 0.0040	[93] 0.0032	[86] 1.049
76	IDEMIA-002	[239] -	[239] -	[91] 0.0096	[94] 0.0045	[95] 0.0036	[90] 1.053	[99] 0.0100	[96] 0.0050	[106] 0.0043	[94] 1.058
77	IDEMIA-003	[239] -	[239] -	[59] 0.0051	[47] 0.0027	[44] 0.0019	[46] 1.030	[76] 0.0069	[83] 0.0039	[82] 0.0027	[78] 1.043
78	IDEMIA-004	[239] -	[239] -	[55] 0.0049	[36] 0.0022	[34] 0.0014	[36] 1.026	[71] 0.0066	[70] 0.0032	[61] 0.0021	[69] 1.038
79	IDEMIA-005	[239] -	[239] -	[68] 0.0059	[39] 0.0025	[47] 0.0020	[50] 1.031	[84] 0.0081	[79] 0.0036	[86] 0.0030	[80] 1.044
80	IDEMIA-006	[239] -	[239] -	[76] 0.0067	[53] 0.0029	[61] 0.0025	[67] 1.036	[92] 0.0096	[88] 0.0042	[100] 0.0037	[88] 1.052
81	IDEMIA-007	[239] -	[239] -	[41] 0.0041	[68] 0.0034	[77] 0.0032	[53] 1.032	[26] 0.0026	[17] 0.0014	[14] 0.0012	[19] 1.015
82	IMAGUS-000	[239] -	[239] -				[204] 10.000	[220] 0.3035	[220] 0.1728	[216] 0.1112	[220] 2.958
83	IMAGUS-002	[239] -	[239] -	[162] 0.1830	[159] 0.0877	[157] 0.0507	[161] 2.067	[212] 0.2203	[207] 0.1090	[200] 0.0632	[209] 2.308
84	IMAGUS-003	[239] -	[239] -	[168] 0.3006	[166] 0.1732	[166] 0.1121	[167] 2.949	[223] 0.3559	[223] 0.2132	[222] 0.1397	[223] 3.363
85	IMPERIAL-000	[239] -	[239] -	[42] 0.0041	[25] 0.0037	[92] 0.0036	[61] 1.034	[25] 0.0024	[30] 0.0018	[44] 0.0017	[25] 1.018
86	INCODE-000	[239] -	[239] -	[140] 0.0373	[137] 0.0155	[129] 0.0086	[136] 1.198	[173] 0.0489	[163] 0.0204	[156] 0.0117	[166] 1.262
87	INCODE-001	[239] -	[239] -	[109] 0.0128	[98] 0.0049	[76] 0.0032	[100] 1.065	[125] 0.0166	[109] 0.0067	[107] 0.0043	[115] 1.086
88	INCODE-002	[239] -	[239] -	[105] 0.0117	[91] 0.0044	[66] 0.0026	[96] 1.058	[129] 0.0178	[111] 0.0070	[108] 0.0043	[121] 1.092
89	INCODE-003	[239] -	[239] -	[88] 0.0086	[63] 0.0032	[46] 0.0020	[78] 1.042	[115] 0.0129	[98] 0.0051	[89] 0.0031	[103] 1.066
90	INCODE-004	[239] -	[239] -	[56] 0.0049	[79] 0.0038	[93] 0.0036	[70] 1.037	[35] 0.0035	[46] 0.0021	[53] 0.0019	[41] 1.023
91	INNOVATRICS-000	[239] -	[239] -				[229] 10.000	[160] 0.0395	[156] 0.0164	[149] 0.0098	[159] 1.211
92	INNOVATRICS-001	[239] -	[239] -				[194] 10.000	[161] 0.0395	[157] 0.0164	[150] 0.0098	[158] 1.211
93	INNOVATRICS-002	[239] -	[239] -	[145] 0.0496	[148] 0.0351	[152] 0.0323	[149] 1.352	[170] 0.0451	[175] 0.0322	[180] 0.0297	[174] 1.321
94	INNOVATRICS-003	[239] -	[239] -	[131] 0.0298	[126] 0.0103	[115] 0.0053	[131] 1.144	[147] 0.0263	[132] 0.0095	[115] 0.0053	[141] 1.129
95	INNOVATRICS-004	[239] -	[239] -	[80] 0.0078	[52] 0.0029	[45] 0.0019	[74] 1.039	[114] 0.0123	[95] 0.0050	[92] 0.0032	[102] 1.064
96	INNOVATRICS-005	[239] -	[239] -				[238] 10.000	[24] 0.0024	[24] 0.0017	[30] 0.0014	[23] 1.017
97	INTSYSMSU-000	[239] -	[239] -	[157] 0.1291	[162] 0.1126	[164] 0.1024	[160] 2.067	[197] 0.1457	[211] 0.1272	[219] 0.1163	[205] 2.203
98	ISYSTEMS-000	[239] -	[239] -	[85] 0.0082	[104] 0.0054	[109] 0.0047	[95] 1.055	[104] 0.0110	[113] 0.0073	[129] 0.0063	[110] 1.075
99	ISYSTEMS-001	[239] -	[239] -	[84] 0.0082	[103] 0.0054	[110] 0.0047	[94] 1.055	[103] 0.0110	[112] 0.0072	[128] 0.0063	[111] 1.075
100	ISYSTEMS-002	[239] -	[239] -	[46] 0.0044	[51] 0.0029	[65] 0.0025	[45] 1.030	[70] 0.0064	[84] 0.0039	[98] 0.0034	[77] 1.041
101	ISYSTEMS-003	[239] -	[239] -	[35] 0.0037	[46] 0.0027	[60] 0.0025	[37] 1.027	[60] 0.0052	[80] 0.0036	[94] 0.0033	[68] 1.037
102	KEDACOM-001	[239] -	[239] -	[95] 0.0099	[124] 0.0095	[132] 0.0094	[113] 1.086	[80] 0.0077	[114] 0.0073	[135] 0.0072	[104] 1.067
103	KNERON-000	[239] -	[239] -				[220] 10.000	[65] 0.0059	[102] 0.0059	[122] 0.0059	[89] 1.053
104	LOOKMAN-003	[239] -	[239] -	[82] 0.0086	[111] 0.0076	[123] 0.0073	[106] 1.071	[89] 0.0088	[119] 0.0076	[138] 0.0074	[106] 1.071
105	LOOKMAN-004	[239] -	[239] -	[89] 0.0088	[110] 0.0075	[122] 0.0072	[107] 1.071	[91] 0.0091	[118] 0.0076	[137] 0.0073	[107] 1.072
106	LOOKMAN-005	[239] -	[239] -	[98] 0.0102	[125] 0.0096	[133] 0.0094	[115] 1.088	[83] 0.0080	[116] 0.0074	[136] 0.0072	[105] 1.068
107	MEGVII-000	[239] -	[239] -	[93] 0.0097	[67] 0.0034	[42] 0.0018	[83] 1.047	[79] 0.0073	[59] 0.0026	[38] 0.0016	[67] 1.036
108	MEGVII-001	[239] -	[239] -				[190] 10.000	[110] 0.0118	[126] 0.0087	[145] 0.0080	[116] 1.086
109	MEGVII-002	[239] -	[239] -				[232] 10.000	[111] 0.0118	[128] 0.0088	[144] 0.0080	[117] 1.087
110	MICROFOCUS-000	[239] -	[239] -				[207] 10.000	[230] 0.5961	[230] 0.4237	[230] 0.3138	[230] 5.385
111	MICROFOCUS-001	[239] -	[239] -				[231] 10.000	[231] 0.5961	[231] 0.4239	[231] 0.3142	[231] 5.385
112	MICROFOCUS-002	[239] -	[239] -				[233] 10.000	[232] 0.6262	[232] 0.4863	[232] 0.4080	[232] 5.828
113	MICROFOCUS-003	[239] -	[239] -	[176] 0.5387	[175] 0.3649	[174] 0.2622	[175] 4.847	[229] 0.5942	[229] 0.4204	[229] 0.3095	[229] 5.361
114	MICROFOCUS-004	[239] -	[239] -	[174] 0.5189	[174] 0.3482	[173] 0.2488	[174] 4.686	[228] 0.5763	[228] 0.4026	[228] 0.2957	[228] 5.199
115	MICROFOCUS-005	[239] -	[239] -	[170] 0.3699	[169] 0.2182	[168] 0.1419	[170] 3.435	[224] 0.4242	[224] 0.2606	[225] 0.1724	[224] 3.861
116	MICROFOCUS-006	[239] -	[239] -	[171] 0.3729	[170] 0.2195	[170] 0.1439	[171] 3.450	[225] 0.4268	[225] 0.2623	[226] 0.1746	[225] 3.880
117	MICROSOFT-000	[239] -	[239] -	[20] 0.0025	[14] 0.0011	[11] 0.0009	[16] 1.014	[40] 0.0038	[27] 0.0017	[23] 0.0013	[34] 1.021
118	MICROSOFT-001	[239] -	[239] -	[18] 0.0024	[12] 0.0011	[10] 0.0009	[13] 1.013	[36] 0.0035	[25] 0.0017	[18] 0.0013	[31] 1.020
119	MICROSOFT-002	[239] -	[239] -	[22] 0.0028	[17] 0.0012	[12] 0.0009	[20] 1.015	[43] 0.0040	[36] 0.0019	[24] 0.0013	[40] 1.023
120	MICROSOFT-003	[239] -	[239] -	[4] 0.0011	[3] 0.0005	[4] 0.0004	[3] 1.006	[7] 0.0016	[4] 0.0009	[2] 0.0006	[5] 1.009
121	MICROSOFT-004	[239] -	[239] -	[2] 0.0010	[1] 0.0005	[1] 0.0004	[1] 1.006	[5] 0.0015	[1] 0.0008	[1] 0.0006	[4] 1.009
122	MICROSOFT-005	[239] -	[239] -	[7] 0.0013	[2] 0.0005	[3] 0.0004	[4] 1.007	[16] 0.0019	[2] 0.0008	[3] 0.0006	[6] 1.010
123	MICROSOFT-006	[239] -	[239] -	[8] 0.0013	[4] 0.0006	[2] 0.0004	[5] 1.007	[17] 0.0020	[7] 0.0010	[4] 0.0007	[7] 1.011
124	NEC-000	[239] -	[239] -	[108] 0.0124	[97] 0.0049	[72] 0.0027	[99] 1.064	[126] 0.0170	[108] 0.0066	[102] 0.0038	[118] 1.087
125	NEC-001	[239] -	[239] -	[117] 0.0160	[121] 0.0090	[126] 0.0076	[116] 1.099	[138] 0.0209	[145] 0.0128	[154] 0.0113	[143] 1.135
126	NEC-002	[239] -	[239] -	[3] 0.0010	[7] 0.0008	[9] 0.0008	[7] 1.008	[2] 0.0010	[3] 0.0008	[5] 0.0008	[1] 1.008
127	NEC-003	[239] -	[239] -	[6] 0.0012	[11] 0.0011	[21] 0.0010	[9] 1.010	[4] 0.0014	[10] 0.0012	[13] 0.0012	[8] 1.011
128	NEUROTECHNOLOGY-000	[239] -	[239] -				[210] 10.000	[172] 0.0471	[164] 0.0204	[158] 0.0121	[165] 1.255
129	NEUROTECHNOLOGY-001	[239] -	[239] -				[200] 10.000	[169] 0.0441	[160] 0.0172	[148] 0.0091	[162] 1.227
130	NEUROTECHNOLOGY-002	[239] -	[239] -				[228] 10.000	[168] 0.0440	[159] 0.0171	[147] 0.0090	[161] 1.226
131	NEUROTECHNOLOGY-003	[239] -	[239] -	[124] 0.0196	[116] 0.0083	[112] 0.0048	[120] 1.105	[141] 0.0225	[137] 0.0100	[121] 0.0057	[139] 1.125
132	NEUROTECHNOLOGY-004	[239] -	[239] -	[63] 0.0055	[54] 0.0030	[49] 0.0021	[59] 1.034	[61] 0.0056	[72] 0.0032	[76] 0.0025	[65] 1.035
133	NEUROTECHNOLOGY-005	[239] -	[239] -	[39] 0.0039	[34] 0.0021	[38] 0.0016	[33] 1.023	[47] 0.0043	[61] 0.0027	[69] 0.0023	[55] 1.028
134	NEUROTECHNOLOGY-006	[239] -	[239] -	[115] 0.0151	[95] 0.0046	[62] 0.0025	[104] 1.068	[130] 0.0180	[101] 0.0059	[95] 0.0033	[114] 1.083
135	NEUROTECHNOLOGY-007	[239] -	[239] -	[184] 1.0000	[224] 1.0000	[216] 1.0000	[195] 10.000	[41] 0.0039	[56] 0.0025	[64] 0.0022	[50] 1.026
136	NEWLAND-002	[239] -	[239] -				[198] 10.000	[184] 0.0786	[183] 0.0397	[178] 0.0263	[185] 1.468
137	NOBLIS-001	[239] -	[239] -	[164] 0.2046	[163] 0.1290	[163] 0.0947	[164] 2.387	[216] 0.2492	[218] 0.1542	[217] 0.1112	[216] 2.679
138	NOBLIS-002	[239] -	[239] -	[161] 0.1562	[158] 0.0832	[158] 0.0516	[159] 1.964	[204] 0.1794	[198] 0.0903	[196] 0.0535	[200] 2.077
139	NTECHLAB-000	[239] -	[239] -	[79] 0.0075	[44] 0.0026	[35] 0.0015	[66] 1.036	[95] 0.0094	[74] 0.0035	[62] 0.0021	[83] 1.046
140	NTECHLAB-001	[239] -	[239] -	[90] 0.0095	[59] 0.0031	[40] 0.0017	[81] 1.044	[112] 0.0119	[87] 0.0042	[71] 0.0023	[93] 1.057
141	NTECHLAB-003	[239] -	[239] -	[58] 0.0050	[32] 0.0018	[26] 0.0011	[34] 1.023	[66] 0.0062	[53] 0.0023	[39] 0.0016	[62] 1.030
142	NTECHLAB-004	[239] -	[239] -	[37] 0.0038	[20] 0.0013	[13] 0.0009	[30] 1.018	[57] 0.0048	[33] 0.0019	[25] 0.0013	[46] 1.024
143	NTECHLAB-005	[239] -	[239] -	[36] 0.0038	[18] 0.0013	[8] 0.0008	[27] 1.017	[54] 0.0047	[26] 0.0017	[11] 0.0011	[42] 1.023
144	NTECHLAB-006	[239] -	[239] -	[28] 0.0033	[10] 0.0011	[7] 0.0007	[19] 1.015	[46] 0.0041	[20] 0.0015	[7] 0.0009	[30] 1.019

Table 19: **Rank-based accuracy for the FRVT 2018 mugshot sets**. *In columns 3 and 4 are template size and template generation duration. Thereafter values are rank-based FNIR with T = 0 and FPIR = 1. This is appropriate to investigational uses but not those with higher volumes where candidates from all searches would need review. Columns 5 - 9 show FRVT 2018 accuracy for various ranks for galleries unenrolled with all lifetime images. Column 10 is a workload statistic, a small value shows an algorithm front-loads mates into the first 10 candidates. The last four columns gives analogous results for enrollment only of the most recent image - see Figure 7. Throughout, blue superscripts indicate the rank of the algorithm for that column, and the best value is highlighted in yellow.*

MISSES OUTSIDE RANK R		RESOURCE USAGE		ENROLL LIFETIME CONSOLIDATED = 1.6M				ENROL MOST RECENT, N = 1.6M			
FNIR(N, T=0, R)		TEMPLATE		FRVT 2018 MUGSHOTS							
#	ALGORITHM	BYTES	MSEC	R=1	R=10	R=50	WORK-10	R=1	R=10	R=50	WORK-10
145	NTECHLAB-007	[239] -	[239] -	[45] 0.0043	[70] 0.0034	[78] 0.0032	[56] 1.033	[27] 0.0027	[18] 0.0014	[15] 0.0012	[21] 1.016
146	NTECHLAB-008	[239] -	[239] -	[33] 0.0037	[62] 0.0032	[75] 0.0031	[47] 1.030	[9] 0.0017	[9] 0.0012	[10] 0.0010	[9] 1.012
147	PARAVISION-000	[239] -	[239] -	[118] 0.0165	[134] 0.0152	[143] 0.0149	[130] 1.140	[131] 0.0188	[158] 0.0167	[170] 0.0164	[147] 1.156
148	PARAVISION-001	[239] -	[239] -	[21] 0.0026	[28] 0.0015	[30] 0.0013	[23] 1.017	[38] 0.0038	[47] 0.0022	[54] 0.0019	[44] 1.023
149	PARAVISION-002	[239] -	[239] -	[23] 0.0028	[30] 0.0016	[31] 0.0014	[28] 1.018	[45] 0.0040	[51] 0.0022	[55] 0.0019	[47] 1.025
150	PARAVISION-003	[239] -	[239] -	[17] 0.0022	[26] 0.0015	[28] 0.0012	[21] 1.015	[31] 0.0031	[41] 0.0020	[46] 0.0017	[33] 1.021
151	PARAVISION-004	[239] -	[239] -	[32] 0.0035	[65] 0.0033	[80] 0.0033	[49] 1.030	[8] 0.0016	[13] 0.0013	[21] 0.0013	[12] 1.013
152	PARAVISION-005	[239] -	[239] -	[31] 0.0034	[64] 0.0033	[79] 0.0032	[48] 1.030	[6] 0.0015	[14] 0.0013	[22] 0.0013	[11] 1.013
153	PIXELALL-002	[239] -	[239] -	[82] 0.0080	[100] 0.0052	[106] 0.0045	[93] 1.054	[50] 0.0045	[57] 0.0025	[57] 0.0019	[56] 1.028
154	PIXELALL-003	[239] -	[239] -	[50] 0.0047	[81] 0.0039	[97] 0.0037	[71] 1.037	[19] 0.0021	[22] 0.0015	[29] 0.0014	[18] 1.015
155	QUANTASOFT-001	[239] -	[239] -	[180] 0.9857	[180] 0.9848	[180] 0.9843	[180] 9.866	[211] 0.2177	[214] 0.1468	[218] 0.1116	[215] 2.539
156	RANKONE-000	[239] -	[239] -	[135] 0.0316	[135] 0.0153	[135] 0.0097	[135] 1.185	[162] 0.0429	[165] 0.0212	[161] 0.0133	[164] 1.252
157	RANKONE-001	[239] -	[239] -	[123] 0.0191	[120] 0.0086	[114] 0.0052	[121] 1.106	[140] 0.0221	[135] 0.0097	[123] 0.0059	[137] 1.121
158	RANKONE-002	[239] -	[239] -	[113] 0.0146	[107] 0.0069	[103] 0.0043	[110] 1.083	[132] 0.0194	[130] 0.0093	[126] 0.0060	[131] 1.111
159	RANKONE-003	[239] -	[239] -	[114] 0.0146	[108] 0.0069	[104] 0.0043	[109] 1.083	[133] 0.0194	[131] 0.0093	[127] 0.0060	[132] 1.111
160	RANKONE-004	[239] -	[239] -	[134] 0.0315	[133] 0.0132	[125] 0.0076	[134] 1.168	[166] 0.0415	[161] 0.0177	[152] 0.0102	[160] 1.225
161	RANKONE-005	[239] -	[239] -	[78] 0.0069	[66] 0.0033	[55] 0.0022	[73] 1.039	[96] 0.0094	[91] 0.0046	[91] 0.0032	[90] 1.054
162	RANKONE-006	[239] -	[239] -	[71] 0.0061	[88] 0.0043	[99] 0.0038	[79] 1.043	[59] 0.0050	[62] 0.0027	[59] 0.0021	[61] 1.030
163	RANKONE-007	[239] -	[239] -	[54] 0.0048	[78] 0.0038	[89] 0.0035	[69] 1.037	[32] 0.0034	[44] 0.0021	[41] 0.0017	[37] 1.022
164	REALNETWORKS-000	[239] -	[239] -	[142] 0.0440	[138] 0.0161	[128] 0.0081	[138] 1.219	[165] 0.0402	[151] 0.0149	[142] 0.0077	[155] 1.201
165	REALNETWORKS-001	[239] -	[239] -	[138] 0.0326	[129] 0.0117	[119] 0.0060	[133] 1.161	[164] 0.0402	[150] 0.0149	[141] 0.0077	[156] 1.201
166	REALNETWORKS-002	[239] -	[239] -	[136] 0.0318	[128] 0.0114	[118] 0.0060	[132] 1.157	[159] 0.0393	[149] 0.0142	[140] 0.0076	[154] 1.195
167	REALNETWORKS-003	[239] -	[239] -	[128] 0.0216	[123] 0.0094	[120] 0.0067	[127] 1.117	[144] 0.0242	[129] 0.0090	[116] 0.0054	[136] 1.120
168	REALNETWORKS-004	[239] -	[239] -	[122] 0.0188	[119] 0.0085	[117] 0.0058	[119] 1.103	[142] 0.0236	[127] 0.0087	[114] 0.0050	[133] 1.116
169	REMARKAI-000	[239] -	[239] -	[51] 0.0047	[73] 0.0036	[83] 0.0034	[63] 1.036	[33] 0.0034	[32] 0.0019	[35] 0.0015	[32] 1.020
170	REMARKAI-000	[239] -	[239] -	[73] 0.0063	[42] 0.0026	[41] 0.0017	[54] 1.032	[87] 0.0086	[77] 0.0036	[78] 0.0025	[81] 1.045
171	REMARKAI-002	[239] -	[239] -	[70] 0.0060	[38] 0.0023	[33] 0.0014	[44] 1.029	[86] 0.0081	[68] 0.0031	[60] 0.0021	[76] 1.041
172	SCANOVATE-000	[239] -	[239] -	[177] 0.7786	[177] 0.7781	[177] 0.7780	[177] 8.004	[58] 0.0050	[49] 0.0022	[37] 0.0015	[52] 1.026
173	SENSETIME-000	[239] -	[239] -	[12] 0.0016	[19] 0.0013	[27] 0.0012	[14] 1.013	[21] 0.0023	[35] 0.0019	[47] 0.0017	[27] 1.018
174	SENSETIME-001	[239] -	[239] -	[11] 0.0016	[16] 0.0012	[24] 0.0011	[12] 1.012	[22] 0.0023	[34] 0.0019	[40] 0.0016	[26] 1.018
175	SENSETIME-002	[239] -	[239] -	[107] 0.0120	[130] 0.0120	[141] 0.0120	[123] 1.108	[118] 0.0137	[148] 0.0136	[162] 0.0136	[138] 1.122
176	SENSETIME-003	[239] -	[239] -	[24] 0.0030	[55] 0.0030	[74] 0.0030	[39] 1.027	[1] 0.0010	[6] 0.0010	[8] 0.0009	[2] 1.009
177	SHAMAN-000	[239] -	[239] -				[189] 10.000	[200] 0.1685	[200] 0.0958	[206] 0.0679	[199] 2.071
178	SHAMAN-001	[239] -	[239] -				[201] 10.000	[201] 0.1696	[199] 0.0925	[201] 0.0642	[198] 2.056
179	SHAMAN-002	[239] -	[239] -				[193] 10.000	[217] 0.2600	[217] 0.1517	[215] 0.1034	[217] 2.691
180	SHAMAN-003	[239] -	[239] -	[154] 0.0966	[155] 0.0548	[154] 0.0401	[155] 1.611	[189] 0.1243	[195] 0.0708	[195] 0.0518	[194] 1.789
181	SHAMAN-004	[239] -	[239] -	[163] 0.1865	[161] 0.1012	[160] 0.0672	[162] 2.161	[213] 0.2221	[209] 0.1241	[207] 0.0825	[212] 2.411
182	SHAMAN-006	[239] -	[239] -	[133] 0.0309	[144] 0.0259	[146] 0.0245	[141] 1.246	[163] 0.0398	[178] 0.0332	[184] 0.0315	[173] 1.316
183	SHAMAN-007	[239] -	[239] -	[132] 0.0307	[143] 0.0259	[147] 0.0245	[139] 1.245	[162] 0.0396	[177] 0.0331	[183] 0.0314	[171] 1.315
184	SIAT-000	[239] -	[239] -				[226] 10.000	[81] 0.0079	[66] 0.0031	[56] 0.0019	[75] 1.040
185	SIAT-001	[239] -	[239] -	[167] 0.2637	[172] 0.2635	[175] 0.2634	[169] 3.372	[11] 0.0018	[11] 0.0013	[12] 0.0011	[13] 1.013
186	SIAT-002	[239] -	[239] -	[165] 0.2127	[168] 0.2124	[171] 0.2123	[166] 2.912	[12] 0.0018	[15] 0.0013	[17] 0.0012	[15] 1.013
187	SMILART-000	[239] -	[239] -				[191] 10.000	[205] 0.1910	[203] 0.1021	[202] 0.0642	[203] 2.183
188	SMILART-001	[239] -	[239] -				[182] 10.000	[210] 0.2167	[212] 0.1277	[210] 0.0908	[213] 2.415
189	SMILART-002	[239] -	[239] -				[237] 10.000	[206] 0.1924	[202] 0.0995	[198] 0.0612	[202] 2.175
190	SMILART-004	[239] -	[239] -	[178] 0.9530	[178] 0.9523	[179] 0.9521	[178] 9.572	[233] 0.9648	[233] 0.9640	[234] 0.9638	[233] 9.678
191	SMILART-005	[239] -	[239] -				[196] 10.000				[235] 10.000
192	SYNESIS-000	[239] -	[239] -				[230] 10.000	[199] 0.1599	[215] 0.1491	[223] 0.1487	[210] 2.360
193	SYNESIS-003	[239] -	[239] -	[159] 0.1347	[157] 0.0788	[159] 0.0629	[157] 1.865	[202] 0.1700	[205] 0.1047	[209] 0.0869	[201] 2.120
194	SYNESIS-003	[239] -	[239] -				[185] 10.000	[124] 0.0162	[153] 0.0160	[169] 0.0160	[145] 1.144
195	TECH5-001	[239] -	[239] -	[65] 0.0055	[80] 0.0038	[87] 0.0035	[72] 1.039	[44] 0.0040	[45] 0.0021	[45] 0.0017	[45] 1.024
196	TEVIAN-000	[239] -	[239] -				[183] 10.000	[137] 0.0203	[123] 0.0080	[113] 0.0049	[129] 1.103
197	TEVIAN-001	[239] -	[239] -				[235] 10.000	[136] 0.0203	[122] 0.0080	[112] 0.0049	[130] 1.103
198	TEVIAN-002	[239] -	[239] -				[221] 10.000	[135] 0.0202	[121] 0.0079	[109] 0.0049	[128] 1.102
199	TEVIAN-003	[239] -	[239] -	[96] 0.0100	[82] 0.0040	[63] 0.0025	[87] 1.051	[121] 0.0147	[100] 0.0059	[101] 0.0037	[112] 1.075
200	TEVIAN-004	[239] -	[239] -	[81] 0.0078	[60] 0.0032	[48] 0.0021	[76] 1.040	[105] 0.0113	[92] 0.0047	[85] 0.0030	[95] 1.058
201	TEVIAN-005	[239] -	[239] -	[61] 0.0052	[35] 0.0022	[37] 0.0016	[38] 1.027	[78] 0.0073	[67] 0.0031	[68] 0.0023	[72] 1.038
202	TIGER-000	[239] -	[239] -	[144] 0.0478	[139] 0.0183	[134] 0.0095	[140] 1.245	[179] 0.0616	[168] 0.0236	[157] 0.0120	[172] 1.315
203	TIGER-001	[239] -	[239] -				[208] 10.000				[238] 10.000
204	TIGER-002	[239] -	[239] -	[43] 0.0042	[31] 0.0017	[25] 0.0011	[32] 1.022	[62] 0.0056	[55] 0.0024	[33] 0.0015	[59] 1.030
205	TIGER-003	[239] -	[239] -				[192] 10.000	[63] 0.0056	[54] 0.0024	[34] 0.0015	[60] 1.030
206	TONGYITRANS-000	[239] -	[239] -	[66] 0.0057	[50] 0.0028	[56] 0.0023	[57] 1.033	[75] 0.0069	[73] 0.0032	[80] 0.0026	[70] 1.038
207	TONGYITRANS-001	[239] -	[239] -	[103] 0.0110	[106] 0.0066	[116] 0.0057	[105] 1.071	[74] 0.0069	[71] 0.0032	[79] 0.0026	[71] 1.038
208	TOSHIBA-000	[239] -	[239] -	[25] 0.0031	[24] 0.0014	[23] 0.0011	[24] 1.017	[49] 0.0045	[50] 0.0022	[51] 0.0018	[51] 1.026
209	TOSHIBA-001	[239] -	[239] -	[29] 0.0033	[25] 0.0014	[22] 0.0010	[29] 1.018	[56] 0.0048	[52] 0.0023	[52] 0.0018	[54] 1.027
210	VD-000	[239] -	[239] -	[172] 0.4301	[171] 0.2331	[167] 0.1419	[172] 3.701	[227] 0.4737	[226] 0.2695	[224] 0.1678	[226] 4.058
211	VD-001	[239] -	[239] -	[129] 0.0218	[132] 0.0126	[136] 0.0102	[129] 1.137	[149] 0.0276	[155] 0.0162	[160] 0.0130	[153] 1.174
212	VIGILANTSOLUTIONS-000	[239] -	[239] -				[184] 10.000	[188] 0.1230	[187] 0.0552	[181] 0.0305	[188] 1.690
213	VIGILANTSOLUTIONS-001	[239] -	[239] -				[202] 10.000	[209] 0.2017	[201] 0.0980	[197] 0.0561	[204] 2.189
214	VIGILANTSOLUTIONS-002	[239] -	[239] -				[223] 10.000	[215] 0.2366	[213] 0.1369	[211] 0.0917	[214] 2.535
215	VIGILANTSOLUTIONS-003	[239] -	[239] -	[148] 0.0545	[140] 0.0207	[137] 0.0107	[143] 1.277	[182] 0.0694	[169] 0.0262	[164] 0.0140	[176] 1.355
216	VIGILANTSOLUTIONS-004	[239] -	[239] -	[156] 0.0990	[150] 0.0431	[145] 0.0235	[151] 1.546	[190] 0.1249	[188] 0.0557	[182] 0.0305	[189] 1.699

Table 20: **Rank-based accuracy for the FRVT 2018 mugshot sets**. *In columns 3 and 4 are template size and template generation duration. Thereafter values are rank-based FNIR with T = 0 and FPIR = 1. This is appropriate to investigational uses but not those with higher volumes where candidates from all searches would need review. Columns 5 - 9 show FRVT 2018 accuracy for various ranks for galleries unenrolled with all lifetime images. Column 10 is a workload statistic, a small value shows an algorithm front-loads mates into the first 10 candidates. The last four columns gives analogous results for enrollment only of the most recent image - see Figure 7. Throughout, blue superscripts indicate the rank of the algorithm for that column, and the best value is highlighted in yellow.*

MISSES OUTSIDE RANK R		RESOURCE USAGE		ENROLL LIFETIME CONSOLIDATED = 1.6M				ENROL MOST RECENT, N = 1.6M			
FNIR(N, T=0, R)		TEMPLATE		FRVT 2018 MUGSHOTS							
#	ALGORITHM	BYTES	MSEC	R=1	R=10	R=50	WORK-10	R=1	R=10	R=50	WORK-10
217	VIGILANTSOLUTIONS-005	[239] -	[239] -				[239] 10.000	[92] 0.0092	[75] 0.0036	[65] 0.0022	[82] 1.046
218	VIGILANTSOLUTIONS-006	[239] -	[239] -				[187] 10.000	[98] 0.0099	[82] 0.0038	[67] 0.0022	[87] 1.049
219	VISIONLABS-003	[239] -	[239] -	[57] 0.0049	[87] 0.0043	[102] 0.0041	[75] 1.040	[73] 0.0068	[99] 0.0058	[120] 0.0055	[91] 1.054
220	VISIONLABS-004	[239] -	[239] -	[15] 0.0019	[15] 0.0012	[20] 0.0010	[13] 1.012	[28] 0.0027	[23] 0.0016	[28] 0.0014	[24] 1.017
221	VISIONLABS-005	[239] -	[239] -	[13] 0.0017	[13] 0.0011	[15] 0.0010	[11] 1.011	[23] 0.0024	[21] 0.0015	[20] 0.0013	[20] 1.016
222	VISIONLABS-006	[239] -	[239] -	[10] 0.0014	[9] 0.0010	[16] 0.0010	[10] 1.010	[13] 0.0018	[16] 0.0014	[19] 0.0013	[16] 1.014
223	VISIONLABS-007	[239] -	[239] -	[9] 0.0014	[8] 0.0010	[14] 0.0009	[8] 1.010	[10] 0.0018	[12] 0.0013	[16] 0.0012	[14] 1.013
224	VISIONLABS-008	[239] -	[239] -	[38] 0.0039	[74] 0.0037	[94] 0.0036	[58] 1.033	[18] 0.0020	[28] 0.0018	[49] 0.0017	[22] 1.017
225	VOCORD-000	[239] -	[239] -				[188] 10.000	[187] 0.0378	[173] 0.0282	[177] 0.0261	[169] 1.279
226	VOCORD-001	[239] -	[239] -				[199] 10.000	[156] 0.0377	[172] 0.0281	[176] 0.0259	[168] 1.277
227	VOCORD-002	[239] -	[239] -				[214] 10.000	[154] 0.0357	[170] 0.0274	[175] 0.0257	[167] 1.268
228	VOCORD-003	[239] -	[239] -	[74] 0.0064	[56] 0.0031	[57] 0.0023	[64] 1.036	[67] 0.0062	[65] 0.0030	[70] 0.0023	[64] 1.035
229	VOCORD-004	[239] -	[239] -	[83] 0.0082	[93] 0.0044	[85] 0.0034	[86] 1.049	[82] 0.0079	[89] 0.0043	[96] 0.0034	[85] 1.048
230	VOCORD-005	[239] -	[239] -	[64] 0.0055	[61] 0.0032	[69] 0.0027	[60] 1.034	[77] 0.0070	[86] 0.0041	[99] 0.0035	[79] 1.044
231	VOCORD-006	[239] -	[239] -				[218] 10.000	[235] 1.0000	[235] 1.0000	[235] 1.0000	[239] 10.000
232	YISHENG-000	[239] -	[239] -				[213] 10.000	[145] 0.0243	[136] 0.0099	[125] 0.0060	[140] 1.127
233	YISHENG-001	[239] -	[239] -	[126] 0.0205	[113] 0.0077	[105] 0.0045	[118] 1.102	[148] 0.0265	[138] 0.0102	[124] 0.0059	[142] 1.134
234	YITU-000	[239] -	[239] -	[47] 0.0044	[49] 0.0028	[59] 0.0024	[43] 1.029	[55] 0.0047	[64] 0.0027	[73] 0.0024	[58] 1.029
235	YITU-001	[239] -	[239] -	[44] 0.0043	[48] 0.0027	[58] 0.0024	[41] 1.028	[51] 0.0045	[63] 0.0027	[72] 0.0024	[57] 1.029
236	YITU-002	[239] -	[239] -	[5] 0.0012	[6] 0.0007	[6] 0.0006	[6] 1.007	[15] 0.0018	[8] 0.0011	[9] 0.0010	[10] 1.012
237	YITU-003	[239] -	[239] -	[16] 0.0021	[29] 0.0016	[36] 0.0015	[22] 1.015	[30] 0.0029	[48] 0.0022	[63] 0.0021	[35] 1.021
238	YITU-004	[239] -	[239] -	[1] 0.0008	[5] 0.0006	[5] 0.0006	[2] 1.006	[3] 0.0013	[5] 0.0009	[6] 0.0009	[3] 1.009
239	YITU-005	[239] -	[239] -	[14] 0.0017	[27] 0.0015	[32] 0.0014	[17] 1.014	[20] 0.0023	[39] 0.0020	[58] 0.0020	[28] 1.019

Table 21: **Rank-based accuracy for the FRVT 2018 mugshot sets**. *In columns 3 and 4 are template size and template generation duration. Thereafter values are rank-based FNIR with T = 0 and FPIR = 1. This is appropriate to investigational uses but not those with higher volumes where candidates from all searches would need review. Columns 5 - 9 show FRVT 2018 accuracy for various ranks for galleries unenrolled with all lifetime images. Column 10 is a workload statistic, a small value shows an algorithm front-loads mates into the first 10 candidates. The last four columns gives analogous results for enrollment only of the most recent image - see Figure 7. Throughout, blue superscripts indicate the rank of the algorithm for that column, and the best value is highlighted in yellow.*

MISSES BELOW THRESHOLD, T		ENROL MOST RECENT MUGSHOT, N = 1.6M								
FNIR(N, T> 0, R >L)		DATASET: FRVT 2018 MUGSHOTS			DATASET: WEBCAM PROBES			DATASET: PROFILE PROBES		
#	ALGORITHM	FPIR=0.001	FPIR=0.01	FPIR=0.1	FPIR=0.001	FPIR=0.01	FPIR=0.1	FPIR=0.001	FPIR=0.01	FPIR=0.1
1	3DIVI-000	[159]0.254	[168]0.158	[169]0.083	[143]0.425	[146]0.302	[145]0.180			
2	3DIVI-001	[158]0.254	[169]0.158	[170]0.084						
3	3DIVI-002	[155]0.253	[170]0.161	[171]0.086						
4	3DIVI-003	[180]0.400	[186]0.282	[186]0.166	[159]0.626	[162]0.497	[159]0.343			
5	3DIVI-004	[138]0.169	[141]0.093	[133]0.045	[135]0.343	[137]0.237	[139]0.138			
6	3DIVI-005	[135]0.166	[140]0.093	[134]0.045	[133]0.339	[136]0.234	[138]0.137	[81]0.996	[83]0.990	[98]0.974
7	3DIVI-006	[137]0.168	[143]0.096	[142]0.048	[134]0.342	[138]0.238	[140]0.142			
8	ALCHERA-000	[125]0.138	[126]0.070	[123]0.032	[101]0.216	[104]0.146	[107]0.087	[98]0.999	[116]0.996	[105]0.979
9	ALCHERA-001	[232]0.999	[233]0.999	[234]0.995	[201]1.000	[225]1.000	[191]1.000			
10	ALCHERA-002	[189]0.486	[189]0.302	[188]0.182	[156]0.591	[156]0.442	[156]0.295	[120]1.000	[136]0.999	[144]0.997
11	ALCHERA-003	[128]0.155	[127]0.070	[116]0.028	[108]0.239	[109]0.152	[102]0.081	[111]0.999	[121]0.997	[94]0.969
12	ALLGOVISION-000	[99]0.088	[108]0.045	[105]0.021	[89]0.166	[94]0.106	[91]0.062	[55]0.990	[68]0.982	[87]0.962
13	ANKE-000	[113]0.117	[120]0.063	[119]0.030	[102]0.220	[107]0.151	[110]0.088	[65]0.994	[81]0.990	[118]0.982
14	ANKE-001	[119]0.119	[121]0.063	[120]0.030	[103]0.220	[108]0.151	[109]0.088	[69]0.994	[92]0.992	[126]0.984
15	ANKE-002	[31]0.032	[29]0.014	[28]0.006	[24]0.079	[23]0.050	[26]0.028	[21]0.948	[20]0.795	[27]0.657
16	AWARE-000	[229]0.983	[160]0.126	[167]0.082	[171]0.817	[140]0.253	[144]0.178	[137]1.000	[130]0.998	[114]0.981
17	AWARE-001	[228]0.996	[159]0.124	[166]0.078				[141]1.000	[139]0.999	[112]0.980
18	AWARE-002	[225]0.977	[156]0.117	[164]0.076				[139]1.000	[124]0.998	[109]0.980
19	AWARE-003	[123]0.128	[132]0.082	[141]0.048	[126]0.298	[129]0.204	[137]0.132	[46]0.984	[61]0.977	[90]0.965
20	AWARE-004	[160]0.269	[173]0.175	[178]0.104	[151]0.509	[154]0.375	[154]0.253	[123]1.000	[138]0.999	[107]0.979
21	AWARE-005	[173]0.364	[135]0.085	[139]0.048	[112]0.253	[112]0.163	[115]0.099	[128]1.000	[137]0.999	[146]0.998
22	AWARE-006	[161]0.276	[174]0.175	[180]0.106	[140]0.398	[144]0.283	[146]0.188	[119]0.999	[134]0.999	[143]0.996
23	AYONIX-000	[213]0.811	[221]0.724	[224]0.597	[181]0.939	[183]0.892	[185]0.802	[91]0.998	[113]0.995	[138]0.991
24	AYONIX-001	[216]0.824	[219]0.701	[222]0.525	[176]0.920	[179]0.845	[181]0.703	[115]0.999	[117]0.996	[122]0.984
25	AYONIX-002	[215]0.824	[220]0.702	[221]0.525	[177]0.920	[178]0.845	[180]0.702	[114]0.999	[118]0.996	[123]0.984
26	CAMVI-001	[206]0.684	[213]0.548	[212]0.373	[168]0.770	[173]0.648	[174]0.488	[64]0.994	[71]0.984	[85]0.961
27	CAMVI-002	[193]0.536	[198]0.400	[195]0.240				[50]0.989	[53]0.973	[63]0.931
28	CAMVI-003	[82]0.071	[115]0.058	[149]0.053	[66]0.132	[95]0.108	[113]0.094	[26]0.970	[35]0.940	[56]0.914
29	CAMVI-004	[83]0.072	[112]0.054	[138]0.048	[68]0.136	[82]0.100	[103]0.083	[112]0.999	[125]0.998	[59]0.915
30	CAMVI-005	[104]0.099	[131]0.076	[157]0.067	[97]0.179	[101]0.132	[124]0.110	[121]1.000	[132]0.998	[55]0.904
31	COGENT-000	[62]0.053	[76]0.029	[92]0.018	[71]0.140	[85]0.100	[97]0.069	[75]0.995	[88]0.991	[124]0.984
32	COGENT-001	[63]0.053	[73]0.029	[91]0.018	[70]0.140	[86]0.100	[98]0.069	[74]0.995	[89]0.991	[125]0.984
33	COGENT-002	[46]0.044	[35]0.017	[33]0.007	[39]0.098	[41]0.063	[44]0.036	[86]0.998	[97]0.994	[128]0.986
34	COGENT-003	[49]0.046	[33]0.016	[32]0.007	[35]0.095	[39]0.061	[47]0.037	[89]0.998	[111]0.995	[132]0.988
35	COGNITEC-000	[132]0.161	[142]0.095	[145]0.050	[127]0.303	[127]0.200	[127]0.115	[58]0.992	[47]0.971	[76]0.953
36	COGNITEC-001	[106]0.102	[109]0.053	[110]0.024	[106]0.230	[103]0.135	[99]0.071	[159]1.000	[42]0.965	[71]0.947
37	COGNITEC-002	[64]0.053	[66]0.025	[61]0.011	[96]0.178	[89]0.101	[77]0.050	[132]1.000	[39]0.956	[69]0.941
38	COGNITEC-003	[61]0.053	[68]0.025	[66]0.011	[87]0.162	[83]0.100	[75]0.050	[135]1.000	[36]0.946	[61]0.924
39	CYBERLINK-000	[70]0.056	[57]0.023	[45]0.009	[53]0.116	[53]0.070	[51]0.038	[78]0.995	[67]0.981	[54]0.900
40	CYBERLINK-001	[65]0.054	[55]0.022	[43]0.008	[48]0.109	[48]0.067	[41]0.036	[73]0.995	[70]0.984	[66]0.934
41	DAHUA-000	[93]0.086	[101]0.045	[99]0.020	[67]0.135	[70]0.083	[68]0.046			
42	DAHUA-001	[85]0.073	[87]0.037	[82]0.016	[61]0.122	[62]0.075	[60]0.042	[39]0.980	[32]0.933	[36]0.790
43	DAHUA-002	[12]0.015	[10]0.006	[7]0.003	[11]0.046	[11]0.029	[11]0.017	[6]0.638	[9]0.522	[10]0.394
44	DEEPGLINT-001				[222]1.000	[205]1.000	[233]1.000	[204]1.000	[218]1.000	[196]1.000
45	DEEPSEA-001	[48]0.046	[52]0.022	[48]0.009	[41]0.101	[35]0.059	[31]0.031	[47]0.985	[54]0.973	[70]0.942
46	DERMALOG-000	[188]0.486	[193]0.362	[194]0.231	[163]0.657	[168]0.528	[164]0.362	[77]0.995	[84]0.991	[104]0.978
47	DERMALOG-001	[191]0.527	[199]0.403	[199]0.266				[56]0.990	[69]0.983	[88]0.964
48	DERMALOG-002	[190]0.502	[195]0.376	[196]0.242				[51]0.990	[65]0.981	[84]0.960
49	DERMALOG-003	[187]0.482	[192]0.360	[192]0.229	[161]0.655	[167]0.526	[163]0.361			
50	DERMALOG-004	[186]0.480	[191]0.358	[191]0.228	[162]0.657	[165]0.526	[162]0.359	[79]0.995	[91]0.991	[111]0.980
51	DERMALOG-005	[98]0.088	[94]0.043	[106]0.022	[78]0.154	[80]0.096	[84]0.057	[54]0.990	[38]0.950	[39]0.816
52	DERMALOG-006	[50]0.052	[70]0.026	[69]0.012	[43]0.105	[46]0.067	[54]0.039	[40]0.981	[33]0.933	[35]0.758
53	DERMALOG-007	[94]0.086	[92]0.040	[90]0.017	[76]0.152	[77]0.093	[29]0.051			
54	EYEDEA-000	[214]0.812	[218]0.679	[218]0.483	[175]0.914	[176]0.783	[177]0.619	[85]0.998	[87]0.991	[106]0.979
55	EYEDEA-001	[201]0.630	[203]0.479	[207]0.333				[105]0.999	[101]0.994	[103]0.978
56	EYEDEA-002	[211]0.794	[205]0.488	[208]0.336				[116]0.999	[115]0.996	[108]0.980
57	EYEDEA-003	[177]0.388	[184]0.265	[184]0.157	[153]0.543	[155]0.404	[155]0.264	[70]0.994	[80]0.990	[113]0.981
58	F8-001	[133]0.166	[85]0.036	[88]0.017				[97]0.998	[114]0.995	[68]0.935
59	GLORY-000	[174]0.367	[188]0.295	[193]0.231	[154]0.547	[159]0.470	[168]0.390	[72]0.995	[95]0.993	[139]0.991
60	GLORY-001	[166]0.305	[181]0.236	[187]0.177	[152]0.537	[157]0.448	[160]0.352	[62]0.993	[86]0.991	[134]0.989
61	GORILLA-000									
62	GORILLA-001	[181]0.406	[182]0.246	[181]0.133	[146]0.453	[148]0.314	[148]0.191	[138]1.000	[152]1.000	[140]0.993
63	GORILLA-002	[141]0.188	[148]0.106	[140]0.048	[119]0.268	[118]0.170	[112]0.093	[148]1.000	[96]0.993	[58]0.915
64	GORILLA-003	[168]0.318	[167]0.157	[158]0.071	[145]0.434	[139]0.247	[135]0.131	[222]1.000	[148]1.000	[110]0.980
65	GORILLA-004	[102]0.089	[95]0.043	[89]0.017	[85]0.160	[87]0.101	[82]0.053	[22]0.959	[27]0.903	[37]0.796
66	HBINNO-000	[210]0.765	[216]0.631	[217]0.457				[133]1.000	[144]1.000	[148]0.998
67	HIK-000	[112]0.112	[125]0.068	[127]0.037	[79]0.155	[91]0.103	[90]0.061	[41]0.981	[48]0.971	[73]0.949
68	HIK-001	[117]0.118	[125]0.065	[122]0.032				[53]0.990	[66]0.981	[86]0.961
69	HIK-002	[118]0.119	[124]0.065	[121]0.032				[59]0.992	[72]0.985	[92]0.966
70	HIK-003	[107]0.103	[114]0.057	[117]0.028	[81]0.158	[92]0.105	[89]0.061	[25]0.969	[30]0.925	[42]0.835
71	HIK-004	[103]0.099	[111]0.054	[114]0.027	[77]0.153	[88]0.101	[85]0.059	[31]0.976	[37]0.947	[48]0.879
72	HIK-005	[42]0.044	[40]0.019	[50]0.009	[23]0.077	[22]0.048	[28]0.028	[118]0.999	[127]0.998	[41]0.831

Table 22: **Threshold-based accuracy**. *Values are FNIR(N, T, L) with N = 1.6 million with thresholds set to produce FPIR = 0.001, 0.01, and 0.1 in non-mate searches. Columns 3-5 apply to FRVT-2018 mugshots: Columns 6-8 show the corresponding FNIR values for webcam images searched against the FRVT-2018 mugshot gallery. Finally, the three rightmost columns show FNIR for profile view images searched against the FRVT-2018 frontal gallery. Throughout blue superscripts indicate the rank of the algorithm for that column. Caution: The Power-low models are mostly intended to draw attention to the kind of behavior, not as a model to be used for prediction.*

MISSES BELOW THRESHOLD, T		ENROL MOST RECENT MUGSHOT, N = 1.6M								
FNIR(N, T> 0, R >L)		DATASET: FRVT 2018 MUGSHOTS			DATASET: WEBCAM PROBES			DATASET: PROFILE PROBES		
#	ALGORITHM	FPIR=0.001	FPIR=0.01	FPIR=0.1	FPIR=0.001	FPIR=0.01	FPIR=0.1	FPIR=0.001	FPIR=0.01	FPIR=0.1
73	HIK-006	[50]0.047	[43]0.020	[49]0.009	[26]0.086	[26]0.052	[29]0.029	[147]1.000	[140]0.999	[40]0.819
74	IDEMIA-000	[111]0.111	[117]0.059	[113]0.027	[109]0.240	[110]0.156	[106]0.085	[52]0.990	[73]0.986	[100]0.976
75	IDEMIA-001	[58]0.051	[74]0.029	[79]0.015				[28]0.971	[41]0.964	[79]0.955
76	IDEMIA-002	[60]0.052	[77]0.029	[84]0.016				[27]0.970	[43]0.965	[74]0.952
77	IDEMIA-003	[51]0.047	[48]0.021	[62]0.011	[88]0.165	[65]0.079	[78]0.050		[206]1.000	[142]0.996
78	IDEMIA-004	[36]0.037	[47]0.021	[67]0.011	[57]0.118	[64]0.079	[76]0.050	[30]0.973	[44]0.968	[82]0.960
79	IDEMIA-005	[44]0.044	[67]0.026	[75]0.014	[75]0.150	[90]0.102	[96]0.065	[35]0.978	[52]0.973	[93]0.967
80	IDEMIA-006	[41]0.043	[67]0.025	[78]0.015	[105]0.226	[111]0.161	[123]0.108	[42]0.982	[64]0.980	[101]0.976
81	IDEMIA-007	[15]0.018	[15]0.008	[21]0.004	[15]0.055	[14]0.033	[14]0.021	[181]1.000	[180]1.000	[212]1.000
82	IMAGUS-000	[208]0.734	[215]0.607	[216]0.452	[173]0.872	[175]0.779	[178]0.635	[126]1.000	[142]1.000	[149]0.999
83	IMAGUS-002	[209]0.749	[213]0.564	[213]0.375	[170]0.816	[172]0.645	[172]0.460	[150]1.000	[149]1.000	[153]0.999
84	IMAGUS-003	[212]0.807	[217]0.669	[220]0.511	[174]0.909	[177]0.809	[179]0.667	[134]1.000	[145]1.000	[151]0.999
85	IMPERIAL-000	[25]0.026	[19]0.009	[22]0.004	[19]0.068	[18]0.041	[18]0.024	[101]0.999	[102]0.995	[12]0.441
86	INCODE-000	[167]0.310	[178]0.199	[177]0.104	[142]0.420	[147]0.304	[147]0.191	[94]0.998	[99]0.994	[121]0.984
87	INCODE-001	[147]0.212	[149]0.112	[136]0.047	[123]0.296	[125]0.198	[125]0.110	[153]1.000	[143]1.000	[51]0.885
88	INCODE-002	[140]0.184	[146]0.100	[132]0.044	[120]0.269	[120]0.176	[116]0.100	[63]0.993	[60]0.976	[60]0.918
89	INCODE-003	[136]0.167	[133]0.084	[126]0.034	[116]0.264	[114]0.164	[108]0.087	[117]0.999	[119]0.996	[53]0.899
90	INCODE-004	[67]0.054	[60]0.023	[44]0.008	[60]0.120	[54]0.070	[45]0.036	[71]0.995	[31]0.929	[24]0.630
91	INNOVATRICS-000	[157]0.253	[171]0.163	[173]0.087	[136]0.361	[141]0.258	[143]0.159	[43]0.983	[58]0.975	[78]0.953
92	INNOVATRICS-001	[156]0.253	[172]0.163	[172]0.087				[44]0.983	[59]0.975	[77]0.953
93	INNOVATRICS-002	[153]0.234	[166]0.139	[165]0.077	[128]0.310	[131]0.209	[131]0.126	[149]1.000	[141]0.999	[117]0.982
94	INNOVATRICS-003	[149]0.221	[162]0.132	[156]0.065	[124]0.297	[128]0.203	[128]0.116	[125]1.000	[131]0.998	[65]0.933
95	INNOVATRICS-004	[124]0.132	[130]0.074	[125]0.033	[104]0.222	[105]0.149	[105]0.085	[38]0.980	[50]0.973	[81]0.957
96	INNOVATRICS-005	[32]0.034	[30]0.014	[26]0.005						
97	INTSYSMSU-000	[230]0.998	[231]0.990	[231]0.921	[188]1.000	[188]0.998	[50]0.038	[124]1.000	[126]0.998	[31]0.705
98	ISYSTEMS-000	[100]0.089	[99]0.044	[103]0.021	[93]0.173	[96]0.110	[94]0.065	[61]0.993	[79]0.989	[116]0.981
99	ISYSTEMS-001	[96]0.088	[98]0.044	[102]0.020				[60]0.993	[78]0.989	[115]0.981
100	ISYSTEMS-002	[88]0.078	[82]0.032	[71]0.013	[62]0.126	[67]0.080	[70]0.046	[83]0.998	[94]0.993	[89]0.965
101	ISYSTEMS-003	[74]0.059	[64]0.024	[58]0.010	[46]0.107	[50]0.068	[52]0.039	[129]1.000	[123]0.997	[75]0.953
102	KEDACOM-001	[22]0.023	[28]0.013	[52]0.009	[21]0.072	[28]0.054	[61]0.042	[48]0.986	[55]0.973	[96]0.972
103	KNERON-000		[84]0.033	[73]0.013						
104	LOOKMAN-003	[43]0.044	[65]0.025	[76]0.014	[50]0.112	[68]0.082	[83]0.057			
105	LOOKMAN-004	[47]0.045	[62]0.024	[72]0.013	[45]0.105	[60]0.075	[81]0.052	[32]0.977	[56]0.974	[97]0.972
106	LOOKMAN-005	[30]0.030	[34]0.017	[60]0.011	[25]0.086	[42]0.063	[69]0.046	[34]0.978	[51]0.973	[95]0.971
107	MEGVII-000	[110]0.106	[113]0.055	[109]0.023	[52]0.116	[47]0.067	[37]0.034			
108	MEGVII-001	[84]0.072	[86]0.037	[97]0.019	[38]0.097	[37]0.061	[35]0.033			
109	MEGVII-002	[87]0.077	[88]0.037	[96]0.019	[37]0.096	[34]0.059	[34]0.033	[96]0.998	[26]0.872	[26]0.644
110	MICROFOCUS-000	[221]0.933	[227]0.867	[228]0.748	[187]0.985	[186]0.950	[188]0.877			
111	MICROFOCUS-001	[222]0.933	[226]0.867	[229]0.748						
112	MICROFOCUS-002	[223]0.934	[228]0.869	[230]0.758						
113	MICROFOCUS-003	[220]0.931	[225]0.866	[227]0.747	[186]0.979	[185]0.948	[187]0.876			
114	MICROFOCUS-004	[231]0.999	[234]0.999	[233]0.994	[184]0.975	[184]0.940	[186]0.862			
115	MICROFOCUS-005	[217]0.835	[223]0.736	[223]0.587	[179]0.928	[181]0.865	[184]0.748			
116	MICROFOCUS-006	[226]0.978	[229]0.963	[225]0.640	[178]0.923	[180]0.858	[183]0.739			
117	MICROSOFT-000	[38]0.041	[39]0.019	[38]0.008	[51]0.115	[55]0.071	[55]0.040			
118	MICROSOFT-001	[39]0.042	[41]0.020	[42]0.008						
119	MICROSOFT-002	[53]0.047	[59]0.023	[56]0.010						
120	MICROSOFT-003	[29]0.028	[26]0.012	[20]0.004	[31]0.091	[32]0.056	[27]0.028			
121	MICROSOFT-004	[26]0.026	[24]0.011	[16]0.004	[27]0.087	[27]0.053	[24]0.026			
122	MICROSOFT-005	[24]0.026	[23]0.010	[17]0.004	[20]0.070	[19]0.041	[13]0.021	[5]0.587	[5]0.354	[6]0.222
123	MICROSOFT-006	[8]0.012	[9]0.006	[12]0.003	[8]0.037	[9]0.024	[7]0.016	[1]0.386	[2]0.281	[3]0.198
124	NEC-000	[89]0.079	[106]0.047	[115]0.027	[72]0.140	[75]0.093	[86]0.059	[36]0.979	[46]0.969	[80]0.956
125	NEC-001	[109]0.106	[119]0.060	[124]0.033	[99]0.197	[102]0.133	[104]0.083	[49]0.986	[49]0.972	[83]0.960
126	NEC-002	[3]0.003	[2]0.002	[2]0.001	[3]0.020	[3]0.013	[2]0.010	[113]0.999	[105]0.995	[14]0.474
127	NEC-003	[2]0.002	[3]0.002	[3]0.002	[2]0.017	[2]0.013	[3]0.011	[12]0.824	[10]0.628	[13]0.450
128	NEUROTECHNOLOGY-000	[163]0.293	[179]0.194	[179]0.105	[147]0.465	[149]0.317	[150]0.196	[104]0.999	[112]0.995	[99]0.974
129	NEUROTECHNOLOGY-001	[164]0.296	[176]0.193	[175]0.103				[87]0.998	[107]0.995	[133]0.989
130	NEUROTECHNOLOGY-002	[165]0.297	[175]0.193	[176]0.103				[84]0.998	[110]0.995	[135]0.989
131	NEUROTECHNOLOGY-003	[203]0.636	[145]0.099	[144]0.050	[118]0.266	[113]0.164	[111]0.088	[194]1.000	[229]1.000	[197]1.000
132	NEUROTECHNOLOGY-004	[78]0.063	[72]0.028	[68]0.012	[54]0.117	[56]0.073	[56]0.040	[67]0.994	[82]0.990	[127]0.984
133	NEUROTECHNOLOGY-005	[68]0.054	[54]0.022	[51]0.009	[64]0.130	[59]0.074	[62]0.042	[90]0.998	[77]0.989	[91]0.965
134	NEUROTECHNOLOGY-006	[154]0.249	[157]0.121	[143]0.049	[141]0.418	[130]0.206	[118]0.103			
135	NEUROTECHNOLOGY-007	[77]0.062	[51]0.021	[41]0.008	[92]0.173	[49]0.068	[48]0.038	[131]1.000	[122]0.997	[102]0.977
136	NEWLAND-002	[183]0.438	[187]0.294	[183]0.155	[148]0.466	[151]0.335	[152]0.213	[107]0.999	[129]0.998	[129]0.986
137	NOBLIS-001	[233]1.000	[232]0.991	[214]0.418	[221]1.000	[206]1.000	[190]1.000	[146]1.000	[155]1.000	[157]1.000
138	NOBLIS-002	[229]0.997	[207]0.488	[203]0.307	[232]1.000	[198]1.000	[176]0.565	[152]1.000	[154]1.000	[156]1.000
139	NTECHLAB-000	[90]0.080	[102]0.045	[100]0.020	[86]0.162	[93]0.105	[88]0.061	[18]0.900	[24]0.826	[32]0.720
140	NTECHLAB-001	[105]0.100	[110]0.053	[111]0.025				[19]0.909	[25]0.842	[34]0.734
141	NTECHLAB-003	[66]0.054	[73]0.028	[70]0.013	[55]0.118	[61]0.075	[63]0.043	[14]0.837	[19]0.752	[22]0.628
142	NTECHLAB-004	[37]0.041	[40]0.021	[54]0.009	[44]0.105	[45]0.065	[43]0.036	[13]0.833	[17]0.746	[23]0.629
143	NTECHLAB-005	[40]0.042	[50]0.021	[55]0.009	[42]0.102	[43]0.063	[39]0.034	[11]0.771	[13]0.661	[19]0.516
144	NTECHLAB-006	[34]0.037	[37]0.018	[40]0.008	[33]0.094	[33]0.059	[32]0.032	[10]0.754	[11]0.635	[15]0.490

Table 23: **Threshold-based accuracy**. *Values are FNIR(N, T, L) with N = 1.6 million with thresholds set to produce FPIR = 0.001, 0.01, and 0.1 in non-mate searches. Columns 3-5 apply to FRVT-2018 mugshots: Columns 6-8 show the corresponding FNIR values for webcam images searched against the FRVT-2018 mugshot gallery. Finally, the three rightmost columns show FNIR for profile view images searched against the FRVT-2018 frontal gallery. Throughout blue superscripts indicate the rank of the algorithm for that column. Caution: The Power-low models are mostly intended to draw attention to the kind of behavior, not as a model to be used for prediction.*

MISSES BELOW THRESHOLD, T		ENROL MOST RECENT MUGSHOT, N = 1.6M								
FNIR(N, T> 0, R >L)		DATASET: FRVT 2018 MUGSHOTS			DATASET: WEBCAM PROBES			DATASET: PROFILE PROBES		
#	ALGORITHM	FPIR=0.001	FPIR=0.01	FPIR=0.1	FPIR=0.001	FPIR=0.01	FPIR=0.1	FPIR=0.001	FPIR=0.01	FPIR=0.1
145	NTECHLAB-007	[23]0.026	[27]0.012	[27]0.005	[18]0.067	[17]0.041	[17]0.023	[9]0.750	[12]0.642	[17]0.498
146	NTECHLAB-008	[10]0.014	[11]0.007	[13]0.003	[10]0.045	[12]0.029	[9]0.017	[4]0.529	[6]0.391	[7]0.252
147	PARAVISION-000	[101]0.089	[104]0.045	[112]0.025	[90]0.170	[84]0.100	[87]0.060	[109]0.999	[120]0.997	[30]0.702
148	PARAVISION-001	[55]0.049	[45]0.020	[36]0.008	[63]0.128	[58]0.074	[53]0.039	[100]0.999	[98]0.994	[21]0.530
149	PARAVISION-002	[56]0.050	[56]0.022	[46]0.009	[58]0.119	[63]0.076	[57]0.041	[45]0.983	[18]0.748	[16]0.495
150	PARAVISION-003	[33]0.035	[32]0.016	[30]0.006	[36]0.096	[36]0.060	[36]0.034	[68]0.994	[14]0.733	[11]0.395
151	PARAVISION-004	[7]0.010	[6]0.004	[6]0.002	[9]0.038	[8]0.024	[6]0.015	[143]1.000	[22]0.797	[2]0.170
152	PARAVISION-005	[4]0.004	[4]0.002	[4]0.002	[4]0.024	[4]0.016	[5]0.012	[37]0.980	[1]0.181	[1]0.109
153	PIXELALL-002	[108]0.105	[78]0.030	[64]0.011	[138]0.388	[69]0.083	[65]0.044	[136]1.000	[147]1.000	[143]0.997
154	PIXELALL-003	[19]0.022	[17]0.009	[15]0.003	[22]0.073	[21]0.043	[19]0.024	[122]1.000	[128]0.998	[33]0.720
155	QUANTASOFT-001	[204]0.639	[209]0.493	[206]0.333						
156	RANKONE-000	[148]0.217	[161]0.127	[161]0.075	[139]0.391	[145]0.291	[149]0.195			
157	RANKONE-001	[134]0.166	[134]0.084	[130]0.040						
158	RANKONE-002	[115]0.118	[129]0.071	[129]0.039	[114]0.261	[124]0.190	[130]0.126			
159	RANKONE-003	[116]0.118	[128]0.071	[128]0.039	[113]0.255	[122]0.187	[129]0.122			
160	RANKONE-004	[142]0.193	[158]0.124	[159]0.074	[144]0.426	[150]0.324	[153]0.221			
161	RANKONE-005	[75]0.059	[83]0.033	[93]0.018	[94]0.173	[98]0.119	[101]0.074	[92]0.998	[100]0.994	[136]0.990
162	RANKONE-006	[35]0.037	[42]0.020	[57]0.010				[33]0.977	[34]0.937	[47]0.870
163	RANKONE-007	[21]0.022	[25]0.011	[29]0.006	[34]0.095	[38]0.061	[42]0.036	[24]0.967	[29]0.924	[44]0.850
164	REALNETWORKS-000	[151]0.234	[165]0.138	[162]0.075	[131]0.319	[132]0.209	[133]0.129			
165	REALNETWORKS-001	[152]0.234	[164]0.138	[163]0.075	[130]0.319	[133]0.209	[132]0.129			
166	REALNETWORKS-002	[150]0.231	[163]0.137	[160]0.074	[129]0.315	[134]0.209	[134]0.129			
167	REALNETWORKS-003	[131]0.159	[137]0.090	[137]0.048	[117]0.266	[119]0.172	[117]0.102	[95]0.998	[74]0.987	[57]0.914
168	REALNETWORKS-004	[130]0.158	[136]0.090	[135]0.047	[115]0.263	[116]0.169	[114]0.099	[110]0.999	[93]0.992	[67]0.935
169	REMARKAI-000	[69]0.055	[58]0.023	[39]0.008	[59]0.120	[52]0.070	[46]0.037	[108]0.999	[103]0.995	[49]0.880
170	REMARKAI-000	[122]0.128	[118]0.059	[108]0.022	[100]0.203	[100]0.123	[93]0.064			
171	REMARKAI-002	[121]0.124	[116]0.059	[107]0.022	[98]0.196	[99]0.122	[92]0.063	[57]0.991	[63]0.980	[64]0.932
172	SCANOVATE-000	[81]0.067	[79]0.030	[63]0.011	[111]0.240	[106]0.150	[100]0.073	[17]0.893	[23]0.803	[29]0.683
173	SENSETIME-000	[17]0.021	[18]0.009	[23]0.004	[16]0.063	[16]0.040	[20]0.025	[166]1.000	[75]0.988	[46]0.869
174	SENSETIME-001	[20]0.022	[20]0.010	[25]0.005	[17]0.064	[20]0.041	[23]0.025			
175	SENSETIME-002	[11]0.015	[31]0.014	[77]0.014	[6]0.028	[7]0.023	[16]0.021	[66]0.994	[62]0.979	[43]0.842
176	SENSETIME-003	[1]0.002	[1]0.001	[1]0.001	[1]0.012	[1]0.009	[1]0.007	[2]0.477	[3]0.311	[3]0.212
177	SHAMAN-000	[183]0.473	[194]0.368	[198]0.257	[158]0.621	[163]0.507	[166]0.375			
178	SHAMAN-001	[192]0.530	[200]0.405	[201]0.272						
179	SHAMAN-002	[207]0.699	[214]0.581	[215]0.423						
180	SHAMAN-003	[184]0.451	[190]0.347	[190]0.223	[157]0.597	[160]0.472	[157]0.317			
181	SHAMAN-004	[198]0.615	[206]0.488	[210]0.342	[167]0.754	[171]0.639	[173]0.480			
182	SHAMAN-006	[126]0.141	[139]0.092	[153]0.058	[107]0.237	[115]0.168	[121]0.108	[29]0.972	[40]0.960	[62]0.931
183	SHAMAN-007	[127]0.141	[138]0.092	[152]0.057	[110]0.240	[117]0.169	[120]0.107			
184	SIAT-000	[97]0.088	[100]0.044	[95]0.019	[47]0.107	[44]0.064	[40]0.035			
185	SIAT-001	[13]0.018	[12]0.007	[11]0.003	[137]0.365	[152]0.348	[158]0.337			
186	SIAT-002	[18]0.022	[13]0.007	[9]0.003	[149]0.478	[158]0.460	[171]0.451			
187	SMILART-000	[199]0.619	[204]0.485	[204]0.320						
188	SMILART-001	[205]0.640	[211]0.504	[209]0.341						
189	SMILART-002	[200]0.628	[208]0.491	[205]0.323						
190	SMILART-004	[224]0.968	[230]0.965	[232]0.964	[185]0.976	[187]0.973	[189]0.973			
191	SMILART-005									
192	SYNESIS-000	[196]0.552	[196]0.376	[189]0.211	[166]0.734	[170]0.598	[170]0.431			
193	SYNESIS-003	[197]0.582	[202]0.443	[202]0.292	[160]0.646	[164]0.524	[165]0.372			
194	SYNESIS-003	[79]0.065	[80]0.032	[83]0.016						
195	TECH5-001	[71]0.057	[36]0.018	[34]0.008	[180]0.935	[31]0.055	[25]0.027	[154]1.000	[146]1.000	[150]0.999
196	TEVIAN-000	[144]0.200	[152]0.112	[147]0.052	[132]0.331	[135]0.227	[136]0.132			
197	TEVIAN-001	[145]0.200	[151]0.112	[148]0.052						
198	TEVIAN-002	[143]0.200	[150]0.112	[146]0.052						
199	TEVIAN-003	[139]0.177	[144]0.096	[131]0.041	[125]0.298	[126]0.198	[126]0.113			
200	TEVIAN-004	[114]0.117	[122]0.063	[118]0.028	[95]0.176	[92]0.115	[95]0.065			
201	TEVIAN-005	[95]0.087	[103]0.045	[98]0.019	[73]0.144	[72]0.089	[74]0.049	[23]0.962	[21]0.796	[25]0.634
202	TIGER-000	[179]0.390	[183]0.261	[182]0.140	[150]0.500	[153]0.366	[151]0.211			
203	TIGER-001				[155]0.580	[161]0.487	[169]0.396			
204	TIGER-002	[92]0.086	[91]0.039	[81]0.015	[83]0.158	[79]0.095	[73]0.048	[103]0.999	[57]0.975	[28]0.678
205	TIGER-003	[91]0.086	[90]0.039	[80]0.015	[82]0.158	[78]0.095	[72]0.048			
206	TONGYITRANS-000	[86]0.074	[89]0.038	[85]0.016	[49]0.112	[51]0.069	[49]0.038			
207	TONGYITRANS-001	[80]0.066	[81]0.032	[74]0.014	[40]0.101	[40]0.062	[38]0.034			
208	TOSHIBA-000	[76]0.062	[71]0.027	[59]0.011	[56]0.118	[57]0.074	[59]0.041	[76]0.995	[76]0.988	[72]0.949
209	TOSHIBA-001	[73]0.058	[38]0.019	[37]0.008	[32]0.092	[29]0.054	[33]0.032			
210	VD-000	[219]0.917	[224]0.827	[226]0.668	[182]0.946	[182]0.871	[182]0.725			
211	VD-001	[146]0.201	[155]0.116	[151]0.056	[121]0.281	[123]0.188	[119]0.106			
212	VIGILANTSOLUTIONS-000	[194]0.537	[197]0.393	[197]0.245	[165]0.695	[169]0.557	[167]0.389	[88]0.998	[104]0.995	[137]0.990
213	VIGILANTSOLUTIONS-001	[202]0.636	[210]0.501	[211]0.347				[127]1.000	[133]0.998	[141]0.995
214	VIGILANTSOLUTIONS-002	[218]0.876	[222]0.730	[219]0.488				[102]0.999	[108]0.995	[131]0.987
215	VIGILANTSOLUTIONS-003	[182]0.408	[185]0.282	[185]0.161	[164]0.660	[166]0.526	[161]0.356	[99]0.999	[106]0.995	[130]0.986
216	VIGILANTSOLUTIONS-004	[195]0.549	[201]0.422	[200]0.266	[172]0.817	[174]0.709	[175]0.523	[80]0.996	[90]0.991	[120]0.984

Table 24: **Threshold-based accuracy**. *Values are FNIR(N, T, L) with N = 1.6 million with thresholds set to produce FPIR = 0.001, 0.01, and 0.1 in non-mate searches. Columns 3-5 apply to FRVT-2018 mugshots: Columns 6-8 show the corresponding FNIR values for webcam images searched against the FRVT-2018 mugshot gallery. Finally, the three rightmost columns show FNIR for profile view images searched against the FRVT-2018 frontal gallery. Throughout blue superscripts indicate the rank of the algorithm for that column. Caution: The Power-low models are mostly intended to draw attention to the kind of behavior, not as a model to be used for prediction.*

MISSES BELOW THRESHOLD, T		ENROL MOST RECENT MUGSHOT, N = 1.6M								
FNIR(N, T> 0, R >L)		DATASET: FRVT 2018 MUGSHOTS			DATASET: WEBCAM PROBES			DATASET: PROFILE PROBES		
#	ALGORITHM	FPIR=0.001	FPIR=0.01	FPIR=0.1	FPIR=0.001	FPIR=0.01	FPIR=0.1	FPIR=0.001	FPIR=0.01	FPIR=0.1
217	VIGILANTSOLUTIONS-005	[178]0.388	[93]0.043	[101]0.020				[142]1.000	[150]1.000	[152]0.999
218	VIGILANTSOLUTIONS-006	[171]0.353	[96]0.043	[104]0.021				[145]1.000	[156]1.000	[147]0.998
219	VISIONLABS-003	[54]0.048	[61]0.023	[65]0.011	[69]0.137	[73]0.091	[80]0.051	[106]0.999	[109]0.995	[38]0.811
220	VISIONLABS-004	[72]0.058	[63]0.024	[35]0.008	[84]0.159	[81]0.097	[66]0.045	[16]0.890	[16]0.742	[20]0.525
221	VISIONLABS-005	[57]0.050	[44]0.020	[31]0.006	[74]0.147	[71]0.087	[58]0.041	[15]0.888	[15]0.736	[18]0.514
222	VISIONLABS-006	[28]0.027	[22]0.010	[19]0.004	[30]0.090	[25]0.051	[22]0.025	[7]0.672	[8]0.511	[9]0.328
223	VISIONLABS-007	[27]0.027	[21]0.010	[18]0.004	[29]0.090	[24]0.051	[21]0.025	[8]0.672	[7]0.511	[8]0.328
224	VISIONLABS-008	[9]0.013	[8]0.006	[8]0.003	[13]0.051	[13]0.032	[12]0.019	[3]0.481	[4]0.317	[4]0.203
225	VOCORD-000	[176]0.381	[154]0.114	[155]0.060	[122]0.285	[121]0.181	[122]0.108	[144]1.000	[157]1.000	[155]1.000
226	VOCORD-001	[162]0.291	[153]0.113	[154]0.060				[151]1.000	[153]1.000	[154]1.000
227	VOCORD-002	[169]0.336	[147]0.105	[150]0.055				[140]1.000	[151]1.000	[158]1.000
228	VOCORD-003	[120]0.122	[107]0.048	[87]0.017	[80]0.155	[76]0.093	[71]0.048	[93]0.998	[85]0.991	[52]0.891
229	VOCORD-004	[172]0.355	[108]0.051	[94]0.019	[91]0.173	[74]0.093	[67]0.046	[130]1.000	[135]0.999	[119]0.982
230	VOCORD-005	[129]0.158	[97]0.044	[86]0.017	[65]0.130	[66]0.080	[64]0.043	[82]0.997	[45]0.968	[45]0.865
231	VOCORD-006	[238]1.000	[236]1.000	[238]1.000	[194]1.000	[232]1.000	[206]1.000	[158]1.000	[184]1.000	[239]1.000
232	YISHENG-000	[175]0.378	[180]0.206	[168]0.083	[183]0.974	[143]0.275	[142]0.146			
233	YISHENG-001	[170]0.346	[179]0.206	[174]0.087	[169]0.808	[142]0.269	[141]0.144			
234	YITU-000	[52]0.047	[53]0.022	[53]0.009	[28]0.090	[30]0.054	[30]0.030			
235	YITU-001	[45]0.044	[46]0.021	[47]0.009						
236	YITU-002	[14]0.018	[14]0.008	[14]0.003	[12]0.049	[10]0.028	[8]0.016			
237	YITU-003	[16]0.019	[16]0.009	[24]0.004	[14]0.052	[15]0.033	[15]0.021			
238	YITU-004	[5]0.010	[5]0.004	[5]0.002	[5]0.027	[5]0.017	[4]0.011	[20]0.936	[28]0.913	[50]0.880
239	YITU-005	[6]0.010	[7]0.005	[10]0.003	[7]0.032	[6]0.023	[10]0.017			

Table 25: **Threshold-based accuracy**. *Values are FNIR(N, T, L) with N = 1.6 million with thresholds set to produce FPIR = 0.001, 0.01, and 0.1 in non-mate searches. Columns 3-5 apply to FRVT-2018 mugshots: Columns 6-8 show the corresponding FNIR values for webcam images searched against the FRVT-2018 mugshot gallery. Finally, the three rightmost columns show FNIR for profile view images searched against the FRVT-2018 frontal gallery. Throughout blue superscripts indicate the rank of the algorithm for that column. Caution: The Power-low models are mostly intended to draw attention to the kind of behavior, not as a model to be used for prediction.*

		INVESTIGATION MODE				IDENTIFICATION MODE				FAILURE TO EXTRACT			
		RANK ONE MISS RATE, FNIR(N, 0, 1)				HIGH T → FPIR = 0.01, FNIR(N, T, L)				FEATURES			
		N=1.6M	N=1.6M	N=1.6M	N=1.1M	N=1.6M	N=1.6M	N=1.6M	N=1.1M	N=1.6M	N=1.6M	N=1.6M	N=1.1M
#	ALGORITHM	FRVT-18	WEBCAM	PROFILE	WILD	FRVT-18	WEBCAM	PROFILE	WILD+	FRVT-18	WEBCAM	PROFILE	WILD
1	3DIVI-000	[152]0.032	[142]0.086		[59]0.071	[168]0.158	[146]0.302		[63]0.095				
2	3DIVI-001	[153]0.035			[62]0.074	[169]0.158			[64]0.095				
3	3DIVI-002	[158]0.038			[64]0.076	[170]0.161			[65]0.096				
4	3DIVI-003	[186]0.083	[160]0.206		[81]0.094	[186]0.282	[162]0.497		[85]0.136				
5	3DIVI-004	[127]0.018	[127]0.062			[141]0.093	[137]0.237						
6	3DIVI-005	[128]0.018	[126]0.062	[88]0.930	[32]0.052	[140]0.093	[136]0.234	[83]0.990	[42]0.069				
7	3DIVI-006	[143]0.024	[136]0.074		[38]0.060	[143]0.096	[138]0.238		[45]0.072				
8	ALCHERA-000	[123]0.016	[113]0.047	[79]0.870	[77]0.092	[126]0.070	[104]0.146	[116]0.996	[55]0.089				
9	ALCHERA-001	[234]0.987	[195]1.000			[233]0.999	[225]1.000						
10	ALCHERA-002	[187]0.095	[157]0.166	[112]0.954	[84]0.098	[189]0.302	[156]0.442	[136]0.999	[84]0.135				
11	ALCHERA-003	[100]0.010	[90]0.035	[51]0.741	[46]0.064	[127]0.070	[109]0.152	[121]0.997	[40]0.067				
12	ALLGOVISION-000	[107]0.011	[86]0.033	[81]0.894		[105]0.045	[94]0.106	[68]0.982					
13	ANKE-000	[116]0.013	[94]0.038	[92]0.931	[112]0.289	[120]0.063	[107]0.151	[81]0.990					
14	ANKE-001	[117]0.013	[95]0.038	[105]0.946	[111]0.284	[121]0.063	[108]0.151	[92]0.992					
15	ANKE-002	[29]0.003	[26]0.016	[30]0.522		[29]0.014	[23]0.050	[20]0.795					
16	AWARE-000	[178]0.061	[153]0.138	[146]0.978	[125]0.588	[160]0.126	[140]0.253	[130]0.998	[123]0.587				
17	AWARE-001	[175]0.056		[145]0.977	[124]0.580	[159]0.124		[139]0.999	[121]0.580				
18	AWARE-002	[176]0.057		[144]0.977		[156]0.117		[124]0.998					
19	AWARE-003	[150]0.031	[143]0.090	[130]0.966	[122]0.503	[132]0.082	[129]0.204	[61]0.977	[118]0.505				
20	AWARE-004	[181]0.068	[159]0.176	[143]0.976		[173]0.175	[154]0.375	[138]0.999					
21	AWARE-005	[151]0.031	[129]0.067	[147]0.978	[123]0.509	[135]0.085	[112]0.163	[132]0.999	[119]0.508				
22	AWARE-006	[183]0.070	[152]0.128	[150]0.983		[174]0.175	[144]0.283	[134]0.999					
23	AYONIX-000	[226]0.450	[188]0.685	[161]0.996	[120]0.400	[221]0.724	[183]0.892	[113]0.995	[122]0.586				
24	AYONIX-001	[221]0.341	[183]0.527	[155]0.993	[117]0.334	[219]0.701	[179]0.845	[117]0.996	[120]0.555				
25	AYONIX-002	[222]0.341	[184]0.527	[156]0.993		[220]0.702	[178]0.845	[118]0.996					
26	CAMVI-001	[214]0.225	[174]0.337	[110]0.953	[96]0.148	[212]0.548	[173]0.648	[71]0.984	[95]0.196				
27	CAMVI-002	[194]0.127		[83]0.915	[91]0.130	[198]0.400		[53]0.973	[90]0.157				
28	CAMVI-003	[174]0.052	[144]0.090	[82]0.911	[94]0.139	[115]0.058	[95]0.108	[35]0.940	[77]0.130				
29	CAMVI-004	[171]0.047	[138]0.077	[53]0.744	[136]1.000	[112]0.054	[82]0.100	[125]0.998	[134]1.000				
30	CAMVI-005	[180]0.065	[148]0.103	[54]0.746	[181]1.000	[131]0.076	[101]0.132	[132]0.998	[213]1.000				
31	COGENT-000	[101]0.010	[111]0.046	[126]0.965	[78]0.093	[76]0.029	[85]0.100	[80]0.991	[72]0.110				
32	COGENT-001	[102]0.010	[110]0.046	[127]0.965		[75]0.029	[86]0.100	[89]0.991					
33	COGENT-002	[37]0.004	[46]0.020	[86]0.925	[21]0.045	[35]0.017	[41]0.063	[97]0.994	[23]0.051				
34	COGENT-003	[39]0.004	[53]0.021	[103]0.939	[33]0.053	[33]0.016	[39]0.061	[111]0.995	[32]0.063				
35	COGNITEC-000	[146]0.025	[121]0.059	[122]0.964		[142]0.095	[127]0.200	[47]0.971					
36	COGNITEC-001	[108]0.012	[88]0.034	[117]0.958	[61]0.074	[109]0.053	[103]0.135	[42]0.965	[46]0.072				
37	COGNITEC-002	[64]0.006	[73]0.025	[107]0.949	[50]0.065	[66]0.025	[89]0.101	[39]0.956	[28]0.061				
38	COGNITEC-003	[68]0.006	[72]0.025	[91]0.930	[29]0.051	[68]0.025	[83]0.100	[36]0.946	[19]0.049				
39	CYBERLINK-000	[42]0.004	[45]0.020	[49]0.717		[57]0.023	[53]0.070	[67]0.981					
40	CYBERLINK-001	[34]0.004	[35]0.018	[50]0.731		[55]0.022	[48]0.067	[70]0.984					
41	DAHUA-000	[94]0.009	[75]0.026			[101]0.045	[70]0.083						
42	DAHUA-001	[72]0.007	[67]0.024	[48]0.703	[4]0.038	[87]0.037	[62]0.075	[32]0.933	[8]0.043				
43	DAHUA-002	[14]0.002	[11]0.012	[12]0.304		[10]0.006	[11]0.029	[9]0.522					
44	DEEPGLINT-001		[193]0.909	[63]0.796			[205]1.000	[218]1.000					
45	DEEPSEA-001	[48]0.004	[24]0.016	[71]0.814		[52]0.022	[35]0.059	[54]0.973					
46	DERMALOG-000	[195]0.129	[164]0.218	[90]0.930	[63]0.075	[193]0.362	[168]0.528	[84]0.991	[69]0.104				
47	DERMALOG-001	[198]0.154		[104]0.941	[75]0.089	[199]0.403		[69]0.983	[81]0.131				
48	DERMALOG-002	[196]0.135		[93]0.933	[66]0.076	[195]0.376		[65]0.981	[70]0.105				
49	DERMALOG-003	[192]0.126	[163]0.217			[192]0.360	[167]0.526						
50	DERMALOG-004	[191]0.125	[162]0.215	[89]0.930	[53]0.066	[191]0.358	[165]0.526	[91]0.991	[61]0.095				
51	DERMALOG-005	[122]0.015	[93]0.037	[47]0.701	[52]0.066	[94]0.043	[80]0.096	[38]0.950	[38]0.066				
52	DERMALOG-006	[85]0.008	[71]0.024	[40]0.619	[35]0.056	[70]0.026	[46]0.067	[33]0.933	[26]0.054				
53	DERMALOG-007	[93]0.009	[76]0.027			[92]0.040	[77]0.093						
54	EYEDEA-000	[219]0.298	[178]0.443	[141]0.974	[92]0.131	[218]0.679	[176]0.783	[87]0.991	[103]0.249				
55	EYEDEA-001	[207]0.196		[98]0.937	[60]0.072	[203]0.479		[101]0.994	[80]0.131				
56	EYEDEA-002	[208]0.198		[94]0.934	[57]0.070	[205]0.488		[115]0.996	[78]0.130				
57	EYEDEA-003	[185]0.080	[155]0.148	[120]0.960	[48]0.064	[184]0.265	[155]0.404	[80]0.990	[56]0.091				
58	F8-001	[113]0.012		[44]0.669		[85]0.036		[114]0.995					
59	GLORY-000	[203]0.178	[171]0.320	[159]0.994		[188]0.295	[159]0.470	[95]0.993					
60	GLORY-001	[193]0.127	[168]0.267	[154]0.992	[114]0.315	[181]0.236	[157]0.448	[86]0.991	[110]0.353				
61	GORILLA-000				[133]0.994				[131]0.994				
62	GORILLA-001	[177]0.060	[145]0.095	[97]0.936	[37]0.057	[182]0.246	[148]0.314	[152]1.000	[48]0.076				
63	GORILLA-002	[134]0.020	[107]0.044	[55]0.753	[19]0.045	[148]0.106	[118]0.170	[96]0.993	[20]0.049				
64	GORILLA-003	[155]0.036	[132]0.070	[72]0.821	[56]0.069	[167]0.157	[139]0.247	[148]1.000	[51]0.080				
65	GORILLA-004	[69]0.006	[68]0.024	[46]0.697		[95]0.043	[87]0.101	[27]0.903					
66	HBINNO-000	[218]0.273		[153]0.990	[118]0.335	[216]0.631		[144]1.000	[112]0.411				
67	HIK-000	[139]0.021	[85]0.033	[114]0.957	[97]0.153	[125]0.068	[91]0.103	[48]0.971	[89]0.155				
68	HIK-001	[120]0.015		[109]0.952	[101]0.162	[123]0.065		[66]0.981	[92]0.166				
69	HIK-002	[119]0.015		[77]0.857	[83]0.094	[124]0.065		[72]0.985	[68]0.103				
70	HIK-003	[109]0.012	[78]0.027	[45]0.689		[114]0.057	[92]0.105	[30]0.925					
71	HIK-004	[106]0.011	[77]0.027	[52]0.743	[42]0.062	[111]0.054	[88]0.101	[37]0.947	[47]0.075				
72	HIK-005	[52]0.005	[28]0.017	[33]0.535		[40]0.019	[22]0.048	[127]0.998					

Table 26: **Miss rates by dataset:** *At left, rank 1 miss rates relevant to investigations; at right, with threshold set to target FPIR = 0.01 for higher volume, low prior, uses. +For the WILD set, FPIR = 0.1 Yellow indicates most accurate algorithm. Throughout blue superscripts indicate the rank of the algorithm for that column.*

		INVESTIGATION MODE				IDENTIFICATION MODE				FAILURE TO EXTRACT			
		RANK ONE MISS RATE, FNIR(N, 0, 1)				HIGH T → FPIR = 0.01, FNIR(N, T, L)				FEATURES			
		N=1.6M	N=1.6M	N=1.6M	N=1.1M	N=1.6M	N=1.6M	N=1.6M	N=1.1M	N=1.6M	N=1.6M	N=1.6M	N=1.1M
#	ALGORITHM	FRVT-18	WEBCAM	PROFILE	WILD	FRVT-18	WEBCAM	PROFILE	WILD[+]	FRVT-18	WEBCAM	PROFILE	WILD
73	HIK-006	[53]0.005	[27]0.017	[34]0.535	[135]1.000	[43]0.020	[26]0.052	[140]0.999	[133]1.000				
74	IDEMIA-000	[88]0.009	[89]0.034	[95]0.935	[104]0.166	[117]0.059	[110]0.156	[73]0.986	[107]0.288				
75	IDEMIA-001	[90]0.009		[99]0.937	[99]0.157	[74]0.029		[41]0.964	[97]0.205				
76	IDEMIA-002	[99]0.010		[113]0.956	[107]0.198	[77]0.029		[43]0.965	[100]0.242				
77	IDEMIA-003	[76]0.007	[87]0.034	[115]0.958		[48]0.021	[65]0.079	[206]1.000					
78	IDEMIA-004	[71]0.007	[84]0.032	[106]0.947	[27]0.051	[47]0.021	[64]0.079	[44]0.968	[35]0.064				
79	IDEMIA-005	[84]0.008	[100]0.039	[111]0.954	[16]0.044	[69]0.026	[90]0.102	[52]0.973	[27]0.055				
80	IDEMIA-006	[97]0.010	[134]0.072	[133]0.969	[31]0.052	[67]0.025	[111]0.161	[64]0.980	[39]0.067				
81	IDEMIA-007	[26]0.003	[21]0.015	[213]1.000		[15]0.008	[14]0.033	[180]1.000					
82	IMAGUS-000	[220]0.304	[180]0.482	[160]0.994	[109]0.222	[215]0.607	[175]0.779	[142]1.000	[109]0.311				
83	IMAGUS-002	[212]0.220	[169]0.301	[152]0.988	[98]0.154	[213]0.564	[172]0.645	[149]1.000	[105]0.252				
84	IMAGUS-003	[223]0.356	[181]0.513	[157]0.993		[217]0.669	[177]0.809	[145]1.000					
85	IMPERIAL-000	[25]0.002	[18]0.015	[11]0.280		[19]0.009	[18]0.041	[102]0.995					
86	INCODE-000	[173]0.049	[147]0.100	[108]0.951		[178]0.199	[147]0.304	[99]0.994					
87	INCODE-001	[125]0.017	[112]0.046	[56]0.762	[30]0.052	[149]0.112	[125]0.198	[143]1.000	[30]0.062				
88	INCODE-002	[129]0.018	[114]0.048	[73]0.843	[8]0.039	[146]0.100	[120]0.176	[60]0.976	[13]0.045				
89	INCODE-003	[115]0.013	[102]0.040	[57]0.764	[10]0.039	[133]0.084	[114]0.164	[119]0.996	[12]0.044				
90	INCODE-004	[35]0.004	[33]0.017	[25]0.475		[60]0.023	[54]0.070	[31]0.929					
91	INNOVATRICS-000	[160]0.040	[132]0.076	[124]0.964	[105]0.188	[171]0.163	[141]0.258	[58]0.975	[101]0.245				
92	INNOVATRICS-001	[161]0.040		[123]0.964	[106]0.193	[172]0.163		[59]0.975	[99]0.221				
93	INNOVATRICS-002	[170]0.045	[135]0.074	[76]0.853		[166]0.139	[131]0.209	[141]0.999					
94	INNOVATRICS-003	[147]0.026	[117]0.055	[75]0.845	[58]0.071	[162]0.132	[128]0.203	[131]0.998	[52]0.081				
95	INNOVATRICS-004	[114]0.012	[103]0.040	[116]0.958	[55]0.067	[130]0.074	[105]0.149	[50]0.973	[43]0.071				
96	INNOVATRICS-005	[24]0.002				[30]0.014							
97	INTSYSMSU-000	[197]0.146	[66]0.023	[36]0.562		[231]0.990	[188]0.998	[126]0.998					
98	ISYSTEMS-000	[104]0.011	[99]0.038	[135]0.969	[103]0.163	[99]0.044	[96]0.110	[79]0.989	[94]0.169				
99	ISYSTEMS-001	[103]0.011		[134]0.969	[102]0.162	[98]0.044		[78]0.989	[93]0.169				
100	ISYSTEMS-002	[70]0.006	[74]0.026	[74]0.844	[24]0.049	[82]0.032	[67]0.080	[94]0.993	[22]0.051				
101	ISYSTEMS-003	[60]0.005	[63]0.023	[60]0.791	[15]0.043	[64]0.024	[50]0.068	[123]0.997	[10]0.044				
102	KEDACOM-001	[80]0.008	[91]0.036	[138]0.972		[28]0.013	[28]0.054	[55]0.973					
103	KNERON-000	[65]0.006				[84]0.033							
104	LOOKMAN-003	[89]0.009	[98]0.038		[165]1.000	[65]0.025	[68]0.082						
105	LOOKMAN-004	[91]0.009	[101]0.039	[140]0.973	[173]1.000	[62]0.024	[60]0.075	[56]0.974					
106	LOOKMAN-005	[83]0.008	[92]0.036	[139]0.972		[34]0.017	[42]0.063	[51]0.973					
107	MEGVII-000	[79]0.007	[31]0.017		[41]0.061	[113]0.055	[47]0.067		[60]0.094				
108	MEGVII-001	[110]0.012	[32]0.017			[86]0.037	[37]0.061						
109	MEGVII-002	[111]0.012	[34]0.017	[23]0.450		[88]0.037	[34]0.059	[26]0.872					
110	MICROFOCUS-000	[230]0.596	[192]0.782		[115]0.316	[227]0.867	[186]0.950		[115]0.434				
111	MICROFOCUS-001	[231]0.596			[116]0.316	[226]0.867			[116]0.434				
112	MICROFOCUS-002	[232]0.626			[119]0.342	[228]0.869			[117]0.447				
113	MICROFOCUS-003	[229]0.594	[191]0.781		[110]0.279	[225]0.866	[185]0.948		[113]0.412				
114	MICROFOCUS-004	[228]0.576	[190]0.758			[234]0.999	[184]0.940						
115	MICROFOCUS-005	[224]0.424	[187]0.601		[100]0.158	[223]0.736	[181]0.865		[106]0.261				
116	MICROFOCUS-006	[225]0.427	[186]0.583		[95]0.146	[229]0.963	[180]0.858		[102]0.246				
117	MICROSOFT-000	[40]0.004	[49]0.021		[49]0.065	[39]0.019	[55]0.071		[37]0.065				
118	MICROSOFT-001	[36]0.004			[44]0.062	[41]0.020			[29]0.061				
119	MICROSOFT-002	[43]0.004			[45]0.063	[59]0.023			[34]0.063				
120	MICROSOFT-003	[7]0.002	[13]0.012			[26]0.012	[32]0.056						
121	MICROSOFT-004	[5]0.001	[12]0.012		[9]0.039	[24]0.011	[27]0.053		[9]0.043				
122	MICROSOFT-005	[16]0.002	[9]0.011	[4]0.144	[2]0.033	[23]0.010	[19]0.041	[5]0.354	[4]0.041				
123	MICROSOFT-006	[17]0.002	[10]0.011	[6]0.150		[9]0.006	[9]0.024	[2]0.281					
124	NEC-000	[126]0.017	[105]0.041	[119]0.959	[134]0.999	[106]0.047	[75]0.093	[46]0.969	[132]0.999				
125	NEC-001	[138]0.021	[118]0.056	[132]0.967		[119]0.060	[102]0.133	[49]0.972					
126	NEC-002	[2]0.001	[3]0.009	[20]0.363	[80]0.093	[2]0.002	[3]0.013	[105]0.995	[71]0.107				
127	NEC-003	[4]0.001	[6]0.010	[19]0.352	[74]0.088	[3]0.002	[2]0.013	[10]0.628	[58]0.092				
128	NEUROTECHNOLOGY-000	[122]0.047	[149]0.104	[137]0.972	[137]1.000	[177]0.194	[149]0.317	[112]0.995	[135]1.000				
129	NEUROTECHNOLOGY-001	[169]0.044		[129]0.966	[130]0.954	[176]0.193		[107]0.995	[128]0.953				
130	NEUROTECHNOLOGY-002	[168]0.044		[128]0.966	[131]0.983	[175]0.193		[110]0.995	[129]0.983				
131	NEUROTECHNOLOGY-003	[141]0.022	[106]0.042	[121]0.961		[145]0.099	[113]0.164	[229]1.000					
132	NEUROTECHNOLOGY-004	[61]0.006	[44]0.020	[136]0.970	[76]0.090	[72]0.028	[56]0.073	[82]0.990	[74]0.122				
133	NEUROTECHNOLOGY-005	[47]0.004	[70]0.024	[80]0.893	[121]0.408	[54]0.022	[59]0.074	[77]0.989	[114]0.415				
134	NEUROTECHNOLOGY-006	[130]0.018	[109]0.045	[39]0.606	[25]0.050	[157]0.121	[130]0.206		[36]0.065				
135	NEUROTECHNOLOGY-007	[41]0.004	[52]0.021	[64]0.796		[51]0.021	[49]0.068	[122]0.997					
136	NEWLAND-002	[184]0.079	[150]0.117	[96]0.936		[187]0.294	[151]0.335	[129]0.998					
137	NOBLIS-001	[216]0.249	[182]0.522	[158]0.993	[127]0.734	[232]0.991	[206]1.000	[155]1.000	[124]0.744				
138	NOBLIS-002	[204]0.179	[177]0.392	[149]0.982		[207]0.488	[198]1.000	[154]1.000					
139	NTECHLAB-000	[95]0.009	[83]0.031	[38]0.595	[12]0.041	[102]0.045	[93]0.105	[24]0.826	[7]0.043				
140	NTECHLAB-001	[112]0.012		[41]0.630	[20]0.045	[110]0.053		[25]0.842	[21]0.049				
141	NTECHLAB-003	[66]0.006	[60]0.023	[26]0.504		[73]0.028	[61]0.075	[19]0.752					
142	NTECHLAB-004	[57]0.005	[40]0.019	[27]0.506	[14]0.043	[49]0.021	[45]0.065	[17]0.746	[18]0.048				
143	NTECHLAB-005	[54]0.005	[36]0.018	[21]0.367	[7]0.038	[50]0.021	[43]0.063	[13]0.661	[6]0.042				
144	NTECHLAB-006	[46]0.004	[30]0.017	[18]0.347	[6]0.038	[37]0.018	[33]0.059	[11]0.635	[5]0.042				

Table 27: **Miss rates by dataset:** *At left, rank 1 miss rates relevant to investigations; at right, with threshold set to target FPIR = 0.01 for higher volume, low prior, uses. [+]For the WILD set, FPIR = 0.1 Yellow indicates most accurate algorithm. Throughout blue superscripts indicate the rank of the algorithm for that column.*

		INVESTIGATION MODE				IDENTIFICATION MODE				FAILURE TO EXTRACT			
		RANK ONE MISS RATE, FNIR(N, 0, 1)				HIGH T → FPIR = 0.01, FNIR(N, T, L)				FEATURES			
		N=1.6M	N=1.6M	N=1.6M	N=1.1M	N=1.6M	N=1.6M	N=1.6M	N=1.1M	N=1.6M	N=1.6M	N=1.6M	N=1.1M
#	ALGORITHM	FRVT-18	WEBCAM	PROFILE	WILD	FRVT-18	WEBCAM	PROFILE	WILD+	FRVT-18	WEBCAM	PROFILE	WILD
145	NTECHLAB-007	[27] 0.003	[14] 0.012	[13] 0.326		[27] 0.012	[17] 0.041	[12] 0.642					
146	NTECHLAB-008	[9] 0.002	[4] 0.010	[7] 0.157		[11] 0.007	[12] 0.029	[6] 0.391					
147	PARAVISION-000	[131] 0.019	[97] 0.038	[32] 0.534		[104] 0.045	[84] 0.100	[120] 0.997					
148	PARAVISION-001	[38] 0.004	[47] 0.020	[14] 0.329	[129] 0.928	[45] 0.020	[58] 0.074	[98] 0.994	[127] 0.927				
149	PARAVISION-002	[45] 0.004	[55] 0.022	[16] 0.335	[113] 0.302	[56] 0.022	[63] 0.076	[18] 0.748	[108] 0.308				
150	PARAVISION-003	[31] 0.003	[41] 0.019	[10] 0.252	[5] 0.038	[32] 0.016	[36] 0.060	[14] 0.733	[11] 0.044				
151	PARAVISION-004	[8] 0.002	[8] 0.010	[2] 0.104		[6] 0.004	[8] 0.024	[22] 0.797					
152	PARAVISION-005	[6] 0.002	[5] 0.010	[1] 0.079		[4] 0.002	[4] 0.016	[1] 0.181					
153	PIXELALL-002	[50] 0.005	[57] 0.022	[69] 0.810		[78] 0.030	[69] 0.083	[142] 1.000					
154	PIXELALL-003	[19] 0.002	[16] 0.014	[29] 0.515		[17] 0.009	[21] 0.043	[128] 0.998					
155	QUANTASOFT-001	[211] 0.218	[189] 0.727		[126] 0.620	[209] 0.493			[125] 0.760				
156	RANKONE-000	[167] 0.043	[151] 0.117		[89] 0.114	[161] 0.127	[145] 0.291		[91] 0.161				
157	RANKONE-001	[140] 0.022			[68] 0.077	[134] 0.084			[67] 0.102				
158	RANKONE-002	[132] 0.019	[133] 0.071			[129] 0.071	[124] 0.190						
159	RANKONE-003	[133] 0.019	[130] 0.068		[69] 0.078	[128] 0.071	[122] 0.187		[62] 0.095				
160	RANKONE-004	[166] 0.041	[154] 0.141		[82] 0.094	[158] 0.124	[150] 0.324		[75] 0.126				
161	RANKONE-005	[96] 0.009	[104] 0.041	[151] 0.986	[39] 0.061	[83] 0.033	[98] 0.119	[100] 0.994	[41] 0.068				
162	RANKONE-006	[59] 0.005		[66] 0.797		[42] 0.020		[34] 0.937					
163	RANKONE-007	[32] 0.003	[39] 0.019	[62] 0.796		[25] 0.011	[38] 0.061	[29] 0.924					
164	REALNETWORKS-000	[165] 0.040	[141] 0.078		[65] 0.076	[165] 0.138	[132] 0.209		[53] 0.084				
165	REALNETWORKS-001	[164] 0.040	[140] 0.078			[164] 0.138	[133] 0.209						
166	REALNETWORKS-002	[159] 0.039	[139] 0.078		[132] 0.992	[163] 0.137	[134] 0.209		[130] 0.992				
167	REALNETWORKS-003	[144] 0.024	[125] 0.062	[59] 0.771		[137] 0.090	[119] 0.172	[74] 0.987					
168	REALNETWORKS-004	[142] 0.024	[122] 0.059	[65] 0.797		[136] 0.090	[116] 0.169	[93] 0.992					
169	REMARKAI-000	[33] 0.003	[37] 0.018	[43] 0.660		[58] 0.023	[52] 0.070	[103] 0.995					
170	REMARKAI-000	[87] 0.009	[82] 0.030			[118] 0.059	[100] 0.123						
171	REMARKAI-002	[86] 0.008	[80] 0.029	[67] 0.802	[23] 0.046	[116] 0.059	[99] 0.122	[63] 0.980	[25] 0.052				
172	SCANOVATE-000	[58] 0.005	[108] 0.045	[35] 0.560		[79] 0.030	[106] 0.150	[23] 0.803					
173	SENSETIME-000	[21] 0.002	[23] 0.016	[31] 0.528		[18] 0.009	[16] 0.040	[75] 0.988					
174	SENSETIME-001	[22] 0.002	[22] 0.016		[3] 0.038	[20] 0.010	[20] 0.041		[1] -0.796				
175	SENSETIME-002	[118] 0.014	[42] 0.020	[22] 0.384		[31] 0.014	[7] 0.023	[62] 0.979					
176	SENSETIME-003	[1] 0.001	[1] 0.007	[5] 0.150		[1] 0.001	[1] 0.009	[3] 0.311					
177	SHAMAN-000	[200] 0.168	[167] 0.262		[90] 0.115	[194] 0.368	[163] 0.507		[86] 0.146				
178	SHAMAN-001	[201] 0.170			[88] 0.113	[200] 0.405			[88] 0.153				
179	SHAMAN-002	[217] 0.260			[93] 0.132	[214] 0.581			[96] 0.201				
180	SHAMAN-003	[189] 0.124	[158] 0.172		[86] 0.109	[190] 0.347	[160] 0.472		[82] 0.132				
181	SHAMAN-004	[213] 0.222	[170] 0.319			[206] 0.488	[171] 0.639						
182	SHAMAN-006	[163] 0.040	[120] 0.058	[102] 0.938		[139] 0.092	[115] 0.168	[40] 0.960					
183	SHAMAN-007	[162] 0.040	[119] 0.057		[70] 0.078	[138] 0.092	[117] 0.169		[50] 0.079				
184	SIAT-000	[81] 0.008	[51] 0.021		[71] 0.078	[100] 0.044	[44] 0.064		[104] 0.250				
185	SIAT-001	[11] 0.002	[173] 0.333		[11] 0.040	[12] 0.007	[152] 0.348		[3] 0.041				
186	SIAT-002	[12] 0.002	[179] 0.446			[13] 0.007	[158] 0.460						
187	SMILART-000	[205] 0.191	[172] 0.325		[208] 1.000	[204] 0.485			[136] 1.000				
188	SMILART-001	[210] 0.217			[197] 1.000	[211] 0.504			[161] 1.000				
189	SMILART-002	[206] 0.192			[177] 1.000	[208] 0.491			[215] 1.000				
190	SMILART-004	[233] 0.965	[194] 0.974		[128] 0.834	[230] 0.965	[187] 0.973		[126] 0.833				
191	SMILART-005												
192	SYNESIS-000	[199] 0.160	[176] 0.361			[196] 0.376	[170] 0.598						
193	SYNESIS-003	[202] 0.170	[165] 0.235			[202] 0.443	[164] 0.524						
194	SYNESIS-003	[124] 0.016	[64] 0.023			[80] 0.032							
195	TECH5-001	[44] 0.004	[29] 0.017	[37] 0.584		[36] 0.018	[31] 0.055	[146] 1.000					
196	TEVIAN-000	[137] 0.020	[128] 0.066		[34] 0.054	[152] 0.112	[135] 0.227		[44] 0.072				
197	TEVIAN-001	[136] 0.020			[43] 0.062	[151] 0.112			[49] 0.078				
198	TEVIAN-002	[135] 0.020			[79] 0.093	[150] 0.112			[73] 0.118				
199	TEVIAN-003	[121] 0.015	[115] 0.052			[144] 0.096	[126] 0.198						
200	TEVIAN-004	[105] 0.011	[96] 0.038		[26] 0.050	[122] 0.063	[97] 0.115		[33] 0.063				
201	TEVIAN-005	[78] 0.007	[79] 0.028	[24] 0.467		[103] 0.045	[72] 0.089	[21] 0.796					
202	TIGER-000	[179] 0.062	[146] 0.095		[172] 1.000	[183] 0.261	[153] 0.366		[230] 1.000				
203	TIGER-001		[175] 0.351				[161] 0.487						
204	TIGER-002	[62] 0.006	[62] 0.023	[28] 0.514		[91] 0.039	[79] 0.095	[57] 0.975					
205	TIGER-003	[63] 0.006	[61] 0.023			[90] 0.039	[78] 0.095						
206	TONGYITRANS-000	[75] 0.007	[59] 0.022			[89] 0.038	[51] 0.069						
207	TONGYITRANS-001	[74] 0.007	[58] 0.022		[87] 0.112	[81] 0.032	[40] 0.062		[83] 0.134				
208	TOSHIBA-000	[49] 0.004	[54] 0.022	[58] 0.766		[71] 0.027	[57] 0.074	[76] 0.988					
209	TOSHIBA-001	[56] 0.005	[56] 0.022			[38] 0.019	[29] 0.054						
210	VD-000	[227] 0.474	[185] 0.551		[108] 0.217	[224] 0.827	[182] 0.871		[111] 0.362				
211	VD-001	[149] 0.028	[116] 0.053			[155] 0.116	[123] 0.188						
212	VIGILANTSOLUTIONS-000	[188] 0.123	[161] 0.212	[148] 0.980	[67] 0.076	[197] 0.393	[169] 0.557	[104] 0.995	[87] 0.152				
213	VIGILANTSOLUTIONS-001	[209] 0.202		[142] 0.975	[85] 0.103	[210] 0.501		[133] 0.998	[98] 0.209				
214	VIGILANTSOLUTIONS-002	[215] 0.237		[131] 0.966	[47] 0.064	[222] 0.730		[108] 0.995	[76] 0.129				
215	VIGILANTSOLUTIONS-003	[182] 0.069	[156] 0.151	[118] 0.958	[51] 0.065	[185] 0.282	[166] 0.526	[106] 0.995	[79] 0.131				
216	VIGILANTSOLUTIONS-004	[190] 0.125	[166] 0.244	[125] 0.965		[201] 0.422	[174] 0.709	[90] 0.991					

Table 28: **Miss rates by dataset:** *At left, rank 1 miss rates relevant to investigations; at right, with threshold set to target FPIR = 0.01 for higher volume, low prior, uses. +For the WILD set, FPIR = 0.1 Yellow indicates most accurate algorithm. Throughout blue superscripts indicate the rank of the algorithm for that column.*

		INVESTIGATION MODE				IDENTIFICATION MODE				FAILURE TO EXTRACT			
		RANK ONE MISS RATE, FNIR(N, 0, 1)				HIGH T → FPIR = 0.01, FNIR(N, T, L)				FEATURES			
		N=1.6M	N=1.6M	N=1.6M	N=1.1M	N=1.6M	N=1.6M	N=1.6M	N=1.1M	N=1.6M	N=1.6M	N=1.6M	N=1.1M
#	ALGORITHM	FRVT-18	WEBCAM	PROFILE	WILD	FRVT-18	WEBCAM	PROFILE	WILD+	FRVT-18	WEBCAM	PROFILE	WILD
217	VIGILANTSOLUTIONS-005	[92] 0.009		[84] 0.920		[93] 0.043		[150] 1.000					
218	VIGILANTSOLUTIONS-006	[98] 0.010		[85] 0.921		[96] 0.043		[156] 1.000					
219	VISIONLABS-003	[73] 0.007	[81] 0.030	[42] 0.640	[28] 0.051	[61] 0.023	[73] 0.091	[109] 0.995	[15] 0.046				
220	VISIONLABS-004	[28] 0.003	[43] 0.020	[17] 0.343		[63] 0.024	[81] 0.097	[16] 0.742					
221	VISIONLABS-005	[23] 0.002	[38] 0.019	[15] 0.334	[13] 0.043	[44] 0.020	[71] 0.087	[15] 0.736	[16] 0.046				
222	VISIONLABS-006	[13] 0.002	[20] 0.015	[9] 0.211		[22] 0.010	[25] 0.051	[8] 0.511					
223	VISIONLABS-007	[10] 0.002	[19] 0.015	[8] 0.211	[1] 0.033	[21] 0.010	[24] 0.051	[7] 0.511	[2] 0.035				
224	VISIONLABS-008	[18] 0.002	[15] 0.014	[3] 0.141		[8] 0.006	[13] 0.032	[4] 0.317					
225	VOCORD-000	[157] 0.038	[131] 0.068	[101] 0.937		[154] 0.114	[121] 0.181	[152] 1.000					
226	VOCORD-001	[156] 0.038		[100] 0.937		[153] 0.113		[153] 1.000					
227	VOCORD-002	[154] 0.036		[87] 0.929		[147] 0.105		[151] 1.000					
228	VOCORD-003	[67] 0.006	[69] 0.024	[68] 0.804	[36] 0.057	[107] 0.048	[76] 0.093	[85] 0.991	[31] 0.062				
229	VOCORD-004	[82] 0.008	[50] 0.021	[61] 0.792		[108] 0.051	[74] 0.093	[135] 0.999					
230	VOCORD-005	[77] 0.007	[65] 0.023	[70] 0.812	[17] 0.044	[97] 0.044	[66] 0.080	[45] 0.968	[14] 0.045				
231	VOCORD-006	[235] 1.000	[203] 1.000	[238] 1.000		[236] 1.000	[232] 1.000	[184] 1.000					
232	YISHENG-000	[145] 0.024	[123] 0.060		[54] 0.067	[180] 0.206	[143] 0.275		[66] 0.100				
233	YISHENG-001	[148] 0.027	[124] 0.060		[40] 0.061	[179] 0.206	[142] 0.269		[54] 0.087				
234	YITU-000	[55] 0.005	[48] 0.020		[73] 0.086	[53] 0.022	[30] 0.054		[59] 0.094				
235	YITU-001	[51] 0.005			[72] 0.086	[46] 0.021			[57] 0.092				
236	YITU-002	[15] 0.002	[7] 0.010		[22] 0.046	[14] 0.008	[10] 0.028		[24] 0.051				
237	YITU-003	[30] 0.003	[25] 0.016			[16] 0.009	[15] 0.033						
238	YITU-004	[3] 0.001	[2] 0.008	[78] 0.866	[18] 0.044	[5] 0.004	[5] 0.017	[28] 0.913	[17] 0.047				
239	YITU-005	[20] 0.002	[17] 0.014			[7] 0.005	[6] 0.023						

Table 29: **Miss rates by dataset:** *At left, rank 1 miss rates relevant to investigations; at right, with threshold set to target FPIR = 0.01 for higher volume, low prior, uses. +For the WILD set, FPIR = 0.1 Yellow indicates most accurate algorithm. Throughout blue superscripts indicate the rank of the algorithm for that column.*

MISSES OUTSIDE RANK R		MUGSHOT SEARCHES, N = 1.6M IDENTITIES							
		INVESTIGATION MODE, T = 0				IDENTIFICATION MODE, T > 0 FOR FPIR = 0.001			
FNIR(N, T, R)		PROPORTION MATED SEARCHES				PROPORTION MATED SEARCHES			
		WITHOUT THE MATE AT RANK 1		WITH NO MATE AT RANK 1	WITH K-TH MATE NOT IN TOP K	WITH THE MATE BELOW THRESHOLD		WITHOUT ANY MATE ABOVE THRESH	WITHOUT ALL MATES ABOVE THRESH
GALLERY		RECENT	CONSOLIDATED	UNCONSOLIDATED		RECENT	CONSOLIDATED	UNCONSOLIDATED	
1	3DIVI-5	[80]0.0176	[69]0.0130	[74]0.0133	[76]0.0449	[83]0.1664	[73]0.1334	[86]0.1339	[91]0.3186
2	3DIVI-6	[85]0.0240	[72]0.0183	[79]0.0172	[75]0.0410	[85]0.1681	[74]0.1339	[87]0.1350	[90]0.3160
3	ALCHERA-2	[99]0.0949	[85]0.0910	[93]0.0734	[94]0.1876	[98]0.4864	[86]0.3719	[105]0.4418	[108]0.6820
4	ALLGOVISION-000	[70]0.0114	[65]0.0106	[71]0.0105	[64]0.0233	[68]0.0881	[61]0.0736	[70]0.0736	[76]0.1995
5	ANKE-0	[76]0.0132	[61]0.0097	[68]0.0100	[73]0.0338	[72]0.1169	[64]0.0982	[76]0.0989	[84]0.2558
6	ANKE-002	[14]0.0028	[36]0.0048	[36]0.0048	[21]0.0087	[24]0.0318	[24]0.0278	[27]0.0278	[40]0.0901
7	ANKE-1	[77]0.0132	[62]0.0097	[69]0.0101	[72]0.0337	[73]0.1192	[65]0.0995	[79]0.1001	[85]0.2581
8	AWARE-5	[89]0.0311	[74]0.0205	[83]0.0230	[87]0.0740	[95]0.3643	[85]0.2895	[102]0.3777	[106]0.6534
9	AWARE-6	[97]0.0697	[84]0.0535	[90]0.0538	[92]0.1551	[92]0.2756	[82]0.2383	[99]0.2465	[103]0.5140
10	AYONIX-1	[106]0.3414	[92]0.3361	[98]0.2841	[99]0.4764	[102]0.8243	[92]0.8533	[110]0.7935	[111]0.9037
11	AYONIX-2	[105]0.3414	[91]0.2603	[99]0.2841	[98]0.4763	[101]0.8242	[90]0.8038	[109]0.7933	[110]0.9036
12	CAMVI-4	[95]0.0468	[82]0.0324	[89]0.0469	[77]0.0475	[58]0.0716	[49]0.0501	[65]0.0661	[47]0.1105
13	CAMVI-5	[96]0.0652	[83]0.0456	[92]0.0633	[84]0.0638	[70]0.0995	[60]0.0724	[73]0.0922	[65]0.1513
14	COGENT-0							[82]0.1046	[8]0.0004
15	COGENT-1							[81]0.1046	[7]0.0004
16	COGENT-2	[18]0.0036	[12]0.0024	[12]0.0027	[20]0.0086	[36]0.0444	[25]0.0296	[41]0.0391	[52]0.1275
17	COGENT-3	[20]0.0038	[19]0.0034	[13]0.0029	[22]0.0091	[39]0.0463	[35]0.0337	[49]0.0450	[64]0.1448
18	COGNITEC-2	[41]0.0057	[28]0.0040	[30]0.0043	[46]0.0145	[44]0.0531	[40]0.0396	[44]0.0400	[57]0.1342
19	COGNITEC-3	[45]0.0062	[33]0.0045	[37]0.0048	[47]0.0148	[43]0.0526	[39]0.0393	[43]0.0397	[56]0.1322
20	CYBERLINK-000	[21]0.0040	[45]0.0056	[46]0.0056	[37]0.0116	[48]0.0565	[46]0.0427	[52]0.0467	[63]0.1415
21	CYBERLINK-001	[17]0.0035	[39]0.0051	[41]0.0053	[33]0.0111	[45]0.0536	[42]0.0396	[53]0.0468	[62]0.1415
22	DAHUA-0	[64]0.0093	[53]0.0068	[58]0.0072	[60]0.0204	[64]0.0861	[55]0.0621	[66]0.0691	[75]0.1967
23	DAHUA-002	[7]0.0018	[27]0.0040	[26]0.0040	[15]0.0063	[9]0.0151	[10]0.0130	[10]0.0139	[25]0.0481
24	DAHUA-1	[49]0.0067	[35]0.0048	[39]0.0052	[52]0.0173	[60]0.0727	[50]0.0518	[61]0.0577	[72]0.1738
25	DEEPGLINT-001		[88]0.1425	[102]0.9269	[102]0.9243		[78]0.1432	[125]1.0000	[125]1.0000
26	DEEPSEA-001	[26]0.0043	[43]0.0055	[48]0.0059	[50]0.0157	[38]0.0462	[34]0.0325	[40]0.0390	[51]0.1263
27	DERMALOG-007	[63]0.0092				[65]0.0863			
28	DERMALOG-5	[78]0.0149	[66]0.0110	[76]0.0139	[69]0.0254	[67]0.0880	[56]0.0646	[71]0.0767	[80]0.2072
29	DERMALOG-6	[56]0.0081	[46]0.0058	[50]0.0061	[38]0.0119	[42]0.0517	[38]0.0380	[46]0.0416	[53]0.1280
30	EVERAI-0							[107]0.5477	[2]0.0001
31	EVERAI-2	[22]0.0040	[13]0.0028	[15]0.0032	[25]0.0099	[41]0.0501	[37]0.0367	[45]0.0410	[55]0.1312
32	EVERAI-3	[15]0.0031	[11]0.0022	[11]0.0024	[18]0.0073	[26]0.0351	[23]0.0254	[28]0.0285	[42]0.0978
33	EVERAI-PARAVISION-004	[4]0.0016	[24]0.0039	[23]0.0039	[11]0.0050	[7]0.0101	[8]0.0100	[7]0.0107	[22]0.0345
34	F8-001	[73]0.0120	[95]0.5364	[72]0.0115	[56]0.0181	[82]0.1658	[88]0.5949	[94]0.1559	[96]0.3507
35	GORILLA-004	[46]0.0063	[55]0.0070	[60]0.0075	[62]0.0216	[69]0.0892	[57]0.0656	[69]0.0718	[77]0.2013
36	GORILLA-2	[84]0.0197	[70]0.0134	[78]0.0153	[83]0.0570	[87]0.1880	[76]0.1376	[92]0.1537	[97]0.3589
37	GORILLA-3	[90]0.0361	[77]0.0242	[85]0.0283	[90]0.1032	[93]0.3175	[84]0.2706	[100]0.3043	[104]0.5786
38	HIK-4							[85]0.1258	[5]0.0004
39	HIK-5	[29]0.0046	[15]0.0032	[21]0.0037	[43]0.0140	[33]0.0436	[27]0.0304	[38]0.0364	[49]0.1228
40	HIK-6	[30]0.0046	[16]0.0032	[20]0.0037	[42]0.0140	[40]0.0469	[33]0.0321	[42]0.0392	[54]0.1310
41	IDEMIA-007	[13]0.0026	[31]0.0044	[34]0.0045	[23]0.0093	[15]0.0181	[13]0.0155	[12]0.0160	[28]0.0567
42	IDEMIA-3							[32]0.0324	[14]0.0007
43	IDEMIA-4							[31]0.0324	[13]0.0007
44	IDEMIA-5	[53]0.0081	[47]0.0059	[52]0.0064	[59]0.0192	[35]0.0440	[31]0.0315	[37]0.0348	[48]0.1125
45	IDEMIA-6	[66]0.0096	[52]0.0067	[61]0.0076	[58]0.0188	[32]0.0433	[29]0.0312	[34]0.0342	[44]0.1032
47	IMPERIAL-000	[35]0.0051	[32]0.0044	[33]0.0045	[19]0.0076	[23]0.0285	[20]0.0218	[24]0.0244	[39]0.0802
48	INCODE-004	[44]0.0062	[42]0.0052	[42]0.0054	[35]0.0113	[46]0.0538	[43]0.0408	[50]0.0457	[59]0.1395
49	INCODE-2	[81]0.0178	[67]0.0117	[75]0.0137	[78]0.0480	[86]0.1839	[75]0.1357	[91]0.1507	[95]0.3500
50	INCODE-3	[75]0.0129	[59]0.0086	[70]0.0103	[74]0.0368	[84]0.1672	[72]0.1222	[89]0.1388	[93]0.3290
51		[36]0.0051				[27]0.0366			
52	INNOVATRICS-4	[74]0.0123	[56]0.0078	[63]0.0081	[71]0.0293	[76]0.1317	[62]0.0925	[74]0.0927	[83]0.2479
53	INTSYSMSU-000	[100]0.1480	[86]0.1294	[94]0.1074	[91]0.1458	[107]0.9984	[97]0.9981	[117]0.9976	[116]0.9987
54	ISYSTEMS-3	[37]0.0052	[21]0.0037	[27]0.0041	[29]0.0106	[51]0.0590	[41]0.0396	[55]0.0500	[66]0.1519
55	KEDACOM-001	[68]0.0104	[63]0.0102	[64]0.0085	[28]0.0105	[18]0.0253	[22]0.0228	[18]0.0198	[26]0.0545
56		[58]0.0086							
57	LOOKMAN-005	[69]0.0107	[64]0.0105	[65]0.0088	[36]0.0114	[25]0.0327	[30]0.0314	[26]0.0255	[35]0.0738
58	LOOKMAN-3	[60]0.0088	[58]0.0086	[56]0.0067	[30]0.0109	[34]0.0437	[45]0.0421	[33]0.0338	[43]0.1015
59	LOOKMAN-4	[61]0.0091	[60]0.0088	[57]0.0072	[41]0.0134	[37]0.0446	[44]0.0413	[35]0.0346	[45]0.1086
60	MEGVII-1	[71]0.0118		[66]0.0096	[63]0.0231	[59]0.0722		[62]0.0577	[71]0.1688
61	MEGVII-2	[72]0.0118		[67]0.0097	[66]0.0236	[61]0.0772		[64]0.0623	[73]0.1810
62	MICROFOCUS-5	[107]0.4242	[93]0.3699	[100]0.3701	[100]0.5522	[103]0.8354	[94]0.9835	[111]0.8139	[112]0.9189
63	MICROFOCUS-6	[108]0.4268	[94]0.3729	[101]0.3732	[101]0.5566	[105]0.9779	[91]0.8191	[112]0.8195	[113]0.9215
64	MICROSOFT-4							[25]0.0245	[10]0.0006
65	MICROSOFT-5	[8]0.0019	[4]0.0013	[6]0.0015	[14]0.0062	[19]0.0256	[15]0.0169	[16]0.0193	[36]0.0755
66	MICROSOFT-6	[9]0.0020	[5]0.0013	[7]0.0015	[13]0.0060	[8]0.0120	[7]0.0079	[22]0.0213	[37]0.0772
67	NEC-0							[108]0.6921	[4]0.0003
68	NEC-2	[1]0.0010	[2]0.0010	[1]0.0008	[1]0.0019	[2]0.0026	[2]0.0021	[1]0.0021	[18]0.0086
69	NEC-3	[3]0.0014	[3]0.0012	[2]0.0010	[2]0.0019	[1]0.0024	[1]0.0020	[2]0.0022	[17]0.0080
70	NEUROTECHNOLOGY-007	[47]0.0066	[116]1.0000	[43]0.0054	[32]0.0110	[55]0.0648	[116]1.0000	[59]0.0551	[69]0.1614
71	NEUROTECHNOLOGY-4							[78]0.1000	[6]0.0004
72	NEUROTECHNOLOGY-5	[25]0.0043	[25]0.0039	[14]0.0032	[24]0.0094	[47]0.0538	[52]0.0522	[47]0.0438	[58]0.1364
73	NEUROTECHNOLOGY-6	[82]0.0180	[71]0.0151	[77]0.0142	[80]0.0534	[91]0.2494	[83]0.2659	[98]0.2125	[102]0.4458
74	NEWLAND-2	[98]0.0786		[91]0.0599	[93]0.1562	[97]0.4385		[103]0.3790	[105]0.6252

Table 30: **Comparing enrollment styles for the FRVT 2018 mugshot sets**. *Consolidated refers to enrollment of all lifetime images in one template Unconsolidated refers to enrollment of those images separately under different identifiers. Columns 3 - 6 values are FNIR at rank 1 and with* T *= 0. Columns 7 - 10 values are high threshold FNIR. Throughout, blue superscripts indicate the rank of the algorithm for that column, and the best three values are highlighted in yellow and green.*

MISSES OUTSIDE RANK R		MUGSHOT SEARCHES, N = 1.6M IDENTITIES							
		INVESTIGATION MODE, T = 0				IDENTIFICATION MODE, T > 0 FOR FPIR = 0.001			
FNIR(N, T, R)		PROPORTION MATED SEARCHES				PROPORTION MATED SEARCHES			
		WITHOUT THE MATE AT RANK 1		WITH NO MATE AT RANK 1	WITH K-TH MATE NOT IN TOP K	WITH THE MATE BELOW THRESHOLD		WITHOUT ANY MATE ABOVE THRESH	WITHOUT ALL MATES ABOVE THRESH
GALLERY		RECENT	CONSOLIDATED	UNCONSOLIDATED		RECENT	CONSOLIDATED	UNCONSOLIDATED	
75	NOBLIS-1	[104]0.2492	[90]0.2046	[96]0.2032	[96]0.3631	[108]0.9996	[98]0.9998	[118]0.9994	[118]0.9997
76	NOBLIS-2	[103]0.1794	[89]0.1562	[97]0.2517	[97]0.3944	[106]0.9973	[96]0.9959	[116]0.9967	[117]0.9987
77	NTECHLAB-007	[38]0.0053	[34]0.0047	[35]0.0047	[27]0.0103	[22]0.0282	[21]0.0223	[23]0.0223	[38]0.0776
78	NTECHLAB-008	[27]0.0044	[26]0.0040	[25]0.0040	[17]0.0073	[11]0.0171	[12]0.0151	[11]0.0151	[27]0.0554
79	NTECHLAB-3							[51]0.0480	[15]0.0007
80	NTECHLAB-4							[39]0.0386	[12]0.0007
81	NTECHLAB-5	[32]0.0047	[23]0.0038	[24]0.0039	[55]0.0179	[31]0.0424	[36]0.0344	[36]0.0347	[50]0.1235
82	NTECHLAB-6	[23]0.0041	[17]0.0033	[17]0.0034	[49]0.0154	[29]0.0367	[26]0.0298	[29]0.0301	[46]0.1088
83	PARAVISION-005	[24]0.0042	[22]0.0038	[22]0.0038	[10]0.0046	[4]0.0068	[4]0.0056	[4]0.0060	[19]0.0158
84	PIXELALL-002	[51]0.0072	[57]0.0084	[49]0.0060	[44]0.0142	[71]0.1076	[71]0.1206	[75]0.0949	[82]0.2475
85	PIXELALL-003	[34]0.0048	[37]0.0050	[28]0.0042	[16]0.0067	[16]0.0244	[32]0.0320	[21]0.0202	[32]0.0658
86	QUANTASOFT-1	[103]0.2177	[98]0.9857	[103]0.9426	[103]0.9502	[100]0.6387	[95]0.9915	[113]0.9640	[115]0.9801
87	RANKONE-006	[54]0.0077	[51]0.0065	[54]0.0065	[48]0.0149	[30]0.0397	[28]0.0310	[30]0.0310	[41]0.0967
88	RANKONE-007	[42]0.0060	[40]0.0052	[40]0.0052	[26]0.0101	[17]0.0248	[19]0.0194	[17]0.0194	[30]0.0622
89	RANKONE-3							[101]0.3144	[3]0.0002
90	RANKONE-4	[94]0.0415	[80]0.0315	[88]0.0318	[89]0.0945	[88]0.1929	[79]0.1539	[93]0.1545	[98]0.3590
91	RANKONE-5	[65]0.0094	[54]0.0069	[59]0.0072	[67]0.0237	[52]0.0592	[47]0.0443	[48]0.0447	[61]0.1404
92	REALNETWORKS-003	[87]0.0268	[76]0.0220	[82]0.0224	[86]0.0722	[81]0.1617	[77]0.1405	[90]0.1415	[94]0.3368
93	REALNETWORKS-004	[86]0.0262	[73]0.0192	[81]0.0222	[85]0.0713	[80]0.1604	[70]0.1179	[88]0.1360	[92]0.3288
94	REALNETWORKS-2	[91]0.0393	[81]0.0318	[84]0.0268	[88]0.0903	[90]0.2314	[81]0.2037	[97]0.1775	[101]0.3949
95	REMARKAI-0	[59]0.0086	[50]0.0063	[55]0.0065	[68]0.0238	[75]0.1278	[66]0.1016	[80]0.1020	[89]0.2671
96	REMARKAI-000	[43]0.0060	[38]0.0051	[38]0.0051	[34]0.0111	[49]0.0577	[48]0.0461	[51]0.0461	[60]0.1399
97	REMARKAI-2	[57]0.0081	[49]0.0060	[51]0.0062	[65]0.0235	[74]0.1239	[63]0.0982	[77]0.0991	[86]0.2615
98	SCANOVATE-000	[53]0.0076	[96]0.7787	[53]0.0064	[51]0.0159	[57]0.0692	[89]0.7902	[60]0.0551	[68]0.1599
99	SENSETIME-0	[11]0.0023	[9]0.0016	[9]0.0018	[4]0.0037	[14]0.0208	[14]0.0161	[13]0.0168	[29]0.0603
100	SENSETIME-002	[79]0.0163	[68]0.0124	[73]0.0124	[40]0.0127	[12]0.0174	[11]0.0134	[9]0.0134	[20]0.0160
101	SENSETIME-003	[19]0.0036	[20]0.0034	[18]0.0034	[5]0.0039	[3]0.0045	[3]0.0040	[3]0.0041	[16]0.0078
102	SENSETIME-1	[12]0.0023	[8]0.0016	[8]0.0018	[8]0.0041	[15]0.0219	[16]0.0172	[15]0.0177	[31]0.0628
103	SHAMAN-6	[93]0.0398	[79]0.0309	[87]0.0312	[81]0.0542	[77]0.1409	[68]0.1106	[83]0.1109	[88]0.2629
104	SHAMAN-7	[92]0.0396	[78]0.0307	[86]0.0310	[79]0.0529	[78]0.1413	[69]0.1109	[84]0.1112	[87]0.2624
105	SIAT-1							[114]0.9663	[1]0.0001
106	SMILART-4	[109]0.9648	[97]0.9530	[104]0.9722	[104]0.9738	[104]0.9682	[93]0.9569	[115]0.9740	[114]0.9781
107	SYNESIS-003	[83]0.0188				[56]0.0677			
108	SYNESIS-3	[101]0.1700	[87]0.1347	[95]0.1350	[95]0.2571	[90]0.5821	[87]0.5294	[106]0.5295	[109]0.7459
109	TECH5-001	[48]0.0066	[48]0.0059	[45]0.0056	[45]0.0144	[53]0.0599	[54]0.0590	[58]0.0537	[70]0.1641
110	TEVIAN-5	[52]0.0073	[41]0.0052	[47]0.0058	[61]0.0213	[66]0.0873	[58]0.0663	[72]0.0770	[81]0.2079
111	TIGER-2	[40]0.0056	[30]0.0042	[32]0.0044	[54]0.0177	[63]0.0861	[59]0.0690	[67]0.0698	[79]0.2016
112	TIGER-3	[39]0.0056		[31]0.0044	[53]0.0177	[62]0.0861		[68]0.0698	[78]0.2015
113	TOSHIBA-0	[28]0.0045	[14]0.0031	[16]0.0033	[31]0.0110	[54]0.0620	[51]0.0519	[57]0.0529	[67]0.1599
114	TOSHIBA-1	[33]0.0048	[18]0.0033	[19]0.0035	[39]0.0120	[50]0.0580	[53]0.0552	[63]0.0585	[74]0.1819
115	VD-1	[88]0.0276	[75]0.0218	[80]0.0221	[82]0.0560	[89]0.2015	[80]0.1650	[95]0.1658	[99]0.3657
116	VIGILANTSOLUTIONS-5	[62]0.0092				[96]0.3880			
117	VIGILANTSOLUTIONS-6	[67]0.0099		[62]0.0077	[70]0.0258	[94]0.3534		[104]0.4155	[107]0.6577
118	VISIONLABS-008	[31]0.0046	[29]0.0042	[29]0.0043	[12]0.0055	[10]0.0157	[9]0.0117	[8]0.0129	[24]0.0424
119	VISIONLABS-5							[56]0.0501	[9]0.0006
120	VISIONLABS-6	[6]0.0018	[7]0.0014	[5]0.0015	[7]0.0040	[21]0.0267	[18]0.0182	[20]0.0201	[34]0.0737
121	VISIONLABS-7	[5]0.0018	[6]0.0014	[4]0.0014	[6]0.0039	[20]0.0266	[17]0.0182	[19]0.0201	[33]0.0737
122	VOCORD-5	[50]0.0070	[44]0.0055	[44]0.0054	[57]0.0182	[79]0.1577	[67]0.1043	[96]0.1717	[100]0.3775
123	YITU-2							[14]0.0173	[11]0.0006
124	YITU-4	[2]0.0013	[1]0.0008	[3]0.0012	[3]0.0033	[5]0.0096	[5]0.0070	[5]0.0080	[21]0.0337
125	YITU-5	[10]0.0023	[10]0.0017	[10]0.0020	[9]0.0041	[6]0.0101	[6]0.0072	[6]0.0088	[23]0.0350

Table 31: **Comparing enrollment styles for the FRVT 2018 mugshot sets**. *Consolidated refers to enrollment of all lifetime images in one template Unconsolidated refers to enrollment of those images separately under different identifiers. Columns 3 - 6 values are FNIR at rank 1 and with* T = 0. *Columns 7 - 10 values are high threshold FNIR. Throughout, blue superscripts indicate the rank of the algorithm for that column, and the best three values are highlighted in yellow and green.*

2020/03/27	FNIR(N, R, T) =	False neg. identification rate	N = Num. enrolled subjects	T = Threshold	$T = 0 \rightarrow$ Investigation
10:40:09	FPIR(N, T) =	False pos. identification rate	R = Num. candidates examined		$T > 0 \rightarrow$ Identification

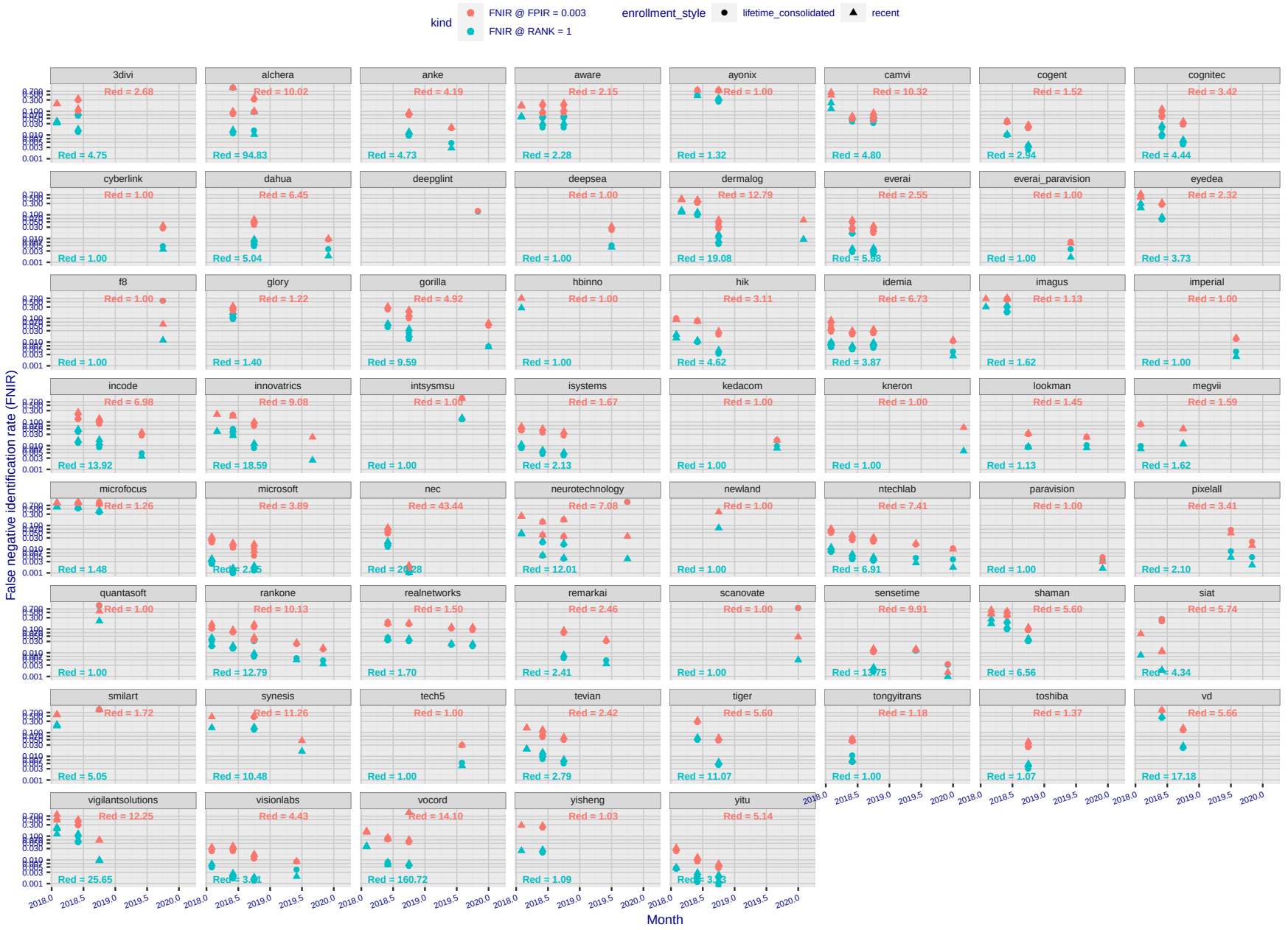

Figure 18: **[Mugshot Dataset] Error rate reductions in 2018**. *For each* FRVT*2018 participant, the plot shows accuracy gains between Phase 1 (Feb 2018), Phase 2 (Jun 2018) and Phase 3 (Nov 2018) according to two metrics: rank one miss rate, FNIR(N, 1, 0), and high threshold, FNIR(N, L, T), with T set to achieve FPIR = 0.003. The text "Red=" gives the best reduction multiplier for the given metric on the recent enrollment strategy - a smaller value is better.*

2020/03/27 10:40:09
FNIR(N, R, T) = False neg. identification rate
FPIR(N, T) = False pos. identification rate
N = Num. enrolled subjects
R = Num. candidates examined
T = Threshold
T = 0 → Investigation
T > 0 → Identification

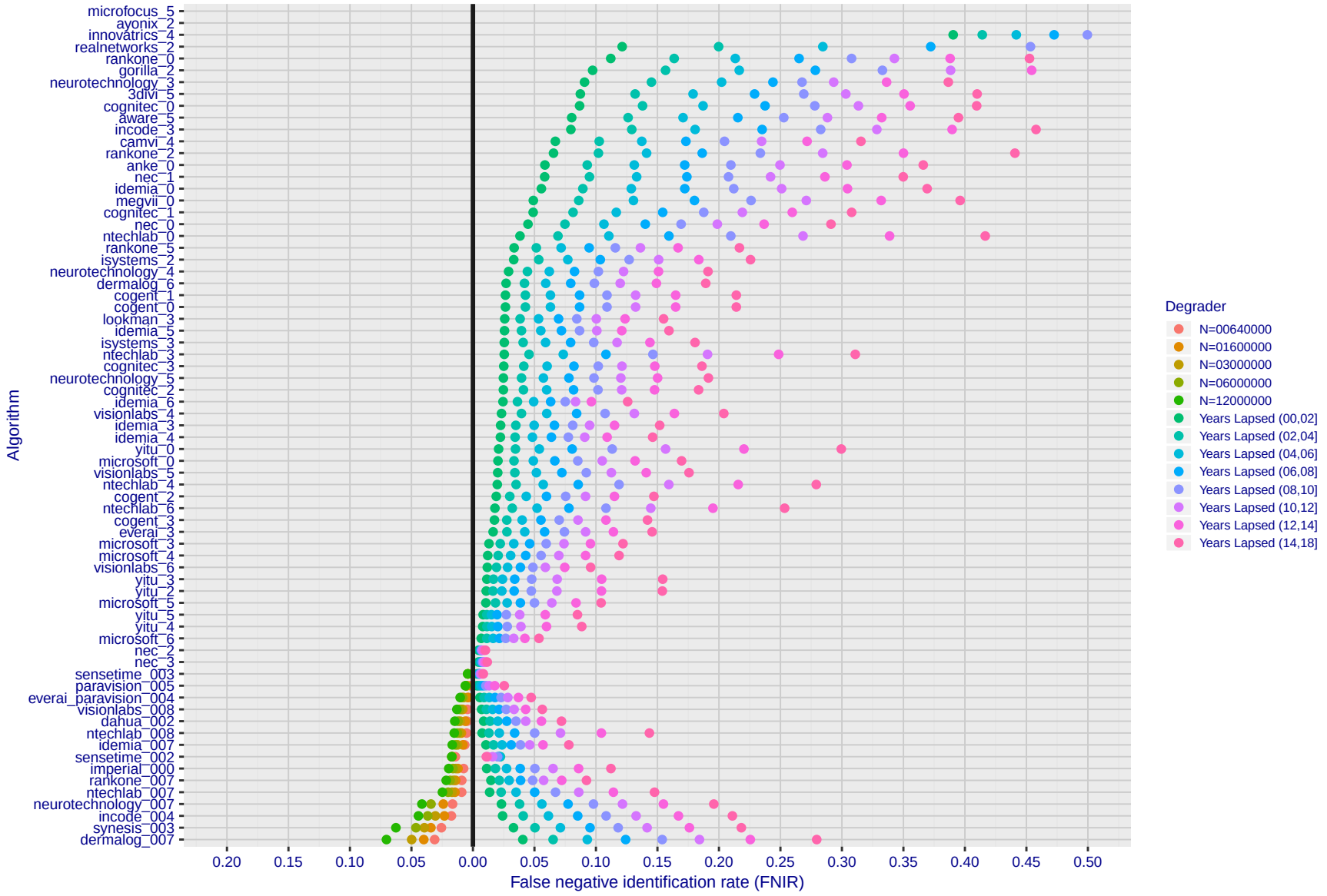

Figure 19: **[FRVT-2018 Mugshot Ageing Dataset] Contrast of ageing and population size dependency.** *The Figure shows, at left, the dependence FNIR(N) for the FRVT-2018, as tabulated in Table 12. At right, is FNIR(N = 3 000 000, ΔT) from Figure 61. Ageing miss rates are computed over all searches binned by number of years between search and initial enrollment. In all cases, FPIR = 0.01.*

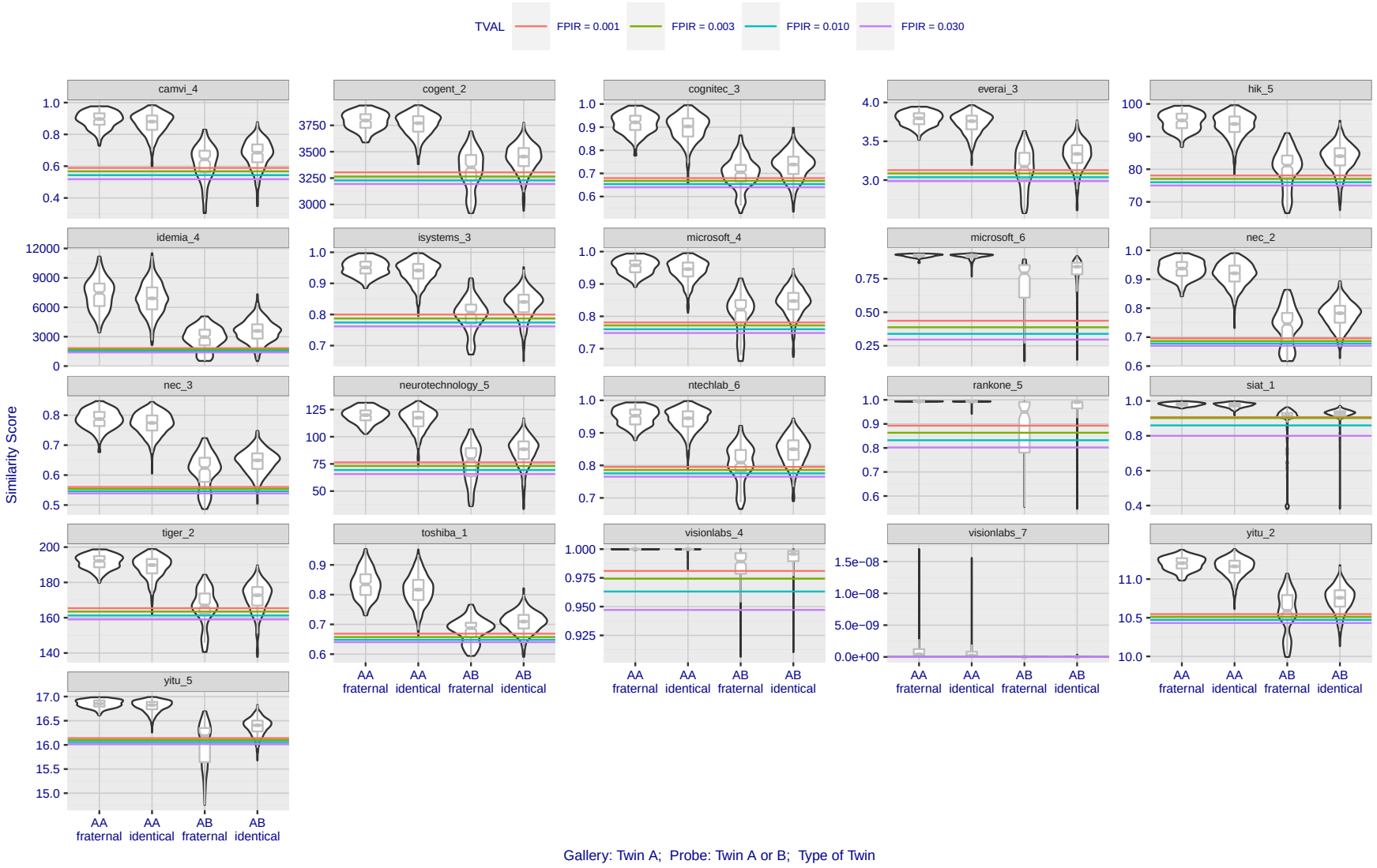

Figure 20: **[Twins Dataset] High scores from twins.** *The Figure shows native similarity scores from searches into a dataset of N = 640 000 background mugshot images plus 104 portrait images, one from each of one of a pair of twins. Two distributions of scores are plotted for each of monozygotic (identical) and dizygotic (fraternal) twins. The first distribution ("AA") shows the mate score from Twin A against their own enrollment. The second ("AB") shows scores from searches of Twin B against the Twin A enrollment: As these are non-mate scores they should be below the various thresholds shown as horizontal lines. That they usually are not is an indication that twins produce very high non-mate scores. Note in theory half of dizygotic (fraternal) twins are different sex. In the sample used here some fraternal twins are correctly rejected.*

Appendices

Appendix A Accuracy on large-population FRVT 2018 mugshots

2020/03/27	FNIR(N, R, T) =	False neg. identification rate	N = Num. enrolled subjects	T = Threshold	$T = 0 \rightarrow$ Investigation
10:40:09	FPIR(N, T) =	False pos. identification rate	R = Num. candidates examined		$T > 0 \rightarrow$ Identification

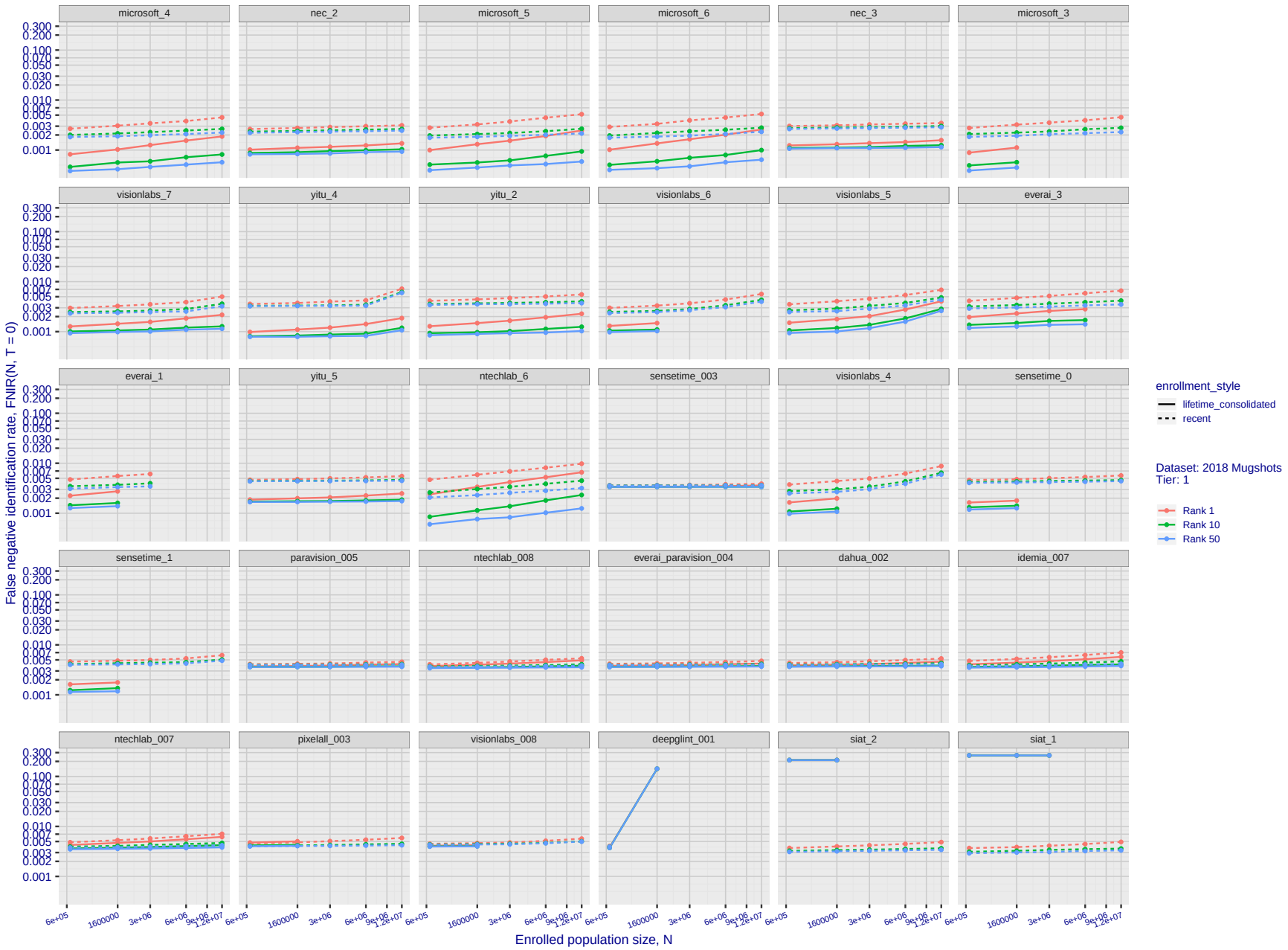

Figure 21: **[FRVT-2018 Mugshot Dataset] Rank-based identification miss rates vs. number of enrolled subjects**. *The figure shows false negative identification rates, FNIR(N, R), across various gallery sizes and ranks 1, 10 and 50. The threshold is set to zero, so this metric rewards even weak scoring rank 1 mates. This also means FPIR = 1, so any search without an enrolled mate will return non-mated candidates. For clarity, results are sorted and reported into tiers spanning multiple pages, the tiering criteria being rank 1 hit rate on a gallery size of 640 000.*

2020/03/27
10:40:09

FNIR(N, R, T) = False neg. identification rate
FPIR(N, T) = False pos. identification rate

N = Num. enrolled subjects
R = Num. candidates examined

T = Threshold

T = 0 → Investigation
T > 0 → Identification

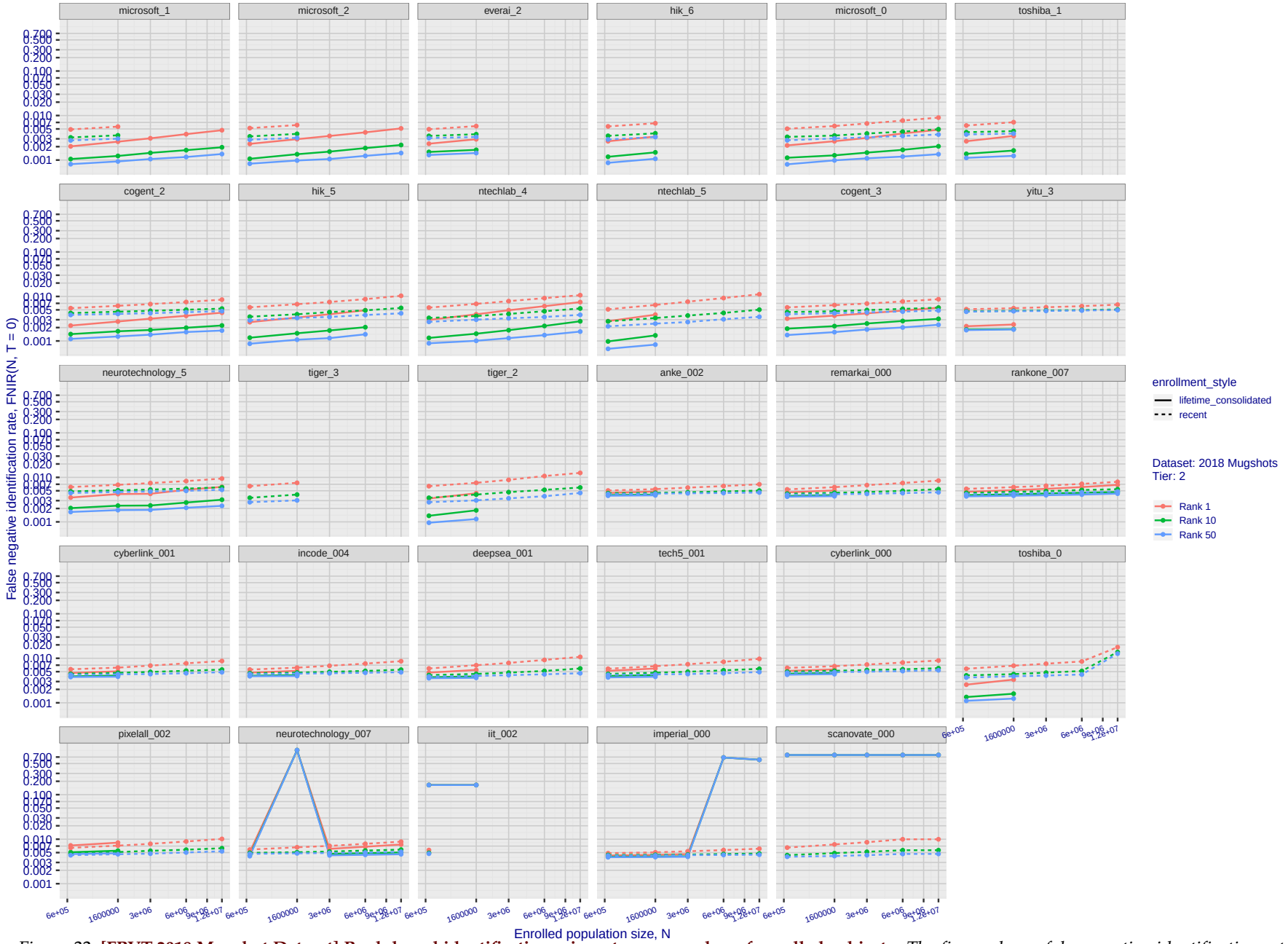

Figure 22: **[FRVT-2018 Mugshot Dataset] Rank-based identification miss rates vs. number of enrolled subjects**. *The figure shows false negative identification rates, FNIR(N, R), across various gallery sizes and ranks 1, 10 and 50. The threshold is set to zero, so this metric rewards even weak scoring rank 1 mates. This also means FPIR = 1, so any search without an enrolled mate will return non-mated candidates. For clarity, results are sorted and reported into tiers spanning multiple pages, the tiering criteria being rank 1 hit rate on a gallery size of 640 000.*

2020/03/27 10:40:09

FNIR(N, R, T) = False neg. identification rate
FPIR(N, T) = False pos. identification rate
N = Num. enrolled subjects
R = Num. candidates examined
T = Threshold
T = 0 → Investigation
T > 0 → Identification

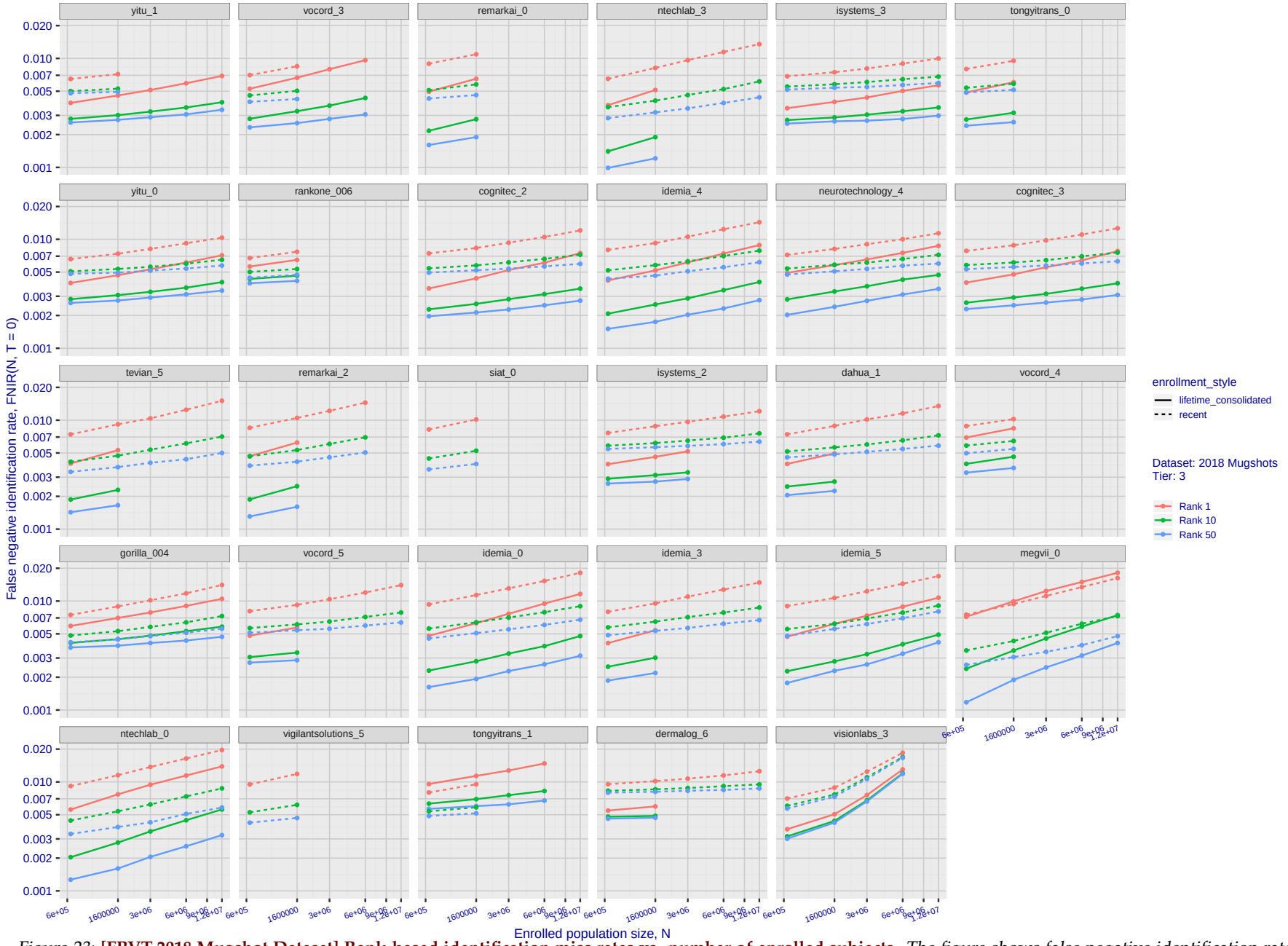

Figure 23: **[FRVT-2018 Mugshot Dataset] Rank-based identification miss rates vs. number of enrolled subjects**. *The figure shows false negative identification rates, FNIR(N, R), across various gallery sizes and ranks 1, 10 and 50. The threshold is set to zero, so this metric rewards even weak scoring rank 1 mates. This also means FPIR = 1, so any search without an enrolled mate will return non-mated candidates. For clarity, results are sorted and reported into tiers spanning multiple pages, the tiering criteria being rank 1 hit rate on a gallery size of 640 000.*

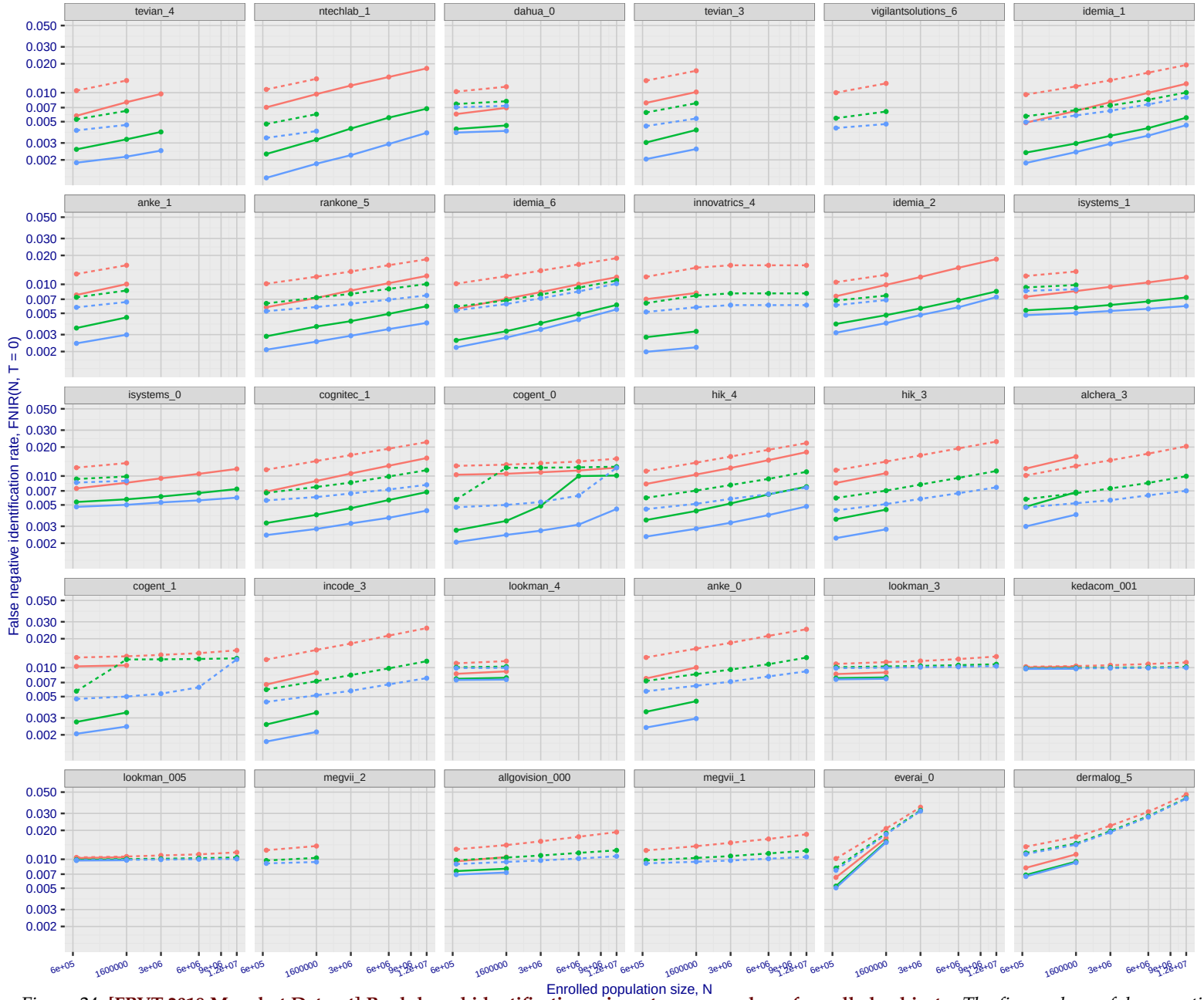

Figure 24: **[FRVT-2018 Mugshot Dataset] Rank-based identification miss rates vs. number of enrolled subjects**. *The figure shows false negative identification rates, FNIR(N, R), across various gallery sizes and ranks 1, 10 and 50. The threshold is set to zero, so this metric rewards even weak scoring rank 1 mates. This also means FPIR = 1, so any search without an enrolled mate will return non-mated candidates. For clarity, results are sorted and reported into tiers spanning multiple pages, the tiering criteria being rank 1 hit rate on a gallery size of 640 000.*

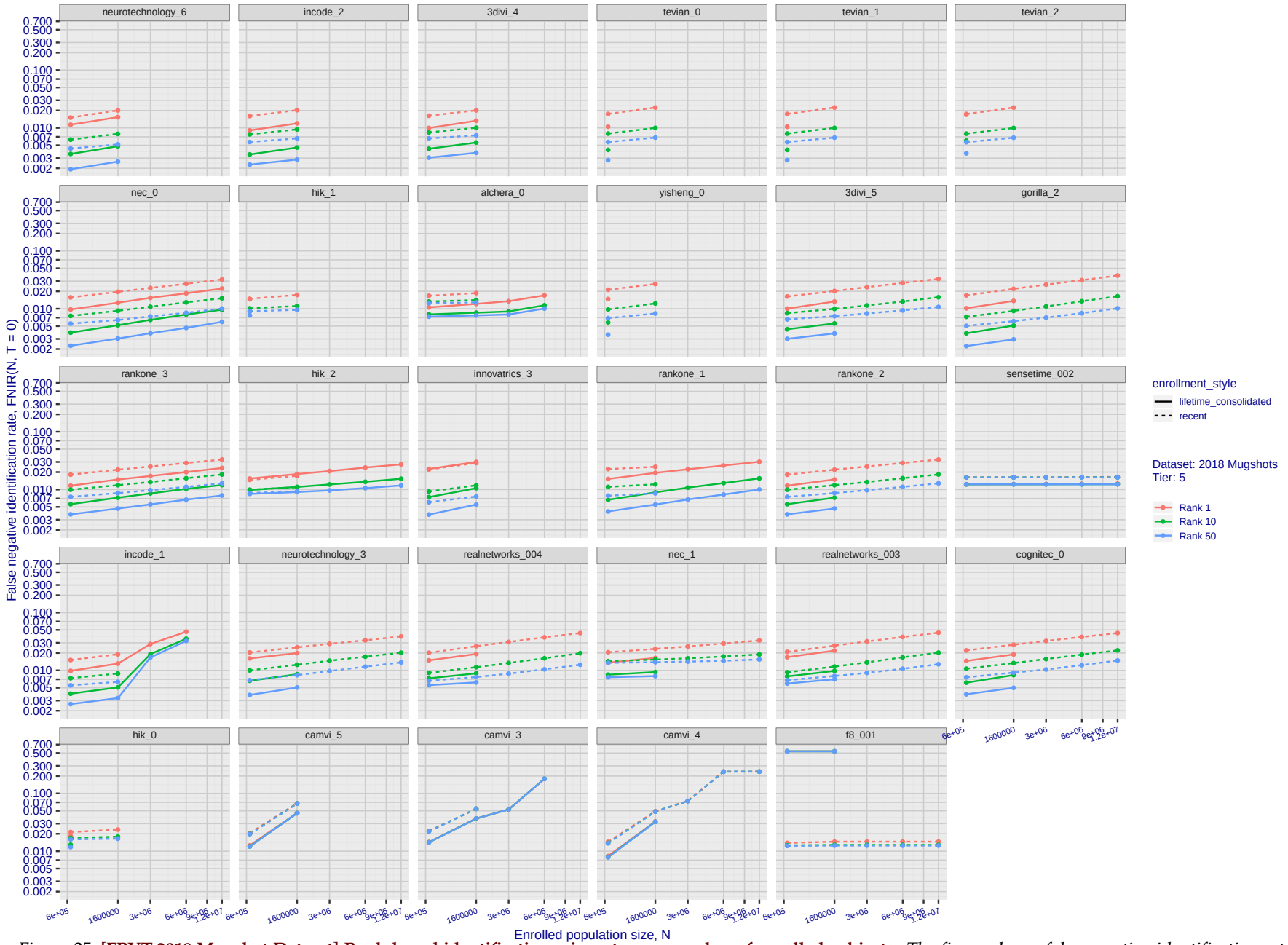

Figure 25: **[FRVT-2018 Mugshot Dataset] Rank-based identification miss rates vs. number of enrolled subjects**. *The figure shows false negative identification rates, FNIR(N, R), across various gallery sizes and ranks 1, 10 and 50. The threshold is set to zero, so this metric rewards even weak scoring rank 1 mates. This also means FPIR = 1, so any search without an enrolled mate will return non-mated candidates. For clarity, results are sorted and reported into tiers spanning multiple pages, the tiering criteria being rank 1 hit rate on a gallery size of 640 000.*

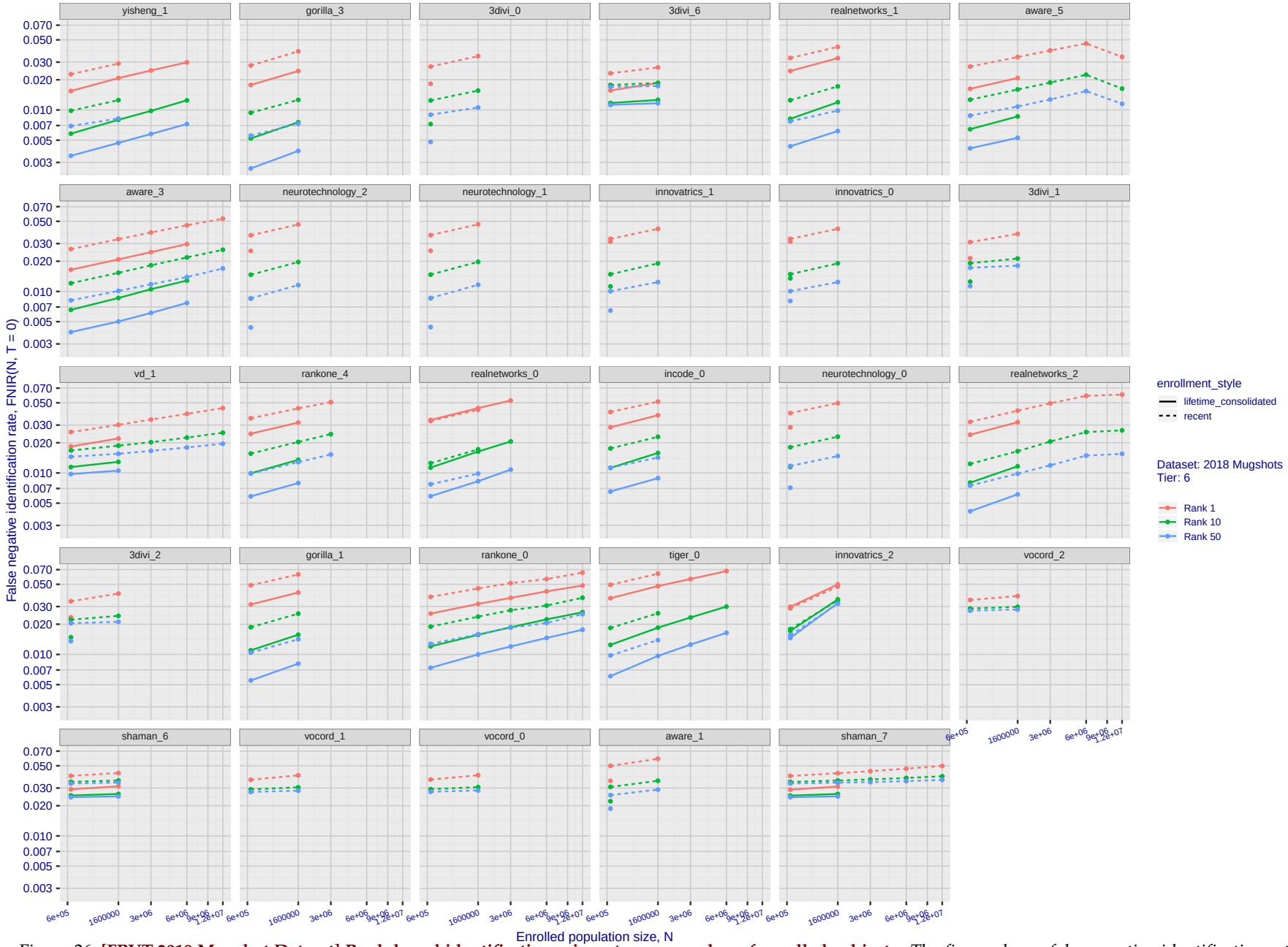

Figure 26: **[FRVT-2018 Mugshot Dataset] Rank-based identification miss rates vs. number of enrolled subjects**. *The figure shows false negative identification rates, FNIR(N, R), across various gallery sizes and ranks 1, 10 and 50. The threshold is set to zero, so this metric rewards even weak scoring rank 1 mates. This also means FPIR = 1, so any search without an enrolled mate will return non-mated candidates. For clarity, results are sorted and reported into tiers spanning multiple pages, the tiering criteria being rank 1 hit rate on a gallery size of 640 000.*

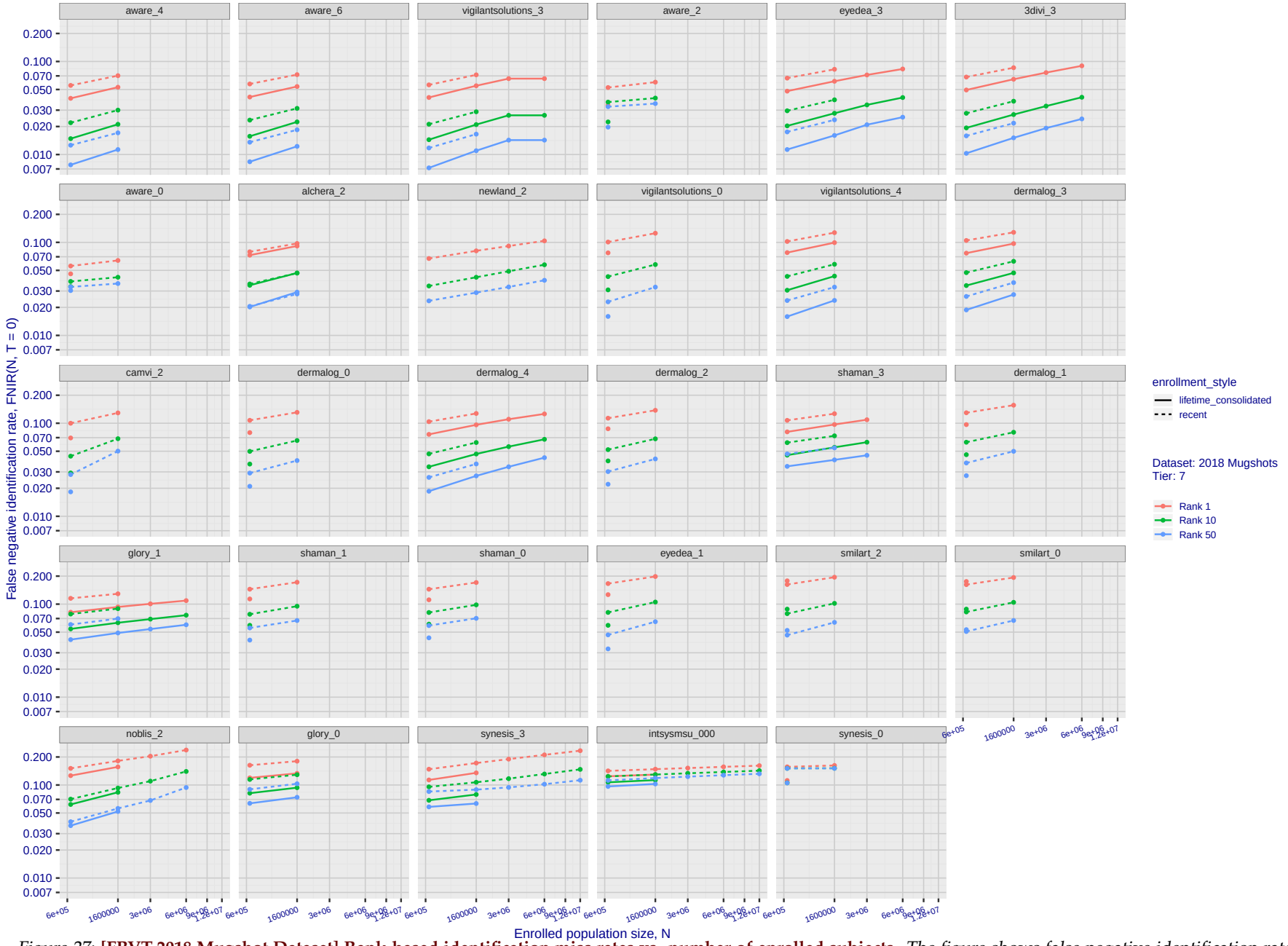

Figure 27: **[FRVT-2018 Mugshot Dataset] Rank-based identification miss rates vs. number of enrolled subjects**. *The figure shows false negative identification rates, FNIR(N, R), across various gallery sizes and ranks 1, 10 and 50. The threshold is set to zero, so this metric rewards even weak scoring rank 1 mates. This also means FPIR = 1, so any search without an enrolled mate will return non-mated candidates. For clarity, results are sorted and reported into tiers spanning multiple pages, the tiering criteria being rank 1 hit rate on a gallery size of 640 000.*

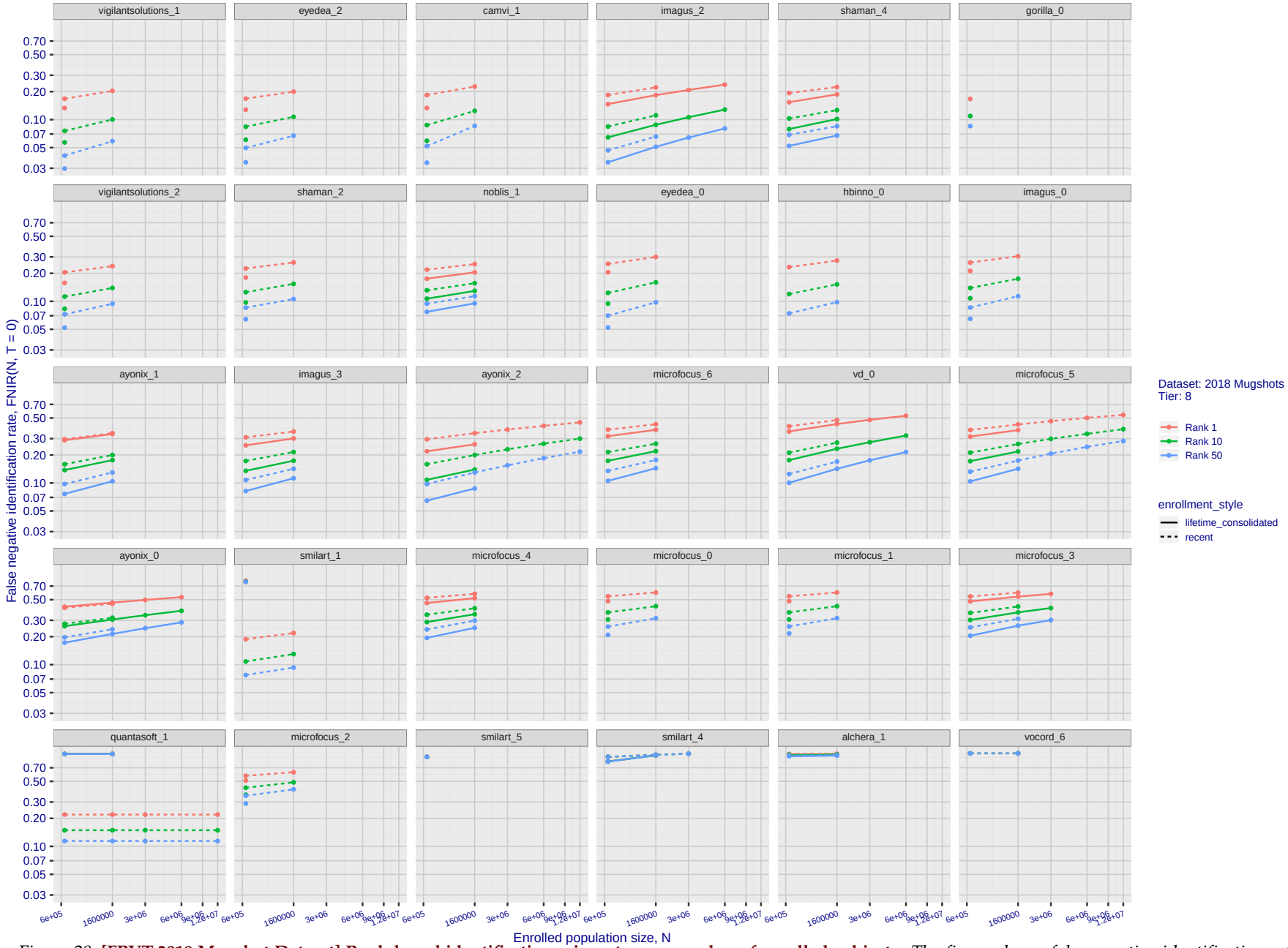

Figure 28: **[FRVT-2018 Mugshot Dataset] Rank-based identification miss rates vs. number of enrolled subjects**. *The figure shows false negative identification rates, FNIR(N, R), across various gallery sizes and ranks 1, 10 and 50. The threshold is set to zero, so this metric rewards even weak scoring rank 1 mates. This also means FPIR = 1, so any search without an enrolled mate will return non-mated candidates. For clarity, results are sorted and reported into tiers spanning multiple pages, the tiering criteria being rank 1 hit rate on a gallery size of 640 000.*

2020/03/27	FNIR(N, R, T) =	False neg. identification rate	N = Num. enrolled subjects	T = Threshold	$T = 0 \rightarrow$ Investigation
10:40:09	FPIR(N, T) =	False pos. identification rate	R = Num. candidates examined		$T > 0 \rightarrow$ Identification

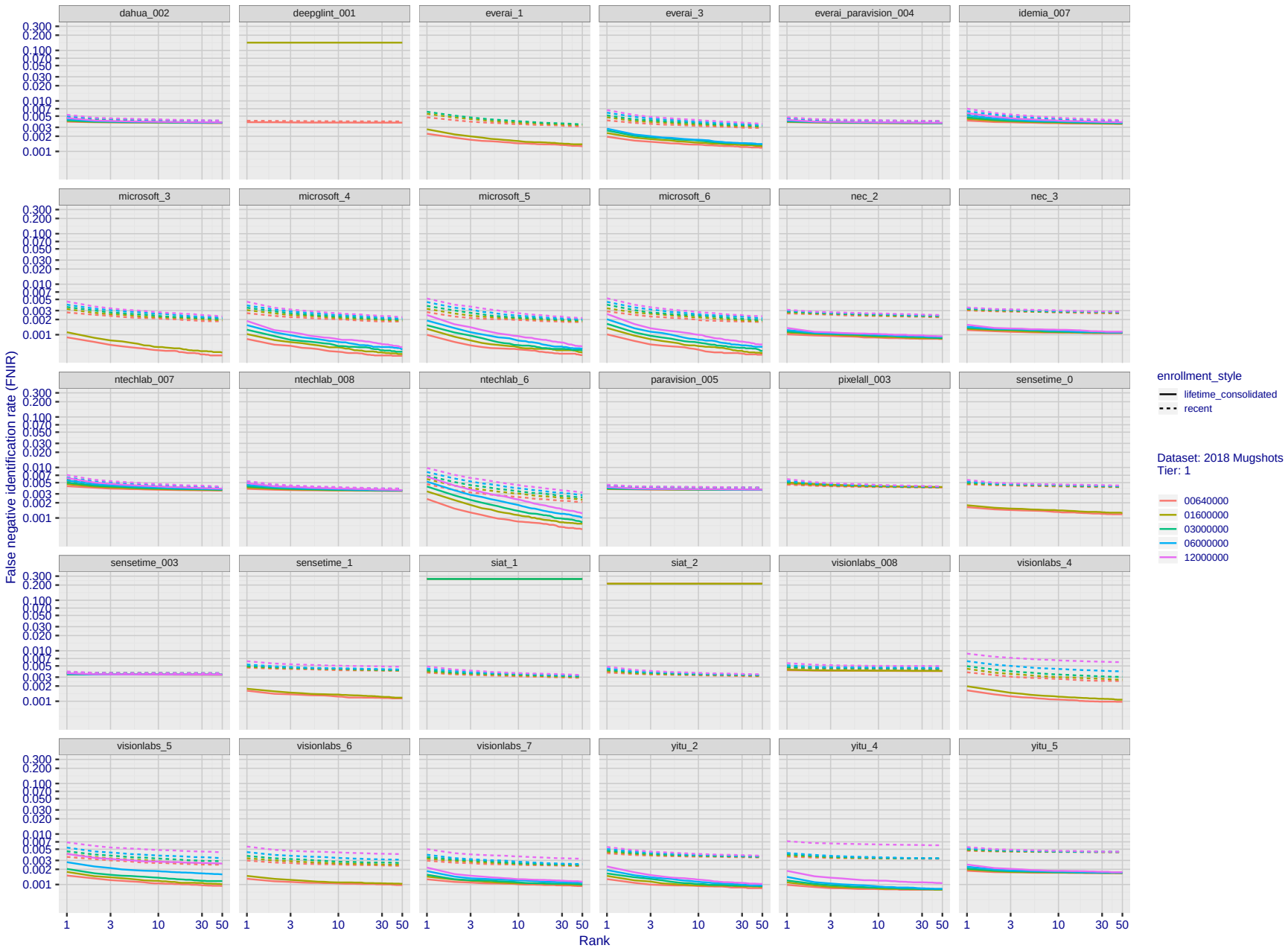

Figure 29: **[FRVT-2018 Mugshot Dataset] Rank-based identification miss rates vs. rank**. *The figure shows false negative identification rates (FNIR) for ranks up to 50. This metric is appropriate to investigational applications where human reviewers will adjudicate sorted candidate lists. Note that with threshold set to zero, FPIR = 1, i.e. any search without an enrolled mate will return non-mated candidates. Results are sorted and reported into tiers for clarity, with the tiering criteria being rank 1 hit rate on a gallery size of N = 640 000 subjects.*

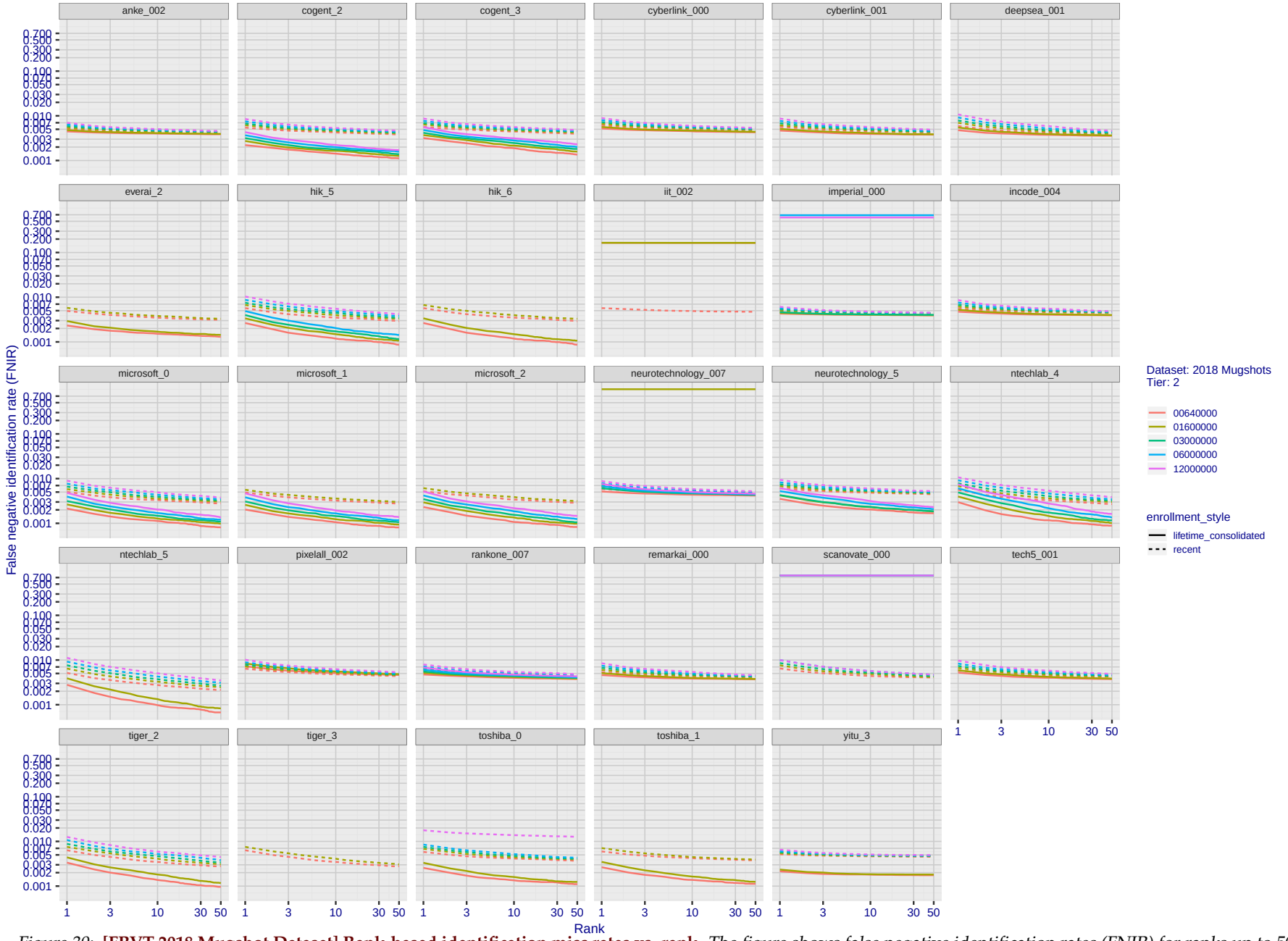

Figure 30: **[FRVT-2018 Mugshot Dataset] Rank-based identification miss rates vs. rank**. *The figure shows false negative identification rates (FNIR) for ranks up to 50. This metric is appropriate to investigational applications where human reviewers will adjudicate sorted candidate lists. Note that with threshold set to zero, FPIR = 1, i.e. any search without an enrolled mate will return non-mated candidates. Results are sorted and reported into tiers for clarity, with the tiering criteria being rank 1 hit rate on a gallery size of N = 640 000 subjects.*

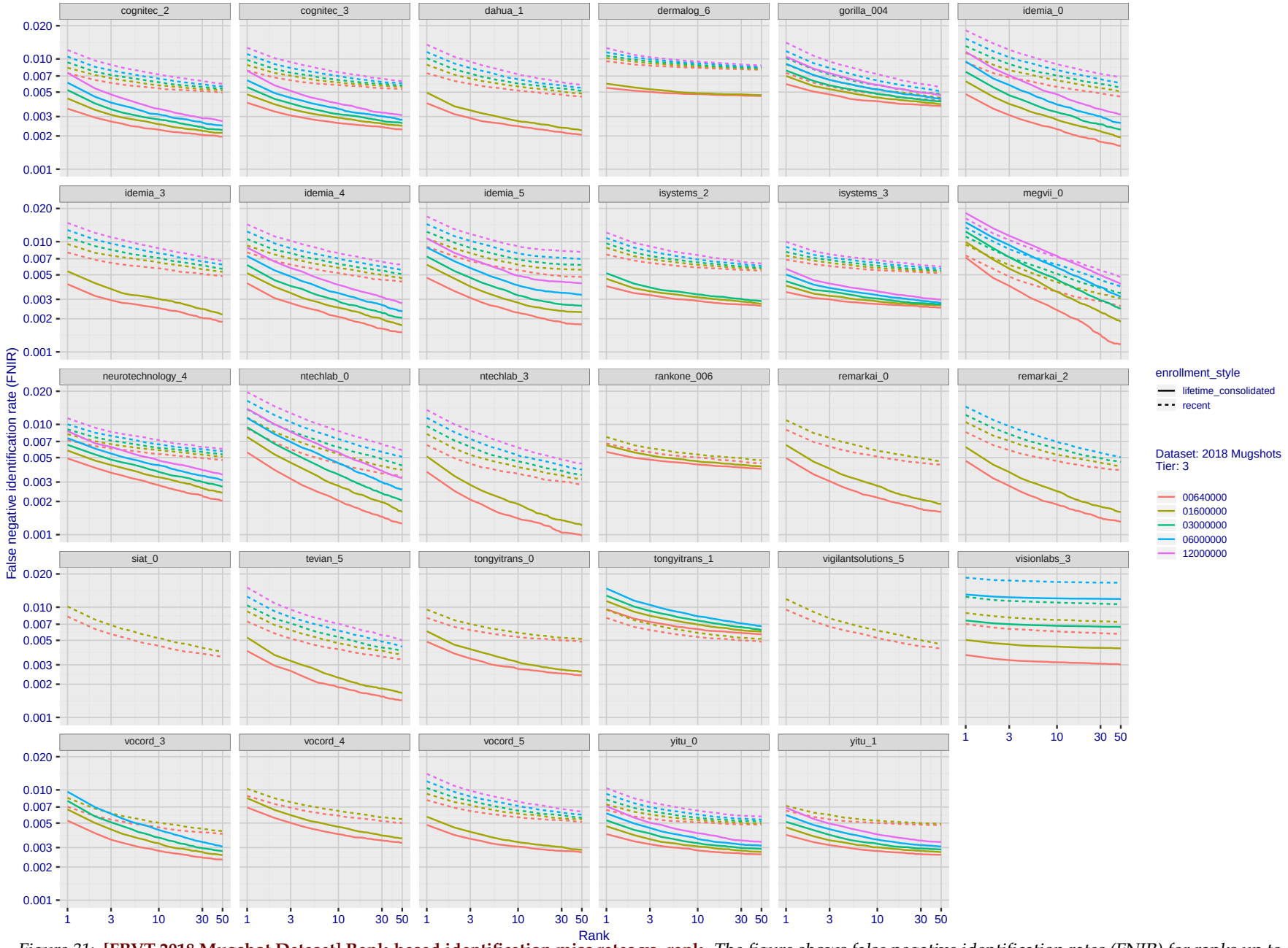

Figure 31: **[FRVT-2018 Mugshot Dataset] Rank-based identification miss rates vs. rank**. *The figure shows false negative identification rates (FNIR) for ranks up to 50. This metric is appropriate to investigational applications where human reviewers will adjudicate sorted candidate lists. Note that with threshold set to zero, FPIR = 1, i.e. any search without an enrolled mate will return non-mated candidates. Results are sorted and reported into tiers for clarity, with the tiering criteria being rank 1 hit rate on a gallery size of N = 640 000 subjects.*

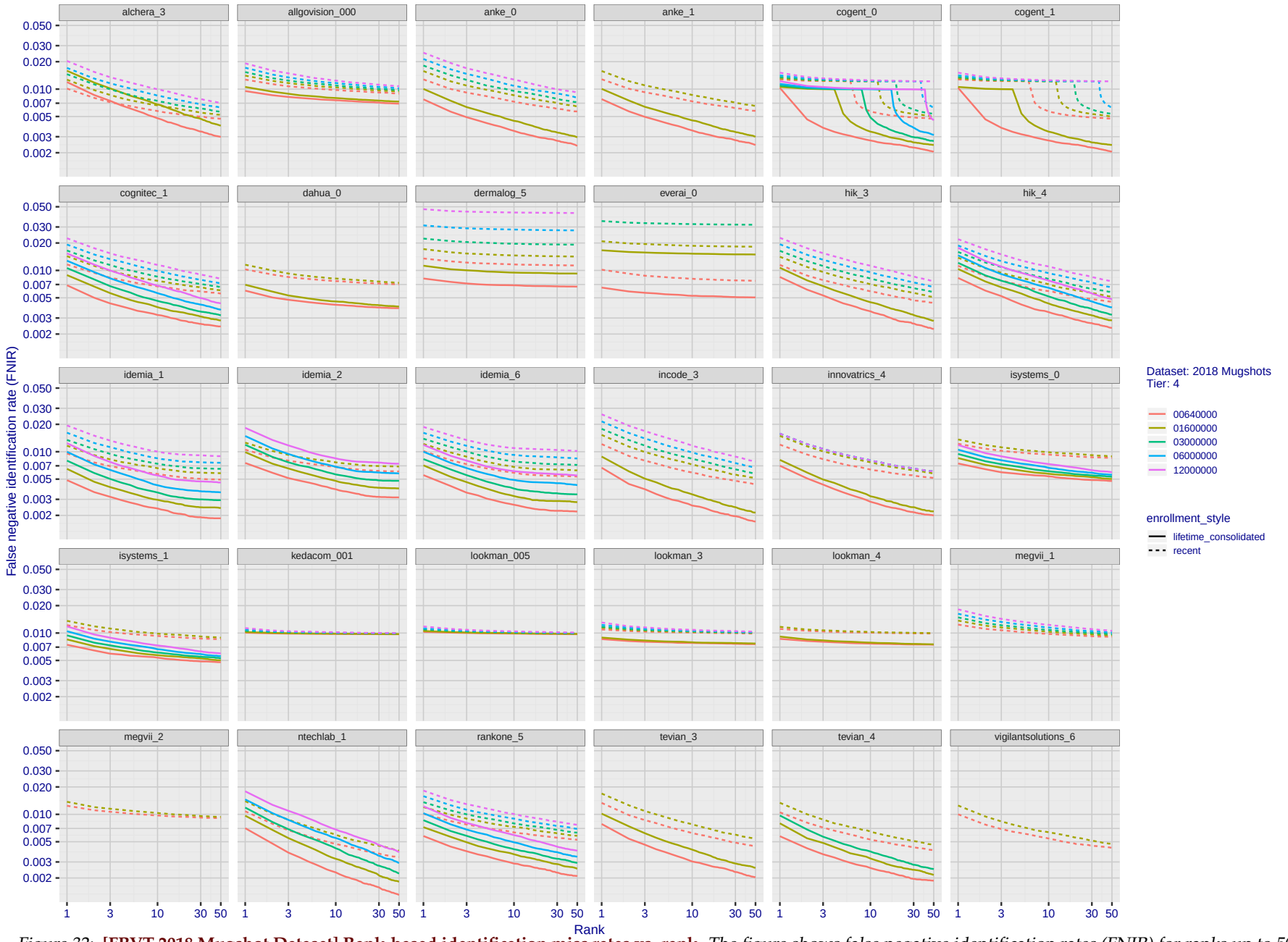

Figure 32: **[FRVT-2018 Mugshot Dataset] Rank-based identification miss rates vs. rank**. *The figure shows false negative identification rates (FNIR) for ranks up to 50. This metric is appropriate to investigational applications where human reviewers will adjudicate sorted candidate lists. Note that with threshold set to zero, FPIR = 1, i.e. any search without an enrolled mate will return non-mated candidates. Results are sorted and reported into tiers for clarity, with the tiering criteria being rank 1 hit rate on a gallery size of N = 640 000 subjects.*

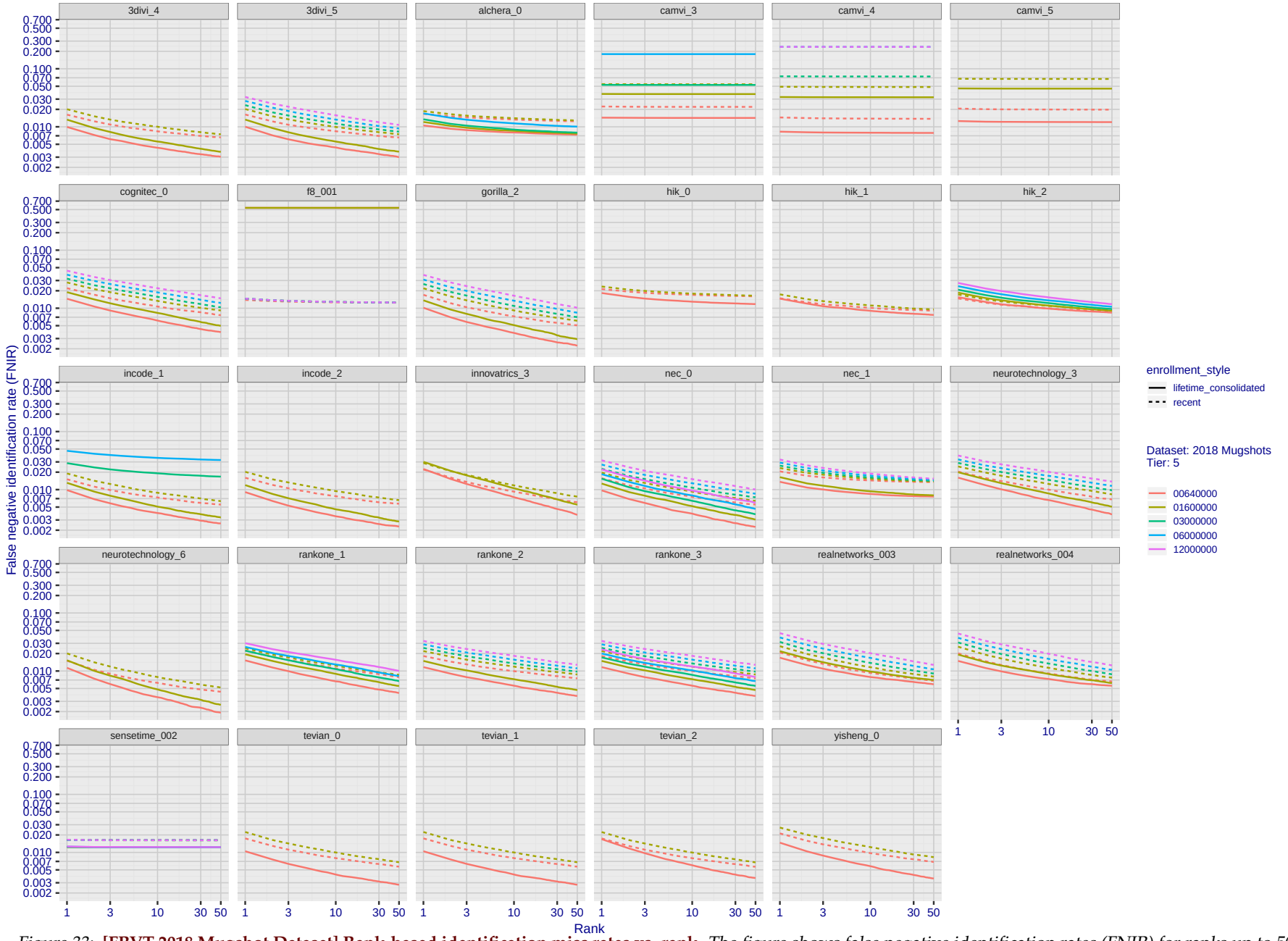

Figure 33: **[FRVT-2018 Mugshot Dataset] Rank-based identification miss rates vs. rank**. *The figure shows false negative identification rates (FNIR) for ranks up to 50. This metric is appropriate to investigational applications where human reviewers will adjudicate sorted candidate lists. Note that with threshold set to zero, FPIR = 1, i.e. any search without an enrolled mate will return non-mated candidates. Results are sorted and reported into tiers for clarity, with the tiering criteria being rank 1 hit rate on a gallery size of N = 640 000 subjects.*

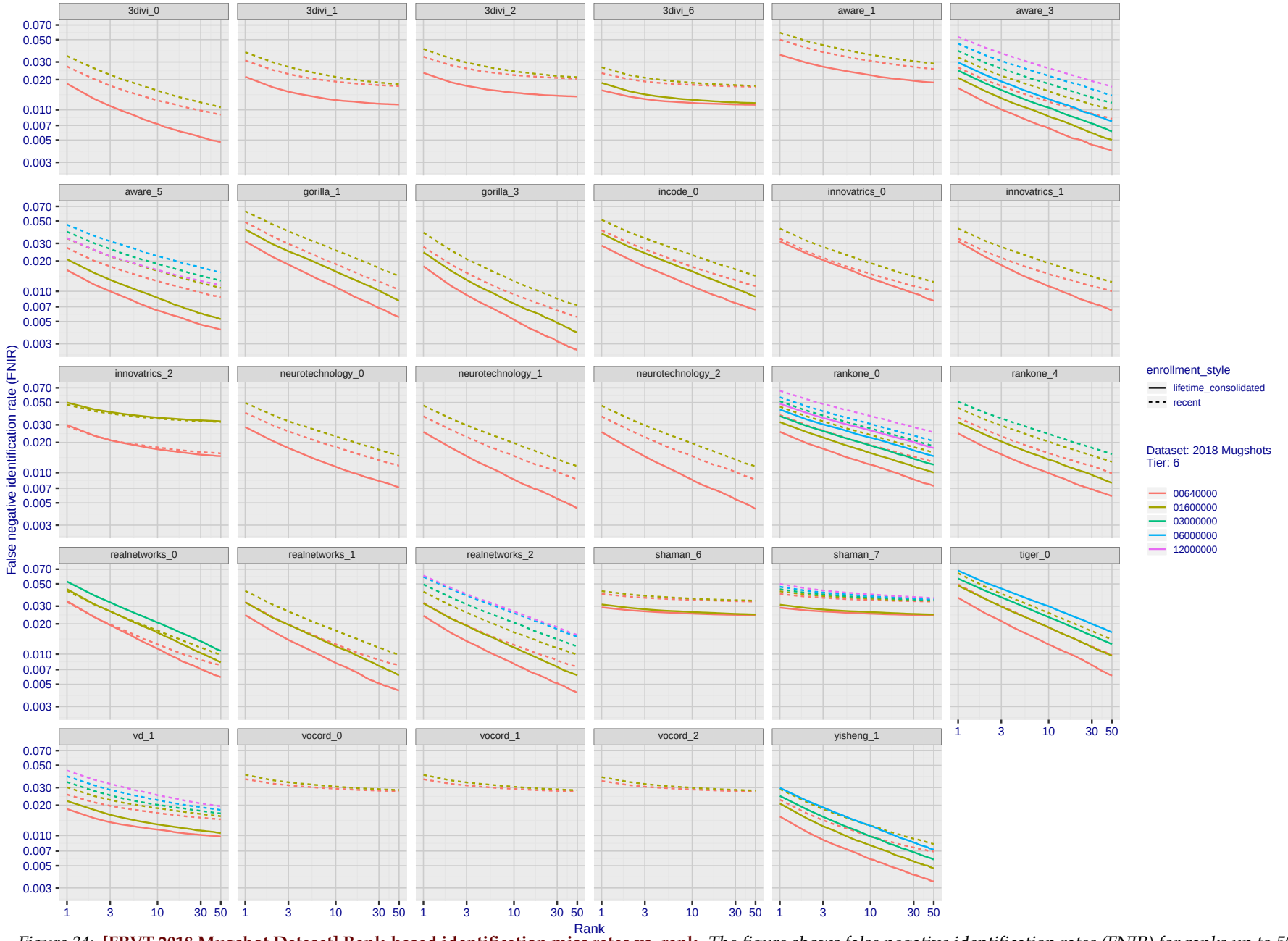

Figure 34: **[FRVT-2018 Mugshot Dataset] Rank-based identification miss rates vs. rank**. *The figure shows false negative identification rates (FNIR) for ranks up to 50. This metric is appropriate to investigational applications where human reviewers will adjudicate sorted candidate lists. Note that with threshold set to zero, FPIR = 1, i.e. any search without an enrolled mate will return non-mated candidates. Results are sorted and reported into tiers for clarity, with the tiering criteria being rank 1 hit rate on a gallery size of N = 640 000 subjects.*

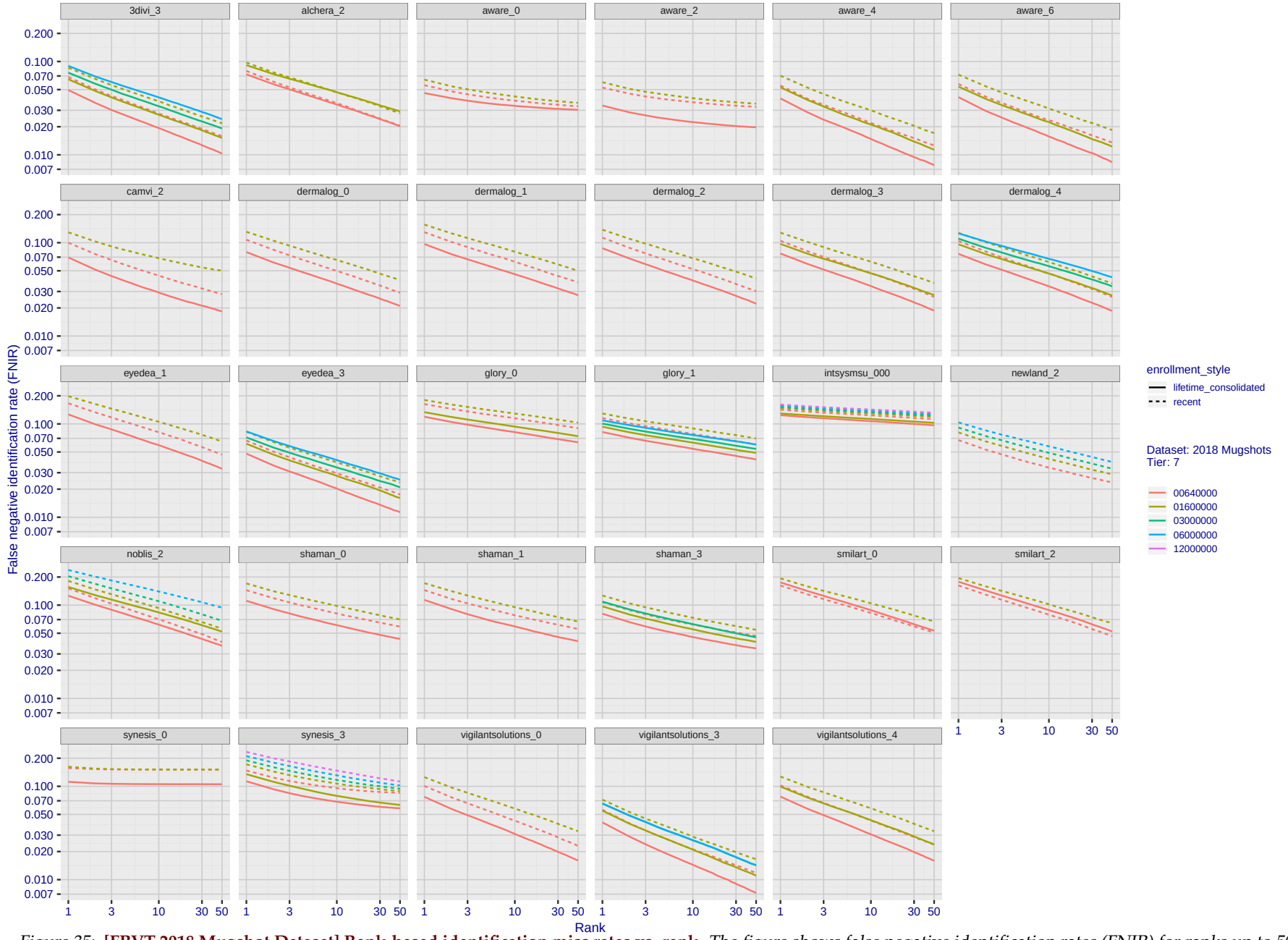

Figure 35: **[FRVT-2018 Mugshot Dataset] Rank-based identification miss rates vs. rank**. *The figure shows false negative identification rates (FNIR) for ranks up to 50. This metric is appropriate to investigational applications where human reviewers will adjudicate sorted candidate lists. Note that with threshold set to zero, FPIR = 1, i.e. any search without an enrolled mate will return non-mated candidates. Results are sorted and reported into tiers for clarity, with the tiering criteria being rank 1 hit rate on a gallery size of N = 640 000 subjects.*

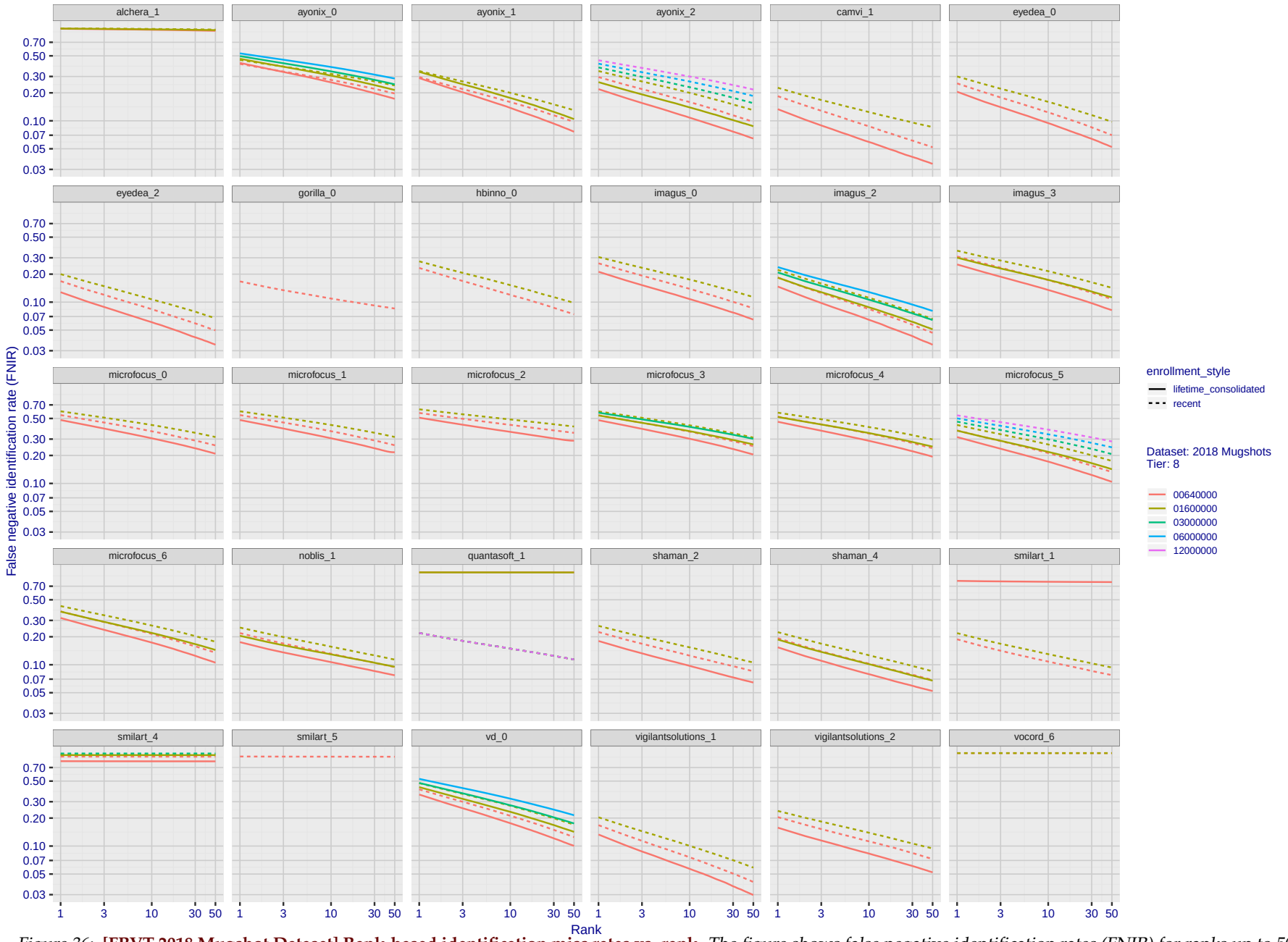

Figure 36: **[FRVT-2018 Mugshot Dataset] Rank-based identification miss rates vs. rank**. *The figure shows false negative identification rates (FNIR) for ranks up to 50. This metric is appropriate to investigational applications where human reviewers will adjudicate sorted candidate lists. Note that with threshold set to zero, FPIR = 1, i.e. any search without an enrolled mate will return non-mated candidates. Results are sorted and reported into tiers for clarity, with the tiering criteria being rank 1 hit rate on a gallery size of N = 640 000 subjects.*

2020/03/27	FNIR(N, R, T) =	False neg. identification rate	N = Num. enrolled subjects	T = Threshold	$T = 0 \rightarrow$ Investigation
10:40:09	FPIR(N, T) =	False pos. identification rate	R = Num. candidates examined		$T > 0 \rightarrow$ Identification

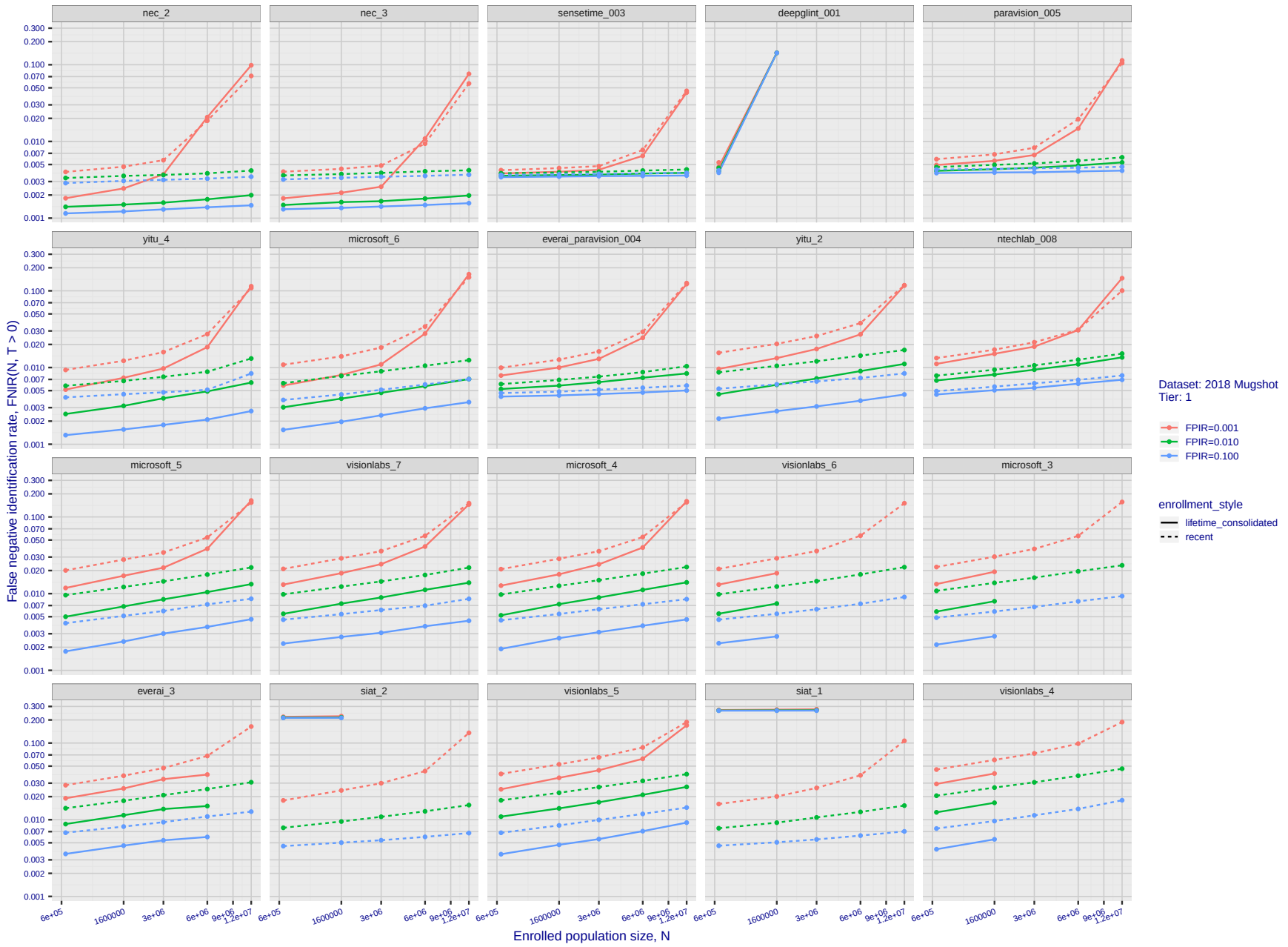

Figure 37: **[FRVT-2018 Mugshot Dataset] Threshold-based identification miss rates vs. number of enrolled subjects**. *The figure shows FNIR(N, T) across various gallery sizes when the threshold is set to achieve the given FPIRs. The rank criterion is irrelevant at high thresholds as mates are always at rank 1. The results are computed from the trials listed in rows 1-10 of Table 1. Less accurate algorithms were not run on large N, so results are missing. For clarity, results are sorted and reported into tiers spanning multiple pages. The tiering criteria is complicated: First paging by FNIR(N_b, 1, 0), then sorting by median FNIR(N_b, T), N_b = 640 000.*

FNIR(N, R, T) = False neg. identification rate
FPIR(N, T) = False pos. identification rate
N = Num. enrolled subjects
R = Num. candidates examined
T = Threshold
T = 0 → Investigation
T > 0 → Identification

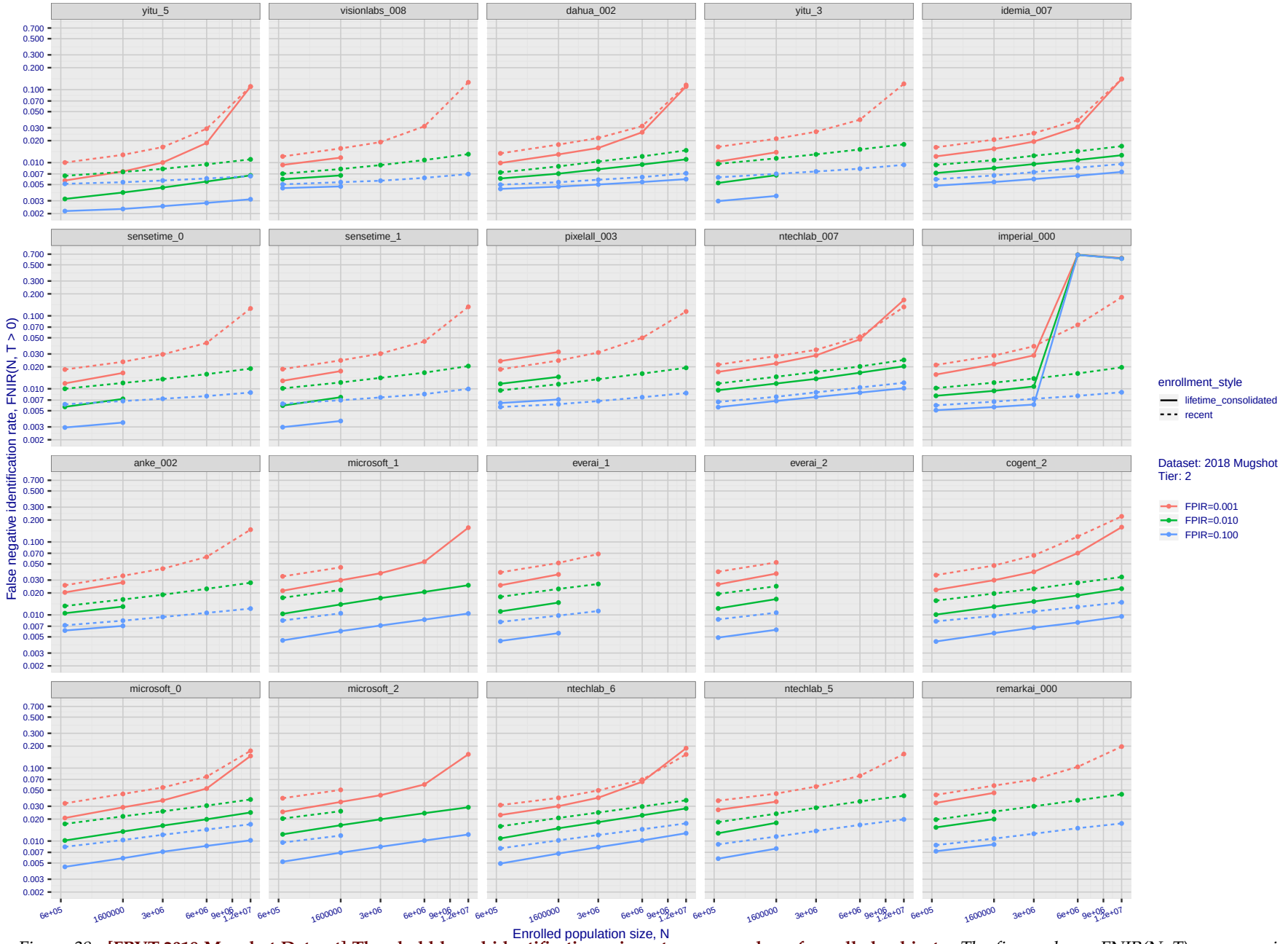

Figure 38: **[FRVT-2018 Mugshot Dataset] Threshold-based identification miss rates vs. number of enrolled subjects**. *The figure shows FNIR(N, T) across various gallery sizes when the threshold is set to achieve the given FPIRs. The rank criterion is irrelevant at high thresholds as mates are always at rank 1. The results are computed from the trials listed in rows 1-10 of Table 1. Less accurate algorithms were not run on large N, so results are missing. For clarity, results are sorted and reported into tiers spanning multiple pages. The tiering criteria is complicated: First paging by FNIR(N_b, 1, 0), then sorting by median FNIR(N_b, T), N_b = 640 000.*

2020/03/27 10:40:09

FNIR(N, R, T) = False neg. identification rate
FPIR(N, T) = False pos. identification rate
N = Num. enrolled subjects
R = Num. candidates examined
T = Threshold
T = 0 → Investigation
T > 0 → Identification

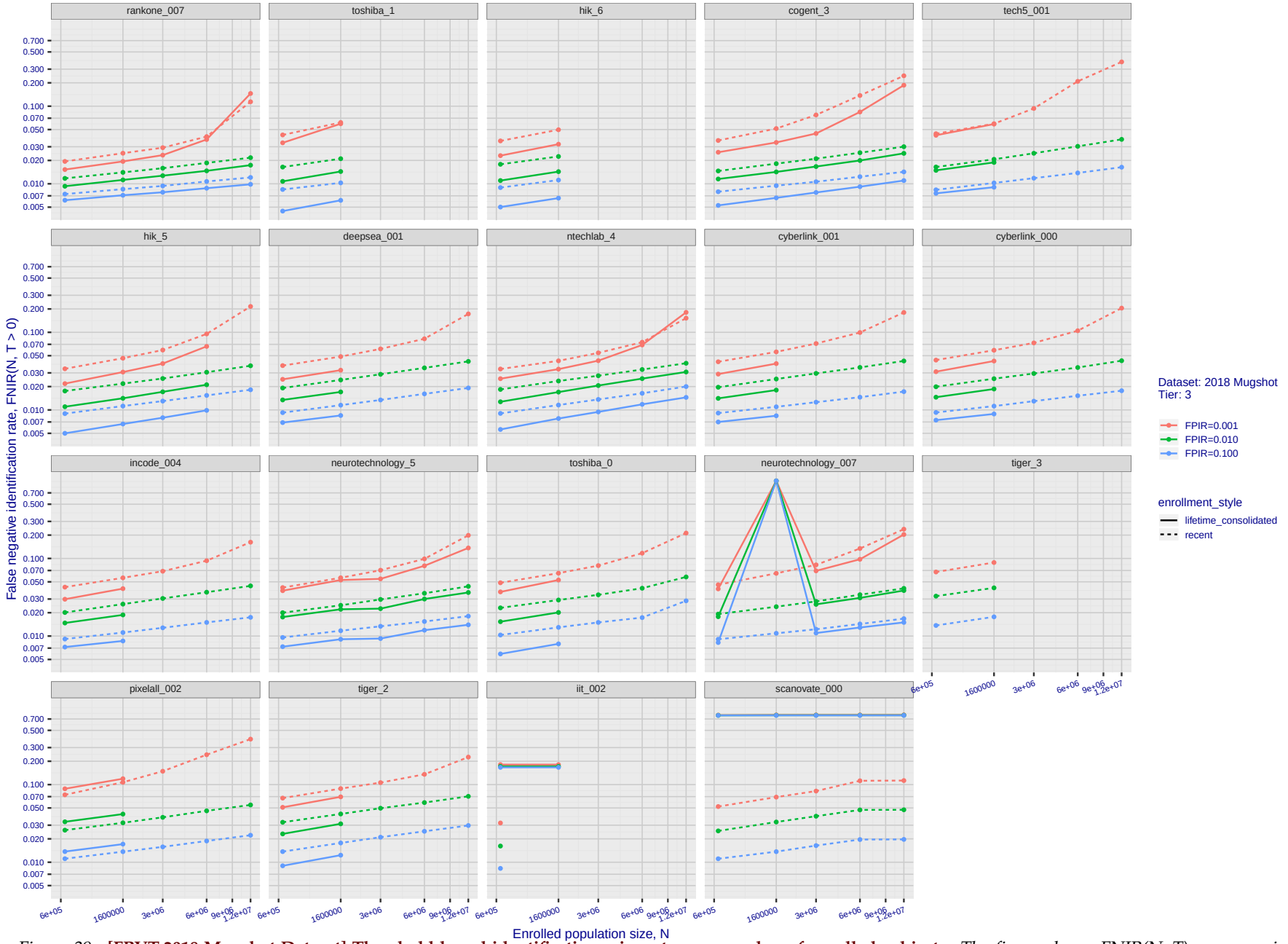

Figure 39: **[FRVT-2018 Mugshot Dataset] Threshold-based identification miss rates vs. number of enrolled subjects**. *The figure shows FNIR(N, T) across various gallery sizes when the threshold is set to achieve the given FPIRs. The rank criterion is irrelevant at high thresholds as mates are always at rank 1. The results are computed from the trials listed in rows 1-10 of Table 1. Less accurate algorithms were not run on large N, so results are missing. For clarity, results are sorted and reported into tiers spanning multiple pages. The tiering criteria is complicated: First paging by FNIR(N_b, 1, 0), then sorting by median FNIR(N_b, T), N_b = 640 000.*

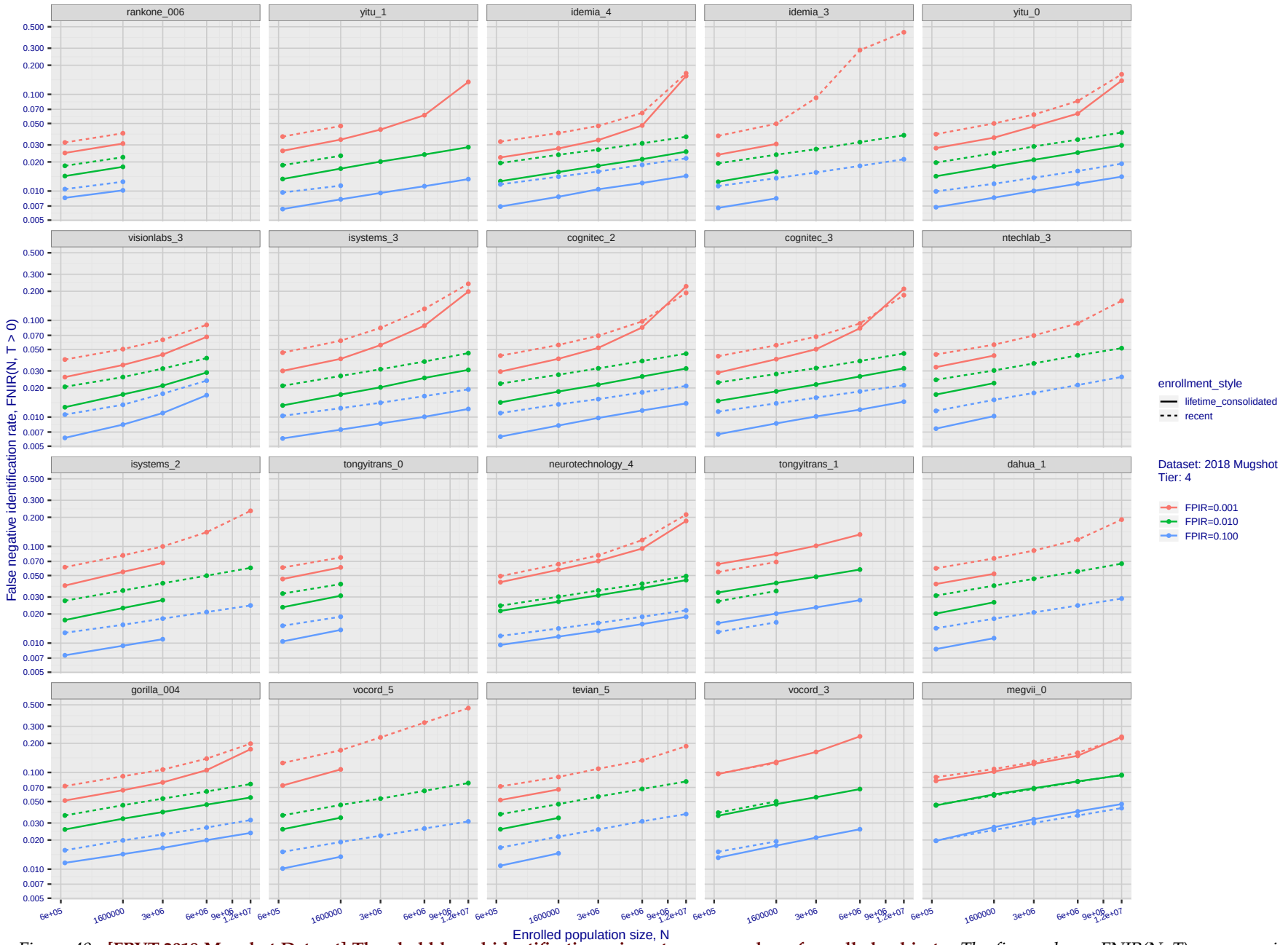

Figure 40: **[FRVT-2018 Mugshot Dataset] Threshold-based identification miss rates vs. number of enrolled subjects**. *The figure shows FNIR(N, T) across various gallery sizes when the threshold is set to achieve the given FPIRs. The rank criterion is irrelevant at high thresholds as mates are always at rank 1. The results are computed from the trials listed in rows 1-10 of Table 1. Less accurate algorithms were not run on large N, so results are missing. For clarity, results are sorted and reported into tiers spanning multiple pages. The tiering criteria is complicated: First paging by FNIR(N_b, 1, 0), then sorting by median FNIR(N_b, T), N_b = 640 000.*

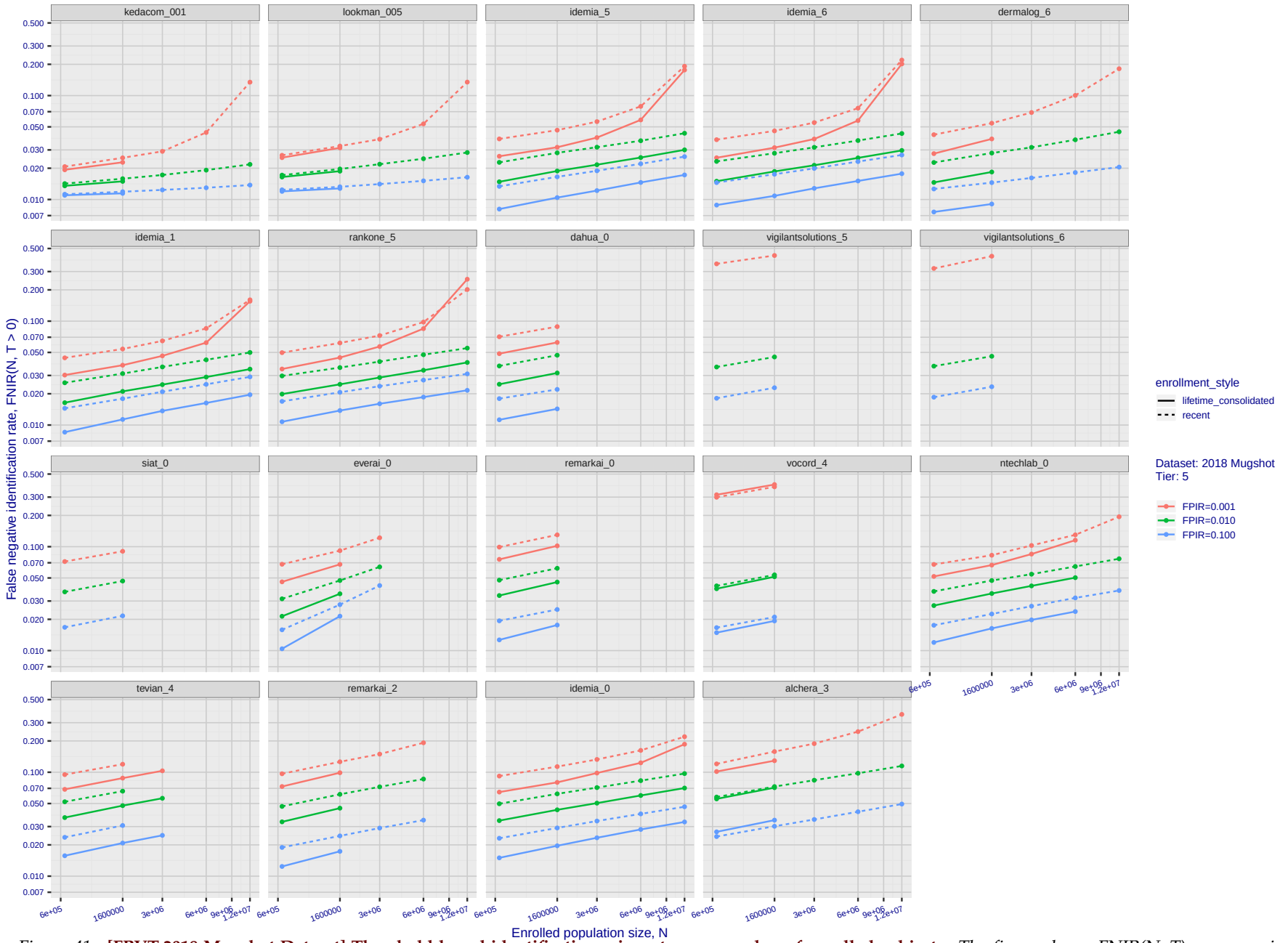

Figure 41: **[FRVT-2018 Mugshot Dataset] Threshold-based identification miss rates vs. number of enrolled subjects**. *The figure shows FNIR(N, T) across various gallery sizes when the threshold is set to achieve the given FPIRs. The rank criterion is irrelevant at high thresholds as mates are always at rank 1. The results are computed from the trials listed in rows 1-10 of Table 1. Less accurate algorithms were not run on large N, so results are missing. For clarity, results are sorted and reported into tiers spanning multiple pages. The tiering criteria is complicated: First paging by FNIR(N_b, 1, 0), then sorting by median FNIR(N_b, T), N_b = 640 000.*

2020/03/27 10:40:09
FNIR(N, R, T) = False neg. identification rate
FPIR(N, T) = False pos. identification rate
N = Num. enrolled subjects
R = Num. candidates examined
T = Threshold
T = 0 → Investigation
T > 0 → Identification

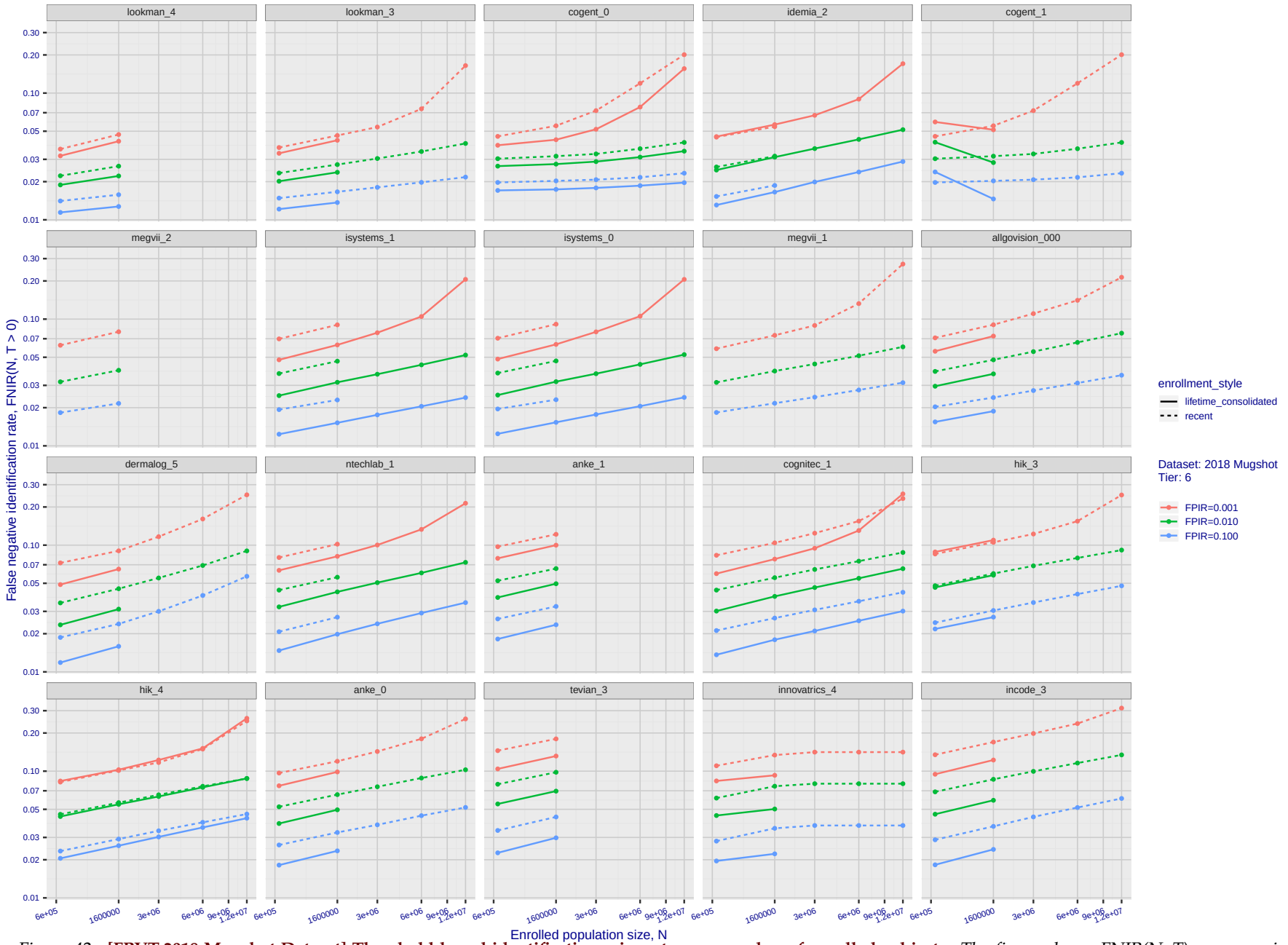

Figure 42: **[FRVT-2018 Mugshot Dataset] Threshold-based identification miss rates vs. number of enrolled subjects**. *The figure shows FNIR(N, T) across various gallery sizes when the threshold is set to achieve the given FPIRs. The rank criterion is irrelevant at high thresholds as mates are always at rank 1. The results are computed from the trials listed in rows 1-10 of Table 1. Less accurate algorithms were not run on large N, so results are missing. For clarity, results are sorted and reported into tiers spanning multiple pages. The tiering criteria is complicated: First paging by FNIR(N_b, 1, 0), then sorting by median FNIR(N_b, T), N_b = 640 000.*

FNIR(N, R, T) = False neg. identification rate
FPIR(N, T) = False pos. identification rate
N = Num. enrolled subjects
R = Num. candidates examined
T = Threshold
T = 0 → Investigation
T > 0 → Identification

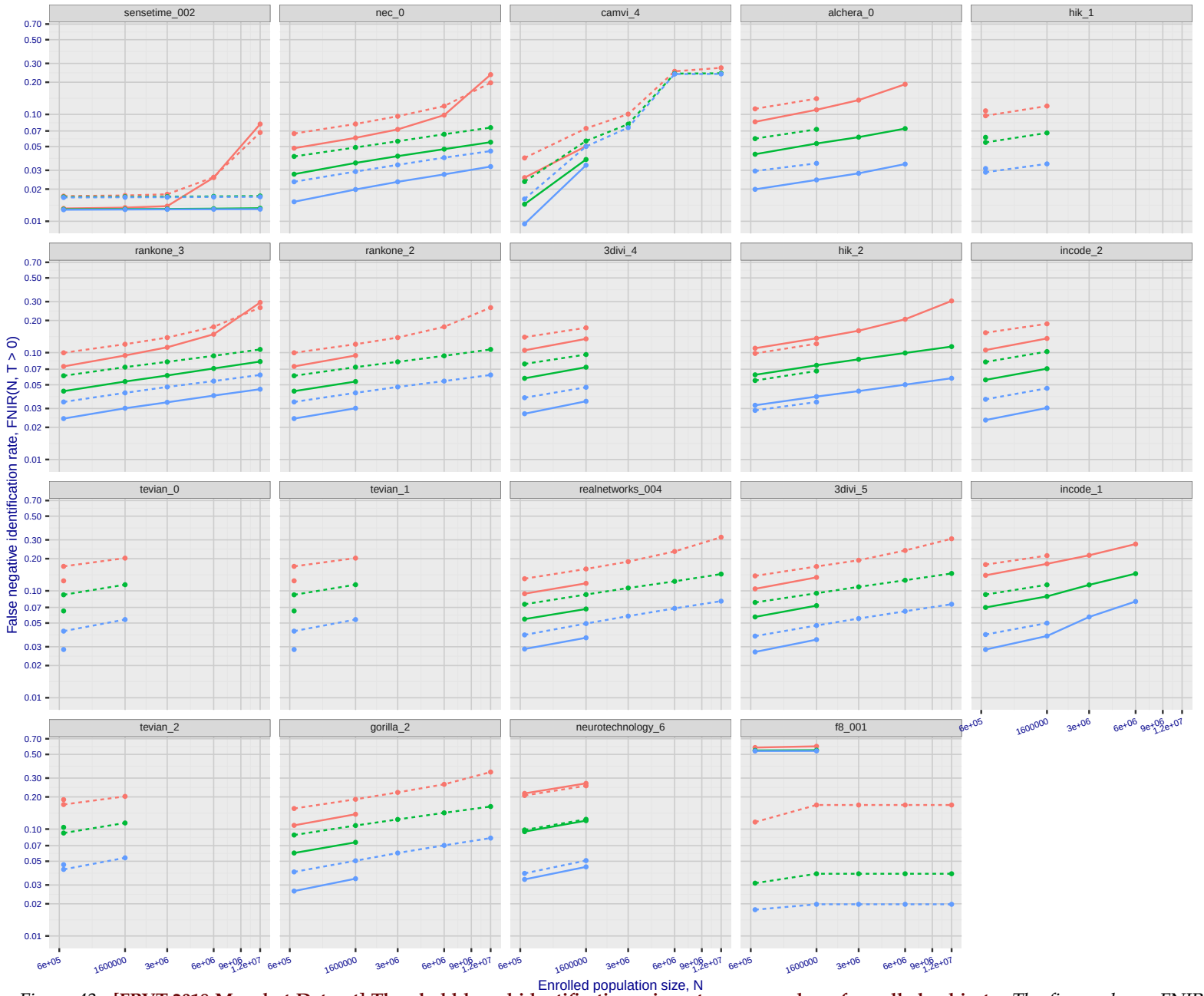

Figure 43: **[FRVT-2018 Mugshot Dataset] Threshold-based identification miss rates vs. number of enrolled subjects**. *The figure shows FNIR(N, T) across various gallery sizes when the threshold is set to achieve the given FPIRs. The rank criterion is irrelevant at high thresholds as mates are always at rank 1. The results are computed from the trials listed in rows 1-10 of Table 1. Less accurate algorithms were not run on large N, so results are missing. For clarity, results are sorted and reported into tiers spanning multiple pages. The tiering criteria is complicated: First paging by FNIR(N_b, 1, 0), then sorting by median FNIR(N_b, T), N_b = 640 000.*

2020/03/27 10:40:09

FNIR(N, R, T) = False neg. identification rate
FPIR(N, T) = False pos. identification rate

N = Num. enrolled subjects
R = Num. candidates examined

T = Threshold

T = 0 → Investigation
T > 0 → Identification

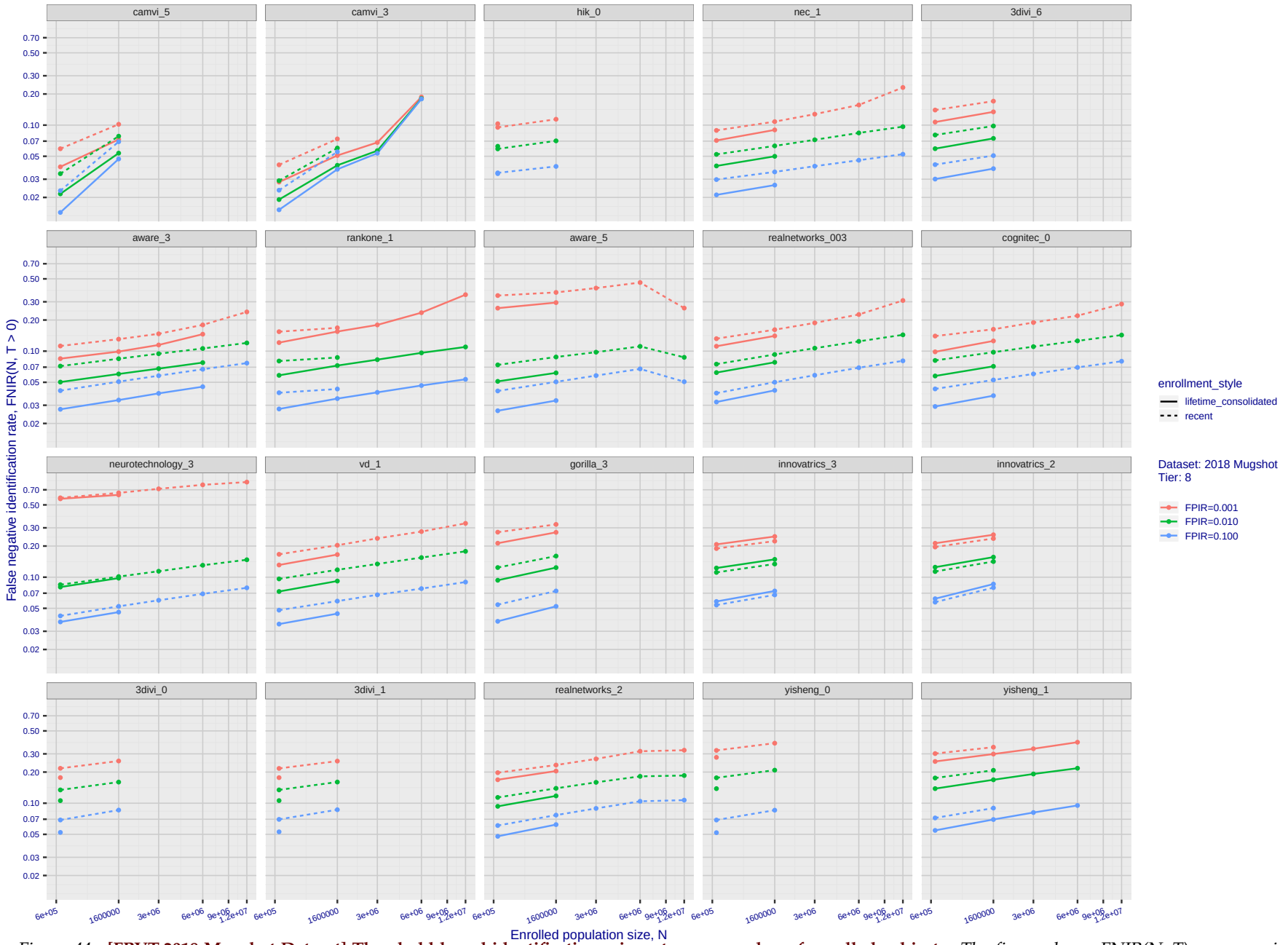

Figure 44: **[FRVT-2018 Mugshot Dataset] Threshold-based identification miss rates vs. number of enrolled subjects**. *The figure shows FNIR(N, T) across various gallery sizes when the threshold is set to achieve the given FPIRs. The rank criterion is irrelevant at high thresholds as mates are always at rank 1. The results are computed from the trials listed in rows 1-10 of Table 1. Less accurate algorithms were not run on large N, so results are missing. For clarity, results are sorted and reported into tiers spanning multiple pages. The tiering criteria is complicated: First paging by FNIR(N_b, 1, 0), then sorting by median FNIR(N_b, T), N_b = 640 000.*

2020/03/27 10:40:09
FNIR(N, R, T) = False neg. identification rate
FPIR(N, T) = False pos. identification rate
N = Num. enrolled subjects
R = Num. candidates examined
T = Threshold
T = 0 → Investigation
T > 0 → Identification

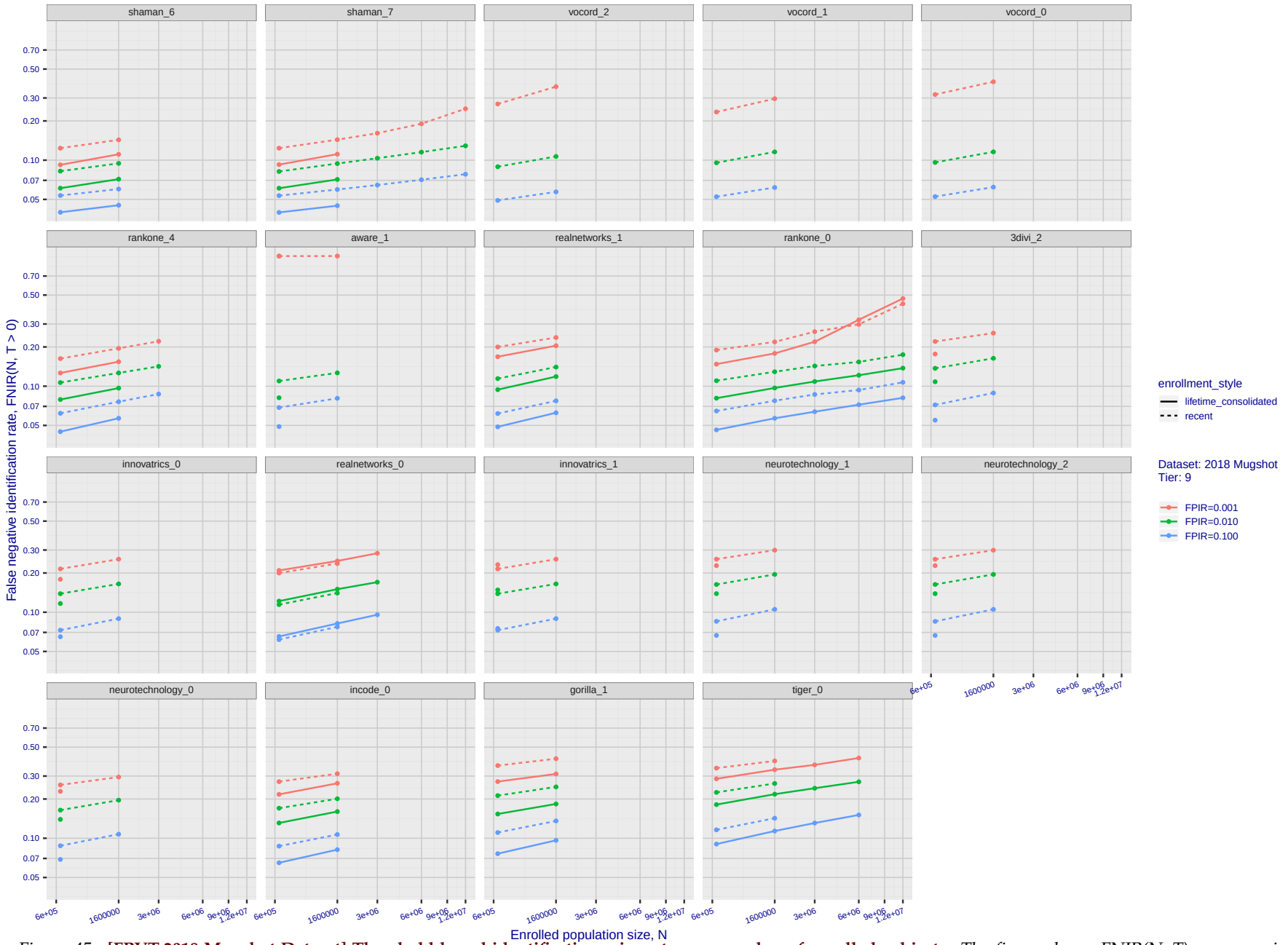

Figure 45: **[FRVT-2018 Mugshot Dataset] Threshold-based identification miss rates vs. number of enrolled subjects**. *The figure shows FNIR(N, T) across various gallery sizes when the threshold is set to achieve the given FPIRs. The rank criterion is irrelevant at high thresholds as mates are always at rank 1. The results are computed from the trials listed in rows 1-10 of Table 1. Less accurate algorithms were not run on large N, so results are missing. For clarity, results are sorted and reported into tiers spanning multiple pages. The tiering criteria is complicated: First paging by FNIR(N_b, 1, 0), then sorting by median FNIR(N_b, T), N_b = 640 000.*

2020/03/27 10:40:09
FNIR(N, R, T) = False neg. identification rate
FPIR(N, T) = False pos. identification rate
N = Num. enrolled subjects
R = Num. candidates examined
T = Threshold
T = 0 → Investigation
T > 0 → Identification

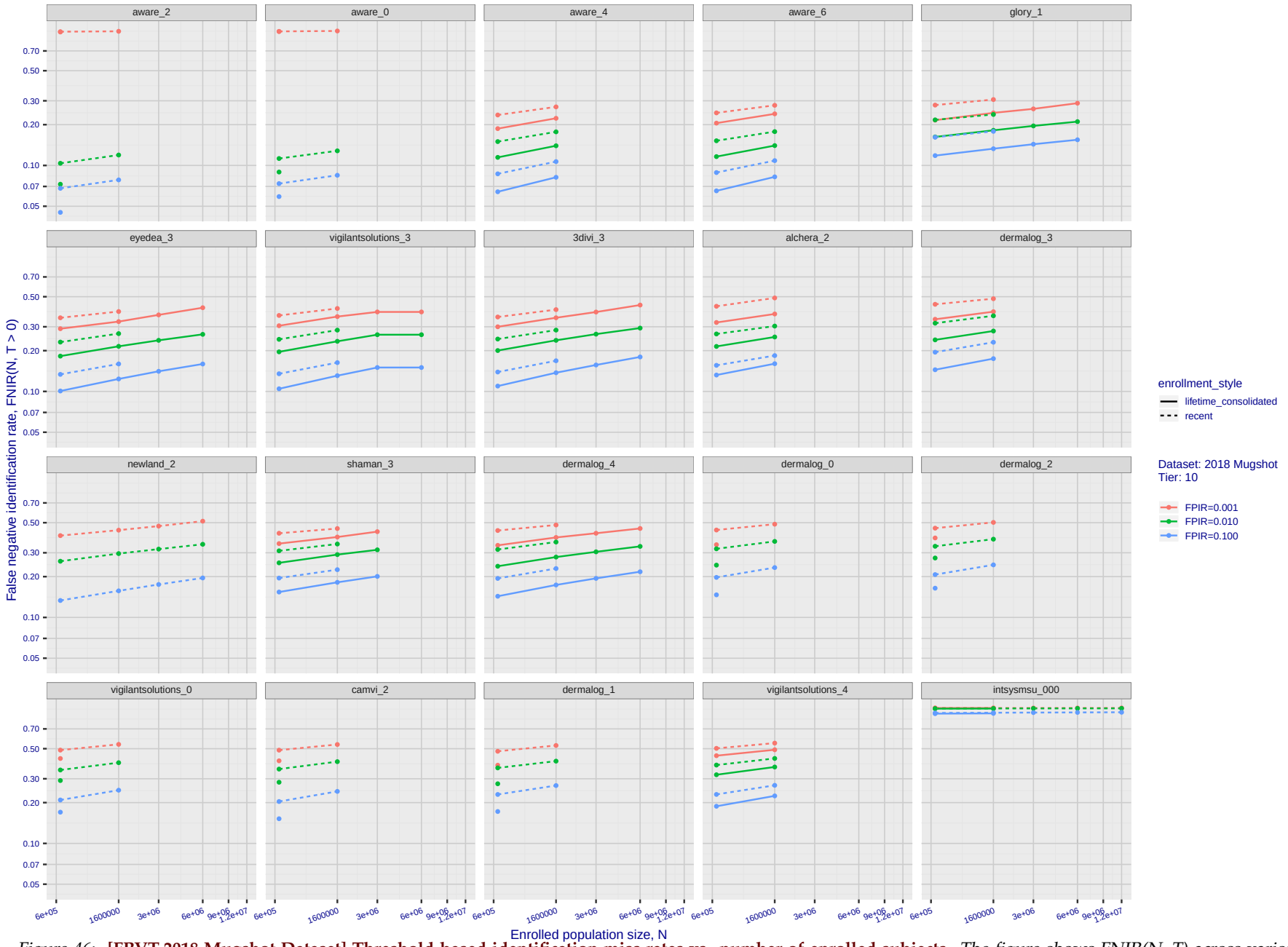

Figure 46: **[FRVT-2018 Mugshot Dataset] Threshold-based identification miss rates vs. number of enrolled subjects**. *The figure shows FNIR(N, T) across various gallery sizes when the threshold is set to achieve the given FPIRs. The rank criterion is irrelevant at high thresholds as mates are always at rank 1. The results are computed from the trials listed in rows 1-10 of Table 1. Less accurate algorithms were not run on large N, so results are missing. For clarity, results are sorted and reported into tiers spanning multiple pages. The tiering criteria is complicated: First paging by FNIR(N_b, 1, 0), then sorting by median FNIR(N_b, T), N_b = 640 000.*

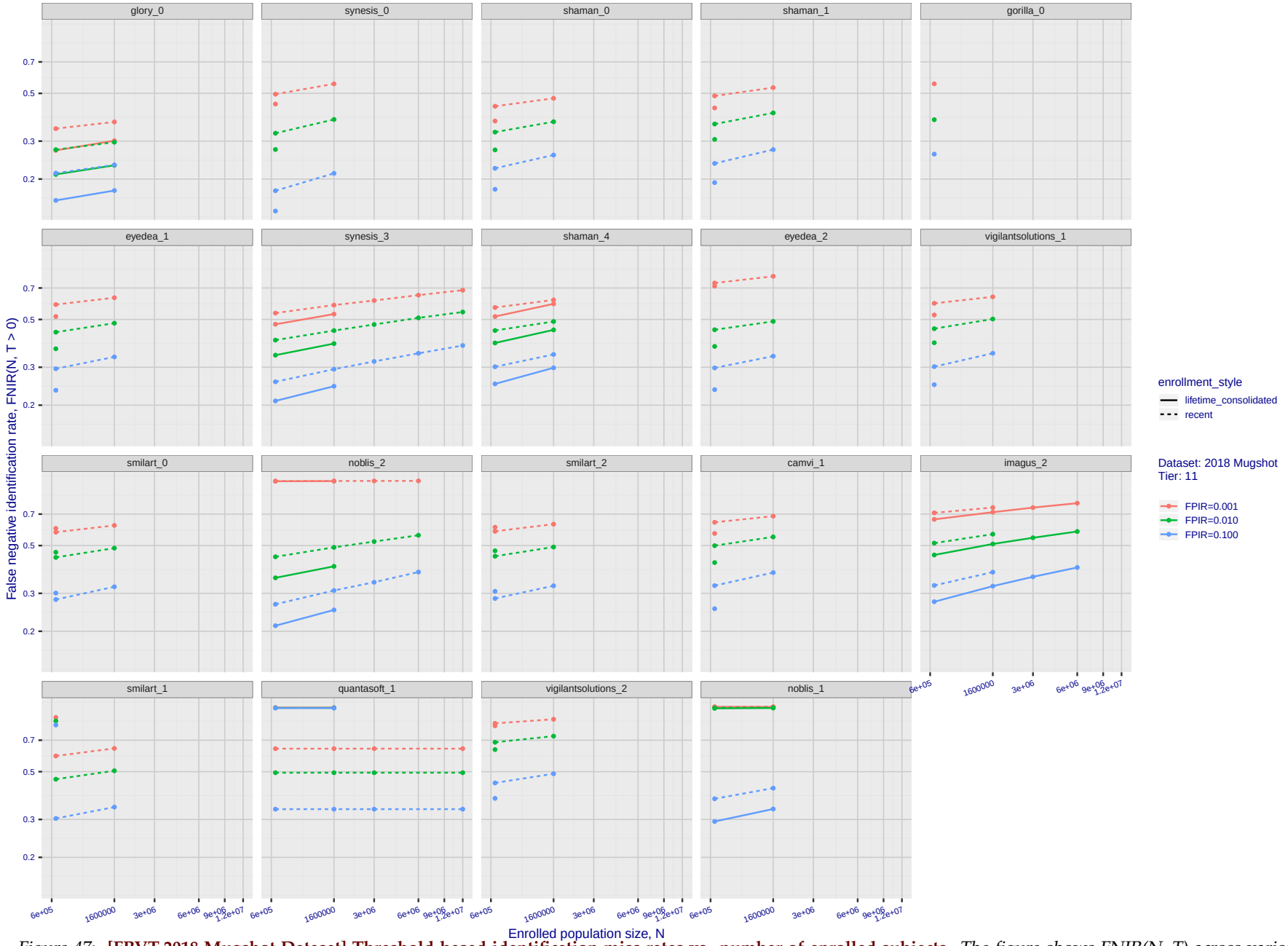

Figure 47: **[FRVT-2018 Mugshot Dataset] Threshold-based identification miss rates vs. number of enrolled subjects**. *The figure shows FNIR(N, T) across various gallery sizes when the threshold is set to achieve the given FPIRs. The rank criterion is irrelevant at high thresholds as mates are always at rank 1. The results are computed from the trials listed in rows 1-10 of Table 1. Less accurate algorithms were not run on large N, so results are missing. For clarity, results are sorted and reported into tiers spanning multiple pages. The tiering criteria is complicated: First paging by FNIR(N_b, 1, 0), then sorting by median FNIR(N_b, T), N_b = 640 000.*

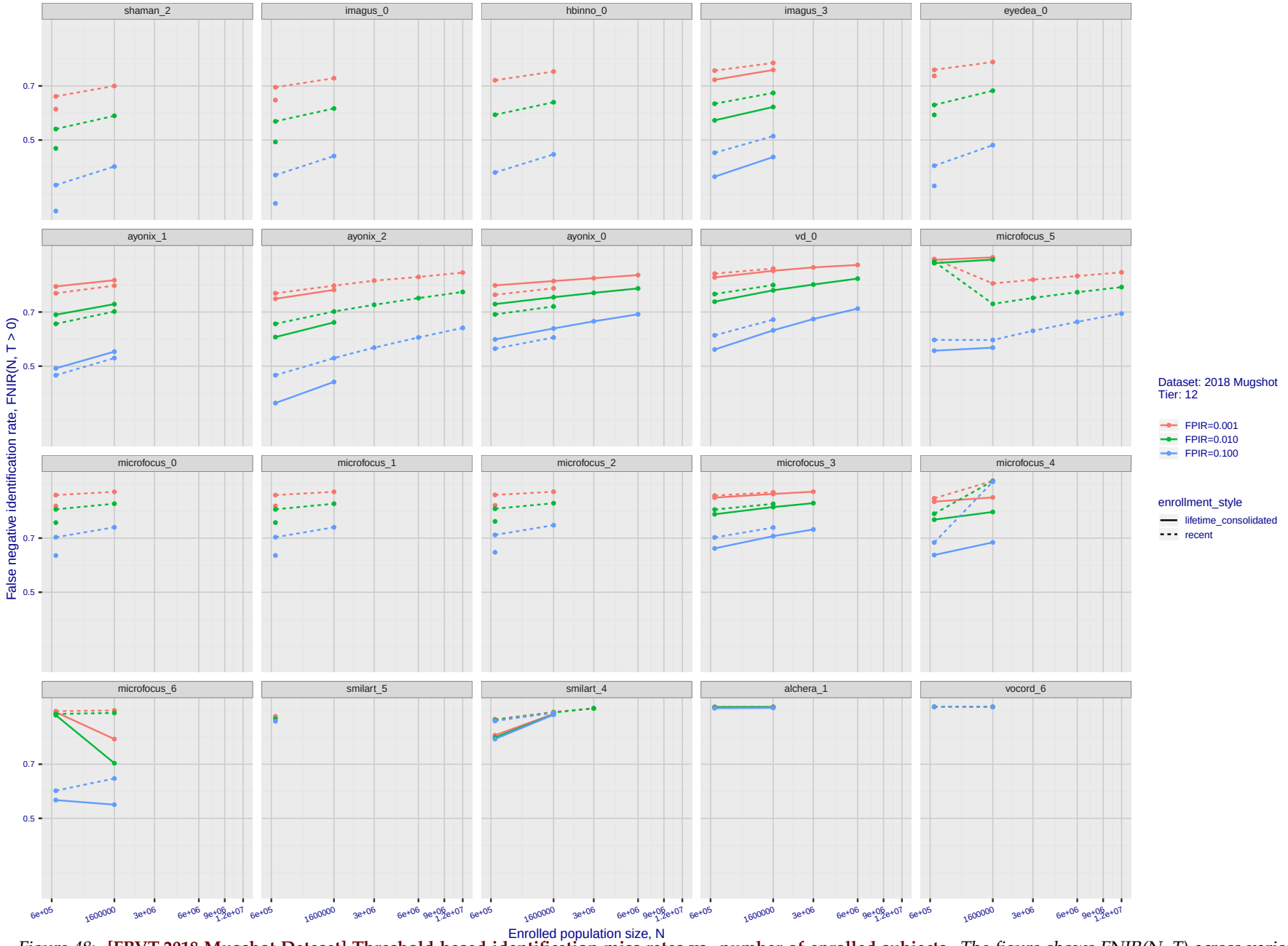

Figure 48: **[FRVT-2018 Mugshot Dataset] Threshold-based identification miss rates vs. number of enrolled subjects**. *The figure shows FNIR(N, T) across various gallery sizes when the threshold is set to achieve the given FPIRs. The rank criterion is irrelevant at high thresholds as mates are always at rank 1. The results are computed from the trials listed in rows 1-10 of Table 1. Less accurate algorithms were not run on large N, so results are missing. For clarity, results are sorted and reported into tiers spanning multiple pages. The tiering criteria is complicated: First paging by FNIR(N_b, 1, 0), then sorting by median FNIR(N_b, T), N_b = 640 000.*

2020/03/27	FNIR(N, R, T) =	False neg. identification rate	N = Num. enrolled subjects	T = Threshold	$T = 0 \rightarrow$ Investigation
10:40:09	FPIR(N, T) =	False pos. identification rate	R = Num. candidates examined		$T > 0 \rightarrow$ Identification

FNIR(N, R, T) = False neg. identification rate
FPIR(N, T) = False pos. identification rate

N = Num. enrolled subjects
R = Num. candidates examined

T = Threshold

T = 0 → Investigation
T > 0 → Identification

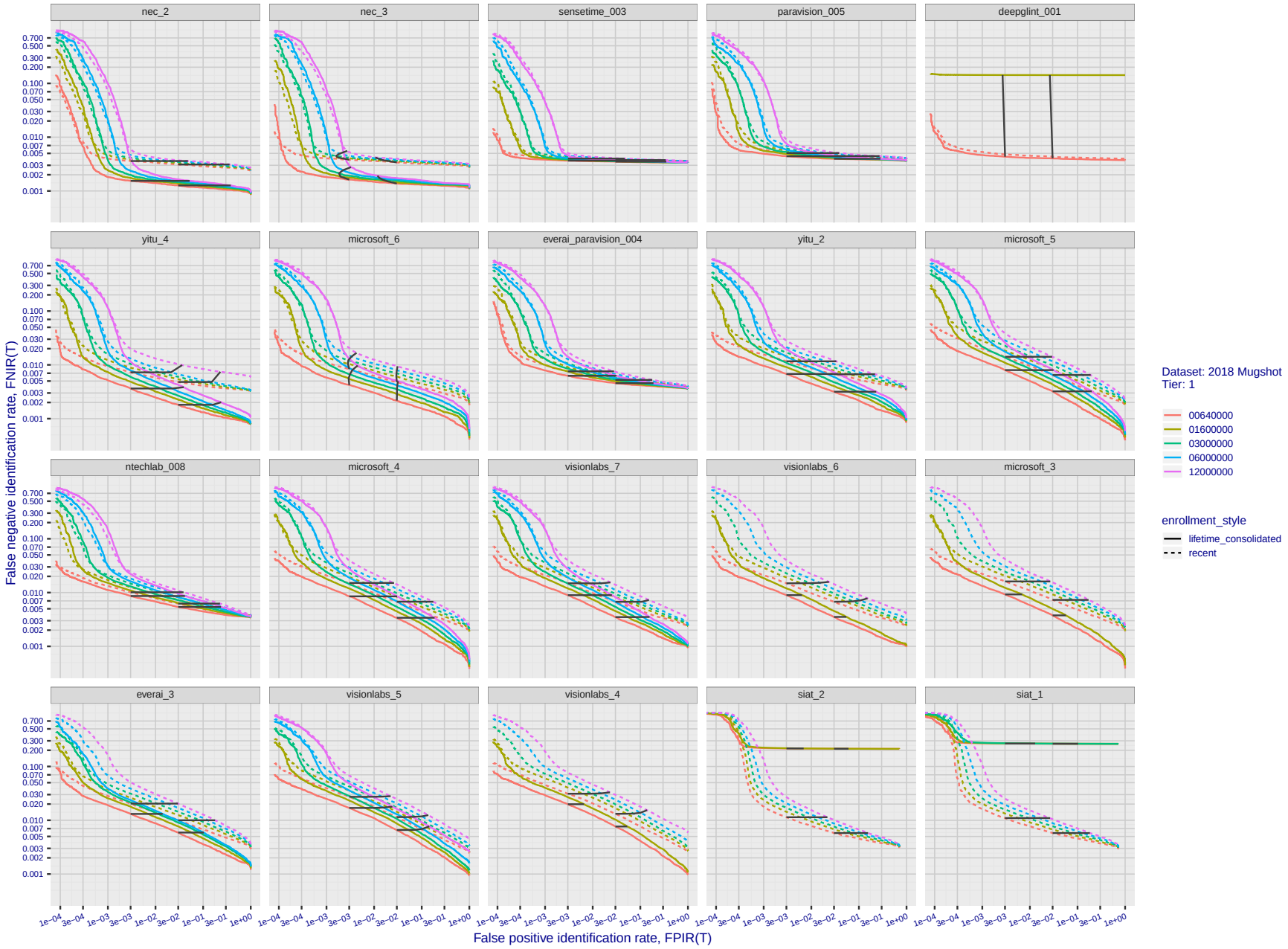

Figure 49: **[FRVT-2018 Mugshot Dataset] Identification miss rates vs. false positive rates**. *The figure shows miss rates FNIR(N, L, T) as a function of FPIR(N, T), with N ranging from 640 000 to 12 000 000 as noted in rows 1-10 of Table 1. These error tradeoff characteristics are useful for applications where a threshold must be elevated to limit false positives, such as when human reviewer labor is not matched to the volume of searches. Dark lines join points of equal threshold: If horizontal, FPIR(T) rises with N, and mate scores are independent of N. Other algorithms adjust scores in an attempt to make FPIR independent of N.*

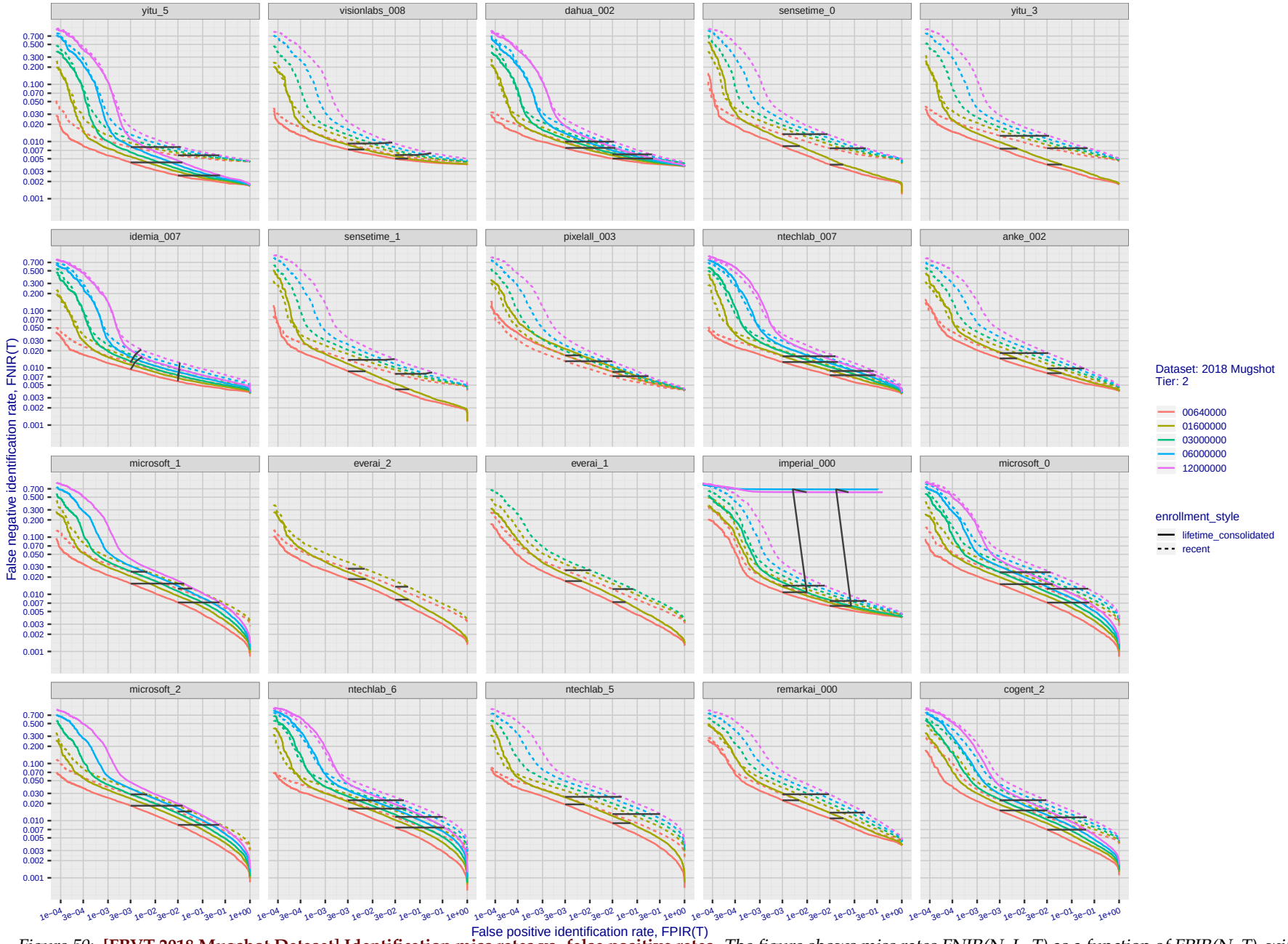

Figure 50: **[FRVT-2018 Mugshot Dataset] Identification miss rates vs. false positive rates**. *The figure shows miss rates FNIR(N, L, T) as a function of FPIR(N, T), with N ranging from 640 000 to 12 000 000 as noted in rows 1-10 of Table 1. These error tradeoff characteristics are useful for applications where a threshold must be elevated to limit false positives, such as when human reviewer labor is not matched to the volume of searches. Dark lines join points of equal threshold: If horizontal, FPIR(T) rises with N, and mate scores are independent of N. Other algorithms adjust scores in an attempt to make FPIR independent of N.*

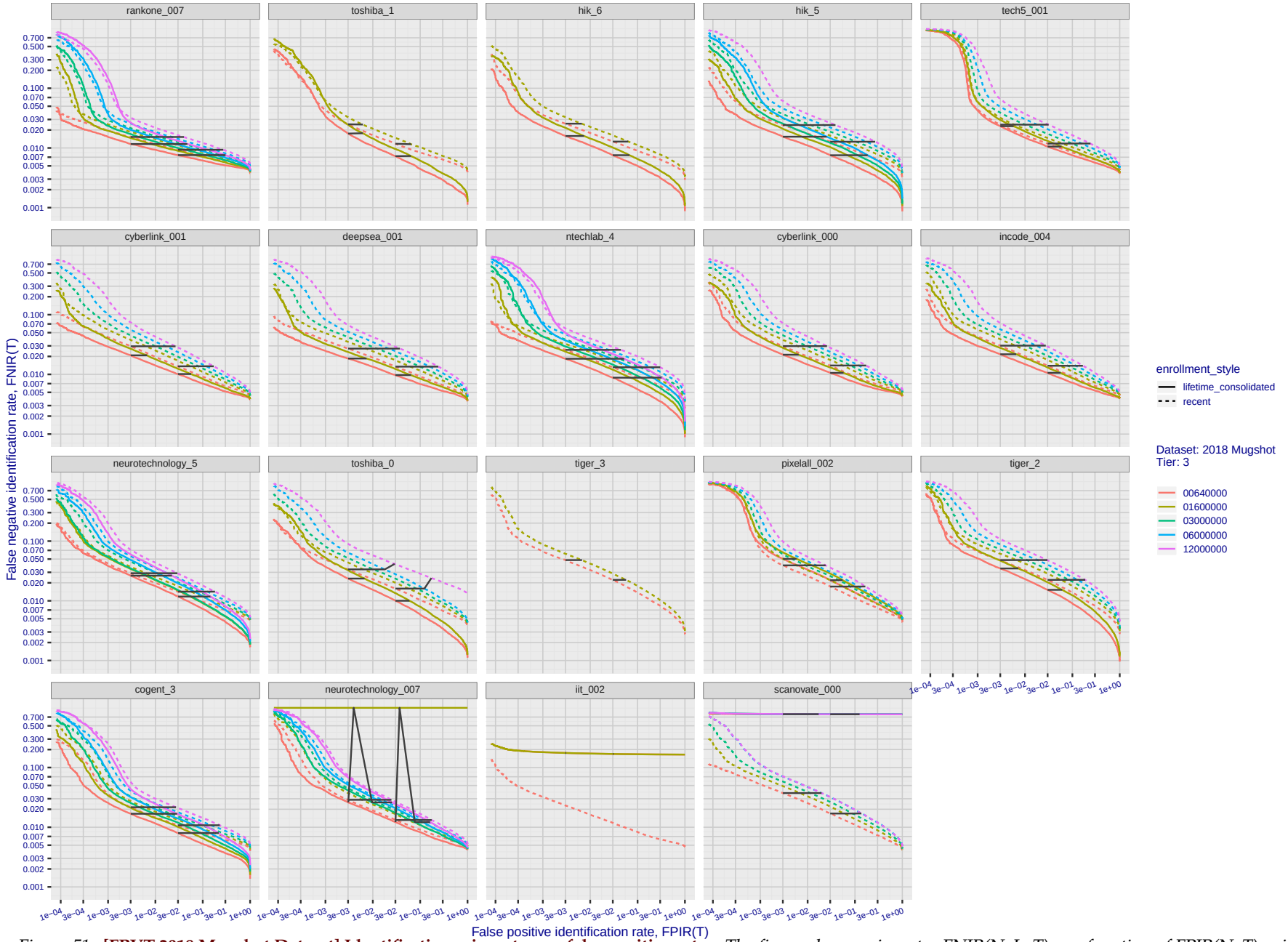

Figure 51: **[FRVT-2018 Mugshot Dataset] Identification miss rates vs. false positive rates**. *The figure shows miss rates FNIR(N, L, T) as a function of FPIR(N, T), with N ranging from 640 000 to 12 000 000 as noted in rows 1-10 of Table 1. These error tradeoff characteristics are useful for applications where a threshold must be elevated to limit false positives, such as when human reviewer labor is not matched to the volume of searches. Dark lines join points of equal threshold: If horizontal, FPIR(T) rises with N, and mate scores are independent of N. Other algorithms adjust scores in an attempt to make FPIR independent of N.*

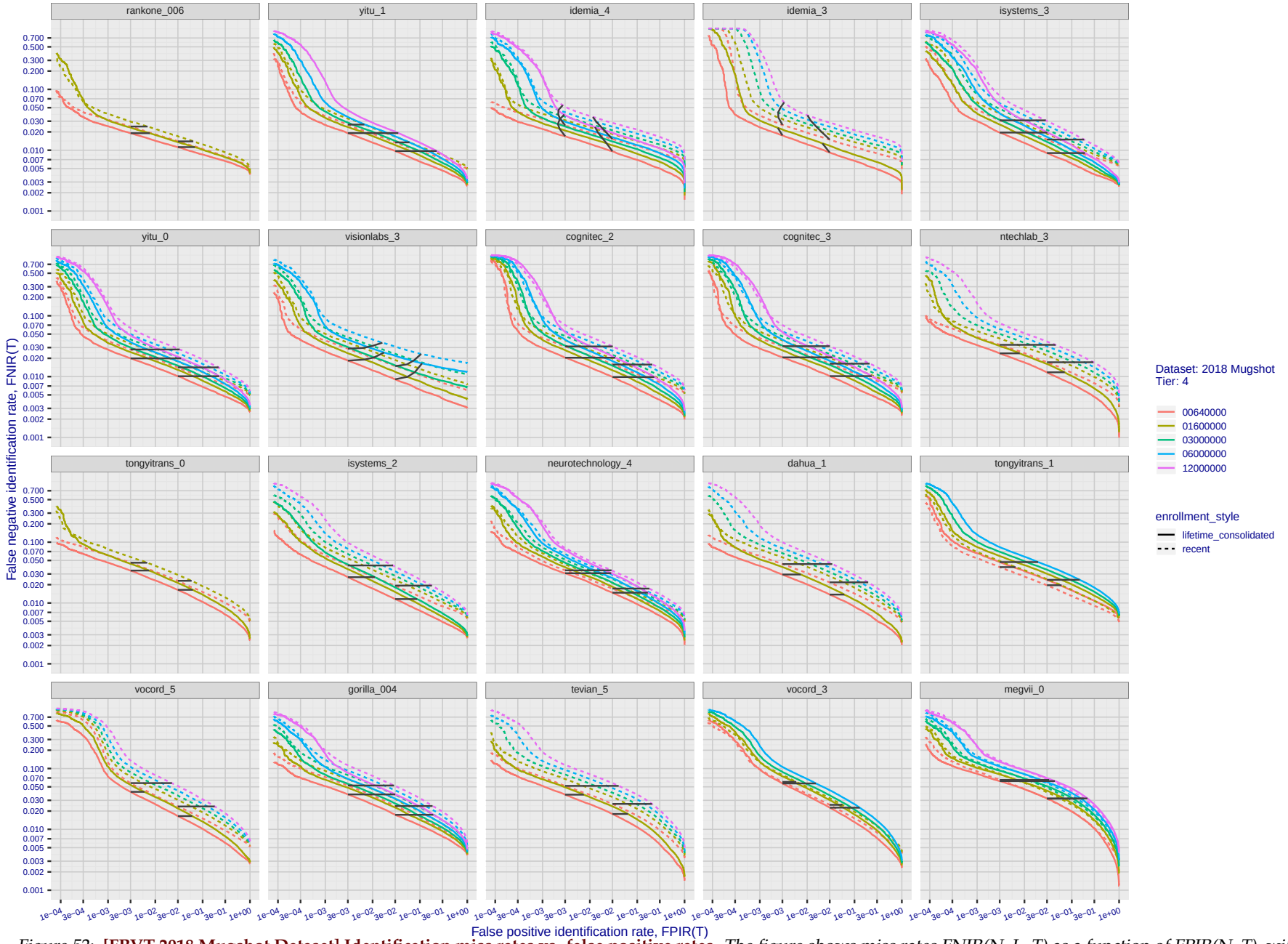

Figure 52: **[FRVT-2018 Mugshot Dataset] Identification miss rates vs. false positive rates**. *The figure shows miss rates FNIR(N, L, T) as a function of FPIR(N, T), with N ranging from 640 000 to 12 000 000 as noted in rows 1-10 of Table 1. These error tradeoff characteristics are useful for applications where a threshold must be elevated to limit false positives, such as when human reviewer labor is not matched to the volume of searches. Dark lines join points of equal threshold: If horizontal, FPIR(T) rises with N, and mate scores are independent of N. Other algorithms adjust scores in an attempt to make FPIR independent of N.*

2020/03/27 10:40:09

FNIR(N, R, T) = False neg. identification rate
FPIR(N, T) = False pos. identification rate

N = Num. enrolled subjects
R = Num. candidates examined

T = Threshold

T = 0 → Investigation
T > 0 → Identification

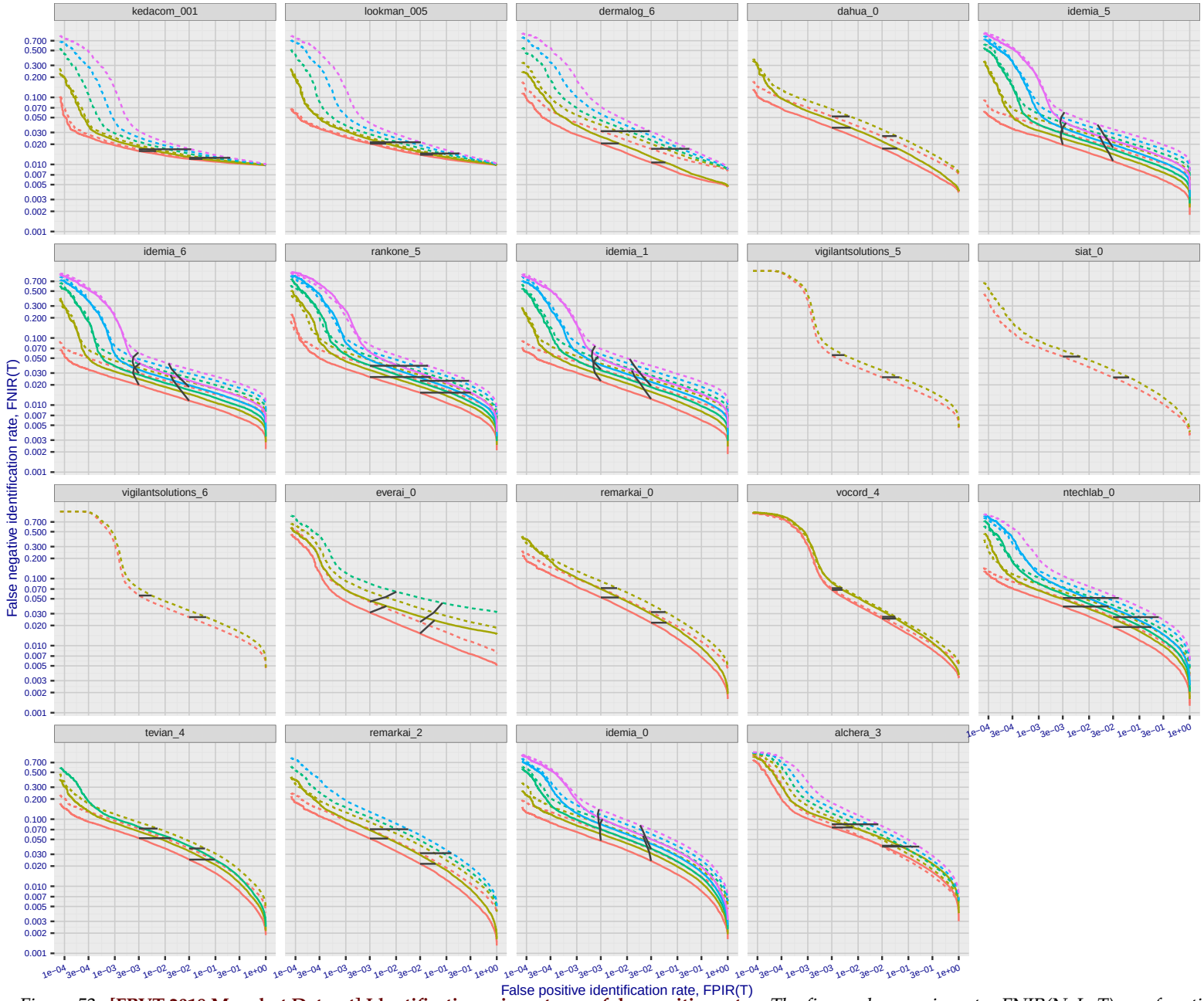

Figure 53: **[FRVT-2018 Mugshot Dataset] Identification miss rates vs. false positive rates**. *The figure shows miss rates FNIR(N, L, T) as a function of FPIR(N, T), with N ranging from 640 000 to 12 000 000 as noted in rows 1-10 of Table 1. These error tradeoff characteristics are useful for applications where a threshold must be elevated to limit false positives, such as when human reviewer labor is not matched to the volume of searches. Dark lines join points of equal threshold: If horizontal, FPIR(T) rises with N, and mate scores are independent of N. Other algorithms adjust scores in an attempt to make FPIR independent of N.*

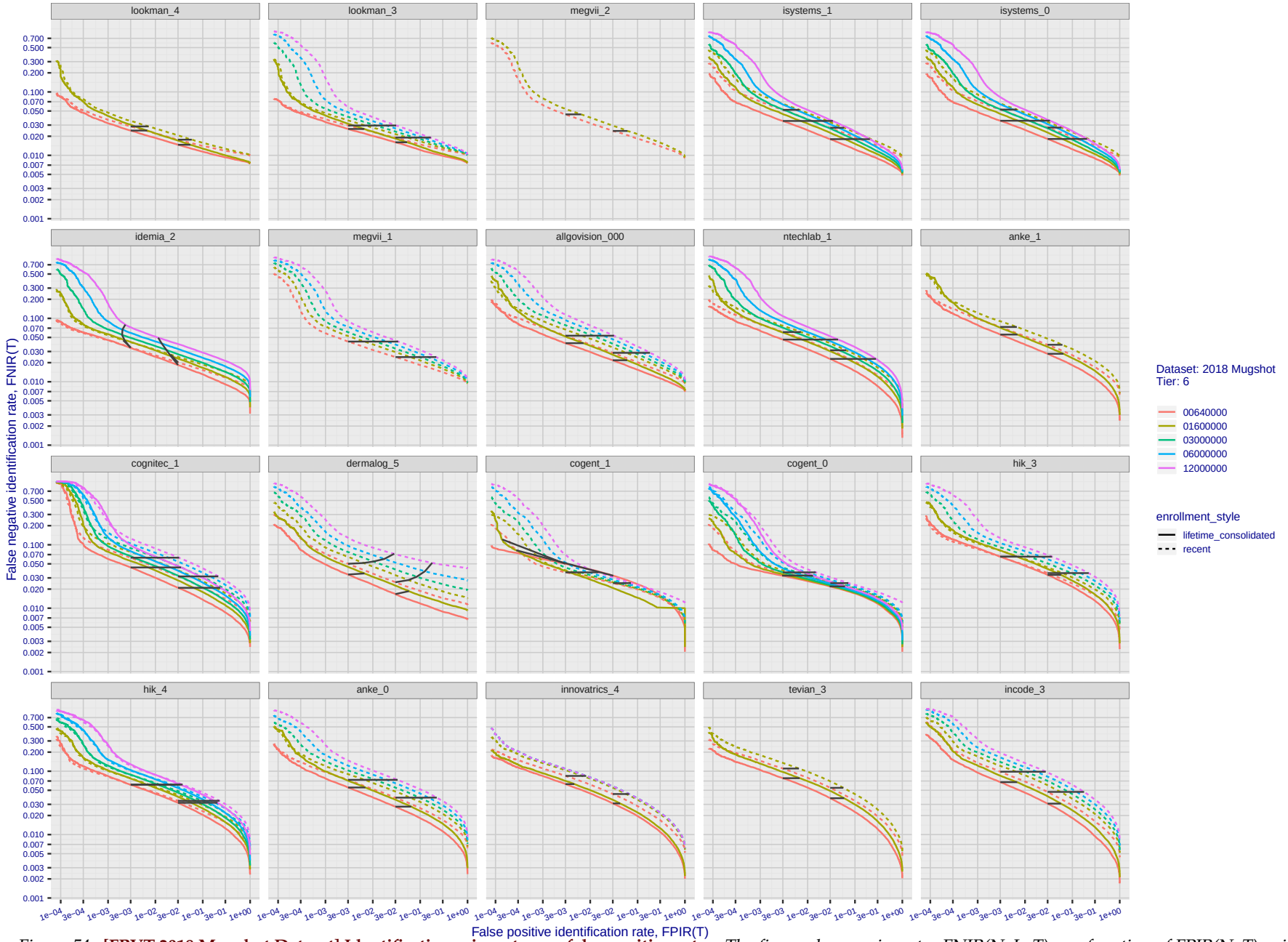

Figure 54: **[FRVT-2018 Mugshot Dataset] Identification miss rates vs. false positive rates**. *The figure shows miss rates FNIR(N, L, T) as a function of FPIR(N, T), with N ranging from 640 000 to 12 000 000 as noted in rows 1-10 of Table 1. These error tradeoff characteristics are useful for applications where a threshold must be elevated to limit false positives, such as when human reviewer labor is not matched to the volume of searches. Dark lines join points of equal threshold: If horizontal, FPIR(T) rises with N, and mate scores are independent of N. Other algorithms adjust scores in an attempt to make FPIR independent of N.*

2020/03/27 10:40:09

FNIR(N, R, T) = False neg. identification rate
FPIR(N, T) = False pos. identification rate

N = Num. enrolled subjects
R = Num. candidates examined

T = Threshold

T = 0 → Investigation
T > 0 → Identification

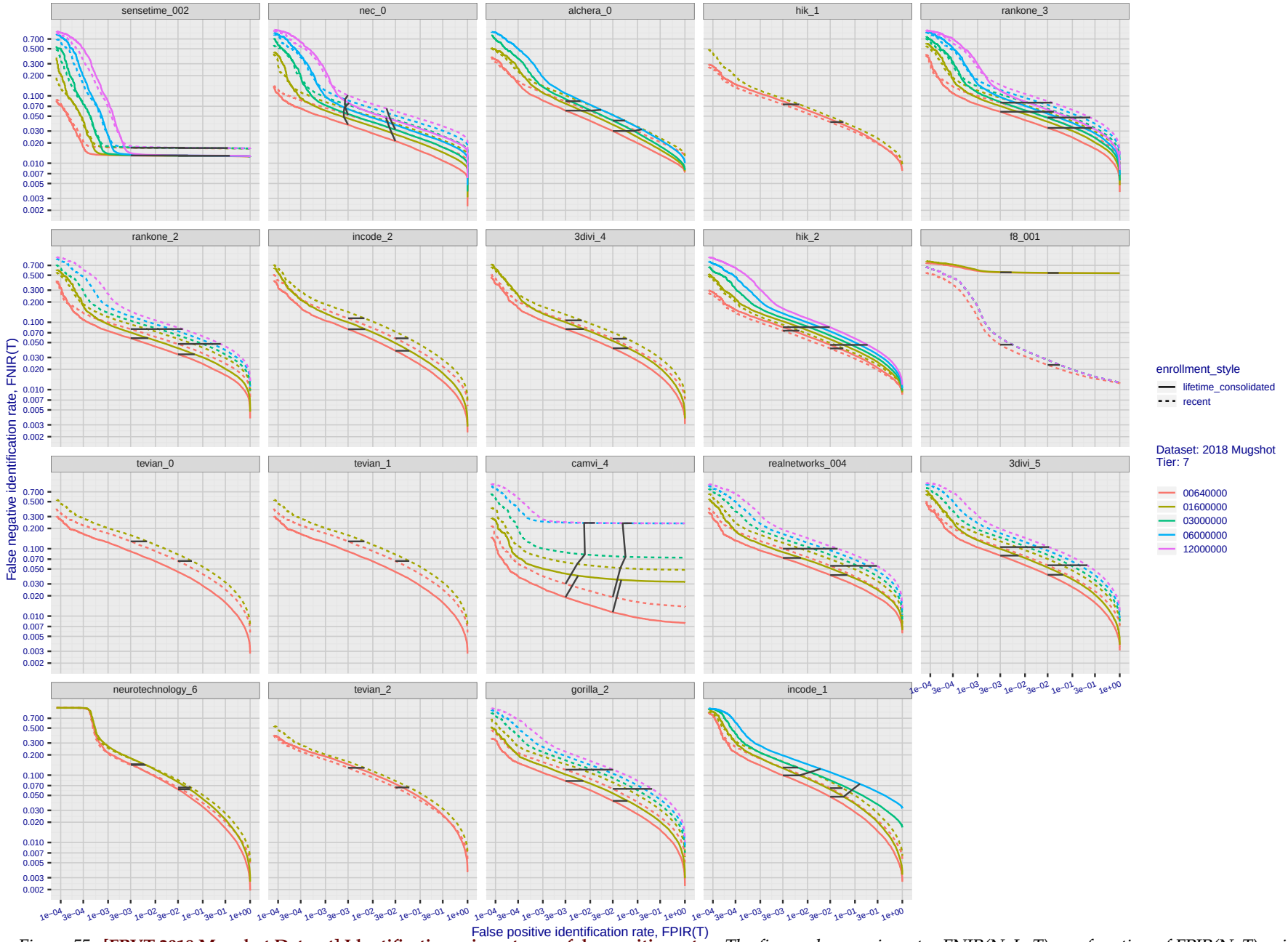

Figure 55: **[FRVT-2018 Mugshot Dataset] Identification miss rates vs. false positive rates**. *The figure shows miss rates FNIR(N, L, T) as a function of FPIR(N, T), with N ranging from 640 000 to 12 000 000 as noted in rows 1-10 of Table 1. These error tradeoff characteristics are useful for applications where a threshold must be elevated to limit false positives, such as when human reviewer labor is not matched to the volume of searches. Dark lines join points of equal threshold: If horizontal, FPIR(T) rises with N, and mate scores are independent of N. Other algorithms adjust scores in an attempt to make FPIR independent of N.*

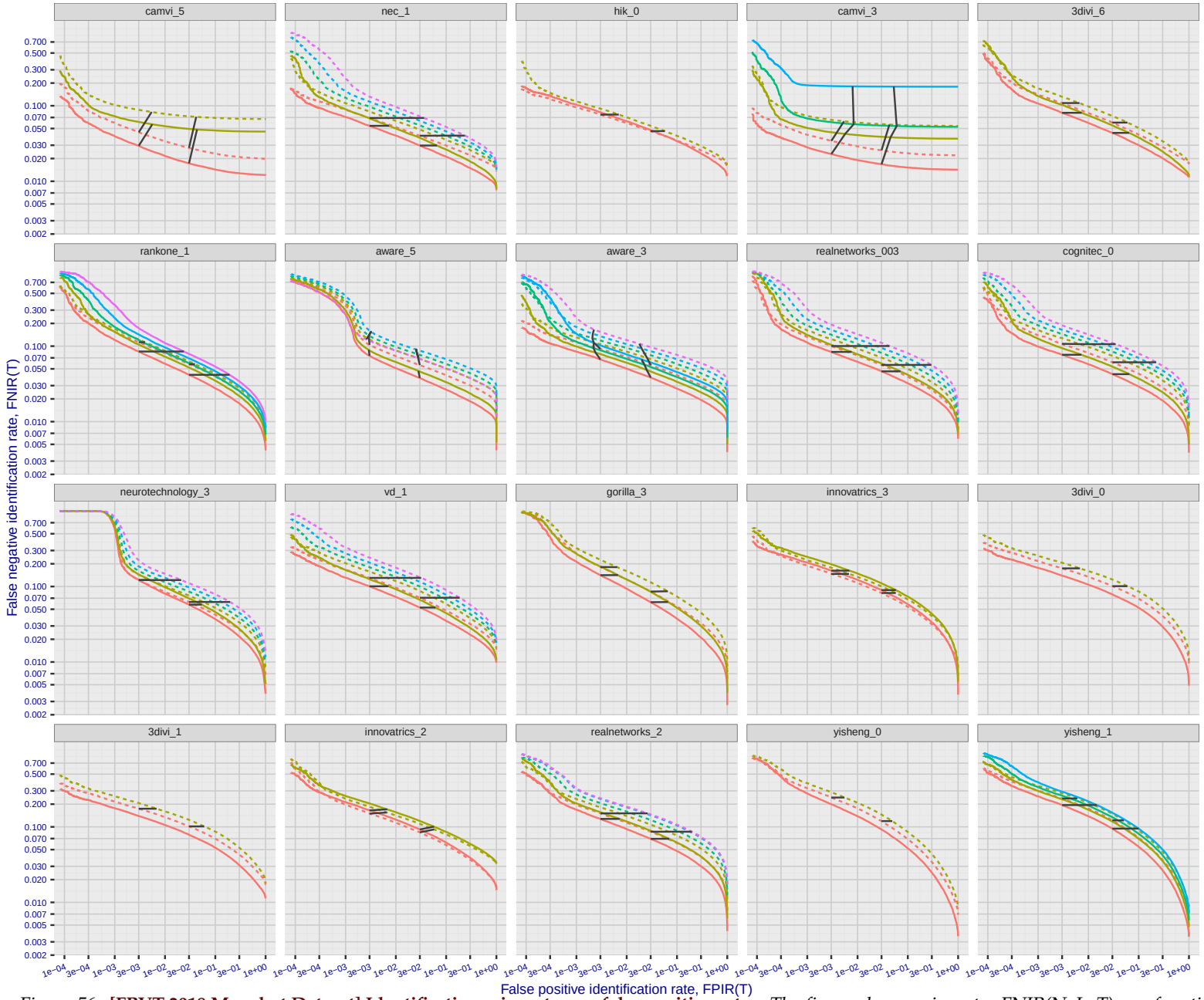

Figure 56: **[FRVT-2018 Mugshot Dataset] Identification miss rates vs. false positive rates**. *The figure shows miss rates FNIR(N, L, T) as a function of FPIR(N, T), with N ranging from 640 000 to 12 000 000 as noted in rows 1-10 of Table 1. These error tradeoff characteristics are useful for applications where a threshold must be elevated to limit false positives, such as when human reviewer labor is not matched to the volume of searches. Dark lines join points of equal threshold: If horizontal, FPIR(T) rises with N, and mate scores are independent of N. Other algorithms adjust scores in an attempt to make FPIR independent of N.*

2020/03/27 10:40:09

FNIR(N, R, T) = False neg. identification rate
FPIR(N, T) = False pos. identification rate
N = Num. enrolled subjects
R = Num. candidates examined
T = Threshold
T = 0 → Investigation
T > 0 → Identification

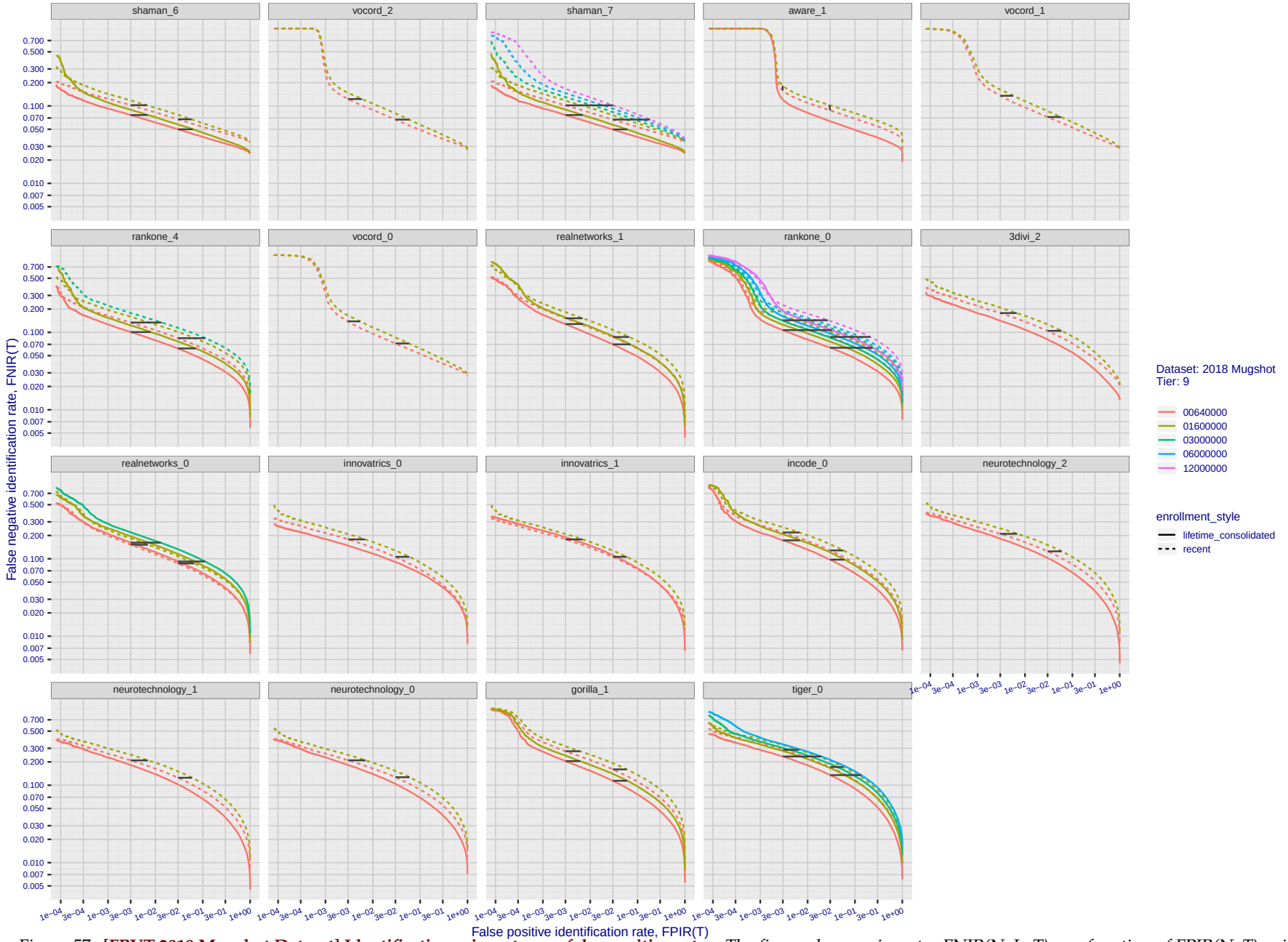

Figure 57: **[FRVT-2018 Mugshot Dataset] Identification miss rates vs. false positive rates**. *The figure shows miss rates FNIR(N, L, T) as a function of FPIR(N, T), with N ranging from 640 000 to 12 000 000 as noted in rows 1-10 of Table 1. These error tradeoff characteristics are useful for applications where a threshold must be elevated to limit false positives, such as when human reviewer labor is not matched to the volume of searches. Dark lines join points of equal threshold: If horizontal, FPIR(T) rises with N, and mate scores are independent of N. Other algorithms adjust scores in an attempt to make FPIR independent of N.*

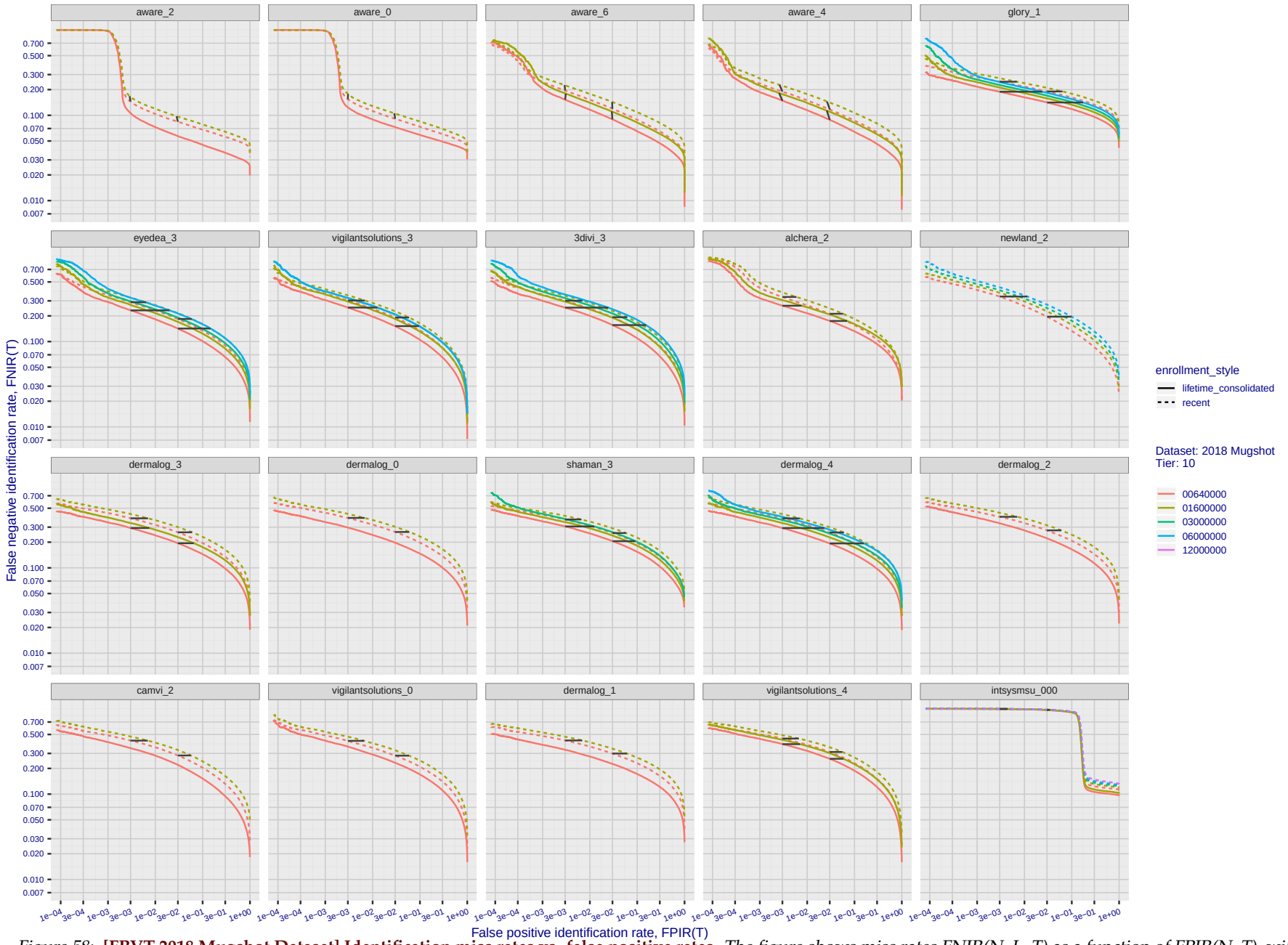

Figure 58: **[FRVT-2018 Mugshot Dataset] Identification miss rates vs. false positive rates**. *The figure shows miss rates FNIR(N, L, T) as a function of FPIR(N, T), with N ranging from 640 000 to 12 000 000 as noted in rows 1-10 of Table 1. These error tradeoff characteristics are useful for applications where a threshold must be elevated to limit false positives, such as when human reviewer labor is not matched to the volume of searches. Dark lines join points of equal threshold: If horizontal, FPIR(T) rises with N, and mate scores are independent of N. Other algorithms adjust scores in an attempt to make FPIR independent of N.*

2020/03/27 10:40:09

FNIR(N, R, T) = False neg. identification rate
FPIR(N, T) = False pos. identification rate

N = Num. enrolled subjects
R = Num. candidates examined

T = Threshold

T = 0 → Investigation
T > 0 → Identification

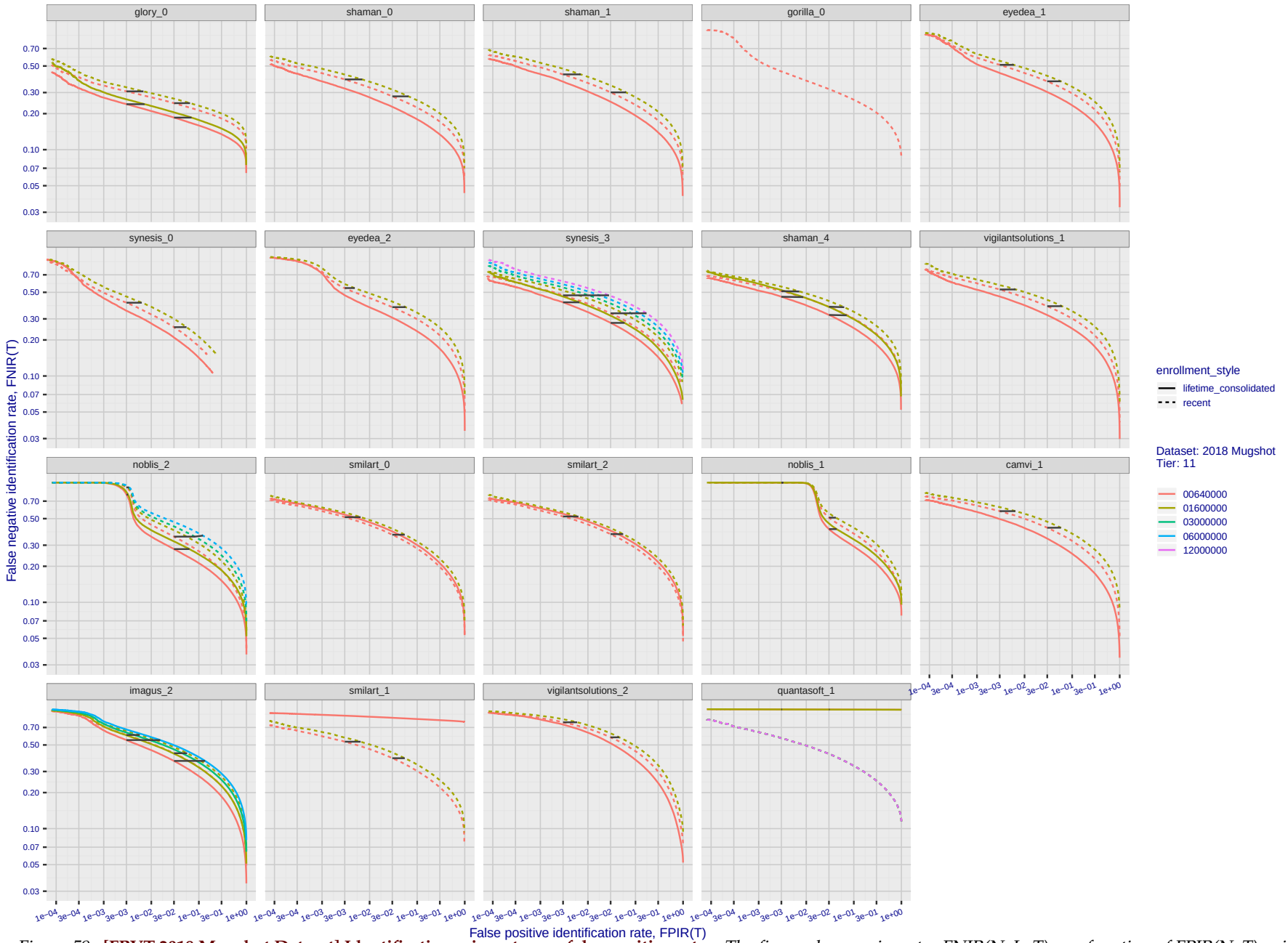

Figure 59: **[FRVT-2018 Mugshot Dataset] Identification miss rates vs. false positive rates**. *The figure shows miss rates FNIR(N, L, T) as a function of FPIR(N, T), with N ranging from 640 000 to 12 000 000 as noted in rows 1-10 of Table 1. These error tradeoff characteristics are useful for applications where a threshold must be elevated to limit false positives, such as when human reviewer labor is not matched to the volume of searches. Dark lines join points of equal threshold: If horizontal, FPIR(T) rises with N, and mate scores are independent of N. Other algorithms adjust scores in an attempt to make FPIR independent of N.*

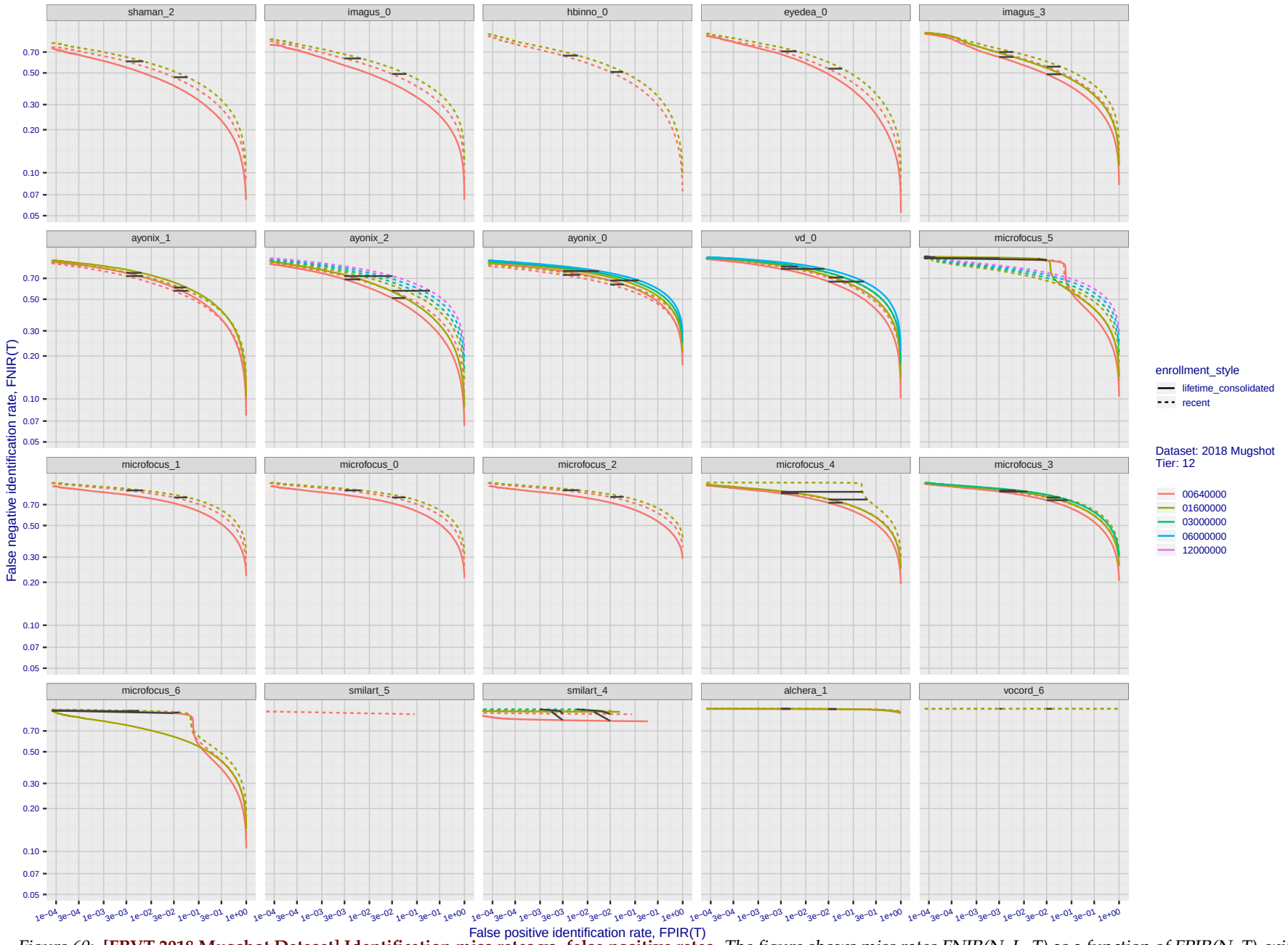

Figure 60: **[FRVT-2018 Mugshot Dataset] Identification miss rates vs. false positive rates**. *The figure shows miss rates FNIR(N, L, T) as a function of FPIR(N, T), with N ranging from 640 000 to 12 000 000 as noted in rows 1-10 of Table 1. These error tradeoff characteristics are useful for applications where a threshold must be elevated to limit false positives, such as when human reviewer labor is not matched to the volume of searches. Dark lines join points of equal threshold: If horizontal, FPIR(T) rises with N, and mate scores are independent of N. Other algorithms adjust scores in an attempt to make FPIR independent of N.*

Appendix B Effect of time-lapse: Accuracy after face ageing

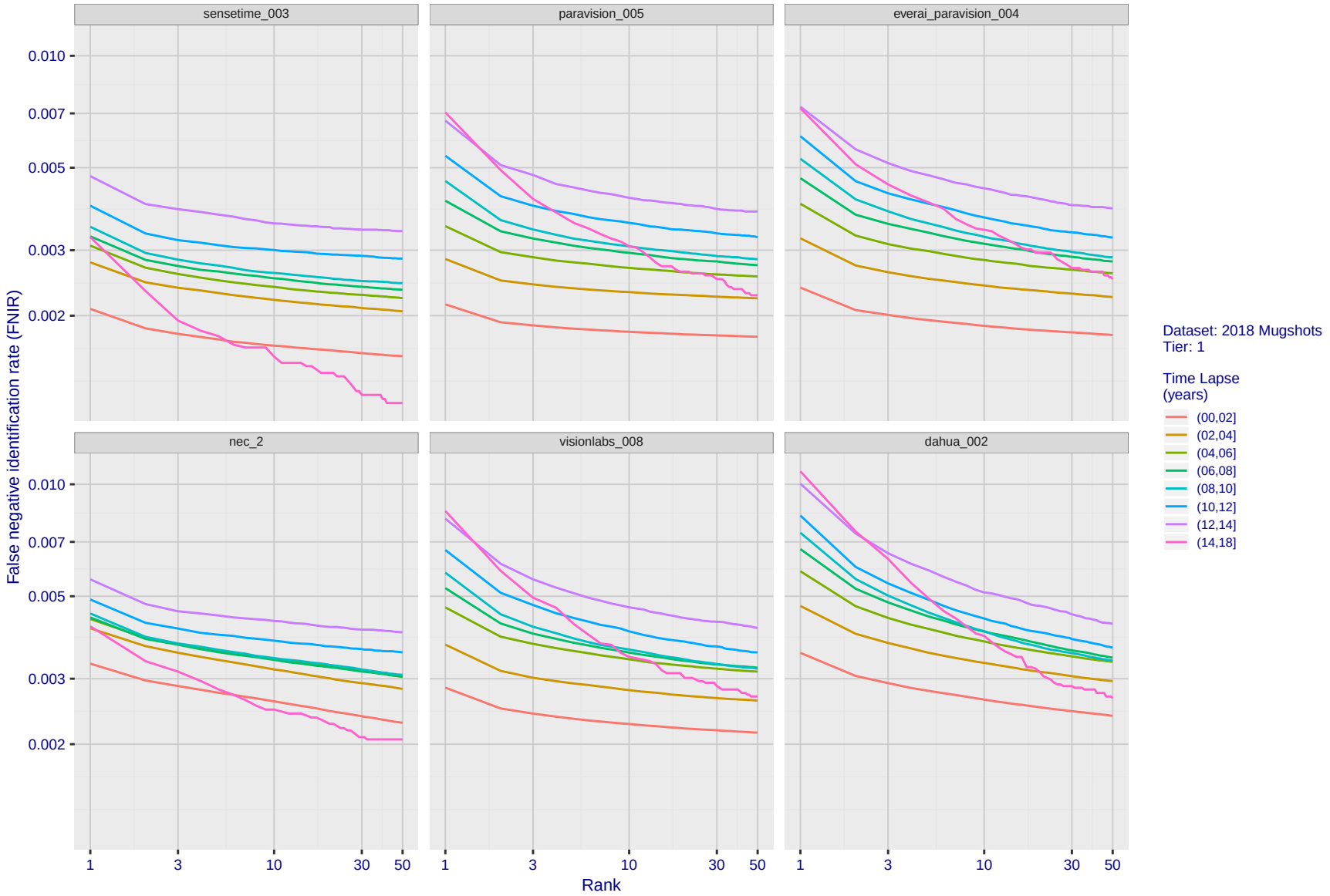

Figure 61: **[FRVT-2018 Mugshot Ageing Dataset] Identification miss rates vs. rank by time-elapsed**. *The oldest image of each individual is enrolled. Thereafter, all more recent images are searched. Miss rates are computed over all searches noted in row 17 of Table 1 and binned by number of years between search and initial enrollment.*

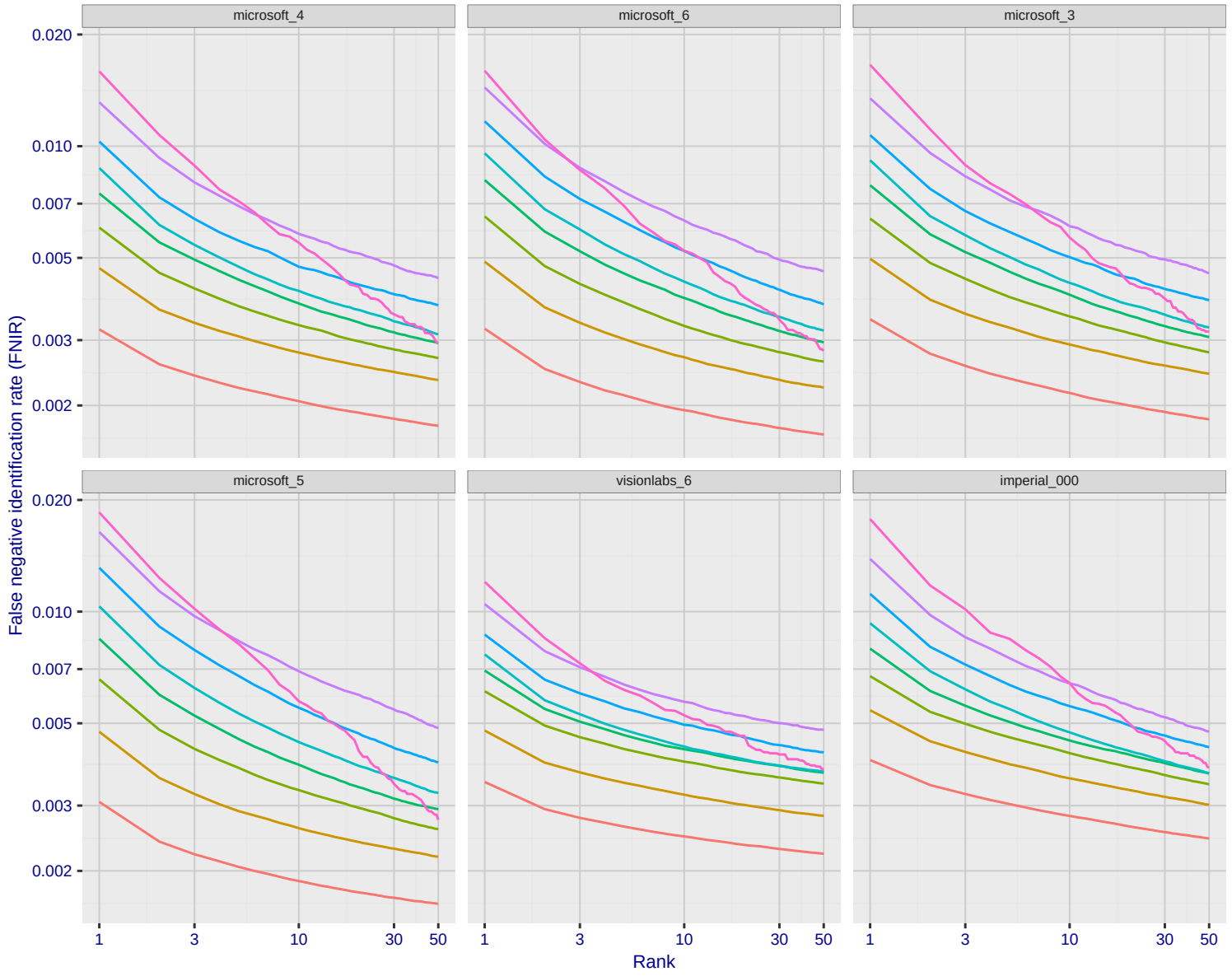

Figure 62: **[FRVT-2018 Mugshot Ageing Dataset] Identification miss rates vs. rank by time-elapsed**. *The oldest image of each individual is enrolled. Thereafter, all more recent images are searched. Miss rates are computed over all searches noted in row 17 of Table 1 and binned by number of years between search and initial enrollment.*

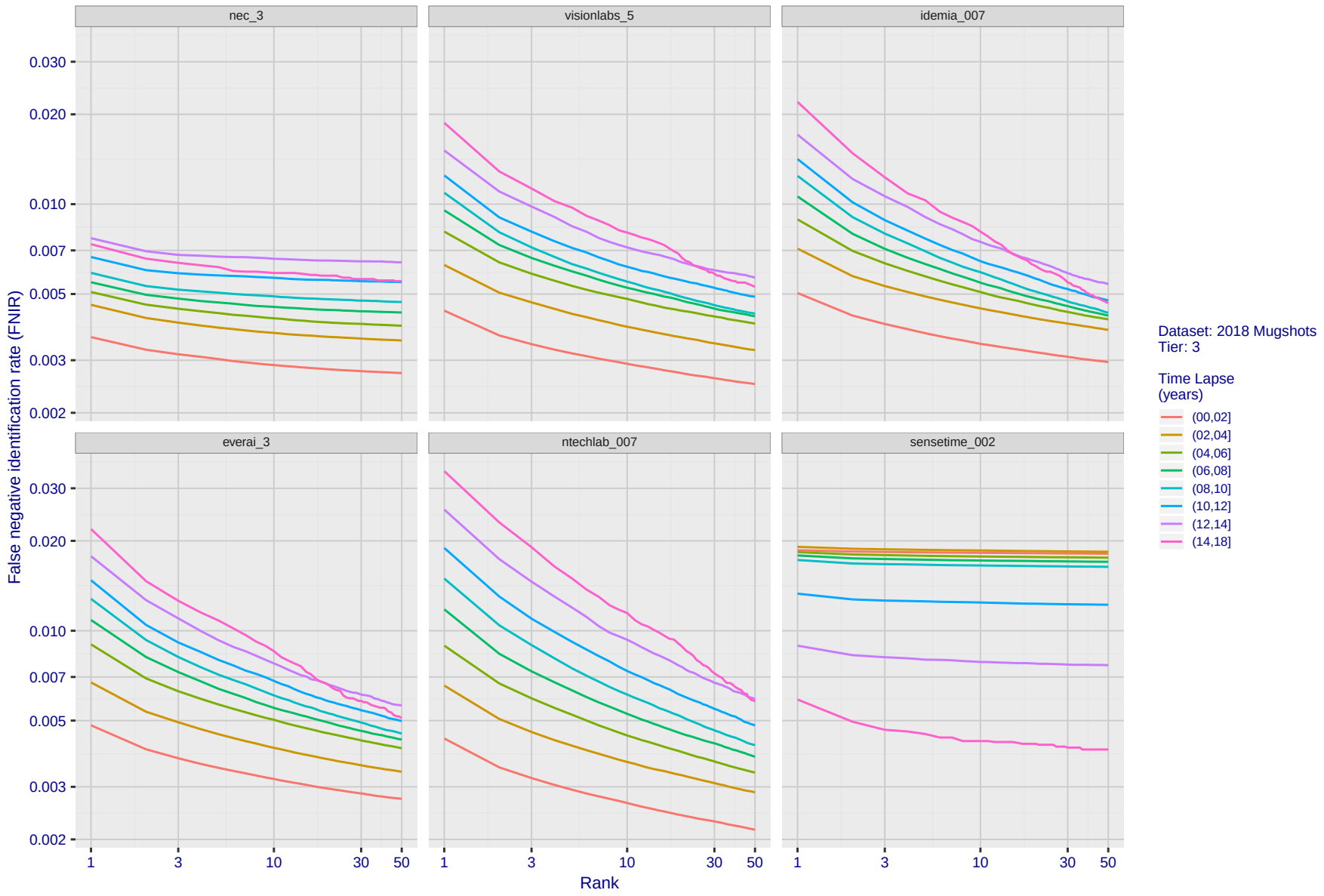

Figure 63: **[FRVT-2018 Mugshot Ageing Dataset] Identification miss rates vs. rank by time-elapsed**. *The oldest image of each individual is enrolled. Thereafter, all more recent images are searched. Miss rates are computed over all searches noted in row 17 of Table 1 and binned by number of years between search and initial enrollment.*

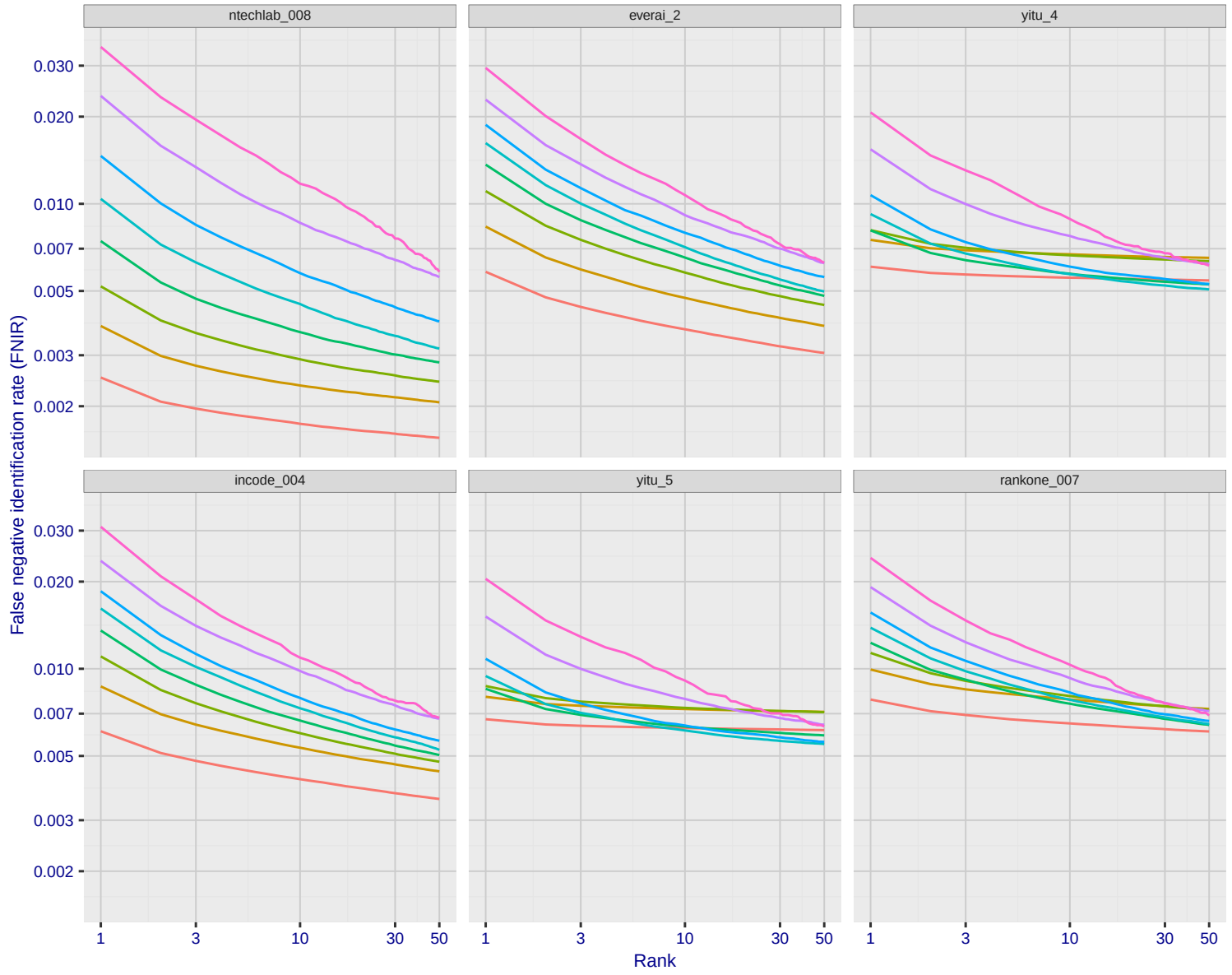

Figure 64: **[FRVT-2018 Mugshot Ageing Dataset] Identification miss rates vs. rank by time-elapsed**. *The oldest image of each individual is enrolled. Thereafter, all more recent images are searched. Miss rates are computed over all searches noted in row 17 of Table 1 and binned by number of years between search and initial enrollment.*

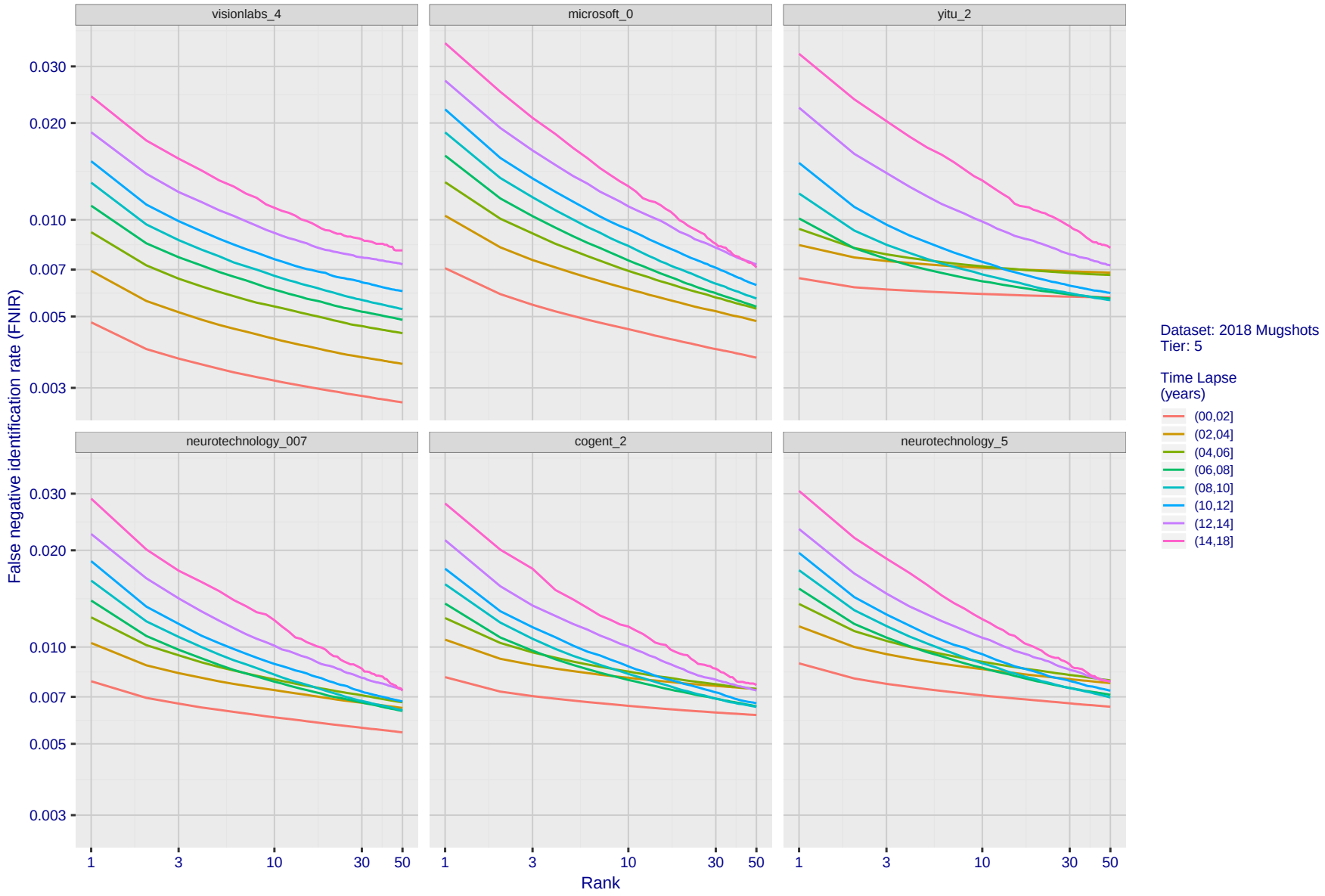

Figure 65: **[FRVT-2018 Mugshot Ageing Dataset] Identification miss rates vs. rank by time-elapsed**. *The oldest image of each individual is enrolled. Thereafter, all more recent images are searched. Miss rates are computed over all searches noted in row 17 of Table 1 and binned by number of years between search and initial enrollment.*

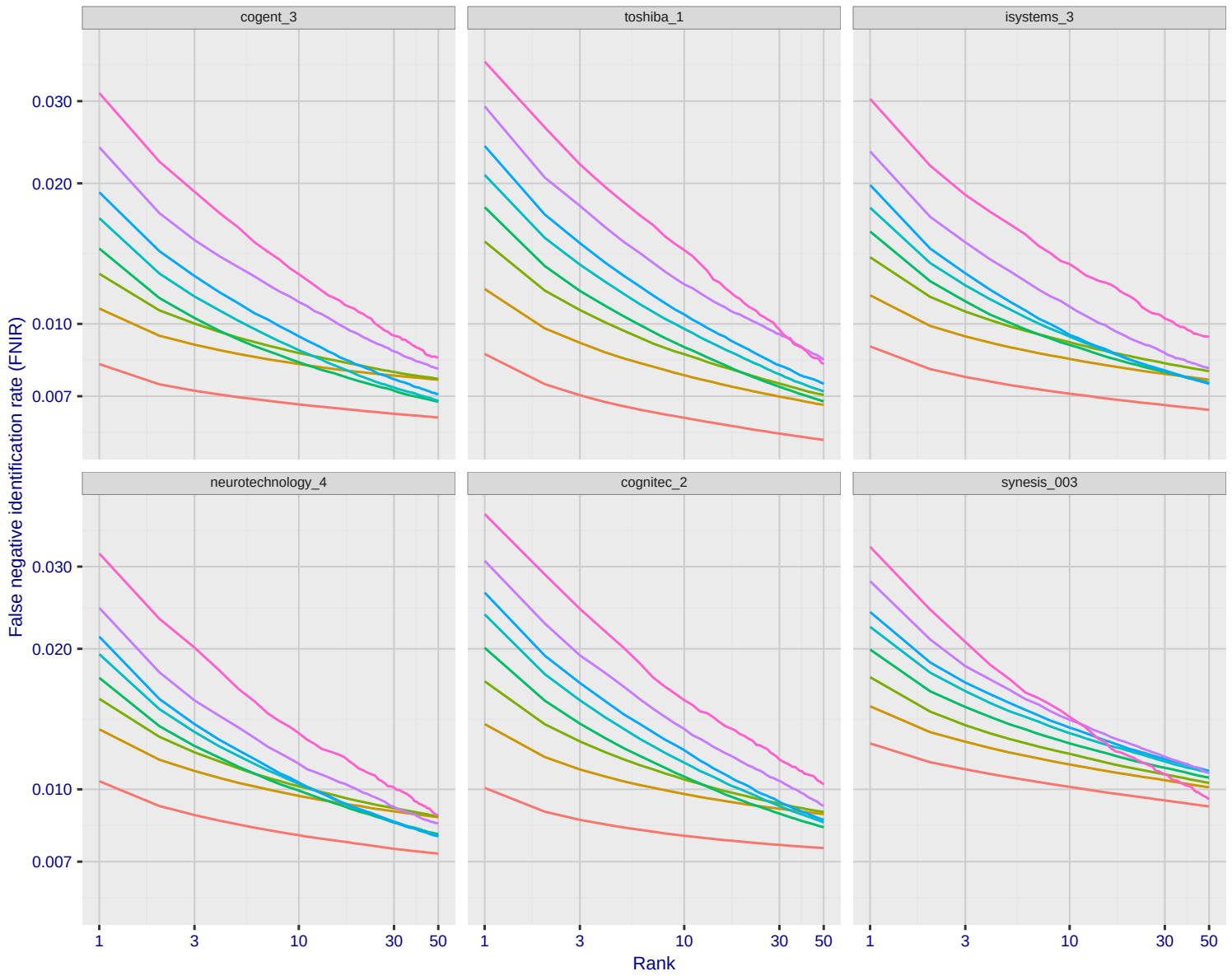

Figure 66: **[FRVT-2018 Mugshot Ageing Dataset] Identification miss rates vs. rank by time-elapsed**. *The oldest image of each individual is enrolled. Thereafter, all more recent images are searched. Miss rates are computed over all searches noted in row 17 of Table 1 and binned by number of years between search and initial enrollment.*

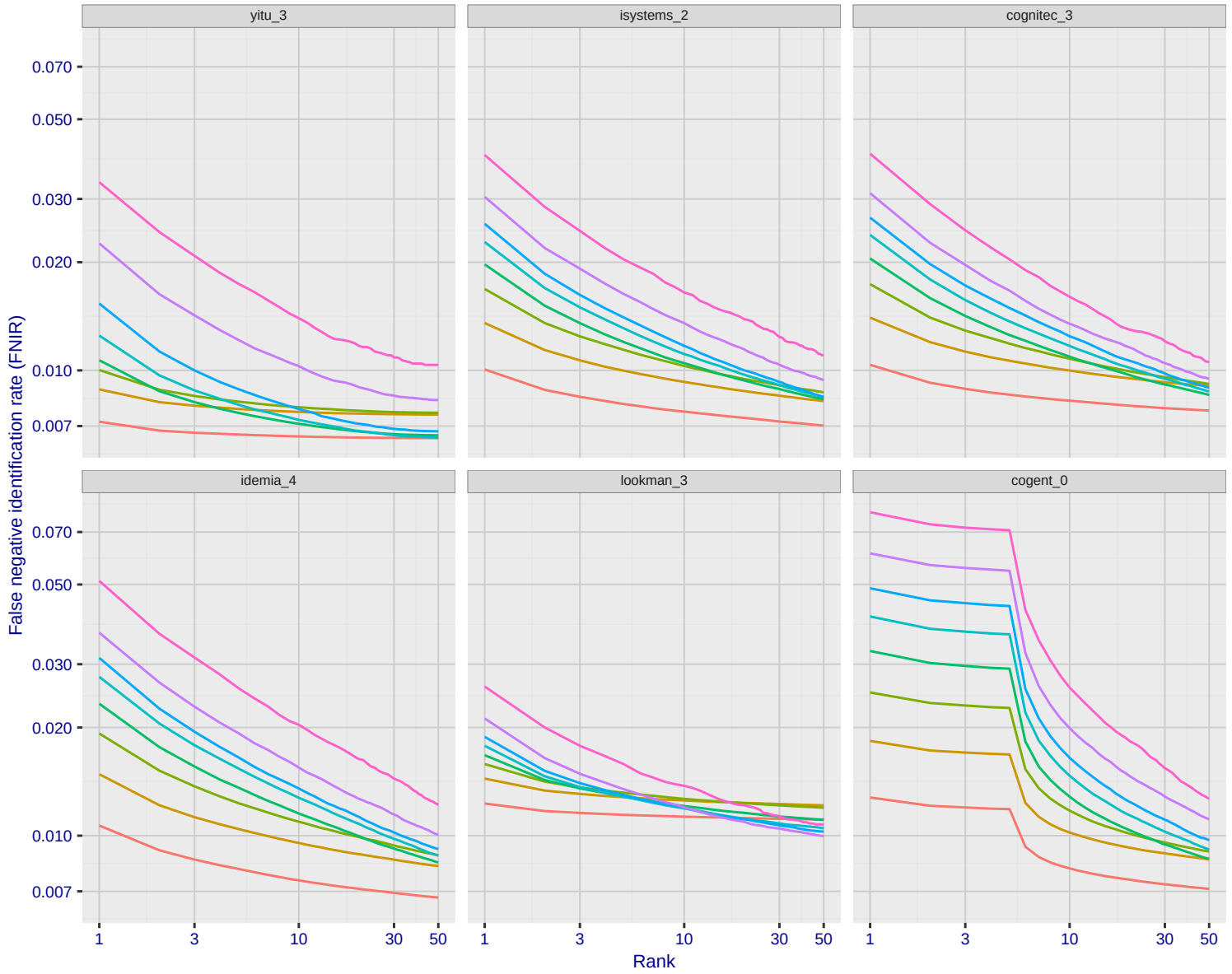

Figure 67: **[FRVT-2018 Mugshot Ageing Dataset] Identification miss rates vs. rank by time-elapsed**. *The oldest image of each individual is enrolled. Thereafter, all more recent images are searched. Miss rates are computed over all searches noted in row 17 of Table 1 and binned by number of years between search and initial enrollment.*

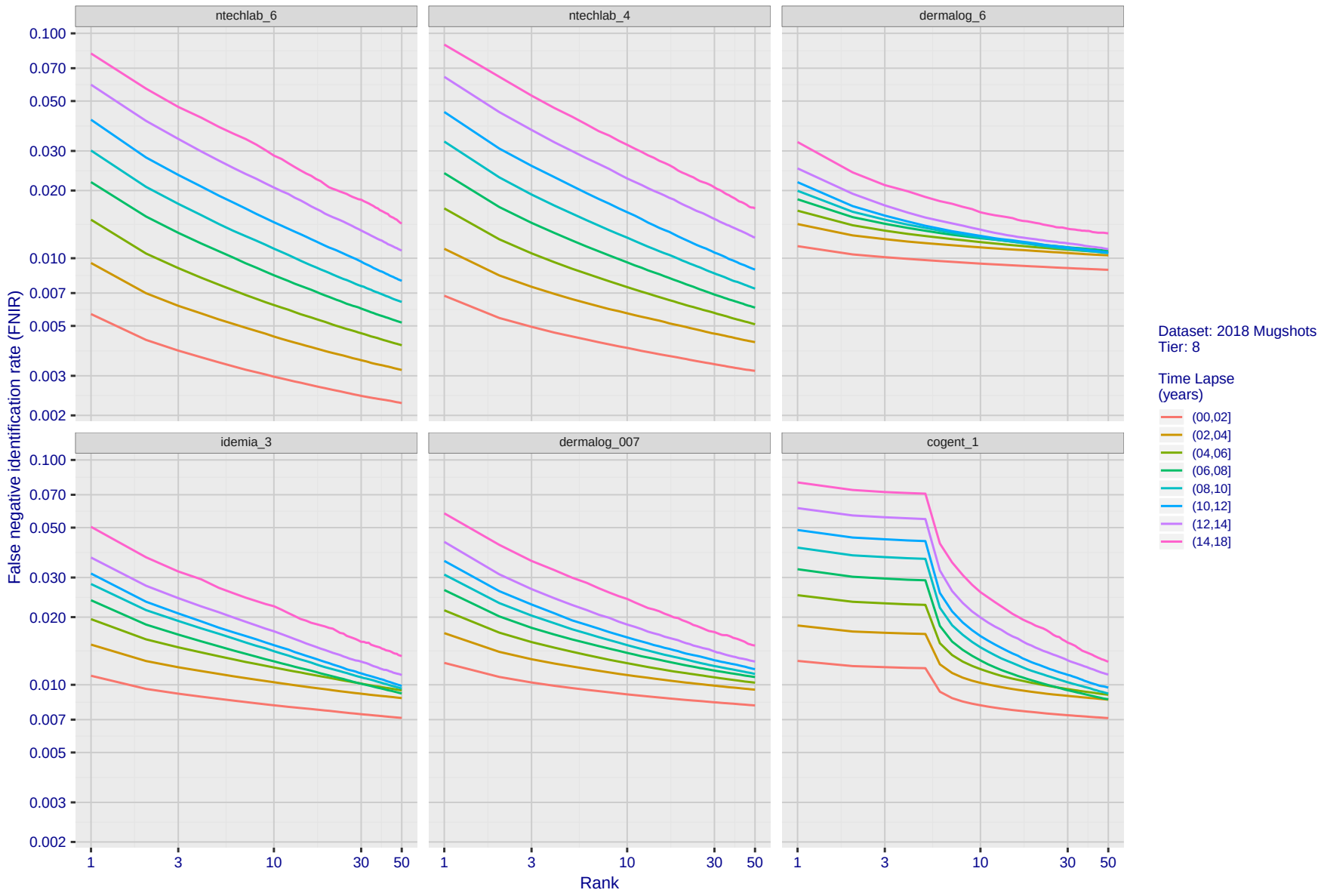

Figure 68: **[FRVT-2018 Mugshot Ageing Dataset] Identification miss rates vs. rank by time-elapsed**. *The oldest image of each individual is enrolled. Thereafter, all more recent images are searched. Miss rates are computed over all searches noted in row 17 of Table 1 and binned by number of years between search and initial enrollment.*

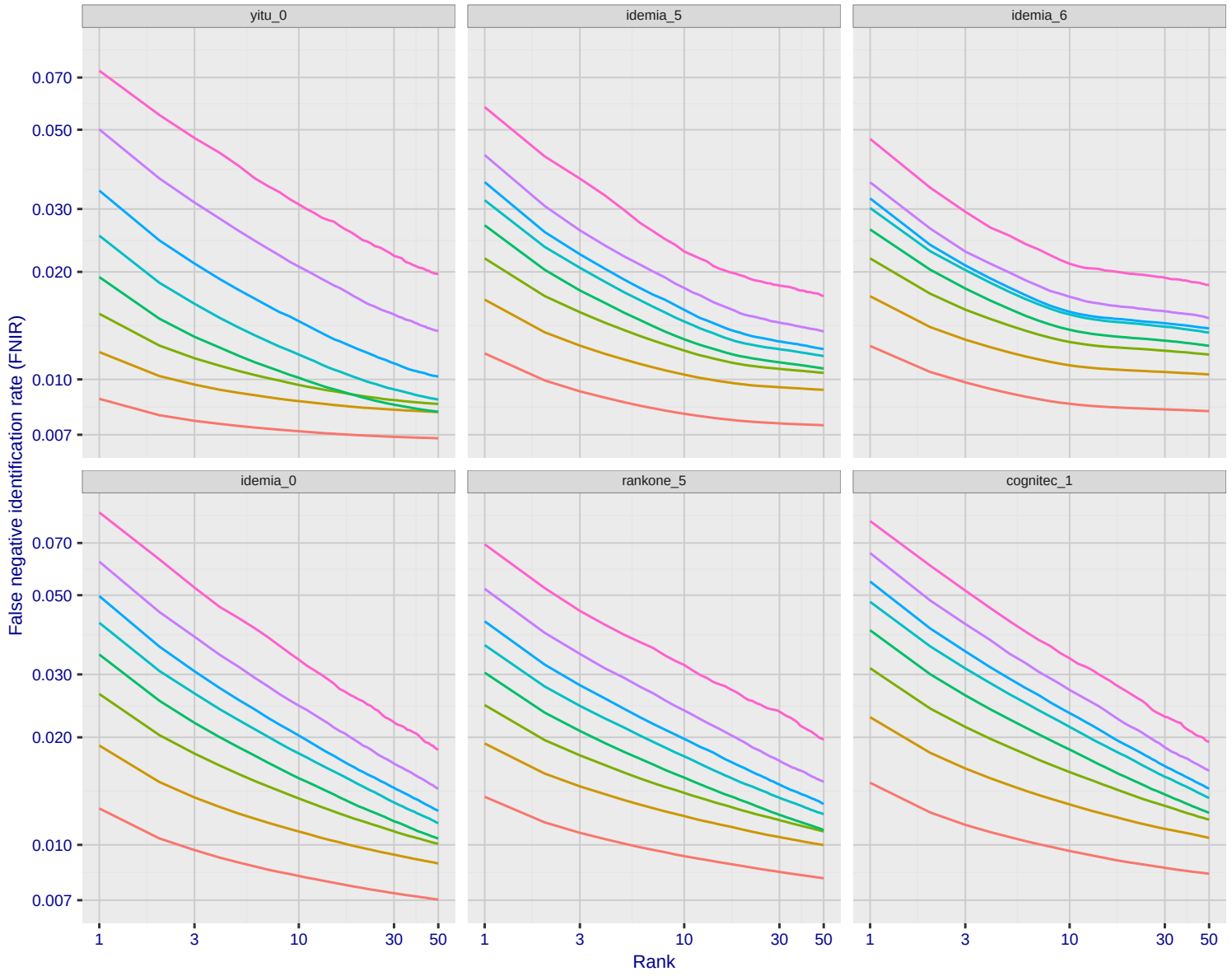

Figure 69: **[FRVT-2018 Mugshot Ageing Dataset] Identification miss rates vs. rank by time-elapsed**. *The oldest image of each individual is enrolled. Thereafter, all more recent images are searched. Miss rates are computed over all searches noted in row 17 of Table 1 and binned by number of years between search and initial enrollment.*

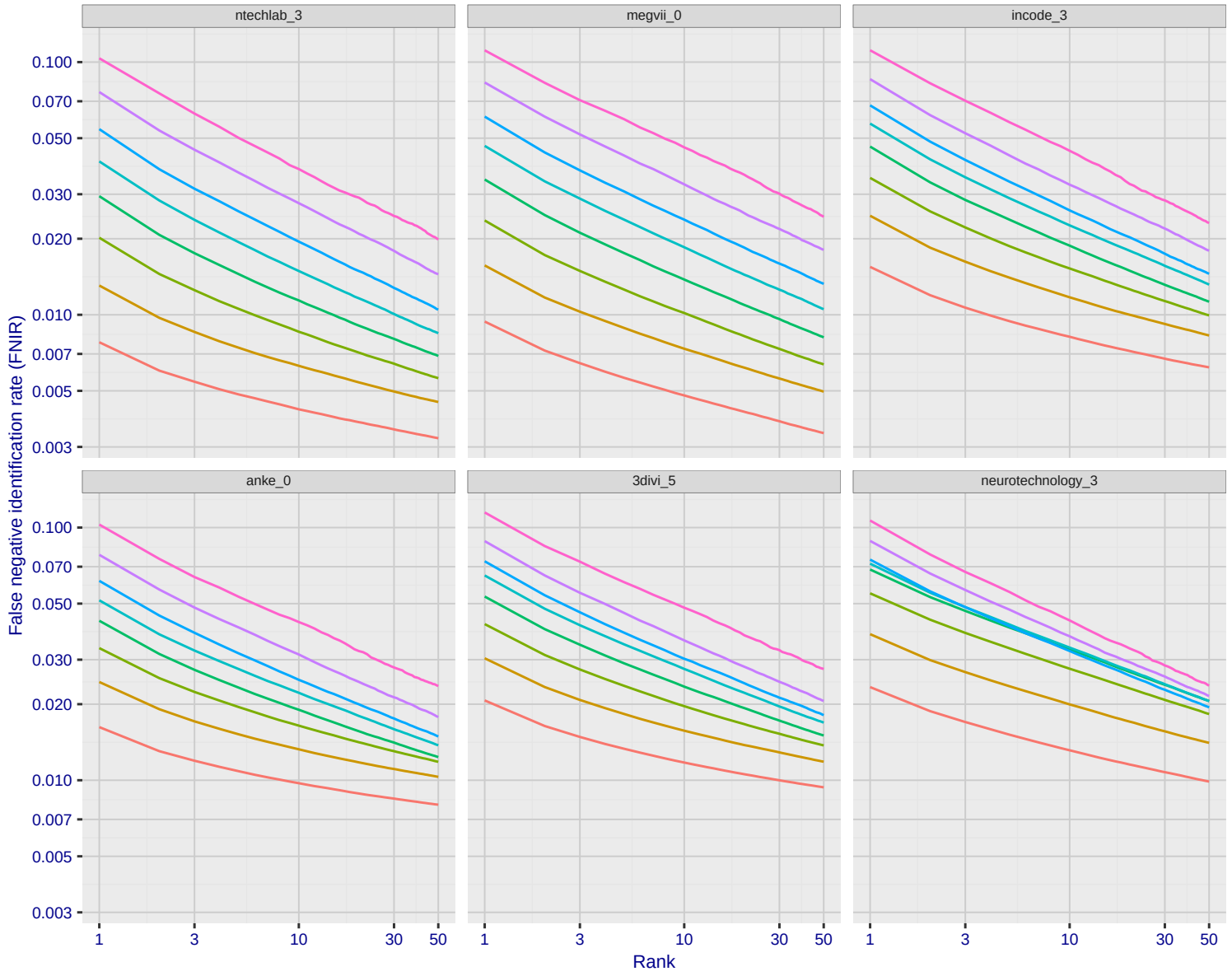

Figure 70: **[FRVT-2018 Mugshot Ageing Dataset] Identification miss rates vs. rank by time-elapsed**. *The oldest image of each individual is enrolled. Thereafter, all more recent images are searched. Miss rates are computed over all searches noted in row 17 of Table 1 and binned by number of years between search and initial enrollment.*

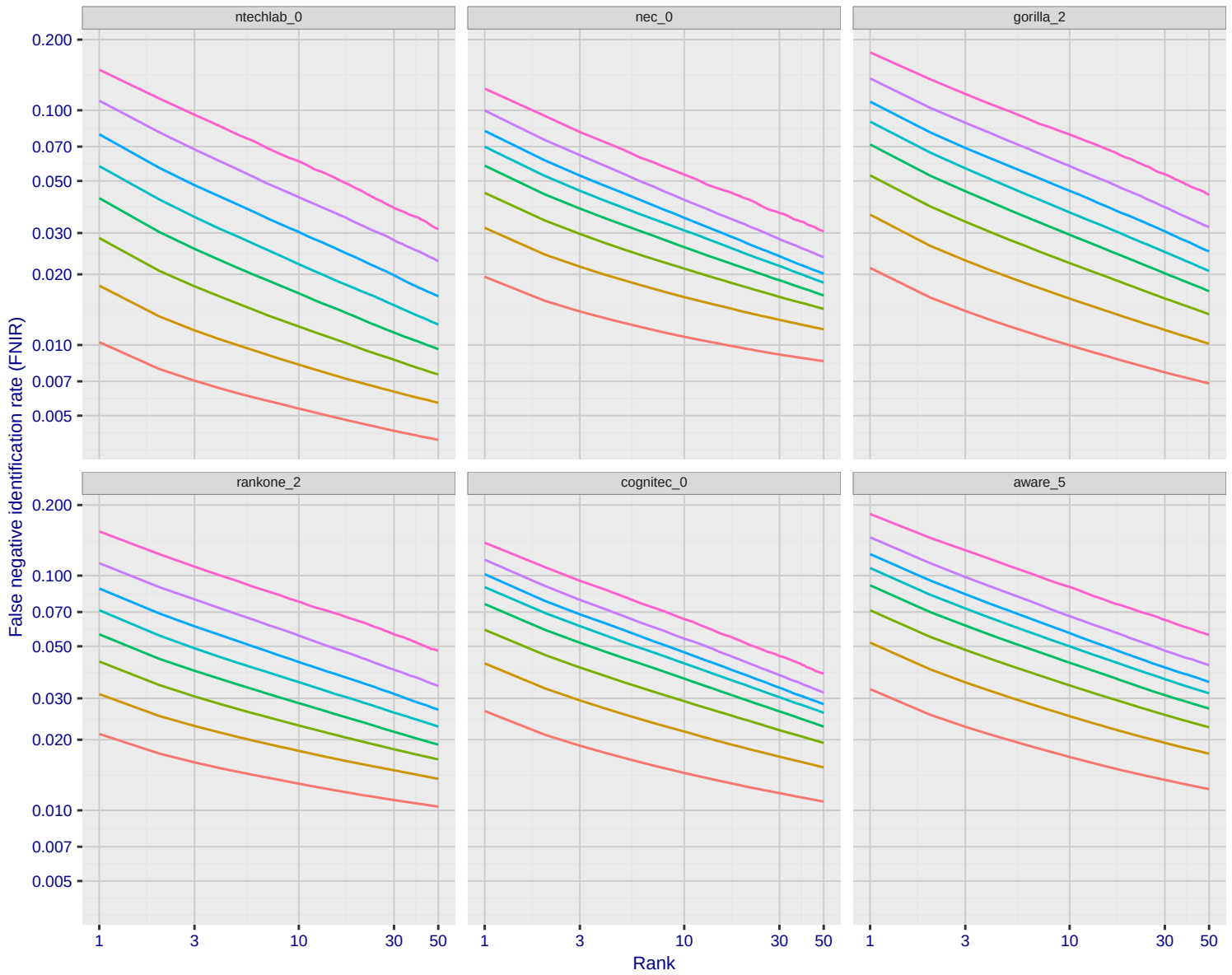

Figure 71: **[FRVT-2018 Mugshot Ageing Dataset] Identification miss rates vs. rank by time-elapsed**. *The oldest image of each individual is enrolled. Thereafter, all more recent images are searched. Miss rates are computed over all searches noted in row 17 of Table 1 and binned by number of years between search and initial enrollment.*

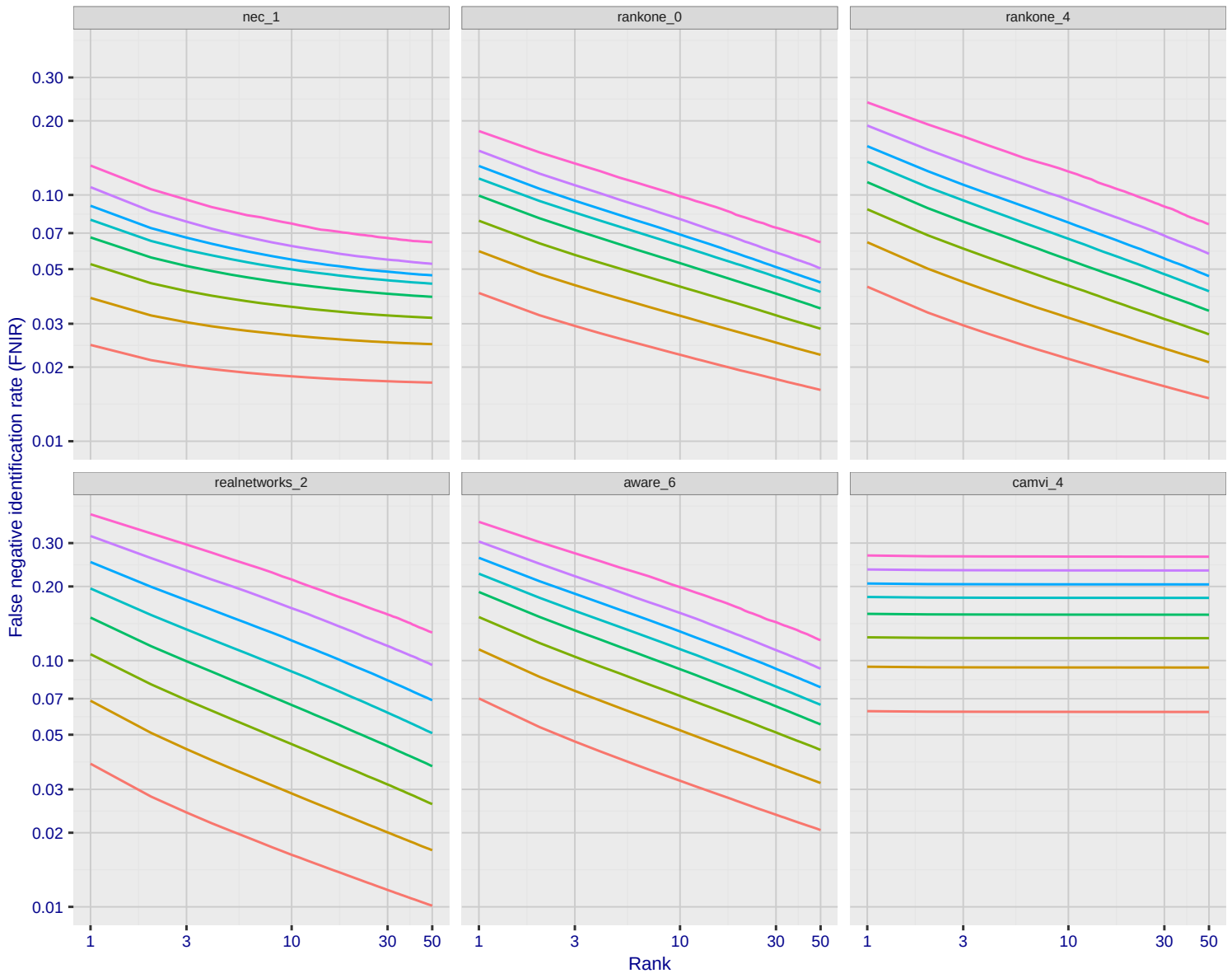

Figure 72: **[FRVT-2018 Mugshot Ageing Dataset] Identification miss rates vs. rank by time-elapsed**. *The oldest image of each individual is enrolled. Thereafter, all more recent images are searched. Miss rates are computed over all searches noted in row 17 of Table 1 and binned by number of years between search and initial enrollment.*

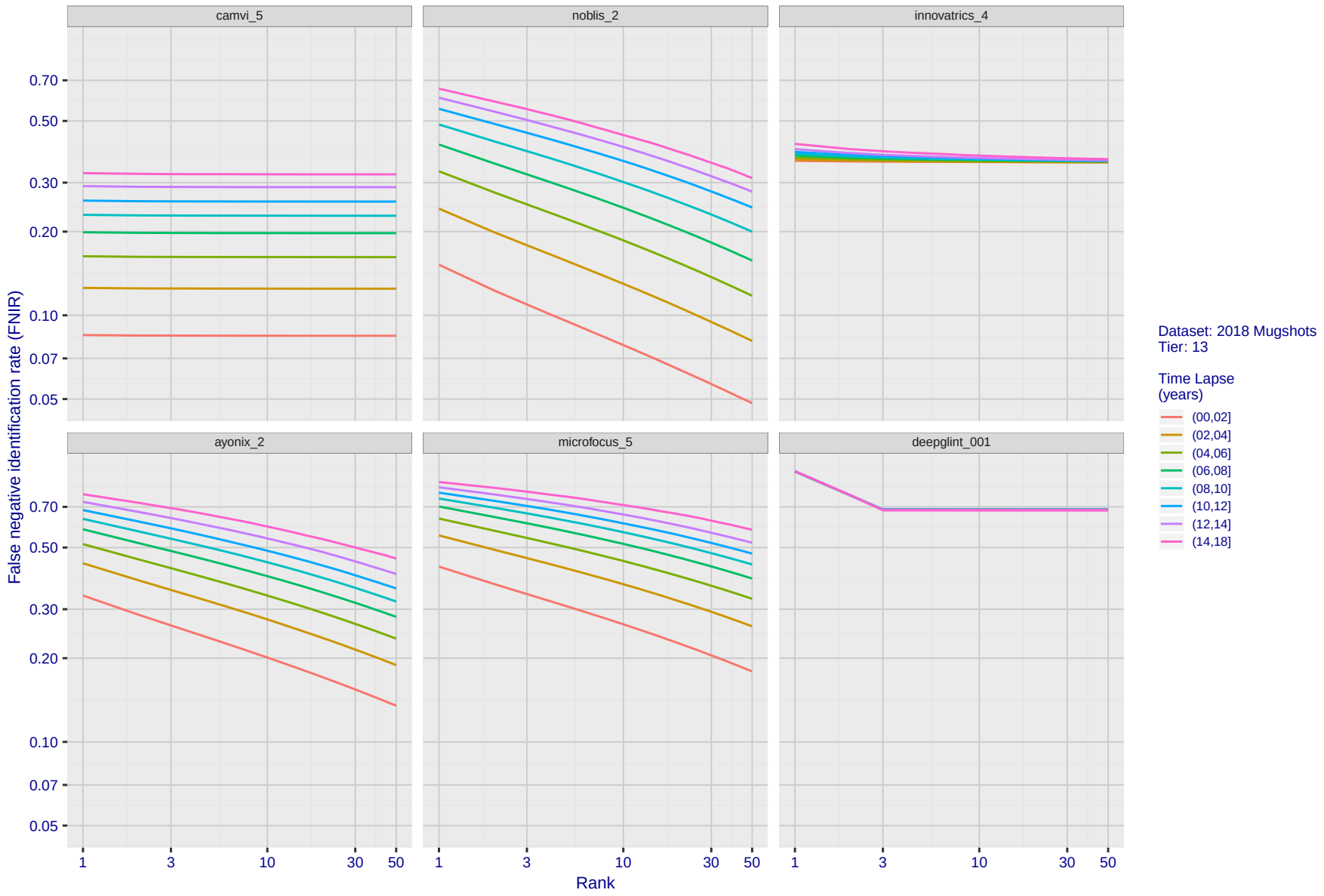

Figure 73: **[FRVT-2018 Mugshot Ageing Dataset] Identification miss rates vs. rank by time-elapsed**. *The oldest image of each individual is enrolled. Thereafter, all more recent images are searched. Miss rates are computed over all searches noted in row 17 of Table 1 and binned by number of years between search and initial enrollment.*

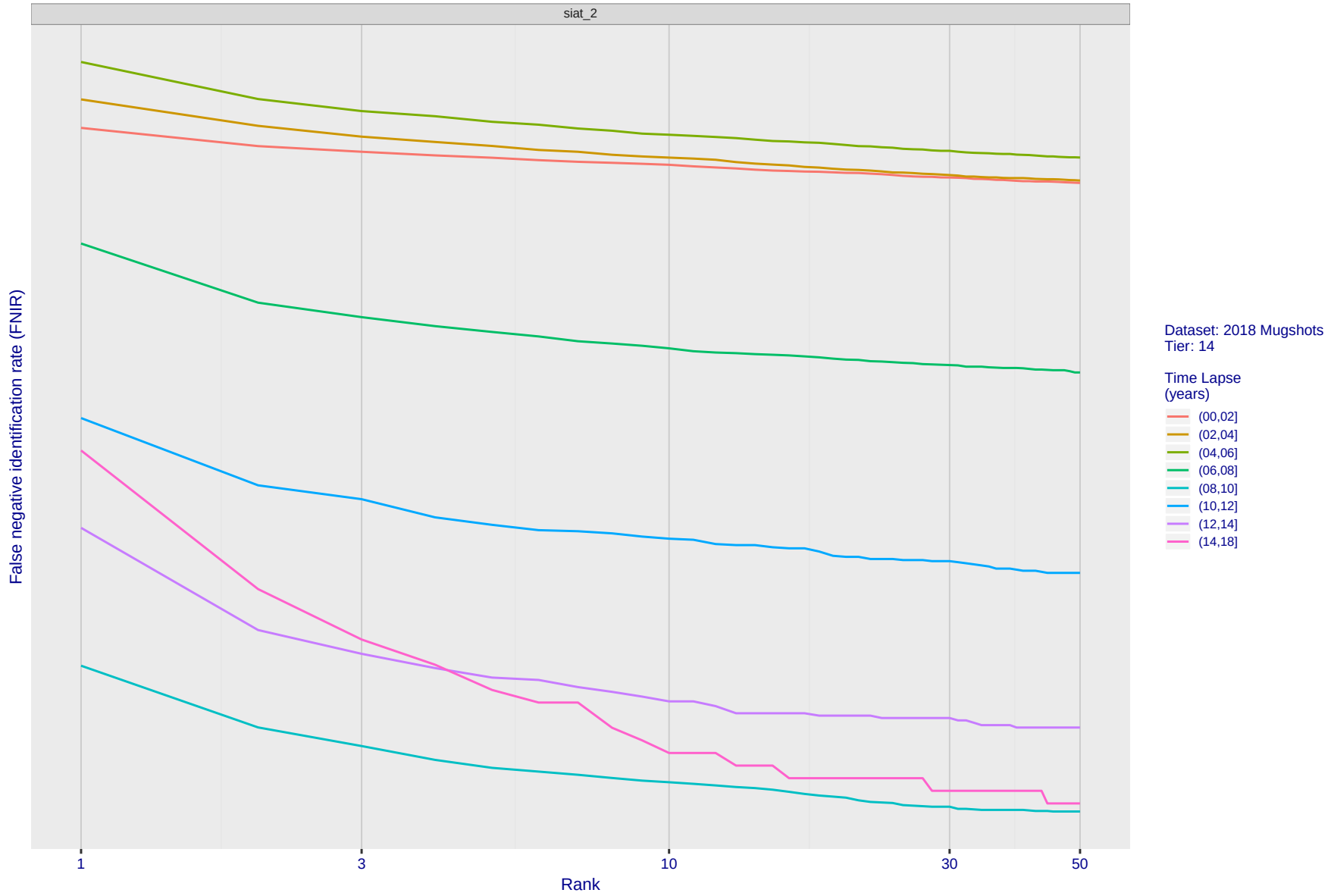

Figure 74: **[FRVT-2018 Mugshot Ageing Dataset] Identification miss rates vs. rank by time-elapsed**. *The oldest image of each individual is enrolled. Thereafter, all more recent images are searched. Miss rates are computed over all searches noted in row 17 of Table 1 and binned by number of years between search and initial enrollment.*

2020/03/27	FNIR(N, R, T) =	False neg. identification rate	N = Num. enrolled subjects	T = Threshold	$T = 0 \rightarrow$ Investigation
10:40:09	FPIR(N, T) =	False pos. identification rate	R = Num. candidates examined		$T > 0 \rightarrow$ Identification

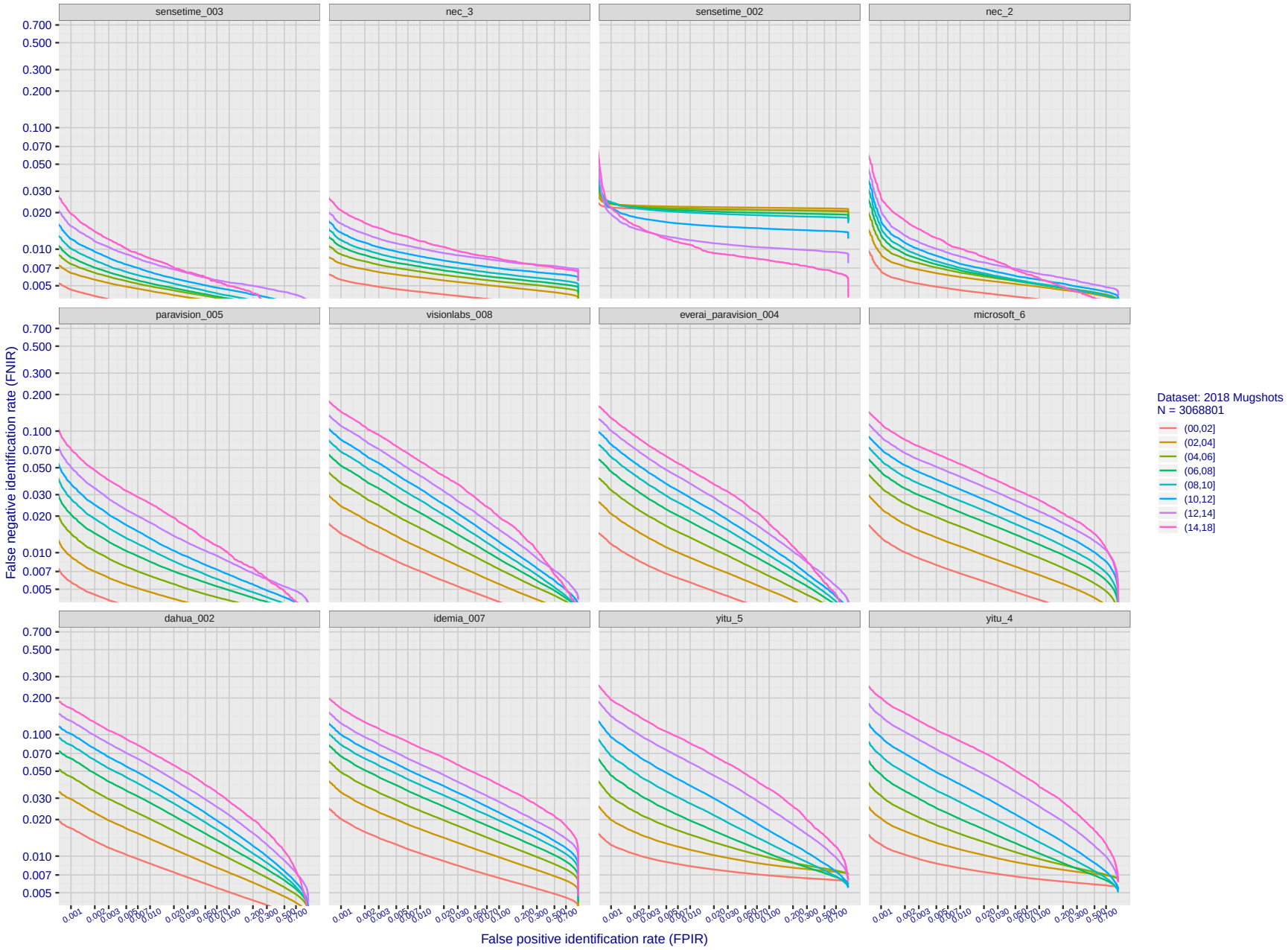

Figure 75: **[FRVT-2018 Mugshot Ageing Dataset] Identification miss rates vs. FPIR by time-elapsed**. *The oldest image of each individual is enrolled. Thereafter, all more recent images are searched. Miss rates are computed over all searches noted in row 17 of Table 1 and binned by number of years between search and initial enrollment. FPIR is computed from the same FRVT 2018 non-mates noted in row 3 of Table 1 with N = 3 000 000.*

2020/03/27 10:40:09

FNIR(N, R, T) = False neg. identification rate
FPIR(N, T) = False pos. identification rate

N = Num. enrolled subjects
R = Num. candidates examined

T = Threshold

T = 0 → Investigation
T > 0 → Identification

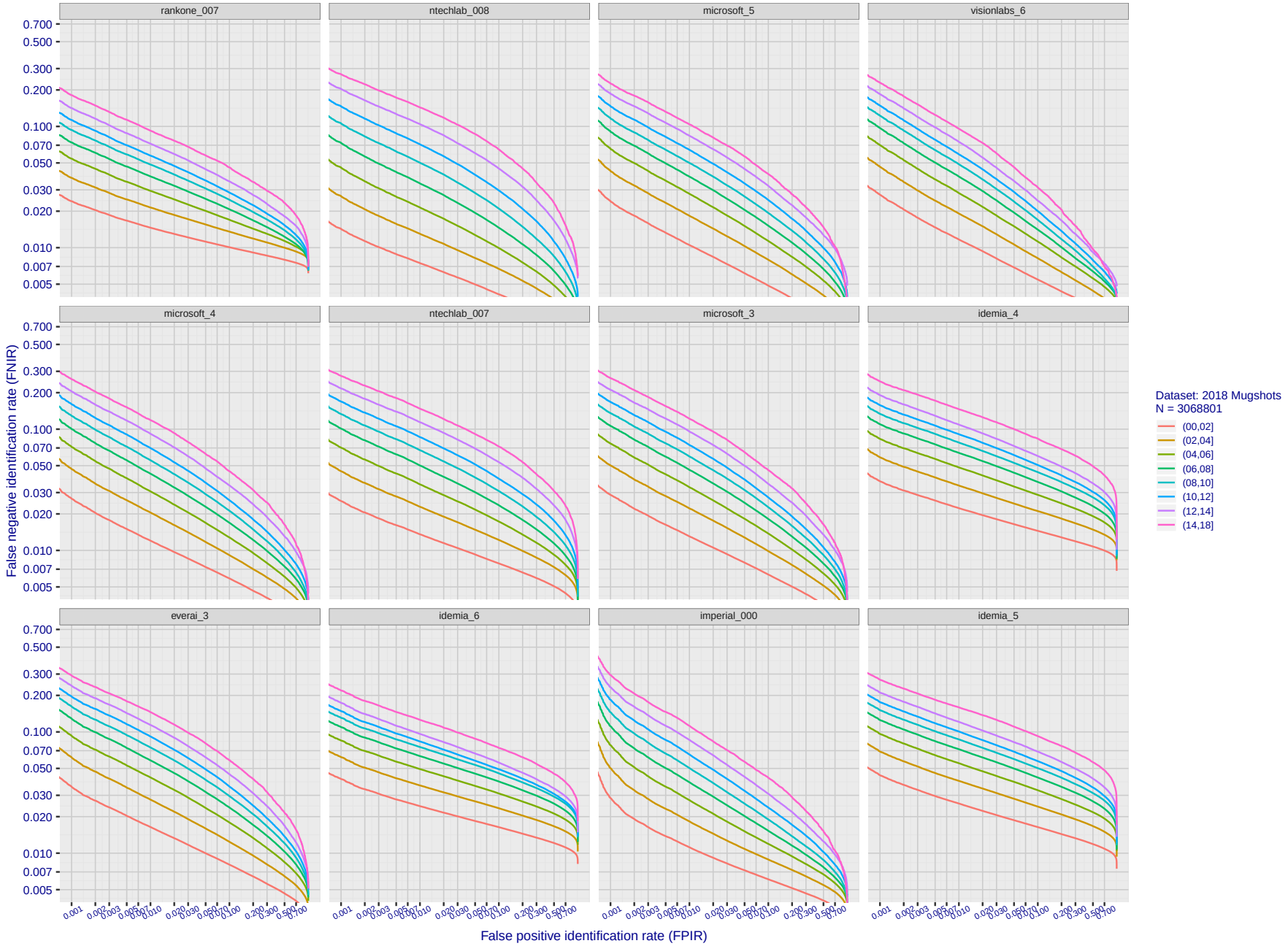

Figure 76: **[FRVT-2018 Mugshot Ageing Dataset] Identification miss rates vs. FPIR by time-elapsed**. *The oldest image of each individual is enrolled. Thereafter, all more recent images are searched. Miss rates are computed over all searches noted in row 17 of Table 1 and binned by number of years between search and initial enrollment. FPIR is computed from the same FRVT 2018 non-mates noted in row 3 of Table 1 with N = 3 000 000.*

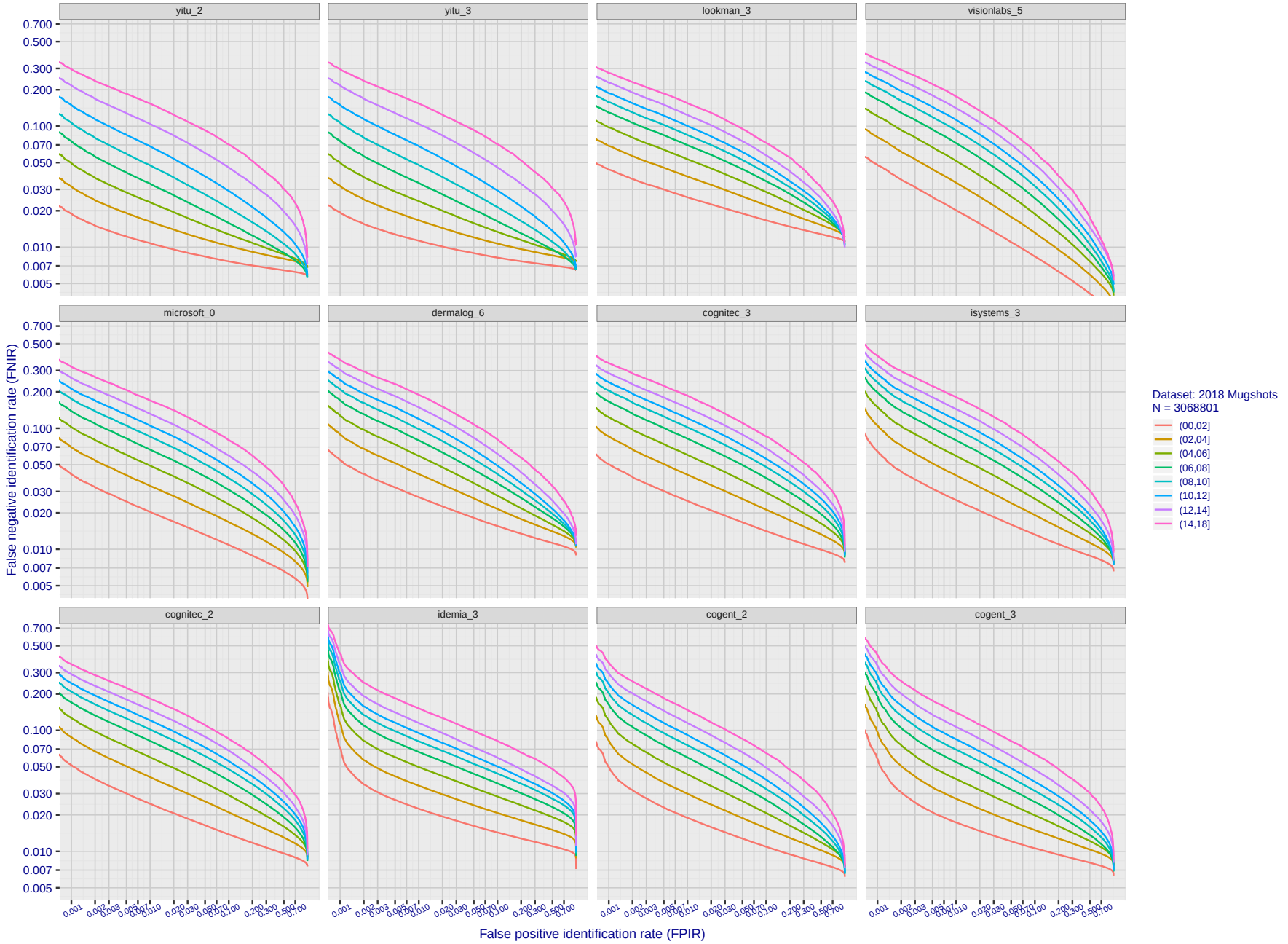

Figure 77: **[FRVT-2018 Mugshot Ageing Dataset] Identification miss rates vs. FPIR by time-elapsed**. *The oldest image of each individual is enrolled. Thereafter, all more recent images are searched. Miss rates are computed over all searches noted in row 17 of Table 1 and binned by number of years between search and initial enrollment. FPIR is computed from the same FRVT 2018 non-mates noted in row 3 of Table 1 with N = 3 000 000.*

2020/03/27 10:40:09

FNIR(N, R, T) = False neg. identification rate
FPIR(N, T) = False pos. identification rate

N = Num. enrolled subjects
R = Num. candidates examined

T = Threshold

T = 0 → Investigation
T > 0 → Identification

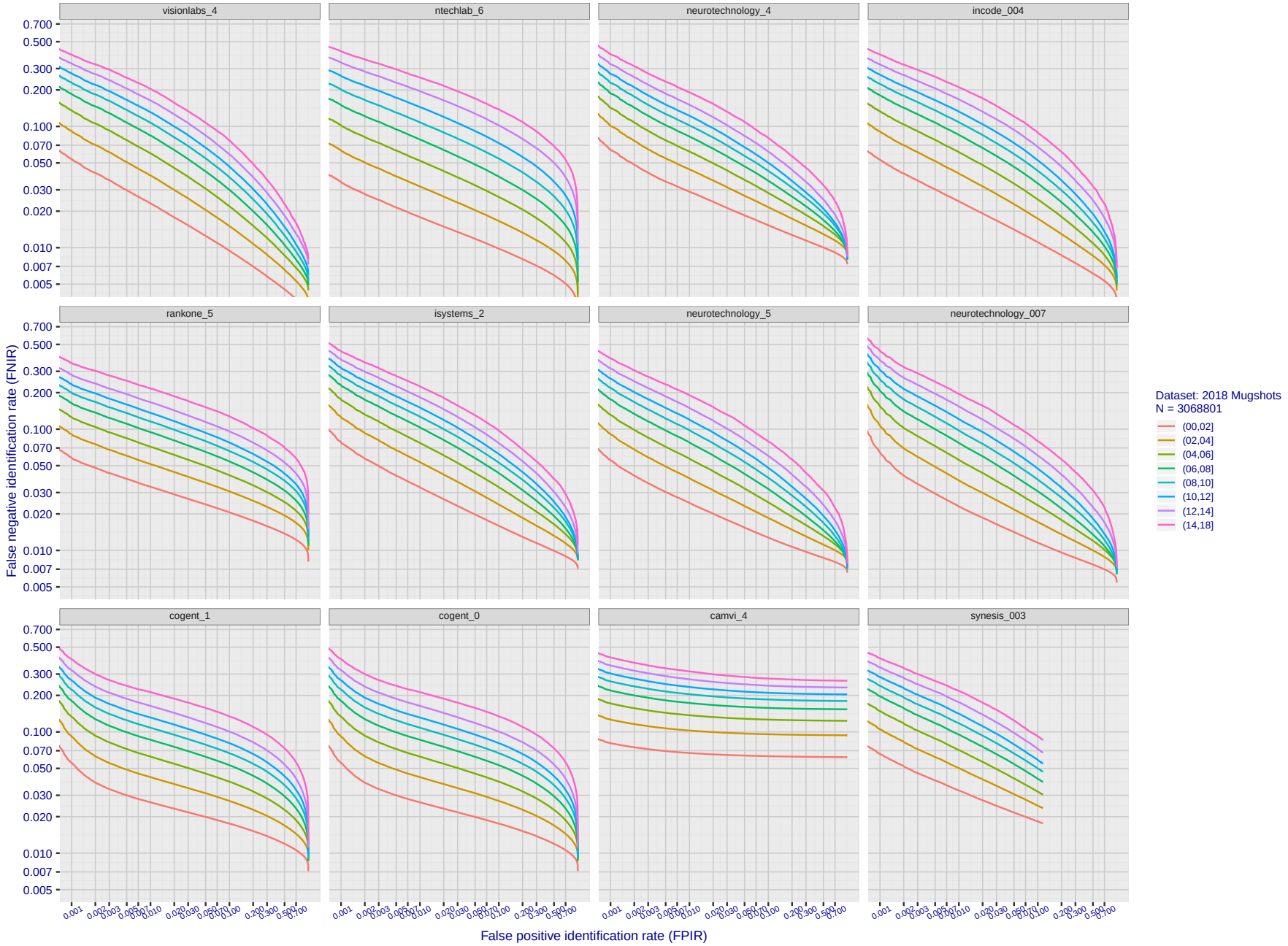

Figure 78: **[FRVT-2018 Mugshot Ageing Dataset] Identification miss rates vs. FPIR by time-elapsed**. *The oldest image of each individual is enrolled. Thereafter, all more recent images are searched. Miss rates are computed over all searches noted in row 17 of Table 1 and binned by number of years between search and initial enrollment. FPIR is computed from the same FRVT 2018 non-mates noted in row 3 of Table 1 with N = 3 000 000.*

2020/03/27
10:40:09
FNIR(N, R, T) = False neg. identification rate
FPIR(N, T) = False pos. identification rate
N = Num. enrolled subjects
R = Num. candidates examined
T = Threshold
T = 0 → Investigation
T > 0 → Identification

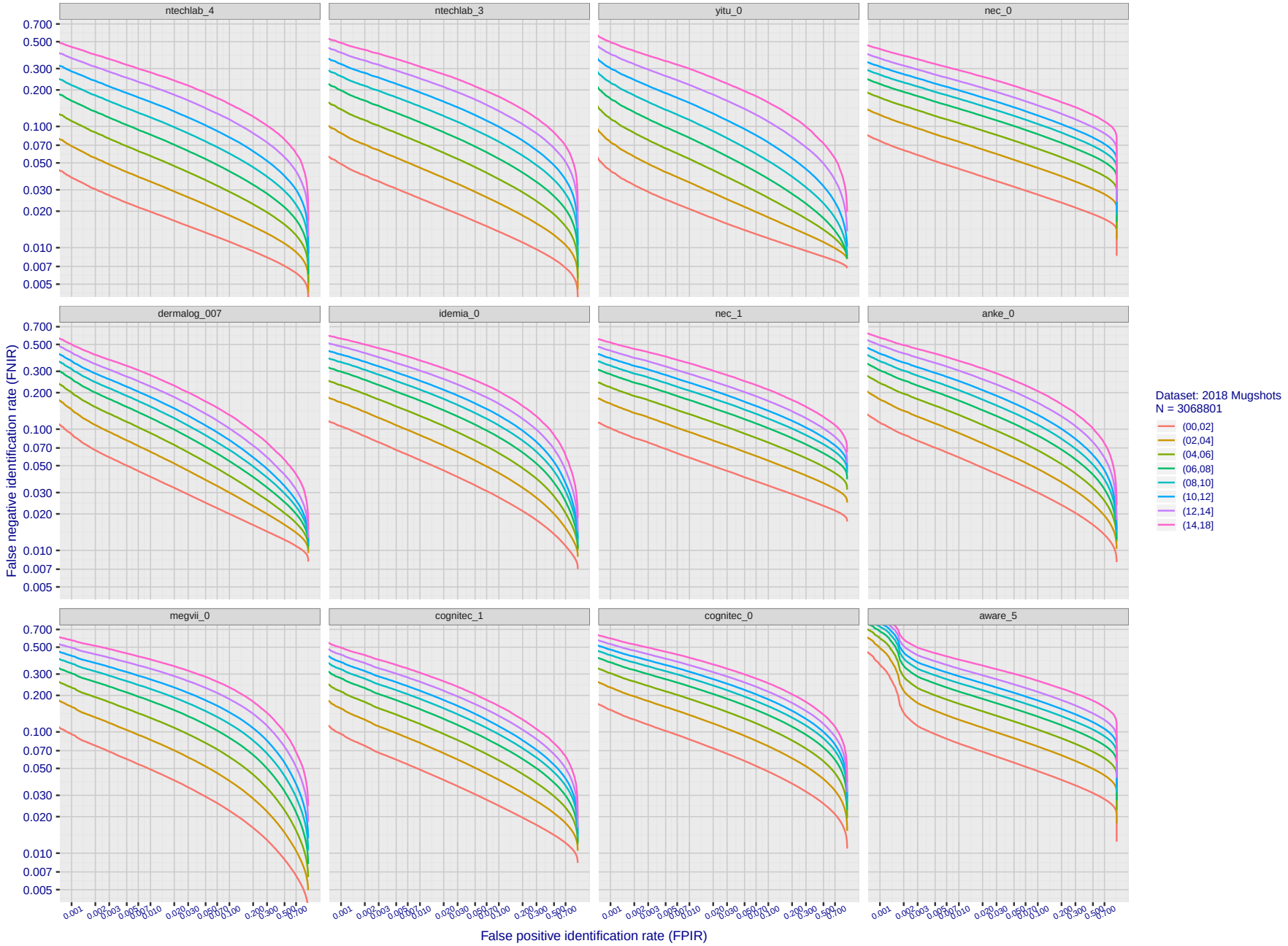

Figure 79: **[FRVT-2018 Mugshot Ageing Dataset] Identification miss rates vs. FPIR by time-elapsed**. *The oldest image of each individual is enrolled. Thereafter, all more recent images are searched. Miss rates are computed over all searches noted in row 17 of Table 1 and binned by number of years between search and initial enrollment. FPIR is computed from the same FRVT 2018 non-mates noted in row 3 of Table 1 with N = 3 000 000.*

2020/03/27
10:40:09
FNIR(N, R, T) = False neg. identification rate
FPIR(N, T) = False pos. identification rate
N = Num. enrolled subjects
R = Num. candidates examined
T = Threshold
T = 0 → Investigation
T > 0 → Identification

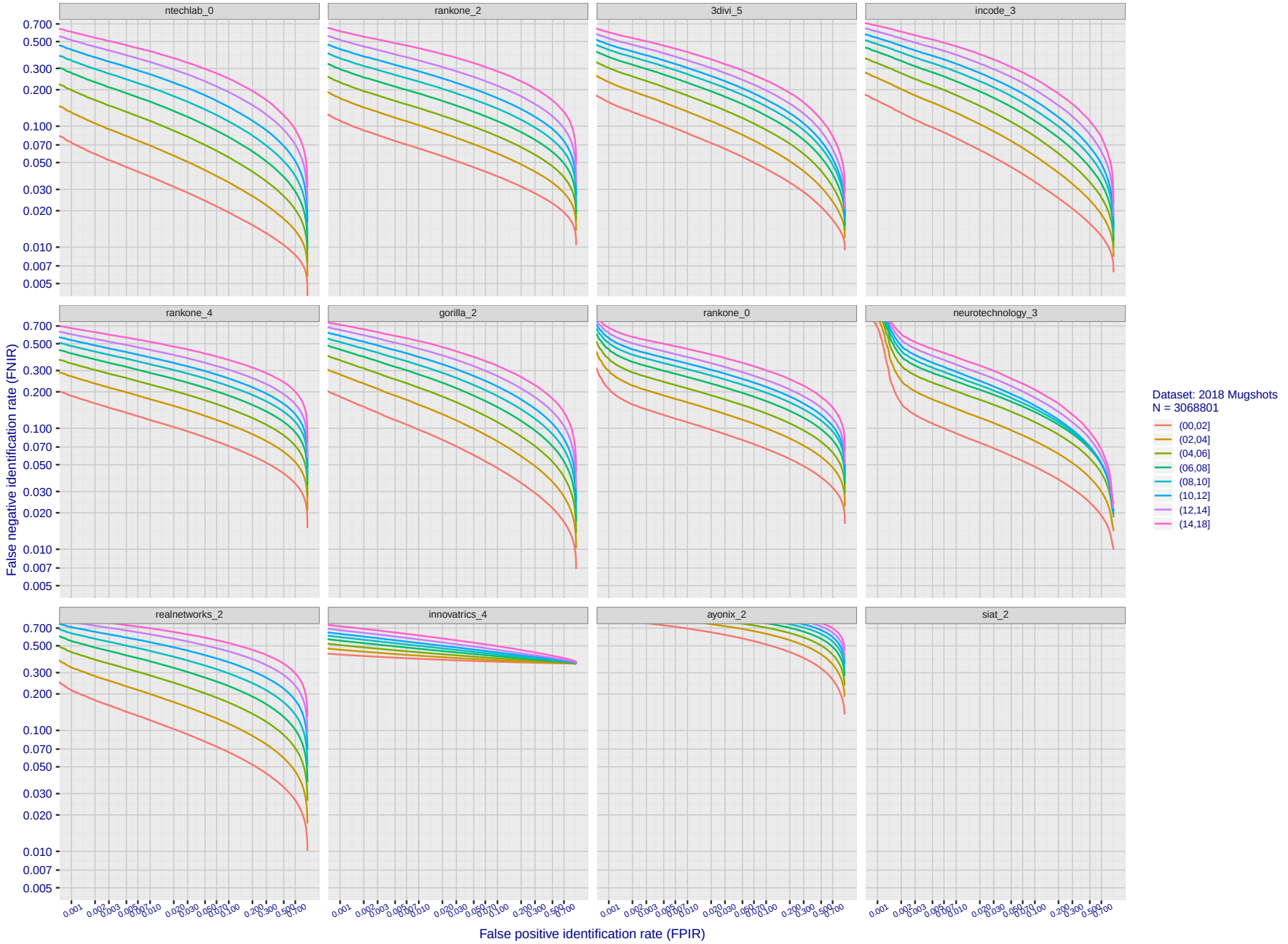

Figure 80: **[FRVT-2018 Mugshot Ageing Dataset] Identification miss rates vs. FPIR by time-elapsed**. *The oldest image of each individual is enrolled. Thereafter, all more recent images are searched. Miss rates are computed over all searches noted in row 17 of Table 1 and binned by number of years between search and initial enrollment. FPIR is computed from the same FRVT 2018 non-mates noted in row 3 of Table 1 with N = 3 000 000.*

2020/03/27 10:40:09

FNIR(N, R, T) = False neg. identification rate
FPIR(N, T) = False pos. identification rate

N = Num. enrolled subjects
R = Num. candidates examined

T = Threshold

T = 0 → Investigation
T > 0 → Identification

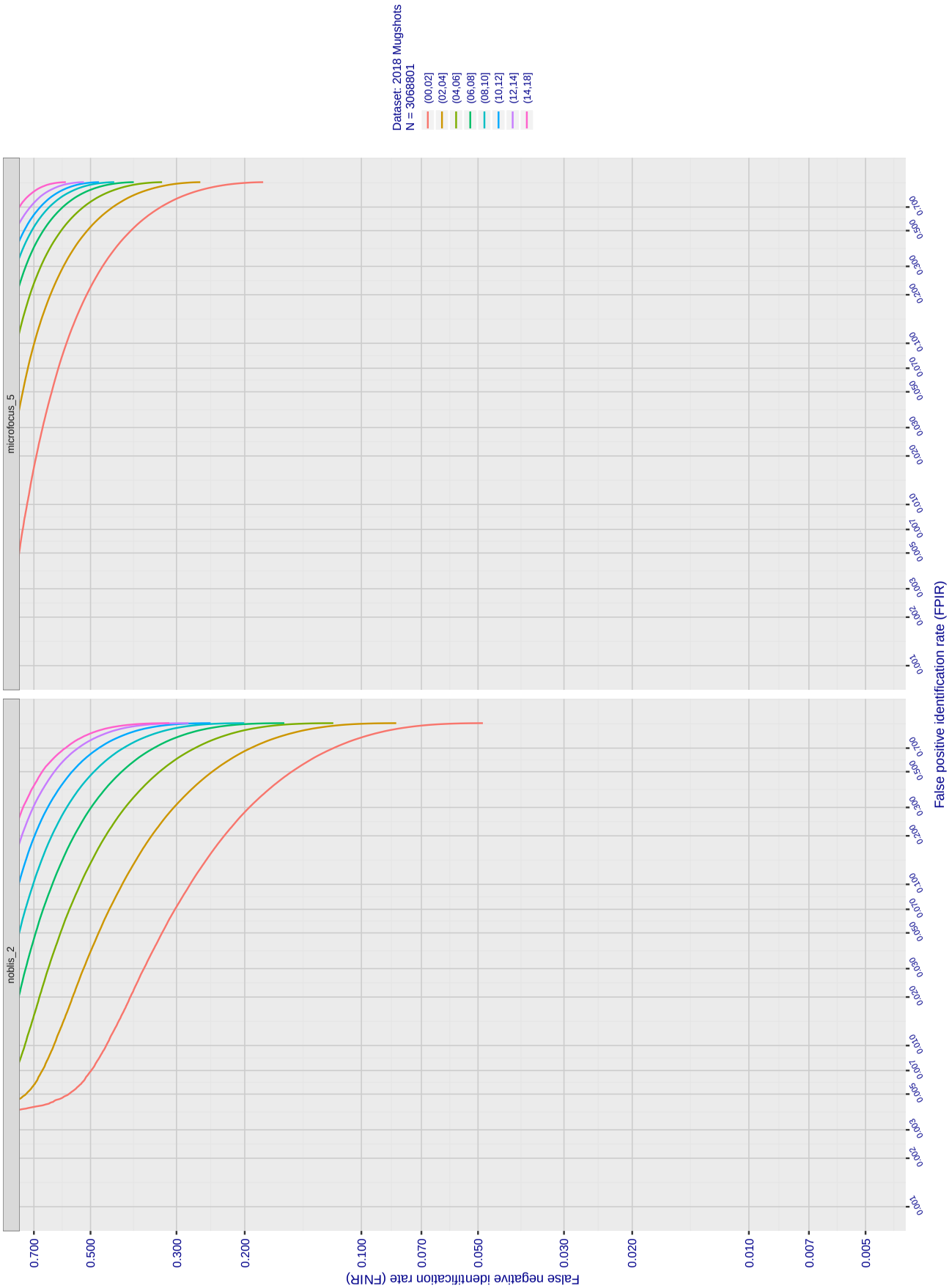

Figure 81: **[FRVT-2018 Mugshot Ageing Dataset] Identification miss rates vs. FPIR by time-elapsed.** *The oldest image of each individual is enrolled. Thereafter, all more recent images are searched. Miss rates are computed over all searches noted in row 17 of Table 1 and binned by number of years between search and initial enrollment. FPIR is computed from the same FRVT 2018 non-mates noted in row 3 of Table 1 with N = 3 000 000.*

2020/03/27	FNIR(N, R, T) =	False neg. identification rate	N = Num. enrolled subjects	T = Threshold	$T = 0 \rightarrow$ Investigation
10:40:09	FPIR(N, T) =	False pos. identification rate	R = Num. candidates examined		$T > 0 \rightarrow$ Identification

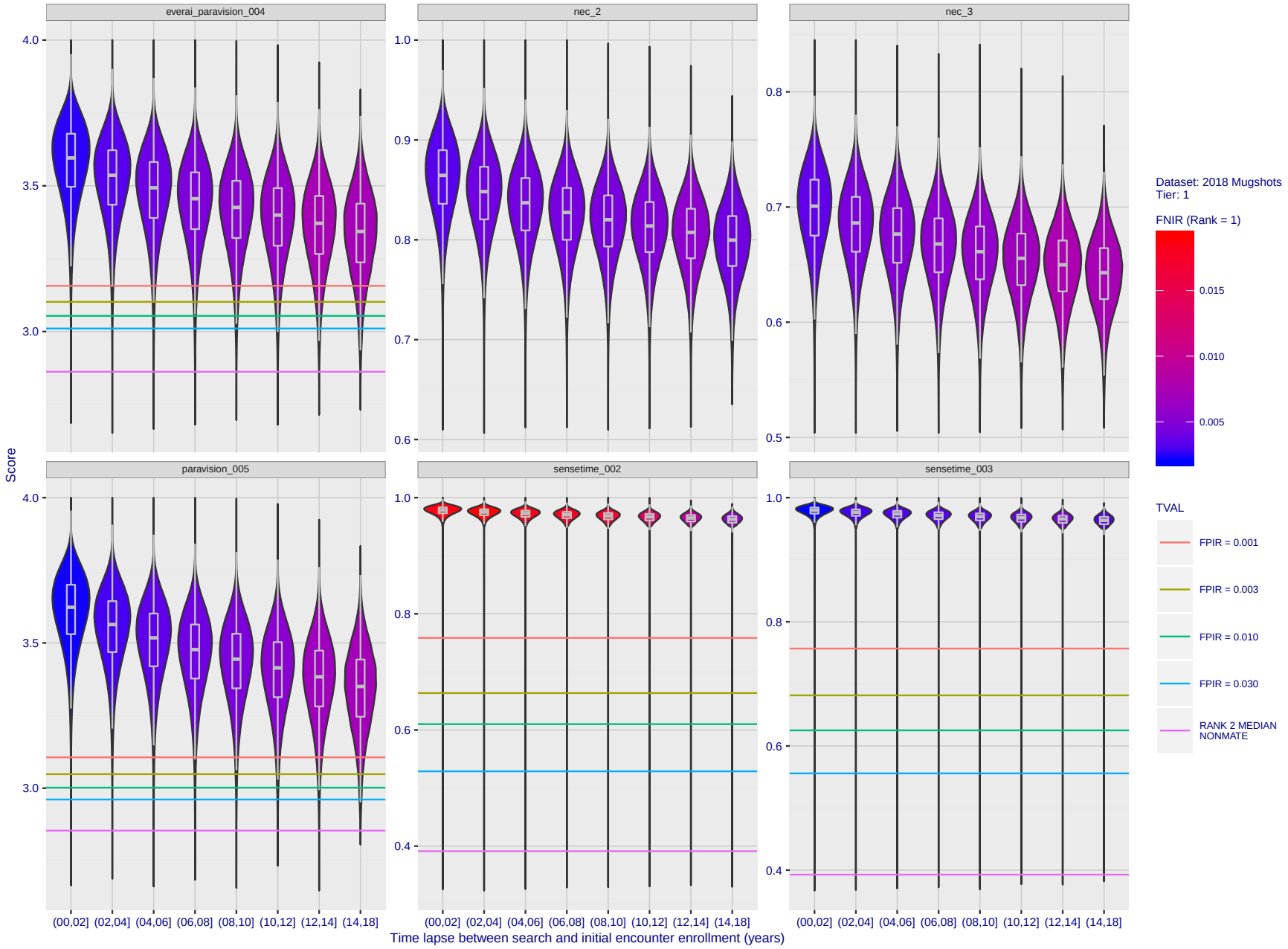

Figure 82: **[FRVT-2018 Mugshot Ageing Dataset] Native mate scores vs. time-elapsed**. *The oldest image of each individual is enrolled. Thereafter, all more recent images are searched. Mated score distributions are computed over all searches noted in row 17 of Table 1 binned by number of years between search and initial enrollment.*

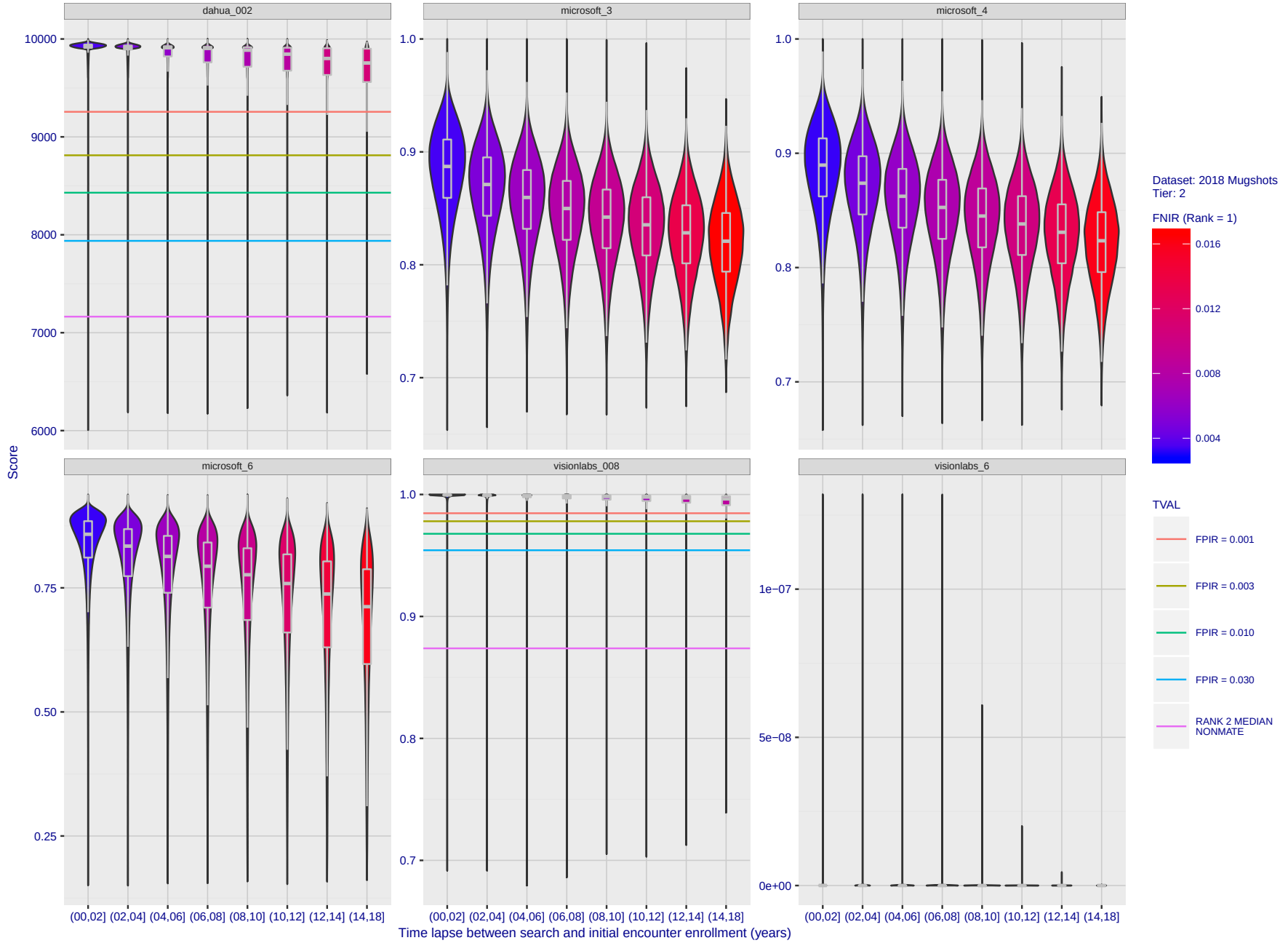

Figure 83: **[FRVT-2018 Mugshot Ageing Dataset] Native mate scores vs. time-elapsed**. *The oldest image of each individual is enrolled. Thereafter, all more recent images are searched. Mated score distributions are computed over all searches noted in row 17 of Table 1 binned by number of years between search and initial enrollment.*

2020/03/27 10:40:09
FNIR(N, R, T) = False neg. identification rate
FPIR(N, T) = False pos. identification rate
N = Num. enrolled subjects
R = Num. candidates examined
T = Threshold
T = 0 → Investigation
T > 0 → Identification

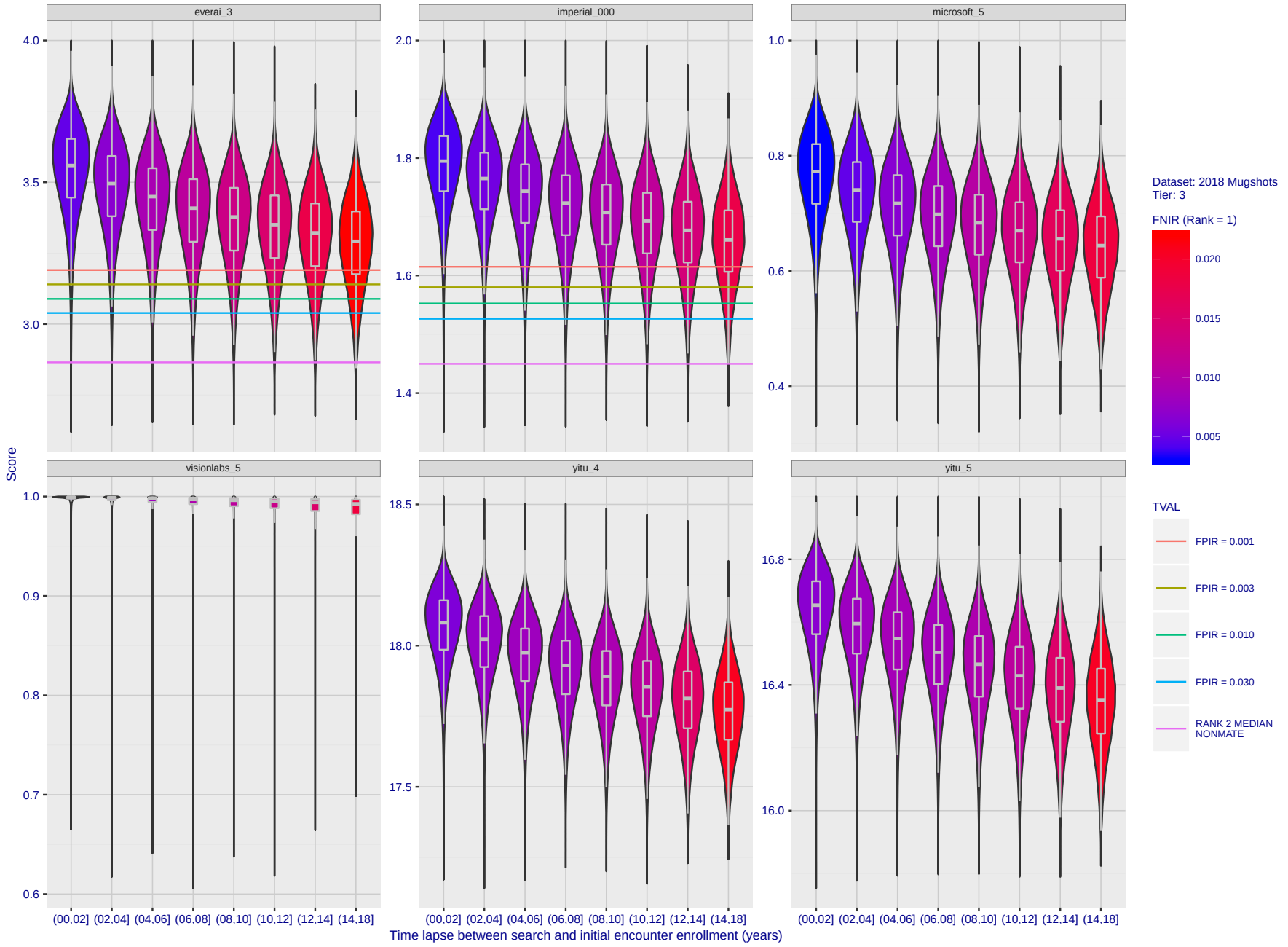

Figure 84: **[FRVT-2018 Mugshot Ageing Dataset] Native mate scores vs. time-elapsed**. *The oldest image of each individual is enrolled. Thereafter, all more recent images are searched. Mated score distributions are computed over all searches noted in row 17 of Table 1 binned by number of years between search and initial enrollment.*

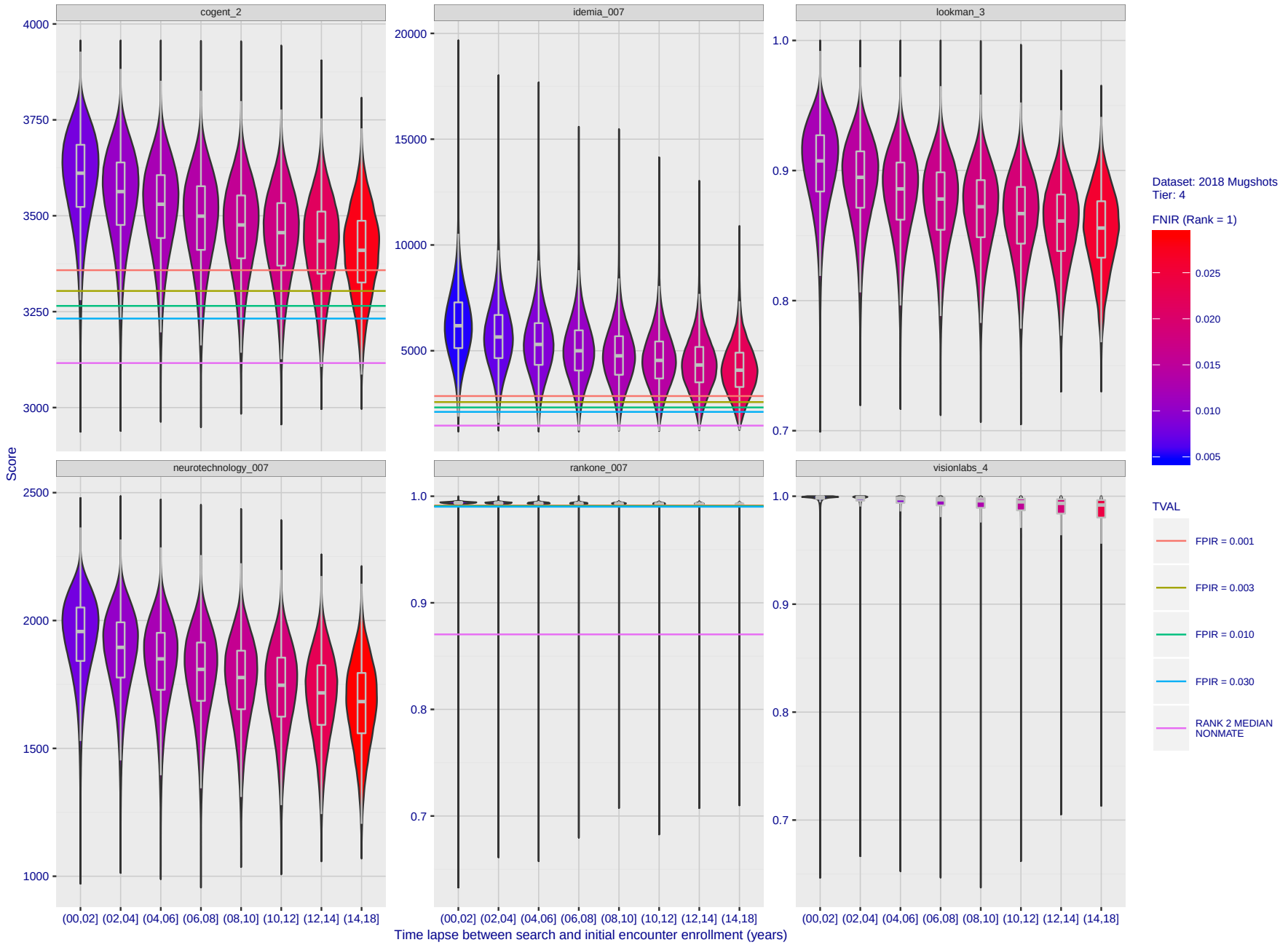

Figure 85: **[FRVT-2018 Mugshot Ageing Dataset] Native mate scores vs. time-elapsed**. *The oldest image of each individual is enrolled. Thereafter, all more recent images are searched. Mated score distributions are computed over all searches noted in row 17 of Table 1 binned by number of years between search and initial enrollment.*

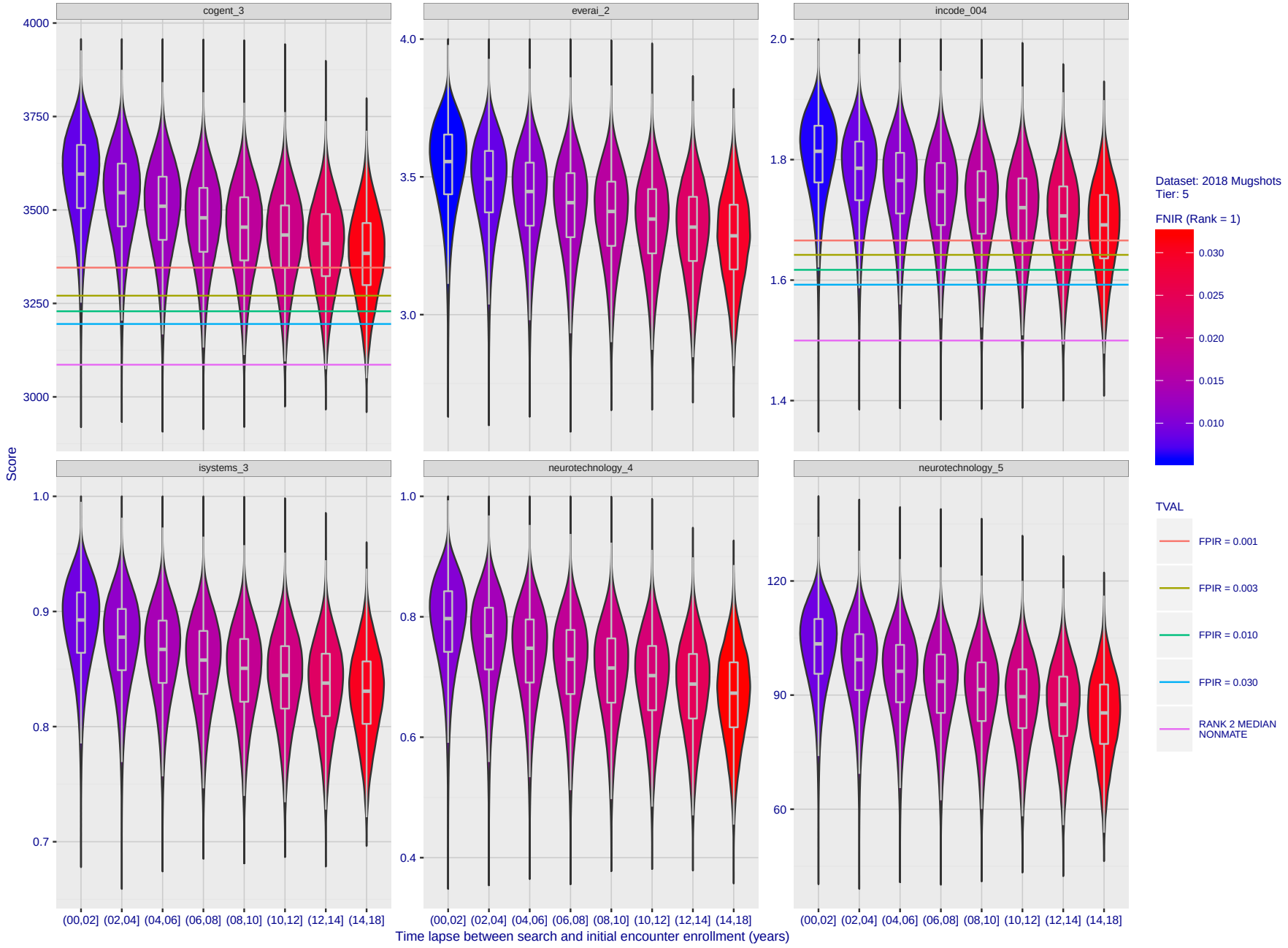

Figure 86: **[FRVT-2018 Mugshot Ageing Dataset] Native mate scores vs. time-elapsed**. *The oldest image of each individual is enrolled. Thereafter, all more recent images are searched. Mated score distributions are computed over all searches noted in row 17 of Table 1 binned by number of years between search and initial enrollment.*

2020/03/27 10:40:09
FNIR(N, R, T) = False neg. identification rate
FPIR(N, T) = False pos. identification rate
N = Num. enrolled subjects
R = Num. candidates examined
T = Threshold
T = 0 → Investigation
T > 0 → Identification

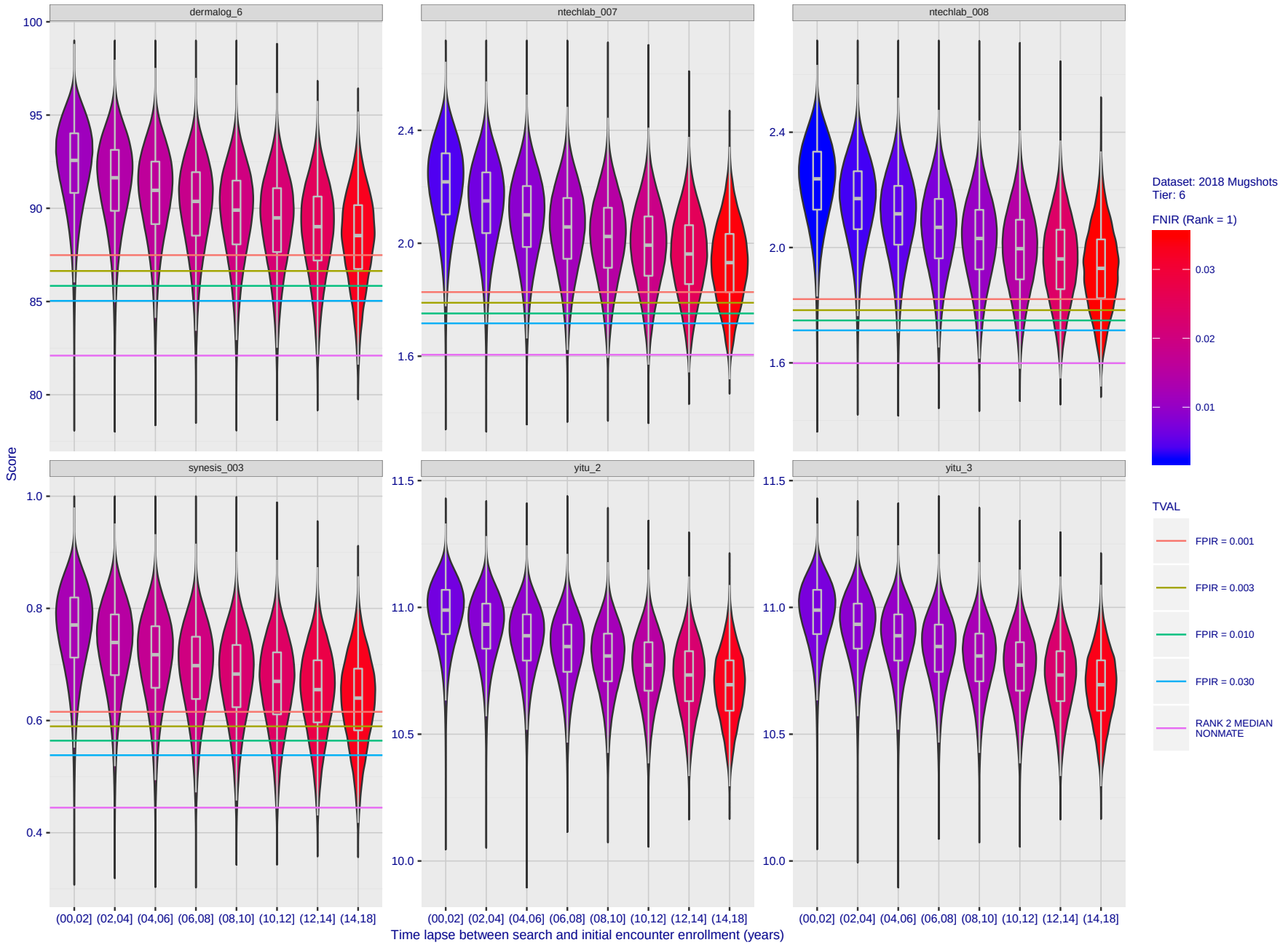

Figure 87: **[FRVT-2018 Mugshot Ageing Dataset] Native mate scores vs. time-elapsed**. *The oldest image of each individual is enrolled. Thereafter, all more recent images are searched. Mated score distributions are computed over all searches noted in row 17 of Table 1 binned by number of years between search and initial enrollment.*

2020/03/27 10:40:09

FNIR(N, R, T) = False neg. identification rate
FPIR(N, T) = False pos. identification rate

N = Num. enrolled subjects
R = Num. candidates examined

T = Threshold

T = 0 → Investigation
T > 0 → Identification

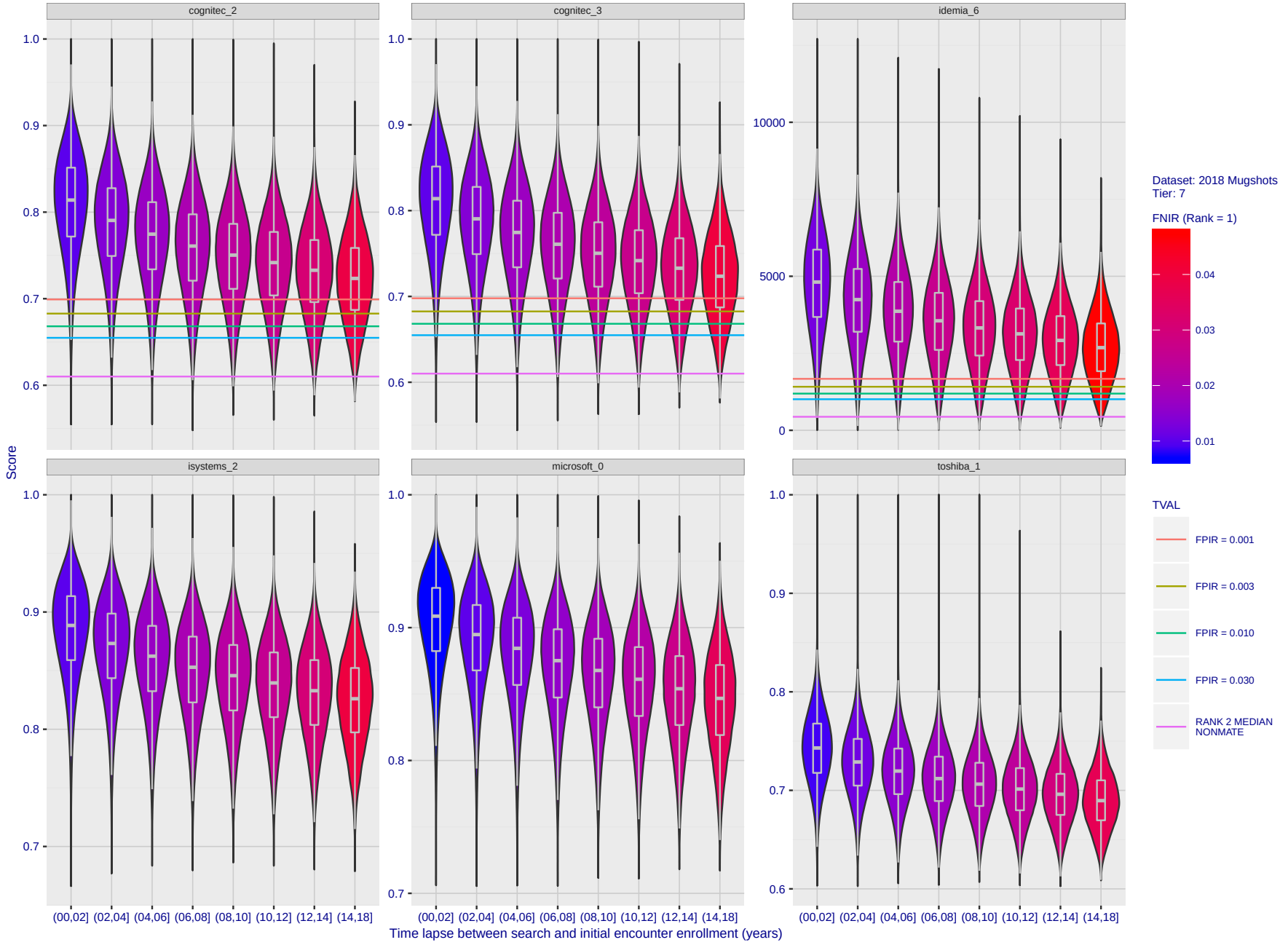

Figure 88: **[FRVT-2018 Mugshot Ageing Dataset] Native mate scores vs. time-elapsed**. *The oldest image of each individual is enrolled. Thereafter, all more recent images are searched. Mated score distributions are computed over all searches noted in row 17 of Table 1 binned by number of years between search and initial enrollment.*

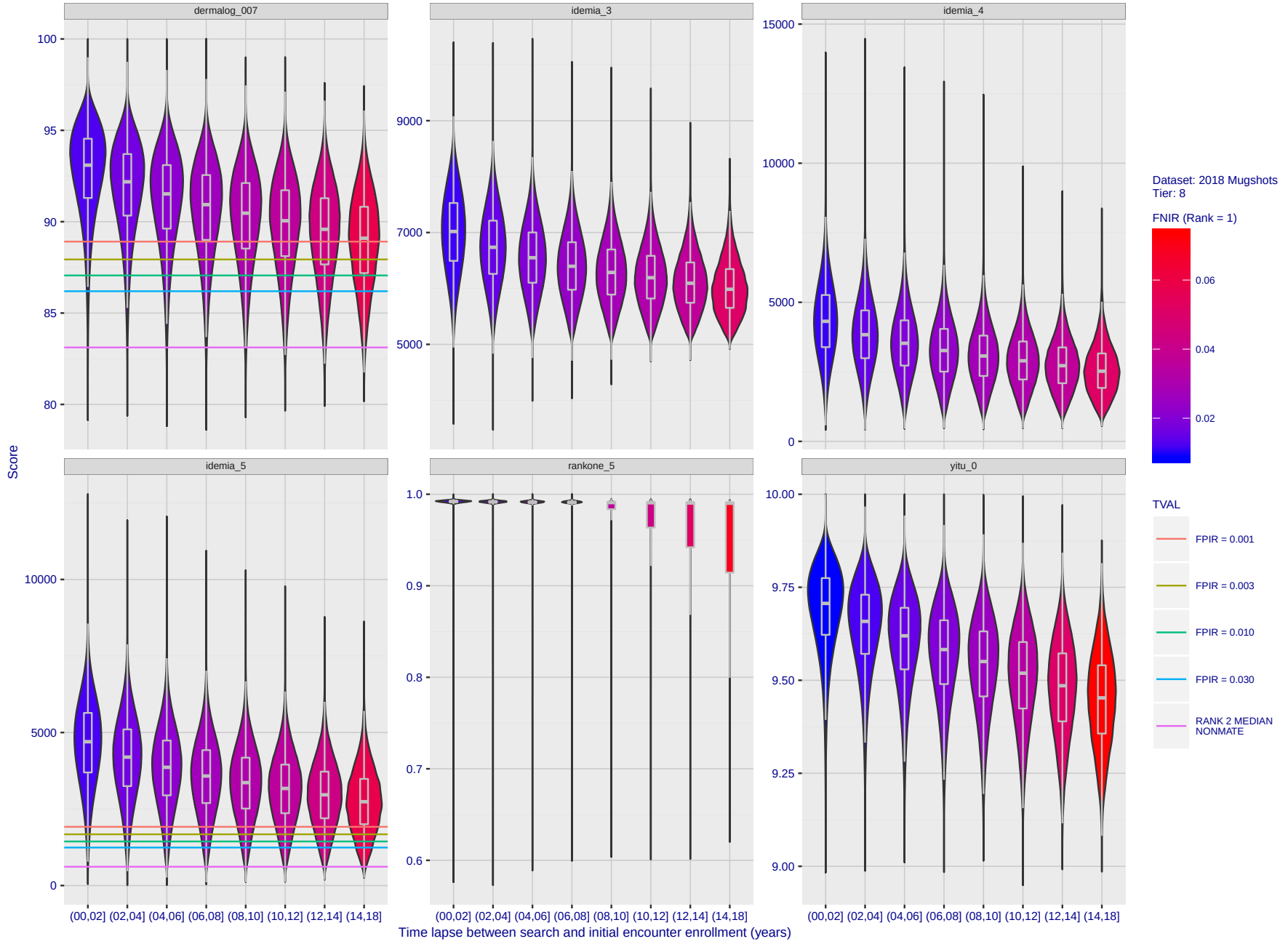

Figure 89: **[FRVT-2018 Mugshot Ageing Dataset] Native mate scores vs. time-elapsed**. *The oldest image of each individual is enrolled. Thereafter, all more recent images are searched. Mated score distributions are computed over all searches noted in row 17 of Table 1 binned by number of years between search and initial enrollment.*

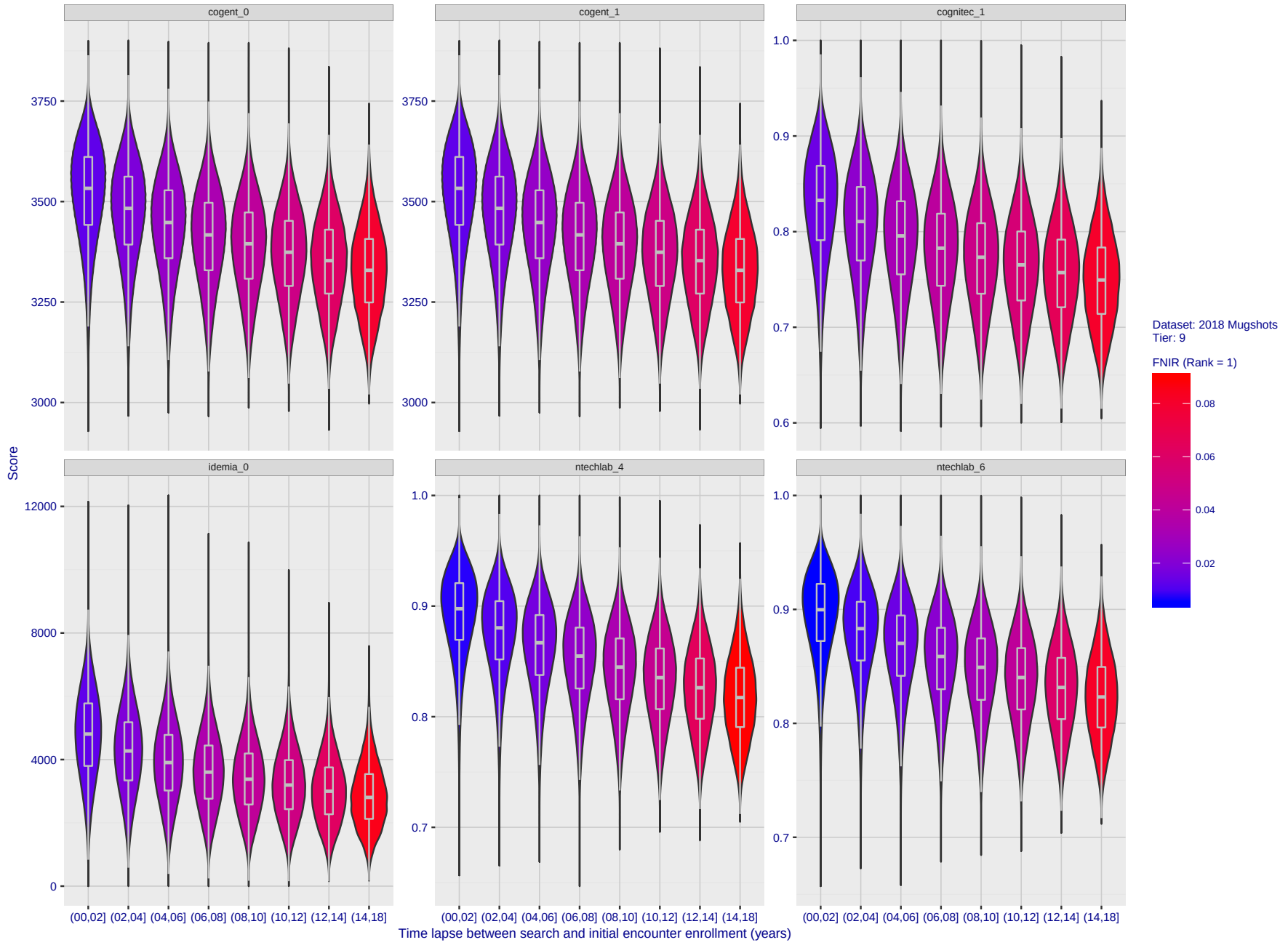

Figure 90: **[FRVT-2018 Mugshot Ageing Dataset] Native mate scores vs. time-elapsed**. *The oldest image of each individual is enrolled. Thereafter, all more recent images are searched. Mated score distributions are computed over all searches noted in row 17 of Table 1 binned by number of years between search and initial enrollment.*

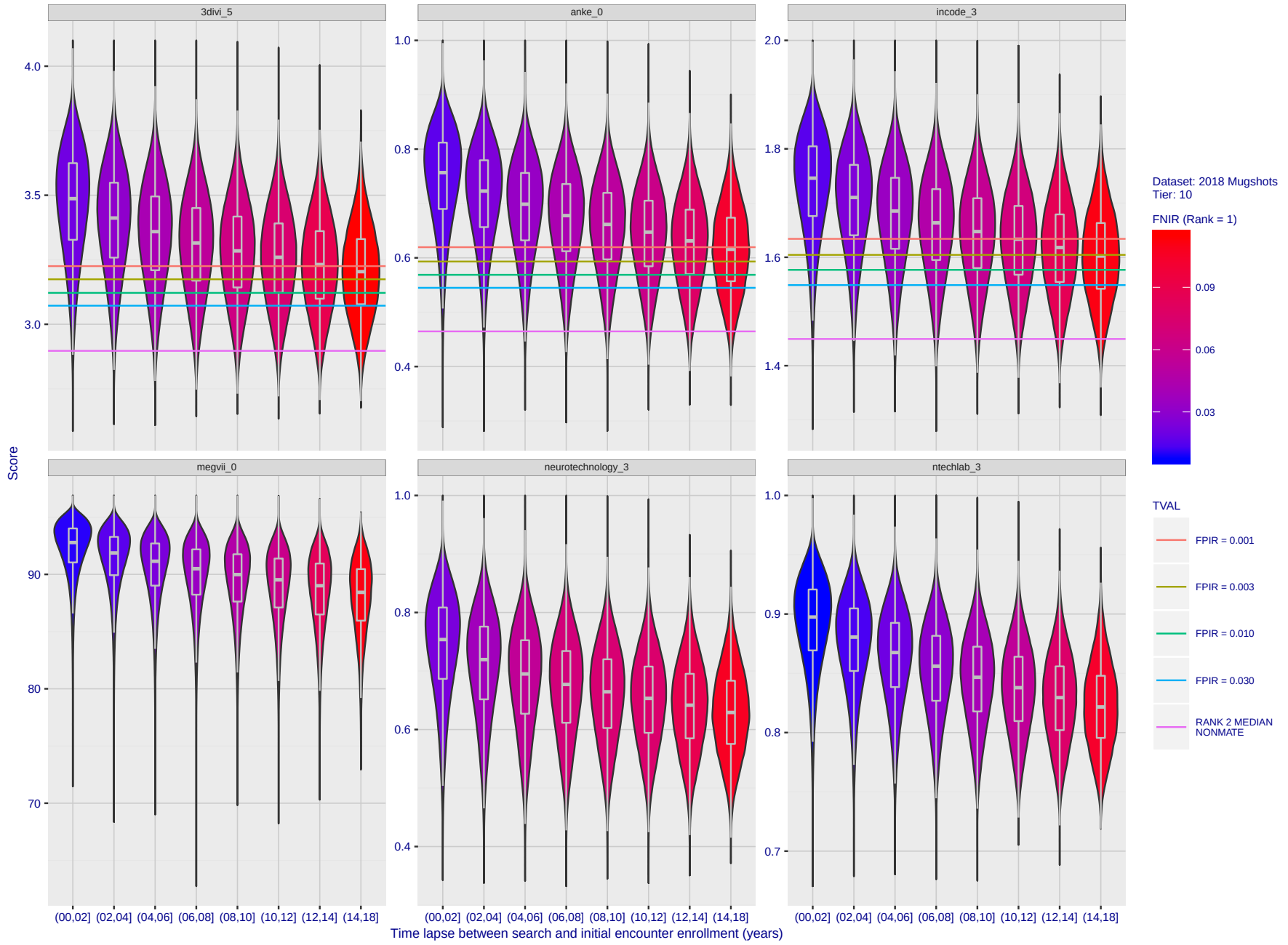

Figure 91: **[FRVT-2018 Mugshot Ageing Dataset] Native mate scores vs. time-elapsed**. *The oldest image of each individual is enrolled. Thereafter, all more recent images are searched. Mated score distributions are computed over all searches noted in row 17 of Table 1 binned by number of years between search and initial enrollment.*

2020/03/27 10:40:09
FNIR(N, R, T) = False neg. identification rate
FPIR(N, T) = False pos. identification rate
N = Num. enrolled subjects
R = Num. candidates examined
T = Threshold
T = 0 → Investigation
T > 0 → Identification

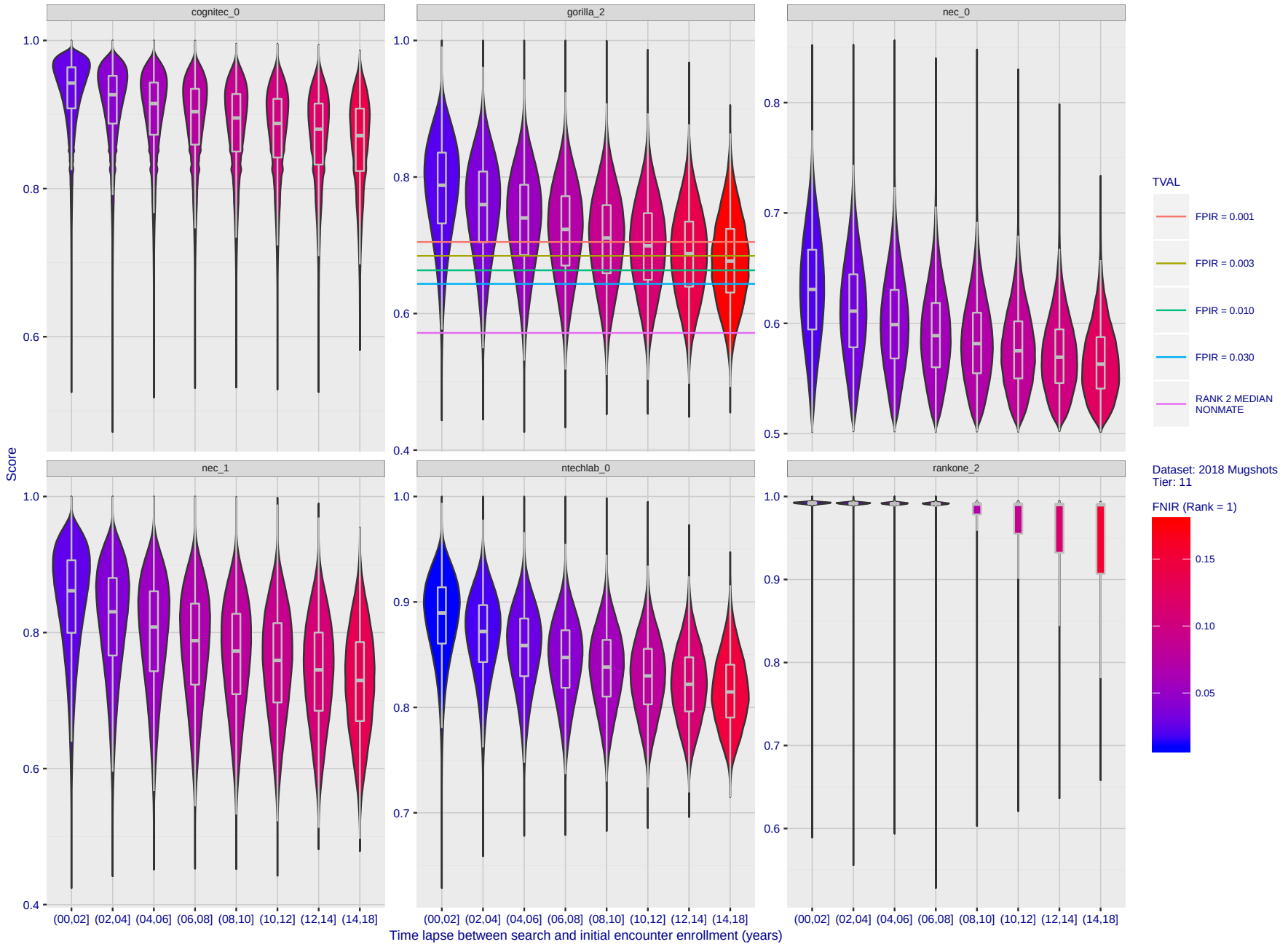

Figure 92: **[FRVT-2018 Mugshot Ageing Dataset] Native mate scores vs. time-elapsed**. *The oldest image of each individual is enrolled. Thereafter, all more recent images are searched. Mated score distributions are computed over all searches noted in row 17 of Table 1 binned by number of years between search and initial enrollment.*

2020/03/27 10:40:09
FNIR(N, R, T) = FPIR(N, T) = False neg. identification rate / False pos. identification rate
N = Num. enrolled subjects
R = Num. candidates examined
T = Threshold
T = 0 → Investigation
T > 0 → Identification

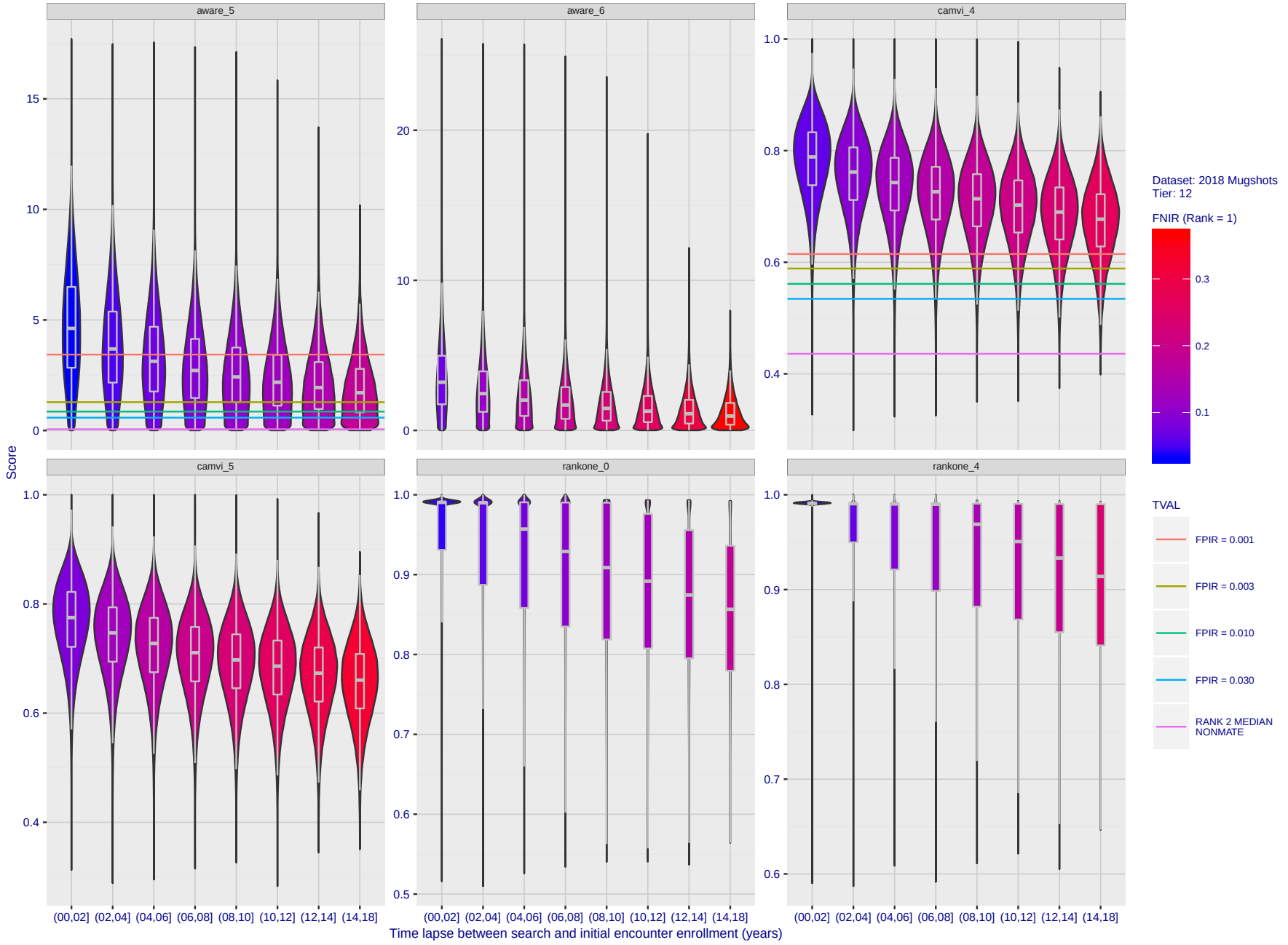

Figure 93: **[FRVT-2018 Mugshot Ageing Dataset] Native mate scores vs. time-elapsed**. *The oldest image of each individual is enrolled. Thereafter, all more recent images are searched. Mated score distributions are computed over all searches noted in row 17 of Table 1 binned by number of years between search and initial enrollment.*

2020/03/27 10:40:09
FNIR(N, R, T) = False neg. identification rate
FPIR(N, T) = False pos. identification rate
N = Num. enrolled subjects
R = Num. candidates examined
T = Threshold
T = 0 → Investigation
T > 0 → Identification

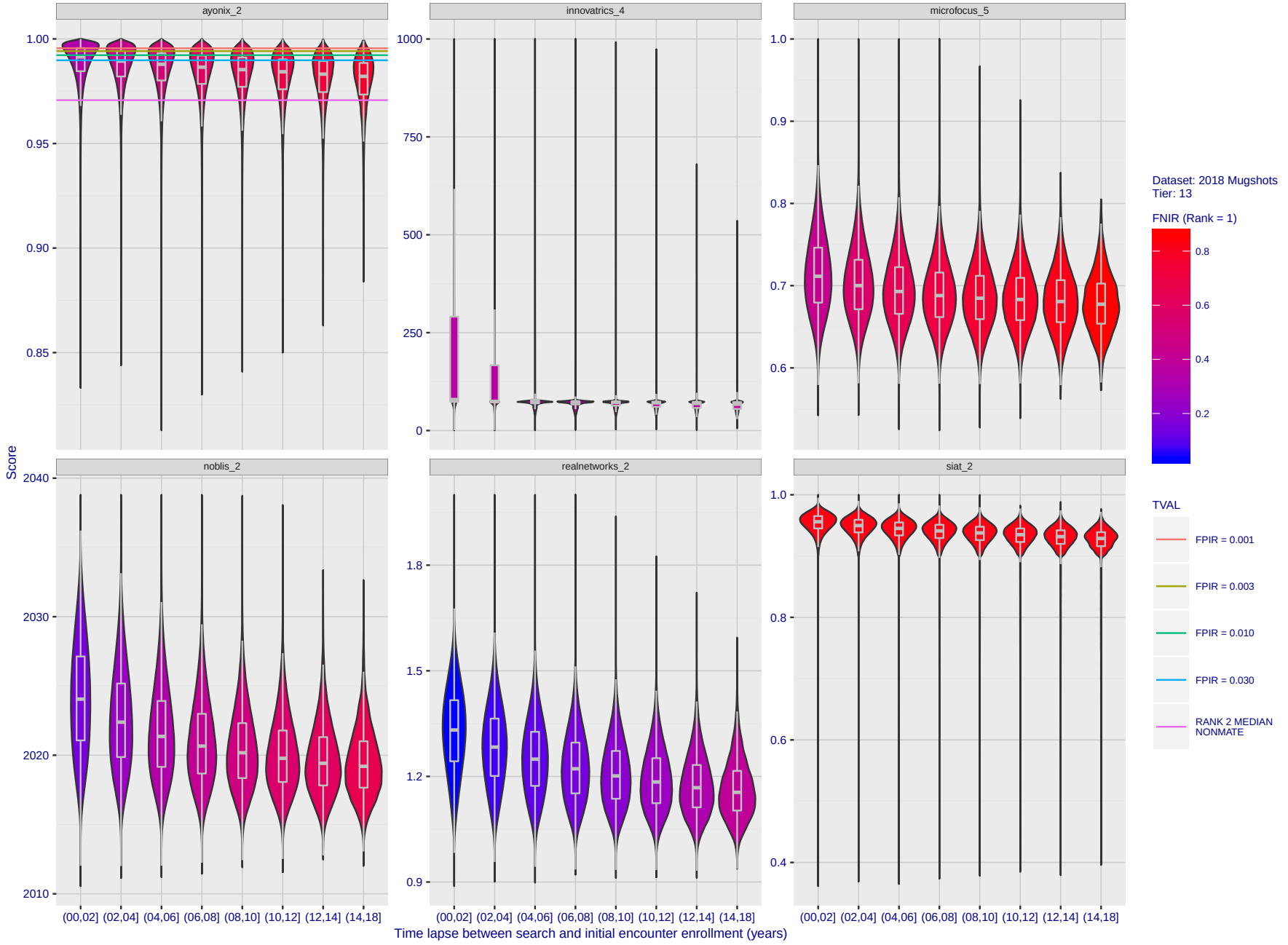

Figure 94: **[FRVT-2018 Mugshot Ageing Dataset] Native mate scores vs. time-elapsed**. *The oldest image of each individual is enrolled. Thereafter, all more recent images are searched. Mated score distributions are computed over all searches noted in row 17 of Table 1 binned by number of years between search and initial enrollment.*

2020/03/27 10:40:09

FNIR(N, R, T) = False neg. identification rate
FPIR(N, T) = False pos. identification rate
N = Num. enrolled subjects
R = Num. candidates examined
T = Threshold
T = 0 → Investigation
T > 0 → Identification

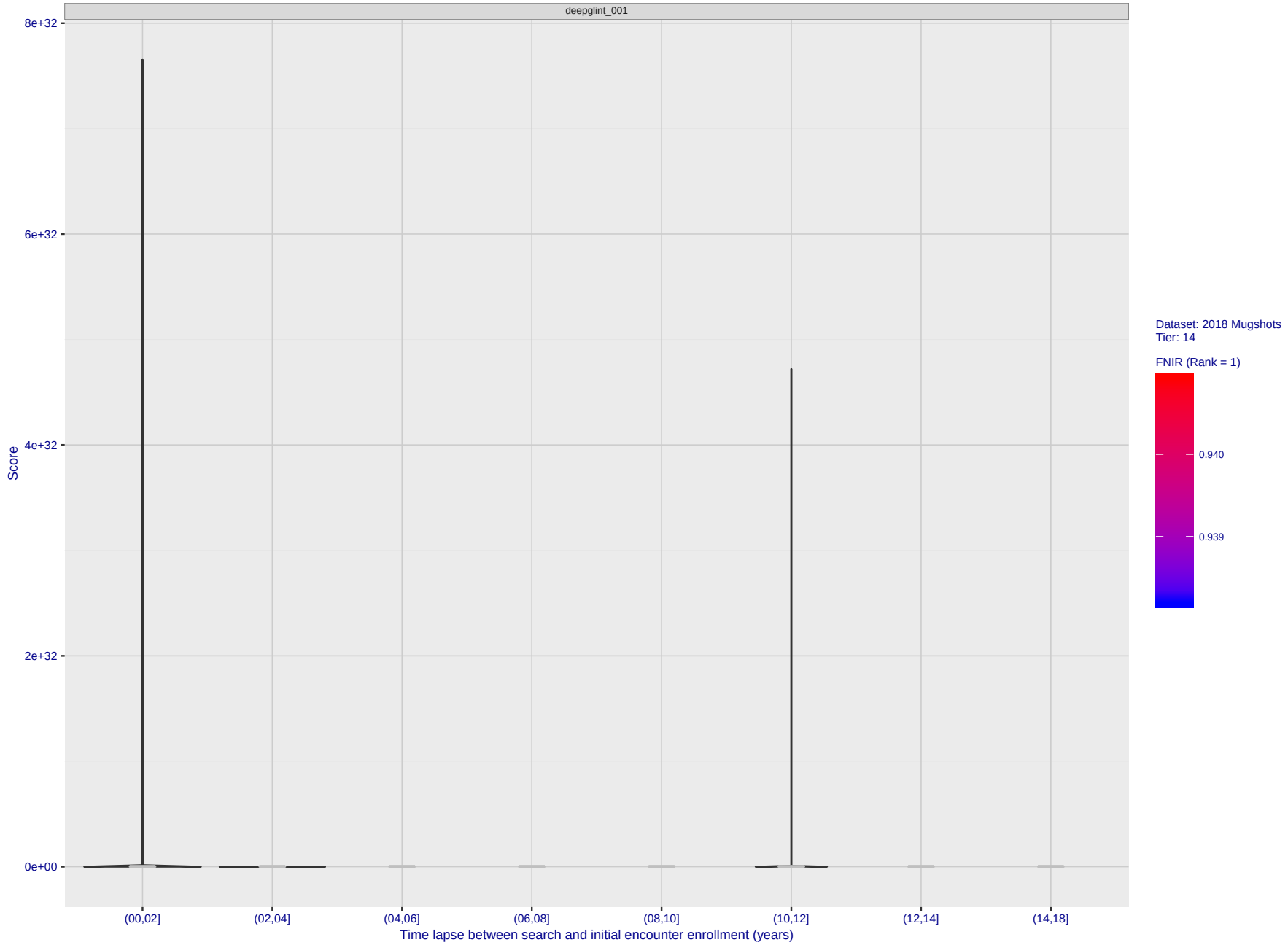

Figure 95: **[FRVT-2018 Mugshot Ageing Dataset] Native mate scores vs. time-elapsed**. *The oldest image of each individual is enrolled. Thereafter, all more recent images are searched. Mated score distributions are computed over all searches noted in row 17 of Table 1 binned by number of years between search and initial enrollment.*

Appendix C Effect of enrolling multiple images

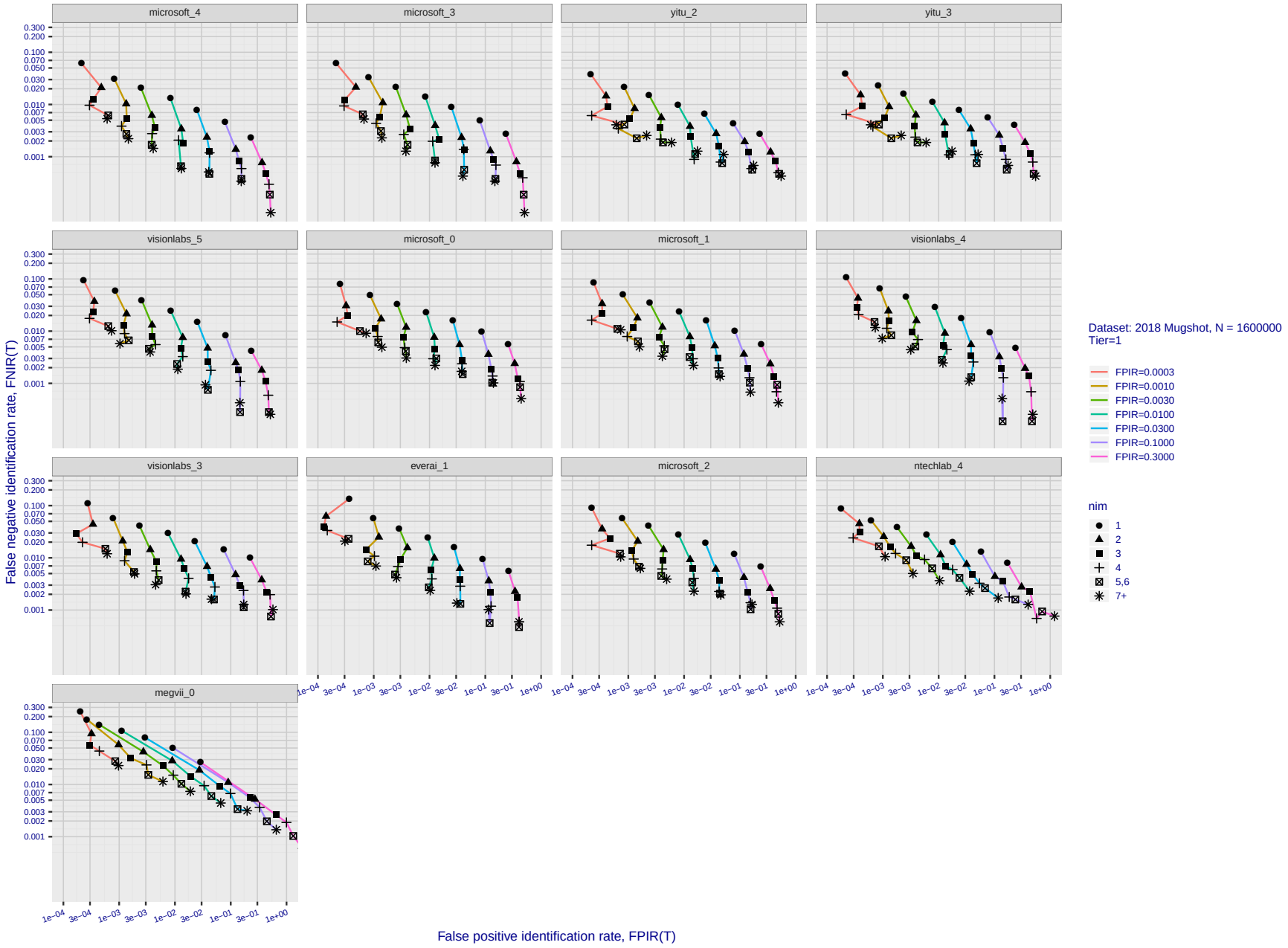

Figure 96: **[FRVT-2018 Mugshot Dataset] Effect of enrolling multiple images for each identity**. *The plot shows an identification miss rates vs. false positive rates, at seven operating thresholds. The enrolled population size is fixed. The images are enrolled with lifetime-consolidation - see section 2.2.*

2020/03/27 10:40:09

FNIR(N, R, T) = False neg. identification rate
FPIR(N, T) = False pos. identification rate

N = Num. enrolled subjects
R = Num. candidates examined

T = Threshold

T = 0 → Investigation
T > 0 → Identification

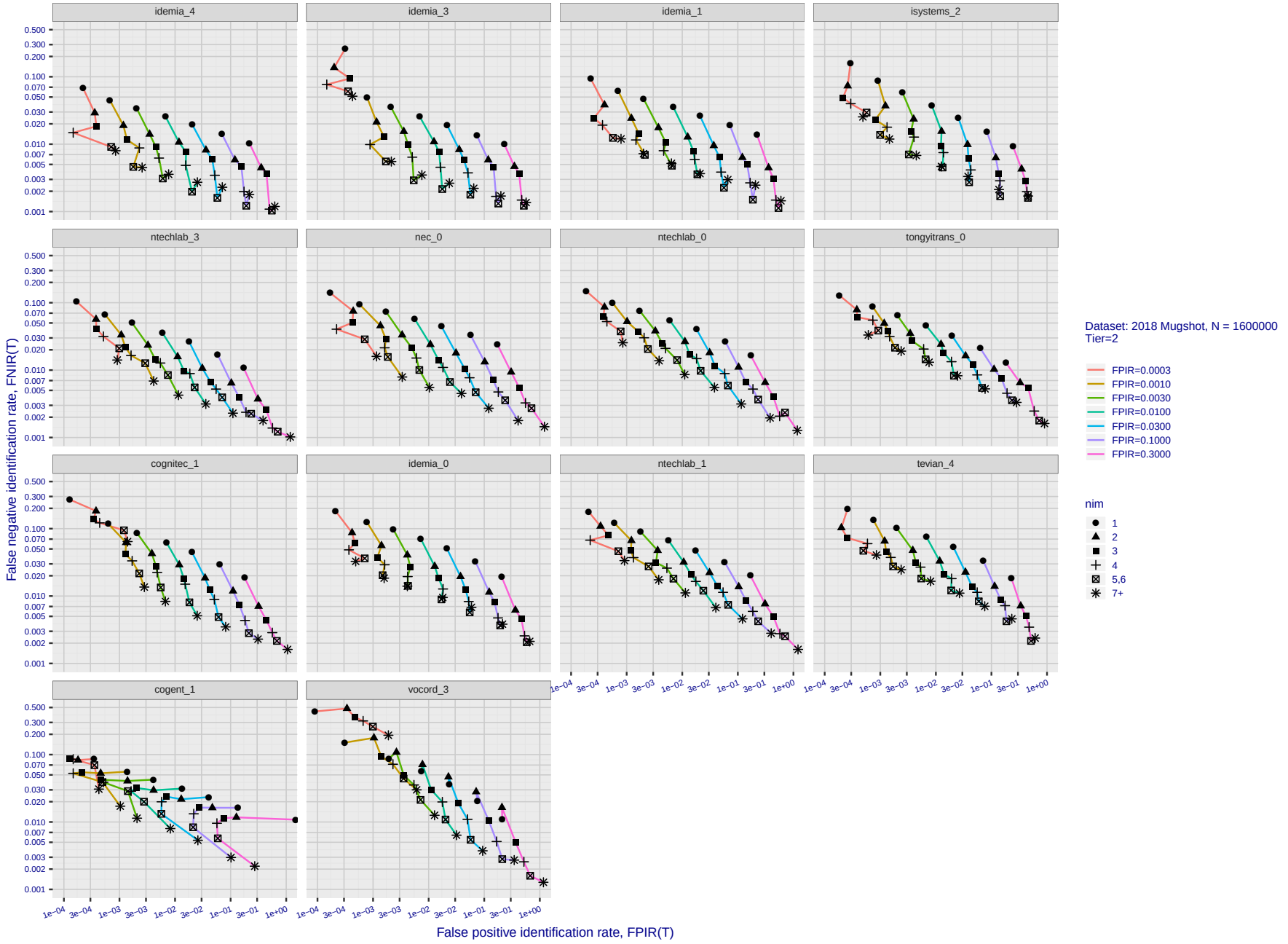

Figure 97: **[FRVT-2018 Mugshot Dataset] Effect of enrolling multiple images for each identity**. *The plot shows an identification miss rates vs. false positive rates, at seven operating thresholds. The enrolled population size is fixed. The images are enrolled with lifetime-consolidation - see section 2.2.*

2020/03/27 10:40:09

FNIR(N, R, T) = False neg. identification rate
FPIR(N, T) = False pos. identification rate

N = Num. enrolled subjects
R = Num. candidates examined

T = Threshold

T = 0 → Investigation
T > 0 → Identification

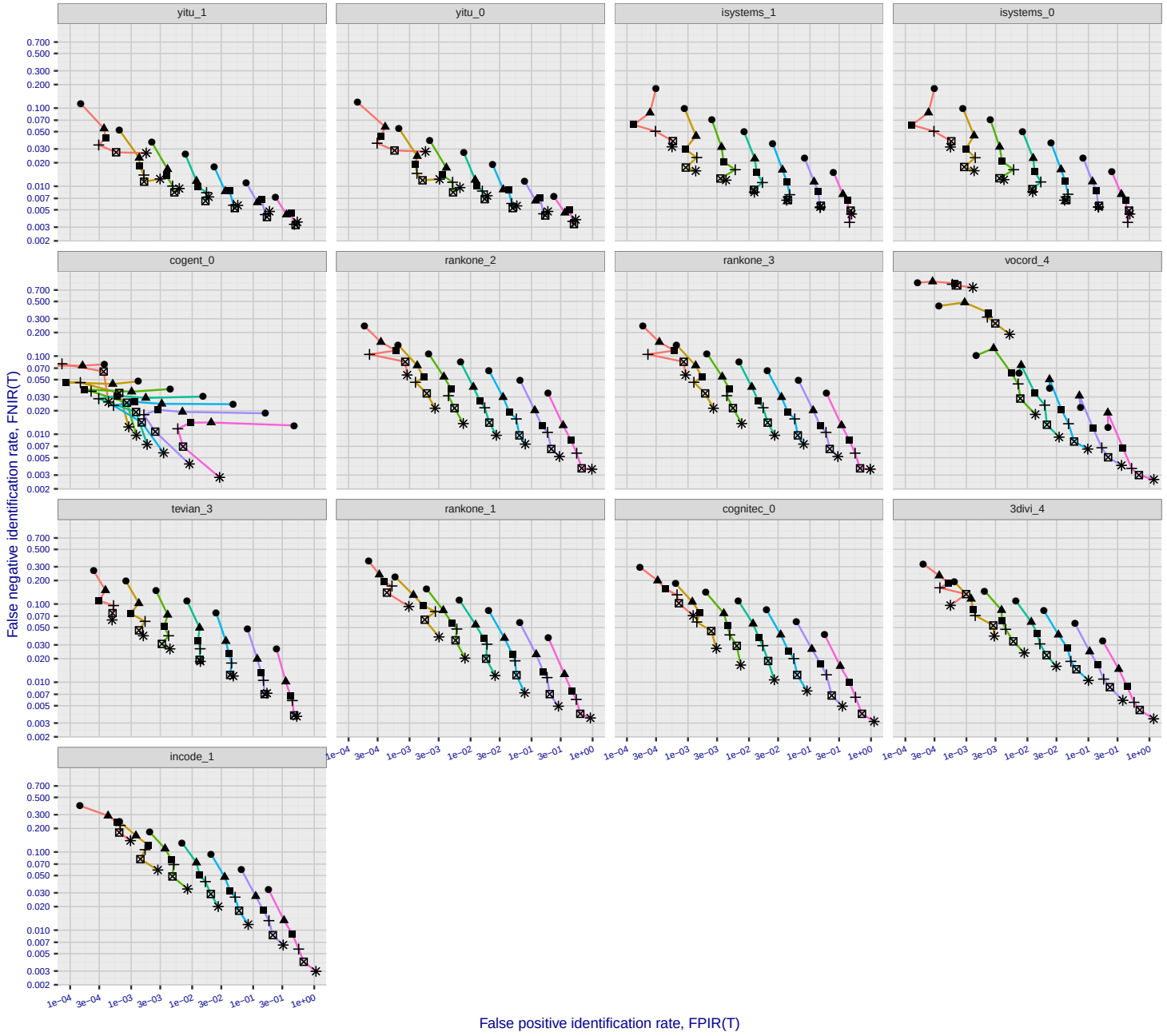

Figure 98: **[FRVT-2018 Mugshot Dataset] Effect of enrolling multiple images for each identity**. *The plot shows an identification miss rates vs. false positive rates, at seven operating thresholds. The enrolled population size is fixed. The images are enrolled with lifetime-consolidation - see section 2.2.*

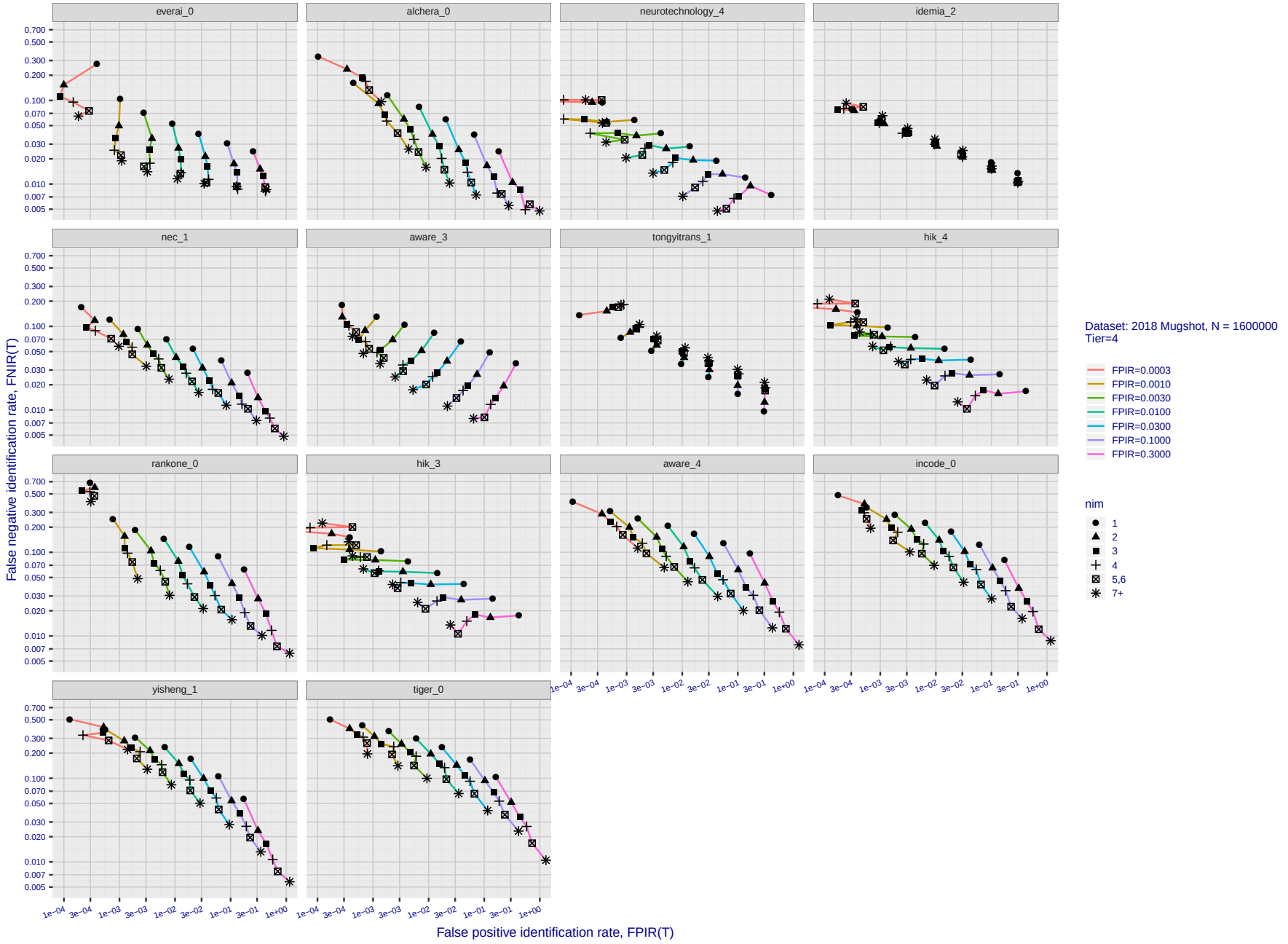

Figure 99: **[FRVT-2018 Mugshot Dataset] Effect of enrolling multiple images for each identity**. *The plot shows an identification miss rates vs. false positive rates, at seven operating thresholds. The enrolled population size is fixed. The images are enrolled with lifetime-consolidation - see section 2.2.*

2020/03/27 10:40:09

FNIR(N, R, T) = False neg. identification rate
FPIR(N, T) = False pos. identification rate
N = Num. enrolled subjects
R = Num. candidates examined
T = Threshold
T = 0 → Investigation
T > 0 → Identification

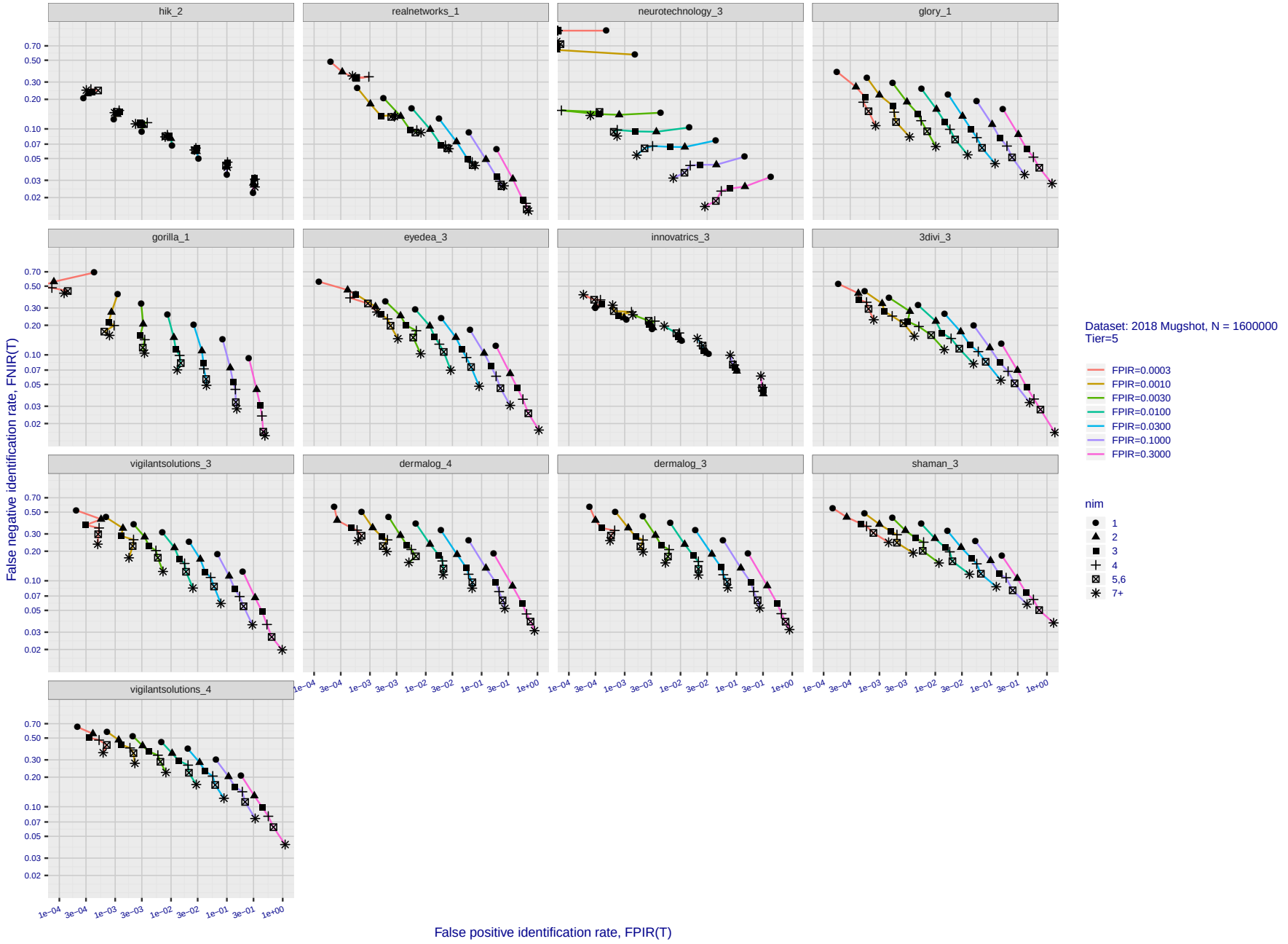

Figure 100: **[FRVT-2018 Mugshot Dataset] Effect of enrolling multiple images for each identity**. *The plot shows an identification miss rates vs. false positive rates, at seven operating thresholds. The enrolled population size is fixed. The images are enrolled with lifetime-consolidation - see section 2.2.*

2020/03/27 10:40:09

FNIR(N, R, T) = False neg. identification rate
FPIR(N, T) = False pos. identification rate
N = Num. enrolled subjects
R = Num. candidates examined
T = Threshold
T = 0 → Investigation
T > 0 → Identification

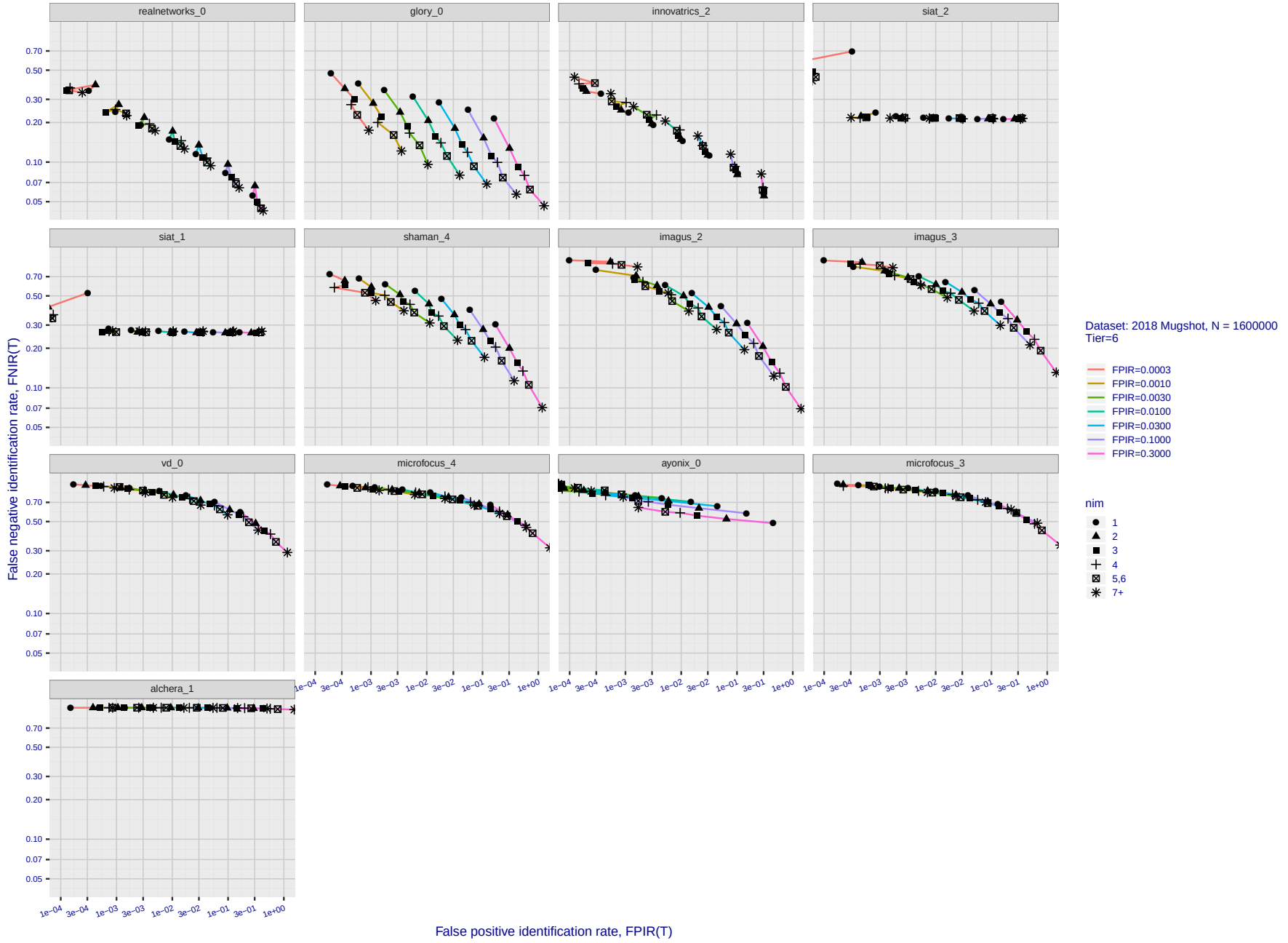

Figure 101: **[FRVT-2018 Mugshot Dataset] Effect of enrolling multiple images for each identity**. *The plot shows an identification miss rates vs. false positive rates, at seven operating thresholds. The enrolled population size is fixed. The images are enrolled with lifetime-consolidation - see section 2.2.*

2020/03/27 10:40:09

FNIR(N, R, T) = False neg. identification rate
FPIR(N, T) = False pos. identification rate

N = Num. enrolled subjects
R = Num. candidates examined

T = Threshold

T = 0 → Investigation
T > 0 → Identification

Appendix D Accuracy with poor quality webcam images

2020/03/27	FNIR(N, R, T) =	False neg. identification rate	N = Num. enrolled subjects	T = Threshold	$T = 0 \rightarrow$ Investigation
10:40:09	FPIR(N, T) =	False pos. identification rate	R = Num. candidates examined		$T > 0 \rightarrow$ Identification

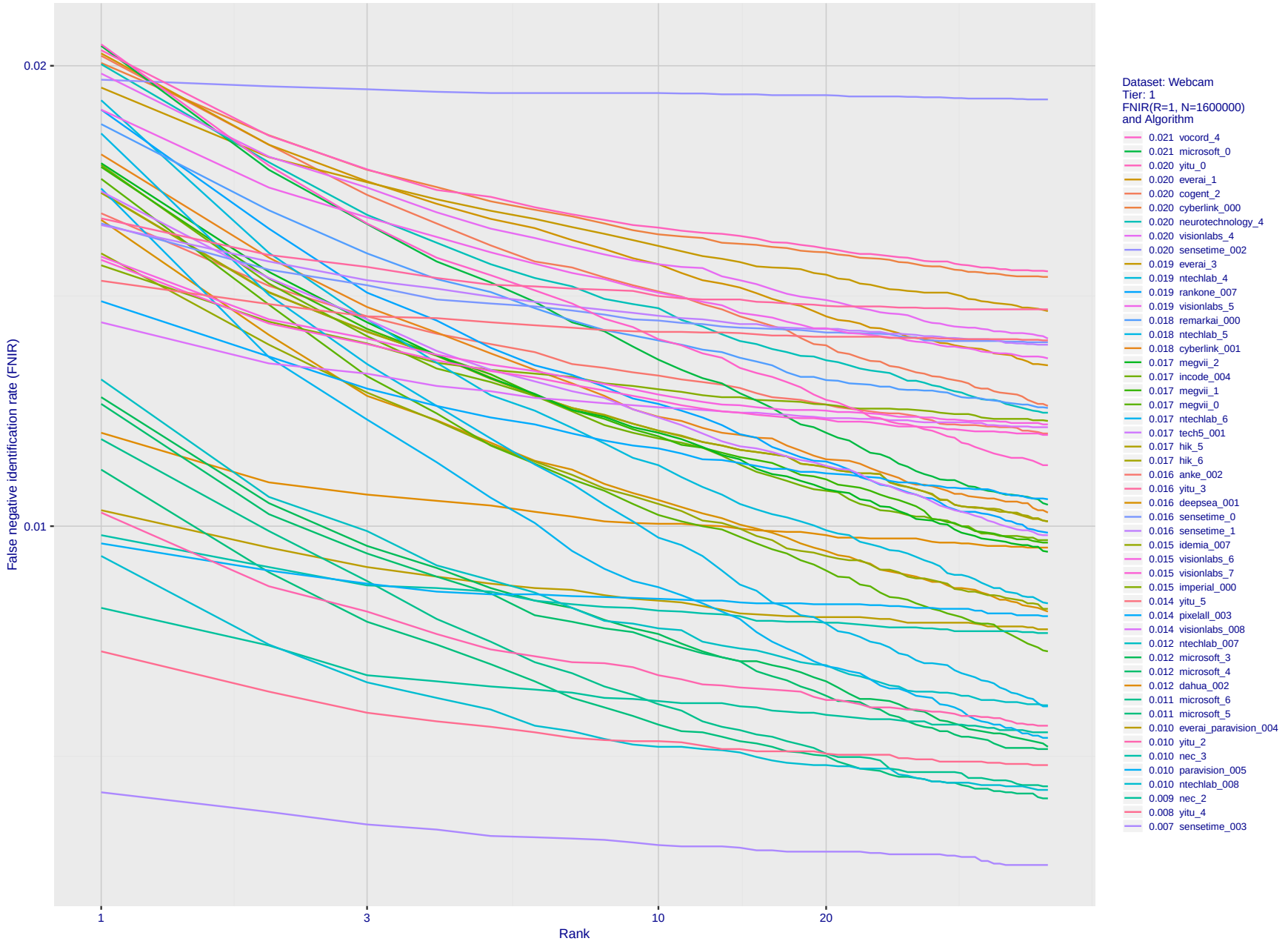

2020/03/27 10:40:09

FNIR(N, R, T) = False neg. identification rate
FPIR(N, T) = False pos. identification rate

N = Num. enrolled subjects
R = Num. candidates examined

T = Threshold

T = 0 → Investigation
T > 0 → Identification

Figure 102: **[Webcam Dataset] Identification miss rates vs. rank**. *The results apply to cross-domain recognition in which webcams are searched against enrolled mugshots. The FNIR values are higher than those for mugshot-mugshot identification due to low image resolution, lighting and less constrained subject pose in webcam images - see Figure 4.*

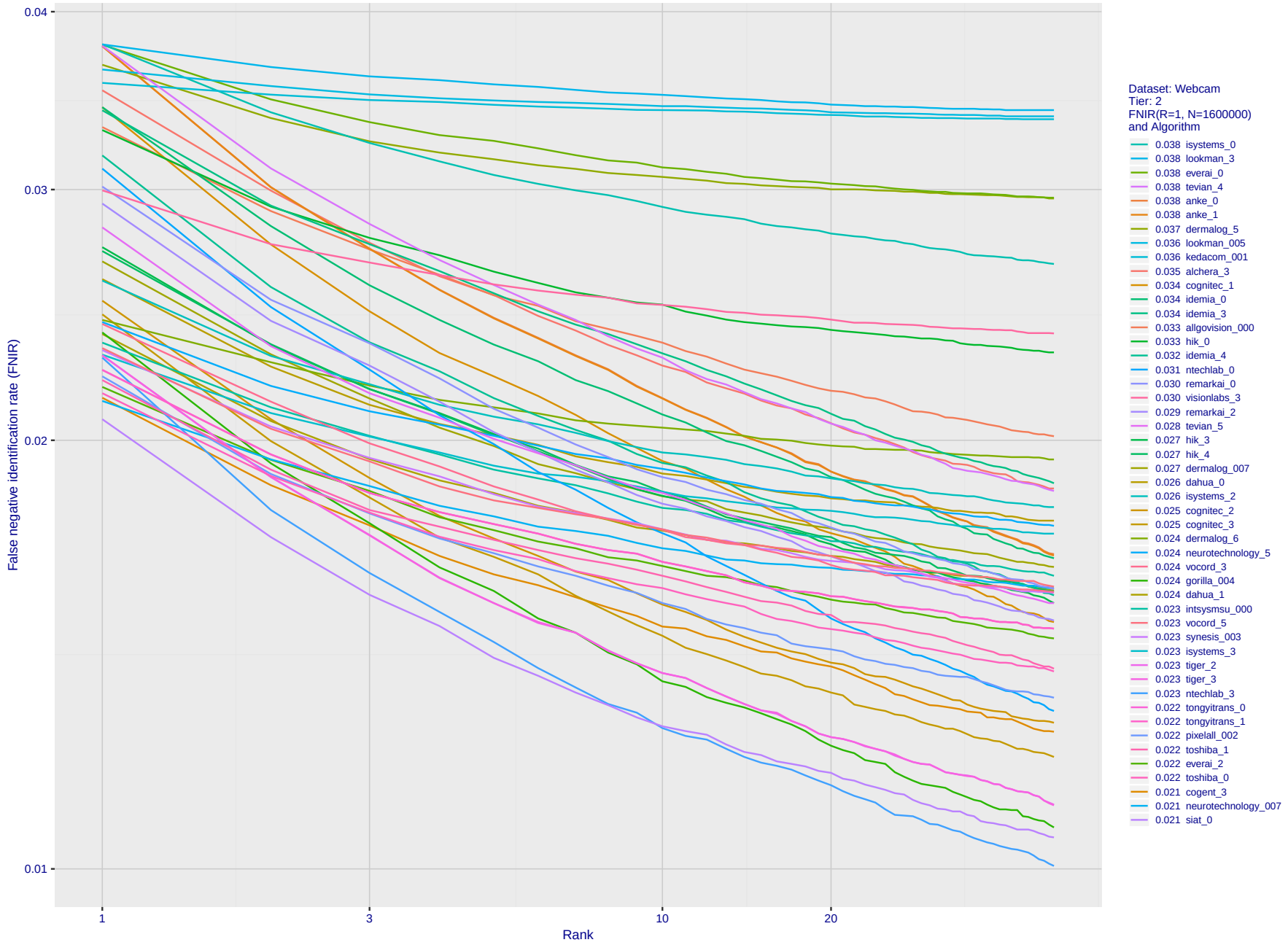

Figure 103: **[Webcam Dataset] Identification miss rates vs. rank**. *The results apply to cross-domain recognition in which webcams are searched against enrolled mugshots. The FNIR values are higher than those for mugshot-mugshot identification due to low image resolution, lighting and less constrained subject pose in webcam images - see Figure 4.*

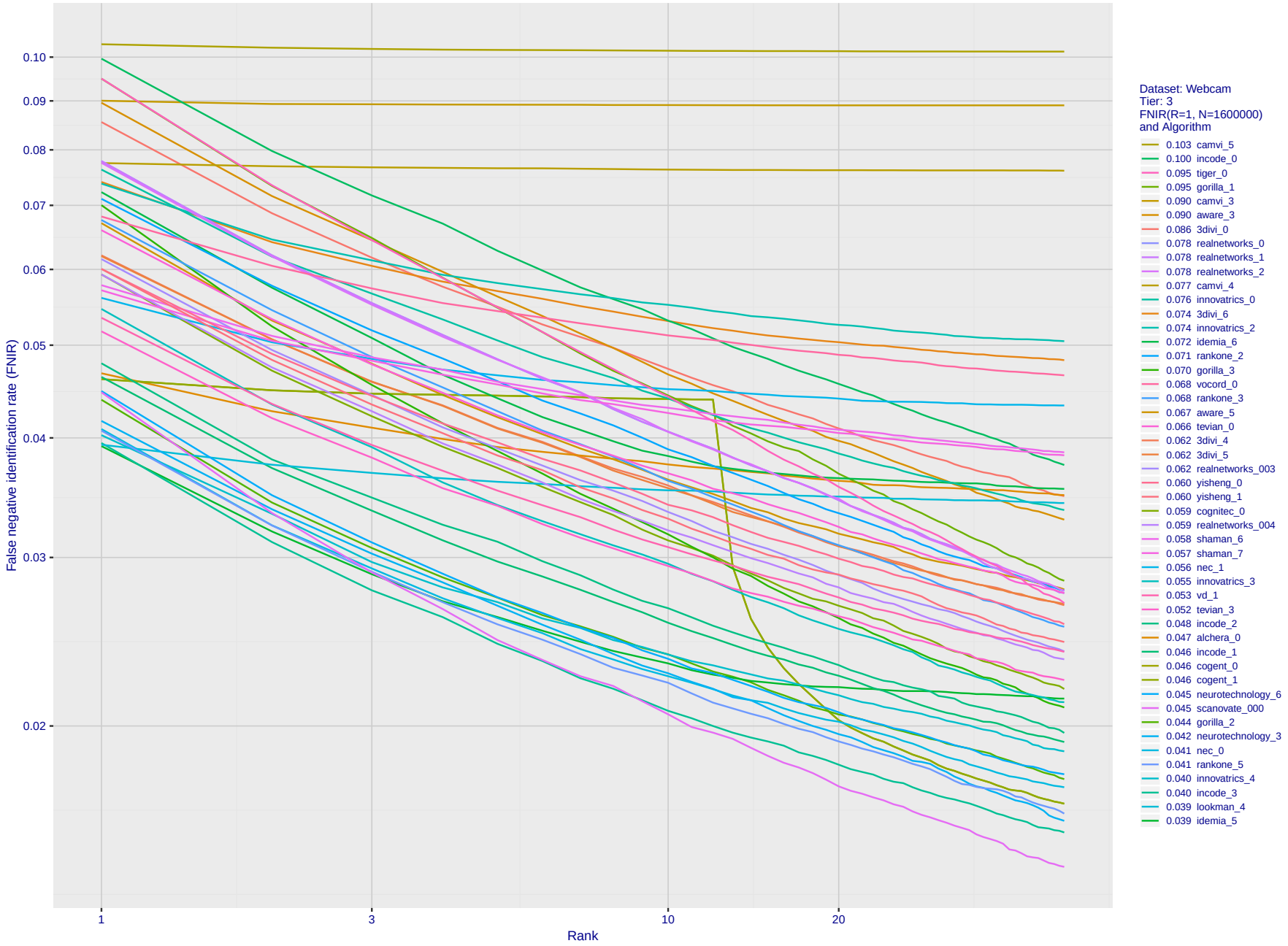

Figure 104: **[Webcam Dataset] Identification miss rates vs. rank**. *The results apply to cross-domain recognition in which webcams are searched against enrolled mugshots. The FNIR values are higher than those for mugshot-mugshot identification due to low image resolution, lighting and less constrained subject pose in webcam images - see Figure 4.*

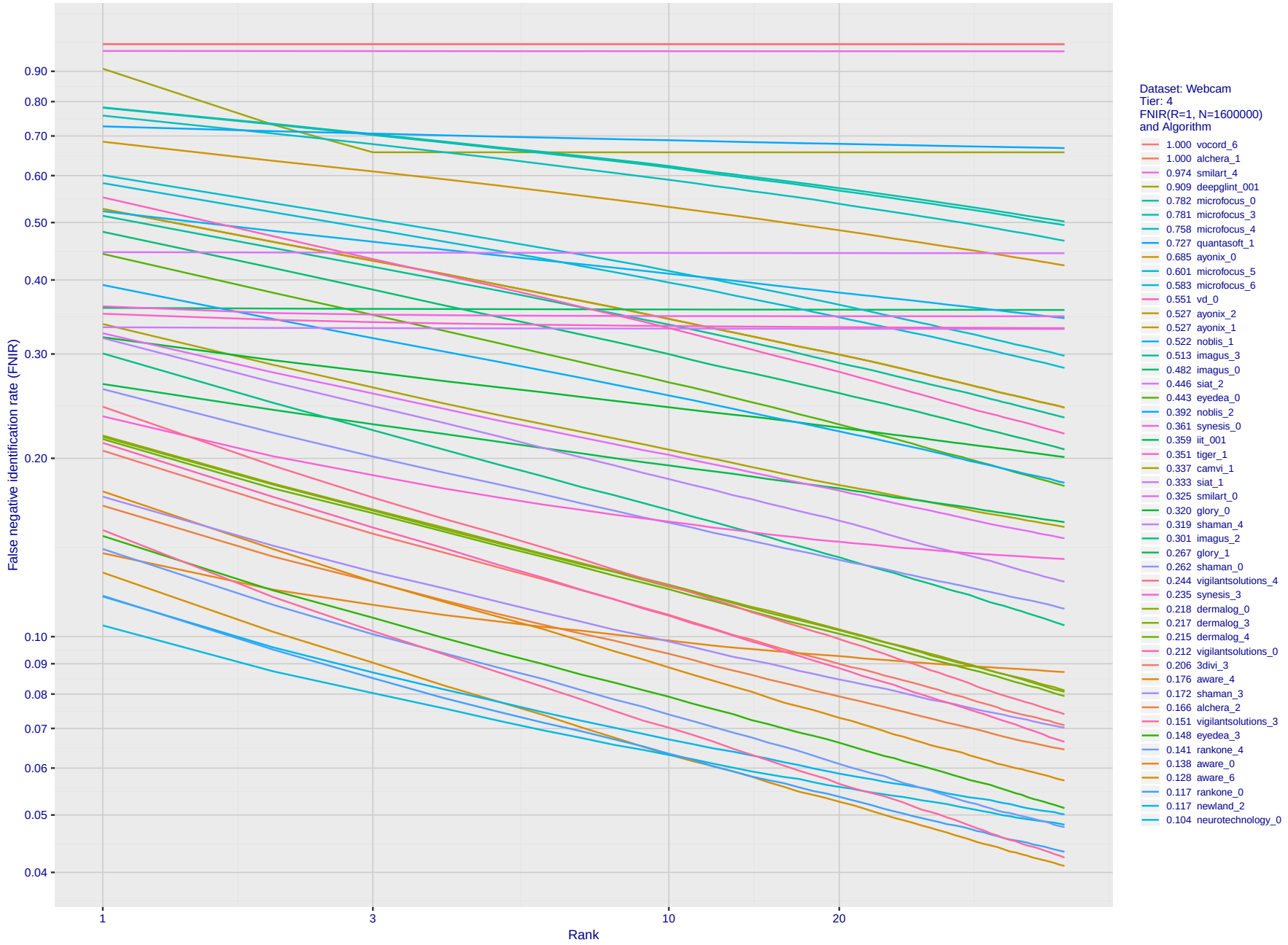

Figure 105: **[Webcam Dataset] Identification miss rates vs. rank**. *The results apply to cross-domain recognition in which webcams are searched against enrolled mugshots. The FNIR values are higher than those for mugshot-mugshot identification due to low image resolution, lighting and less constrained subject pose in webcam images - see Figure 4.*

2020/03/27	FNIR(N, R, T) =	False neg. identification rate	N = Num. enrolled subjects	T = Threshold	$T = 0 \rightarrow$ Investigation
10:40:09	FPIR(N, T) =	False pos. identification rate	R = Num. candidates examined		$T > 0 \rightarrow$ Identification

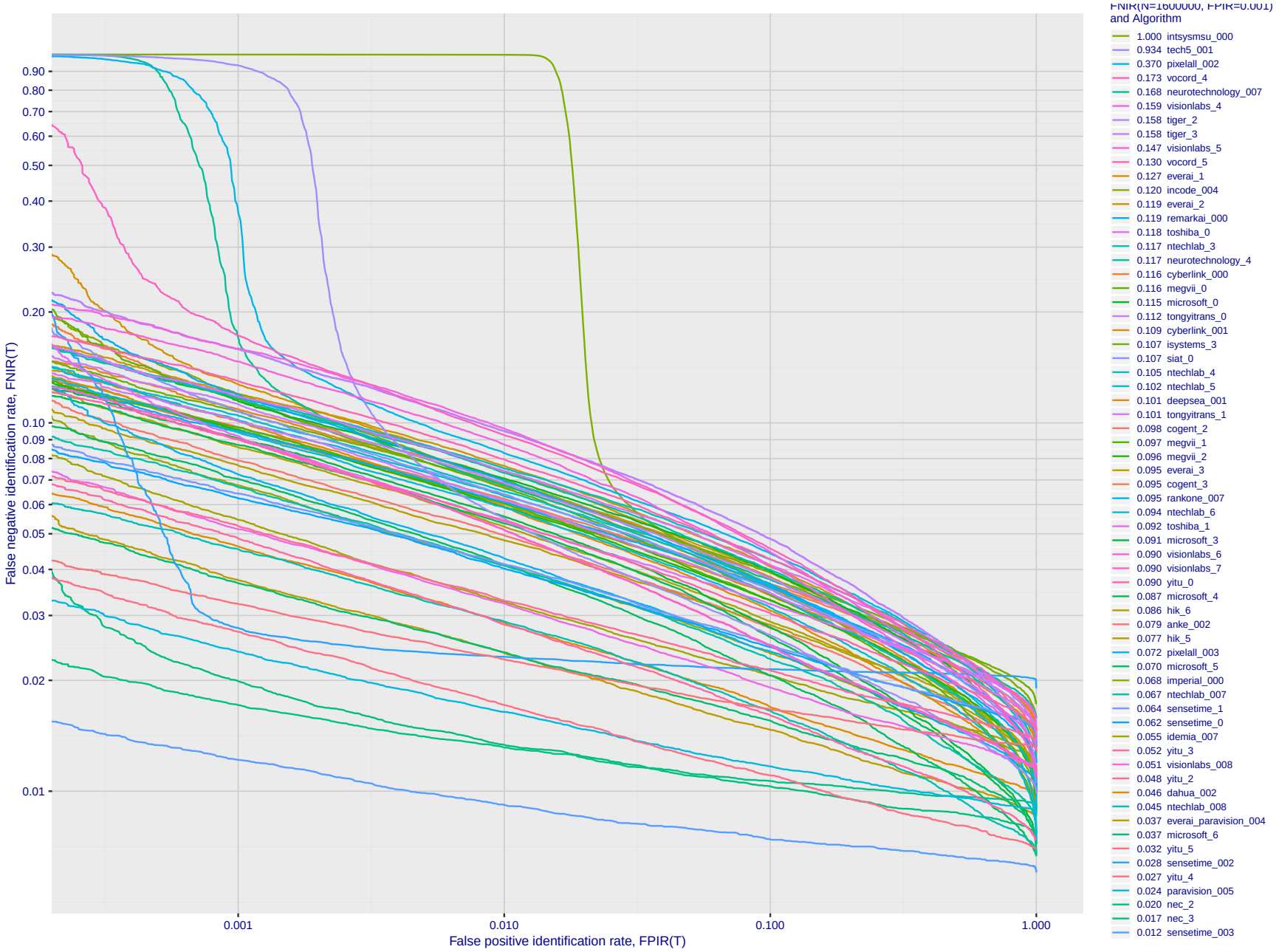

Figure 106: **[Webcam Dataset] Identification miss rates vs. false positive rates**. *The results apply to cross-domain recognition in which webcams are searched against enrolled mugshots. The FNIR values are higher than those for mugshot-mugshot identification due to low image resolution, lighting and less constrained subject pose in webcam images - see Figure 4.*

2020/03/27 10:40:09

FNIR(N, R, T) = False neg. identification rate
FPIR(N, T) = False pos. identification rate

N = Num. enrolled subjects
R = Num. candidates examined

T = Threshold

T = 0 → Investigation
T > 0 → Identification

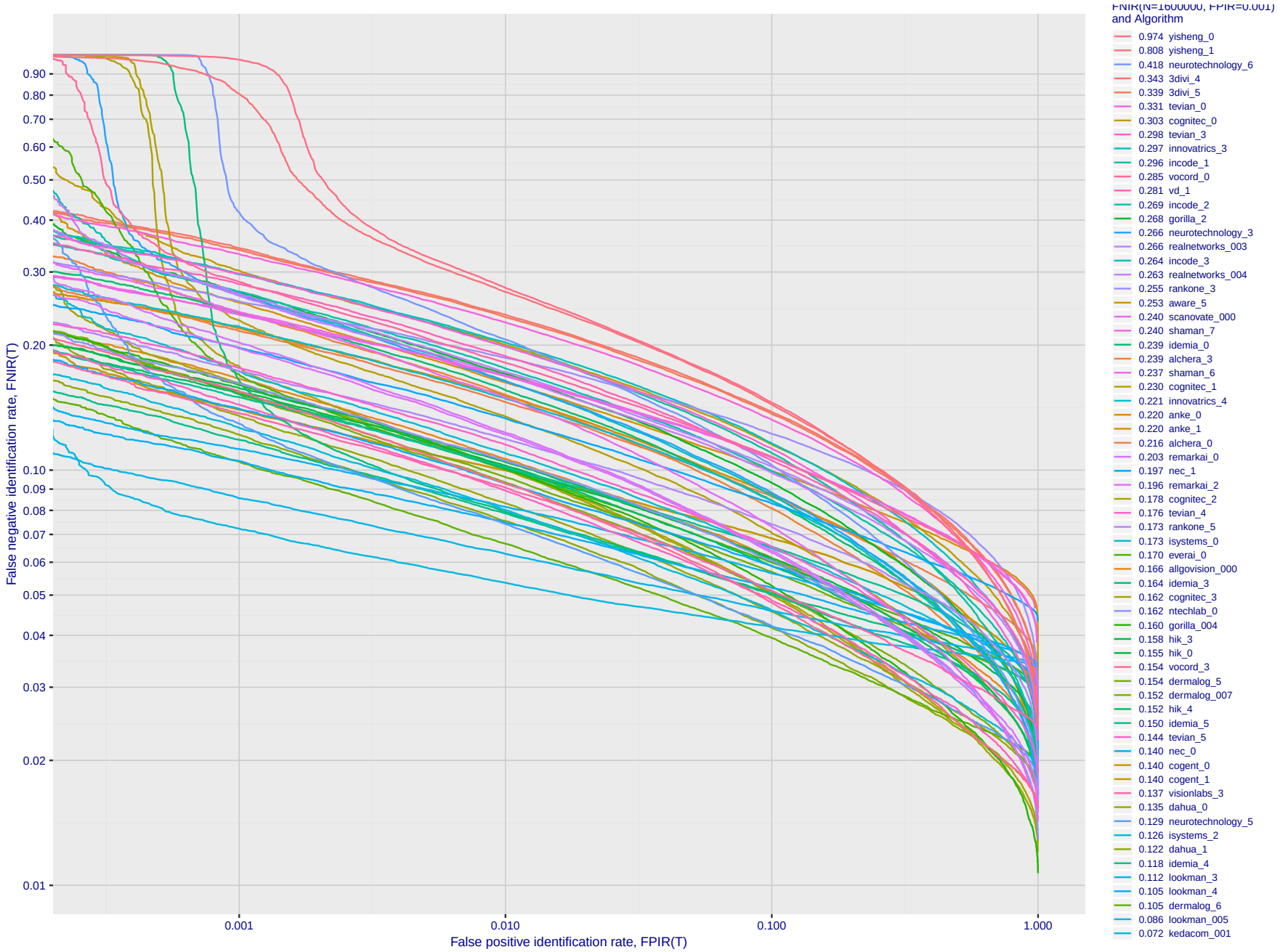

Figure 107: **[Webcam Dataset] Identification miss rates vs. false positive rates**. *The results apply to cross-domain recognition in which webcams are searched against enrolled mugshots. The FNIR values are higher than those for mugshot-mugshot identification due to low image resolution, lighting and less constrained subject pose in webcam images - see Figure 4.*

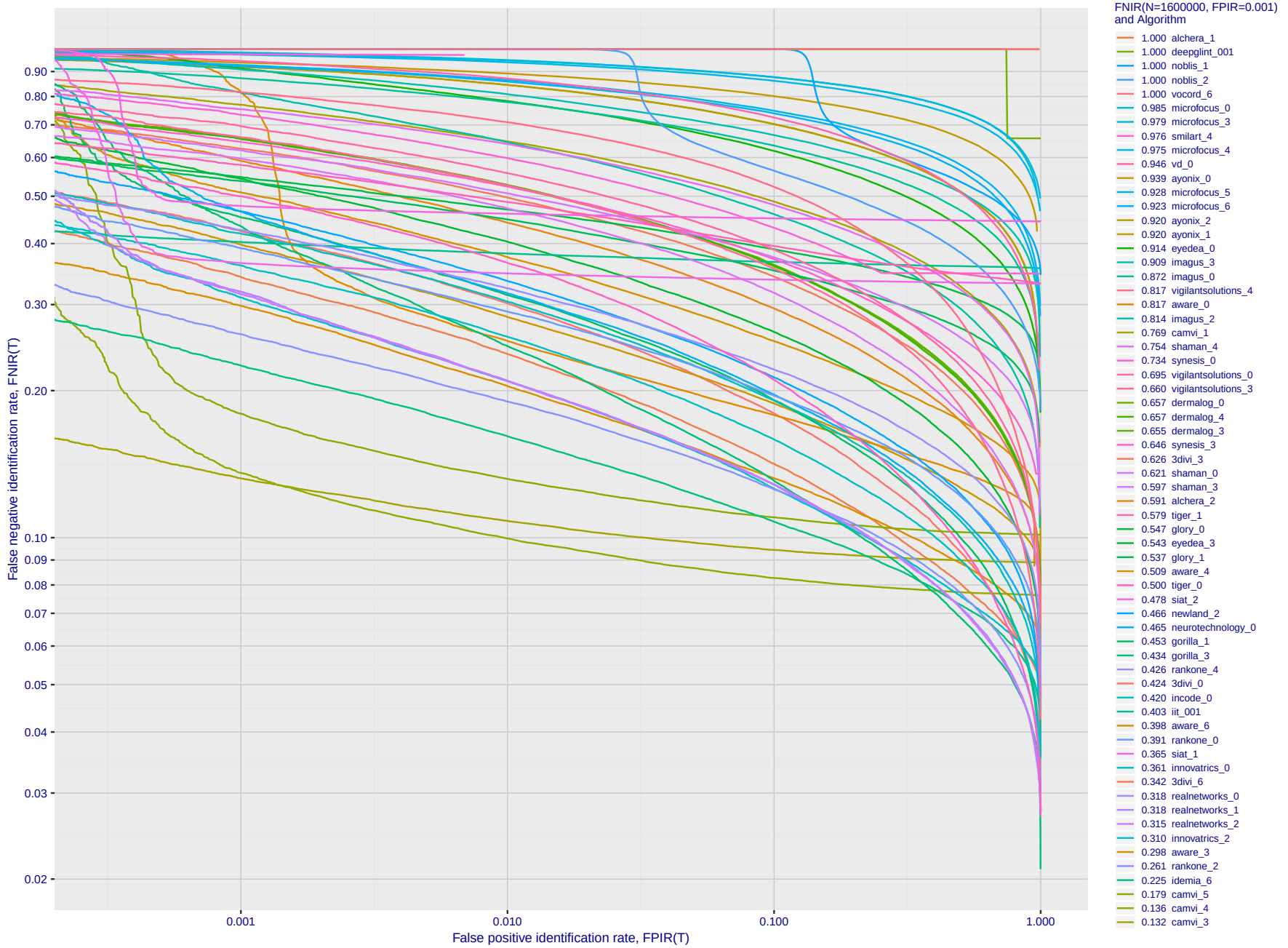

Figure 108: **[Webcam Dataset] Identification miss rates vs. false positive rates**. *The results apply to cross-domain recognition in which webcams are searched against enrolled mugshots. The FNIR values are higher than those for mugshot-mugshot identification due to low image resolution, lighting and less constrained subject pose in webcam images - see Figure 4.*

Appendix E Accuracy for profile-view to frontal recognition

Figures 109 - 111 gives accuracy results for searching 100 000 mated and 100 000 non-mated profile-view images against the same FRVT 2018 frontal enrollment dataset, N = 1 600 000, used in the main mugshot trials. This experiment corresponds to row-13 of Table 1. An example of profile-view image is given in Figure 5.

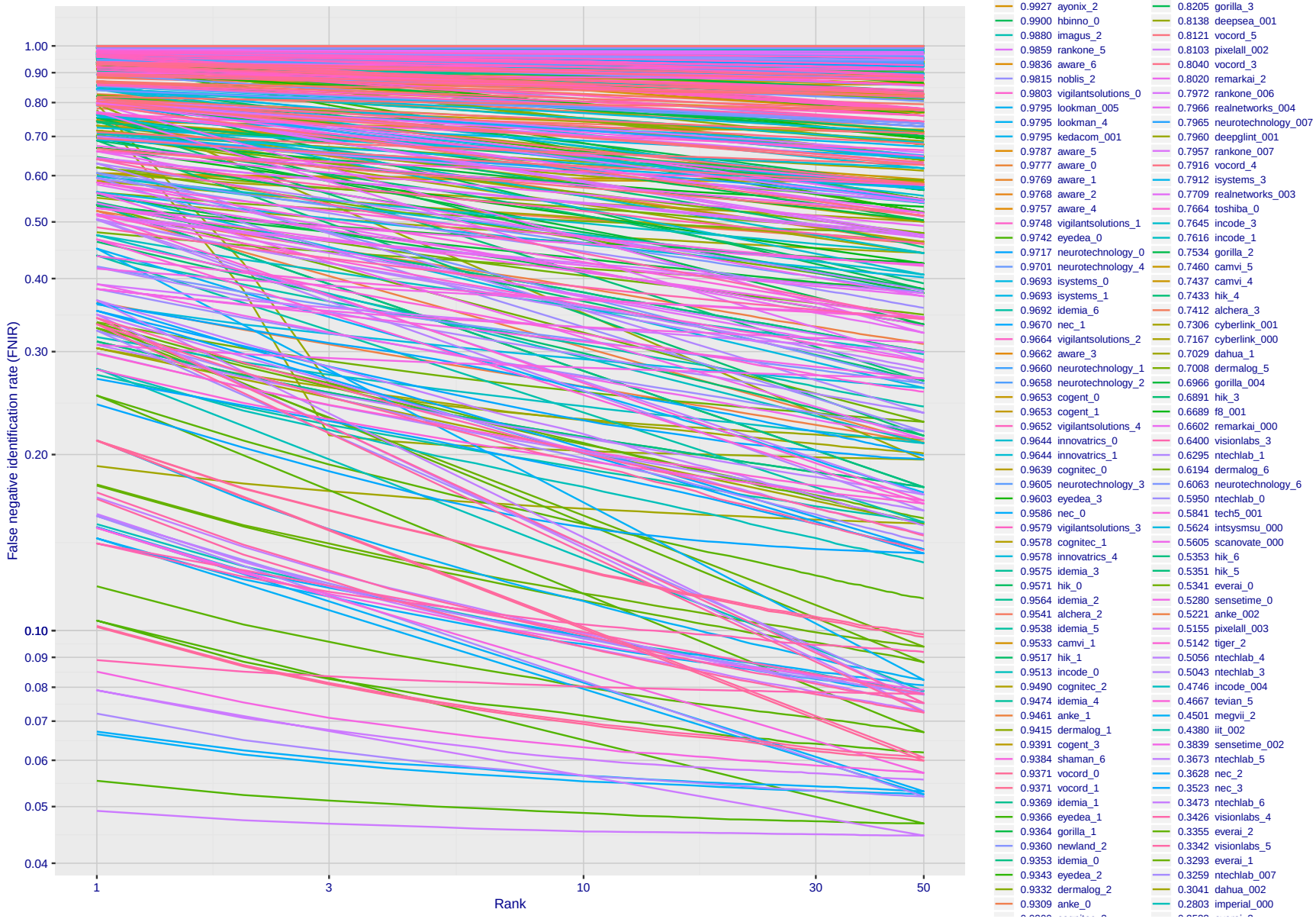

Figure 109: **[Mugshot and profile-view dataset] Rank-based accuracy**. *For some of the more accurate Phase 3 algorithms the figure plots error tradeoff characteristics for frontal and profile-view searches into an enrolled set of N = 1 600 000 frontal images. Note that some algorithms fail on profile-view images with FNIR → 1 - this evaluation did not ask developers to provide profile-view capability. Some algorithms, on the other hand, give FNIR approaching that for frontal-view searches using c. 2010 algorithms. The best result is that 91% of profile-view searches yield the correct mate at rank 1, and better than 94% in the top-50 candidates.*

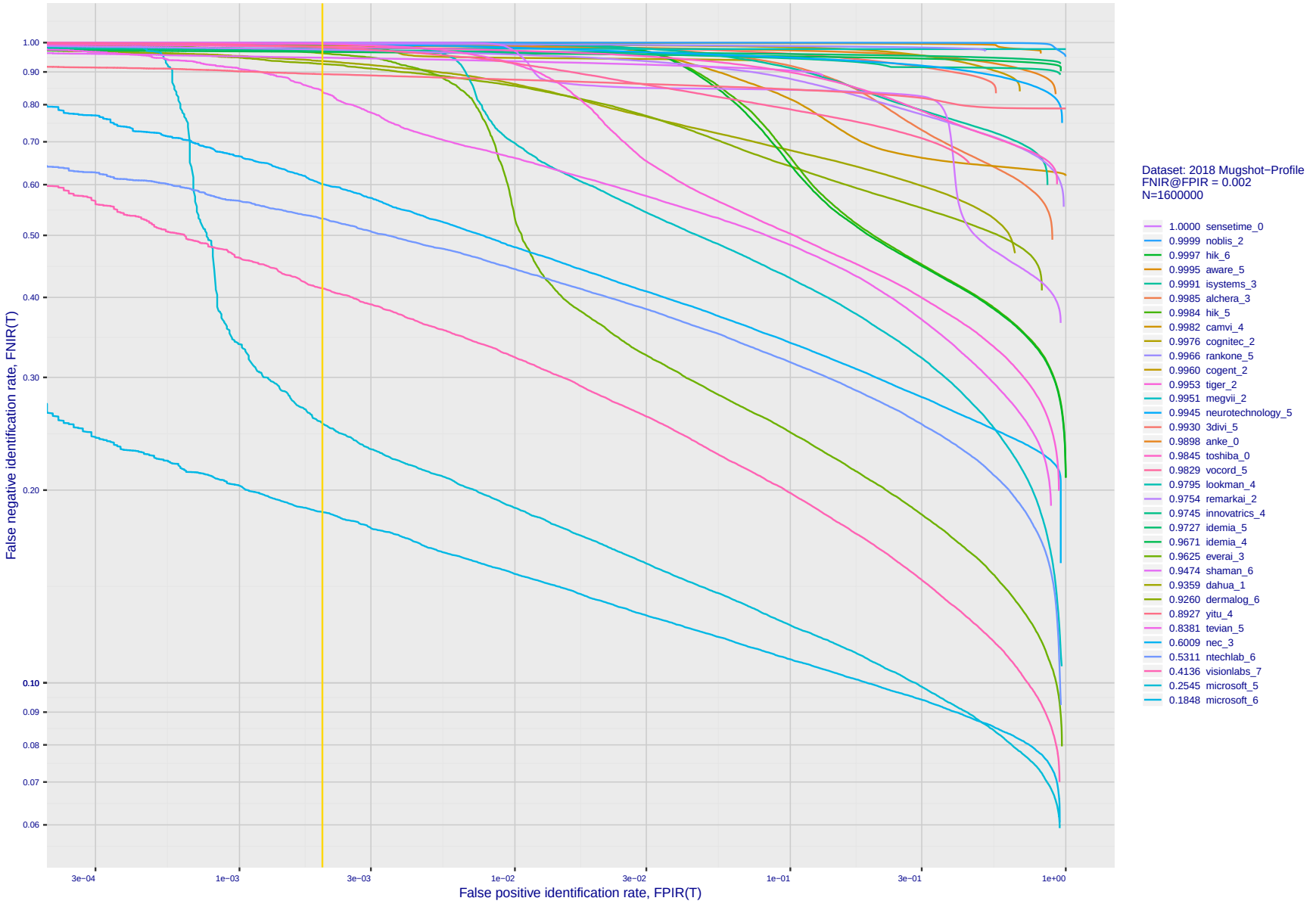

Figure 110: **[Mugshot and profile-view dataset] Threshold-based accuracy**. *For some of the more accurate Phase 3 algorithms the figure plots error tradeoff characteristics for frontal and profile-view searches into an enrolled set of N = 1 600 000 frontal images. Note that some algorithms fail on profile-view images with FNIR → 1 - this evaluation did not ask developers to provide profile-view capability. Some algorithms, on the other hand, give FNIR approaching that for frontal-view searches using c. 2010 algorithms.*

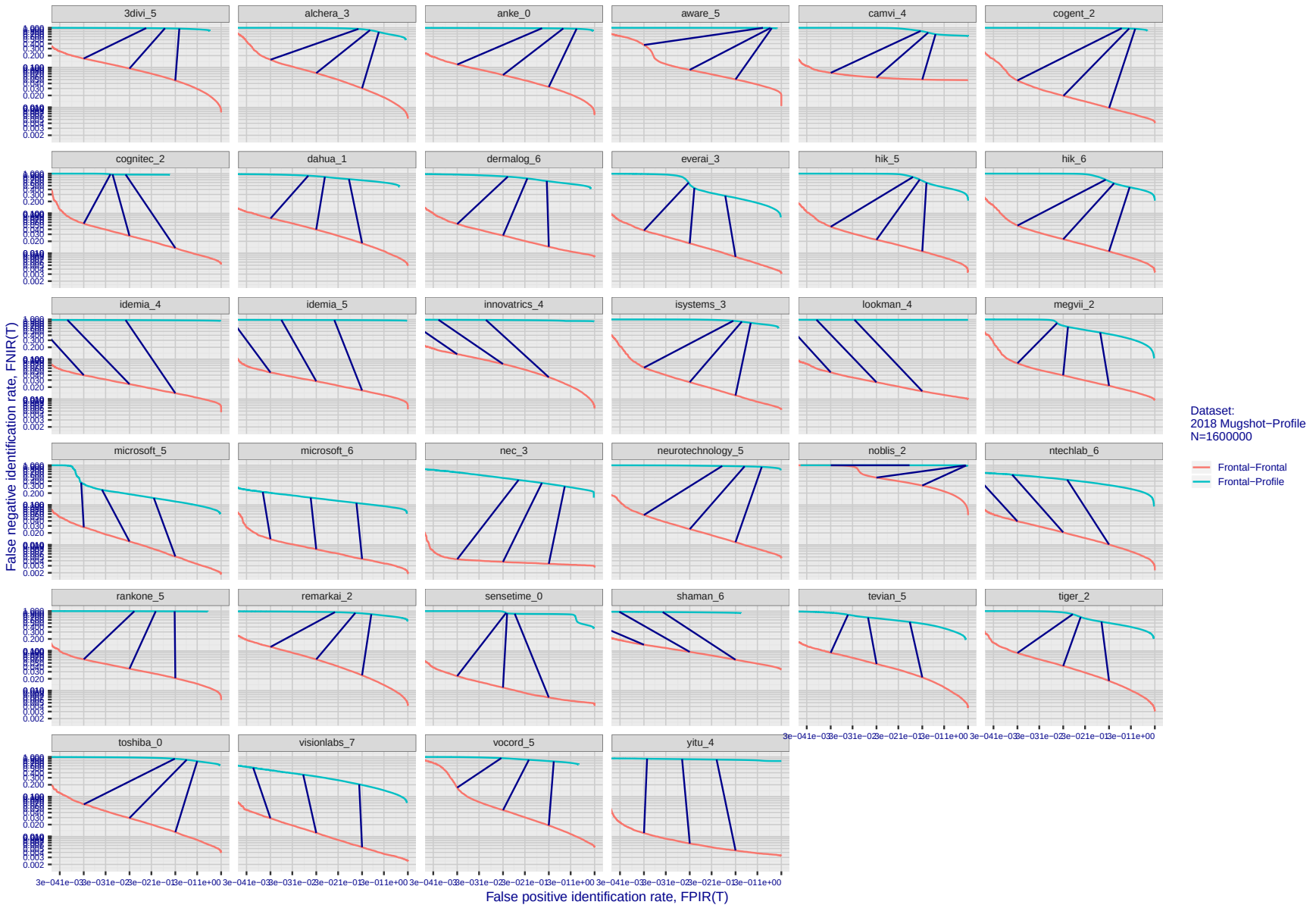

Figure 111: **[Mugshot and profile-view dataset] Speed-accuracy tradeoff**. *For some of the more accurate Phase 3 algorithms the figure plots error tradeoff characteristics for frontal and profile-view searches into an enrolled set of N = 1 600 000 frontal images. Some algorithms fail on profile-view images with FNIR → 1 - this evaluation did not ask developers to provide profile-view capability. Some algorithms, on the other hand, give FNIR approaching that for frontal-view searches using c. 2010 algorithms. Blue lines connect points of equal threshold from which it is evident that some algorithms would give markedly higher false positive outcomes if profile-view images were searched in a system configured for frontal searches. This would be a vulnerability in an access control system.*

Appendix F Search duration

As in and prior tests, this section documents search speeds spanning three orders of magnitude. In applications where search volumes are high enough, this will have implications for hardware requirements especially for large N or when search duration is appreciably larger than the time it takes to prepare a template from the search image(s). Further, given very large (and growing) operational databases, the scalability of algorithms is important. It has been reported previously [7] that search duration can scale sublinearly with enrolled population size N. Further there has been considerable recent research on indexing, exact [12] and approximate nearest neighbor search [1,12] and fast-search [13,15].

Figure 112 charts the search duration measurements presented earlier in Tables 2 - 5.

- ▷ Most algorithms scale linearly. For those in that category, there is a wide range in speed with search durations ranging from 82 milliseconds for a 12 million gallery (for NEC-3) to more than 40 seconds (for Yitu-3, Toshiba-2) and even higher for less accurate algorithms.
- ▷ Some developers (Camvi, Dermalog, EverAI, Innovatrics, and Visionlabs) provide algorithms whose template search durations grow logarithmically i.e. approximately $T(N) = a \log N$ with the constant a varying between implementations. In the figure this model is fit using the point $T(1) = 0$, and $T(640\,000)$. This very sublinear behaviour affords extremely fast search times in very large galleries. One caveat for the sublinear algorithms is that the fast-search data structures require considerable computation time - on the order of hours - for N in the millions, and this scales mildy super-linearly, i.e. $O(N^b), b > 1$. There are exceptions: the Camvi algorithms take minutes; and Innvovatrics' scale sublinearly.

2020/03/27	FNIR(N, R, T) =	False neg. identification rate	N = Num. enrolled subjects	T = Threshold	$T = 0 \rightarrow$ Investigation
10:40:09	FPIR(N, T) =	False pos. identification rate	R = Num. candidates examined		$T > 0 \rightarrow$ Identification

FNIR(N, R, T) = False neg. identification rate
FPIR(N, T) = False pos. identification rate

N = Num. enrolled subjects
R = Num. candidates examined

T = Threshold

T = 0 → Investigation
T > 0 → Identification

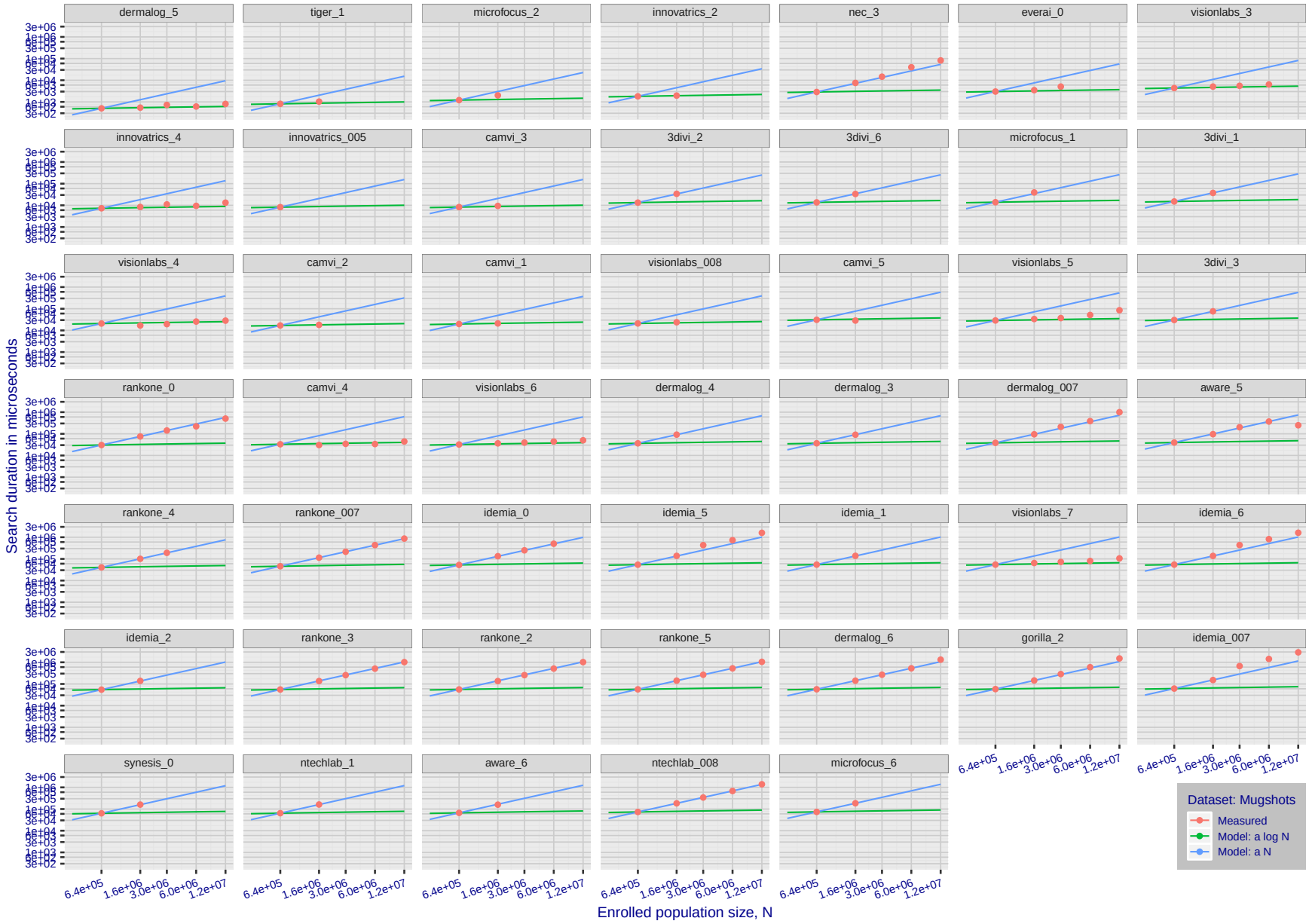

Figure 112: **[Mugshot Dataset] Search duration vs. enrolled population size**. *In red are the actual point durations measured on a single c. 2016 core. The blue shows linear growth from $N = 640\,000$. The green line shows logathmic growth from that point to $N = 1\,600\,000$. Note the sublinear growth from algorithms from Camvi, Dermalog, EverAI, Innovatrics, and Visionlabs. The tiger_1 algorithm is also sublinear, but inaccurate and inoperable at $N \geq 3000000$. This capability sometimes comes at the additional expense of converting a linear gallery data structure into whatever fast-search data structure is used. Note that search times are sometimes dominated by the template generation times shown in Table 18.*

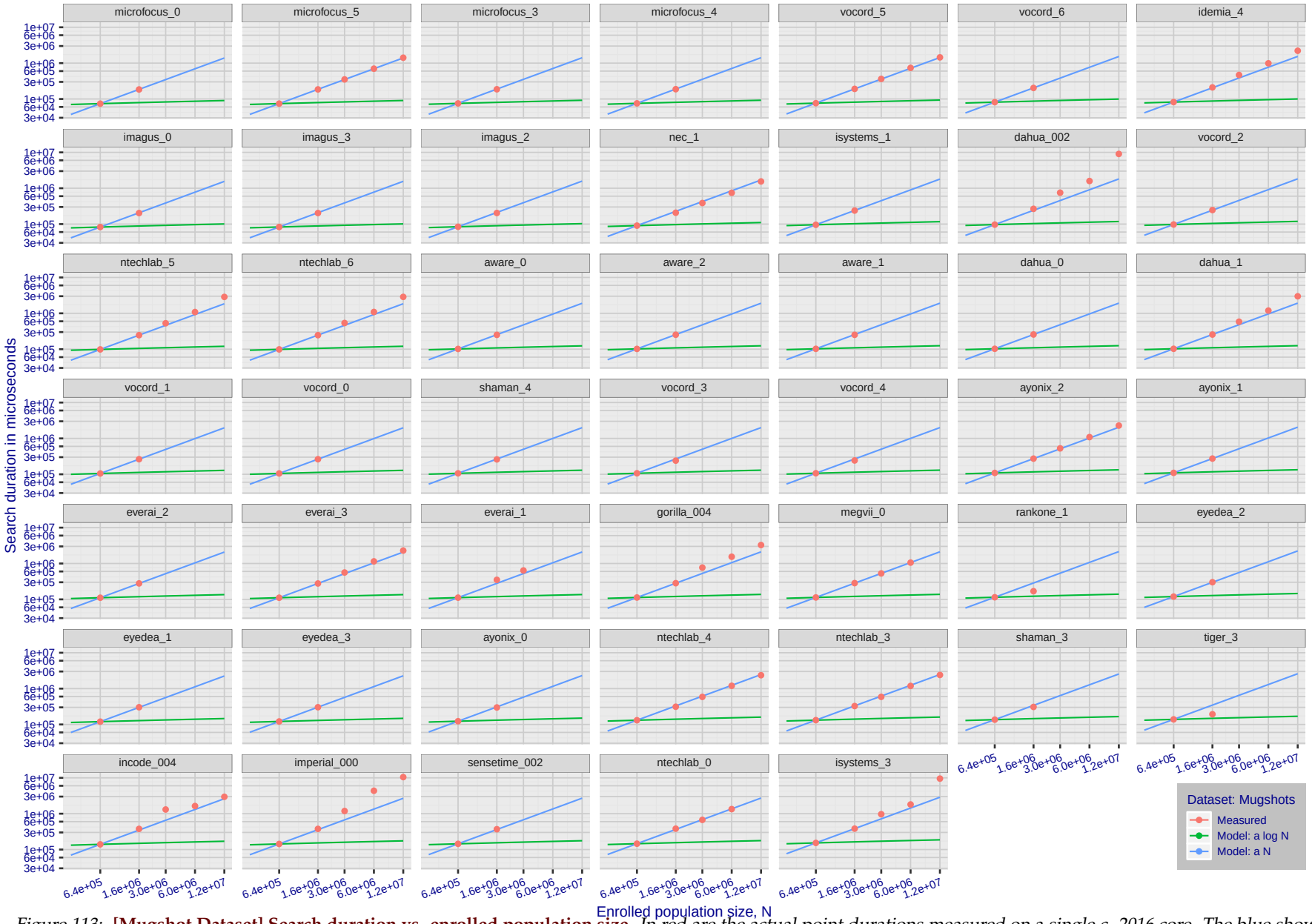

Figure 113: **[Mugshot Dataset] Search duration vs. enrolled population size**. *In red are the actual point durations measured on a single c. 2016 core. The blue shows linear growth from $N = 640\,000$. The green line shows logathmic growth from that point to $N = 1\,600\,000$. Note the sublinear growth from algorithms from Camvi, Dermalog, EverAI, Innovatrics, and Visionlabs. The tiger_1 algorithm is also sublinear, but inaccurate and inoperable at $N \geq 3000000$. This capability sometimes comes at the additional expense of converting a linear gallery data structure into whatever fast-search data structure is used. Note that search times are sometimes dominated by the template generation times shown in Table 18.*

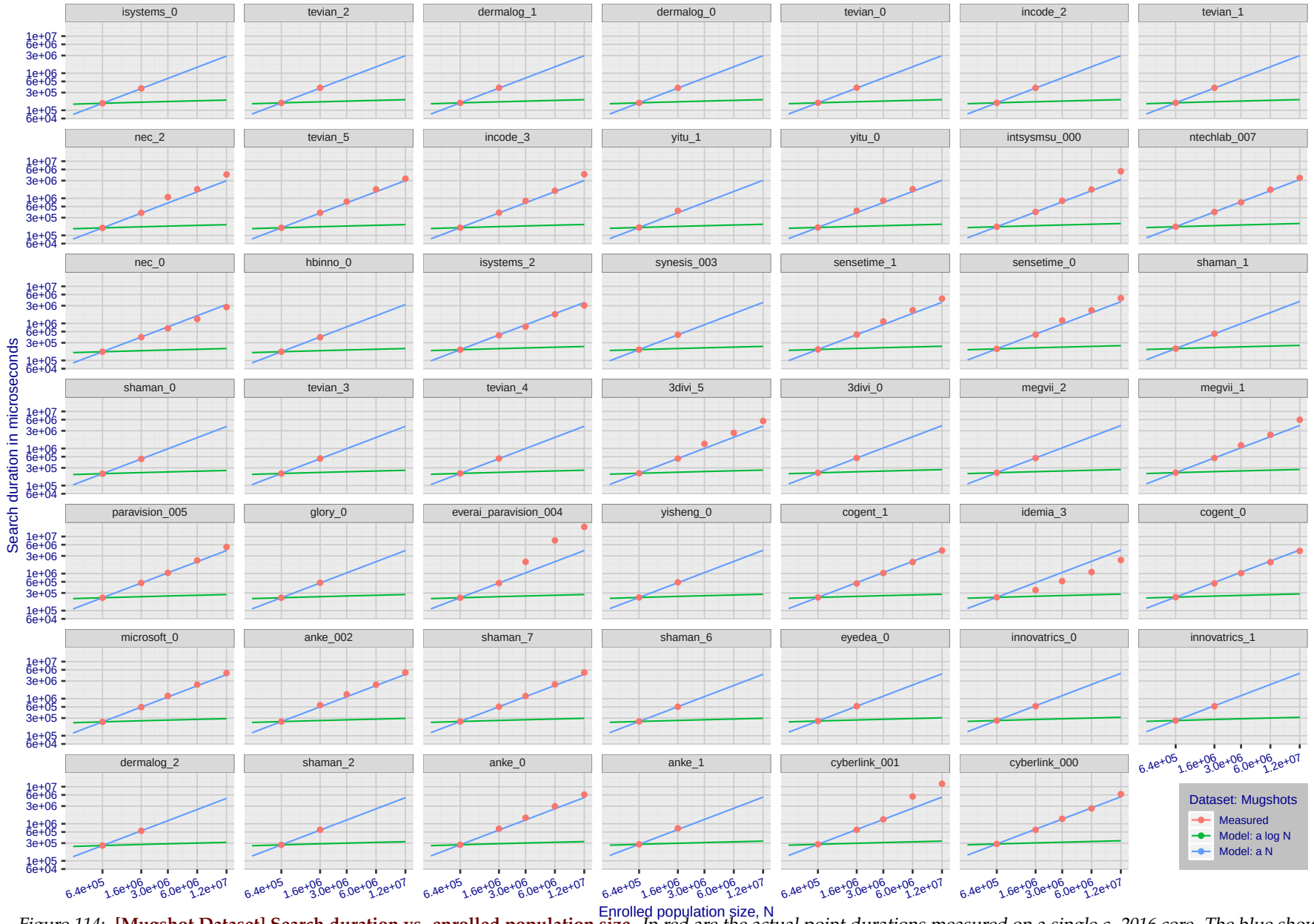

Figure 114: **[Mugshot Dataset] Search duration vs. enrolled population size**. *In red are the actual point durations measured on a single c. 2016 core. The blue shows linear growth from $N = 640\,000$. The green line shows logathmic growth from that point to $N = 1\,600\,000$. Note the sublinear growth from algorithms from Camvi, Dermalog, EverAI, Innovatrics, and Visionlabs. The tiger_1 algorithm is also sublinear, but inaccurate and inoperable at $N \geq 3000000$. This capability sometimes comes at the additional expense of converting a linear gallery data structure into whatever fast-search data structure is used. Note that search times are sometimes dominated by the template generation times shown in Table 18.*

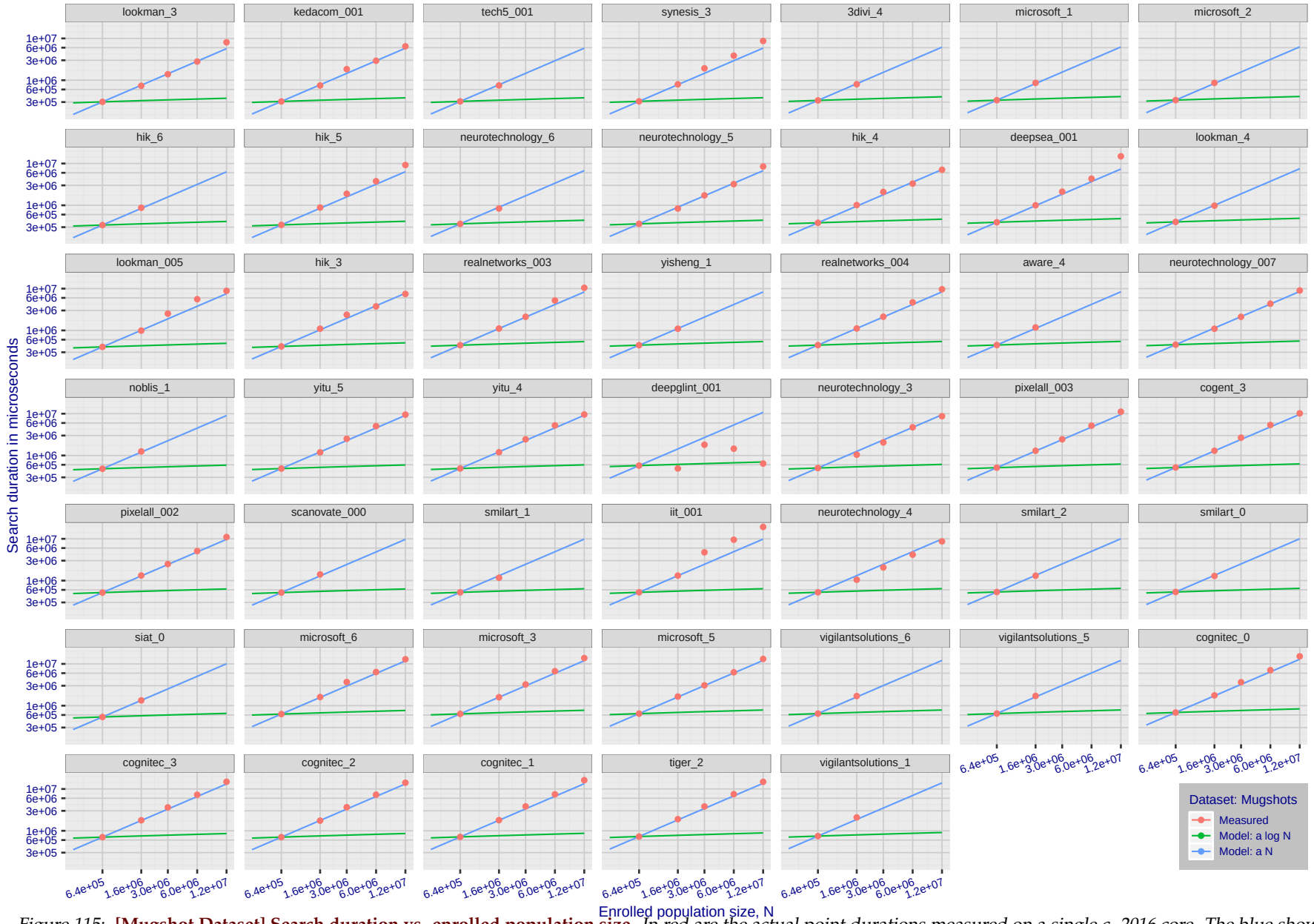

Figure 115: **[Mugshot Dataset] Search duration vs. enrolled population size**. *In red are the actual point durations measured on a single c. 2016 core. The blue shows linear growth from $N = 640\,000$. The green line shows logathmic growth from that point to $N = 1\,600\,000$. Note the sublinear growth from algorithms from Camvi, Dermalog, EverAI, Innovatrics, and Visionlabs. The tiger_1 algorithm is also sublinear, but inaccurate and inoperable at $N \geq 3000000$. This capability sometimes comes at the additional expense of converting a linear gallery data structure into whatever fast-search data structure is used. Note that search times are sometimes dominated by the template generation times shown in Table 18.*

2020/03/27 10:40:09

FNIR(N, R, T) = False neg. identification rate
FPIR(N, T) = False pos. identification rate

N = Num. enrolled subjects
R = Num. candidates examined

T = Threshold

T = 0 → Investigation
T > 0 → Identification

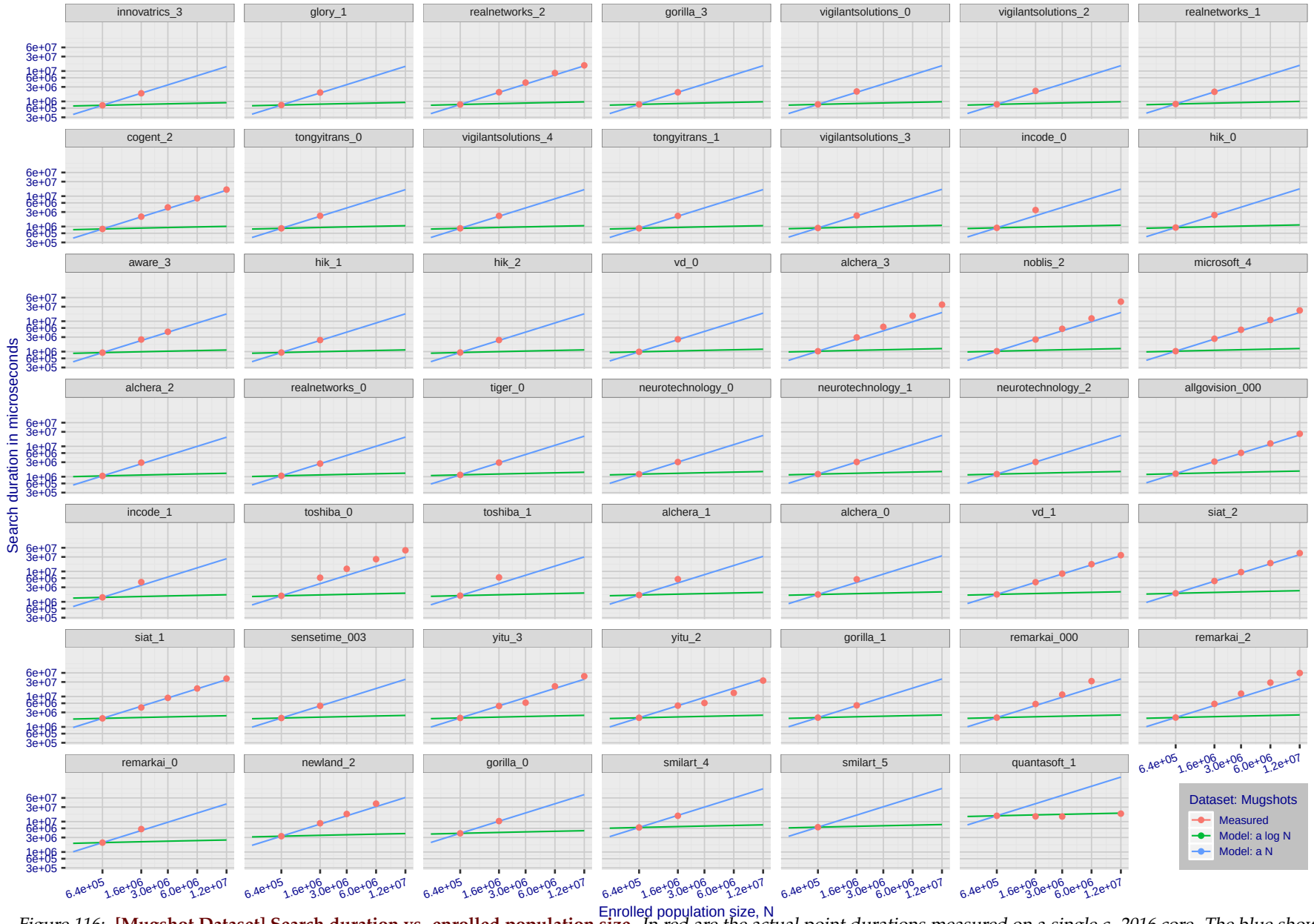

Figure 116: **[Mugshot Dataset] Search duration vs. enrolled population size**. *In red are the actual point durations measured on a single c. 2016 core. The blue shows linear growth from $N = 640\,000$. The green line shows logathmic growth from that point to $N = 1\,600\,000$. Note the sublinear growth from algorithms from Camvi, Dermalog, EverAI, Innovatrics, and Visionlabs. The tiger_1 algorithm is also sublinear, but inaccurate and inoperable at $N \geq 3000000$. This capability sometimes comes at the additional expense of converting a linear gallery data structure into whatever fast-search data structure is used. Note that search times are sometimes dominated by the template generation times shown in Table 18.*

Appendix G Gallery Insertion Timing

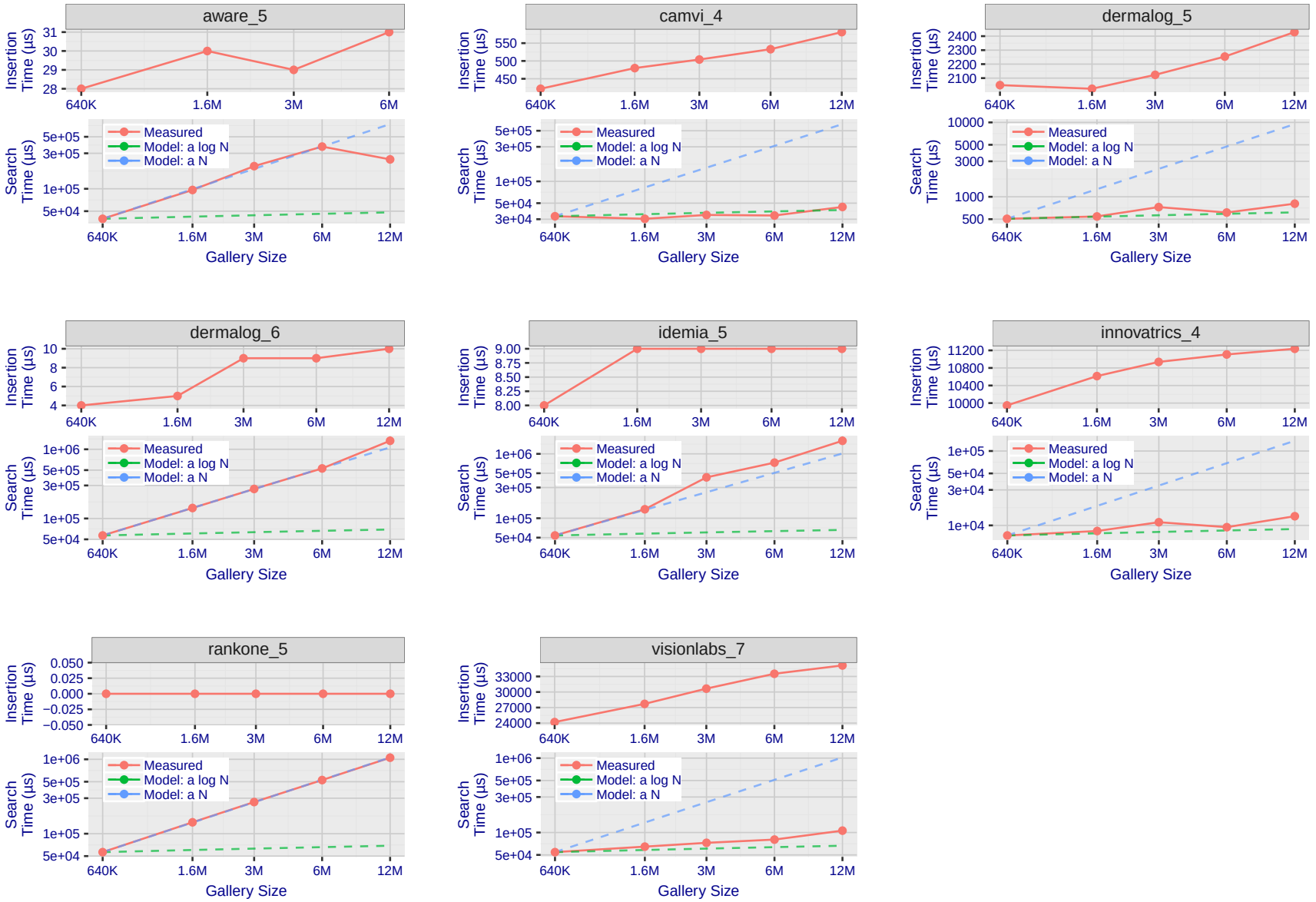

Figure 117: **[Mugshot Dataset] Gallery insertion duration vs. enrolled population size**. *This chart plots the time it takes to insert a single template into a finalized gallery, illustrated over increasing gallery sizes. For reference, search times on finalized galleries of corresponding sizes are plotted right underneath. Gallery insertion time plots were generated on algorithms that 1) successfully implemented gallery insertion with no errors and 2) that were run on galleries with N up to* 12 000 000. *Generally, only the more accurate algorithms were run on galleries with N up to* 12 000 000.

2020/03/27
10:40:09

FNIR(N, R, T) = False neg. identification rate
FPIR(N, T) = False pos. identification rate
N = Num. enrolled subjects
R = Num. candidates examined
T = Threshold
T = 0 → Investigation
T > 0 → Identification

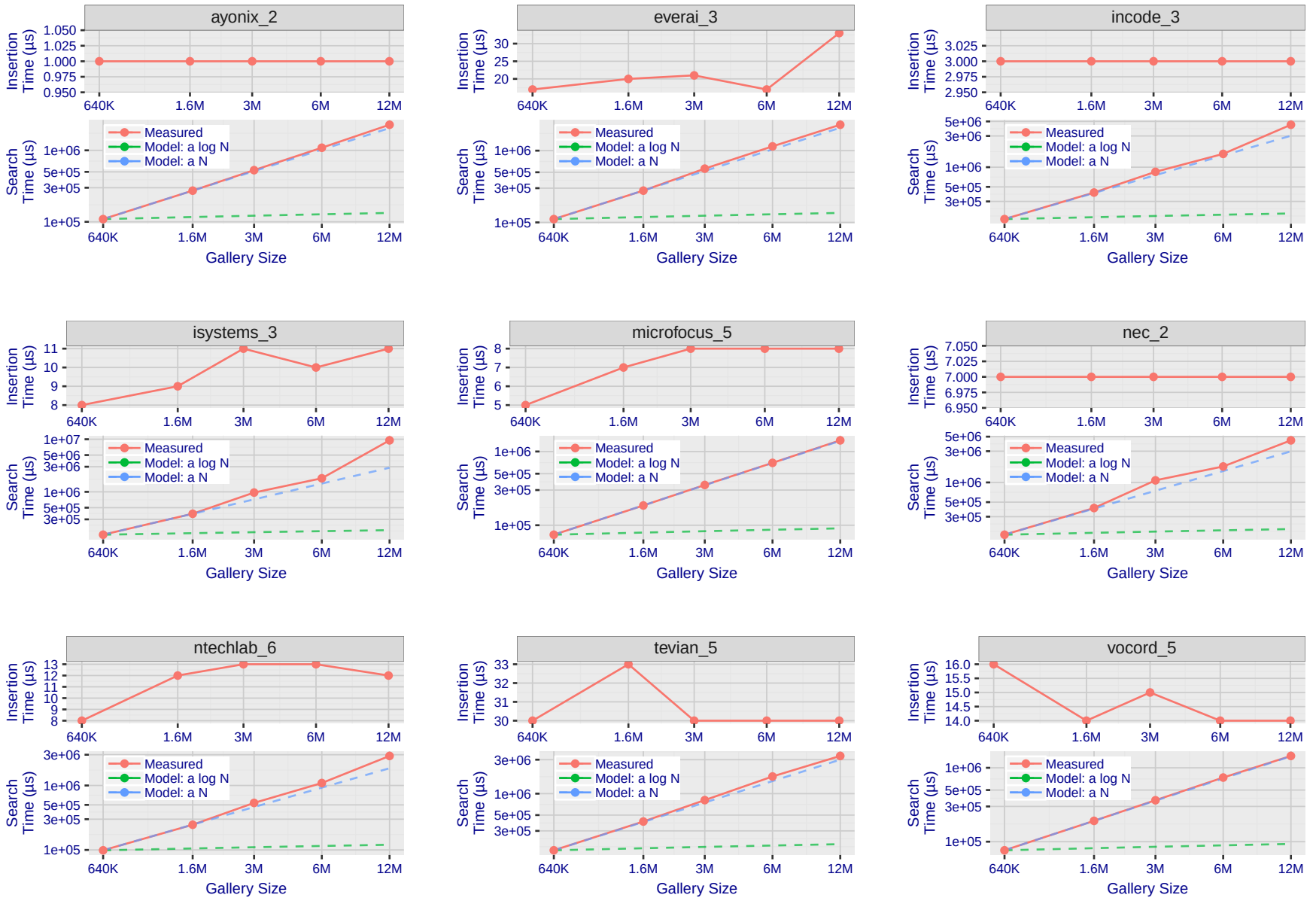

Figure 118: **[Mugshot Dataset] Gallery insertion duration vs. enrolled population size**. *This chart plots the time it takes to insert a single template into a finalized gallery, illustrated over increasing gallery sizes. For reference, search times on finalized galleries of corresponding sizes are plotted right underneath. Gallery insertion time plots were generated on algorithms that 1) successfully implemented gallery insertion with no errors and 2) that were run on galleries with N up to* 12 000 000. *Generally, only the more accurate algorithms were run on galleries with N up to* 12 000 000.

2020/03/27 10:40:09
FNIR(N, R, T) = False neg. identification rate
FPIR(N, T) = False pos. identification rate
N = Num. enrolled subjects
R = Num. candidates examined
T = Threshold
T = 0 → Investigation
T > 0 → Identification

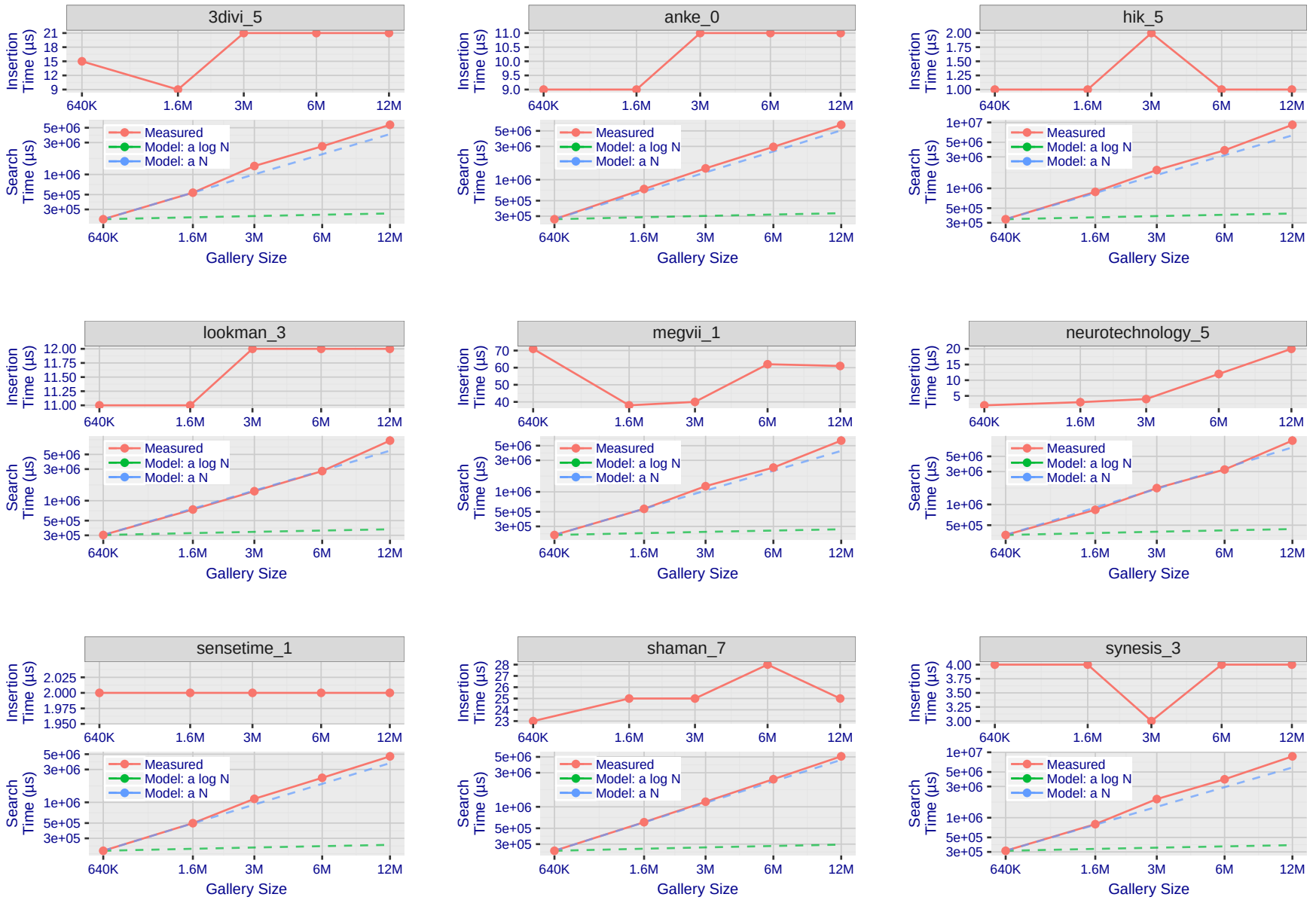

Figure 119: **[Mugshot Dataset] Gallery insertion duration vs. enrolled population size**. *This chart plots the time it takes to insert a single template into a finalized gallery, illustrated over increasing gallery sizes. For reference, search times on finalized galleries of corresponding sizes are plotted right underneath. Gallery insertion time plots were generated on algorithms that 1) successfully implemented gallery insertion with no errors and 2) that were run on galleries with N up to* 12 000 000. *Generally, only the more accurate algorithms were run on galleries with N up to* 12 000 000.

2020/03/27 10:40:09
FNIR(N, R, T) = False neg. identification rate
FPIR(N, T) = False pos. identification rate
N = Num. enrolled subjects
R = Num. candidates examined
T = Threshold
T = 0 → Investigation
T > 0 → Identification

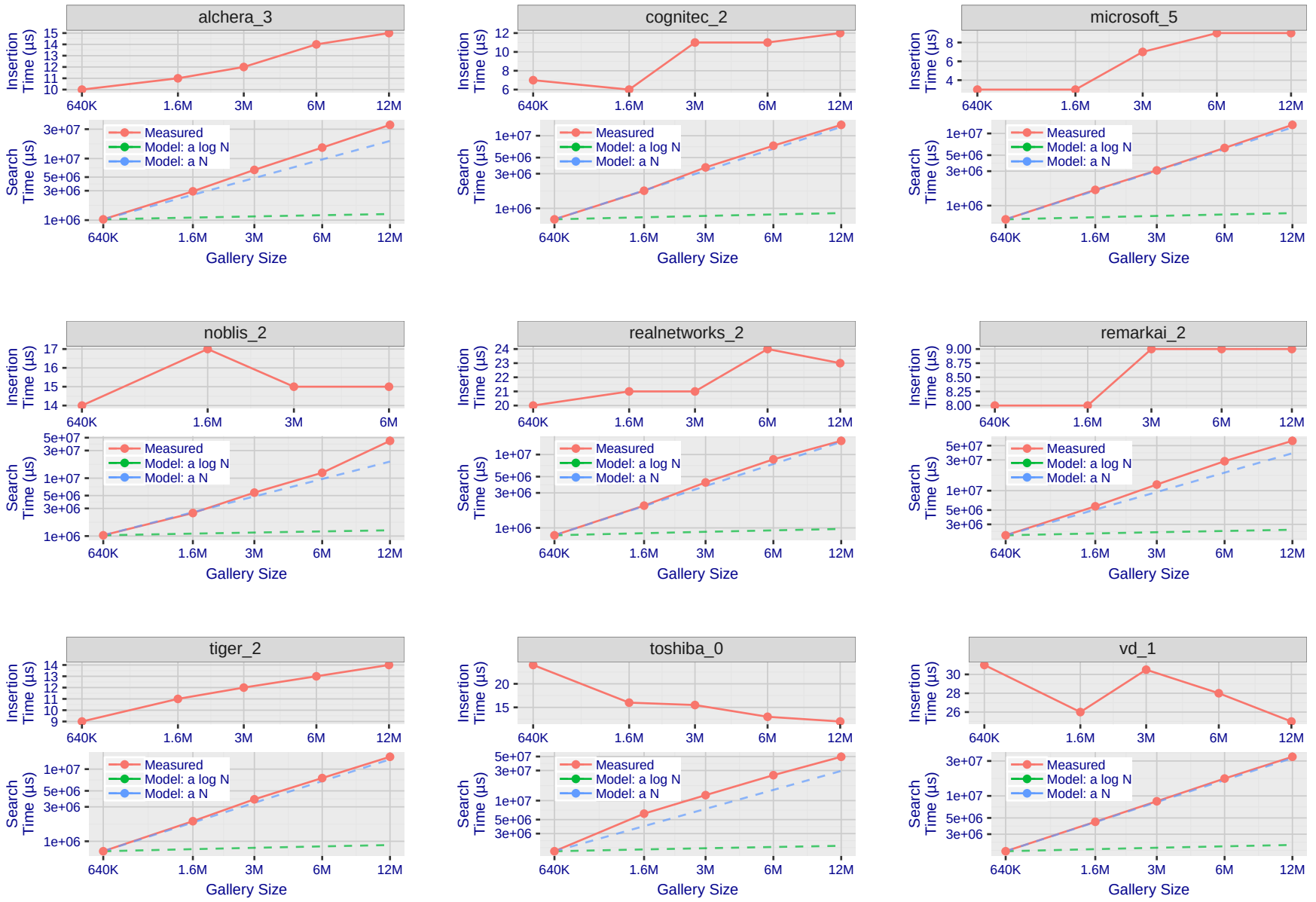

Figure 120: **[Mugshot Dataset] Gallery insertion duration vs. enrolled population size**. *This chart plots the time it takes to insert a single template into a finalized gallery, illustrated over increasing gallery sizes. For reference, search times on finalized galleries of corresponding sizes are plotted right underneath. Gallery insertion time plots were generated on algorithms that 1) successfully implemented gallery insertion with no errors and 2) that were run on galleries with N up to* 12 000 000. *Generally, only the more accurate algorithms were run on galleries with N up to* 12 000 000.

2020/03/27 10:40:09
FNIR(N, R, T) = FPIR(N, T) = False neg. identification rate / False pos. identification rate
N = Num. enrolled subjects
R = Num. candidates examined
T = Threshold
T = 0 → Investigation
T > 0 → Identification

References

[1] Artem Babenko and Victor Lempitsky. Efficient indexing of billion-scale datasets of deep descriptors. In *The IEEE Conference on Computer Vision and Pattern Recognition (CVPR)*, June 2016.

[2] Blumstein, Cohen, Roth, and Visher, editors. *Random parameter stochastic models of criminal careers*. National Academy of Sciences Press, 1986.

[3] Thomas P. Bonczar and Lauren E. Glaze. Probation and parole in the united statesm 2007, statistical tables. Technical report, Bureau of Justice Statistics, December 2008.

[4] White D., Kemp R. I., Jenkins R., Matheson M, and Burton A. M. Passport officers' errors in face matching. *PLoS ONE*, 9(8), 2014. e103510. doi:10.1371/journal. pone.0103510.

[5] P. Grother, G. W. Quinn, and P. J. Phillips. Evaluation of 2d still-image face recognition algorithms. NIST Interagency Report 7709, National Institute of Standards and Technology, 8 2010. http://face.nist.gov/mbe as MBE2010 FRVT2010.

[6] P. J. Grother, R. J. Micheals, and P. J. Phillips. Performance metrics for the frvt 2002 evaluation. In *Proceedings of Audio and Video Based Person Authentication Conference (AVBPA)*, June 2003.

[7] Patrick Grother and Mei Ngan. Interagency report 8009, performance of face identification algorithms. *Face Recognition Vendor Test (FRVT)*, May 2014.

[8] Patrick Grother, George Quinn, and Mei Ngan. Face in video evaluation (five) face recognition of non-cooperative subjects. Interagency Report 8173, National Institute of Standards and Technology, March 2017. https://doi.org/10.6028/NIST.IR.8173.

[9] Patrick Grother, George W. Quinn, and Mei Ngan. Face recognition vendor test - still face image and video concept, evaluation plan and api. Technical report, National Institute of Standards and Technology, 7 2013. http://biometrics.nist.gov/cs_links/face/frvt/frvt2012/NIST_FRVT2012_api_Aug15.pdf.

[10] K. He, X. Zhang, S. Ren, and J. Sun. Deep residual learning for image recognition. In *2016 IEEE Conference on Computer Vision and Pattern Recognition (CVPR)*, pages 770–778, June 2016.

[11] Gary B. Huang, Manu Ramesh, Tamara Berg, and Erik Learned-Miller. Labeled faces in the wild: A database for studying face recognition in unconstrained environments. Technical Report 07-49, University of Massachusetts, Amherst, October 2007.

[12] Masato Ishii, Hitoshi Imaoka, and Atsushi Sato. Fast k-nearest neighbor search for face identification using bounds of residual score. In *2017 12th IEEE International Conference on Automatic Face & Gesture Recognition (FG 2017)*, pages 194–199, Los Alamitos, CA, USA, May 2017. IEEE Computer Society.

[13] Jeff Johnson, Matthijs Douze, and Hervé Jégou. Billion-scale similarity search with gpus. *CoRR*, abs/1702.08734, 2017.

[14] Ira Kemelmacher-Shlizerman, Steven M. Seitz, Daniel Miller, and Evan Brossard. The megaface benchmark: 1 million faces for recognition at scale. *CoRR*, abs/1512.00596, 2015.

[15] Yury A. Malkov and D. A. Yashunin. Efficient and robust approximate nearest neighbor search using hierarchical navigable small world graphs. *CoRR*, abs/1603.09320, 2016.

[16] Joyce A. Martin, Brady E. Hamilton, Michelle J.K. Osterman, Anne K. Driscoll, , and Patrick Drake. National vital statistics reports. Technical Report 8, Centers for Disease Control and Prevention, National Center for Health Statistics, National Vital Statistics System, Division of Vital Statistics, November 2018.

[17] O. M. Parkhi, A. Vedaldi, and A. Zisserman. Deep face recognition. In *British Machine Vision Conference*, 2015.

[18] P. Jonathon Phillips, Amy N. Yates, Ying Hu, Carina A. Hahn, Eilidh Noyes, Kelsey Jackson, Jacqueline G. Cavazos, Géraldine Jeckeln, Rajeev Ranjan, Swami Sankaranarayanan, Jun-Cheng Chen, Carlos D. Castillo, Rama Chellappa, David White, and Alice J. O'Toole. Face recognition accuracy of forensic examiners, superrecognizers, and face recognition algorithms. *Proceedings of the National Academy of Sciences*, 115(24):6171–6176, 2018.

[19] Florian Schroff, Dmitry Kalenichenko, and James Philbin. Facenet: A unified embedding for face recognition and clustering. *CoRR*, abs/1503.03832, 2015.

[20] Jeroen Smits and Christiaan Monden. Twinning across the developing world. *PLOS ONE*, 6(9):1–5, 09 2011.

[21] Yaniv Taigman, Ming Yang, Marc'Aurelio Ranzato, and Lior Wolf. Deepface: Closing the gap to human-level performance in face verification. In *Proceedings of the 2014 IEEE Conference on Computer Vision and Pattern Recognition*, CVPR '14, pages 1701–1708, Washington, DC, USA, 2014. IEEE Computer Society.

[22] A. Towler, R. I. Kemp, and D White. *Unfamiliar face matching systems in applied settings*. Nova Science, 2017.

[23] Working Group 3. Ed. M. Werner. *ISO/IEC 19794-5 Information Technology - Biometric Data Interchange Formats - Part 5: Face image data*. JTC1 :: SC37, 2 edition, 2011. http://webstore.ansi.org.

[24] David White, James D. Dunn, Alexandra C. Schmid, and Richard I. Kemp. Error rates in users of automatic face recognition software. *PLoS ONE*, 10:1–14, October 2015.

[25] Bradford Wing and R. Michael McCabe. Special publication 500-271: American national standard for information systems data format for the interchange of fingerprint, facial, and other biometric information part 1. Technical report, NIST, September 2015. ANSI/NIST ITL 1-2015.

[26] Andreas Wolf. Portrait quality - (reference facial images for mrtd). Technical report, ICAO, April 2018.